

# **TECHNICAL REPORT 93-01**

## **Geology and Hydrogeology of the Crystalline Basement of Northern Switzerland**

Synthesis of Regional Investigations  
1981-1993 within the Nagra Radioactive  
Waste Disposal Programme

May 1994

M. Thury, A. Gautschi, M. Mazurek, W.H. Müller  
H. Naef, F.J. Pearson, S. Vomvoris, W. Wilson



# TECHNICAL REPORT 93-01

## Geology and Hydrogeology of the Crystalline Basement of Northern Switzerland

Synthesis of Regional Investigations  
1981-1993 within the Nagra Radioactive  
Waste Disposal Programme

May 1994

M. Thury<sup>1)</sup>, A. Gautschi<sup>1)</sup>, M. Mazurek<sup>2)</sup>, W.H. Müller<sup>1)</sup>,  
H. Naef<sup>3)</sup>, F.J. Pearson<sup>4)</sup>, S. Vomvoris<sup>1)</sup>, W. Wilson<sup>5)</sup>

1) Nagra, CH-5430 Wettingen

2) Mineralogisch-petrographisches Institut der Universität Bern,  
CH-3012 Bern

3) Büro für angewandte Geologie, CH-9042 Speicher

4) Ground-Water Geochemistry, 1304 Walnut Hill Lane, Suite 210,  
Irving, Texas 75038

5) P.O. Box 914, Georgetown, Colorado 80444, USA

This report was prepared as an account of work sponsored by Nagra. The viewpoints presented and conclusions reached are those of the author(s) and do not necessarily represent those of Nagra.

"Copyright (c) 1994 by Nagra, Wettingen (Switzerland). / All rights reserved.

All parts of this work are protected by copyright. Any utilisation outwith the remit of the copyright law is unlawful and liable to prosecution. This applies in particular to translations, storage and processing in electronic systems and programs, microfilms, reproductions, etc."

## ABSTRACT

This report summarizes the results of regional geological investigations that were carried out by Nagra (Swiss National Cooperative for the Disposal of Radioactive Waste) in Northern Switzerland. These investigations assessed the suitability of the crystalline basement as a host rock for a repository for high-level and long-lived intermediate-level radioactive waste. The investigation programme was conducted during 1981 - 1993 and included the following:

- a deep drilling campaign that consisted of seven boreholes, predominantly cored, with depths that range from 1306 to 2482 m (5900 meters in the crystalline basement and 6400 meters in the overlying sediments) and an extensive programme of logging, packer tests and water sampling
- geophysical investigations that consisted of 400 km of reflection seismics and 230 km of refraction seismics, gravimetry and aeromagnetic surveys
- long-term monitoring of hydraulic pressures
- hydrogeological modeling
- hydrochemical investigations
- geological mapping and compilation of geological maps
- geological studies of outcrops of the crystalline basement in the Southern Black Forest (Germany)
- neotectonic studies, including installation of a network of seven stations for measuring microearthquakes, geodetic measurements, geomorphological studies and stress measurements.

Data from the investigation programme were analysed in detail and the resulting information is contained in more than 100 Nagra Technical Reports. This report synthesises all of those results.

The present-day geological setting of Central Northern Switzerland is the product of a geological evolution that can be traced back more than 400 million years. The most significant events occurred during the Paleozoic Era and Tertiary Period. During the Variscan orogeny, the crystalline basement underwent strong structural and metamorphic/hydrothermal overprinting, which was accompanied by plutonic and volcanic activity. Since then, the lithology and structure of the basement have not changed significantly. The Permo-Carboniferous Trough of Northern Switzerland formed during the late phase of the Variscan orogeny, about 245 million years ago. During the Tertiary Period, after a time of relative tectonic inactivity that lasted about 200 million years, further changes occurred in the region, namely the formation of the Upper Rhine Graben, the updoming of the Black Forest and the formation of the Folded Jura.

The tectonic-structural regime in the crystalline basement cannot be mapped accurately due to the presence of the sedimentary overburden and because current exploration techniques are inadequate. A deterministic characterization of the

conditions in the basement is thus not feasible. For this reason, data from surface-based investigations of the neighboring Southern Black Forest and from boreholes and seismic investigations in Northern Switzerland were used to construct a schematic fault model, which then served as a basis for developing the local hydrogeological model and deriving the explorability study.

On the basis of a detailed analysis of drillcores in the vicinity of water-inflow points, water flow in the crystalline basement correlates with the following structural and lithological discontinuities (water-conducting features):

- cataclastic zones
- fractured zones with open joints
- aplites and aplitic gneisses with brittle deformation

Major water-conducting faults consist of local concentrations of cataclastic zones accompanied by open joints. Due to extensive hydrothermal alteration, the rock in the immediate vicinity of water-conducting features generally has an enhanced microporosity and clay minerals that formed under hydrothermal conditions usually are present; this situation is favorable for the retention of radionuclides.

From a hydrogeological viewpoint, the crystalline basement consists of (1) an upper, higher-permeability domain that is several hundred meters thick and that has a mean hydraulic conductivity of about  $K=1E-7$  m/s; and (2) a lower, low-permeability domain with  $K<1E-10$  m/s. Large subvertical water-conducting faults transect both hydrogeological domains. The deep Permo-Carboniferous Trough of Northern Switzerland functions as a hydraulic barrier that separates the groundwater in the crystalline basement of the Swiss Plateau, which presumably infiltrated in the Alps, from the groundwater in the crystalline basement north of the Permo-Carboniferous Trough, which infiltrated in the Southern Black Forest. The main discharge zone for the latter groundwater is the Rhine River valley.

On the basis of chemical and isotopic compositions, groundwater of the crystalline basement is subdivided into four groups: recent calcium-bicarbonate water with low mineralization (dissolved solids  $< 0.2$  g/l) in the Black Forest; sodium-bicarbonate-sulphate water (dissolved solids about 0.5 g/l) in the area around the Siblingen borehole, which infiltrated during a cold climatic period at least 10,000 years ago; sodium-sulfate water (dissolved solids 0.9-1.4 g/l) in the region Zurzach-Leuggern-Böttstein-Kaisten, which infiltrated before the last ice age, i.e., at least 70,000 years ago; and highly-mineralized, probably in part very old saline waters in low-permeability areas of the crystalline basement (Böttstein, Leuggern, Weiach) or in the vicinity of the Permo-Carboniferous Trough (Säckingen, Schafisheim). The low-mineralized groundwater and some saline groundwater probably evolved entirely within the crystalline basement (Weiach, Leuggern), whereas other saline water contains a component of sedimentary origin (Schafisheim, Säckingen, possibly Böttstein). The understanding of the groundwater flow regime in the basement that is derived from hydrochemical considerations is generally consistent with the understanding derived from hydrogeological modeling.

The long-term geological and climatic evolution of Northern Switzerland was evaluated by considering a range of plausible scenarios. These scenarios were formulated on the basis of data derived from the tectonic history of the region and from neotectonic studies. The updoming of the Southern Black Forest is expected to continue. This process will result in the Rhine river being displaced southwards, in some places as much as 2 km in 1 million years. Fluvial erosion of the Rhine, which is associated with uplift, is estimated to be a maximum of 200 m in the Koblenz region. Differential movements along first order faults (e.g. the Vorwald fault) are predicted to be a maximum of 100 m per million years. Movements along smaller faults (cataclastic zones) will probably be less than 1 m for the same time period.

The geological dataset for the performance assessment model chain was compiled from the results of the regional investigation programme and is presented in the form of conceptual models with a range of parameters; uncertainties are also discussed. The dataset includes hydrogeological information, such as water flow through a repository, distribution of flow among individual water-conducting features and dilution potential of near-surface aquifers and rivers; conceptual models of water-conducting features, with relevant data on their geometry, mineralogy and porosity; an estimate of in situ hydrochemical conditions (reference water); data on concentrations and compositions of colloids in groundwater and geotechnical parameters for studies of repository design and layout.

As part of an explorability study, an investigation concept was formulated that will be used to identify the locations of subvertical, layout-determining water-conducting faults and the extent of suitable blocks of low-permeability crystalline basement. The concept includes reflection seismic surveys and a vertical borehole with a "star" array of four inclined boreholes, all drilled from the same site. Hydraulic testing will be carried out in the boreholes and seismic tomography measurements will be made among the boreholes and between the boreholes and the earth's surface. Statistical analyses indicate that, if the schematic fault model for Northern Switzerland reflects the actual conditions in the crystalline basement of the region, then there is a good chance that at least one sufficiently large block that is suitable for hosting part of a repository can be identified using the above concept. It may be necessary, in a later investigation phase, to drill additional boreholes before underground characterization of the crystalline basement can be done using a shaft and exploratory drifts.

The geological synthesis indicates that potentially suitable crystalline rock at appropriate depths occurs in two regions of Northern Switzerland. The most promising siting options are in a strip of land that is a few kilometers wide south of the Rhine river (area West: Kaisten-Leuggern-Böttstein). A second-priority potential siting region is in Canton Schaffhausen (area East: Siblingen). Area East is less well-characterized and, based on current results, it is recommended that for the time being no further investigations be carried out in this area. Taking into consideration the project-specific boundary conditions set by the Swiss high-level waste-disposal programme, it is proposed that the next investigation phase should include 3D seismics in the Böttstein-Leuggern region and drilling of a "star" of inclined boreholes at the former deep drilling site at Leuggern or Böttstein. These two deep boreholes have already revealed the presence of large sections of low-permeability crystalline basement that are considered suitable for hosting a repository.

## ZUSAMMENFASSUNG

Dieser Bericht fasst die Ergebnisse eines regionalen geologischen Untersuchungsprogramms zusammen, welches die Nationale Genossenschaft für die Lagerung radioaktiver Abfälle (Nagra) in der Nordschweiz zur Abklärung der Eignung des kristallinen Grundgebirges als Wirtgestein für ein Endlager für hochradioaktive und langlebige mittelaktive Abfälle durchgeführt hat. Das Programm erstreckte sich über die Jahre 1981 - 1993 und umfasste:

- ein Tiefbohrprogramm mit sieben Bohrungen mit Endtiefen zwischen 1306 und 2482 m, 5900 Bohrmeter im Kristallin, 6400 Bohrmeter im überlagernden Sediment, vorwiegend gekernt, mit umfangreichem Logging, Packertest- und Wasserprobenahmeprogramm
- geophysikalische Untersuchungen (400 km Reflexionsseismik und 230 km Refraktionsseismik, Gravimetrie, Aeromagnetik)
- Langzeitbeobachtung der Druckverhältnisse der Tiefengrundwässer
- hydrogeologische Modellierungen
- hydrochemische Untersuchungen
- geologische Kartierungen und Kompilation geologischer Karten
- geologische Studien an Aufschlüssen des kristallinen Grundgebirges im Südschwarzwald (Deutschland)
- neotektonische Untersuchungen (Installation von sieben Erdbebenmessstationen zur Erfassung der Mikroerdbeben, geodätische Messungen, geomorphologische Studien, Spannungsmessungen).

Die Untersuchungsergebnisse wurden detailliert ausgewertet. Die Ergebnisse sind in über 100 technischen Berichten der Nagra publiziert worden. Im vorliegenden Bericht wird die Synthese dieser Arbeiten dargestellt.

Die heutigen geologischen Verhältnisse in der zentralen Nordschweiz sind das Ergebnis einer geologischen Entwicklungsgeschichte, die sich über eine Zeitspanne von mehr als 400 Mio. Jahren zurückverfolgen lässt. Die bedeutendsten Ereignisse fallen ins Paläozoikum und ins Tertiär. Während der Variskischen Orogenese erfuhr das kristalline Grundgebirge eine starke strukturelle und metamorphe/hydrothermale Überprägung, begleitet von plutonischer und vulkanischer Aktivität. Bezüglich Lithologie und Struktur ist das Grundgebirge seither nicht mehr wesentlich verändert worden. In diesem Grundgebirge entwickelte sich in einer Spätphase der Variskischen Orogenese bis vor ca. 245 Mio. Jahren der Permokarbon-Trog der Nordschweiz. Nach einer rund 200 Mio. Jahre dauernden, tektonisch relativ ruhigen Periode, kam es im Tertiär zu einer erneuten Umgestaltung der Region, nämlich zur Bildung des Oberrheingrabens, der Aufdomung des Schwarzwaldes und der Entstehung des Faltenjuras.

Die tektonisch-strukturellen Verhältnisse im kristallinen Grundgebirge sind wegen der Sedimentbedeckung nicht kartierbar und mit den heutigen Explorationsmethoden nur

unvollständig erfassbar. Eine deterministische Charakterisierung ist deshalb nicht möglich. Aus diesem Grund musste auf der Basis von Oberflächendaten aus dem benachbarten Südschwarzwald sowie Bohrungen und seismischen Untersuchungen aus der Nordschweiz ein schematisches Störungsmodell erstellt werden, das als Grundlage für das lokale hydrogeologische Modell und die Explorierbarkeitsstudie diene.

Die Wasserführung im Kristallin kann aufgrund einer detaillierten Analyse von Bohrkernen im Bereich von Wasserzuflussstellen mit folgenden strukturellen und lithologischen Diskontinuitäten (wasserführenden Systemen) korreliert werden:

- kataklastische Zonen
- geklüftete Zonen mit offenen Klüften
- spröd deformierte Aplite und aplitische Gneise

Grössere wasserführende Störungen können als lokale Akkumulationen von kataklastischen Zonen, begleitet von offenen Klüften, betrachtet werden. Wegen der extensiven hydrothermalen Umwandlung des Kristallins zeigt das Gestein in der unmittelbaren Umgebung der wasserführenden Systeme im allgemeinen eine erhöhte Mikroporosität sowie hydrothermal gebildete Tonminerale, was sich günstig auf die Radionuklid-Retention auswirkt.

Hydrogeologisch kann das Kristallin in einen mehrere hundert Meter mächtigen, oberen, höherdurchlässigen Bereich mit einer durchschnittlichen hydraulischen Leitfähigkeit in der Grössenordnung von  $K=1E-7$  m/s und in einen unteren, geringdurchlässigen Bereich von  $K<1E-10$  m/s unterteilt werden. Subvertikale, grössere wasserführende Störungen durchschlagen beide hydrogeologischen Einheiten. Der tiefe Nordschweizer Permokarbon-Trog wirkt als hydraulische Barriere und trennt die vermutlich in den Alpen infiltrierten Grundwässern des Kristallins des Mittellandes von den im Südschwarzwald infiltrierten Grundwässern des Kristallins nördlich des Permokarbon-Trogs. Vorfluter dieser letzten Wässer ist der Rhein.

Aufgrund der chemischen Zusammensetzung und der Isotopengehalte lassen sich die Grundwässer im Kristallin in vier Gruppen unterteilen: Junge, schwachmineralisierte Calcium-Hydrogenkarbonat-Grundwässer (gelöste Feststoffe  $<0.2$  g/l) im Schwarzwald, kaltzeitlich (vor mindestens 10'000 Jahren) infiltrierte Natrium-Hydrogenkarbonat-Sulfat-Grundwässer (gelöste Feststoffe um 0.5 g/l) im Gebiet der Bohrung Siblingen, vor der letzten Eiszeit (vor mindestens 70'000 Jahren) infiltrierte Natrium-Sulfat-Grundwässer (gelöste Feststoffe 0.9 - 1.4 g/l) im Gebiet Zurzach-Leuggern-Böttstein-Kaisten sowie höhermineralisierte, zum Teil vermutlich sehr alte saline Grundwässer in geringdurchlässigen Bereichen des Kristallins (Böttstein, Leuggern, Weiach) oder in der Nähe des Permokarbon-Trogs (Säckingen, Schafisheim). Die schwachmineralisierten Grundwässer und ein Teil der salinen Grundwässer zeigen eine chemische Evolution innerhalb des Kristallins (Weiach, Leuggern), der übrige Teil der salinen Wässer enthält eine Komponente sedimentären Ursprungs (Schafisheim, Säckingen, ev. Böttstein). Die hydrochemischen Verhältnisse ergeben generell ein konsistentes Bild mit dem aus den hydrogeologischen Modellen abgeleiteten, regionalen Grundwasserströmungsfeld im Kristallin.

Die geologische und klimatische Langzeitentwicklung der Nordschweiz wird in Form verschiedener möglicher Szenarien diskutiert. Ihre Erarbeitung basiert einerseits auf Erkenntnissen aus der tektonischen Geschichte der Region, andererseits auf Daten der Neotektonik. Zukünftig wird mit einer weiteren Aufdomung des Südschwarzwaldes gerechnet. Dadurch kommt es zu einer Verlagerung des Rheins gegen Süden, stellenweise bis zu 2 km im betrachteten Zeitraum von 1 Mio. Jahre. Die mit der Hebung verbundene Tiefenerosion des Rheins wird auf maximal 200 m im Raume Koblenz geschätzt. Differentialbewegungen entlang von Störungen erster Ordnung (z.B. Vorwaldstörung) werden auf maximal 100 m pro Mio. Jahre prognostiziert. Bewegungen entlang kleinerer Störungen (kataklastische Zonen) dürften im gleichen Zeitraum weniger als 1 m betragen.

Der geologische Datensatz für die Modellkette der Sicherheitsanalyse wurde aus den Ergebnissen des regionalen Untersuchungsprogramms extrahiert und in Form von konzeptuellen Modellen mit einem Spektrum von Parametern dargestellt und bezüglich Unsicherheiten diskutiert. Der Datensatz umfasst hydrogeologische Daten (Wasserfluss durch ein Endlager, Verteilung des Flusses auf die einzelnen wasserführenden Systeme, Verdünnungspotential der oberflächennahen Aquifere und des Vorfluters), konzeptuelle Modelle der wasserführenden Systeme mit entsprechenden Daten über ihre Geometrie, Mineralogie und Porosität, eine Abschätzung der hydrochemischen 'in-situ' Bedingungen (Referenzwasser), Angaben über Konzentration und Zusammensetzung der Kolloide im Grundwasser und geotechnische Parameter für Endlagerbau und -auslegung.

In einer Explorierbarkeitsstudie wurde ein Untersuchungskonzept erarbeitet, mit welchem die räumliche Lage von subvertikalen, auslegungsbestimmenden wasserführenden Störungszonen, respektive die Ausdehnung von geeigneten geringdurchlässigen Kristallinblöcken, nachgewiesen werden kann. Das Konzept sieht neben reflexionsseismischen Untersuchungen eine Vertikalbohrung und vier vom gleichen Bohrplatz aus sternförmig angeordnete Schrägbohrungen vor, in welchen hydraulische Tests und seismisch-tomographische Messungen zwischen den Bohrungen und von den Bohrungen zur Erdoberfläche durchgeführt werden können. Statistische Analysen haben gezeigt, dass, falls das Störungsmodell der Nordschweiz die tatsächlichen Verhältnisse im kristallinen Grundgebirge der Nordschweiz widerspiegelt, eine gute Chance besteht, dass mit obigem Konzept mindestens ein Block mit einer Grösse gefunden werden kann, der für die Aufnahme eines Teils eines Endlagers geeignet sein könnte. In einer weiteren Untersuchungsphase müssten nach Bedarf weitere Bohrungen abgeteuft werden bevor dann, mittels Schacht und Sondierstollen, eine Charakterisierung des Kristallins untertage erfolgen kann.

Insgesamt hat die geologische Synthese ergeben, dass potentiell geeignetes Kristallin in geeigneter Tiefenlage in zwei Gebieten der Nordschweiz vorkommt. Die meistversprechenden Standortmöglichkeiten liegen in einem wenige Kilometer breiten Streifen südlich des Rheins (Gebiet West: Kaisten-Leuggern-Böttstein). Eine potentielle Standortregion zweiter Priorität liegt im Kanton Schaffhausen (Gebiet Ost: Siblingen). Das Gebiet Ost ist weniger gut charakterisiert, und es werden, basierend auf den heute verfügbaren Untersuchungsergebnissen, gegenwärtig keine weiteren Untersuchungen empfohlen. Unter Berücksichtigung der projektspezifischen Randbedingungen des

schweizerischen Programms für die Entsorgung hochradioaktiver Abfälle wird für die unmittelbar nachfolgende Untersuchungsphase die Durchführung von 3D-Seismik im Gebiet Böttstein-Leuggern und die Abteufung von Schrägbohrungen gemäss obigem Konzept an den ehemaligen Bohrlokalationen Leuggern oder Böttstein vorgeschlagen. In diesen beiden Bohrungen wurden bereits grössere Strecken von geringdurchlässigem Kristallin nachgewiesen, das für ein Endlager als geeignet betrachtet wird.

## RÉSUMÉ

Ce rapport présente les résultats du programme régional d'investigations géologiques que la Société coopérative nationale pour l'entreposage de déchets radioactifs (Cédra) a réalisé dans le nord de la Suisse en vue d'examiner l'aptitude du socle cristallin à abriter un dépôt final pour déchets de haute activité et de moyenne activité à vie longue. Ce programme qui s'est étendu de 1981 à 1993 comprenait:

- un programme d'exploration comptant sept forages profonds de 1306 à 2482 m, à savoir 5900 m dans le cristallin et 6400 m dans les couches sédimentaires sus-jacentes, presque entièrement carottés et incluant un programme substantiel de diagraphies (logging), d'essais avec obturateurs (packer) et de prélèvements d'échantillons d'eau,
- des investigations géophysiques (400 km de sismique réflexion et 230 km de sismique réfraction, gravimétrie, géomagnétique aérienne),
- l'observation à long terme de l'évolution de la pression des eaux souterraines profondes,
- la modélisation hydrogéologique,
- des investigations hydrochimiques,
- une cartographie géologique et une compilation de cartes géologiques,
- des études géologiques d'affleurements du socle cristallin dans la partie méridionale de la Forêt Noire (Allemagne),
- des investigations néotectoniques (implantation de sept stations de mesures sismiques pour l'enregistrement des microséismes, mesures géodésiques, études géomorphologiques, mesures de tensions).

Les résultats des investigations ont été analysés en détail. Ils ont été publiés dans plus de 100 rapports techniques de la Cédra. Le présent rapport fait la synthèse de ces travaux.

La situation géologique dans la partie centrale du nord de la Suisse est le résultat de l'évolution géologique que l'on peut suivre sur plus de 400 millions d'années. Les événements les plus déterminants se situent au Paléozoïque et au Tertiaire. L'orogénèse varisque a laissé une profonde marque structurelle et métamorphique/hydrothermale dans le socle cristallin, accompagnée d'activités plutoniques et volcaniques. Depuis lors le socle n'a plus été modifié de façon importante sur les plans lithologique et structural. Le fossé permio-carbonifère du nord de la Suisse s'est développé durant la phase tardive de l'orogénèse varisque jusqu'à il y a environ 245 millions d'années. Après une période de 200 millions d'années relativement calme sur le plan tectonique, la région a subi un réaménagement au Tertiaire, à savoir la formation du fossé rhéan supérieur, le soulèvement de la Forêt Noire et le développement du Jura plissé.

La situation tectonique et structurale du socle cristallin ne peut être cartographiée en raison de sa couverture sédimentaire, et elle ne peut être appréhendée que de façon incomplète avec les techniques d'exploration disponibles à ce jour. Une caractérisation déterministe n'est par conséquent pas possible. Il a fallu pour cette raison élaborer un modèle schématique des failles importantes, sur la base d'indications de surface relevées dans la partie méridionale de la Forêt Noire voisine, ainsi que d'informations tirées de forages et d'investigations sismiques dans le nord de la Suisse. Le modèle a servi de base pour l'établissement d'un modèle hydrogéologique local et pour l'étude des possibilités d'exploration.

Par l'analyse détaillée des carottes de forage dans les zones d'arrivées d'eau, la circulation des eaux dans le cristallin peut être attribuée aux discontinuités structurales et lithologiques (systèmes de circulation d'eau) suivantes:

- zones cataclastiques
- zones fissurées avec fissures ouvertes
- aplites et gneiss aplitiques déformés de manière cassante.

Les zones de failles présentant d'importantes circulations d'eau peuvent être considérées comme des accumulations locales de zones cataclastiques accompagnées de fissures ouvertes. En raison des transformations hydrothermales pénétratives du cristallin, la roche présente de façon générale, dans les environs immédiats des systèmes de circulation d'eau, une microporosité plus élevée ainsi que des minéraux argileux d'origine hydrothermale, constituant ainsi une situation favorable pour la rétention de radionucléides.

Du point de vue hydrogéologique, le cristallin peut être subdivisé en une zone supérieure plus perméable, épaisse de plusieurs centaines de mètres, d'une conductivité hydraulique moyenne de l'ordre de  $K = 1E-7$  m/s, et en une zone inférieure, moins perméable avec  $K < 1E-10$  m/s. Des failles subverticales, présentant d'importantes circulations d'eau, traversent ces deux unités hydrogéologiques superposées. Le profond fossé permo-carbonifère du nord de la Suisse constitue une barrière hydraulique séparant les eaux souterraines du cristallin du Plateau suisse, qui se sont probablement infiltrées dans les Alpes, des eaux souterraines du cristallin situé au nord du fossé permo-carbonifère, qui se sont infiltrées dans la partie méridionale de la Forêt Noire et dont le Rhin constitue l'exutoire.

Les eaux souterraines du cristallin peuvent être subdivisées en quatre groupes sur la base de leur composition chimique et isotopique: eaux souterraines bicarbonatées calciques, peu minéralisées (minéralisation  $< 0.2$  g/l) dans la Forêt Noire, eaux souterraines bicarbonatées sodiques et sulfatées (minéralisation vers 0.5 g/l) dans la région du forage de Siblingen, infiltrées lors d'une période de climat froid (il y a 10'000 ans au moins), eaux souterraines sulfatées sodiques (minéralisation 0.9 -1.4 g/l) dans la région de Zurzach-Leuggern-Böttstein-Kaisten, infiltrées avant la dernière période glaciaire (il y a 70'000 ans au moins) ainsi que des eaux très minéralisées, vraisemblablement en partie des eaux souterraines salines très anciennes, dans les zones peu perméables du cristallin (Böttstein, Leuggern, Weiach) ou à proximité du fossé permo-carbonifère (Säckingen, Schafisheim). Les eaux souterraines peu minéralisées,

ainsi qu'une partie des eaux souterraines salines, montrent une évolution chimique à l'intérieur du cristallin (Weiach, Leuggern), alors que les autres eaux salines contiennent une composante d'origine sédimentaire (Schafisheim, Säcking, év. Böttstein). De façon générale, la situation hydrochimique offre une image cohérente avec le champ de circulation régional des eaux souterraines dans le cristallin déduit des modèles hydrogéologiques.

L'évolution géologique et climatique à long terme du nord de la Suisse est discutée sur la base de différents scénarios possibles. Leur élaboration se fonde d'une part sur les connaissances relatives à l'histoire tectonique de la région et d'autre part sur des informations néotectoniques. On table sur une continuation du soulèvement de la partie méridionale de la Forêt Noire (dôme). Il s'en suit un déplacement du cours du Rhin vers le sud, localement jusqu'à 2 km en un million d'années. On évalue la profondeur de l'érosion du Rhin résultant de ce soulèvement à 200 m au maximum dans la région de Koblenz. Des mouvements différentiels de 100 m au maximum par million d'années sont pronostiqués le long de failles de premier ordre (par ex. la faille de Vorwald). Les mouvements le long de failles plus modestes (zones cataclastiques) devraient être limités à moins de 1 m durant le même laps de temps.

Les données géologiques pour la chaîne de modèles de l'analyse de sûreté ont été tirées des résultats du programme régional d'investigation, et sont présentées sous forme de modèles conceptuels comprenant une fourchette de paramètres et dont les incertitudes sont commentées. L'ensemble des informations comprend des données hydrogéologiques (flux d'eau à travers un dépôt final, distribution du flux entre les différents systèmes de circulation, potentiel de dilution des aquifères proches de la surface et des rivières), des modèles conceptuels des systèmes de circulation des eaux avec les données correspondantes relatives à leur géométrie, minéralogie et porosité, une estimation de la situation hydrochimique "in situ" (eaux de référence), des données concernant la concentration et la composition des colloïdes dans les eaux souterraines, ainsi que des paramètres géotechniques relatifs à la réalisation et la disposition du dépôt final.

Dans le cadre d'une étude d'explorabilité, un concept d'investigations a été élaboré. Ce concept doit permettre de localiser les zones de failles subverticales aquifères ainsi que l'extension de blocs cristallins peu perméables adéquats entre ces failles, qui sont tous deux déterminants pour l'implantation d'un dépôt final. En plus d'investigations par sismique réflexion, ce concept prévoit un forage vertical et quatre forages obliques, foncés à partir d'un même point, dans lesquels pourront être réalisés des tests hydrauliques ainsi que des tomographies par sismique entre les forages de même qu'entre forages et surface du sol. Des analyses statistiques ont montré que si le modèle des failles importantes du nord de la Suisse représente la situation réelle dans le socle cristallin, il existe de bonnes chances pour qu'à l'aide du concept mentionné ci-dessus on puisse trouver au moins un bloc d'extension adéquate afin d'accueillir une partie au moins d'un dépôt final. Lors d'une phase d'investigations ultérieure il faudra, le cas échéant, réaliser encore d'autres forages avant que l'on puisse entreprendre la caractérisation du cristallin en sous-sol à partir d'un puits et de galeries d'exploration.

La synthèse géologique a montré que le cristallin comporte des zones potentiellement adéquates à une profondeur acceptable dans deux régions du nord de la Suisse. Les possibilités de sites les plus prometteuses se situent à l'intérieur d'une bande large de quelques kilomètres au sud du Rhin (zone ouest: Kaisten-Leuggern-Böttstein). Une zone de sites potentiels de seconde priorité se trouve dans le canton de Schaffhouse (zone est: Siblingen). Cette dernière zone est moins bien caractérisée. Sur la base des résultats actuellement disponibles, il n'est pas recommandé d'y poursuivre d'autres investigations pour le moment. Considérant les conditions spécifiques du projet helvétique de stockage final de déchets de haute radioactivité, une campagne de sismique 3D dans la région de Böttstein-Leuggern et des forages inclinés selon le concept ci-dessus sur un des anciens sites de forage de Leuggern ou de Böttstein sont proposés lors d'une prochaine phase d'investigations. Ces forages ont en effet déjà permis d'identifier d'importants tronçons de cristallin peu perméable pouvant être considérés comme adéquat pour un dépôt final.



**CONTENTS**

	page
ABSTRACT	I
ZUSAMMENFASSUNG	IV
RÉSUMÉ	VIII
CONTENTS	XIII
FIGURES	XXI
TABLES	XXVIII
APPENDICES	XXXI
1 INTRODUCTION	1-1
1.1 Contribution of geology to repository safety	1-1
1.2 Historical evolution of the Swiss HLW repository programme	1-2
1.3 Content and structure of the present report	1-3
2 THE GEOLOGICAL INVESTIGATION PROGRAMME 1981 - 1993	2-1
2.1 Overview of the programme	2-1
2.2 Deep drilling programme	2-3
2.3 Geophysical investigations	2-12
2.4 Hydrogeological investigations	2-13
2.4.1 Hydrogeological data	2-14
2.4.2 Hydrodynamic models	2-15
2.5 Hydrochemical investigations	2-16
2.6 Geological map of Central Northern Switzerland 1:100,000 and geological mapping campaigns	2-19
2.6.1 Geological map of Central Northern Switzerland	2-19
2.6.2 Additional geological mapping	2-19
2.7 Geological studies in the Southern Black Forest	2-19
2.8 Neotectonic studies	2-20
2.8.1 Geological-tectonic documentation	2-21
2.8.2 Microearthquake measurement network	2-21
2.8.3 Geomorphological investigations	2-23
2.8.4 Geodetic investigations	2-23
2.8.5 Determining the recent stress field	2-24

3	STRUCTURE AND GEOLOGICAL EVOLUTION OF NORTHERN SWITZERLAND	3-1
3.1	The pre-Mesozoic evolution of the basement	3-3
3.2	Northern Switzerland during the Mesozoic and Early Tertiary	3-11
3.3	Tertiary tectonics in Northern Switzerland	3-13
3.3.1	The formation of the Upper Rhine Graben	3-13
3.3.2	Uplift of the Black Forest	3-16
3.3.3	The subsidence of the Molasse Basin	3-16
3.3.4	Alpine décollement thrust and formation of the Folded Jura	3-17
3.4	Young to recent movements	3-18
3.5	Present-day geothermal conditions	3-19
3.5.1	Introduction	3-19
3.5.2	The temperature field in Northern Switzerland	3-19
3.5.3	Interpretation	3-20
4	GEOLOGICAL EVOLUTION AND PETROGENESIS OF THE CRYSTALLINE BASEMENT	4-1
4.1	The pre-Alpine basement of Central Europe	4-1
4.2	Pre-Variscan and Variscan geology of the Black Forest	4-2
4.2.1	Large-scale subdivision	4-2
4.2.2	Geological evolution of pre-Variscan gneisses	4-4
4.2.3	Evolution of magmatic activity	4-10
4.2.4	Tectonics of Paleozoic sediment zones	4-12
4.2.5	Summary: Succession of magmatic and metamorphic events in the Black Forest	4-12
4.3	Sources of data for the investigation of the crystalline basement of Northern Switzerland	4-13
4.4	Lithological units in the crystalline basement of Northern Switzerland	4-13
4.4.1	Paragneisses	4-16
4.4.2	Orthogneisses	4-17
4.4.3	Variscan intrusives: granites and basic batholiths - occurrence and comparison with the Southern Black Forest	4-17
4.4.4	Variscan intrusives: dykes	4-19
4.4.5	Lithological correlations between boreholes in Northern Switzerland	4-20
4.5	Post-metamorphic/post-magmatic (Late and post-Variscan) evolution of the crystalline basement of Northern Switzerland	4-20

4.5.1	Retrograde effects of cooling in gneisses	4-21
4.5.2	Retrograde effects of cooling in granites	4-21
4.5.3	Tourmaline-quartz veins	4-21
4.5.4	Ductile quartz deformation	4-23
4.5.5	Alteration related to dyke intrusion	4-23
4.5.6	High-temperature cataclasis and hydrothermal alteration	4-23
4.5.7	Formation of ore and mineral veins in the Black Forest	4-26
4.5.8	Low-temperature cataclasis and hydrothermal alteration	4-31
4.5.9	Surface weathering	4-33
4.5.10	Kaolinitic alteration	4-33
4.5.11	Generation of vugs/channels and mineralizations	4-34
4.5.12	Summary: Late- and post-Variscan evolution of the basement of Northern Switzerland	4-35
5	STRUCTURAL ELEMENTS OF NORTHERN SWITZERLAND AND SCHEMATIC FAULT MODELS FOR THE CRYSTALLINE BASEMENT	5-1
5.1	Glossary of terms	5-1
5.2	Inventory of regional structures	5-2
5.2.1	The Upper Rhine Graben (URG) and the Rhenish Fault Pattern of Northern Switzerland	5-2
5.2.2	The fault pattern of the sedimentary cover of Northern Switzerland	5-3
5.2.3	The Permo-Carboniferous Trough of Northern Switzerland (PCT)	5-8
5.2.4	Structural elements in the southern Black Forest and the crystalline basement of Northern Switzerland	5-9
5.2.5	Description of the key structures	5-13
5.3	Schematic fault models	5-20
5.3.1	Introduction	5-20
5.3.2	Classification and description of relevant structural features	5-21
5.3.3	Modeling faults	5-23
5.3.4	Schematic fault model in area West (Fig. 5-7)	5-24
5.3.5	Schematic fault model in area East (Fig. 5-8)	5-26
6	GEOLOGICAL CHARACTERIZATION OF WATER-CONDUCTING FEATURES IN THE CRYSTALLINE BASEMENT	6-1
6.1	Comments on the scale of observation	6-1

6.2	Identification of water-inflow points in Nagra's deep boreholes: Definitions and methodology	6-2
6.2.1	Sources and treatment of hydraulic data	6-2
6.2.2	Results	6-3
6.3	Geological classification of inflow points	6-6
6.3.1	Concept	6-6
6.3.2	Structural elements and their regional correlation	6-6
6.4	Types of water-conducting features in the basement of Northern Switzerland	6-14
6.4.1	Comments on fractured aplite/pegmatite dykes and aplitic gneisses	6-16
6.4.2	Distinction between plutonites and gneisses	6-16
6.5	How representative are the borehole observations ? Comparison with geological and hydrological evidence from the Black Forest	6-17
6.5.1	Ore and mineral veins in the Black Forest	6-17
6.5.2	Hydrogeological parameters derived from boreholes in the Black Forest	6-18
6.5.3	Geometric and hydrogeological characterization of dykes	6-19
6.6	Mineralogy of water-conducting features	6-21
6.6.1	Mineralogy of cataclastic and jointed zones	6-22
6.6.2	Mineralogy of fractured aplite/pegmatite dykes and aplitic gneisses	6-24
6.7	Porosity of water-conducting features	6-26
6.7.1	Microscopic pore-space geometry	6-26
6.7.2	Quantitative porosimetry	6-30
6.8	Spatial orientation of water-conducting features	6-37
6.8.1	Orientation of cataclastic zones	6-37
6.8.2	Orientation of joints	6-37
6.8.3	Orientation of aplite/pegmatite dykes	6-37
6.8.4	Orientation of aplitic gneiss layers	6-38
6.9	Depth dependence of water-conducting features, geological and hydraulic parameters	6-40
6.10	3-dimensional spatial arrangement of higher- and low-permeability crystalline basement	6-42
6.11	Water-conducting features in large-scale faults	6-43
6.12	Relative abundances of water-conducting features	6-44
6.13	Spatial heterogeneity of water-conducting features: Fracture apertures and channeling	6-45

6.13.1	Conceptual models of natural fractures	6-45
6.13.2	Possible channeling in water-conducting features in the crystalline basement in Northern Switzerland	6-46
6.14	Summary	6-47
7	CHEMISTRY, ORIGIN AND RESIDENCE TIME OF GROUND-WATER IN THE CRYSTALLINE BASEMENT	7-1
7.1.	Scope of investigations and data presented	7-1
7.2	Hydrochemistry of groundwater in the crystalline basement and adjacent units	7-4
7.2.1	Description of water chemistry	7-4
7.2.2	Chemical evolution	7-9
7.3	Isotope hydrogeology	7-23
7.3.1	Scope and objectives of isotope studies	7-23
7.3.2	Groundwater mixing and sample contamination	7-23
7.3.3	Recharge areas and conditions	7-24
7.3.4	Isotopic composition, geochemistry and origin of solutes	7-26
7.3.5	Groundwater residence and travel times	7-31
7.4	Hydrochemical and isotopic evidence of cross-formational flow between the pre-Mesozoic basement and overlying sedimentary aquifers	7-32
7.5	Summary of conclusions	7-33
8	HYDROGEOLOGY OF THE CRYSTALLINE BASEMENT	8-1
8.1	Hydraulic data from boreholes	8-1
8.1.1	Hydraulic properties	8-3
8.1.2	Hydraulic head	8-8
8.2	Conceptual hydrogeological model	8-10
8.2.1	Sedimentary rock components	8-13
8.2.2	Crystalline rock components	8-14
8.3	Approach to the quantification of groundwater flow	8-19
8.4	Regional groundwater flow system	8-20
8.4.1	Hydraulic boundary conditions	8-22
8.4.2	Hydraulic properties	8-26
8.4.3	Model results (base case)	8-27
8.4.4	Sensitivity analyses	8-30
8.4.5	Flux analyses	8-33

8.4.6	Addition of first order faults	8-35
8.4.7	Evaluation of regional flow	8-36
8.5	Local groundwater flow system - area West	8-39
8.5.1	Input to the local-scale model	8-39
8.5.2	Model results	8-42
8.5.3	Evaluation of local groundwater flow	8-51
8.6	Flow within blocks of low-permeability domain - area West	8-52
8.6.1	Effective hydraulic conductivity	8-55
8.6.2	Properties of transmissive elements	8-57
8.6.3	Characteristics of flow paths	8-58
8.6.4	Evaluation of flow in blocks	8-60
8.7	Groundwater flow conditions in area East	8-61
8.7.1	Modification of the regional-scale model	8-61
8.7.2	Properties of transmissive elements in blocks of crystalline rock	8-62
8.8	Underground constructions in the crystalline basement: hydrogeological effects	8-62
8.9	Conclusions	8-64
9	NEOTECTONICS AND SCENARIOS OF GEOLOGICAL PROCESSES	9-1
9.1	Introduction	9-1
9.2	Neotectonics	9-2
9.2.1	General aspects	9-2
9.2.2	Geology, geomorphology and analysis of drainage patterns	9-3
9.2.3	Geodetic and geophysical data	9-4
9.2.4	Conclusion	9-16
9.3	Long-term scenarios of geological development	9-17
9.3.1	Endogenous scenarios	9-17
9.3.2	Exogenous scenarios	9-19
9.4	Safety-relevant aspects	9-22
9.4.1	Overview	9-22
9.4.2	Safety-relevant aspects of the endogenous scenarios	9-22
9.4.3	The safety-relevant aspects of exogenous scenarios	9-30
9.5	Evaluation of potential changes in groundwater flow conditions in the crystalline basement	9-35

10	GEOLOGIC DATA BASE FOR SAFETY ASSESSMENT MODELS AND REPOSITORY DESIGN	10-1
10.1	Overview of geologic data requirements	10-1
10.1.1	Geological input for near-field modeling	10-1
10.1.2	Data for geosphere transport models and biosphere modeling	10-2
10.1.3	Data for repository design and construction	10-3
10.2	Groundwater flow	10-4
10.2.1	Area West	10-4
10.2.2	Area East	10-11
10.2.3	Discussion	10-16
10.3	Small-scale characterization of the geosphere: conceptual model of water-conducting features	10-19
10.3.1	The need to simplify	10-20
10.3.2	Simplified geometry of cataclastic zones	10-20
10.3.3	Simplified geometry of jointed zones	10-22
10.3.4	Simplified geometry of deformed aplite/pegmatite dykes	10-23
10.3.5	Mineralogy and open porosity of water-conducting features	10-26
10.3.6	Cation exchange capacities	10-27
10.3.7	Comments on regional variations of water-conducting features	10-30
10.4	Hydrogeochemical database	10-30
10.4.1	Reference waters	10-30
10.4.2	Colloids	10-49
10.5	Geotechnical data	10-54
10.5.1	Introduction	10-54
10.5.2	Geotechnical properties of the rock	10-55
10.5.3	The recent stress field in the Böttstein - Kaisten - Leuggern area	10-57
10.5.4	Geothermal conditions	10-58
11	EXPLORABILITY OF THE CRYSTALLINE ROCKS OF NORTHERN SWITZERLAND AND PROPOSED INVESTIGATION CONCEPT	11-1
11.1	Objectives of the investigation programme	11-1
11.2	Overview of potential investigation methods	11-2
11.3	Proposed investigation concept	11-6
11.4	Chances of success	11-11

12	CONCLUSIONS RELEVANT TO A REPOSITORY	12-1
12.1	Conceptual geological model of the crystalline basement for area West (Kaisten - Leuggern - Böttstein area)	12-3
12.1.1	Structure of the crystalline basement and adjoining sedimentary formations	12-3
12.1.2	Hydrochemical and isotopic characteristics of groundwater	12-8
12.1.3	Conditions of groundwater circulation	12-8
12.1.4	Extent of low-permeability blocks of crystalline rock	12-9
12.1.5	Long-term changes of the geological setting	12-10
12.2	Repository design and safety concept	12-11
12.2.1	Repository design	12-11
12.2.2	Safety concept and contribution of the crystalline basement to repository safety	12-13
12.3	Siting possibilities for a repository in the crystalline basement of Northern Switzerland	12-15
12.3.1	Potential siting area Kaisten - Leuggern - Böttstein (area West)	12-17
12.3.2	Potential siting area Siblingen (area East)	12-20
12.4	Investigation concept	12-20
	REFERENCES	Ref. 1
	LIST OF ABBREVIATIONS	

**FIGURES**

	page
2-1a :	Nagra investigation area with locations of reflection seismics lines and deep boreholes in Northern Switzerland. 2-2
2-1b :	Geological cross-section through the Nagra investigation area. 2-2
2-2a :	Böttstein borehole: geological overview, testing and sampling. 2-4
2-2b :	Weiach borehole: geological overview, testing and sampling. 2-5
2-2c :	Riniken borehole: geological overview, testing and sampling. 2-6
2-2d :	Schafisheim borehole: geological overview, testing and sampling. 2-7
2-2e :	Kaisten borehole: geological overview, testing and sampling. 2-8
2-2f :	Leuggern borehole: geological overview, testing and sampling. 2-9
2-2g :	Siblingen borehole: geological overview, testing and sampling. 2-10
2-3 :	Location map of hydrochemical sampling points or groups of sampling points. 2-17
2-4 :	Microearthquake network for Northern Switzerland. 2-22
3-1 :	Overview of the tectonic division of Northern Switzerland and neighboring areas. 3-2
3-2 :	Chronology of Variscan orogenic phases and timetable for basement evolution in the region of Northern Switzerland. 3-5
3-3 :	Tectonic history of Northern Switzerland. 3-8/9
3-4 :	Scheme of the tectonic evolution of Northern Switzerland during the Mesozoic and the Cenozoic. 3-12
3-5 :	Schematic synopsis of sedimentation and crustal movements during the Tertiary. 3-14
3-6 :	Vertical crustal movements in Northern Switzerland: Tertiary and Quaternary 3-15
3-7 :	The heat flux in Northern Switzerland. 3-21
4-1 :	Tectonic map of the Black Forest. 4-3

4-2 :	Pressure - Temperature - time (P-T-t) path of the crystalline rocks of the Black Forest.	4-8
4-3 :	Vertical profile across the "Grube Clara" hydrothermal ore mine from the Central Black Forest.	4-29
4-4 :	Distribution of hydrothermal ore veins near Haslach in the Central Black Forest.	4-30
5-1 :	Evolution of Rhenish striking structures in the Rhine Graben and adjacent areas.	5-4
5-2 :	Simplified depth map of the seismic marker "Base Mesozoic".	5-6
5-3 :	Tectonic sketch map of the eastern end of the Folded Jura.	5-9
5-4 :	Geological profiles through the potential siting area West according to seismic sections.	5-10
5-5 :	Overview of the basement of the Black Forest - Northern Switzerland and adjacent units.	5-11
5-6 :	Fault zones in the crystalline basement as mapped on reflection seismics line 82-NF-10.	5-15
5-7a :	Inventory of structures in the area West.	5-25
5-7b :	Schematic fault network of the area West.	5-25
5-8a :	Inventory of structures in the area East around Siblingen.	5-28
5-8b :	Schematic fault network in the area East.	5-28
5-9 :	Schematic fault models of the areas West (Kaisten - Leuggern - Böttstein) and East (Siblingen).	5-30
6-1 :	Identification of inflow points in the Siblingen borehole by fluid logging.	6-4
6-2 :	Illustrations of structural elements in the crystalline basement.	6-9
6-3 :	Occurrence of aplite and pegmatite dykes in borehole sections north of the Permo-Carboniferous Trough.	6-13
6-4 :	Types of pore-spaces in crystalline rocks in transmitted and fluorescent light.	6-27/28
6-5 :	Quantification of wallrock porosity by Hg injection and U/Th disequilibrium measurements.	6-32

6-6 :	Open porosities of wallrocks as a function of rock types and type of alteration.	6-35
6-7 :	Spatial orientation of aplite/pegmatite dykes in the boreholes of Böttstein, Kaisten and Leuggern.	6-39
6-8 :	Borehole sections with higher and low permeability in the crystalline basement of Northern Switzerland.	6-41
6-9 :	Concepts representing channel flow through fractures.	6-46
7-1 :	Map showing major tectonic units of Northern Switzerland with locations of water samples.	7-2
7-2a :	Schoeller diagram of waters of the alkaline earth-HCO <sub>3</sub> chemical type from the crystalline basement of the Black Forest.	7-6
7-2b :	Schoeller diagram of waters of the Na-HCO <sub>3</sub> -SO <sub>4</sub> chemical type from the crystalline basement of the Siblingen borehole.	7-6
7-2c :	Schoeller diagram of waters of the Na-SO <sub>4</sub> chemical type from the thermal boreholes at Zurzach and the upper crystalline basement of the Böttstein borehole.	7-6
7-2d :	Schoeller diagram of waters of the Na-SO <sub>4</sub> chemical type from the crystalline basement at Leuggern.	7-6
7-2e :	Schoeller diagram of waters of the Na-SO <sub>4</sub> chemical type from the Permian and crystalline basement of the Kaisten borehole.	7-7
7-2f :	Schoeller diagram of waters of Na-SO <sub>4</sub> and Na-Cl chemical types from the crystalline basement at Leuggern, Böttstein, Schafisheim, Weiach and Säckingern.	7-7
7-2g :	Schoeller diagram of waters of Na-Cl chemical types from the Buntsandstein and Permian of the Weiach, Riniken, and Schafisheim boreholes.	7-7
7-3 :	Graph of sodium concentration against mobile anion (Cl + SO <sub>4</sub> ) concentrations.	7-12
7-4 :	Graph of sulphate and chloride contents of water from the crystalline basement and adjacent sedimentary units.	7-12
7-5 :	Graph of dissolved helium and dissolved chloride contents.	7-14
7-6 :	Graph of magnesium and calcium contents.	7-14

7-7 :	Graph of bromide and chloride contents.	7-15
7-8 :	Graph showing dissolved silica concentrations and formation temperatures of waters, and the solubilities of quartz and chalcedony.	7-17
7-9 :	Graph showing Na/K ratios and formation temperatures of waters, and two Na/K geothermometer equations.	7-18
7-10 :	Graph of the $\delta^2\text{H}$ and $\delta^{18}\text{O}$ values of water from the crystalline basement and adjacent and sedimentary units and the meteoric water line for Switzerland.	7-25
7-11 :	Graphs illustrating the correspondence between the measured $\delta^{18}\text{O}$ values of calcite from the Kaisten borehole, and calculated $\delta^{18}\text{O}$ values for calcite at equilibrium with waters sampled.	7-27
7-12 :	Graph of $\delta^{13}\text{C}$ values and $^{14}\text{C}$ contents of waters.	7-27
7-13 :	Graph of $\delta^{34}\text{S}$ and $\delta^{18}\text{O}$ of sulphate minerals and dissolved sulphate.	7-29
8-1 :	Approach to the evaluation of the hydrogeology of the crystalline basement.	8-2
8-2 :	Hydraulic conductivity, as determined from packer tests, versus depth below ground surface for the 6 Nagra boreholes that penetrate the crystalline basement.	8-4/5
8-3 :	Log transmissivity of the water-conducting features and log hydraulic conductivity of the matrix versus depth.	8-7
8-4 :	Potentiometric surface in the upper part of the crystalline basement.	8-11
8-5 :	Transmissivity of water-conducting features versus depth.	8-15
8-6 :	Conceptual model of the crystalline basement and its representation for numerical modeling of groundwater flow at various scales.	8-21
8-7 :	Boundary conditions and hydraulic properties, regional-scale model, base case.	8-23
8-8 :	Structure of the regional-scale model, base case.	8-25
8-9 :	Areal distribution of simulated hydraulic head in upper crystalline basement, regional-scale model, base case.	8-28

8-10 :	Distribution of simulated hydraulic head in selected vertical sections, regional-scale model, base case.	8-29
8-11 :	Example of sensitivity runs with the regional-scale model.	8-34
8-12 :	Effect of permeable major water-conducting faults of first order on the regional-scale groundwater flow system.	8-36
8-13 :	Local-scale model, area West; summary of main components and definition of the two bounding scenarios.	8-13
8-14 :	Simplified section showing boundary conditions, geometric relationships and hydraulic properties, local-scale model, area West.	8-43
8-15 :	Distributions of simulated hydraulic gradient in the low-permeability domain, local-scale model, area West.	8-45
8-16 :	Horizontal component (logarithmic scale) of simulated Darcy flux in the low-permeability domain and major water-conducting faults, local-scale model, area West.	8-46
8-17 :	Contours of vertical component (logarithm) of simulated Darcy flux in the low-permeability domain and major water-conducting faults, local-scale model, area West.	8-47
8-18 :	Projection of simulated Darcy flux vectors in selected vertical sections, local-scale model, area West.	8-49
8-19 :	Typical fracture network in the low-permeability domain of area West, generated by NAPSAC.	8-53
8-20 :	Distributions of number, spacing, trace lengths and conductances of transmissive elements intersecting a tunnel segment.	8-59
9-1 :	A N-S cross section from the Southern Black Forest into Northern Switzerland showing geomorphological evidence for the young uplift of the Southern Black Forest.	9-6/7
9-2 :	Uplift of the Southeastern Black Forest and the evolution of the Plio-Pleistocene drainage pattern in the region of Northern Switzerland.	9-8
9-3 :	First order levelling net and recent crustal movements in Switzerland relative to a reference point at Aarburg based on data from 1903 to 1990.	9-9

9-4 :	Precision levelling in the Southern Black Forest and adjacent N Switzerland according to the German levelling programme, calculated for a common reference point at Laufenburg (CH).	9-10
9-5 :	The epicenters of seismicity in Northern Switzerland (1983 - 1993).	9-12
9-6a :	Fault plane solutions in Northern Switzerland 1977-1989.	9-14
9-6b :	The fault planes of the Läuelfingen earthquakes series.	9-15
9-6c :	Rose diagramm compiling the orientation of the 28 fault plane solutions.	9-15
9-7 :	Relationship between young reactivated fault pattern and geothermal gradient in Northern Switzerland and the Permo-Carboniferous Trough.	9-24
9-8 :	Potential ground acceleration values as expected from earthquakes in Switzerland.	9-27
9-9 :	Damage in underground tunnels in relation to earthquake magnitude.	9-28
9-10 :	Erosion history for a NW-SE section through the Black Forest.	9-31
9-11 :	Distribution of simulated hydraulic head in selected vertical sections, modified regional-scale model.	9-37
10-1 :	Processes taken into account in the safety assessment of geosphere transport and the relation to input data from geological, hydrogeological and hydrochemical investigations.	10-3
10-2 :	Geometric approach for the derivation of the hydrogeologic input for safety analysis, reference area West.	10-5
10-3 :	Normalized flux distributions in a single transmissive element.	10-8
10-4 :	Distributions of flux in a single transmissive element.	10-9
10-5 :	Distributions of total flux in transmissive elements in a tunnel segment.	10-10
10-6 :	Methodology for the derivation of the hydrogeologic input for safety analysis, area East.	10-15
10-7 :	Small-scale conceptual model of cataclastic zones in the crystalline basement of Northern Switzerland.	10-21

10-8 :	Small-scale conceptual model of jointed zones in the crystalline basement of Northern Switzerland.	10-24
10-9 :	Small-scale conceptual model of fractured aplite/pegmatite dykes and aplitic gneisses in the crystalline basement of Northern Switzerland.	10-25
10-10 :	Cation exchange capacities of altered wallrock samples.	10-28
10-11 :	Schoeller diagram of reference waters and more saline waters from the crystalline basement.	10-32
10-12 :	Micrograph of Leuggern groundwater colloids.	10-50
10-13 :	Example of colloid size distributions.	10-52
11-1 :	Illustration of the investigation concept.	11-8
11-2 :	Example of a realization of a synthetic fault network.	11-13
12-1 :	Process steps and relationships involved in planning a repository in the crystalline basement of Northern Switzerland.	12-2
12-2 :	Conceptual geological model of the crystalline basement of Northern Switzerland.	12-4
12-3 :	Sketch showing a repository concept for HLW/TRU in the crystalline basement of Northern Switzerland.	12-12
12-4 :	Potential siting area Kaisten - Leuggern - Böttstein (area West).	12-18
12-5 :	Potential siting area Siblingen (area East).	12-21

**TABLES**

		page
2-1 :	Overview of the main Nagra technical reports (NTB-series) of the deep drilling programme.	2-12
4-1 :	Metamorphic, magmatic and tectonic history of the Black Forest.	4-5
4-2 :	Granite suites in the Black Forest.	4-11
4-3 :	Overview of deep boreholes in Northern Switzerland that penetrated the crystalline basement.	4-14/15
4-4 :	Mineralogical compositions of fresh rock types in the crystalline basement of Northern Switzerland.	4-18
4-5 :	Overview of post-magmatic/post-metamorphic effects (deformations and alterations) in boreholes of Northern Switzerland.	4-22
4-6 :	Compilation of absolute age datings of minerals and whole-rocks in the Nagra boreholes in Northern Switzerland.	4-27/28
4-7 :	Post-metamorphic/post-magmatic evolution of the basement of Northern Switzerland and of the Black Forest.	4-36
5-1 :	Systematics of faults and lithological discontinuities in the basement.	5-14
6-1 :	Depths of all inflow points identified in deep boreholes penetrating the crystalline basement of Northern Switzerland and classification according to type of water-conducting features.	6-5
6-2 :	Dependence of inflow point frequency on rock type within the gneiss series of Leuggern and Kaisten.	6-10
6-3 :	Average mineralogy of water-conducting feature types 1 and 2 (cataclastic and jointed zones).	6-25
6-4 :	Average mineralogy of water-conducting feature type 3 (fractured aplite/pegmatite dykes and aplitic gneisses).	6-26
6-5 :	Summary of porosimetric data from the crystalline basement of Northern Switzerland.	6-33
6-6 :	Porosimetric data grouped according to rock types.	6-34
6-7 :	Porosimetric data grouped according to state of alteration.	6-34

6-8 :	Relative abundances of water-conducting features.	6-44
7-1 :	Summary of location, sampling points and chemical character of water types in the crystalline basement and adjacent units.	7-3
7-2 :	Comparison of modelled and analyzed compositions of water from the crystalline basement at Weiach.	7-20
7-3 :	Possible mineral dissolution and precipitation by which Recharge Group water could evolve to the Eastern Group.	7-22
8-1 :	Hydraulic heads in long-term monitored zones of Nagra boreholes.	8-9
8-2 :	Hydraulic parameters of crystalline rock components, derived from borehole data.	8-17
8-3 :	Observed and simulated hydraulic heads in Nagra boreholes.	8-30
8-4 :	Results of sensitivity analyses, regional-scale model.	8-32
8-5 :	Distributions of simulated Darcy fluxes in second order faults and in low-permeability domain, local-scale model, area West.	8-50
8-6 :	Input characteristics of transmissive elements (TE's) for evaluation of effective hydraulic conductivity - area West, low-permeability domain.	8-54
9-1 :	Summary of endogenous (tectonic) bounding scenarios A and B.	9-18
9-2 :	Principal erosion scenarios.	9-21
9-3 :	Safety-relevant aspects of the endogenous and exogenous scenarios.	9-23
9-4 :	Endogenous scenarios (time horizon 1 Ma): quantitative estimates of total displacements.	9-29
9-5 :	Exogenous scenarios (time horizon: 1 Ma): quantitative estimates of erosion and denudation.	9-33
10-1 :	Geometric and hydraulic results relevant to safety analysis, area West.	10-12/13
10-2 :	Geometric and hydraulic results relevant to safety analysis, area East.	10-17/18

10-3 :	Summary of exchangeable cations, cation exchange capacities, surface areas and mineralogical compositions of altered wallrock samples.	10-29
10-4 :	Reference water chemistry: area West.	10-35/36/37
10-5 :	Reference water chemistry: area East.	10-43/44/45
10-6 :	Böttstein 1326 m and Leuggern 923 m waters.	10-47/48
10-7 :	Comparison of groundwater chemistry and colloid data from the Northern Switzerland study.	10-54
10-8 :	Geotechnical properties of the crystalline basement.	10-56
11-1 :	Key aspects to be answered for the assessment of feasibility and safety of a repository.	11-3
11-2 :	Contribution of investigation methods to the characterisation of the crystalline basement of Northern Switzerland.	11-4
11-3 :	Exploration concept for the crystalline basement.	11-7
11-4 :	Parameters of the families of major water-conducting faults used for statistical analysis.	11-12
11-5 :	Simulated block size distribution in an area of 6 km x 10 km.	11-14
11-6 :	Simulated chances of existence of blocks of different sizes in a randomly located area of 1 km x 1 km and in an area of 1 km x 2 km.	11-14
11-7 :	Mean number of faults intersected by boreholes.	11-14
12-1 :	Size distribution of low-permeability crystalline blocks between major water-conducting faults.	12-9
12-2 :	Depth of rock temperatures of 50 °C and 55 °C in selected Nagra boreholes.	12-16

**APPENDICES**

- 3-1 : Geological-tectonic overview map.
- 4-1 : Mesozoic subcrop map Northern Switzerland - Southern Black Forest.
- 5-1 : Geological overview of the sedimentary cover.
- 5-2 : Overview of Permo-Carboniferous Trough of Northern Switzerland
- 5-3 : Mapped structures in the crystalline basement of Northern Switzerland and the Southern Black Forest.
- 9-1 : Neotectonics of Northern Switzerland.
- 9-2 : Bounding scenario B.



## 1 INTRODUCTION

The Swiss concept for nuclear waste management envisages deep disposal of high-level radioactive waste (HLW) and long-lived intermediate-level waste<sup>1)</sup> (TRU) in suitable geological formations in Northern Switzerland. The assessment of the feasibility and safety of such disposal therefore requires detailed characterization of the geosphere in the repository area.

This report summarizes the results of a comprehensive geological investigation programme in the crystalline basement of Northern Switzerland which was initiated by Nagra in 1978. It represents a major component of the so-called 'Kristallin-I' synthesis of the regional phase of the repository siting programme (cf. section 1.2).

This synthesis report draws on information contained in more than 100 Nagra reports, which are referenced in the appropriate sections.

### 1.1 Contribution of geology to repository safety

The direct contribution of geology to repository safety is discussed in great detail in the Project Gewähr Report Series (NAGRA 1985b) and in NAGRA (1994a) and can be summarized as follows:

- protection of the engineered disposal system (waste and technical barriers)
- radionuclide retardation in the geosphere and dilution in deep and shallow aquifers.

Protection of the disposal system from external influences is ensured in suitable geological formations by the following factors:

- the thickness of the overburden protects the repository from intentional or accidental human intrusion (minimized by absence of resources in host rock), from sabotage and from other external influences (e.g. acts of war)
- the deep location of the repository protects the technical barriers and the waste from the effects of erosion by water and ice and also minimizes the effects of extreme events such as earthquakes
- siting the repository in a tectonically inactive area enhances long-term mechanical integrity of the technical barriers and the stability of the geological ones.

In addition, the longevity of the engineered barriers is enhanced by a geological environment with low groundwater fluxes and favorable hydrochemistry.

Retardation of the transport of radionuclides through the geosphere to the surface environment is ascribed an additional role in the overall safety concept. The geological barriers may retard radionuclide transport with the effect that a large proportion of the nuclides will have decayed to a significant extent before they reach the biosphere. In addition, as nuclides approach the biosphere they undergo substantial dilution in groundwaters circulating near the surface.

---

1) Swiss classification is LMA (langlebige mittelaktive Abfälle - long-lived intermediate-level waste), which is effectively equivalent to TRU wastes (transuranic-containing wastes) as usually defined.

## 1.2 Historical evolution of the Swiss HLW repository programme

The Federal Government Ruling of 6th October 1978 on the Atomic Act designates the guaranteeing of "permanent safe management and final disposal" of radioactive waste as a prerequisite to future development and use of nuclear energy in Switzerland.

In 1978 a first comprehensive desk study covering all areas of Switzerland and a wide range of potential host rocks was performed (VSE et al. 1978). Due to requirements for long-term tectonic stability, site selection for a HLW/TRU repository was concentrated in the northern part of Switzerland (Fig. 2-1a) (THURY 1980). A three-phase siting programme was defined in which an initial regional analysis would lead to a detailed investigation of a more limited area and, eventually, underground characterization of a potential site.

In 1980, the crystalline basement was allocated first priority as a potential host rock and a Phase I regional characterization programme was initiated (Chapter 2). Factors leading to the selection of the crystalline basement were:

- the low seismicity of the area
- the hydrogeology of a basement overlain by low-permeability sedimentary rocks can be favorable
- the gravel aquifers in the discharge area and the Rhine river offer a large dilution potential
- the geochemical conditions in the crystalline basement are expected to be favorable
- natural resources are not known (a possible exception is geothermal energy)
- many foreign disposal projects are based on a crystalline host rock and there is therefore a lot of international experience in this area, as well as an extensive database which is partly applicable to the Swiss situation
- granite and gneiss are attractive rock types from an engineering point of view.

Most effort was devoted to gathering data on the crystalline basement in the chosen investigation area, but care was taken to characterize also the overlying sedimentary rocks at the selected borehole locations.

Coupling the continuation of operating licenses for the nuclear power plants to demonstration of the safety and feasibility of radioactive waste disposal provided the incentive for the major Project Gewähr 1985 analysis (NAGRA 1985b). The Project Gewähr 1985 study introduced the concept of very deep disposal (c. 1200 m below surface) in the crystalline basement of Northern Switzerland, with massive engineered barriers. In their review of this project, the licensing authorities concluded that the basic safety of this concept had been demonstrated (HSK 1987). Project Gewähr 1985 was published at a relatively early stage in the regional characterization of the crystalline basement and hence, as noted by the licensing authorities, it demonstrated the feasibility and safety of the general disposal concept for a site that has characteristics based on analysis of very limited information (mainly data from the Böttstein borehole). However, extrapolation of these data to a wider region or identification of particular

locations that would be suitable as a site was not possible. In addition, the authorities also recommended the characterization of sedimentary formations. This resulted in a parallel sediment programme in which an initial desk study led to the selection of two favored formations, the Opalinus Clay and the Lower Freshwater Molasse (NAGRA 1988b). A characterization of the Opalinus Clay, involving field work (seismic surveys, deep borehole investigations), was initiated recently.

The Phase I regional characterization of the crystalline basement has now been completed and is being documented as part of the project called Kristallin-I (NAGRA 1994b). Kristallin-I is an update of the HLW analysis in Project Gewähr 1985 and has three main components: a synthesis of the very extensive field investigation programme, a performance assessment which quantifies the level of safety provided by a specific repository design and an analysis of exploration strategies for subsequent phases of more localized site characterization from the surface (Phase II) and from underground (Phase III). More details of the strategy for management of Swiss high-level waste are given by McCOMBIE et al. (1993) and McKINLEY et al. (1993).

### **1.3 Content and structure of the present report**

This report presents an overview of the geological investigations performed for the Kristallin-I project. Here the term 'geology' is taken to include tectonics, petrography, stratigraphy, hydrogeology and geochemistry. The report comprises a description of the geological investigation programme carried out from 1981 to 1993 (Chapter 2), an outline of the geological evolution of Northern Switzerland (Chapter 3) with special emphasis on the evolution of the crystalline basement (Chapter 4), a description of structural geology (Chapter 5), a detailed characterization of discrete small-scale water-conducting features in the crystalline basement (Chapter 6) and the results of the regional hydrogeochemical and hydrogeological investigations (Chapter 7 and 8). An assessment of long-term geological evolution scenarios is presented in Chapter 9. The geological database for the safety analysis calculations and the performance assessment is extracted from the bulk dataset and discussed in Chapter 10 of the report. Chapter 11 is devoted to the explorability of the crystalline basement with respect to future phases of the site selection and characterization programme. Finally, the conclusions relevant to siting a HLW repository in the crystalline basement are summarized in Chapter 12.

The results of the Kristallin-I safety assessment, including geosphere transport modeling based on input data from this synthesis, are presented in a separate report (NAGRA 1994a) and an overview of the entire project is given in NAGRA (1994b).

The present report was prepared by a working group comprising Nagra staff, contractors and consultants under the project management of Marc Thury. All members of this group are listed as authors of the full report. Individual sections were prepared by various members of the group. The main responsibility for the individual Chapters is as follows:

- Chapter 1: M. Thury, A. Gautschi  
Chapter 2: M. Thury, A. Gautschi, W.H. Müller, S. Vomvoris  
Chapter 3: H. Naef, W.H. Müller  
Chapter 4: M. Mazurek, A. Gautschi  
Chapter 5: H. Naef, W.H. Müller  
Chapter 6: M. Mazurek, A. Gautschi  
Chapter 7: F.J. Pearson, A. Gautschi  
Chapter 8: S. Vomvoris, W. Wilson  
Chapter 9: H. Naef, W.H. Müller, S. Vomvoris  
Chapter 10: M. Mazurek, F.J. Pearson, A. Gautschi, S. Vomvoris, W.H. Müller  
Chapter 11: M. Thury, S. Vomvoris, W.H. Müller, A. Gautschi  
Chapter 12: M. Thury, A. Gautschi, W.H. Müller, S. Vomvoris,

All Chapters received scrutiny from all members of the group. An editorial board comprising Marc Thury, Andreas Gautschi, Walter Müller and Stratis Vomvoris was responsible for the overall scientific content of the report.

The report has been much improved by the thoughtful and detailed review comments of Ian McKinley, Charles McCombie and Piet Zuidema (all from Nagra), Peter Diebold (Herznach), Felice Jaffé (Geneva), Hansjörg Schmassmann (Geologisches Institut Dr. Schmassmann AG, Liestal) and Andreas Haug (Geotechnisches Institut AG, Zürich).

The authors wish to acknowledge the contribution of numerous other Nagra staff members and external contractors who prepared the various drafts and the final version of the report.

## 2 THE GEOLOGICAL INVESTIGATION PROGRAMME 1981 - 1993

### 2.1 Overview of the programme

The investigation area for the Phase I regional investigations of the crystalline basement of Northern Switzerland was selected in 1979 (THURY 1980) and is shown in Figure 2-1a. To the north, the area is limited by the national border of Switzerland; the southern border is in the region where the maximum depth to the top of the crystalline basement was expected to be around 1500 m. The investigation area is in a zone of relatively low seismic activity between two more active areas around Basel in the west and Schaffhausen in the east (cf. section 2.8). Figure 2-1b shows a geological cross-section of the area, based on information available following Project Gewähr 85.

Originally, a series of 12 deep boreholes spread over the investigation area (supplemented by geophysical, hydrogeological and hydrochemical surveys) was planned to explore the practically unknown crystalline basement below the sedimentary cover. The seismic surveys and the first boreholes led to the discovery of a several kilometer deep Permo-Carboniferous Trough (cf. Fig. 2-1b, Permo-Carboniferous Trough of Northern Switzerland), the existence of which was not previously known (cf. e.g. geological cross-sections in LAUBSCHER [1977, Fig. 2], BUSER & WILDI [1981, Abb. 13] and ZIEGLER [1982, Fig. 26]). Based on this finding, the deep drilling programme was reduced to seven boreholes.

The wide range of investigations carried out in the region from 1981 to 1993 can be divided into the following programmes, which are described in detail in the following sections (2.2 to 2.8):

- a deep drilling programme, comprising seven deep boreholes;
- geophysical investigations: reflection and refraction seismics surveys, gravity surveys;
- hydrogeological investigations;
- hydrochemical investigations;
- regional geological investigations: mapping and compilations of geological maps;
- geological studies on outcrops in the Southern Black Forest, Germany;
- neotectonic studies (microearthquake survey, precision leveling, geomorphology).

The scientific programme was designed by Nagra and its consultants and was carried out, under Nagra management, by more than 50 university institutes, consulting companies and contractors, involving more than 200 scientists from 8 countries. The results of these investigations are presented in great detail in numerous reports and papers; key publications are referenced in the appropriate Chapters of the present report.

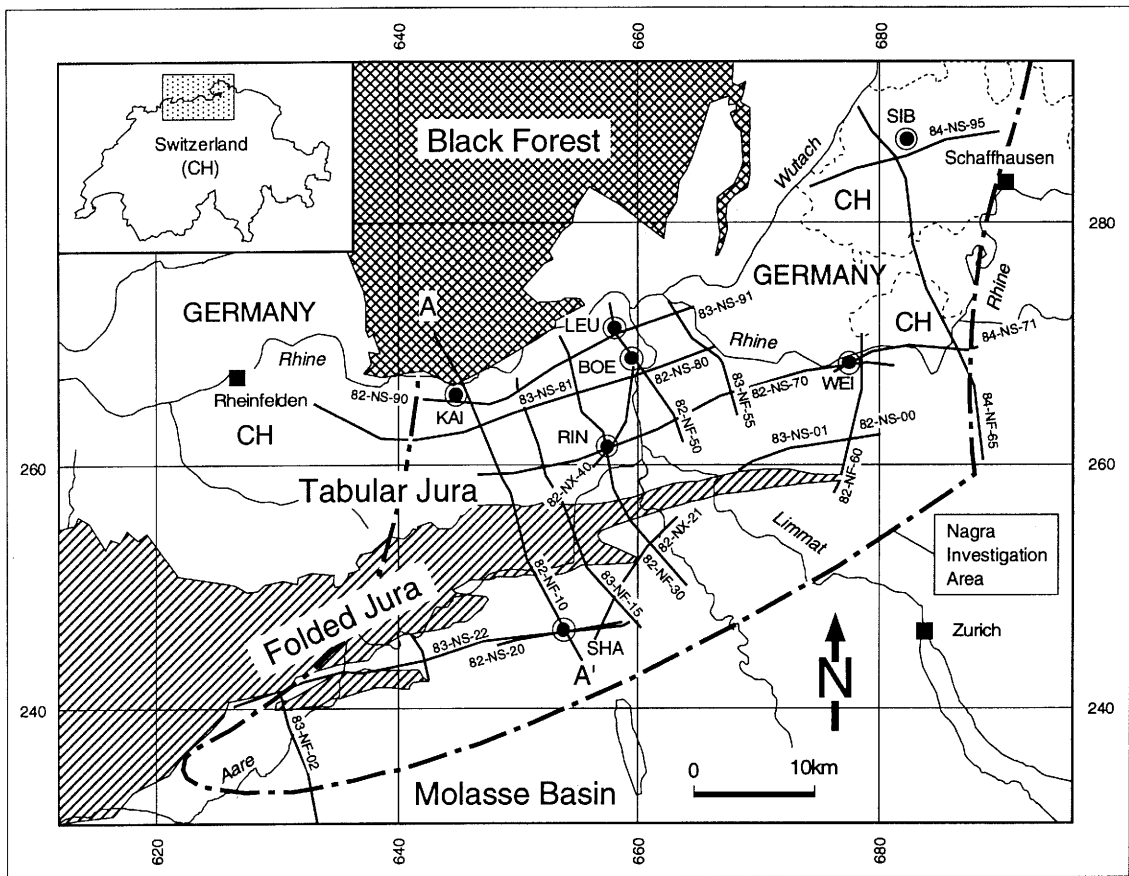


**Fig. 2-1a :** Nagra investigation area with locations of reflection seismics lines and deep boreholes in Northern Switzerland (Nagra boreholes: BOE = Böttstein, WEI = Weiach, RIN = Riniken, SHA = Schafisheim, KAI = Kaisten, LEU = Leuggern, SIB = Siblingen).

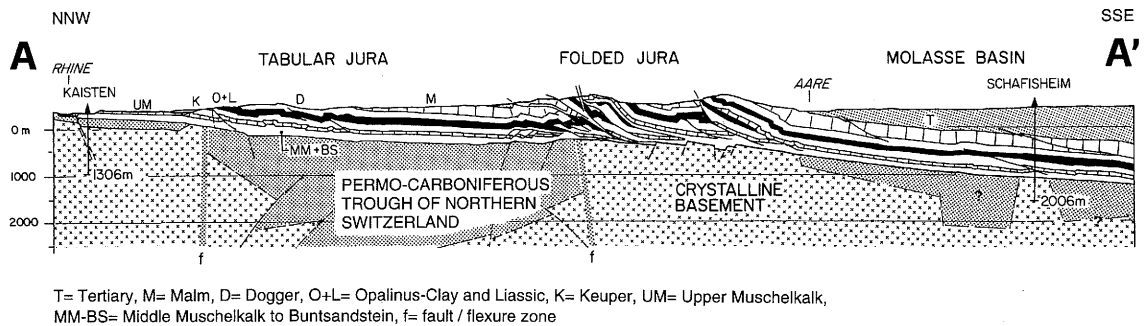


**Fig. 2-1b :** Geological cross-section A-A' (cf. Fig. 2-1a) through the Nagra investigation area along reflection seismics line 82-NF-10. From DIEBOLD (1986).

## 2.2 Deep drilling programme

The objective of the deep drilling programme was to acquire data on the geological, hydrogeological and hydrogeochemical properties of the crystalline basement and the overlying sedimentary rocks, using the most appropriate investigation tools. The programme comprises a mineralogical, structural and stratigraphic characterization of the different rock types, determination of hydraulic parameters (such as hydraulic conductivity and head), determination of the chemical composition and the isotopic signature of the deep groundwaters, acquisition of data on rock mechanical properties, investigation of the geothermal conditions, determination of the neotectonic stress field and acquisition of data for the depth calibration of the regional geophysical surveys.

### Investigations

Seven boreholes were drilled, with depths ranging from 1306 to 2482 m (Fig. 2-2a - g, THURY & AMMANN 1990). The geographic locations of the drill sites are given in Figure 2-1a. From a tectonic point of view, the Kaisten, Riniken, Leuggern, Böttstein and Siblingen boreholes are all located in the Tabular Jura, the Schafisheim borehole in the Molasse Basin and the Weiach borehole in the transition zone between the Tabular Jura and the Molasse Basin.

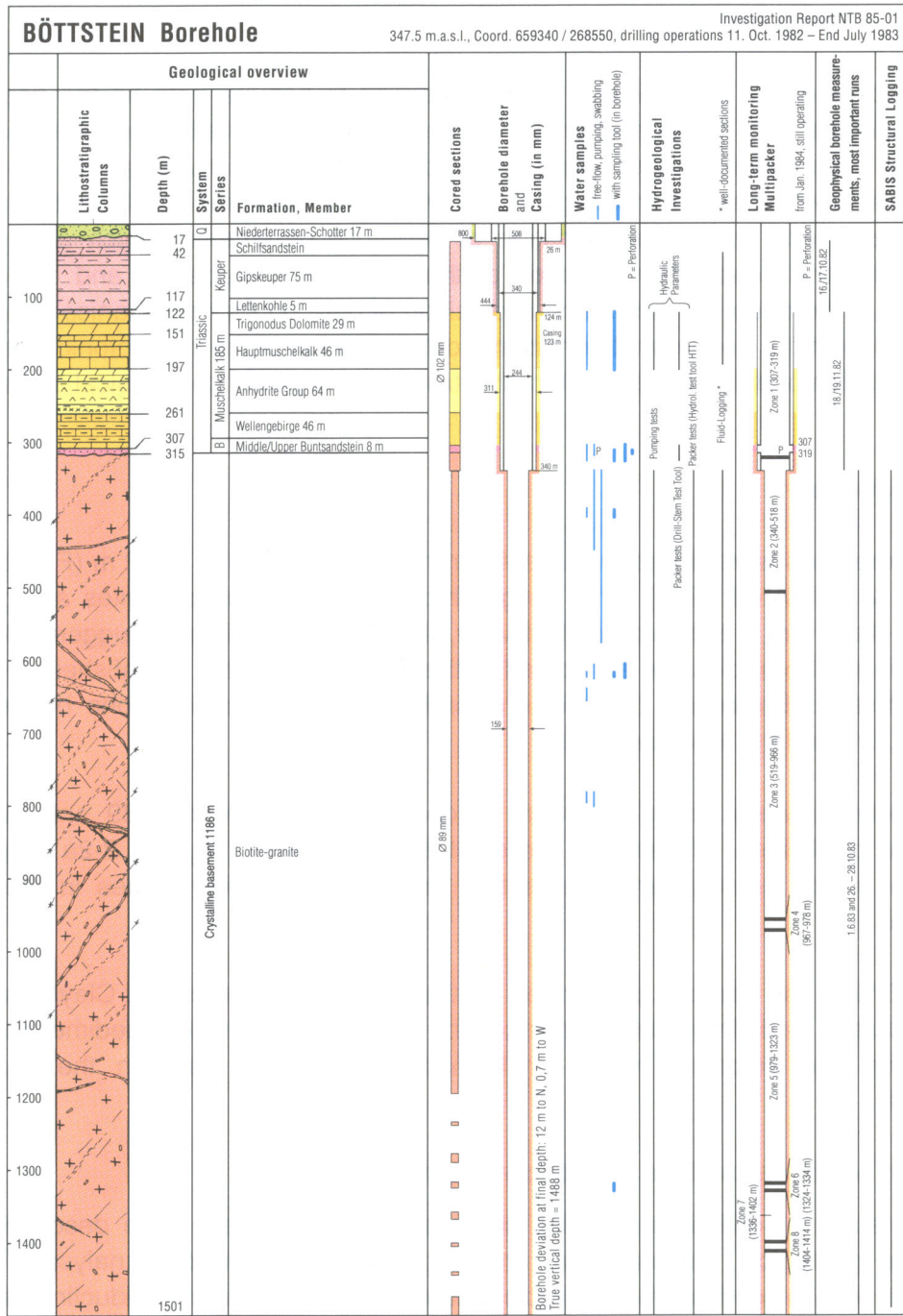
The boreholes were drilled between October 1982 and April 1989 and, with the exception of Riniken, all reached the crystalline basement. Figures 2-2a - g give an overview of the geology and the testing and sampling programmes in the seven boreholes.

About 80 % of the sections penetrated by the boreholes were cored. Clay/freshwater, clay/saltwater and freshwater drilling-fluids were used in the sedimentary rock formations and deionized water or formation fluid were used in the crystalline basement.

The main components of the scientific programme were:

Detailed study of drillcores and drill cuttings, including on-site core description and extensive geological, mineralogical and petrophysical laboratory analyses. Special emphasis was placed on the characterization of discrete water-conducting features. The data from a large set of borehole geophysical logs were used to prepare synthetic lithological logs.

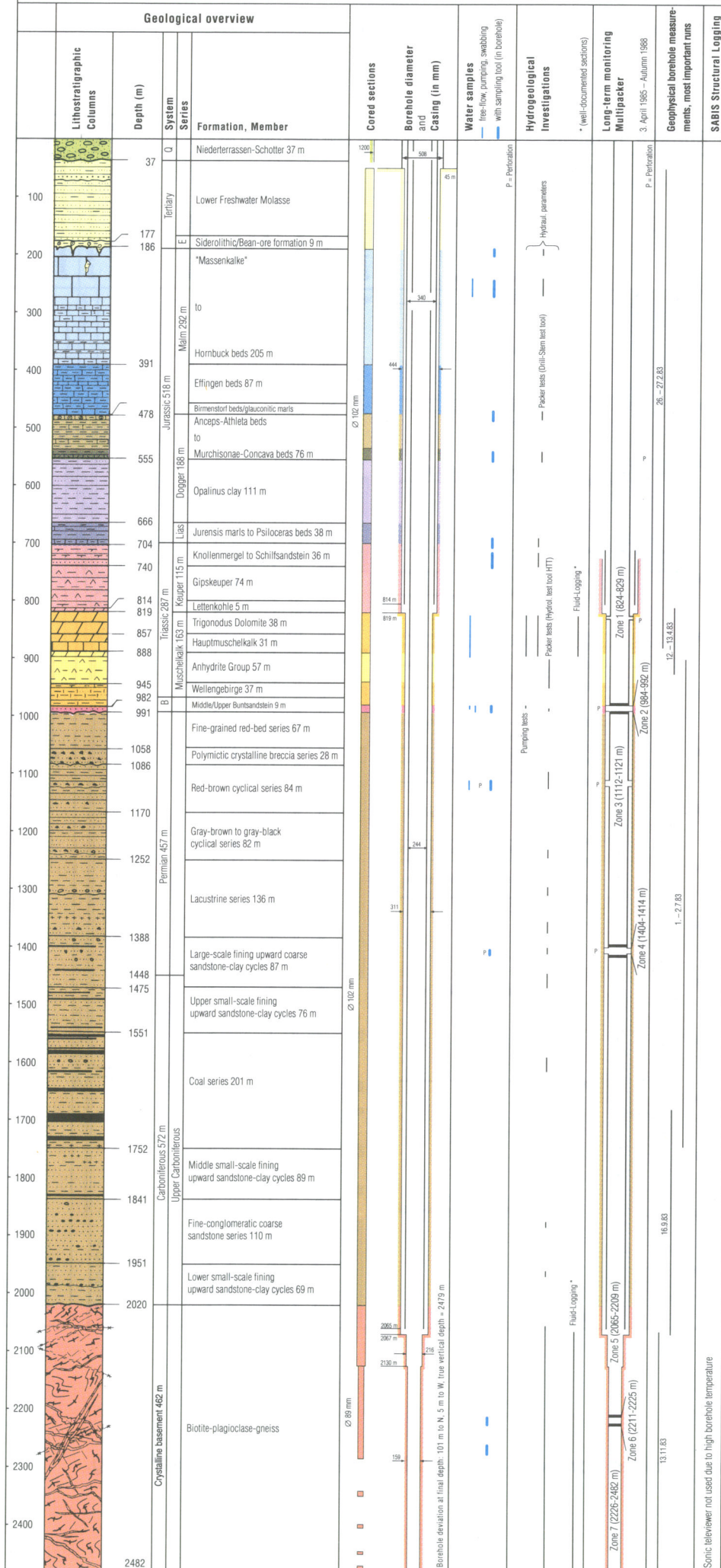
Investigation of structural discontinuities (fractures, lithological boundaries) using some of the most up-to-date geophysical logging techniques. For example, the orientation of fractures was registered by acoustic televiewer, and a variety of electrical/ electromagnetic Schlumberger prototype tools provided spatially oriented structural images of the borehole wall. The structures observed in the cores could then be oriented.



# WEIACH Borehole

368.7 m.a.s.l., Coord. 676750 / 268620, drilling operations 10. Jan. 1983 – 12. Nov. 1983

Investigation Report NTB 88-08



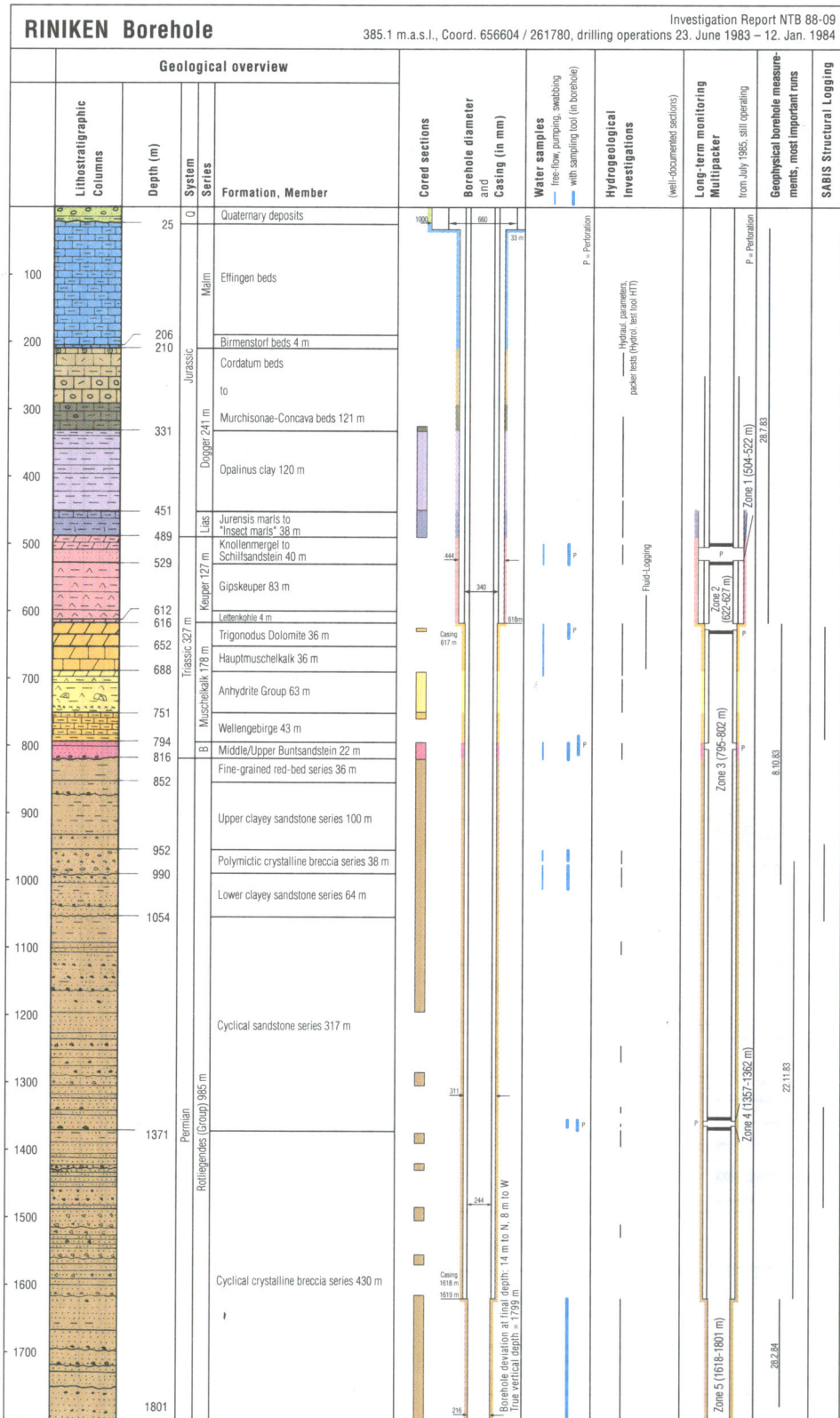
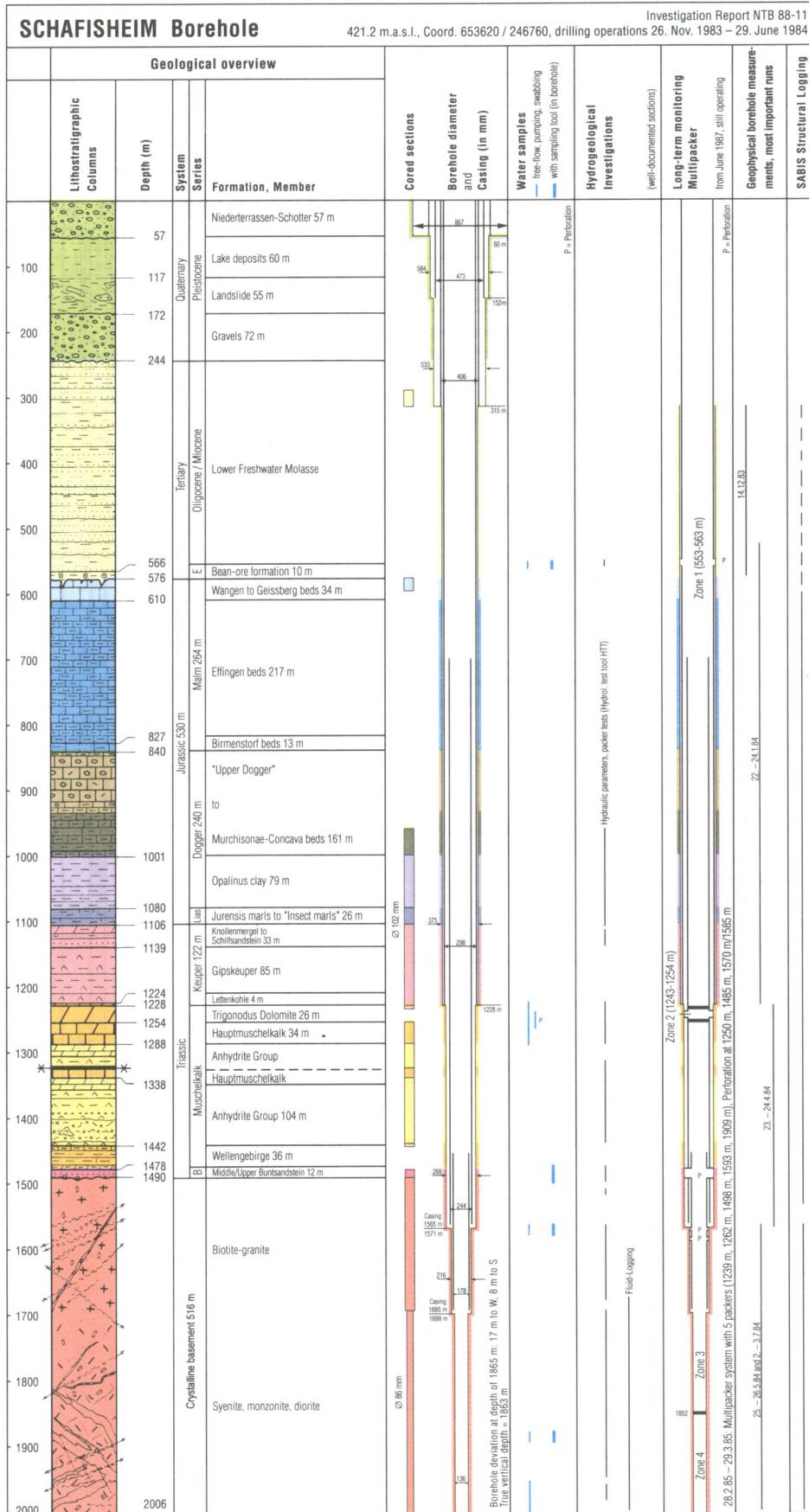


Fig. 2-2c : Riniken borehole: geological overview, testing and sampling.



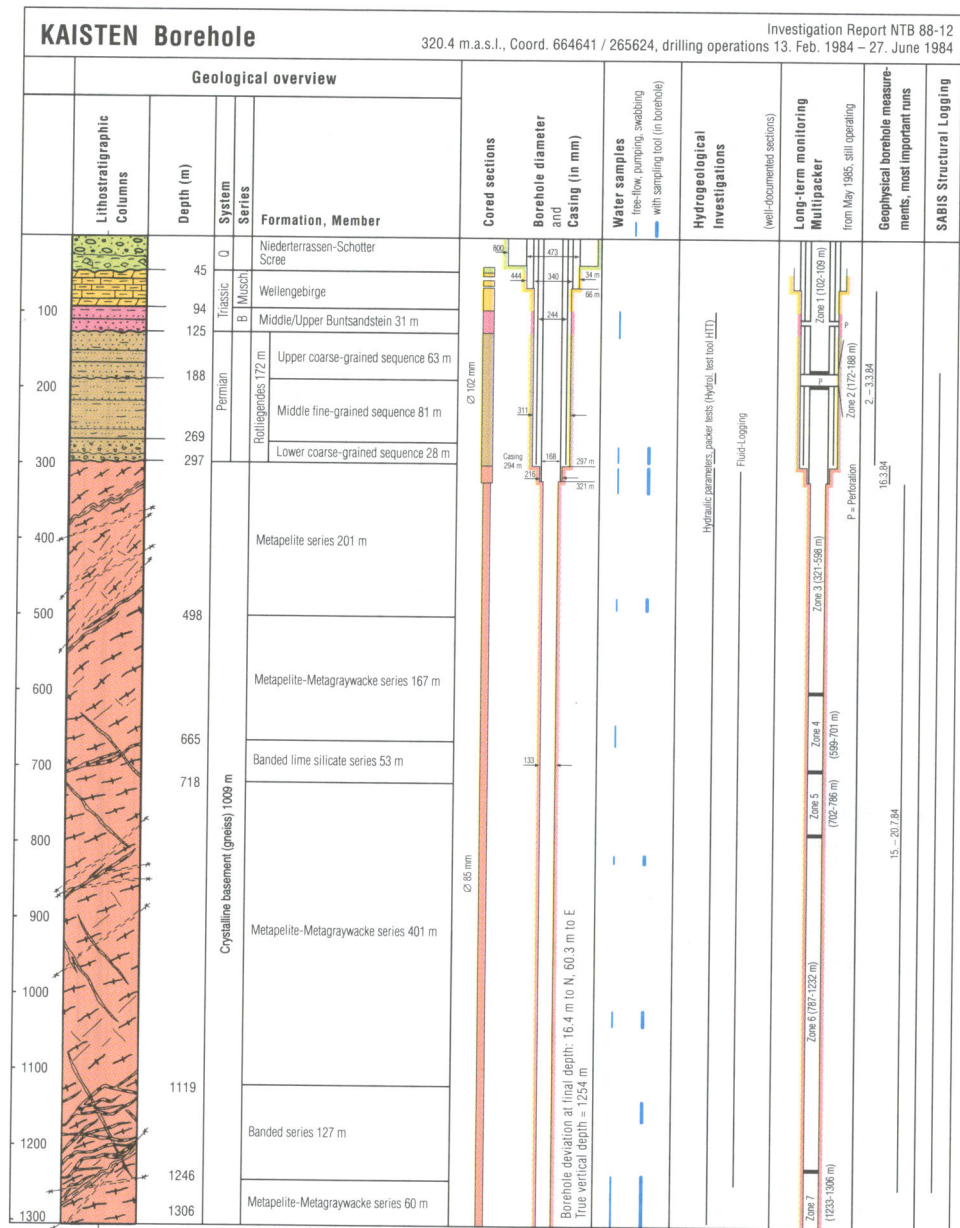


Fig. 2-2e : Kaisten borehole: geological overview, testing and sampling.

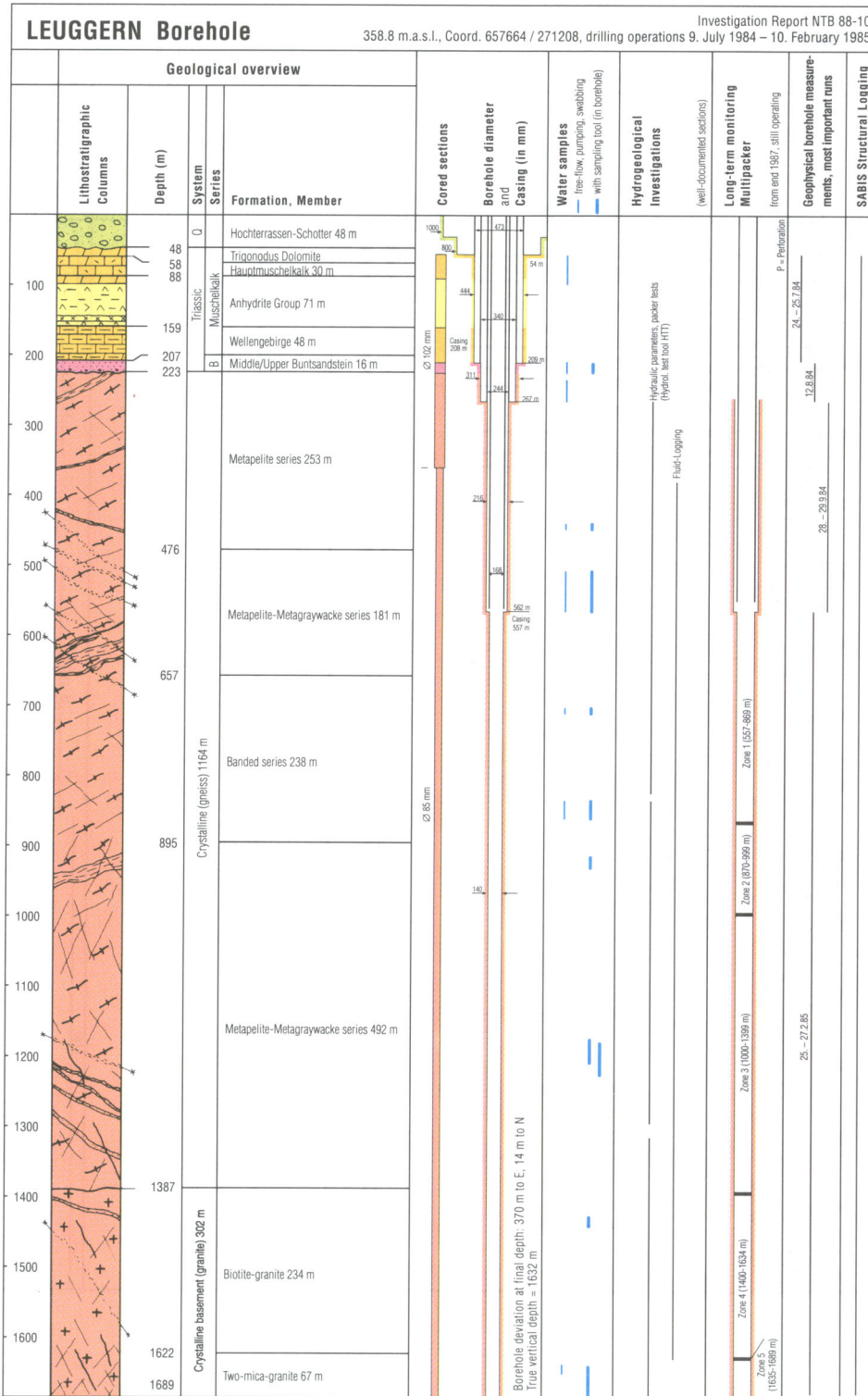


Fig. 2-2f : Leuggern borehole: geological overview, testing and sampling.

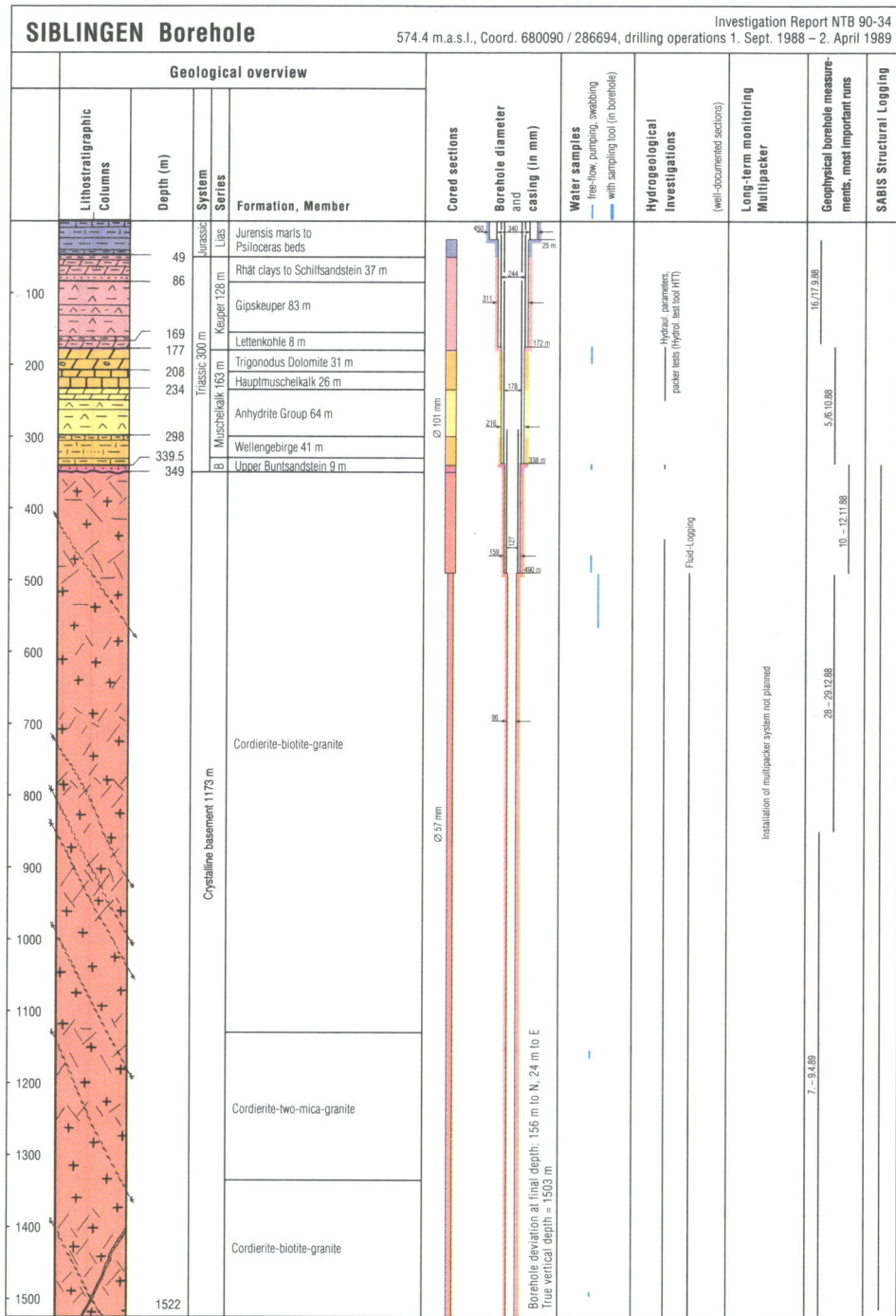


Fig. 2-2g : Siblingen borehole: geological overview, testing and sampling.

A comprehensive programme was carried out for investigating hydraulic parameters. Single- and double-packer tests provided data on the transmissivities and hydraulic heads in different straddle intervals (KÜPFER et al. 1989). Fluid logging techniques, i. e. measurements of electrical conductivity and temperature in the borehole under pumping conditions, were used to locate groundwater inflow points in the borehole with high precision ( $\pm 1$  m in the later boreholes of Leuggern, Kaisten and Siblingen) (BLÜMLING & HUFSCHMIED 1989, KELLEY et al. 1991). Based on these results, the discrete water-conducting features could be identified and characterized. In the majority of the boreholes, multipacker systems have been installed for long-term monitoring of hydraulic pressures. Most of them are still in operation today and will continue to operate until a decision is made to decommission these holes (HUFSCHMIED & FRIEG 1989, PASQUIER et al. 1993).

Numerous groundwater samples were collected for hydrochemical and isotopic analyses in order to investigate the in-situ geochemical conditions as well as the origin and subsurface residence times of the groundwater. The samples were taken either at the well-head or in the borehole, using suitable down-hole sampling tools (HAUG 1985, GAUTSCHI & SCHOLTIS 1989). Addition of tracers to the drilling-fluid was used to allow assessment of the extent of drilling-fluid contamination in each sample.

Conventional geomechanical methods such as uniaxial and triaxial pressure tests, tensile tests and creep tests were performed to provide input for geotechnical purposes (planning of shaft and tunnel constructions). Another technique, developed in recent years, allows the direction of the maximum horizontal rock stress to be determined on the basis of oriented borehole diameter measurements (borehole wall breakouts, BECKER et al. 1984).

In each borehole, temperature was recorded continuously along-hole by single measurements at specific depths and during hydraulic tests. These measurements allow the geothermal conditions to be characterized accurately.

Finally, a variety of measurements including sonic, resistivity, neutron and gamma logs, borehole seismics and borehole gravimetry was carried out in order to complement and calibrate surface geophysical investigations.

Detailed descriptions of all investigation methods mentioned above and all borehole-specific results are presented in various technical reports on the Nagra deep boreholes (Tab. 2-1).

Nagra NTB	Böttstein	Weiach	Riniken	Schafisheim	Kaisten	Leuggern	Sibingen
Drilling Technology	NAGRA 1985c	NAGRA 1986b	NAGRA 1988c	NAGRA 1991a	NAGRA 1986c	NAGRA 1989b	NAGRA 1992a
Geology	PETERS et al. 1986	MATTER et al. 1988a	MATTER et al. 1987	MATTER et al. 1988b	PETERS et al. 1989b	PETERS et al. 1989a	
Geophysical Logging	WEBER et al. 1986						
Fluid Logging	NAGRA 1988a						KELLEY et al. 1991
Gas in Drilling-fluid	HINZE et al. 1989						
Packer Tests	LEECH et al. 1985	BUTLER et al. 1989	BELANGER et al. 1989a	MOE et al. 1990	McCORD & MOE 1990	BELANGER et al. 1989b	OSTROWSKI & KLOSKA 1989
Long-term Monitoring Multipacker	SCHNEIDER & SCHLANKE 1986						
Interpretation Multipacker	PICKENS et al. 1985	BELANGER et al. 1990		McNEISH et al. 1990		BELANGER et al. 1990	
Water Sampling	WITTWER 1986						BLASER & SCHOLTIS 1991
Hydrochemical Data Set	PEARSON 1985	PEARSON et al. 1989					
Isotope Hydrogeology	PEARSON et al. 1991						
Investigation Report (Extended Summary)	NAGRA 1985a	NAGRA 1989c	NAGRA 1990b	NAGRA 1992b	NAGRA 1991c	NAGRA 1990b	NAGRA 1992a

**Tab. 2-1 :** Overview of the main Nagra technical reports (NTB-series) of the deep drilling programme.

### 2.3 Geophysical investigations

The objective of the geophysical investigation programme was to obtain as comprehensive an inventory as possible of relevant, reliable data on the deep geology of the investigation region. When interpreted in conjunction with the results from the deep boreholes and surface mapping campaigns, these data should provide a detailed picture of the tectonic regime of Northern Switzerland.

In the region of Northern Switzerland, Nagra's interests coincided with the work being carried out by the Swiss Geophysical Commission, which is charged by the Federal Government with geophysical surveying of Switzerland. Both organizations therefore decided in summer 1981 to combine their efforts in a joint investigation programme.

#### Investigation programme

The regional geophysical programme comprised the following components:

**Gravimetry:** A total of 4952 gravimetric stations were surveyed in the region during 1981/82. Evaluation of the data showed a significant mass deficit in the Riniken-Weiach area (KLINGELE & SCHWENDENER 1984).

**Aeromagnetics:** In 1981, a line network totalling 6250 km with a mesh size of 1 km (N - S) and 5 km (E - W) was surveyed from flying altitudes of 1100 and 1500 m. No significant magnetic anomalies were identified in the investigation area (KLINGELE et al. 1984).

**Magnetotellurics:** Also in 1981, magnetotelluric pilot measurements were carried out in the Black Forest (Schönau-Kaisten), the Tabular Jura (Herznach) and at the Baldeggersee (FISCHER et al. 1984). However, the results of the survey were inconclusive and no further measurements have been carried out.

**Refraction seismics:** The surveys carried out in 1981/82 were based on a seismometer array covering a total of 232 km and provided the first indications of the existence of the Permo-Carboniferous Trough of Northern Switzerland (SIERRO et al. 1983). Its presence was later confirmed using reflection seismics and it was encountered in the Weiach and Riniken boreholes; further refraction measurements were carried out in 1984 with a view to mapping the Permo-Carboniferous Trough (FROMM et al. 1985).

**Reflection seismics:** The network for the reflection seismics survey, which was carried out in three phases between 1982 and 1984, totalled 400 km (Fig. 2-1a). The geophysical data processing of the field recordings resulted in high-quality seismic profiles. The results were first published in SPRECHER & MÜLLER (1986) and interpreted in detail in DIEBOLD et al. (1991).

In the area to the east of the crystalline basement investigation region, a further reflection seismics campaign was carried out in 1991/92; the network totalled around 230 km. These measurements were carried out in connection with site investigations in the Opalinus Clay and are still undergoing interpretation.

## **2.4 Hydrogeological investigations**

Any radionuclides released from a repository will be transported to the biosphere primarily with circulating groundwater. For this reason, Nagra's investigation programme has assigned particular importance to hydrogeological investigations. The term hydrogeological investigations is used here in a broad sense to include:

- hydraulic testing and observations in the Nagra deep boreholes
- analysis of hydrogeological data from other wells or boreholes within the Nagra investigation area
- synthesis of all available information and conceptualization of the hydrogeological framework
- hydrodynamic modeling of the groundwater flow on different scales.

The aim of the hydrogeological investigations, and particularly of the hydrodynamic modeling, is to provide a quantitative characterization of the groundwater flow regime within a given region based on available measurements. Models are thus used both in an interpretive and a predictive manner; in the former case, the models are used to discriminate among various plausible hypotheses in order to interpret the data - e.g.

could a hydraulic boundary or connection exist in some areas, should hydraulic conductivity values strongly decrease with depth; in the latter case, hydraulic characteristics of the flow regime are quantified, e.g. what is the magnitude of groundwater flow in an area, what are the flow path directions and lengths. The results form the basis for the hydrogeological database required for the performance assessment calculations. Finally, the models help to illustrate and quantify the uncertainty existing for critical input parameters, as well as the impact of the uncertainty on the predictions.

Nagra developed a first set of conceptual hydrogeological models and the corresponding hydrodynamic models in connection with Project Gewähr (see below). With the additional information collected and analyzed since then, the conceptual models have been updated and a second set of studies have been performed in connection with the Kristallin-I project. Hydraulic data analysis, conceptual model development and results are summarized in Chapter 8.

#### **2.4.1 Hydrogeological data**

To obtain the input data required for modeling, it is necessary to make a systematic inventory of all relevant geological and hydrogeological data available from the region and to evaluate these data with the aim of formulating one (or possibly more) conceptual hydrogeological model(s) which allow a consistent interpretation of all measurements.

Some data on the hydraulic conductivity of the different formations were available before the Nagra investigations began. These data were, however, insufficient to allow determination of the spatial distribution of the hydraulic conductivities in the key features; there were virtually no data pertaining to aquitards or low-permeability crystalline basement sections and data for the hydraulic characterization of tectonically disturbed zones (faults) were also lacking. For this reason, extensive hydraulic testing was performed in the deep boreholes, both in the crystalline basement and in the overlying sedimentary formations.

The hydrogeological data acquired within Nagra's deep drilling programme are summarized in the reports mentioned in Table 2-1. The data include i) hydraulic properties such as hydraulic conductivities and storage coefficients of the sedimentary formations and crystalline basement penetrated by the boreholes, ii) hydraulic head estimates from the test programme as well as from long-term measurements. Hydrochemical data such as residence times of groundwaters were also used for determining certain boundary conditions during the stage of the conceptual hydrogeological model development; at a later stage they also allowed an independent check to be made of the consistency of the hydrodynamic model results.

Information from other wells and boreholes in the area was also analyzed to expand and complement the hydrogeological database. For example, additional information on hydraulic heads in the investigation area comes from mineral and thermal water boreholes in the region, from drill-stem tests in oil industry boreholes and from

hydrological data (e.g. river elevations). A monitoring programme carried out for mineral and thermal springs in the investigation area provides data on volumetric flow rate, electrical conductivity and temperature based on both periodic and continuous measurements (section 2.5).

#### **2.4.2 Hydrodynamic models**

The first hydrodynamic models for the investigation area were developed in connection with Project Gewähr between 1981 and 1984 by the Centre d'Hydrogéologie of the University of Neuchâtel under contract from Nagra (KIRALY 1985; KIMMEIER et al. 1985).

The first, or so-called "regional", model comprised all the infiltration zones of the crystalline basement and extended from the Aar Massif to the Black Forest and from the Bernese Jura to Lake Constance. The discretization selected for this area took into account surface topography, river networks, geological structures and stratigraphic outcrops. The model extended in a vertical direction from the surface down to a depth of 8000 m below sea-level; the vertical discretization was based on lithostratigraphic boundaries.

The second, or "local", model allowed complex geological structures and stratigraphic and topographic correlations to be identified over a smaller area. This model extended from the Rhine in the north to the Aare along the southern foot of the Jura in the south, and from the line Olten-Augst in the west to the eastern boundary of the Lägeren in the east. The external boundary conditions for the local model were derived from the regional model.

Once the field investigations had been completed and the relevant data analyzed, a new set of hydrodynamic models based on the updated hydrogeological conceptualization was prepared (Fig. 8-6) and the area of interest for a HLW repository in the crystalline basement was somewhat modified. The southern boundary is now defined by the northern margin of the Permo-Carboniferous Trough, and to the west the region extends to the Zeiningen-Wehr fault zone. These changes in the geometric situation, together with an improved hydrogeological dataset, served as the basis for characterizing groundwater flow in an area of approximately 1000 km<sup>2</sup> (Fig. 8-8). Two regions were defined within this area, one in the west and one in the east (cf. Chapter 8), and detailed hydrodynamic modeling was carried out. The numerical hydrodynamic models were constructed in such a way that current structural geology model concepts could be taken into account, and a further refinement was undertaken on the so-called block scale. The low-permeability blocks in the crystalline basement, which are bounded by major water-conducting faults and are foreseen for the location of the disposal tunnels, were characterized hydrogeologically using fracture network models. Consistent combination of results from the local models and modeling on a block scale allowed the development of a database which could be used for further safety analysis calculations, as described in Chapters 8 and 10.

## 2.5 Hydrochemical investigations

Hydrochemical and isotopic analyses of groundwaters in a repository area and its surroundings are an important part of a waste repository safety assessment. Three types of information can be derived from these data:

- The regional distribution of groundwater types and their hydrochemical and isotopic composition give estimates of groundwater residence times and provide constraints on provenance, e. g. location of recharge areas and climatic conditions during recharge. This information can be used for consistency checks of hydrodynamic models.
- The longevity of the engineered barriers in a repository, the solubility of radionuclides in groundwater and the retardation of radionuclides in the engineered barriers and in the geosphere strongly depend on the hydrogeochemical environment. Careful sampling and analysis of groundwaters from deep boreholes is necessary to assess the in-situ hydrochemical conditions in the near- and far-field of a potential repository.
- Continuous hydrogeological and hydrochemical monitoring of commercially exploited thermal and mineral springs and wells in a site investigation area provides information on possible perturbations (or absence thereof) caused by ongoing research activities (drilling, pumping tests).

### Hydrochemical programme

Nagra's hydrochemical programme started in 1981 with the collection of water samples from about 140 springs and wells of different aquifers in Northern Switzerland and adjacent areas; this was called the 'Regional Programme' (SCHMASSMANN et al. 1984, SCHMASSMANN 1990). Detailed hydrochemical and isotopic analyses were carried out on these samples. About 60 water samples from the seven Nagra deep boreholes were also collected using special methods (HAUG 1985) and analyzed; 50 of these samples gave useful results (WITWER 1986, PEARSON et al. 1989, BLASER & SCHOLTIS 1991). Additional geochemical and isotopic data on rock material are also available from these boreholes. A literature study yielded complementary hydrochemical data from so-called external analyses ('Fremde Analysen'), both from points sampled during the Regional Programme and from additional sampling locations. Figure 2-3 is a map of the region studied showing the sampling locations.

Within the area of Nagra's deep drilling programme, several thermal and mineral water springs and wells are exploited for balneological and bottled drinking water purposes. Nagra set up an extensive hydrogeological and hydrochemical monitoring survey of 16 observation points to study long-term fluctuations, to obtain evidence of possible perturbations caused by the Nagra drilling activities, and to be in a position to evaluate claims of harmful influences (NAGRA 1986a, SCHMASSMANN 1990). Monitoring was carried out at the following locations (Fig. 2-3):

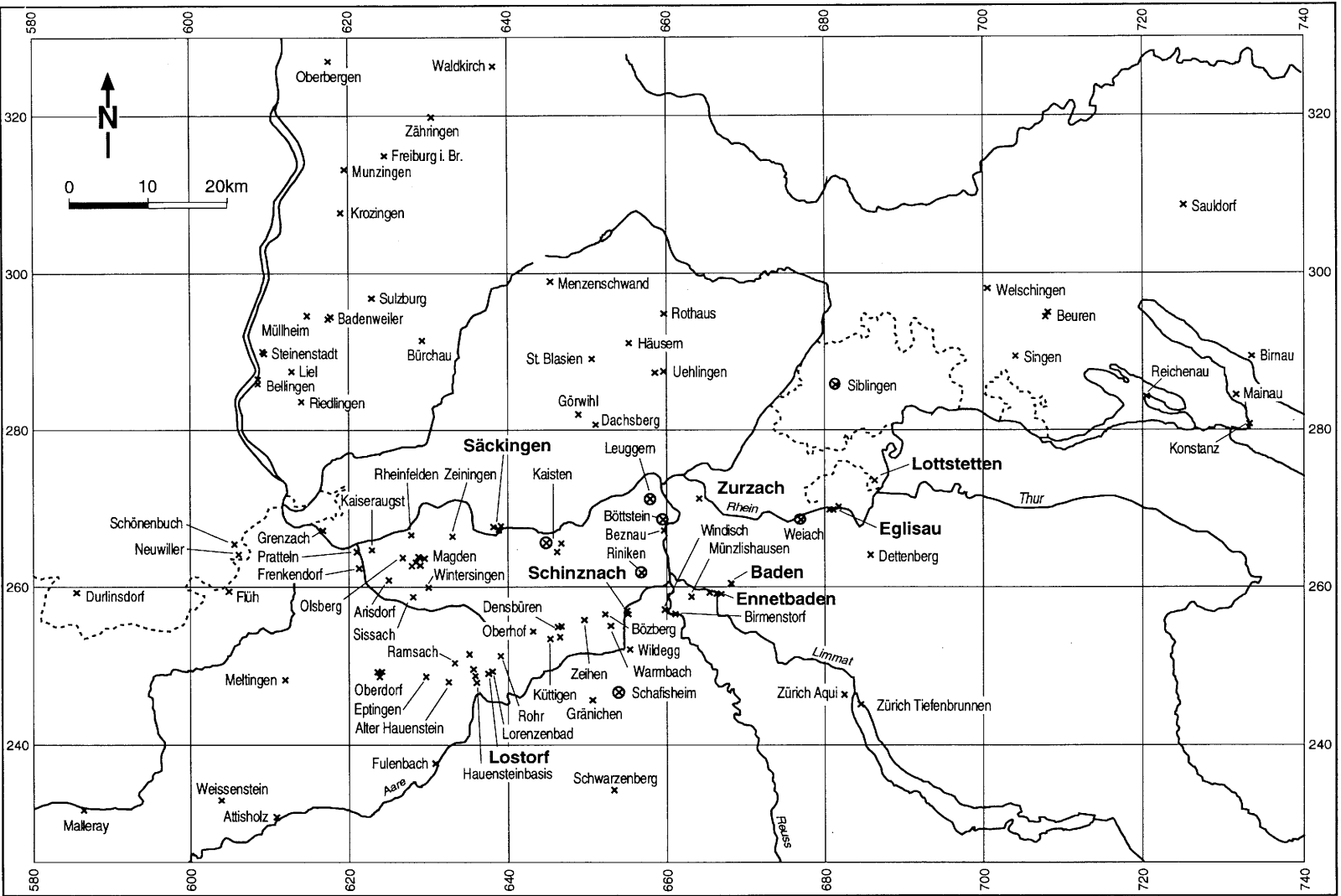


**Fig. 2-3 :** Location map of hydrochemical sampling points or groups of sampling points. Nagra deep borehole locations have a special symbol (cross in circle). Locations of the observation network for mineral and thermal springs and wells are in bold print.

- Säckingen Spa (Germany), crystalline basement, 2 wells;
- Zurzach Spa, crystalline basement, 2 wells;
- Baden/Ennetbaden Spa, Muschelkalk, 19 springs (4 for hydrochemical sampling);
- Schinznach Spa, Muschelkalk, 2 wells;
- Lostorf Spa, Muschelkalk, 2 wells;
- Lottstetten (Germany), planned for prospective use, Upper Jurassic, 1 well;
- Eglisau, bottling plant, Upper Jurassic and Tertiary, 3 wells.

The survey began one year before the drilling of the first Nagra borehole and consisted of periodic measurements and continuous records of hydraulic head, volumetric flow rate, temperature and electric conductivity, supported by periodical hydrochemical sampling. The survey was abandoned after the period of drilling activities. No influence on the thermal and mineral springs and wells could be identified (NAGRA 1986a).

### **Analytical programmes**

Analytical programmes of differing levels of complexity were selected, depending on the quality and quantity of the water samples. Of the four programmes (types A,B,C,D), type D, which originally contained 80 chemical, physical, microbiological and isotopic parameters, was the most comprehensive (GAUTSCHI & SCHOLTIS 1989, SCHMASSMANN 1990). Based on the results of a first set of analyses, some trace elements with very low concentrations in most samples and routine microbiological analyses that could not be interpreted due to contamination problems were omitted in later investigations. Tables 10-4 to 10-5 represent the most comprehensive type D analytical programme, complemented by some trace element analyses originating from a colloid study. For most samples, additional isotopic and dissolved noble gas analyses were performed (PEARSON et al. 1991).

All analyses have been subjected to quality control and are stored in a computer data bank. The procedures are described in GAUTSCHI & SCHOLTIS (1989), PEARSON et al. (1989) and PEARSON et al. (1991).

Most of the chemical and isotopic data, and their interpretation, are published in a series of Nagra Technical Reports (NTBs). The most relevant reports for the Kristallin-I project are PEARSON et al. (1991), SCHMASSMANN et al. (1992) and PEARSON & SCHOLTIS (1993).

## **2.6 Geological map of Central Northern Switzerland 1:100,000 and geological mapping campaigns**

### **2.6.1 Geological map of Central Northern Switzerland**

In 1982, when Nagra began field investigations in the region of Central Northern Switzerland, there was a need for a concise, uniform but sufficiently detailed geological map of the entire region. At that time the area was covered only by an incomplete, heterogeneous mosaic of mostly older geological maps on different scales.

A geological map on a scale 1:100,000 was therefore compiled, which covers the whole Nagra investigation area and the adjoining region of Baden-Württemberg to the north. The topographic basis for this exercise was the Bözberg sheet and the northern half of the Beromünster sheet of the map of Switzerland 1:100,000. The "Geological Map of Central Northern Switzerland" (ISLER et al. 1984) was published with the cooperation of the Swiss Geological Commission.

The explanatory notes to the map (MÜLLER et al. 1984) attempt to provide a concise overview of the rock units to be found in the area and of the geological/tectonic evolution processes. These appendices take account of the most recent information available at the time, including the ongoing Nagra investigations.

### **2.6.2 Additional geological mapping**

In terms of level of detail, there were gaps in the geological mapping along the Rhine in the region covered by the Laufenburg and Zurzach sheets 1:25,000. In this area, there was particular interest in the trend and the structure of large-scale fault zones which traverse the Swiss-German border and are represented morphostructurally in the neighboring Southern Black Forest. For this reason, these areas were mapped geologically on a 1:10,000 scale. The results of these new mapping campaigns were made available to the Swiss National Hydrological and Geological Survey (section: geological mapping) for a series of geological atlas sheets (scale 1:25,000), but could not be taken into consideration in the 1:100,000 map of Northern Switzerland which had already been published.

## **2.7 Geological studies in the Southern Black Forest**

Because of the existence of the sedimentary overburden, the investigation programmes presented in sections 2.2, 2.3 and 2.6 could only investigate the crystalline basement of Northern Switzerland directly at a few outcrops along the Rhine at Laufenburg and in the deep boreholes, and indirectly using geophysical tools. It was therefore decided to carry out certain petrographic and structural geology studies in the geographically adjacent Southern Black Forest, where the basement is exposed. The bedrock and its structures could be studied at outcrops in gorges, valleys, quarries, at

road construction sites, in the tunnels and caverns of the Schluchsee hydro plant and in some still accessible ore mines.

The following objectives were foreseen for the investigations in the Southern Black Forest, with particular attention being paid to potentially water-bearing brittle deformation features:

- studying the geological/tectonic structure of the basement;
- determining the extent of the different rock types and basement blocks (block tectonics);
- detailed structural analysis of brittle deformations in the crystalline basement;
- characterizing the nature of discontinuities (fault zones, fractures, etc.);
- drawing up a pattern of faulting based on morphostructural studies in the directly adjoining region of the Southern Black Forest.

According to current information from the deep boreholes and from the Southern Black Forest, the basement between the tectonic sutures of the Badenweiler-Lenzkirch Zone and the Permo-Carboniferous Trough of Northern Switzerland can be considered as a single unit, both in terms of petrography and tectonics. Some information from the studies in the Southern Black Forest, e.g. classification of fault zones, fault patterns, extent of "intact" crystalline bodies, etc., can thus be applied to the basement of Northern Switzerland, although caution must be exercised in this respect.

The results of this work are documented in several Nagra Technical Reports (HUBER-ALEFFI & HUBER-ALEFFI 1984, HUBER & HUBER 1986, HUBER & HUBER-ALEFFI 1990). Supplementing information from the deep boreholes and the geophysical studies, these results also made an important contribution to the development of the structural model of Northern Switzerland (AMMANN et al. 1992), which served as the basis for the hydrodynamic model of Northern Switzerland and for the exploration study.

## **2.8 Neotectonic studies**

The long-term safety ( $10^5 - 10^6$ a) of a HLW repository depends on possible future changes of its geological environment. As no firm predictions are possible, scenarios are used to investigate possible future developments. Formulating plausible future scenarios of this type requires a fundamental understanding of regional geological structure and of the recent history of the earth, and its dynamics and kinematics, in the investigation area. Considerable importance is thus attached to neotectonic studies, which provide a basis for predicting future geological evolution.

Such long-term scenarios for Northern Switzerland were first presented and discussed in detail within the framework of Project Gewähr (DIEBOLD & MÜLLER 1985). An updated, revised version (NAEF 1992) is presented in Chapter 9.

The aim of the neotectonic programme was to identify, describe and localize recent tectonic events, and to attempt to provide an understanding of the mechanisms of the individual phenomena with a view to assessing their significance. An interdisciplinary approach had to be adopted, with investigations in the following fields contributing data to the neotectonic programme:

- geology/tectonics;
- geomorphology;
- seismology;
- geodesy;
- rock mechanics (determining the recent stress field).

Various aspects of the neotectonic programme have already been completed, whilst others, particularly long-term projects such as monitoring and analyzing earthquakes and verifying the GPS network for Northern Switzerland, are still ongoing.

### **2.8.1 Geological-tectonic documentation**

A comprehensive literature study (ISLER 1984b) brought together all the key information on recent crustal movements in Switzerland and the surrounding regions. This study represented the starting-ground for the new neotectonic studies.

All tectonic features such as faults and overthrusts which are shown on existing geological maps and mentioned in the literature have been inventoried. As part of the geological documentation exercise, the "Geological Map of Central Northern Switzerland" with neighboring region of Baden-Württemberg, scale 1:100,000 (section 2.6), was prepared and geological studies were carried out in the Southern Black Forest (section 2.7).

NAEF et al. (1985) used schematic geological profiles and a stratigraphic division as a basis for preparing subsidence diagrams for the period of the Molasse sedimentation. These showed that different discrete phases of tectonic activity ranging from the Oligocene up to the post-Molasse period can be distinguished.

The reports and maps mentioned, the results of the deep drilling programme (section 2.2) and the interpretation of reflection seismics data (section 2.3) all combine to provide a comprehensive geological-tectonic document which served as the basis for considering neotectonic problems.

### **2.8.2 Microearthquake measurement network**

One of the aims of neotectonic studies is to identify and locate recent active fault zones and fault systems. One recognized method for characterizing active fault systems is accurate mapping of earthquake hypocenters. Analysis of earthquakes and earthquake groups provides information on focal mechanisms, which in turn allows conclusions to be drawn as to the prevailing stress field. Knowledge of this indirectly determined stress field is very helpful in understanding patterns of neotectonic movement.

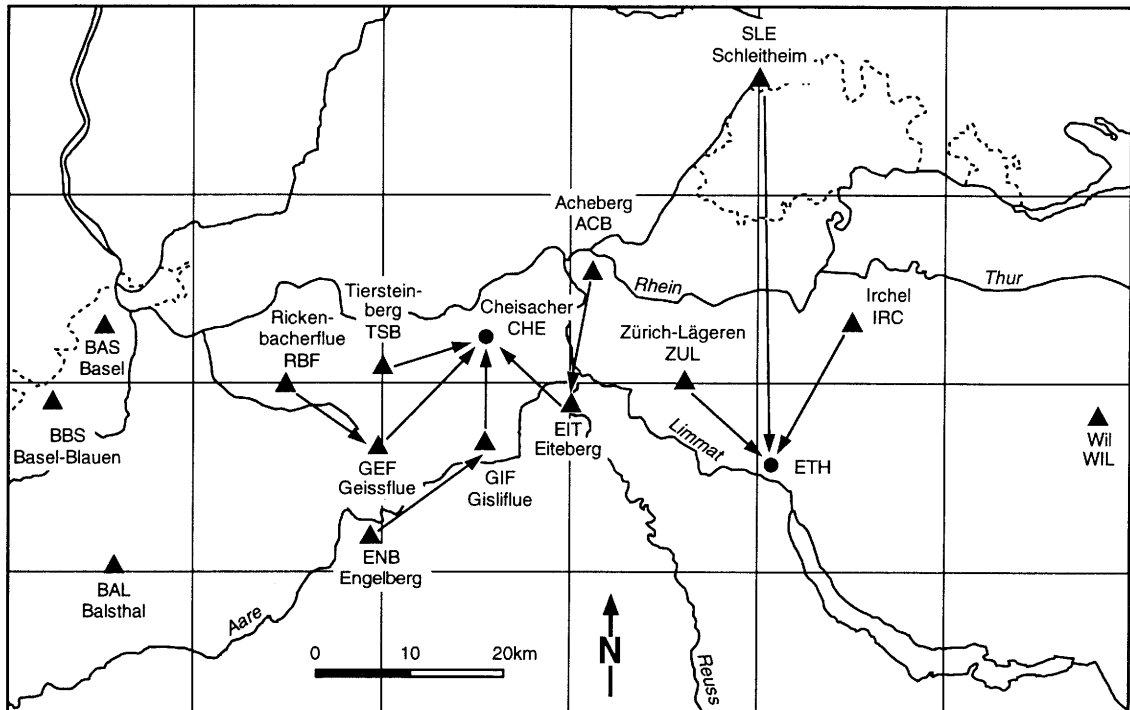


**Fig. 2-4:** Microearthquake network for Northern Switzerland: seismometer locations (triangles), signal transfer (arrows) and registration locations (black points) in Northern Switzerland.

A study on the inventory of seismicity between 1910 and 1982 (MAYER-ROSA et al. 1983) showed that seismic activity in Central Northern Switzerland is very low. In order to obtain a sufficiently comprehensive dataset for present purposes over a period of a few years, it was necessary to measure very low-magnitude earthquakes. In order to achieve this, the density of the existing seismometer station network had to be increased and the Swiss Seismological Service was charged, in cooperation with Nagra, with developing a concept for a new station network for Northern Switzerland.

This new network was installed in 1983 and began operations during the same year (MAYER-ROSA et al. 1984). It consists of a total of 12 seismometers, 9 of which are new (Fig. 2-4). All the stations are equipped with short-period seismometer systems which register ground movements in a vertical direction. Two of the stations are additionally equipped with two horizontal seismometers each, to allow incoming signals to be registered in three-dimensional form; this arrangement also allows better identification of shear waves.

The sensitivity of the new station network to microearthquakes, and the accuracy with which the earthquakes can be localized, show a marked improvement over the previous arrangement (DEICHMANN & RENGGLI 1984); it is now possible to register weak earthquakes with a magnitude of less than 1.0 on the Richter scale.

To date, the results of the microearthquake investigations have fulfilled all expectations, providing Nagra with important information on active fault systems, their deformation character, and the recent stress field. The results are published as they become available in the Nagra Technical Report series (DEICHMANN & RENGGLI 1984, DEICHMANN 1987, 1990) and an overview is provided in section 9.2.3.

### **2.8.3 Geomorphological investigations**

Lineament analyses are available for the region of Northern Switzerland; these were prepared independently by three different specialists on the basis of satellite photographs. However, examination of this lineament pattern did not provide any indication of undiscovered tectonic disturbed zones or of neotectonic activity on any of the lineaments (ISLER 1984a).

An analysis (HALDIMANN et al. 1984) of the rock morphology beneath the Quaternary deposits and of the evolution of accumulation and erosion levels of gravel terraces in the lower Aare valley and the upper Rhine valley provided indications of Upper Pleistocene movements. A study of river history in the Southern Black Forest also indicates active, Quaternary block tectonics (section 9.2.2).

### **2.8.4 Geodetic investigations**

Recent vertical crustal movements can be calculated by comparing repeated, temporally separated precision leveling measurements. The investigations carried out in Northern Switzerland in cooperation with the Federal Office of Topography (GUBLER et al. 1984, SCHNEIDER et al. 1992) and in the neighboring region of Baden-Württemberg by the Geodetic Institute of the University of Karlsruhe (MÄLZER et al. 1988) have indicated regions with significant uplift and subsidence tendencies.

There are virtually no data on recent horizontal movements at faults and overthrusts in Switzerland; this is due to the difficulties associated with performing such measurements (work-intensive, very high costs, insufficiently accurate). With the introduction of the geodetic "Global Positioning System" (GPS), large distances can now be measured with a high degree of precision and repeated measurements at appropriately spaced time intervals make it possible to obtain data on recent horizontal crustal movements. Nagra has therefore installed a high-precision GPS network in Northern Switzerland. All significant fault zones (Eggberg, Vorwald, Mandach and Mettau faults, etc.) and tectonic units are covered by this network, which was measured by the Federal Office of Topography in two subsequent campaigns in October 1988. The results of this double calibration of the GPS network fulfilled all high expectations (SCHNEIDER & WIGET 1990). Since the expected movements are very

small, a sufficiently long period of time should elapse to allow significant displacements to be registered. A first repeat measurement is therefore planned in 1995.

### **2.8.5 Determining the recent stress field**

Information on the recent stress field is important in order to predict the future tectonic evolution of a region. In order to obtain a dataset which is as comprehensive and consistent as possible, a range of different methods is used to determine the stress field:

- seismotectonic analysis of earthquakes or earthquake swarms (PAVONI 1984; DEICHMANN 1987, 1990);
- investigations of borehole-wall breakouts from the deep boreholes drilled in Northern Switzerland (BECKER et al. 1984);
- in situ stress measurements (BECKER et al. 1984).

MÜLLER et al. (1987) provides an overview of the different techniques used, the results and their interpretation.

### **3 STRUCTURE AND GEOLOGICAL EVOLUTION OF NORTHERN SWITZERLAND**

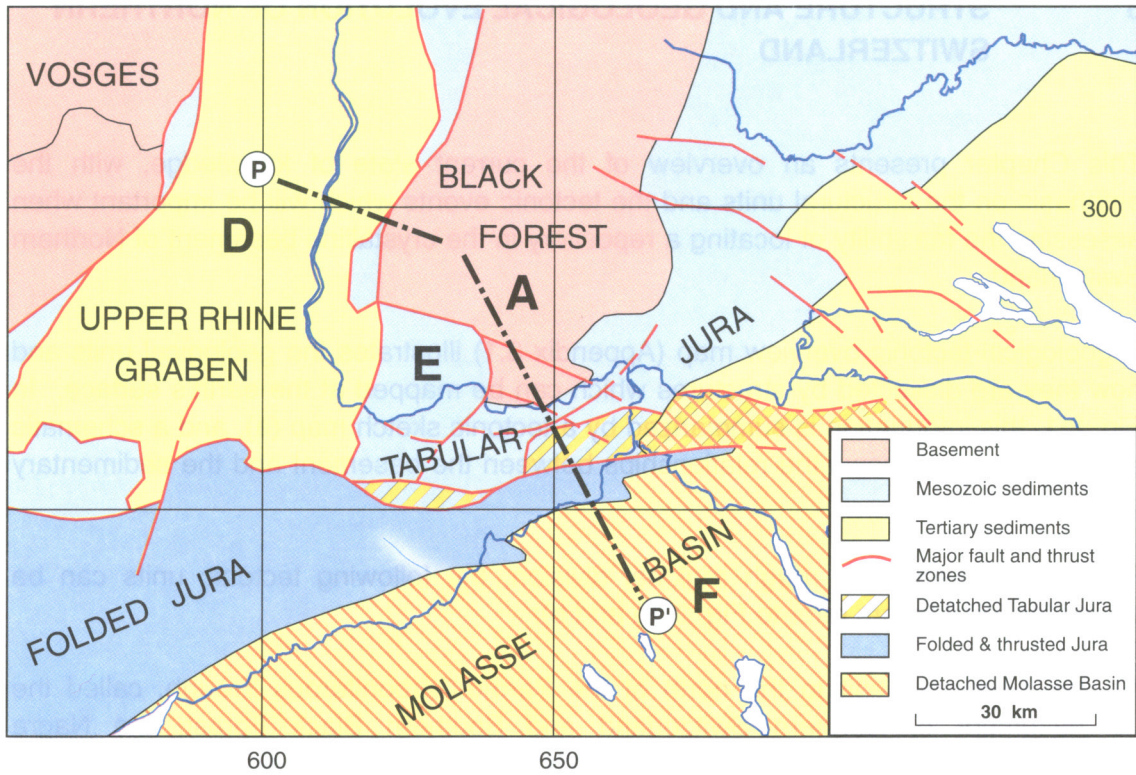
This Chapter presents an overview of the current state of knowledge, with the emphasis on the structural units and the tectonic events which will be important when assessing the feasibility of locating a repository in the crystalline basement of Northern Switzerland.

A geological-tectonic overview map (Appendix 3.1) illustrates the geological units and how they are dissected by structures which can be mapped at the earth's surface. In Fig. 3-1, this information is summarized by a tectonic sketch map (a), and a schematic profile (b), which shows the relationships between the basement and the sedimentary cover.

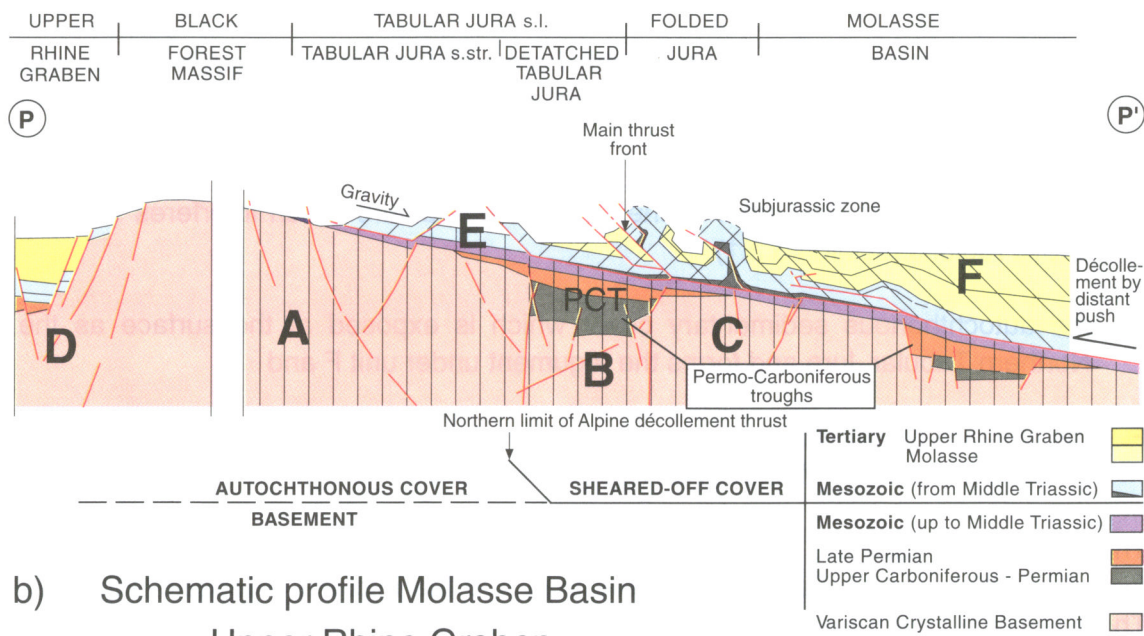
For the purposes of a rough regional division, the following tectonic units can be defined (capital letters refer to Fig. 3-1a and b):

- A the basement unit to the north of the Permo-Carboniferous Trough, called the basement of Northern Switzerland and Southern Black Forest; the Nagra boreholes at Kaisten, Leuggern, Böttstein and Siblingen were drilled near the southern boundary of this region (for details, section 3.1);
- B the zone of the Permo-Carboniferous Trough of Northern Switzerland (PCT) with the Riniken and Weiach boreholes (section 3.2);
- C the basement unit to the south of the Permo-Carboniferous Trough, which was encountered in the Schafisheim borehole, including further Paleozoic sedimentary zones;
- D the Tertiary rift of the Upper Rhine Graben, a structure which interferes with the above regions (section 3.3.1);
- E the autochthonous sedimentary cover which is exposed at the surface as the Northern Tabular Jura and forms the tegument under unit F and
- F the sheared-off overburden comprising the southern or detached Tabular Jura, the Folded Jura and the Molasse Basin (section 3.3).

The present-day structure of Central Northern Switzerland is the result of a geological evolution which can be traced back more than 400 Ma into the Paleozoic (Fig. 3-2). The significant tectonic events occurred at the beginning and at the end of this period, i.e. during the Paleozoic and the Tertiary, with the approximately 200 Ma in between being a period of relative tectonic inactivity (cf. Fig. 3-4). The geological history of Northern Switzerland can thus be divided into three phases, each with its own character:



a) Tectonic Units of Northern Switzerland



b) Schematic profile Molasse Basin - Upper Rhine Graben

Fig. 3-1: Overview of the tectonic division of Northern Switzerland and neighboring areas. Schematic profile not to scale!

1. During the Variscan orogeny, the crystalline basement underwent extensive deformation and metamorphism, accompanied by plutonic and volcanic activity, and has not changed significantly since then in terms of material components and structure. The Permo-Carboniferous Trough of Northern Switzerland formed during the late stage of the Variscan orogeny and represents an important component of the pre-Mesozoically consolidated basement (Fig. 3-2).
2. The time from the beginning of the Mesozoic to the Early Tertiary was marked by a long period without significant tectonic movements; this is reflected in the regional uniformity of the Mesozoic overburden (Fig. 3-4).
3. During the Tertiary, the region of Northern Switzerland underwent renewed tectonic overprinting associated with the Alpine orogeny. The updoming of the Black Forest and the subsidence of both the Upper Rhine Graben and the Alpine foreland (Molasse Basin) resulted in the reactivation of old fault zones in the basement of Northern Switzerland. During the Tertiary, the sedimentary cover was partly detached, thrust and folded by distant push from the Alpine orogen (Folded Jura [Figs. 3-1, 3-3, 3-4]).

The scenario of neotectonic movements includes ongoing uplift in the Black Forest and probably further thrusting in the Folded Jura (cf. Chapter 9).

A series of idealized profile sketches has been drawn in Figure 3-3 to indicate the key stages of structural evolution using the example of the northern margin of the Permo-Carboniferous Trough (cf. also Chapter 4).

### **3.1 The pre-Mesozoic evolution of the basement**

Assuming that the results of recent geological research in the neighboring Black Forest will also be applicable in principle to the region of Northern Switzerland, the Variscan evolution of the basement of Northern Switzerland can then be divided into a series of discrete phases (cf. Fig. 3-2):

- I Formation of the old, pre-Variscan gneiss basement during the Precambrian and Early Paleozoic.
- II Variscan convergence with intrusion of syn-kinematic plutonites and metamorphic overprinting of the gneiss basement during the Devonian-Early Carboniferous.
- III a) Intrusion of post-kinematic plutonites and  
b) Updoming and extension of the central mountain belt (Moldanubian) in the Namurian-Westphalian; retrograde metamorphism.
- IV Late orogenic shearing and forming of sedimentary graben structures accompanied by acid volcanism in the Late Carboniferous-Early Permian (Saalian tectonics).
- V Post-orogenic subsidence (thermal cooling), marine transgression into the marginal zones of the orogen (Zechstein), continental sedimentation in troughs within the mountain range (Upper Rotliegendes).

As proposed by MILNES (1990), these phases can be summarized into two major cycles: during phases I to IIIa the basement was formed by orogenic and magmatic processes (basement-forming events) and during phases IIIb to V and later during the Tertiary the consolidated crust reacted as a more or less rigid body to the large-scale stresses (post-consolidation events, Fig. 3-2). Phase III marks the transition between these two major cycles (unroofing phase according to MILNES 1990), when rapid uplift and erosion of the Variscan mountains made it possible for rocks from deeper levels of the upper crust - e.g. the syn- to post-kinematic granites - to reach the surface within a relatively short period of time. A detailed analysis of the crystalline basement of Northern Switzerland is given in Chapter 4.

*Phase I:* Formation of the old gneiss mass

The gneisses and anatexites which form the framework for the granite intrusions of the Southern Black Forest provide evidence of a multiphase history of metamorphism and deformation which possibly extended as far back as the Precambrian (VON GEHLEN et al. 1986). These are mainly metamorphosed sediments and migmatites, for which isotope dating often gives Variscan ages. This indicates that the basement sections which are exposed today in the Southern Black Forest formed a geochemically open system during the Variscan metamorphism (KROHE & EISBACHER 1988).

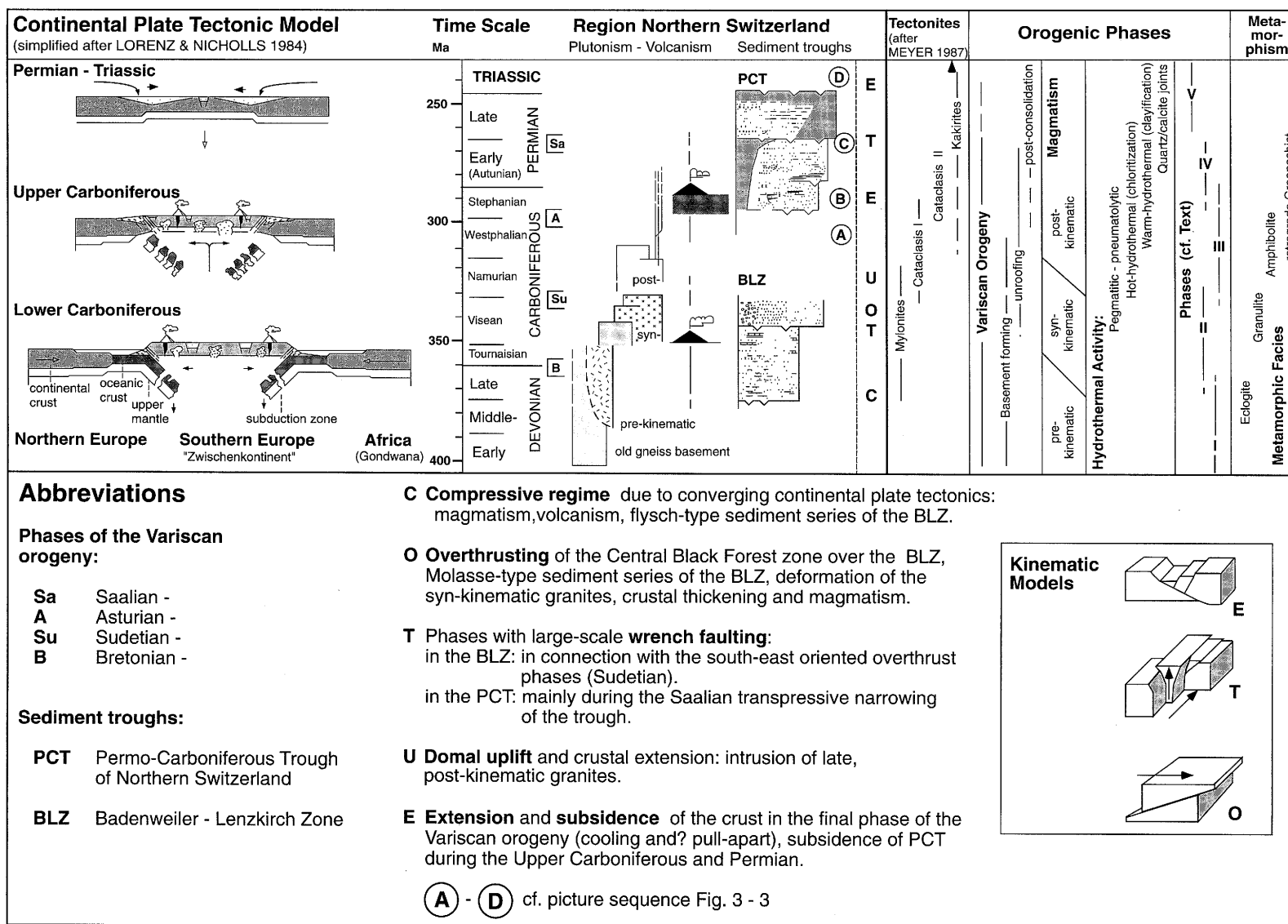
The extremely varied lithological spectrum of the Black Forest gneiss complex, together with the marked contrasts in structure, suggests that the individual large-scale units (blocks, complexes) are of varying origin and took the form of microcontinents which were welded together during the course of the Variscan orogeny. They are delimited by deep-reaching suture zones with a melange character, some containing sedimentary series whose ages and structures provide important information on the character and sequence of the orogeny. The Badenweiler-Lenzkirch Zone can be considered such a remnant of a sedimentary basin which, during the Upper Devonian - Lower Carboniferous, was located between the present-day Central Black Forest and the crystalline block of the Southern Black Forest. The Permo-Carboniferous Trough of Northern Switzerland is a comparable, but significantly younger, suture zone between the crystalline basement of Northern Switzerland and the basement beneath the Molasse Basin.

Following their consolidation, the old gneiss complexes behaved on a regional scale as more or less isotropic bodies intersected unconformably by post-metamorphic fault zones. By way of contrast, the small-scale fabric of later deformation features (fracture systems) was oriented preferentially along numerous lithological and structural anisotropies on a local scale (PETERS et al. 1989a, b).

*Phase II:* Variscan convergence and intrusion of syn-kinematic granites

The Variscan orogeny is the expression of a Late Paleozoic collision of two protocontinents, namely Gondwana in the south and Laurasia in the north (cf. Fig. 3-2, left side, after LORENZ & NICHOLLS 1984). The crustal fragments (microcontinents) lying between the protocontinents were also involved in the collision and largely

Fig. 3-2: Chronology of Variscan orogenic phases and timetable for basement evolution in the region of Northern Switzerland.



retained their original configuration as discrete crystalline zones. Examples of these isolated crustal fragments are the gneiss mass of the Central Black Forest and the SE Black Forest (Hotzenwald complex after KROHE & EISBACHER 1988), which lie to the north and south of the Badenweiler-Lenzkirch Zone respectively (cf. Fig. 5-5).

The older granites of the Southern Black Forest are evidence of large-scale, syn-tectonic plutonism. Typical for this older generation of syn-tectonic granites are strongly deformed, heterogeneous intrusive bodies with complex marginal zones and anisotropic internal fabrics (e.g. granite of Mambach, cf. HUBER-ALEFFI & HUBER-ALEFFI 1984). Their intrusion is associated with large, late-orogenic shear zones along which they were uplifted and then deformed.

The structural inventory which is observed in the region Black Forest - Northern Switzerland today originated during the Variscan convergence and is largely ductile in nature. Large overthrust surfaces and shear horizons are characterized by granulitic mylonites and form discrete zones which separate the individual gneiss nappes (e.g. STENGER et al. 1989). Increasing late-orogenic compression was associated with local steepening of the overthrust structures and the formation of shear zones. This late phase II overthrust regime also resulted in penetrative mylonitization (VON GEHLEN et al. 1986, ECHTLER & CHAUVET 1992). One example of such post-metamorphic shearing with dynamic quartz deformation could possibly be the gneiss series observed in Leuggern (cf. PETERS et al. 1989b).

#### *Phase III: Post-kinematic magmatism and uplift*

During the Upper Carboniferous, the Late Variscan orogeny was characterized by predominantly thermal updoming and extension of the overthickened crust, again accompanied by intensive granitic magmatism. Compared with the older granites, the intrusive bodies of this last phase are largely undeformed (e.g. Albtal Granite); they also partly penetrate the Badenweiler-Lenzkirch Zone (e.g. Ursee Granite) and are therefore younger (335-320 Ma) than the compressional phase (Phase II above) which culminated in the overthrusting of the Central Black Forest gneiss mass over the Badenweiler-Lenzkirch Zone (cf. section 4.2.4).

The continuing domal uplift resulted in rapid erosion of the highest crustal segments. The associated extension concentrated on more or less flat-lying fault zones (low-angle normal faults, inverted overthrust surfaces), divergent shear zones and high-angle normal faults. As deeper-lying crustal sections were exposed, pathways for the younger granites were formed, allowing these to rise to relatively shallow levels. Rapid cooling and a high thermal flux resulted (tectonic unroofing).

Although the results of radiometric dating of the different granites of the Southern Black Forest remain controversial in many respects (cf. MAZUREK & PETERS 1992), the actual intrusive activity probably ceased in the Late Carboniferous (ca. 320-310 Ma) (cf. section 4.2.3). The cycle of basement-forming processes was then largely complete.

As early as 1976, LORENZ & NICHOLLS (1976) proposed a basin and range tectonic model for the Late Variscan scenario in Europe; this has been corroborated by recent research in the Black Forest basement (KROHE & EISBACHER 1988, EISBACHER et al. 1989, ECHTLER & CHAUVET 1992). An expression of these extensional tectonics, termed "detachment faulting", are the early tectonites of cataclasis I after MEYER (1987) at the transition from ductile to brittle deformation behavior (Fig. 3-2 and section 4.5.6).

Typical for detachment horizons is a polyphase tectonite fabric which documents movements at different crustal levels (mylonite → cataclasite → kakirite, cf. Fig. 3-2) through which the individual rock sections pass during the unroofing. This phenomenon can be found in numerous locations, for example in the fault zone encountered in the lower section of the Kaisten borehole (side-branch of the Eggberg fault?).

The cataclasites were subject to continuous mineralization due to intensive hydrothermal alteration and cementation; the later ones (kikirites) are lithified either incompletely or not at all.

#### *Phase IV: Late-orogenic shearing and graben formation in the Permo-Carboniferous*

The final phase of the Variscan orogeny (Westphalian to Permian, around 315-245 Ma) was characterized by continued stretching, thinning and shearing of the crust along normal faults and steeply-inclined divergent wrench faults. Graben structures were formed, particularly along old nappe boundaries, and accompanied by volcanism and hydrothermal activity. The erosion products of the newly-formed mountain ranges were deposited in these depressions.

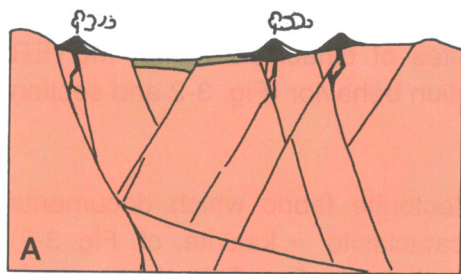
Evidence for this Late Variscan tectonic activity is provided by the numerous continental coal basins of Central Europe, one of which is the PCT. Based on results from the Wintersingen, Riniken and Weiach boreholes, and from reflection seismics campaigns, the PCT shows similarities to the Permo-Carboniferous deposits around the French Massif Central.

Set against the background of these large-scale analogies, a multiphase evolution can also be postulated for the PCT:

Extension and subsidence probably began in the Upper Carboniferous (Stephanian, around 295 Ma) with coal-rich sediments being deposited unconformably in wide basins over the crystalline basement (Fig. 3-3, situations A, B).

Stratigraphic and structural studies in the area of the PCT indicate that after the graben formation - during the Early Permian - there was a phase of transpressive tectonic events correlating to increased tectonic activities in large areas of Central Europe (Saalian tectonics).

These events are also documented in the sedimentary record of the PCT in the form of coarse-clastic sediments (conglomerates and breccias) which contain a large

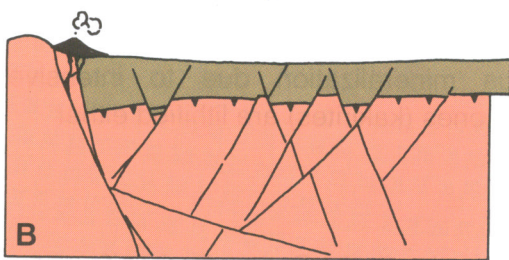


**A Situation in the late Westphalian (around 300 Ma)**

Final phase of post-kinematic granite intrusion: cooling, volcanism and hot-hydrothermal phase. Differential uplift and subsidence, erosional detritus from high zones deposited in evolving basins.

**Stephanian (Upper Carboniferous, around 296-285 Ma)**

(Asturian phase of the Variscan orogeny), continuing crustal extension, beginning of synsedimentary trough formation along normal faults and dextral wrench faults. Erosion of highs in the trough: peripheral alluvial fans and anastomosing river system in wetlands → peat → coal.

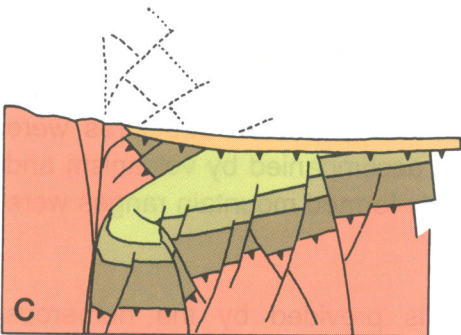


**B Situation in the early Lower Permian (Autunian, around 280 Ma)**

Deposition of the coal series (Stephanian) followed by differential subsidence. Extensive synsedimentary tectonics control sedimentation in the trough. Lakes were wide-spread in the Autunian, anoxic bottom-water → bituminous shales.

**Lower/Upper Permian transition (around 265 Ma)**

Saalian phase of the Variscan orogeny: intensive shearing of the trough along convergent wrench faults → internal folding and thrust, deposition processes continued ("syntectonic" Untere Schuttfächerserie: lower alluvial fan complex).

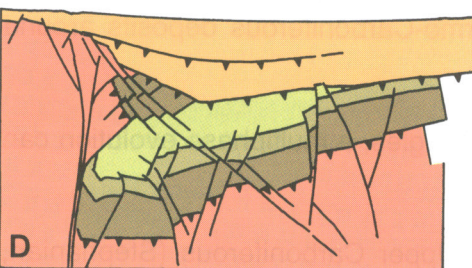


**C Situation in the early Upper Rotliegendes (~260 Ma)**

After the Saalian phase: unconformable deposition of the Obere Trogfüllung (upper trough infill) with extensive tectonic activity. Differential uplift of shoulders (Obere Schuttfächerserie: upper alluvial fan complex). Climatic change from humid to arid (deserts): Rot (red) sediments → Rotliegendes.

**Upper Rotliegendes (around 260-245 Ma)**

Decrease in subsidence due to crustal extension and cooling, as well as compaction of the thick trough infill. In the Upper Permian, the depositional environment extends far beyond the old trough shoulders.



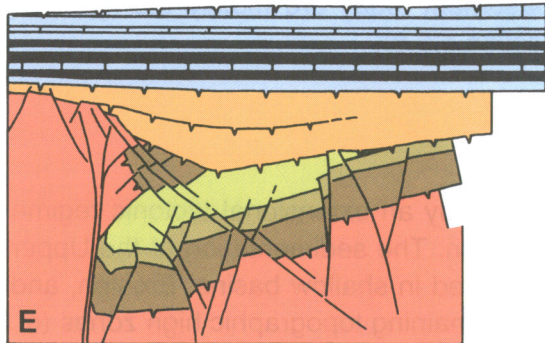
**D Situation at the Permian/Triassic transition (~245 Ma)**

Following completion of the Variscan orogeny and deposition of the Obere Trogfüllung, a state of peneplanation is reached.

**Mesozoic (Triassic-Cretaceous, around 245-66 Ma)**

Continued cooling of the Variscan formations accompanied during a period of relative tectonic inactivity by general subsidence and marine transgression. After a delay during the Triassic, fully marine conditions dominate in the Jurassic.

**Fig. 3-3:** Tectonic history of Northern Switzerland, illustrated for the evolution of a schematic profile through the northern margin of the Permo-Carboniferous Trough (from DIEBOLD 1990).

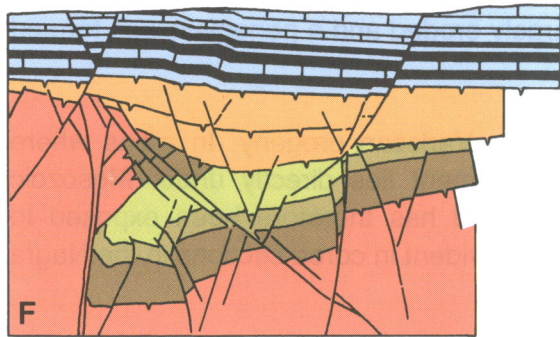


### E Situation at the Cretaceous/Tertiary transition (around 65 Ma)

The tectonic inactivity during the Triassic and Jurassic is evidenced by undisturbed, almost parallel bedding. During the Cretaceous there was large-scale domal uplifting, a retreat of the sea and erosion of the newly-formed land surface. Deposits of the Cretaceous and the earliest Tertiary are absent in Northern Switzerland.

### Early Tertiary (Eocene-Oligocene, around 50-24 Ma)

In the Upper Rhine graben region, the continental period with erosion continued into the Eocene (around 50 Ma). This was followed by renewed tectonic activity: the Upper Rhine graben subsided during the Eocene and Oligocene. The Permo-Carboniferous trough of Northern Switzerland was also affected by this process: peripheral faults which originated in the Palaeozoic were reactivated as faults and/or flexures.

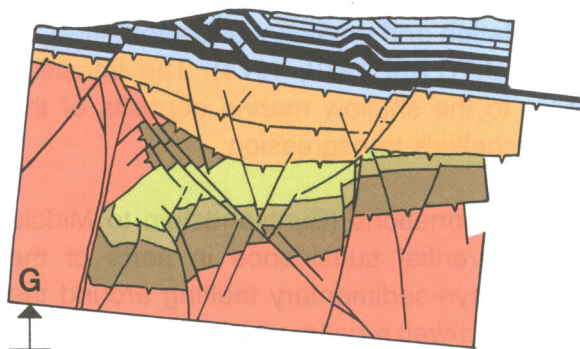


### F Situation in the early Miocene (around 22 Ma)

The old Tertiary to early Miocene reactivation of the old peripheral faults of the Permo-Carboniferous trough is evidence clearly by the deformation of the Mesozoic sediment cover. Continental conditions continued to prevail in many areas of central Northern Switzerland and erosion reached some parts of the Dogger before the deposition of the Upper Freshwater Molasse.

### Middle to late Miocene (20-10 Ma)

Under the influence of the uplift of the Black Forest and the Vosges (which began in the Miocene) and the subsidence of the Molasse basin, the regional SSE-tilting in Northern Switzerland became increasingly pronounced.



### G Situation today, following the Jura folding

During the Jura folding (from ca. 10 Ma), the sedimentary cover in large areas of the Tabular Jura was sheared off along the evaporites of the Middle Triassic and translated NNE. The northern boundary of the sheared-off sedimentary cover (which is also overthrust in the north) overlies the northern margin of the Permo-Carboniferous trough (Mandach thrust). The old disturbed zones, which were reactivated as flexures and/or faults, functioned as weak zones which served as nucleation points for the overthrusting.

Fig. 3-3: (continued)

proportion of crystalline and/or volcanic components (MATTER et al. 1987, 1988a). In particular the gravels of undeformed granites show that the original intrusion level of the post-kinematic granites was uplifted to the surface and exposed to erosion. The brittle structures observed in the crystalline basement today are mainly the result of these Permo-Stephanian tectonic events (cf. section 4.5.8).

#### *Phase V: Post-orogenic differential subsidence*

The Saalian phase of wrench faulting was followed by an extensional tectonic regime with widespread subsidence during the Late Permian. The sedimentation of the Upper Rotliegendes (upper trough infill of the PCT) occurred in shallow basins. Erosion, and particularly intensive weathering, prevailed in the remaining topographic high zones (cf. sections 4.5.9 and 4.5.10), while thin, detrital deposits formed in regions of subsidence. As a rule, only a few 100 meters of fine-grained red beds were deposited (playa sediments). These basins extended far out over the limits of the deep Permo-Carboniferous troughs. As the differential movements died out at the time of the Early Triassic, the Variscan mountain range was largely eroded and a peneplain was formed (Fig. 3-3, situation D).

The Saalian unconformity marks the end of the Variscan orogeny. In areas where Permian was not deposited the crystalline basement lies directly under Mesozoic cover. It was situated at or near the surface and has therefore been exposed to weathering and decompaction processes. This is evident in cored sections in the Nagra boreholes or in the adjacent Southern Black Forest.

The Permian/Triassic boundary between the continental Upper Rotliegendes and the overlying Buntsandstein is, in some locations, a continuous lithological transition rather than a sharp contact. The sedimentary sequence from the Permian to the Lower Triassic is characterized by hiatuses, resedimentation and erosional unconformities, all of which are typical for terrestrial deposits (cf. ORTLAM 1970, 1974). The transition from these Permo-Triassic red bed sediments to the shallow marine deposits of the Middle Triassic took place with the onset of Muschelkalk transgression.

Abrupt thickness changes in the Lower Triassic formations (Buntsandstein to Middle Muschelkalk) are an indication of ongoing differential subsidence in parts of the basement. HAUBER (1971 and 1993) describes syn-sedimentary faulting around the Middle Triassic salt deposits at Rheinfelden and Schweizerhalle, which apparently has a Hercynian strike (WNW-ESE).

On a local scale, the structures associated with this Late Permian - Early Triassic subsidence phase were probably largely normal faults and possibly pull-apart structures (fractures). Reconstructions in the vicinity of the PCT show (App. 36, 38 in DIEBOLD et al. 1991; BLÜM 1989) that subsidence generally followed old structures as guidelines, occurring mainly along Hercynian-striking lineaments (e.g. Vorwald and Eggberg faults) which were already active during the Saalian tectonic phase as dextral shear zones. A cross-section through the western part of the PCT clearly shows how the northern margin of the Trough collapsed during the sedimentation of the upper

trough infill (cf. Fig. 3-3, situation D) and was broken up by normal faulting over a large area (cf. DIEBOLD et al. 1991).

### **3.2 Northern Switzerland during the Mesozoic and Early Tertiary**

During the Triassic and Jurassic, the continued cooling of the Variscan orogen led to a steady, albeit slow, subsidence in Central Europe. In the region of Northern Switzerland, the continental period which had prevailed since the Late Carboniferous came to an end with the marine Muschelkalk transgression (Wellengebirge, ca. 235 Ma). The uniform nature of these deposits, with only small lateral changes in thickness, is evidence of the minimal relief of the Early Triassic peneplain (cf. Fig. 3-3, situation E). The base of the Mesozoic sediments serves as an important reference horizon which formed a plain well into the Tertiary. Its present deformation state must therefore be attributed largely to Tertiary tectonic activity. The almost uniform, well-stratified series of the Triassic and Jurassic were deposited in an epicontinental sea and indicate relative tectonic inactivity for this period of around 100 Ma. However, around the PCT, small-scale, local increases in thickness, particularly of the Middle Triassic and Early Jurassic, could be explained by decreasing compaction and associated normal faulting of the thick (up to 5 km) trough infills.

Cretaceous deposits are absent throughout Northern Switzerland; they were probably never laid down over the limestones of the Malm (e.g. BÜCHI et al. 1965). This seems to correlate with the fact that, during the Cretaceous and the Early Tertiary (Paleocene), continental conditions with weathering and erosion must have prevailed in large areas of Central Europe. At the same time, a supraregional dome-like structure evolved along the axis of what was later the Upper Rhine Graben (Rhenish Massif) and extended south towards the Alps (TRÜMPY 1980). There must have been considerable erosion in this uplift zone since here Tertiary sediments overlie Mesozoic strata of very different ages (Tertiary subcrop, cf. Fig. 5 in TRÜMPY 1980). This marked hiatus covering a period of around 100 Ma between the Jurassic and the Tertiary is shown clearly in Figure 3-4. Supraregional concepts (e.g. ZIEGLER 1982) and, recently, approaches to modeling sediment maturity i.e. burial history in the Mesozoic strata of Northern Switzerland, provide evidence of a significant erosional hiatus between the Malm and Tertiary deposits (e.g. TODOROV et al. 1993, KÄLIN 1990, HURFORD 1993).

Since the top of the Malm corresponds to a karstified erosional surface, over which the Molasse transgressed with angular unconformity, it is clear that some erosion took place; however, the original thicknesses of sediments is still a point of discussion.

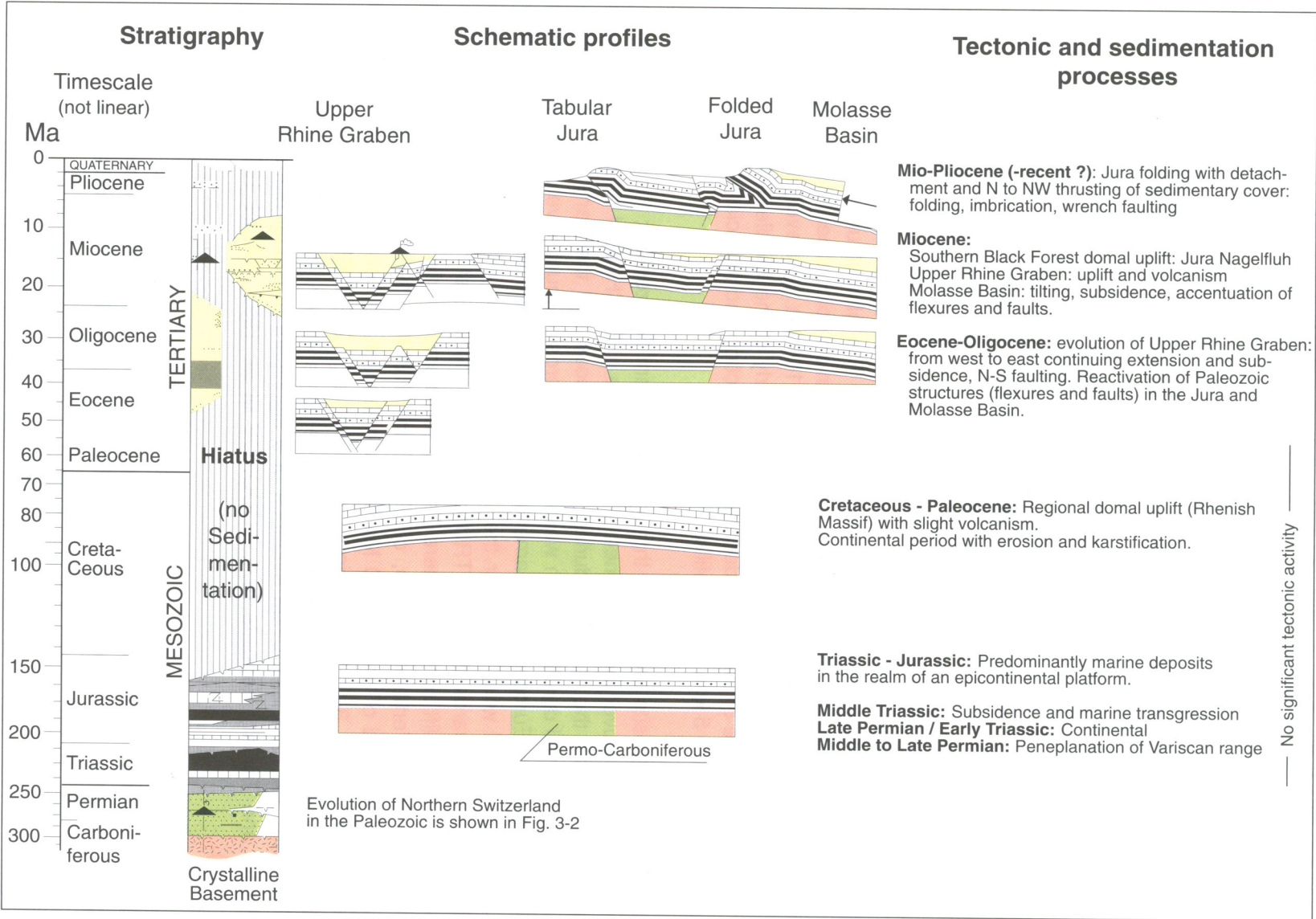


Fig. 3-4: Scheme of the tectonic evolution of Northern Switzerland during the Mesozoic and the Cenozoic (from DIEBOLD 1990).

### 3.3 Tertiary tectonics in Northern Switzerland

The younger geological history of Northern Switzerland is dominated by four regional events whose effects overlap both temporally and spatially in the investigation region:

- the evolution of the Upper Rhine Graben
- the uplift of the Black Forest
- the subsidence of the Molasse Basin
- the folding of the Jura Mountains.

All these events are more or less related to the Alpine orogeny, whose effects extended well into the foreland and are probably still active today. Figure 3-5 shows a synopsis of crustal movements and sedimentation in the area (cf. Fig. 3-6). The events were initially dominated by extensional tectonics, namely subsidence and sedimentation (Oligocene-Early Miocene), but later uplift and large-scale compressional tectonics dominated in the entire region (Middle Miocene-recent; cf. NAEF et al. 1985).

#### 3.3.1 The formation of the Upper Rhine Graben

The Upper Rhine Graben is part of a European rift system which extends from northern Germany to the Mediterranean Sea (for further details cf. section 5.2.1).

The tectonic reactivation of the region began in the Late Eocene with the formation of the Upper Rhine Graben. For the southern section of the Graben between Karlsruhe and Basel, the sedimentary record shows continued subsidence up to the end of the Oligocene (i.e. between 45 and 23 Ma) along predominantly NNE-SSW, i.e. "Rhenish"-trending faults (Fig. 3-5, 3-6; cf. also section 5.2.1).

The Graben infill reaches a thickness of around 2000 meters and consists of marine sediments (Lower Marine Molasse) with evaporites (including potash salt), overlain by Upper Oligocene freshwater deposits. The source of the detrital Graben deposits was mainly Mesozoic sediments of the slightly uplifting Graben shoulders (Black Forest and Vosges).

The center of subsidence in the southern part of the Upper Rhine Graben moved with time from west to east (cf. Fig. 5-1). While the depocenter was located in the Upper Alsace during the Eocene (potash salt basin), subsidence gradually shifted eastwards during the Oligocene. By the end of the Oligocene, the region of the Aargau Tabular Jura (Zeiningen fault zone, Wölflinswil graben, etc.) was probably involved in the Rhenish tectonics (LAUBSCHER 1982, 1987). However in this latter area, corresponding Oligocene deposits are absent.

There is also evidence of Rhenish tectonic activity in the area of the Folded Jura to the south of the Upper Rhine Graben, and in the western Molasse Basin, along Rhenish-striking fault zones (Rauracian depression). Related to Rhenish extensional tectonics are reactivations of peripheral faults along the Permo-Carboniferous Trough.

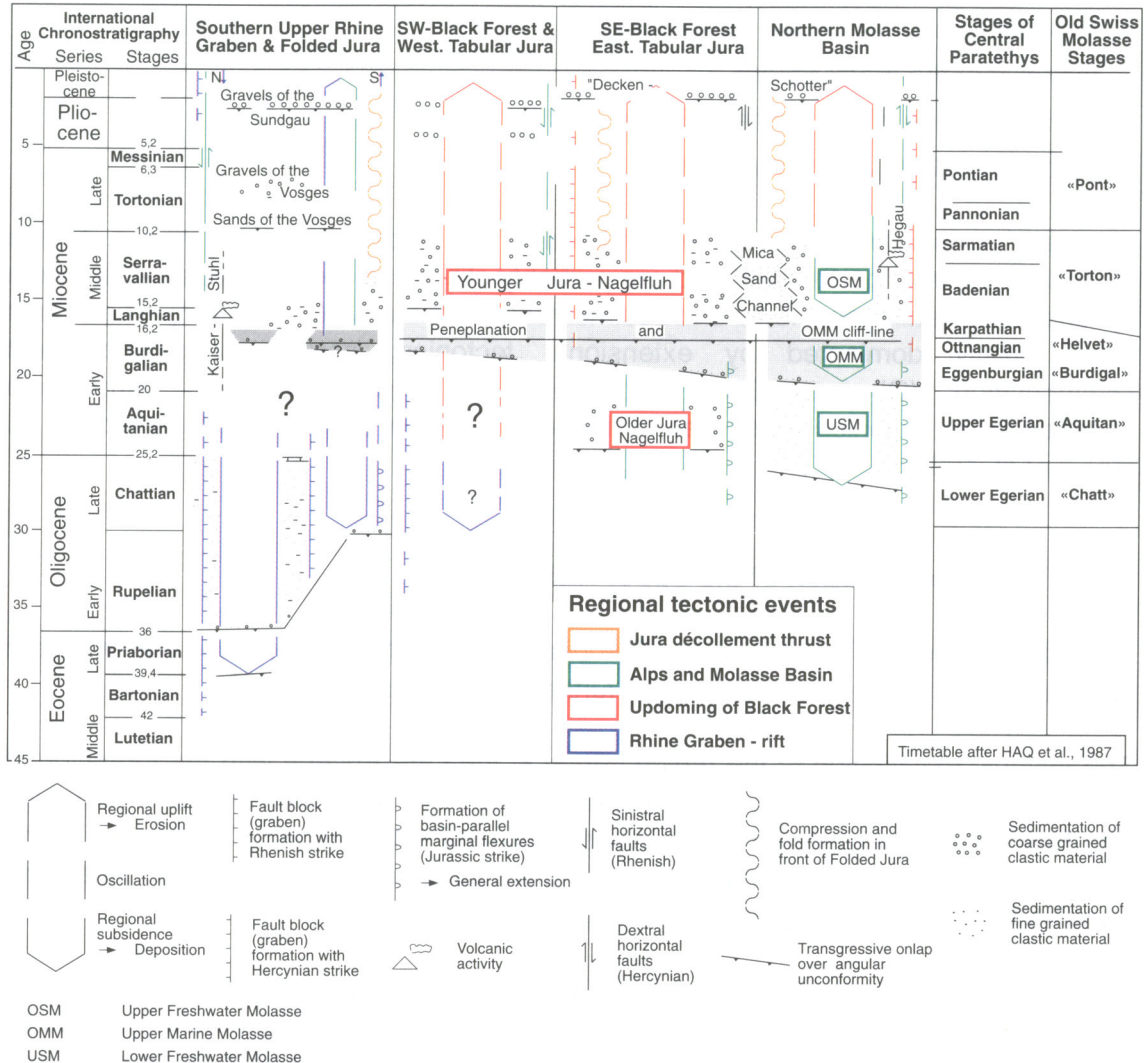


**Fig. 3-5:** Schematic synopsis of sedimentation and crustal movements during the Tertiary. Four temporally and spatially overlapping tectonic events have marked the history of Northern Switzerland since the Late Eocene:

1. The subsidence of the Upper Rhine Graben (blue) in the Eo-Oligocene.
2. The uplift of the Black Forest (red) in 2 phases a) during the Oligocene and b) Miocene-recent.
3. The subsidence of the Alpine foreland (green), at the northern margin of which sediments from the Late Oligocene to the Middle Miocene remain intact.
4. Décollement and uplift of the overburden in the wake of the Alpine thrust (orange).

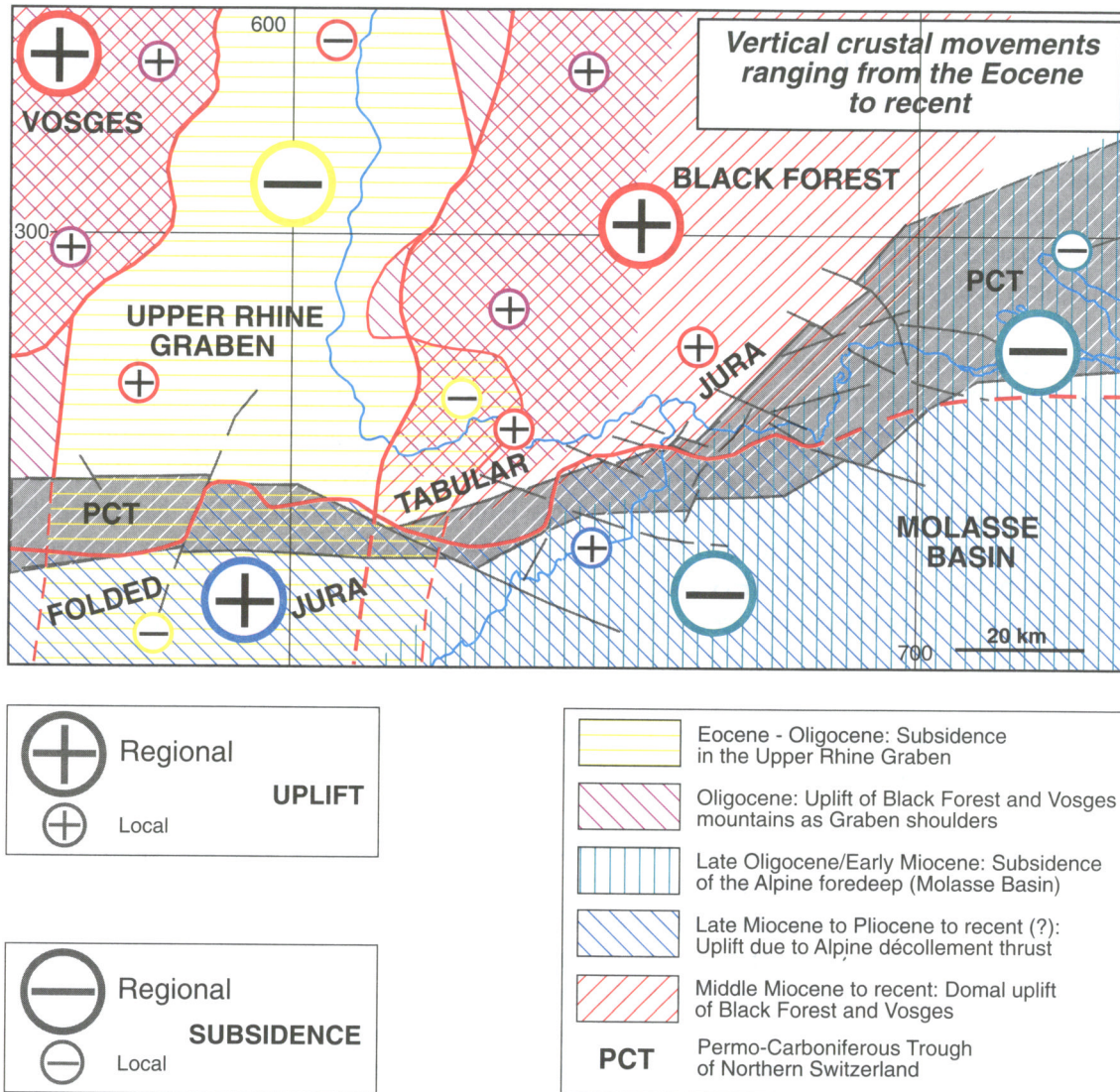


**Fig. 3-6:** Vertical crustal movements in Northern Switzerland: Tertiary and Quaternary.

Results of geological, geomorphological and geodetic-geophysical techniques were used to reconstruct regional vertical movements for various tectonic units. The Permo-Carboniferous Trough of Northern Switzerland (PCT), shaded in gray, separates the northern area with the Black Forest, the Upper Rhine Graben and the Vosges from the Molasse Basin to the south and thus functions as a supraregional structure zone (a suture zone) which determines the orientation of faulting and also the overthrusting of the Folded Jura.

### **3.3.2 Uplift of the Black Forest**

Two uplift phases can be distinguished in the Southern Black Forest. Early and moderate uplifting during the Eo-Oligocene is directly correlated with subsidence of the Upper Rhine Graben (so-called shoulder uplift). The erosional products in the Graben infill show that this uplift phase could only have amounted to a few 100 meters between the Eocene and the Oligocene/Miocene boundary (Older Jura Nagelfluh with almost exclusively Malm gravels). Large-scale uplifting in the Vosges-Black Forest region began in the Middle Miocene and is evidenced in Northern Switzerland by the deposition of the Younger Jura Nagelfluh. This uplifting of the Black Forest resulted in the exposure of large areas of the crystalline basement (cf. Fig. 9-10) and is still continuing today.

During the updoming of the Black Forest, Hercynian-striking lineaments were reactivated. The latter were inherited from the Paleozoic and now form the horst and graben structures of the south-eastern Black Forest, their evolution being documented in the morphogenesis (e.g. SCHMASSMANN in HALDIMANN et al. 1984). Whereas the early uplift phase is directly linked to the Rhine Graben rifting, the Neogene to recent updoming in the Southern Black Forest may be an effect of Alpine tectonics (foreland bulge, cf. LAUBSCHER 1992). The associated extension generated pull-apart structures and possibly reactivated a large part of the pre-existing brittle structures. The faults which were active during the Neogene and can be mapped today in the Schaffhausen Tabular Jura or the Hotzenwald can basically be attributed to the uplift of the Black Forest. This information can also be derived from analysis of Miocene sediments at the northern margin of the Molasse Basin (cf. next section).

Recent apatite fission-track dating (MICHALSKI, 1987) confirms that the uplift of the Black Forest and the Vosges during the Tertiary was not a uniform event. The interpretation of results indicates that the individual blocks uplifted at different rates and also not simultaneously. It shows, for example, that the Southern Black Forest was uplifted later than the Central Black Forest, but with a higher average uplift rate. Differential vertical movements of neighboring blocks could be detected with fission-track dating, indicating displacements of several 100 meters.

### **3.3.3 The subsidence of the Molasse Basin**

A first phase of extensional tectonics at the northern margin of the Molasse Basin is documented for the time of the Lower Freshwater Molasse and is related to rapid subsidence in the center of the Basin (NAEF et al. 1985). General extension in the upper crust led to formation of marked flexures and faults which are oriented primarily along old structural elements in the basement. The reactivation of the marginal zones of the PCT must also be seen in this context; today these represent the most pronounced post-Mesozoic structures in the basement of Northern Switzerland.

Stratigraphic conditions at the northern margin of the Molasse Basin show clearly that depositional edges and facies belts of individual Molasse formations (mainly Lower Freshwater Molasse and Upper Marine Molasse) are oriented along PCT-parallel

flexures. The latter are therefore considered as external boundary flexures of the Molasse Basin and are an expression of active extensional tectonics during the Oligo-Miocene subsidence. The PCT played the role of a hinge zone between the meso-European foreland and the mobilized Alpine foreland (Molasse Basin).

The regional uplift of the Black Forest already mentioned above is simultaneous with the later phases of subsidence of the Alpine foreland since the Middle Miocene (Upper Freshwater Molasse). This led primarily to a regional tilting of the whole area of central Northern Switzerland by 4 - 5° to the SE and to renewed reactivation of basement structures as faults (examples: Vorwald and Eggberg fault zones, Bonndorf graben, Randen fault zone, etc.). The Hegau volcanism (14-7 Ma, App. 3-1) also was active during this phase of extensional tectonics.

The temporal and regional interference of uplift in the Black Forest and subsidence in the Molasse Basin makes it difficult to trace back the Miocene structures of Northern Switzerland clearly to one or other of these events (cf. Fig. 3-5 & 3-6).

### **3.3.4 Alpine décollement thrust and formation of the Folded Jura**

In the Late Miocene, the basement of Northern Switzerland was covered by a stack of Mesozoic, and partly also by Molasse, deposits; this stack dipped moderately to the SE-SSE and was affected by a network of faults and flexures. In the western part of Central Northern Switzerland, a dense set of Rhenish-striking (NNE-SSW) faults is superimposed on the reactivated "Hercynian" (WNW-ESE) and "Variscan" or "Jurassic" (SW-NE) striking systems. While this stack of sediments remained largely intact in the northern and eastern Tabular Jura (E in Fig. 3-1b), the south-western area was affected by the Jura folding and underwent intensive deformation (F in Fig. 3-1b).

As a result of late Alpine movements, the sedimentary cover of the northern Alpine foreland (Molasse Basin and Jura) was detached along the evaporites of the Middle Triassic and transported northwards over the largely passive basement. The northern front of this décollement mass is imbricated and folded in the region of the Folded Jura and thrust over the (autochthonous) Tabular Jura. The décollement thrust (distant push) hypothesis (BUXTORF 1916) has largely been confirmed by results from the Nagra boreholes (Schafisheim: MATTER et al. 1988b, JORDAN & NÜESCH 1989) and from reflection seismic surveys in the eastern Jura and adjacent Plateau Molasse (DIEBOLD et al. 1991, SPRECHER & MÜLLER 1986).

As indicated above, the sediments which had been faulted by Oligocene-Miocene extensional tectonics were subsequently involved in the Jura folding (cf. Fig. 3-3, situation F). During the Jura folding these faults acted as weak zones and determined the location and geometry of folds and overthrusts in the dislocated cover (LAUBSCHER 1965, 1986; SPRECHER & MÜLLER 1986; MÜLLER et al. 1984); this is clearly reflected by the tectonic sketch map of the eastern end of the Folded Jura (cf. Fig. 5-3).

The basement and the Lower Triassic (tegument) behaved passively during the Jura folding. Nevertheless, it must be assumed on the basis of results from neotectonic investigations (stress measurements: BECKER et al. 1984, MÜLLER et al. 1987; earthquakes: PAVONI 1984, 1987, DEICHMANN 1987, 1990) that the basement has been continuously subjected to tectonic processes up to the present day (cf. Chapter 9).

Since the Early Miocene, the maximum horizontal principal stress in the crust of the Alpine foreland appears to have been directed along a NW-SE axis. It is probable that, in addition to normal faulting, there were also horizontal lateral movements in the basement. In the prevailing stress field, the Rhenish- and Hercynian-striking faults in the basement provided locations for sinistral and dextral wrench faulting. This concept has also been postulated in numerous publications (e.g. ILLIES & GREINER 1976, HEGELE 1984, PAVONI 1987) and is confirmed by fault plane solutions, e.g. Fig. 9-6 for earthquakes in Northern Switzerland.

It is safe to assume that the tectonic processes in the basement proceed slowly (cf. NAEF et al. 1985, MICHALSKI 1987); therefore, they appear to be relatively insignificant compared to the movements of the décollement thrust (distant push), with horizontal dislocations of several 100 m per 1 Ma.

### **3.4 Young to recent movements**

Recent crustal movements are the expression of ongoing active tectonics apparent either in short-term events (e.g. earthquakes) or more or less continuous processes (creep). The dynamic processes in the earth's interior take place over geological timescales; the relevant phenomena thus began some time in the recent past and will also be important for the near future. When analyzing such movements, it is therefore appropriate to consider "neotectonics" over a time period of several Ma.

Neotectonic investigations consider both geological-geomorphological data with a large time horizon as well as geodetic-geophysical measurements with a time span of 100 a at the most. The relationships and problems are discussed in more detail in Chapter 9.

Appendix 9-1 also gives an overview of observed young to recent movements. The geodetic (precision levelling) and seismotectonic databases, in particular the analysis of earthquake swarms and the numerous geomorphological indications of recent movements, are important. With current knowledge of regional geology, and after careful weighting of the evidence available, the following key statements can be made:

- Since the Miocene, the Southern Black Forest has been in a continuing state of uplift and erosion, which has led in the SE to tilting and steepening of the relief. This updoming of the Southern Black Forest will probably continue in the future, accompanied by slight extensional and shearing tectonic activity.

- A NW-SE-oriented stress field prevails in the basement of Northern Switzerland and is accompanied by slight seismic activity. Deviatoric stress conditions can be observed in the overburden; together with information from leveling and geomorphology, this provides strong evidence for the argument that the décollement of the Alpine foreland and the Jura folding are still continuing today (e.g. BECKER et al. 1987).

## **3.5 Present-day geothermal conditions**

### **3.5.1 Introduction**

The rock temperatures in the vicinity of a potential repository represent important boundary conditions for the construction and operation of the facility and are also relevant when considering the long-term evolution of safety-relevant chemical and physical processes.

The increase in temperature with depth (the "geothermal gradient") is determined firstly by the large-scale geology and petrophysical properties of the rocks, for example radiogenic heat production or thermal conductivity. Secondly convective heat transport (via fluid phases) also plays an important role. This parameter depends in the first instance on the permeability of the rocks and is caused primarily by thermally driven circulation of deep groundwaters in the uppermost kilometers of the crust.

In areas where groundwater circulation is maintained by marked hydraulic gradients, there is also advective heat transport.

When developing a geothermal model, it must therefore be assumed that the large-scale heat distribution, which is determined primarily by conductive transport and originates from greater depths, is overlain by a small-scale thermal field which is defined by local hydrodynamic conditions.

Temperature data from deep boreholes allow the spatial temperature field to be mapped and geothermal gradients to be derived over specified depth intervals. The average increase in temperature per depth interval is shown on isopleth maps (in K/km). However, before the measured data can be interpreted, it is necessary to take into account the thermal rock parameters. This allows heat flux maps (in mW/m<sup>2</sup>) to be drawn up as a product of temperature gradient (in K/km) and thermal conductivity (in W/mK) in the rock sequences.

### **3.5.2 The temperature field in Northern Switzerland**

RYBACH et al. (1987) have evaluated temperature data from 55 boreholes. They have shown that the vertical temperature gradient itself is depth-dependent; it therefore appeared appropriate to derive the geothermal gradients over two different depth intervals (cf. also VOLLMAYR 1983, STIEFEL & WILHELM 1989). Figure 9-7 shows

the lateral variation in the geothermal gradient in the depth interval 750 - 1500 m after RYBACH et al. (1987). The dataset does not allow direct reconstruction of isotherms for greater depths and recourse has to be made to extrapolation based on plausible models (cf. e.g. GRIESSER 1989).

SCHÄRLI (1989) has recently reprocessed the geothermal data for Northern Switzerland and has prepared a detailed heat flux map using petrophysical parameters. The data from the Nagra boreholes provided the framework for this study.

While the interpretation of RYBACH et al. (1987) shows the known geothermal anomaly of Central Northern Switzerland as a single maximum in the region north of Brugg (Riniken borehole), i.e. above the central Permo-Carboniferous Trough, the heat flux map of SCHÄRLI (1989) shows that this anomaly is made up of two maxima (Fig. 3-7). One maximum is located to the north of the PCT (Kaisten, Leuggern, Böttstein [ $160 \text{ mW/m}^2$ ], Zurzach boreholes) and a second maximum is concentrated in the region Baden-Brugg [ $170 \text{ mW/m}^2$ ], i.e. more or less above the southern margin of the PCT, coinciding here with the main overthrust of the Folded Jura.

The boreholes located within the Trough between these two maxima have clearly lower heat flux values (Riniken [ $110 \text{ mW/m}^2$ ], Beznau, Weiach, Eglisau).

Fig. 3-7 indicates the extent and magnitude of the heat flow anomaly of Northern Switzerland as compared to the Molasse Basin where heat flow values  $\leq 100 \text{ mW/m}^2$  are the rule (GORHAN & GRIESSER 1988).

### 3.5.3 Interpretation

An investigation of the geothermal conditions in Northern Switzerland has shown that the locally observed thermal anomalies can only be explained satisfactorily with the assumption of marked convective heat fluxes in the form of upwelling deep groundwaters. Based on knowledge of the regional geology, a two-dimensional model was developed characterized by the parameters permeability, porosity, heat production, thermal conductivity and hydraulic gradients. Previous calculations assumed that the upwelling deep groundwaters at the northern margin of the PCT, which are responsible here for the positive thermal anomaly, come exclusively from great depths below the PCT (RYBACH et al. 1987). However, GRIESSER (1989) conjectured that inflowing waters from the north, i.e. from an infiltration zone in the Southern Black Forest, also penetrate as far as the northern margin of the PCT (Fig. 9-7). Here they well up together with the deep waters in highly permeable zones within the crystalline basement. The exfiltration zone for these waters is then the region of the Rhine valley. A similar circulation model was proposed by KANZ (1987) on the basis of hydrochemical results and has since been confirmed by numerous data (e.g. PEARSON et al. 1991, TODOROV et al. 1993).

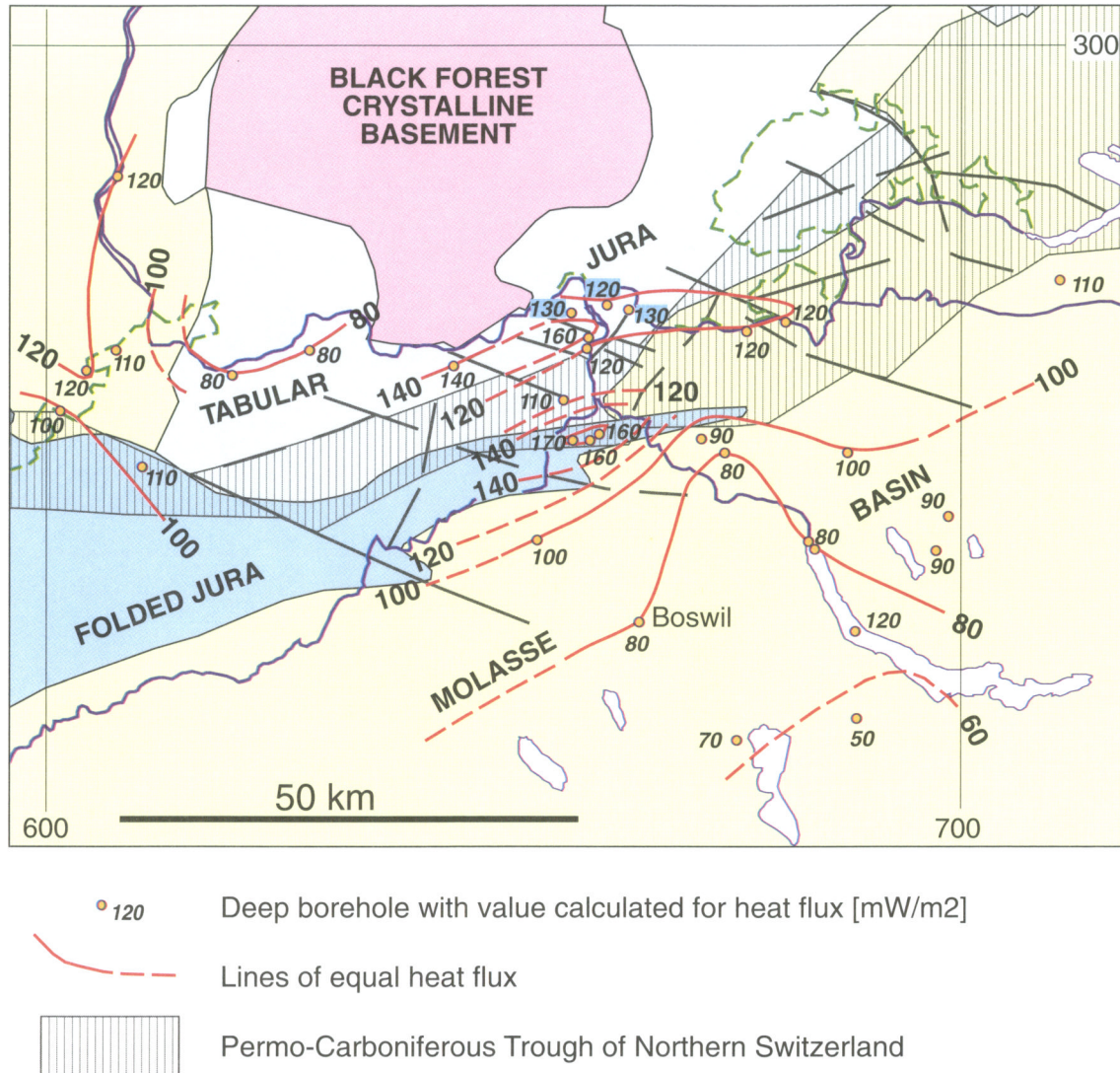


**Fig. 3-7:** The heat flux in Northern Switzerland.

The heat flux (in  $\text{mW/m}^2$ ) is calculated as a product of temperature gradient (in  $\text{K/m}$ ) and thermal conductivity (in  $\text{W/mK}$ ) from the data measured in the deep boreholes. The values are also corrected for the temperature-dependence of heat conduction and the influence on the geothermal temperature field by the Quaternary ice ages. The enhanced heat flux in the strike of the Permo-Carboniferous Trough can be seen clearly, the highest values being concentrated mainly at the southern and northern marginal zones of the Trough (after SCHÄRLI 1989).



## 4 GEOLOGICAL EVOLUTION AND PETROGENESIS OF THE CRYSTALLINE BASEMENT

### 4.1 The pre-Alpine basement of Central Europe

The Black Forest and its southern subsurface continuation in Northern Switzerland are part of the pre-Alpine basement of Central Europe. KOSSMAT (1927) introduced the classical subdivision of Variscan<sup>1)</sup> Europe into three tectonic units:

1. Rhenohercynian belt (e.g. Harz, Rheinisches Schiefergebirge; external, northernmost unit)
2. Saxothuringian belt (e.g. Odenwald-Spessart, northern parts of the Vosges, parts of the Bohemian Massif)
3. Moldanubian belt (e.g. Black Forest, southern parts of the Vosges, southern parts of the Bohemian Massif).

All three tectonic units of Variscan Europe comprise abundant granitoid intrusions documenting crustal thickening and melting during the orogenic events. Overviews of Variscan tectonics are given by BEHR et al. (1984) and KROHE & EISBACHER (1988).

As illustrated in Figure 3-2, the Variscan orogeny is a consequence of a continent-continent collision between Gondwana (specifically Africa) and Laurasia (i.e. Eurasia/North America). Due to the generally very poor outcrop conditions, a geodynamic reconstruction of the European Hercynides (i.e. the Variscan mountain chain) is still disputed. The number and vergence (direction) of subduction zones are not unequivocally established. In contrast to the Alpine orogeny, Variscan ophiolites as markers of oceanic suture zones are lacking. HOLDER & LEVERIDGE (1986) suggest a complex pattern of multiple subduction zones separating the Rhenohercynian, Saxothuringian and Moldanubian belts.

The area investigated here (i.e. the Black Forest and the basement of Northern Switzerland) is part of the Moldanubian belt, which is interpreted as the internal zone of the Hercynides. This belt consists of high-grade gneisses that were intruded by Variscan plutons, mainly granites. The southern parts of the Moldanubian belt, now situated in the Alps, have been overprinted by the Alpine orogeny. Pre-Alpine high-grade gneisses and Variscan intrusives are abundant in the external massifs of the Alps (Aar Massif, Aiguilles Rouges Massif, cf. ABRECHT 1980, SCHALTEGGER 1986, VON RAUMER 1983).

---

1) The terms "Hercynian" and "Variscan" are synonymous and refer to an orogenic event that affected parts of Europe, Asia and North America. Tectonic, metamorphic and magmatic activity extended over a very long period of time, most of the events taking place in the interval 340-280 Ma b.p.

## 4.2 Pre-Variscan and Variscan geology of the Black Forest

This Chapter describes the petrogenesis of the Black Forest basement and ends with the last Variscan magmatic activity. Because the basement of Northern Switzerland is the nearby subsurface continuation of the Southern Black Forest, the regional evolution presented here is presumed to be analogous in both areas, so that evidence from the well-studied Black Forest can be transferred to Northern Switzerland. As far as they are known and comparable, the geological datasets from both regions are fully consistent.

The rocks have been extensively studied by petrographers and petrologists, whereas the study of structural and tectonic aspects is impeded by the modest relief and poor outcrop conditions. Most of the information presented stems from roadcuts and quarries.

### 4.2.1 Large-scale subdivision

Five petrographic-structural sub-units are defined in the Black Forest (KTB 1986, cf. Fig. 4-1):

1. *Zone of Baden-Baden (BBZ)*: The northernmost tip of the Black Forest is occupied by Early Paleozoic, weakly metamorphosed sediments and minor I-type granites<sup>1)</sup>. The Zone of Baden-Baden is correlated with an analogous structure in the Northern Vosges Mountains (zone of Lalaye-Lubine, cf. KTB 1986) and is interpreted as belonging to the Saxothuringian belt. Following the interpretation of HOLDER & LEVERIDGE (1986), a major crustal suture (Variscan subduction zone) separates this sedimentary sequence from the Moldanubian to the south.
2. *Granite zone of the Northern Black Forest (NGC)*: This area is dominated by granites of Early to Late Carboniferous ages.
3. *Gneisses of the Central Black Forest (CGC)*: This gneiss mass is the largest unit in the Black Forest and covers about 3000 km<sup>2</sup>. The gneisses comprise both high-grade para- and orthogneisses (MÜLLER 1989), some of which have been subjected to partial melting (anatexis) during metamorphism. The Triberg granite (Late Carboniferous) is the only large intrusive body of this zone.
4. *The Zone of Badenweiler-Lenzkirch (BLZ)* is an E-W-trending structure separating the gneisses of the Central Black Forest from the granites and gneisses of the Southern Black Forest. This structure dips about 40° to the north and is identified in seismic profiles to depths of at least 10 km (EISBACHER & KROHE 1985) and

---

1) Based on mineralogical and geochemical evidence, several types of granites can be distinguished. I-type ("igneous") granites are differentiated melts derived from the deep crust and the mantle and are typically related to subduction zones.

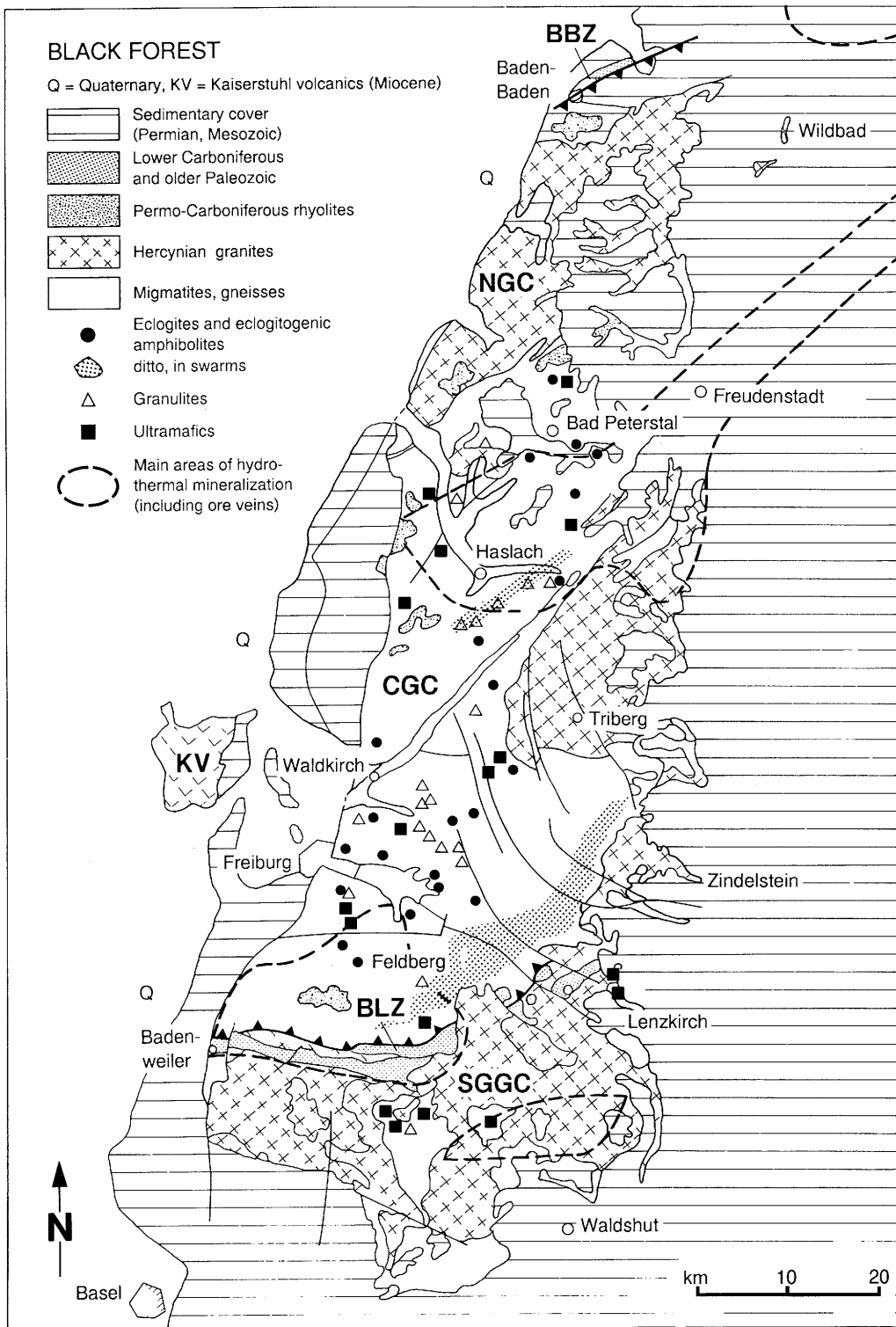


**Fig. 4-1 :** Tectonic map of the Black Forest. Regions with abundant ore vein mineralizations are also indicated. BBZ = Baden-Baden Zone, NGC = Granite Complex of the Northern Black Forest, CGC = Central Gneiss Complex, BLZ = Badenweiler-Lenzkirch Zone, SGGC = Gneiss and Granite Complex of the Southern Black Forest. KV = Kaisterstuhl volcanics (Rhine Graben), Q = Quaternary.

consists of low-grade metamorphic, Early Paleozoic sediments. It represents a major compressive structure within the Moldanubian belt.

5. *Gneisses and granites of the Southern Black Forest (SGGC)*: The petrographic and geochemical characteristics of the gneiss series in the Southern Black Forest are different from those of the Central Black Forest gneiss mass (KTB 1986). Paragneisses, often migmatitic and of metapelitic composition, dominate over orthogneisses and can be correlated with gneisses drilled in the Kaisten and Leuggern boreholes (MAZUREK 1992). Granites are invariably S-type<sup>1)</sup> and have Carboniferous ages. They are subdivided into two groups, the older of which is slightly deformed and schistose.

#### 4.2.2 Geological evolution of pre-Variscan gneisses

The present paragneisses are the polymetamorphic equivalents of clastic sediments. Deposition of these sediments took place in the Proterozoic (about 700 - 900 Ma b.p. estimated from Sr isotope data by HOFMANN & KÖHLER 1973).

##### Eclogite-facies metamorphic stage

Numerous basic lenses have been found in the gneisses and migmatites of the Central Black Forest (KLEIN & WIMMENAUER 1984). These basic rocks, interpreted as relics of basaltic dykes cross-cutting the gneisses, show clear evidence of high-pressure (eclogitic) metamorphism. In recent years, relic high-pressure mineralogies have also been identified in intermediate and acidic rocks (gneisses) embedding the eclogites/amphibolites (WIMMENAUER & STENGER 1989). Even though much of the evidence for a high-pressure metamorphism is overprinted by the younger high-temperature/low-pressure stage (migmatization, see below), it appears that not only the basic intercalations but also large parts of the surrounding gneisses have experienced subduction to depths of up to 50 km. Pressure estimates indicate eclogitic conditions of > 12 - 15 kbar at temperatures > 600 °C (WIMMENAUER & STENGER 1989, STENGER et al. 1989). Whereas eclogites are common in the Central Black Forest, no occurrences are known in the gneisses of the Southern Black Forest.

##### Granulite-facies metamorphic stage

In addition to an eclogite-facies metamorphism, a younger granulite-facies (high-temperature/medium-pressure) stage is documented mainly in high-temperature ductile shear zones. Based on mineral equilibria, temperatures of 650 - 750 °C at pressures of 7 - 10 kbar have been derived (STENGER et al. 1989). There is an evolutionary trend from the eclogites to the granulites, corresponding to a pressure relaxation.

---

1) S-type ("sedimentary") granites are generated by crustal melting of sedimentary rocks, a process that typically takes place in a late orogenic, overthickened continental crust.

equivalent stratigraphic age	age [Ma]	event
Late Carboniferous	290 - 310	Extrusion of rhyolitic sheets.
Early/Late Carboniferous	310 - 330	Melt generation in the overthickened continental crust and intrusion of younger granites (undeformed) and dykes.
Early Carboniferous	330 - 340	Retrograde metamorphism of the gneiss series, cooling below 300 °C; imbrication of the Zones of Baden-Baden and Badenweiler-Lenzkirch; major uplift of the Central Gneiss Complex; regional deformation.
Early Carboniferous	? - 340	Amphibolite-grade metamorphism, deformation and migmatization of the gneiss series. Ages and relation to the older granites poorly constrained.
Early Carboniferous	360 - 340	Intrusion of older granites (deformed).
		Granulite-grade metamorphism of the gneiss series.
Devonian	400	Eclogite-grade metamorphism of the gneiss series.
Ordovician	480 - 490	High-temperature isotopic homogenization (no further characterization possible).
Cambrian	520	Intrusion of granitoids (present today as orthogneisses within the gneiss series).
Late Proterozoic	700 - 900	Deposition of clastic sediments (protoliths of the paragneisses).

**Tab. 4-1 :** Metamorphic, magmatic and tectonic history of the Black Forest. Note that equivalent stratigraphic ages are mostly derived from radiometric dating rather than from stratigraphic evidence.

Eclogites and granulites are not distributed evenly over the gneiss mass of the Central Black Forest and are absent in large areas. STENGER et al. (1989) suggest that the Central Black Forest might be conceived as an accretionary nappe system in which rock bodies from very different tectonic positions (namely subducted and obducted sheets) have been juxtaposed. Such a hypothesis is difficult to prove unequivocally because much of the structural evidence was completely obliterated during the subsequent low-pressure, high-temperature metamorphism and migmatization that affected all rocks of the Black Forest basement.

### **Amphibolite-facies metamorphic stage and migmatization**

In contrast to the eclogite and granulite metamorphic stages, a low-pressure/high-temperature (amphibolite-grade) metamorphic event is present in all regions of the Black Forest and Northern Switzerland. This event left a very strong imprint in the rocks, and it partially obliterates the older metamorphic stages. MAZUREK (1992) distinguishes two successive metamorphic stages:

1. Pervasive ductile deformation and sub-solidus amphibolite-grade metamorphism at 550 - 650 °C/4.5 - 6.5 kbar.
2. Anatectic migmatization at > 650 °C/< 4.5 kbar, postdating ductile deformation.

Migmatization led to partial melting of the gneisses and to the segregation of leucosomes (melt pockets), giving the rocks a very inhomogeneous aspect on the scale of meters. Metapelitic rocks are more strongly affected by migmatization than meta-graywackes and orthogneisses. In the Southern Black Forest and in Northern Switzerland, no evidence exists of the older stages of metamorphism (eclogites, granulites). It is unknown whether the rocks in fact did not experience the older stages or whether all evidence has been completely obliterated by the pervasive migmatization.

### **Retrograde greenschist-facies metamorphic stage**

This stage represents the retrograde path (cooling and uplift) after the peak of amphibolite-grade metamorphism and migmatization. The stage is characterized by an extensive hydration of the high-grade parageneses, which mainly leads to the formation of abundant micas (MAZUREK 1992). Conditions are estimated at < 600 °C / < 2.5 kbar.

### **Age determinations and P-T-t evolution of the gneiss series**

Based on petrographic evidence, the pressure-temperature-time evolution of the gneisses described above is represented as stages of one single P-T loop rather than several polymetamorphic events (Fig. 4-2). Additional evidence is gained from radiometric age determinations, as described below.

#### *High-temperature isotopic homogenization:*

This phase of evolution is documented exclusively by isotopic data (isotope systems with very high closure temperatures); all petrographic evidence has been completely obliterated by younger events.

In a U/Pb study of zircon, STEIGER et al. (1973) obtained an upper intersection with Concordia<sup>1)</sup> at 480 Ma. HOFMANN & KÖHLER (1973) report Rb/Sr whole-rock isochrons yielding 490 Ma. Similar dates (460 - 490 Ma) have been obtained by WERCHAU et al. (1989a) using the U/Pb method on zircon (upper intersection with Concordia). The data show that zircon growth and a large-scale homogenization of the Rb/Sr system took place 480 - 490 Ma before present, which indicates a major high-temperature metamorphic and/or magmatic event. Until recently, this event has been correlated with the regional "Caledonian" migmatization in the Black Forest, as described above. However, some recently published age determinations (discussed below) suggest that migmatization as evident in the entire Black Forest might be much younger (cf. KROHE & EISBACHER 1988). Therefore, it appears that the 480 - 490 Ma phase of metamorphism and magmatism has no petrographic expression in the rocks and has been completely overprinted by the younger phases.

*Eclogite-facies metamorphic stage:*

SCHLEICHER & KRAMM (1986) obtained discordant U/Pb data for zircons from eclogites. They interpret the lower intercept with Concordia at 410 Ma as the age of the eclogite-grade metamorphism. Concordant U/Pb ages of zircons and Rb/Sr small-scale isochrons from the eclogites (WERCHAU et al. 1989a) yield ages around 390 Ma, which is again interpreted as the age of high-pressure metamorphism. Field evidence indicates that high-pressure metamorphism predates regional migmatization, whose age should consequently be < 390 - 410 Ma (see below).

*Granulite-facies metamorphic stage:*

No radiometric age determinations are available for this stage.

*Amphibolite-facies metamorphic stage and migmatization:*

WERCHAU et al. (1989b) obtained concordant U/Pb ages on monazites from granite and high-grade gneiss samples from the whole Black Forest. All ages are in the interval 325 - 335 Ma, irrespective of rock type (granite - gneiss) and sample locality. These dates are interpreted as monazite crystallization ages related to migmatization of the gneisses and coeval intrusion of Variscan granites. Unfortunately, the samples and analytical results are not adequately documented, which precludes conclusive interpretation. Overall, the age of the migmatization is still poorly constrained.

---

1) The U/Pb method of absolute age dating yields two independent ages, based on the decay of <sup>238</sup>U to <sup>206</sup>Pb and of <sup>235</sup>U to <sup>207</sup>Pb. If these ages are identical, they lie on a curve called the *Concordia* in a <sup>206</sup>Pb/<sup>238</sup>U vs <sup>207</sup>Pb/<sup>235</sup>U diagram. If the two ages are not identical, they are called discordant and are geologically meaningless because the U/Pb system was disturbed by rock/fluid interactions (e.g. Pb loss from a zircon). Discordant data points often form arrays that plot on a straight line (called the *Discordia*) in the above-mentioned diagram. Intersections between Concordia and Discordia may date geological events, while in other cases they are meaningless.

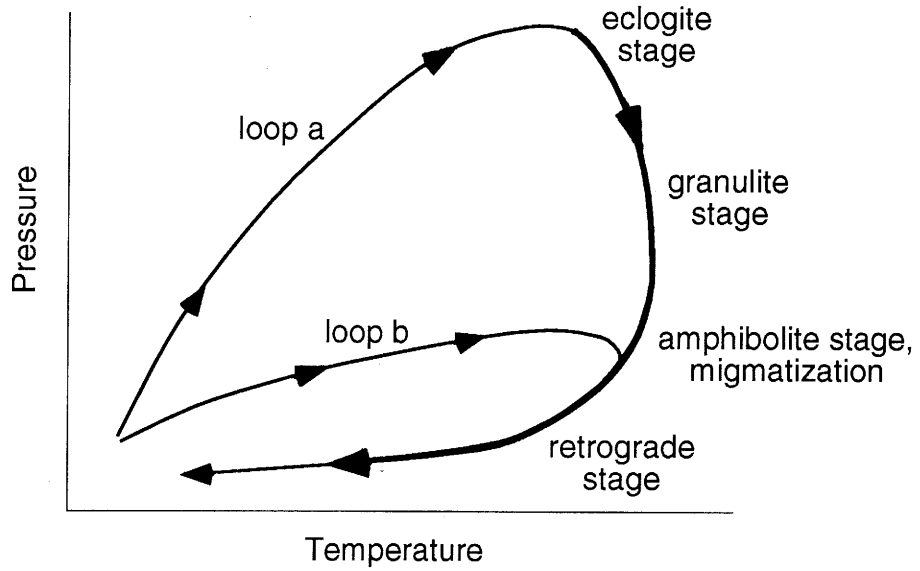
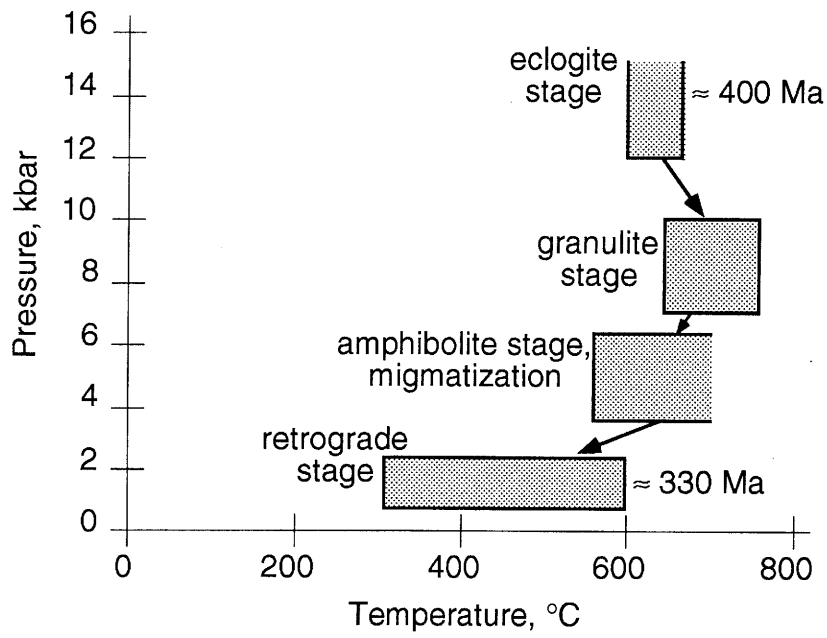


**Fig. 4-2 :** Pressure - Temperature - time (P-T-t) path of the crystalline rocks of the Black Forest. Adapted from STENGER et al. (1989). See text for explanation.

*Retrograde greenschist-facies metamorphic stage (uplift, cooling):*

HRADETZKY et al. (1989) applied the  $^{39}\text{Ar}/^{40}\text{Ar}$  step-degassing technique to amphiboles in basic rocks from the Central and Southern Black Forest. Most ages obtained scattered between 320 and 350 Ma and document the last cooling of the rocks below the closing temperature of amphibole for the K/Ar system (about 500 - 700 °C, depending on grain size; cf. FAURE 1986). Isotope systems with low blocking temperatures around 300 - 350 °C (i.e. Rb/Sr and K/Ar in biotite and K/Ar in muscovite) yield ages of 325 - 330 Ma, which are only slightly less than the age of migmatization. KROHE & EISBACHER (1988) suggest that these dates reflect a rapid differential uplift of the Central Black Forest which was accommodated by major shear zones such as the Badenweiler-Lenzkirch Zone.

## Discussion

Even though more data are needed to establish the geochronology of the Black Forest gneisses, recent evidence suggests that all basement rocks were formed or completely recrystallized during the course of the Variscan orogeny. Some zircon dates reflect older, possibly Caledonian events but are difficult to interpret. A Variscan origin of the migmatites is also consistent with tectonic and petrological considerations. The Variscan continent-continent collision resulted in an overthickened continental crust, which led to partial melting and migmatite formation. Part of the melt products segregated to large magmatic bodies and are present today as Variscan granites. This interpretation is consistent with geochemical evidence, which suggests that all granites from the Moldanubian part of the Black Forest are S-types (MAZUREK & PETERS 1992, definitions cf. section 4.2.1).

A serious point of debate is still the age of migmatization. The monazite dates (cf. above) suggest that migmatization only slightly predates retrograde metamorphism, cooling and rapid uplift of the gneisses. A fast metamorphic evolution has also been suggested by MAZUREK (1992), based on chemical and isotopic disequilibria identified between mineral generations grown during the prograde, migmatitic and retrograde stages of metamorphism. If migmatization really occurred at ~340 Ma before present, it must be younger than the intrusion of the older Variscan granites (intruded 340 - 360 Ma before present, see below). However, no evidence of migmatitic overprint has been reported from these granites to date. More data are needed to establish an estimate for the age of migmatization.

Based on petrological and geochronological evidence, a P-T-t loop can be constructed for all stages of metamorphism discussed above and is presented in Figure 4-2 (loop a). Because the eclogite and granulite stages are known only from certain areas of the Central Black Forest, other regions of the Black Forest may have experienced only the small loop b shown in Figure 4-2. It is emphasized that while the relative ages of the metamorphic stages are well-known, more geochronological work is needed to establish a consistent absolute timescale.

### 4.2.3 Evolution of magmatic activity

#### Pre-Variscan granites

The oldest plutonic rocks are granitoids, known today as orthogneisses within the gneiss series of the Central Black Forest. Their age of intrusion has been dated at 520 Ma by TODT & BÜSCH (1981) (U/Pb on zircon, lower intersection with Concordia). These rocks are overprinted by the low-pressure migmatization.

#### Older Variscan granites

The distinction between older and younger granites in the Black Forest is based on the state of deformation. A major regional deformation affected the older granites (e.g. Klemmbach-Schlächtenhaus and Hauenstein granites) some 330 - 340 Ma before present (Sudetic phase of Variscan deformation, cf. Fig. 3-2), whereas all younger intrusives are post-deformational. The older granites were deformed under greenschist-grade conditions (MAZUREK & PETERS 1992) and seem to be spatially related to major crustal shear zones, such as the Badenweiler-Lenzkirch zone (MAASS 1983). Some of the older granites have been dated (summary in STENGER 1983), yielding ages of 340 - 360 Ma.

#### Younger Variscan granites

The most significant magmatic activity in the Black Forest is represented by the intrusion of the younger Variscan granites, which occupy a large part of the total outcrop area (Fig. 4-1, Tab. 4-2). The granites intruded in a complex, multiphase process (EMMERMANN 1977). The peak of Variscan magmatic activity occurred 310 - 330 Ma before present, i.e. it slightly postdates the cooling ages and the uplift of the Central Black Forest gneisses. LAUBSCHER (1986) suggests that the intrusion of voluminous granites was triggered by right-lateral crustal shear movements that are evident in the Armorican Massif (Brittany, France).

The systematics of Variscan magmatism in the Southern Black Forest and in the basement of Northern Switzerland were investigated by MAZUREK & PETERS (1992). All granites in the Moldanubian Black Forest are S-types, i.e. they originate from crustal melting of sedimentary rocks (cf. section 4.2.1). Metapelitic gneisses and migmatites of the Black Forest are possible source rocks for the granitic melts.

EMMERMANN (1977) distinguished three granite suites in the Black Forest (SW Black Forest, SE Black Forest, N Black Forest; cf. Tab. 4-2). Granites within each suite are related by continuous compositional and evolutionary trends. Progressively deeper magma sources have been deduced in the evolution of each suite.

#### Late Variscan dykes

The intrusion of dykes in the final stages of the orogeny is well-documented throughout Variscan Europe and is interpreted as a consequence of gravity-induced collapse of the overthickened orogen (cf. Chapter 5 and DEWEY 1988, LORENZ & NICHOLLS 1984). Dykes in the Black Forest comprise granite and rhyolite porphyries, lamprophyres, aplites and pegmatites. Judging from cross-cutting relationships, lamprophyres generally are the youngest intrusive rocks (MÜLLER 1984).



describes intrusive rhyolitic dykes that he interprets as feeder dykes of the extrusive sheets. The rhyolites mark the final point in the magmatic evolution of the Black Forest. Volcanism seems to postdate the youngest granites by about 20 Ma in the whole Black Forest. Both granites and volcanites are progressively younger from south to north. Analogous volcanic rocks of Permian age are also known from the Alps (OBERHÄNSLI et al. 1988).

Based on geochemical data, SCHLEICHER (1978) argues against the interpretation that granite porphyry dykes as described above represent feeder conduits for extrusive rhyolitic sheets and suggests separate magmatic events. This interpretation is also corroborated by field evidence: Ore veins cross-cut granite porphyry dykes but do not affect the overlying volcanic rocks, which are therefore younger (HOENES 1937).

#### **4.2.4 Tectonics of Paleozoic sediment zones**

Early Paleozoic clastic sediments and volcanics with varying degrees of metamorphism occur in two NE-SW-trending, narrow structures (Zones of Baden-Baden and Badenweiler-Lenzkirch; cf. Fig. 4-1). Both of these zones are regarded as major crustal sutures (e.g. KROHE & EISBACHER 1988, WICKERT et al. 1990). Age determinations are difficult due to the scarcity of fossils and partly have to rely on analogies with similar formations in the Vosges Mountains. The Baden-Baden zone generally is correlated with the zone of Lalaye-Lubine in the Vosges, where it is interpreted as the boundary between the Saxothuringian and Moldanubian belts.

The Badenweiler-Lenzkirch Zone trends E-W and crops out over about 40 km; it is only ca. 3 km wide and dips to the north. Its subsurface continuation is observed to depths of 10 - 12 km in seismic surveys (KTB 1986). While the Late Devonian and Early Carboniferous sediments are virtually unmetamorphosed, the older schists display a variety of metamorphic grades.

The structure of both sediment zones is quite complex, which is due to tectonic imbrication. The grade of metamorphism is highly variable on a local scale and ranges from unmetamorphosed to amphibolite-grade. The juxtaposition of rocks in contrasting degrees of metamorphism is probably due to Late Variscan imbrication. KROHE & EISBACHER (1988) concluded that the Central Gneiss Complex of the Black Forest was subjected to a rapid upward movement and south-directed thrusting over the Zone of Badenweiler-Lenzkirch about 330 - 340 Ma before present, i.e. shortly after the peak of gneiss metamorphism and anatexis.

#### **4.2.5 Summary: Succession of magmatic and metamorphic events in the Black Forest**

The metamorphic, magmatic and tectonic history of the Black Forest is summarized in Table 4-1.

### **4.3 Sources of data for the investigation of the crystalline basement of Northern Switzerland**

The crystalline basement of Northern Switzerland is the subsurface continuation of the Black Forest basement and is covered by Mesozoic and Tertiary sediments whose thicknesses increase from north to south. Only few surface outcrops exist on the Swiss side of the Rhine (most detailed description in BÜCHI et al. 1984). Therefore, most of the knowledge about the crystalline basement in Northern Switzerland is based on evidence from deep boreholes. Additional information pertinent to the interpretation of the large-scale basement structure and its tectonic evolution was deduced from seismic surveys and surface observations and is discussed in Chapter 3.

Many deep boreholes have been drilled in the last 100 years. The crystalline basement has been penetrated by exploration boreholes seeking coal, oil, gas, salt or thermal water. The geology of the crystalline basement sections penetrated by these boreholes is summarized in MAZUREK & PETERS (1992). The longest and best documented core profiles in Northern Switzerland resulted from Nagra's deep drilling programme, where 6 boreholes yielded about 6 km of cores from the crystalline basement. In contrast, many of the older drilling campaigns were stopped as soon as the basement was reached, or the hole was drilled without coring. In addition, the rock material from these boreholes is sometimes lost or poorly documented. In spite of these limitations, the older boreholes yield valuable geological data that complement the results of Nagra's investigations. Data are available from 22 boreholes that penetrate the crystalline basement of Northern Switzerland. Their locations are shown in Appendix 4-1 and an overview is given in Table 4-3.

### **4.4 Lithological units in the crystalline basement of Northern Switzerland**

With some minor exceptions, an excellent correlation exists between crystalline rock types in Northern Switzerland and those in the adjacent Southern Black Forest (MAZUREK & PETERS 1992). Granites have been drilled in 14 boreholes, gneisses have been encountered seven times and banded series of amphibolite/leucocratic gneiss have been observed in two boreholes. Basic, K-rich intrusives have been encountered once.

Rock types encountered in Northern Switzerland but unknown from the Southern Black Forest comprise:

- K-rich, basic magmatic rocks (diorites, monzonites, syenites) in the Schafisheim borehole
- I-type granites in the Schafisheim and Pfaffnau boreholes (all other granites are S-types; see below and MAZUREK & PETERS 1992)
- High-grade orthogneisses in the Herdern borehole (orthogneisses are unknown from the Southern Black Forest but abundant in the Central Black Forest gneiss mass; cf. section 4.2).

borehole	coordinates	drilled for	year	top crystalline basement		crystalline profile length	crystalline rock types	sediments above top crystalline
				[m] below surface	[m] above sea level			
Böttstein	659341/268556	radioactive waste disposal	1982/83	315 m	33 m	1186 m	biotite granite	Lower Triassic (Buntsandstein)
Herdern	711308/274597	oil/gas	1981/82	2127 m	- 1600 m	27 m	biotite orthogneiss	Lower Triassic (Buntsandstein)
Kaisten	644641/265624	radioactive waste disposal	1984	297 m	23 m	1009 m	mainly metapelitic gneiss	Lower Permian (Rotliegendes)
Koblenz RKK30	661759/273936	hydro power plant project	1954	157 m	164 m	4 m	biotite gneiss	Lower Triassic (Buntsandstein)
Kreuzlingen 1	729201/276169	oil/gas	1962	2534 m	- 1995 m	10 m	cordierite-biotite melagranite	Lower Triassic (Buntsandstein)
Leuggern	657664/271208	radioactive waste disposal	1984/85	223 m	136 m	1466 m	mainly metapelitic gneiss above biotite granite	Lower Triassic (Buntsandstein)
Lindau 1	692815/255098	oil/gas	1964	2365 m	- 1849 m	12 m	cordierite-biotite melagranite	Lower Triassic (Buntsandstein)
Pfaffnau 1	632708/231789	oil/gas	1963	1824 m	- 1324 m	19 m	biotite granite	Lower Triassic (Buntsandstein)
Rheinfelden-Weierfeld	623993/266209	coal	1875	367 m	- 86 m	66 m	banded series	Lower Permian (Rotliegendes)
Rheinfelden-Engerfeld	627650/266680	thermal water	1983	372 m	- 72 m	229 m	banded series above granite	Lower Permian (Rotliegendes)
Rietheim L2	662460/272834	salt	1969/70	319 m	+ 77 m	4 m	biotite gneiss	Lower Triassic (Buntsandstein)
Schafisheim	653620/246760	radioactive waste disposal	1983/84	1490 m	- 1069 m	516 m	granite, syenite, monzonite, diorite	Lower Triassic (Buntsandstein)

Tab. 4-3 : Overview of deep boreholes in Northern Switzerland that penetrated the crystalline basement.

Tab. 4-3 : continued

borehole	coordinates	drilled for	year	top crystalline		crystalline profile length	crystalline rock types	sediments above top crystalline
				[m] below surface	[m] above sea level			
Schleitheim	678160/288980	salt	1823/24	154 m	308 m	4 m	granite	Lower Triassic (Buntsandstein)
Siblingen	680090/286693	radioactive waste disposal	1988/89	349 m	225 m	1173 m	cordierite-biotite granite, andalusite-cordierite-bearing two-mica granite	Lower Triassic (Buntsandstein)
Weiach	676744/268618	radioactive waste disposal	1983	2020 m	- 1651 m	462 m	biotite gneiss	Upper Carboniferous (Stephanian)
Wintersingen	629106/261606	coal	1939	421 m	- 36 m	19 m	andalusite-cordierite-bearing two-mica granite	Lower Permian (Rotliegendes)
Zurzach Z1	663952/271229	salt	1913/14	415 m	- 74 m	1 m	granite	Lower Triassic (Buntsandstein)
Zurzach T1	663972/271224	thermal water	1955	415 m	- 74 m	16 m	andalusite-cordierite-bearing two-mica granite	Lower Triassic (Buntsandstein)
Zurzach T2	664020/271325	thermal water	1965	425 m	- 86 m	45 m	granite	Lower Triassic (Buntsandstein)
Zurzach T3	663742/271482	thermal water	1979/80	402 m	- 56 m	299 m	metapelitic gneiss above cordierite-biotite and andalusite-cordierite-bearing two-mica granite	Lower Triassic (Buntsandstein)
Zuzgen 1	635030/263400	salt	1939/40	256 m	+ 156 m	148 m	andalusite-cordierite-bearing two-mica granite	Lower Permian (Rotliegendes)
Zuzgen 2	635410/263470	salt	1940	243 m	+163 m	16 m	granite	Lower Permian (Rotliegendes)

The I-type granites and basic magmatites are all situated at the southern boundary of the Permo-Carboniferous Trough of Northern Switzerland and seem to be related to the fault system along which the Trough was formed. The Trough represents a major crustal lineament, which could explain the mantle signatures in the geochemistry of the I-type granites (MAZUREK & PETERS 1992). K-rich magmatites and I-type granites have also been described in the Northern Black Forest ("durbachites", SAUER 1893) and in the Vosges (FLUCK 1980).

#### 4.4.1 Paragneisses

Paragneisses, i.e. metamorphic rocks of sedimentary origin, dominate the gneiss series by quantity. They are fully analogous to gneisses encountered in the Southern Black Forest, e.g. to the "Gneisanatexite Typ Hauensteiner Murgtal" (METZ 1980). By analogy to the Black Forest, the age of sedimentation is Proterozoic. The lithological units in the paragneisses are dominated by metapelites and meta-graywackes and minor intercalations of hornblende gneisses, amphibolites, aplitic gneisses<sup>1)</sup> and calc-silicates. The geochemistry of these rocks was investigated in detail by MÜLLER (1989) and WIMMENAUER (1980, 1984). Similar to the Black Forest, the gneiss series of Northern Switzerland was subjected to a high-grade metamorphism and partial melting (migmatization), mainly of the metapelites (MAZUREK 1992).

Detailed petrographic descriptions of all rock types encountered in the boreholes are given in reports by MATTER et al. (1988a) and PETERS et al. (1989a, b). Typical mineralogical compositions are given in Table 4-4.

The *metapelites* consist of biotite, sillimanite, cordierite, plagioclase, K-feldspar and quartz as major constituents and some retrograde muscovite. On the whole, metapelites are very mica-rich and inhomogeneous rocks. Migmatization led to the segregation of dm-size melt pockets (leucosomes), which have a granitic mineralogy and texture. With only insignificant exceptions, all cordierite has been altered by retrograde and hydrothermal events and is only present as pseudomorphs.

*Meta-graywackes* are present as biotite-plagioclase-quartz gneisses with only minor components of Al-rich minerals (sillimanite, cordierite), typical of the metapelites. They are interlayered with the metapelites on the dm - m scale, which is interpreted as a relict bedding. Meta-graywackes are less affected by migmatization than metapelites.

Metapelites and meta-graywackes account for > 90% of all paragneisses, and all other types of gneiss are only minor in abundance.

---

1) The term "aplitic gneiss" is non-standard in geological literature and is used here in a purely descriptive sense. Aplitic gneisses are metamorphosed volcanic rocks deposited as layers in the paragneiss series. Their chemical composition, mineralogy and texture are very similar to that of aplite dykes.

*Aplitic gneisses* form concordant, meter-thick intercalations within the metapelites and meta-graywackes. Structural and geochemical evidence indicates that these layers represent the metamorphosed equivalents of rhyolites rather than intrusive aplite dykes.

*Hornblende-biotite-plagioclase-quartz gneisses* are very similar to the meta-graywackes except for the occurrence of hornblende, which probably indicates a slightly more Ca-rich source rock compared to the meta-graywackes.

*Amphibolites* are very limited in their occurrence and probably represent marly sedimentary layers.

Hornblende-biotite-plagioclase-quartz gneisses, amphibolites and a part of the aplitic gneisses are concentrated in the so-called *banded series* in the Kaisten (1119 - 1246 m) and Leuggern (657 - 895 m) boreholes, where they are interlayered with biotite-plagioclase gneisses. Typically, the banded series also contain numerous pegmatite dykes.

*Calc-silicates and related rock types* are mostly concentrated in thick series consisting of plagioclase-clinopyroxene rocks, biotite gneisses and minor calc-silicates s.str. containing calcite-bearing parageneses. Decimeter-size boudins of calc-silicates are abundant in the whole gneiss series.

#### 4.4.2 Orthogneisses

*Orthogneisses* have only been identified in the Herdern borehole (MAZUREK & PETERS 1992) and represent intensely deformed and high-grade metamorphic equivalents of granitic rocks.

#### 4.4.3 Variscan intrusives: granites and basic batholiths - occurrence and comparison with the Southern Black Forest

Mean mineralogical compositions of granites and basic magmatites are given in Table 4-4.

Analogous to the Black Forest, most of the granites drilled in the crystalline basement of Northern Switzerland are S-types (cf. section 4.2.1 for definition). MAZUREK & PETERS (1992) compared granites from the Southern Black Forest and Northern Switzerland and attempted to establish a genetic classification based on petrographic and geochemical evidence. Due to the large similarities between the Black Forest and Northern Switzerland, granites from both regions can be classified in the following common scheme:

1. *Syn-kinematic granites (e.g. Hauenstein)*: These granites are characterized by a foliation, which is probably due to the regional deformation phase at 330 - 340 Ma before present. An example is the Hauenstein granite in the southernmost Black Forest. All other granite types are undeformed and therefore younger.

data in [vol.-%]	paragneisses						ortho-gneisses	intrusive rocks			
	metapelites	meta-graywackes	hornblende gneisses	amphibolites	aplitic gneisses	calc-silicates	ortho-gneisses	granites	basic intrusives	aplitites, pegmatites, granite and rhyolite porphyries	lamprophyres
quartz	15-35	25-40	15-40	0-5	20-35	5-30	21-25	25-35	0-5	25-40	10-30
K-feldspar	5-10	0-5	0-20	0	20-40	0-5	18-24	25-35	0-45	10-35	5-25
plagioclase	15-25	30-40	25-40	30-40	20-40	20-45	41-45	20-30	5-35	25-35	5-25
sillimanite	0-10	0	0	0	0	0	0	0	0	0	0
biotite	10-25	15-35	10-20	10-20	5-15	0	11-13	5-15	15-40	0-10	20-40
muscovite	10-25	0-5	0	0	0	0	0	0-10	0	0-15	0
chlorite	0-5	0	0	0	0	0	0	0	0	0	0
hornblende	0	0	0-20	35-45	0	0	0	0	5-30	0	0-10
clinopyroxene	0	0	0	0-5	0	20-35	0	0	0-10	0	0-10
titanite	0	0	0-5	3-7	0	2-6	0	0	0	0	0-5
garnet	0-5	0-5	0	0	0	0-5	0	0	0	0	0
others, access.	3-5	2-4	2-5	2-5	2-5	10-20	2-5	2-5	3-5	2-4	5-10

**Tab. 4-4 :** Mineralogical compositions of fresh rock types (i.e. those unaffected or weakly affected by hydrothermal alteration) in the crystalline basement of Northern Switzerland. Data are in [vol.-%].

2. *Inhomogeneous S-type melagranites (Lindau, Kreuzlingen)*: The chemical inhomogeneity of these undifferentiated granites is caused by variable degrees of partial melting and the abundance of metapelitic xenoliths. These granites are probably older than the more leucocratic S-type granites, which are more homogeneous and show clear differentiation trends. No S-type melagranites are known from the Southern Black Forest, and absolute datings are not available.
3. *South-east Black Forest/Northern Switzerland S-type granite series - older plutons*: An excellent geochemical correlation exists between granites of the Black Forest and Northern Switzerland. All of these granites intruded in the interval 315 - 330 Ma before present. This group consists of 2 intrusion suites:
  - a. *S-type biotite granites (St. Blasien, Albtal, Böttstein/Leuggern)*
  - b. *Younger, highly-differentiated, S-type, andalusite-bearing two-mica granite series (Säckingen/Zuzgen/Wintersingen, Zurzach, Siblingen)*. These granites evolved from the same parent magmas as the biotite granites but were subjected to a more intense magmatic differentiation.
4. *South-east Black Forest/Northern Switzerland S-type granite series - younger plutons (Schluchsee, Bärhalde)*: These S-type plutons are dated at 307 - 321 Ma and are therefore younger than the andalusite-two-mica granites. Their composition does not plot on trend lines defined by the older plutons of the South-east Black Forest/Northern Switzerland S-type granite series. To date, this granite type has not been encountered in Northern Switzerland.
5. *K-rich I-type granites (Schafisheim, Pfaffnau)*: The geochemical characteristics of these plutons differ significantly from the S-type granites discussed above. They do not represent pure crustal melts but rather have some mantle signatures. Both plutons of this type are spatially related to large-scale horst structures in the Permo-Carboniferous Trough system and may also be genetically linked to the presence of this large-scale crustal discontinuity.

Basic magmatic rocks drilled in Schafisheim (diorites, monzonites, syenites) are probably genetically related to the (slightly younger) granite of Schafisheim. More details are given in MATTER et al. (1988b) and MAZUREK & PETERS (1992).

#### 4.4.4 Variscan intrusives: dykes

Five types of dykes have been observed in the boreholes:

1. Aplites;
2. Pegmatites;
3. Granite porphyries;
4. Rhyolite porphyries;
5. Lamprophyres.

Relations in Northern Switzerland are fully analogous to those described above for the Black Forest. Petrographic and structural evidence suggests that there are several generations of aplites and pegmatites. Some of them may be older than the Variscan granites while others cross-cut all rock types including the granites. Some aplites in the gneiss series of Leuggern were subjected to the same ductile deformation as the surrounding gneisses and therefore must be older than the intrusion of the Leuggern granite, which is undeformed.

While aplites, pegmatites and lamprophyres are very common in Northern Switzerland, porphyry dykes are of subordinate importance. Only one single swarm of granite porphyries has been identified in Northern Switzerland (Schafisheim, 1614 - 1633 m), and two rhyolite porphyries have been drilled in Böttstein.

Mean mineralogical compositions of all types of dykes are given in Table 4-4.

#### **4.4.5 Lithological correlations between boreholes in Northern Switzerland**

Based on the limited number of boreholes, the understanding of the spatial distribution of granites and gneisses in the basement of Northern Switzerland is very incomplete. In most cases, not enough data exist to define lithological boundaries on a regional scale. There are two important exceptions to this rule:

1. Based on petrographic and geochemical criteria, the granites of Böttstein and Leuggern belong to one single intrusive body. Probably a continuous granitic body occurs between these two boreholes, even though its geometry cannot be further characterized.
2. The granites of Zuzgen and Wintersingen probably correlate genetically with the granite of Säckingen which crops out in the southernmost Black Forest (App. 4-1). MAZUREK & PETERS (1992) suggested that these three sites are part of one single magmatic body. All three sites are made up of Al-rich, andalusite-bearing two-mica granites with identical textures.

The metapelitic gneisses of Kaisten and Leuggern correlate with analogous rocks cropping out in the Southern Black Forest. However, it is not possible to connect these gneiss areas spatially because they have probably been intruded by voluminous granites whose positions and sizes are unknown.

#### **4.5 Post-metamorphic/post-magmatic (Late and post-Variscan) evolution of the crystalline basement of Northern Switzerland**

While the Variscan and pre-Variscan basement evolution is well-studied in the Black Forest, borehole evidence in Northern Switzerland yields only an incomplete picture of the petrogenesis. However, due to the spatial proximity of the two regions, the petrogenetic evolution of the Black Forest can be assumed to be fully analogous to that of the basement of Northern Switzerland. No evidence in the Swiss part of the basement exists that would suggest major petrogenetic differences.

In contrast, the post-metamorphic/post-magmatic evolution has been intensely studied in Northern Switzerland, while only limited information is available from the Black Forest. Therefore, this Chapter is mostly based on data from Swiss boreholes, complemented by some data from the Black Forest. The description is mainly based on the borehole reports by MATTER et al. (1988a, b), PETERS et al. (1986, 1989a, b) and NAGRA (1992a). This Chapter is a continuation of section 4.2, where the Proterozoic to Variscan regional evolution is summarized.

#### **4.5.1 Retrograde effects of cooling in gneisses**

Analogous to the situation in the Black Forest, most of the gneisses of Northern Switzerland underwent some degree of retrograde metamorphism during cooling and uplift after migmatization (Tab. 4-5). Retrograde effects only slightly postdate the peak of metamorphism (migmatization). They are fully penetrative (i.e. they affect the whole rock volume and are not restricted to fractured areas) and comprise mainly the crystallization of muscovite at the expense of K-feldspar, biotite and cordierite. Retrograde effects are ubiquitous in the metapelites (e.g. Kaisten, Leuggern, cf. MAZUREK 1992), but are only minor in biotite-plagioclase gneisses (e.g. Weiach) and most of the other rock types. Minor occurrence of retrograde andalusite indicates an upper pressure limit of 3.5 kbars.

#### **4.5.2 Retrograde effects of cooling in granites**

An analogous, but younger, process of retrogression affected the Variscan granites (e.g. Böttstein, Leuggern, Siblingen, Zuzgen, Wintersingen, Zurzach and others), in which muscovite formed during subsolidus cooling of the plutons. Textures suggest that muscovite did not crystallize from a melt. Retrograde muscovite from the Böttstein granite has been dated at 314 Ma using the K/Ar method, which is a date indistinguishable from the age of intrusion of the granite (cf. Tab. 4-6). Andalusite is an accessory phase in Al-rich S-type granites of Northern Switzerland (i.e. Zuzgen, Wintersingen, Zurzach and Siblingen) and indicates low-pressure conditions during retrogression (MAZUREK & PETERS 1992). Andalusite is also known from the granites of Säckinggen and Hauenstein in the southernmost Black Forest.

#### **4.5.3 Tourmaline-quartz veins**

A first phase of brittle deformation is documented by 0.5 - 2 cm thick, steeply-dipping veins containing tourmaline, quartz and minor muscovite, chlorite, titanite, apatite and arsenopyrite. They are completely healed by the mineralizations but are often reactivated by younger cataclastic movements. The veins occur mostly in metapelitic gneisses (where they cross-cut schistosity), but are also found in Al-rich granites (e.g. Siblingen, Lindau, Leuggern, cf. Tab. 4-5).

Based on petrographic evidence, the veins are retrograde features that only insignificantly postdate the peak of metamorphism in the gneisses (or, in the case of granites,

Phase	Processes and features	Nagra boreholes							older boreholes							
		Kaisten	Leugern	Leugern	Böttstein	Weiach	Sibingen	Schafisheim	Pfaffnau	Herdern	Kreuzlingen	Lindau	Zurzach	Zuzgen	Wintersingen	Weierfeld
		gneiss	gneiss	granite	granite	gneiss	granite	granite/syenite	granite	gneiss	granite	granite	granite, gneiss	granite	granite	banded rocks
<i>retrograde effects (post-metamorphic/post-magmatic cooling)</i>	retrograde muscovite formation	XXX	XXX	X	X	X	XXX	X	-	-	X	X	XXX	XXX	XXX	-
	tourmaline-quartz veins	XX	XX	X	-	-	X	-	-	-	X	-	-	-	-	-
	ductile quartz deformation	X	XX	X	X	X	X	X	XXX	X	XX	X	X	X	XX	X
<i>high-temperature phase</i>	high-temperature cataclasis and jointing	X	XX	X	XX	XX	XXX	XXX	XXX	-	-	-	-	-	-	X
	high-temperature alteration	X	XX	XX	XX	XX	XX	XXX	XXX	XX	-	X	-	-	-	XX
<i>low-temperature phase</i>	low-temperature cataclasis and jointing	XXX	X	-	XX	-	-	-	X	XX	XX	-	?	X	X	-
	low-temperature (illitic) alteration	XXX	XX	XX	XX	X	-	-	X	XX	XX	-	XX	X	X	X
<i>kaolinitic phase</i>	kaolinitic alteration and minor jointing	XXX	X	X	XX	-	XXX	-	XX	XX	-	-	-	X	X	-
	calcite-siderite impregnation	X	X	X	X	X	X	X	XXX	XX	XX	X	-	-	-	-
	vugs/channels with mineralizations	XX	XX	XX	XX	X	XX	XX	-	XX	-	-	-	-	X	X

**Tab. 4-5 :** Overview of post-magmatic/post-metamorphic effects (deformations and alterations) in boreholes of Northern Switzerland. X = weakly developed, XX = strongly developed, XXX = very strongly developed.

the age of intrusion) and that are syn-genetic with the muscovite formation described above. PETERS et al. (1989a) attribute the formation of the veins to a hydraulic fracturing process. Based on arsenopyrite geothermometry (KRETSCHMAR & SCOTT 1984), temperatures of 535 - 600 °C are reported for the formation of the veins in the gneisses of Kaisten.

#### 4.5.4 Ductile quartz deformation

Another retrograde effect, in addition to the mineral reactions and localized fracturing (tourmaline-quartz veins) described above, is the generally weak but penetrative ductile deformation of quartz in the whole region. Quartz is the only mineral affected (feldspars do not show any effects), which suggests temperatures in the interval 300 - 500 °C for this deformation. Ductile quartz deformation is locally very intense in the gneisses of Leuggern and results in mylonitic textures, while the Leuggern granite is less affected (MEYER 1987). In the granite of Pfaffnau, ductile quartz deformation leads to the formation of a weak schistosity of the rock, and some effects also occur in the granites of Kreuzlingen and Wintersingen (Tab. 4-5).

#### 4.5.5 Alteration related to dyke intrusion

This phase of alteration is unique to the gneisses of Weiach and is spatially related to the surroundings of aplite dykes (MATTER et al. 1988a). In contrast to all younger alterations, it has no relation to cataclastic fracture zones. Very probably, it is due to hot fluids that were released during the crystallization of the aplite dykes and that infiltrated the adjacent country rocks. The mineralogical effects comprise mainly the following alterations:

plagioclase	⇒	albite + K-feldspar
biotite	⇒	chlorite ± muscovite
cordierite	⇒	muscovite
K-feldspar	⇒	muscovite

Minor alteration products comprise quartz, titanite, epidote and apophyllite. The temperature of the alteration is estimated at about 400 °C (i.e. greenschist-grade). Based on petrographic criteria, this phase of alteration can be distinguished from all younger phases discussed below.

#### 4.5.6 High-temperature cataclasis and hydrothermal alteration

##### Petrography and physical conditions

High-temperature cataclastic deformation and/or jointing affected crystalline rocks penetrated by most of the boreholes to some extent (Tab. 4-5). Detailed structural analysis and fluid inclusion studies (boiling phenomena) indicate that deformation was facilitated by hydraulic fracturing (MEYER 1987). In general, cataclastic zones dip

steeply and range in thickness from centimeters to meters. Textures on the scale of hand-specimens are often chaotic with no preferred orientation, and rock clasts are embedded in an interconnected fine-grained cataclastic matrix. Shear strain across fractures is often limited (as far as this can be judged in the core material). A detailed description of the geometric patterns is given in MEYER (1987).

Deformation was invariably associated with a syn-genetic hydrothermal alteration by fluids circulating in the fractures. The intensity of alteration varies as a function of primary mineralogy and therefore of the rock type. The following lists the most common rock types in the order of decreasing hydrothermal effects of the high-temperature phase:

calc-silicate rocks (*most strongly affected*)  
 amphibolites  
 meta-graywackes  
 aplitic gneisses  
 metapelites, granites (*least affected*)

Typical hydrothermal effects on mineralogy are:

plagioclase	⇒	sericitic muscovite + albite ± K-feldspar ± prehnite
biotite	⇒	chlorite + sericitic muscovite ± Ti oxides ± titanite ± K-feldspar ± fluorite ± prehnite
cordierite	⇒	sericitic muscovite
hornblende	⇒	chlorite + titanite ± leucoxene ± calcite
pyroxene	⇒	chlorite + sericitic muscovite + calcite

The alteration of plagioclase and biotite is quantitatively the most significant. Minor alteration products comprise epidote, pumpellyite, hydrogrossular and pyrite. The product minerals are all well-crystallized and mostly correspond to greenschist-grade parageneses, for which a temperature interval of 300 - 400 °C can be estimated (extensive discussion in MATTER et al. 1988a).

The high-temperature phase correlates with low-salinity NaCl waters identified in fluid inclusions in rock-forming and fracture-filling quartz and calcite. Within this group of fluid inclusions, a temporal evolution from high to low homogenization temperatures (400 ⇒ 140 °C) and decreasing salinities has been identified (MULLIS 1987). These trends are interpreted in terms of a progressive dilution of the formation waters by infiltrating meteoric waters, which is fully consistent with stable isotope studies (MAZUREK 1992, SIMON 1990, SIMON & HOEFS 1987). Some fluid inclusion samples with high homogenization temperatures show indications of boiling phenomena<sup>1)</sup> and therefore reflect the actual temperatures at which the inclusions

---

1) "Boiling" in the standard usage of fluid inclusions investigations refers to the natural coexistence of two fluid species in a one-component solution, e.g. liquid water and steam. In a pressure-temperature diagram, the two fluids lie on a two-phase curve. When such coexisting fluid phases are trapped in inclusions, the ratio of trapped liquid to gas is largely accidental and varies from inclusion to inclusion. Therefore, boiling phenomena are identified in microthermometric methods by large variations in the gas/liquid ratio (i.e. density) of cogenetic inclusions.

were trapped. Trapping temperatures are about 300 - 380 °C, which is consistent with temperature estimates for the high-temperature hydrothermal phase based on mineral parageneses. The presence of early inclusions without boiling phenomena and high homogenization temperatures was used to constrain the pressure conditions at the time of trapping. Given a maximum fluid temperature of 400 °C (upper limit, based on mineral parageneses), a maximum pressure of 300 - 700 bars was derived, which corresponds to a maximum depth of 3 - 7 km below surface (assuming hydrostatic conditions)<sup>1)</sup>. This means that the maximum possible erosion of the crystalline basement is a few km. Because the pressure estimation is highly sensitive to the poorly constrained difference between homogenization and actual trapping temperature, this overburden is a maximum and may have been much less in reality. Irrespective of the uncertainty of the pressure estimation, geothermal gradients were large during the high-temperature phase (min. 60 °C/km, possibly much higher). Based on vitrinite reflectance data from Weiach, KEMPTER (1987) suggests gradients around 100 °C/km during the Late Carboniferous and Early Permian.

Pressures derived from fluid inclusions showing boiling phenomena can be < 100 bars, which, in several samples, is less than the hydrostatic pressure of the present overburden of the crystalline basement. Sub-hydrostatic conditions reflect transient, probably very short-lived events, such as seismic movements (cf. MUIR WOOD & KING 1993, SIBSON 1993), and corroborate the hypothesis that hydraulic fracturing was an important process of brittle deformation (MEYER 1987).

### **Regional correlation and timing**

In spite of some differences among various sites, petrographic evidence suggests that high-temperature cataclasis and alteration represent an event of regional extent. In the Schafisheim and Pfaffnau boreholes, which were drilled in local horst-like structures in the Permo-Carboniferous Trough system (App. 4-1), high-temperature cataclasis and alteration are extremely strong and affect the entire profiles. Petrographically, the alteration is mostly characterized by an intense albitization and is somewhat different from the alteration characteristics of the other boreholes. Very probably, the uniqueness of the rocks penetrated by these boreholes is due to their tectonic position (App. 4-1), and the extreme cataclastic deformation is probably due to movements along major faults in the Permo-Carboniferous Trough of Northern Switzerland.

High-temperature cataclasis and alteration did not affect the sediments overlying the basement rocks and therefore predate the deposition of the oldest sediments, whose age is Stephanian (ca. 290 Ma). This conclusion is corroborated by evidence from fluid inclusions. Low-salinity NaCl inclusions (correlated above with the high-temperature phase) identified in clastic sediments (Stephanian-Rotliegendes, i.e. 260 - 290 Ma) are features inherited from the protolith (crystalline source rock), i.e. they were trapped prior to the deposition of the sediments. This timing is evident from microtextural

---

1) The principles of quantitative interpretation of microthermometric measurements in fluid inclusions is discussed in detail in ROEDDER (1984).

relations. Inclusion trails containing low-salinity NaCl fluids end at the boundaries of clastic grains and never pass into post-sedimentary (diagenetic) neoformations, such as cements and overgrowths. The ubiquitous occurrence of low-salinity NaCl fluid inclusions both in basement rocks and clastic sediments (Permo-Carboniferous, Buntsandstein) indicates that the high-temperature phase was an event of regional importance.

An uncertainty is whether the high-temperature deformations and alterations in granites and gneisses are genetically correlated or whether they represent a pre-granitic event in the gneisses (e.g. in the course of post-migmatitic, retrograde cooling) and a late to post-intrusive event in the granites. K/Ar age dating of biotite chloritization in the gneisses of Weiach, an alteration clearly attributed to the high-temperature phase, yields 300 - 320 Ma (Tab. 4-6). These dates are consistent with a single event related to the intrusion of Variscan granites. Consistent results were also obtained by HAMMERSCHMIDT & WAGNER (1983) from the Urach III exploration borehole in the Swabian Alb (S Germany). K/Ar ages of biotites from ortho- and paragneisses yield 320 - 330 Ma and are largely independent of the degree of chloritization.

In the intrusive rocks of Schafisheim, K/Ar dates of hornblende, K-feldspar and albite yield 300 Ma and are interpreted as the age of high-temperature hydrothermal alteration. The age of intrusion of the basic magmatites is documented by a Rb/Sr mineral isochron and K/Ar on biotite at 316 Ma (Tab. 4-6).

Taking together the evidence from radiometric age determinations, structural and petrographic relations of fluid inclusions, the age of the high-temperature phase is constrained to the interval 290 - 320 Ma, i.e. to the Late Carboniferous (cf. Fig. 3-2). Deformation and alteration of the high-temperature phase are a consequence of the shallow intrusion of Late Variscan granites during late orogenic basement uplift (DIEBOLD et al. 1991). The Late Carboniferous is characterized by rapid basement uplift, erosion and tectonic unroofing and extremely high geothermal gradients (cf. Chapter 3). Subsequently, differential subsidence in a dilational or right-lateral transpressive regime was initiated in the Uppermost Carboniferous (Stephanian; trough formation, coal seams).

#### **4.5.7 Formation of ore and mineral veins in the Black Forest**

##### **Occurrence**

Ore mineralizations are not evenly distributed over the Black Forest but occur in rather well-defined districts (WIMMENAUER 1985, WALTHER et al. 1986, cf. Fig. 4-1). In the southern part of the Black Forest, two highly mineralized districts are known, namely the Schauinsland and the Urberg districts. Some of the mineral deposits have been mined until recent times (e.g. Menzenschwand, Gottesehre/Urberg). Ore mineralizations in the Black Forest have had a complex, multiphase genesis from the Late Variscan to the Tertiary (e.g. HOFMANN & EIKENBERG 1991). The most common minerals are barite, fluorite, sphalerite, galena, pyrite, pitchblende, calcite and quartz.

## K/Ar age data

loc.	depth [m] sample	lithology	sample description	mineralogy	grain-size fraction $\mu\text{m}$	age in [Ma]	error [Ma]	tentative interpretation
BOE	400.05	altered biotite granite	cataclastic matrix	95 % illite, 5 % chlorite/smectite ML	< 2	229	2	low-T phase, rejuvenated
BOE	400.05	altered biotite granite	cataclastic matrix	illite	6 - 20	261	2	low-T phase, rejuvenated
BOE	481.92	altered biotite granite	whole-rock	65 % illite, 25 % illite/smectite ML, 10 % dioct. chlorite	< 2	157	2	low-T phase, rejuvenated
BOE	481.92	altered biotite granite	whole-rock	biotite	35 - 50	314	6	intrusion
BOE	654.12	altered biotite granite	fracture coating	illite	< 2	269	3	low-T phase, rejuvenated
BOE	671.30	fresh biotite granite	whole-rock	biotite	35 - 50	322	3	intrusion
BOE	696.14	altered biotite granite	cataclasite	95 % illite, 5 % chlorite/smectite	< 2	210	4	low-T phase, rejuvenated
BOE	696.14	altered biotite granite	cataclasite	muscovite	35 - 50	314	6	retrograde cooling
BOE	902.69	altered biotite granite	cataclasite	97 % illite, 3 % chlorite	< 2	246	3	low-T phase, rejuvenated
BOE	1160.15	altered biotite granite	cataclastic matrix	25 % illite, 75 % chlorite	< 2	217	3	low-T phase, rejuvenated
BOE	1439.20	altered biotite granite	cataclastic matrix	50 % illite, 50 % chlorite	< 2	249	3	low-T phase, rejuvenated
BOE	1439.20	altered biotite granite	cataclastic matrix	93 % illite, 7 % chlorite	< 2	289	3	low-T phase
BOE	1490.7-1491.1	fresh biotite granite	whole-rock	biotite	50 - 80	334	3	intrusion
LEU	596.35	biotite-plagioclase gneiss	fracture coating	82 % illite (1M), 18 % chlorite	no grain-size sep.	273	3	low-T phase
LEU	1298.18	aplitic dyke in gneiss	fracture coating	94 % illite (1M), 6 % chlorite	no grain-size sep.	254	3	low-T phase, rejuvenated
LEU	1479.30	altered biotite granite	alteration products in plagioclase	67 % illite (1M), 33 % chlorite	no grain-size sep.	268	3	low-T phase, rejuvenated
LEU	1648.83	altered cordierite-two mica granite	hydrothermal quartz-illite vein	illite	< 6	275	2	low-T phase
LEU	1666.18	altered cordierite-two mica granite	fracture coating	illite	no grain-size sep.	278	3	low-T phase
KAI	580.79	fresh biotite-plagioclase gneiss	fracture coating	95 - 100 % illite (2M1), 0 - 5 % kaolinite	no grain-size sep.	135	1.6	Cretaceous event
KAI	943.51	fresh biotite gneiss	fracture coating	illite (1Md)	no grain-size sep.	126	1.6	Cretaceous event
KAI	1046.36	chloritized biotite gneiss	fracture coating	90 - 95 % illite (2M1), 5 - 10 % kaolinite, smectite, chlorite	no grain-size sep.	138	2	Cretaceous event
SHA	1879.78-1883.76	hornblende-biotite syenite	whole-rock	hornblende albite K-feldspar biotite		299 300 300 316	3.2 3.2 5 3.3	high-T phase high-T phase high-T phase intrusion
WEI	2101.92	biotite gneiss	whole-rock	biotite	80 - 100	320	3.4	high-T phase
WEI	2285.20	biotite gneiss	whole-rock	biotite, partially altered to chlorite	80 - 100	320	3.3	high-T phase
WEI	2346.31	biotite gneiss	whole-rock	biotite, partially altered to chlorite	50 - 90	300	3.2	high-T phase

**Tab. 4-6 :** Compilation of absolute age datings of minerals and whole-rocks in the Nagra boreholes in Northern Switzerland. Data from PETERS et al. (1986, 1989a,b) and MATTER et al. (1988a,b).

**Rb/Sr age data**

loc.	depth [m] sample	lithology	sample description	mineralogy	isochron data			tentative interpretation
					Sr initial	age in [Ma]	error [Ma]	
BOE	1490.7 - 1491.1	fresh biotite granite	whole-rock	whole-rock sample: quartz, K-feldspar, plagioclase, biotite, accessories	0.71475	243	3	system disturbed by Mesozoic/Tertiary event(s)
BOE	1490.7 - 1491.1	fresh biotite granite	whole-rock	biotite				
KAI	1046.36	chloritized biotite gneiss	fracture coating	90 - 95 % illite (2M1), 5 - 10 % kaolinite, smectite, chlorite	model ages	138 129	20 20	Cretaceous event
LEU	1525.97	fresh biotite granite	whole-rock	quartz, K-feldspar, plagioclase, biotite, accessories	0.71428	279	5	low-T phase
LEU	1636.90	fresh cordierite-two mica granite	whole-rock	quartz, K-feldspar, plagioclase, biotite, muscovite, cordierite alteration products, accessories				
LEU	1648.29	altered cordierite-two mica granite	whole-rock	quartz, K-feldspar, plagioclase, biotite, muscovite, cordierite alteration products, other alteration products, accessories				
LEU	1648.83	altered cordierite-two mica granite	hydrothermal quartz-illite vein	quartz, illite				
LEU	1648.83	altered cordierite-two mica granite	hydrothermal quartz-illite vein	illite, fraction < 6 µm				
SHA	1879.78 - 1883.76	hornblende-biotite syenite	whole-rock	apatite	0.7087	315		intrusion
SHA	1879.78 - 1883.76	hornblende-biotite syenite	whole-rock	K-feldspar				
SHA	1879.78 - 1883.76	hornblende-biotite syenite	whole-rock	plagioclase				
SHA	1879.78 - 1883.76	hornblende-biotite syenite	whole-rock	hornblende				
SHA	1879.78 - 1883.76	hornblende-biotite syenite	whole-rock	biotite				
SHA	1879.78 - 1883.76	hornblende-biotite syenite	whole-rock	biotite, K-feldspar, plagioclase, hornblende, accessories				

**Fission track age data**

loc.	depth [m] sample	lithology	sample description	mineralogy	age in [Ma]	error [Ma]
BOE	481.92	altered biotite granite	whole-rock	apatite	143	12
BOE	671.30	fresh biotite granite	whole-rock	apatite	128	12
BOE	696.14	altered biotite granite	whole-rock	apatite	128	12

Tab. 4-6 : continued

Hydrothermal ore mineralizations in the Black Forest are invariably associated with major cataclastic fault zones (e.g. HOFMANN 1989 for Menzenschwand, HUCK 1984 for Grube Clara). HUCK (1984) demonstrated that metallogeny in the Grube Clara was a multiphase process of fault movements and hydrothermal ore deposition, and HOFMANN & EIKENBERG (1991) report similar relations for the Menzenschwand U deposit. Ore minerals were deposited in pre-existing planar structures such as cataclastic shear zones or joints.

Figure 4-3 shows a cross-section through the mining district "Grube Clara" in the Central Black Forest. It can be seen that the mineralized zone extends at least 350 m below the surface and possibly much deeper. The ore veins dip near-vertically towards the north-east. The mineralized zone consists of a complex pattern of single veins with a typical thickness of a few meters, and younger veins cross-cut older generations.

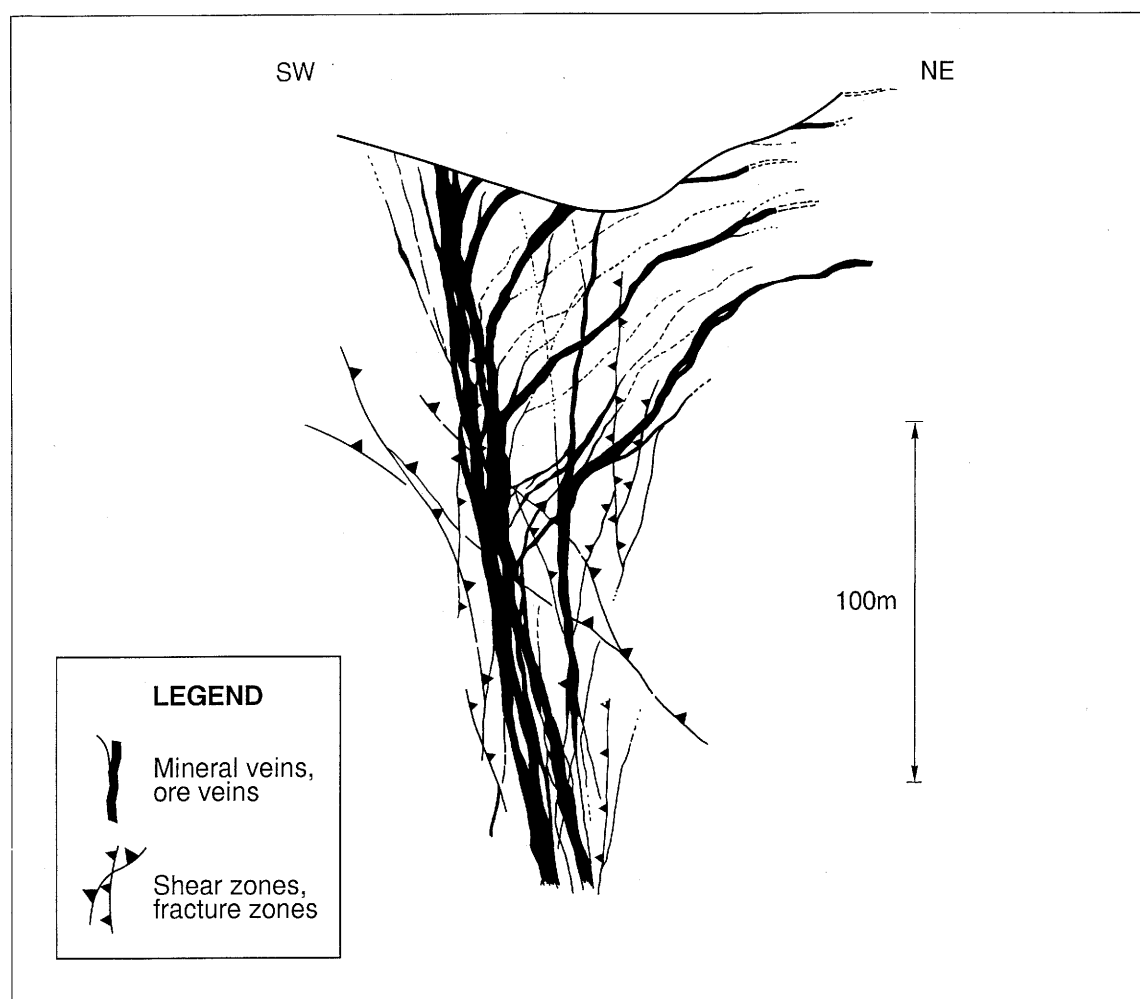


**Fig. 4-3 :** Vertical profile across the "Grube Clara" hydrothermal ore mine from the Central Black Forest. Mineralizations were formed in several phases of different ages, mainly in pre-existing cataclastic zones. Taken from HUCK (1984).

Figure 4-4 shows a map with ore veins in the Kinzig Valley (Central Black Forest). The veins are planar structures and may extend over several kilometers. In the Southern Black Forest, the most common orientations of the ore veins are NE-SW or NNE-SSW with a very steep dip angle (WIMMENAUER 1985).

Large hydrothermal ore and mineral veins have not been observed in the crystalline basement of Northern Switzerland, possibly due to the low probability of drilling through subvertical structures with vertical boreholes. The possible correlation of the deepest borehole section of Leuggern with features similar to ore veins is discussed in section 6.5.

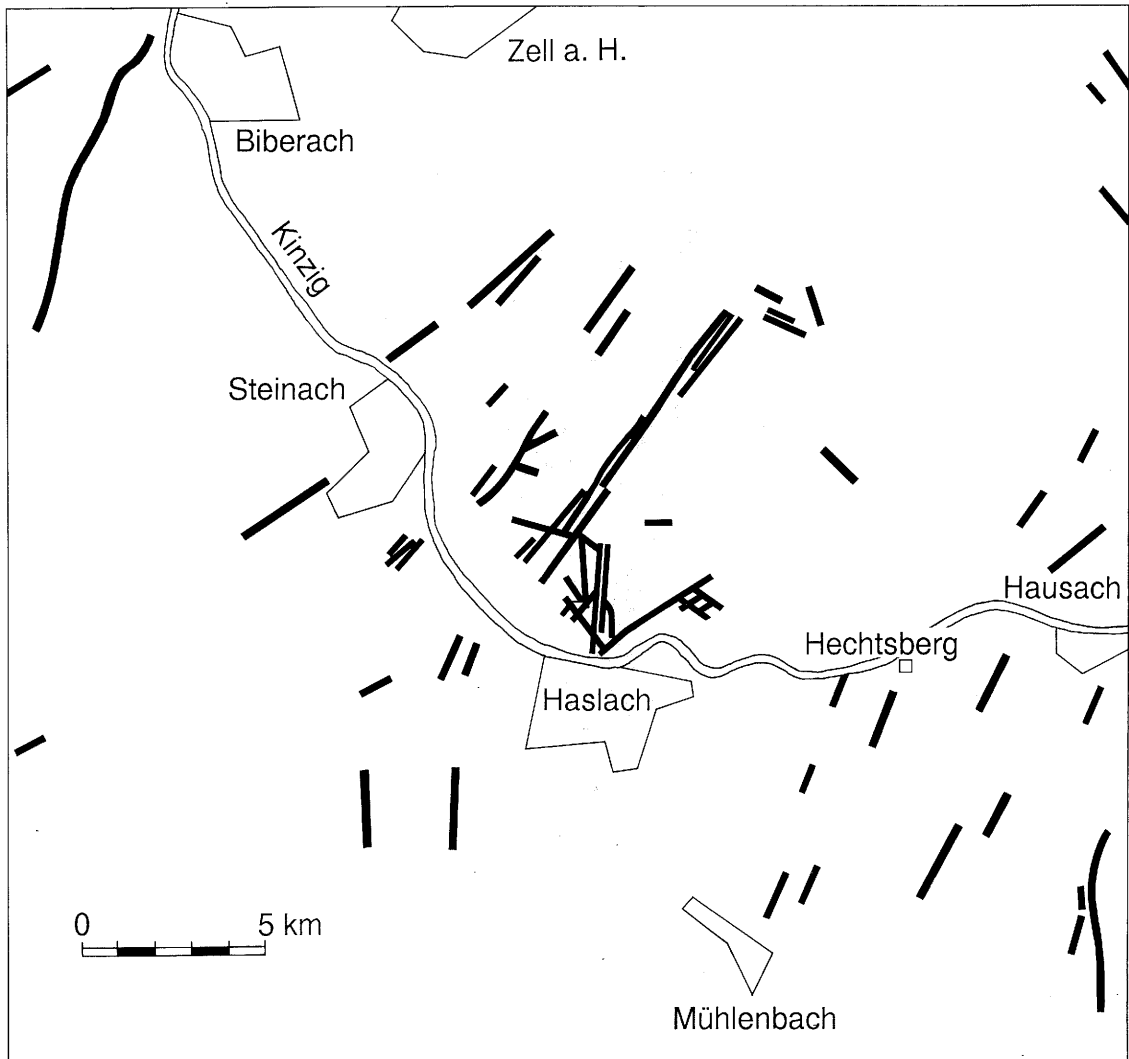


**Fig. 4-4 :** Distribution of hydrothermal ore veins near Haslach in the Central Black Forest. Taken from WIMMENAUER (1985).

## Genetic aspects and timing

Most authors agree that the ore vein systems evolved during the Late Variscan. HOFMANN & EIKENBERG (1991) dated the Menzenschwand U deposit at 295 Ma (U/Pb on pitchblende, upper intersection with Concordia). Therefore, the formation of the deposit in the Late Carboniferous is coeval with the high-temperature phase described above. A genetic correlation is also corroborated by evidence from fluid inclusions. The oldest inclusion type contains salt-poor NaCl waters with homogenization temperatures in the interval 100 - 400 °C; boiling phenomena are commonly observed. These conditions are very similar to those in the fluids attributed above to the high-temperature phase. A Tertiary hydrothermal overprint of the Menzenschwand ore vein system is well-documented by HOFMANN & EIKENBERG (1991). They obtained 50 Ma for this event (U/Pb on pitchblende, lower intersection with Concordia), which they attribute to the formation of the Rhine Graben.

Some mineralizations in the Black Forest cross-cut Early Triassic sediments (Buntsandstein) and are therefore younger than 220 Ma. BONHOMME et al. (1983) dated illites from the Oberwolfach fluorite-barite deposit (Central Black Forest) using the K/Ar method and obtained consistent ages in the interval 185 - 196 Ma. The authors interpret these dates as formation ages of the mineralization. Similar results were obtained by BAUBRON et al. (1980) in the French Massif Central.

### 4.5.8 Low-temperature cataclasis and hydrothermal alteration

#### Petrography and physical conditions

Evidence of low-temperature cataclastic deformation and associated argillic alteration is observed in the crystalline basement in most of the boreholes (Tab. 4-5), and dominates by quantity all other post-magmatic/post-metamorphic events. These effects represent a major crustal deformation of regional extent. Cataclastic deformation was invariably accompanied by jointing that typically reactivated pre-existing mechanical discontinuities such as zones deformed in the high-temperature phase or dyke/wallrock contacts. Low-temperature cataclasis was a multiphase, coupled process of deformation and hydrothermal activity, as demonstrated by the presence of cemented cataclasites as components in cataclastic zones. In contrast to the rather chaotic geometric patterns of the high-temperature cataclasis, shear zones of the low-temperature phase are somewhat more regular planar features (MEYER 1987).

Late movements of the low-temperature phase probably produced the cohesionless cataclastic zones ("kakirites") which, unlike all older deformation features, have not been healed by subsequent hydrothermal cementation and therefore consist of crumbly rock fragments and unconsolidated fault gouges. Similar features have also been recognized in the Black Forest (HUBER-ALEFFI & HUBER-ALEFFI 1984).

Low-temperature alteration postdated the high-temperature phase and produced abundant clay minerals at the expense of primary phases. The most important mineral reactions are:

plagioclase	⇒	illite + illite/smectite mixed-layer phase ± albite ± calcite
biotite	⇒	chlorite ± Ti oxides ± illite ± hematite
cordierite	⇒	illite
sillimanite	⇒	illite

Plagioclase alteration is most common, while biotite is only partially affected. Minor hydrothermal products are quartz, K-feldspar and siderite. The upper several 100 m of the crystalline basement have a penetrating, reddish stain caused by very minor amounts of microcrystalline hematite. Even at deeper levels, localized hematite occurrences, generally related to cataclastic zones, have been observed. Based on petrographic evidence, this hematite impregnation can be attributed to oxidized, presumably meteoric waters that circulated during the low-temperature phase. The presence of mixed-layer illite/smectite with about 80% illite layers imposes an upper temperature limit of about 250 °C. The heat source of this hydrothermal phase probably correlates with rhyolitic volcanism known in the Black Forest (see above, cf. PETERS 1987). KEMPTER (1987) postulates geothermal gradients of about 100 °C/km for the Early Permian, which possibly correlates with the low-temperature phase.

A second, distinct type of water-rich fluid inclusions has been identified in all boreholes and is younger than the dilute NaCl waters discussed above. This inclusion type consists of highly saline brines containing NaCl, CaCl<sub>2</sub> and MgCl<sub>2</sub> as major solutes (MULLIS 1987). Maximum homogenization temperatures scatter between 100 and 140 °C. This type of fluid evolves with time from brines to more dilute solutions. These inclusions are post-Stephanian, but more precise time constraints are uncertain. BEHR & GERLER (1987) and BEHR et al. (1987) argue that highly saline fluids in vein mineralizations are derived from sedimentary basins (Permian and younger) rather than from intense rock/water interactions. Fluids of this type prevailed from the Permian to the Miocene, because they also occur in Mesozoic and Tertiary sediments (MULLIS 1987). It is possible that the highly saline, early fluids of this type are associated with the low-temperature phase, but they could in principle also be younger (e.g. they could be related to the kaolinitic alteration discussed below). PETERS (1987) suggested that the low-temperature phase correlates with the younger, lower-temperature populations of the salt-poor NaCl waters (discussed above). HOFMANN & EIKENBERG (1991) correlate saline hydrothermal fluids from a U vein system in the Black Forest with the Early Tertiary formation of the Rhine Graben.

### Regional correlation and timing

Low-temperature cataclasis and illite-dominated alteration occur throughout Northern Switzerland and have been identified in most of the boreholes (Tab. 4-5). Petrographic and structural observations suggest that the low-temperature phase represents a major regional event and can therefore be genetically correlated over the entire region of interest.

Based on the fact that no cataclastic deformation is present in the Uppermost Permian and Early Triassic sediments directly covering the crystalline rocks in Kaisten,

Böttstein, Leuggern and Schafisheim, the age of the low-temperature cataclasis is greater than 260 Ma (MEYER 1987). Numerous K/Ar age datings of illite are available from the boreholes. In spite of considerable scatter (most dates are from the interval 210 - 280 Ma), many analyses cluster between 260 - 280 Ma (Tab. 4-6). The younger ages are interpreted as rejuvenations in the course of younger hydrothermal events, while the dates between 260 and 280 Ma closely match the age of the low-temperature hydrothermal phase. This pattern is consistent with a Rb/Sr isochron of altered whole-rocks and minerals grown during the low-temperature phase in Leuggern yielding 279 Ma (Tab. 4-6).

This time period (Autunian, Early Permian) is characterized by strong subsidence localized in deep Permo-Carboniferous troughs and is documented by thick piles of clastic sediments in Northern Switzerland as well as in other troughs of Central Europe (e.g. Massif Central, Saar-Nahe, Alps). Very probably, the low-temperature hydrothermal phase and deformation are genetically linked to these crustal movements in a transpressive/transpressive tectonic framework (ARTHAUD & MATTE 1977, DIEBOLD et al. 1991).

#### **4.5.9 Surface weathering**

At the end of the Early Permian, the topographic relief of the Variscan orogen was very low due to uplift, erosion and tectonic unroofing. Transpressive/transpressive crustal movements of the Saalian phase ceased and were followed by quieter sedimentation in the Late Permian, mostly localized in the subsiding troughs (cf. Chapter 3). Basement rocks outside the troughs were exposed to the surface before being covered by Late Permian (Rotliegendes) and/or Early Triassic (Buntsandstein) clastic sediments. At the end of the Paleozoic, Central Europe had virtually no relief, and the Variscan orogen had no topographic expression at all (peneplain). The Late Variscan granites (e.g. Böttstein, Siblingen) have been uplifted about 5 - 8 km since their intrusion in the Carboniferous.

Surface weathering in the crystalline rocks is limited to the uppermost few meters. Typical effects are feldspar dissolution and mica alteration, which are indicated by a decrease of the alkali contents. In some places, a basement grit has developed. Many effects of weathering are difficult to distinguish from those of the hydrothermal alterations.

#### **4.5.10 Kaolinitic alteration**

A different type of argillic alteration (postdating the illite-dominated low-temperature phase of section 4.5.8) is present in some of the boreholes (e.g. Kaisten, Siblingen, Böttstein, cf. Tab. 4-5) and is characterized by the clay paragenesis kaolinite + smectite, which replaces plagioclase or is encountered on fracture coatings. In Kaisten and Siblingen, the entire profiles are affected, while in Böttstein the kaolinitic alteration is restricted to the uppermost 300 m of the crystalline basement. The alteration affects plagioclase alone, while, in contrast to the illite-dominated alteration, biotite remains

unaffected. In addition to the clay minerals, very fine-grained calcite ( $\pm$  siderite) crystallizes both in the altered plagioclases and on fracture coatings. As in the case of the other alteration phases, no depth dependence of the kaolinitic alteration can be identified in the boreholes. In contrast to the older phases, this alteration is not linked to a major cataclastic deformation but rather to jointing. Very often, pre-existing structures of the older phases are reactivated.

No good time constraints are available for this phase, which could be due to a Mesozoic, Tertiary or recent event. K/Ar dates of illites from Kaisten, where this type of alteration is strongly developed, yield 126 - 138 Ma, i.e. Cretaceous dates (cf. Tab. 4-6). A Rb/Sr model age of illite is in the same interval. Dating by the Ar/Ar step-heating method confirmed the significance of these dates (i.e. they are not mixed ages due to rejuvenation). Possibly, these dates represent movements and associated hydrothermal activity along the Eggberg fault system, which is spatially related to the Kaisten borehole. However, a genetic connection to the kaolinitic alteration cannot be demonstrated conclusively. Alternatives for a genetic correlation of the kaolinitic phase comprise:

1. Early Cretaceous ages, as found in Kaisten and also reported by other authors in the Black Forest (cf. BROCKAMP et al. 1994). Possibly related to the opening of the Atlantic Ocean?
2. Cretaceous formation of the Rhine Dome, followed by significant erosion of Mesozoic cover rocks. The "Rhine Dome" high, a major crustal bulge, developed in the Cretaceous and separated the Tethys realm from the North Sea basin (BACHMANN et al. 1987).
3. Early Tertiary formation of the Rhine Graben and Tabular Jura. A mantle plume with associated volcanism developed beneath the Rhine Graben, and the Black Forest was uplifted.
4. Folding of the Jura Mountains about 10 Ma before present. Even though most of the deformation is restricted to Mesozoic and Tertiary sediments, some effects on the crystalline basement cannot be excluded.

It is also possible that kaolinite has been generated in more than one single event. Regardless of the exact timing of the kaolinitic alteration, similar geochemical conditions probably still define the present hydrogeochemical system.

Difficulties in attributing the highly saline fluid inclusions to either the low-temperature or the kaolinitic phase are outlined above.

#### **4.5.11 Generation of vugs/channels and mineralizations**

The timing of the generation of vugs/channels and mineralizations in relation to the kaolinitic alteration is not entirely clear; the two events could in fact be contemporaneous. Similarly to the kaolinitic alteration, no major deformation is linked to this event.

Open channels (mm-cm scale) were generated in pre-existing structures, preferentially cataclastic matrices, by partial dissolution of the very fine-grained and porous infills. Conspicuous, idiomorphic crystals of calcite, fluorite, barite, siderite, celestite and minor ore minerals were deposited in the vugs. These open channels are of prime importance for present-day permeability and hydrodynamics of the crystalline basement. HOFMANN & EIKENBERG (1991) distinguish two phases of barite deposition in the Black Forest, a first in the Late Carboniferous (295 Ma) and a second in the Tertiary (50 Ma).

The kaolinitic alteration and the generation of vugs/channels with mineralizations are the youngest rock/water interactions identified in the rocks, and these processes may still be continuing. For the purpose of geochemical modeling (e.g. groundwater evolution), rock/water interactions characteristic of the kaolinitic alteration and of the mineralizations in vugs are used as representative features of the recent hydrogeochemical system.

#### **4.5.12 Summary: Late- and post-Variscan evolution of the basement of Northern Switzerland**

The post-metamorphic/post-magmatic evolution of the basement of Northern Switzerland and of the Black Forest, based on the above discussion and additional stratigraphic evidence (cf. Fig. 3-2), is summarized in Table 4-7.

stratigraphic age	radiometric age [Ma] (if available)	event
Early Tertiary	50	Secondary remobilization of ore veins (related to the formation of the Rhine Graben), uplift of the Black Forest.
Mesozoic or Tertiary (...recent?)		Kaolinitic phase, jointing, formation of vugs/channels.
Middle Triassic (Muschelkalk)		Marine transgression.
Permian/ Early Triassic		Post-orogenic formation of a peneplain throughout Central Europe, erosion and surface weathering of the crystalline basement.
Late Permian		Dilational subsidence of the Permo-Carboniferous troughs, thick clastic sedimentation.
Early Permian	260 - 280	"Saalian phase" of the Hercynian orogeny: Vertical movements in the crust, locally rapid subsidence -> deformation in deep Permo-Carboniferous troughs; transpressive/transpressive tectonic regime.  Low-temperature phase in granites and gneisses (cataclasis, jointing, alteration).
Stephanian (Uppermost Carboniferous)		Basement uplift, formation of sedimentary troughs along major faults; syn-tectonic sedimentation, coal seams.
Late Carboniferous	290 - 320  ca. 295  290 - 310	High-temperature phase in granites and gneisses (cataclasis, jointing, alteration); significant basement uplift and unroofing.  Formation of ore veins.  Extrusion of rhyolitic sheets in the Black Forest, intrusion of rhyolite porphyry dykes.
Late Carboniferous	ca. 314	Retrograde effects in granites (muscovite formation, tourmaline-quartz veins, ductile quartz deformation).
Early Carboniferous	314 - 334	Intrusion of Late Hercynian granites and basic magmatites, followed by intrusions of dykes.

**Tab 4-7 :** Post-metamorphic/post-magmatic evolution of the basement of Northern Switzerland and of the Black Forest.

## 5 STRUCTURAL ELEMENTS OF NORTHERN SWITZERLAND AND SCHEMATIC FAULT MODELS FOR THE CRYSTALLINE BASEMENT

This Chapter, after a short glossary (5.1), outlines (in 5.2) the structural inventory of the individual tectonic units as defined in Chapter 3 (cf. Fig. 3-1). On the basis of this inventory, schematic fault networks and fault models have been developed for the crystalline basement in the two potential siting areas. These networks and models which served as input for hydrodynamic modeling (cf. Chapter 8) and for developing strategies of future exploration (cf. Chapter 11) are reviewed in the later part of the Chapter (5.3).

### 5.1 Glossary of terms

In this Chapter a specific terminology is used when referring to faults, their characteristics and geometric relationships. These terms are defined in the following short glossary:

**FAULT CLASSIFICATION:** based on present knowledge and in view of the intended applications the following four categories have been distinguished (details are provided in Table 5-1 and in the text):

- 1st and 2nd order faults: large fault zones of regional significance,
- higher order faults (fault zones): smaller faults, generally of local significance and often associated with 1st and 2nd order faults,
- extensional discontinuities without infill (e.g. open joints) and
- extensional discontinuities with infill (e.g. dykes and veins).

**FAULT FAMILY:** a regionally significant set of faults striking roughly parallel; mostly 1st and 2nd order faults (cf. Tab. 5-1); generally, but not necessarily, of the same origin and with a similar geological history.

In the traditional local (German) geological literature proper names are used for some of the regionally consistent strike directions of structural elements. These names are also used in Chapter 5 (e.g. for the strike direction of fault families):

- *Hercynian* (direction), strike approx. WNW-ESE (110°), e.g. Vorwald fault,
- *Eggian* (direction), strike approx. NNW-SSE (150°) and
- *Rhenish* (direction), strike approx. N-S (180°), dominating feature is the URG.

**FAULT MODEL:** the geometric arrangement of faults or fault families in space. A fault model West (Böttstein - Kaisten - Leuggern - Zurzach) and a fault model East (greater Siblingen area) have been defined (cf. section 5.3.4 and 5.3.5).

**FAULT NETWORK:** the geometric arrangement of faults or fault families on a single horizontal plane, e.g. the outcrop pattern of faults on a map. A fault network West (Böttstein - Kaisten - Leuggern - Zurzach, cf. Fig. 5-7) and a fault network East (greater Siblingen area, cf. Fig. 5-8) have been defined.

*SCHEMATIC (fault network):* due to the lack of data in some areas a generalized distribution of faults has to be postulated. It is assumed that, within a single family, the faults are (sub-) parallel and regularly spaced. Although a schematic fault network does not predict the location of individual faults, each (schematic) fault family is fixed geographically in relation to the known features.

## **5.2 Inventory of regional structures**

The inventory of structural elements within the individual tectonic units that were defined in Chapter 3 (cf. Fig 3-1) should give an indication of the prevailing regional and local structural trends.

Emphasis is placed on those tectonic units that provide direct structural information about the crystalline basement in the area of interest to Nagra. A reliable interpretation of relevant data is based either on field data from basement outcrops in the Southern Black Forest or the deep boreholes and/or from reflection seismic surveys. Where such data are unavailable, overburden structures can often be used to infer the structural pattern of the underlying crystalline basement, e.g. in the Tabular Jura.

For a detailed discussion of regional tectonics, reference should be made to HUBER & HUBER-ALEFFI (1990) and DIEBOLD et al. (1991).

### **5.2.1 The Upper Rhine Graben (URG) and the Rhenish fault pattern of Northern Switzerland**

In past decades, the development, structure and neotectonics of the Upper Rhine Graben (URG) have been the subject of intensive investigations, resulting in a comprehensive body of information. The approximately NNE-SSW-striking Paleogene rift graben (cf. section 3.3.1) is controlled by first order (cf. Tab. 5-1) regional fault zones trending in the so-called Rhenish strike direction (N-S to NNE-SSW), which also dominates the basement below the western Tabular Jura and the Dinkelberg block (cf. App. 3-1, Fig. 5-1). The important questions are: To what extent do these Rhenish striking faults also occur in the basement of the Kaisten-Leuggern-Böttstein region and around Siblingen, and what is their character in these areas.

The rifting of the URG in the Early Tertiary was probably oriented along an inherited sinistral shear zone which was produced during a Late Variscan compression phase (cf. section 3.2, e.g. ILLIES 1962, EISBACHER et al. 1989). The Paleogene stress field reactivated this weak zone as an extensional graben structure (cf. LAUBSCHER 1992). The stratigraphic successions in the southern URG, well-known from numerous boreholes, indicate that the western part was first to subside (Graben of Dannemarie, Fig. 5-1). The rift extended eastwards and reached up to the Rhine Graben Flexure east of Basel during the Oligocene (RF in Fig. 5-1). The Rhenish faults of the Dinkelberg and the western Tabular Jura are thus located outside the actual rift. The formation of the numerous Rhenish-striking faults to the east of the Graben area is

probably due to a combination of both the extension reaching out towards the E and an early uplift phase of the Central Black Forest. As a result, large basement blocks were successively broken up along pre-existing basement faults. Furthermore, due to a S tilt, their sedimentary cover became involved in southwards gravity gliding (e.g. Mettau overthrust, Fig. 3-1; HERZOG 1956, LAUBSCHER 1982, GÜRLER et al. 1987, WILDI 1975).

The Paleogene uplift phase of the Black Forest led, at the same time, to an accentuated reactivation of inherited Late Paleozoic, Hercynian-striking faults in the region of the Dinkelberg and Fricktal blocks (e.g. Kandern-Hausen fault, Rheinfeldern fault, K and R in Fig. 5-1). The two most important structural trends of the area were thus superimposed as an expression of the general extension during the Oligocene.

To the east of the Wehra-Zeiningen fault zone (W in Fig. 5-1), the Rhenish faults are of secondary importance only. It may be assumed that the influence of the Oligocene URG rift tectonics decreased in this area. Here, the Rhenish faults are no longer as dominant as in the west. Sediments which cover the crystalline basement in the potential siting regions in Northern Switzerland eastern Tabular Jura illustrate only second order Rhenish-striking faults (cf. App. 5.1). The fault network mapped at the surface in this area is dominated by more or less WNW-ESE trending Hercynian and WSW-ENE to SW-NE (i.e. almost Jura-parallel) structural trends.

The development of the Rhenish fault pattern can be summarized as follows:

- the Rhenish-trending elements are part of the structural plan which was inherited from the Paleozoic. They dominate in the region of the Upper Rhine Graben. The rift structure is superimposed on a Late Variscan (sinistral) shear zone, the Rhenish lineament, which was reactivated during the Early Tertiary;
- to the east of the URG, a Rhenish fault pattern still can be found in the basement and its sedimentary cover, but not as a dominant feature;
- Rhenish-striking fault zones both in the URG and the wider region are being reactivated as neotectonic sinistral shear zones (cf. Chapter 9).

### **5.2.2 The fault pattern of the sedimentary cover of Northern Switzerland (App. 5-1)**

In Northern Switzerland the crystalline basement is concealed below Mesozoic sediments (Tabular Jura), except locally around Laufenburg. Here, deep boreholes and reflection seismics are the only adequate exploration tools. But, as stated in Chapter 3, seismics are not able to provide coherent information about structures such as fault planes within the crystalline basement (cf. Fig. 5-6).

In general the autochthonous sedimentary cover can be mapped by means of reflection seismics. The structural inventory of the Tabular Jura provides indirect information about the basement, because all post-Mesozoic vertical displacements of the basement surface are copied into the overlying sediments.

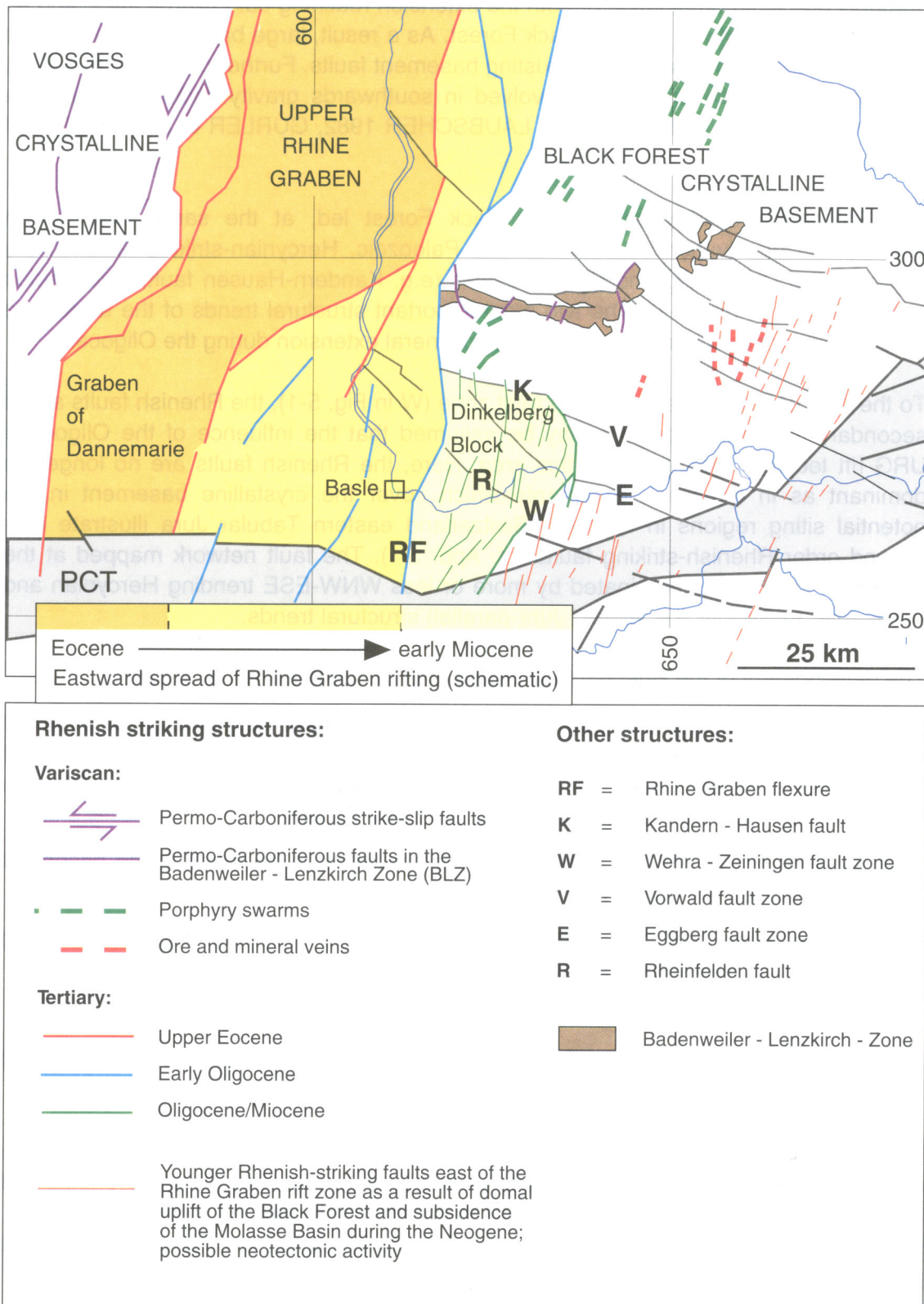


**Fig. 5-1 :** Evolution of Rhenish striking structures in the Rhine Graben and adjacent areas.

Therefore, conclusions can be drawn about the presence and strike of faults (mainly normal faults) which extend from the sediments down into the basement. The fault pattern of the Base Mesozoic (cf. Fig. 5-2) as mapped by seismics should include the main fault families of post-Paleozoic basement tectonics. It provides, with all the inherent uncertainties of the mapping method, the only relevant information about basement structures between the Nagra boreholes of Northern Switzerland.

A synoptic analysis of all the data relating to the sedimentary cover of Northern Switzerland shows a coherent regional picture (cf. NAEF & DIEBOLD 1990).

From N to S the following 3 tectonic units have been distinguished (cf. Fig. 3-1 and App. 5-1):

1. *The Tabular Jura s.str.*, where autochthonous Mesozoic and Cenozoic sediments overly the basement tectonically conformably;
2. *The Detached Tabular Jura*, which has been slightly dislocated due to décollement in front of the Folded Jura
3. *The Folded Jura* as the product of compressive, Late Alpine décollement tectonics during the Neogene.

### **Tabular Jura s.str. and autochthonous Molasse of Northern Switzerland**

The Tabular Jura s.str., which includes the autochthonous northern part of the Molasse Basin, is considered here as one tectonic unit (Fig. 3-1). The structural inventory of this area provides key information on the post-Permian evolution of the basement (App. 5-1, DIEBOLD et al. 1991).

In the area between Kaisten and Leuggern, the original bedding of the Tabular Jura is disturbed along the Mettau thrust. Here, due to SE-vergent gravity gliding, the sedimentary cover is detached from the basement in a narrow zone between the Mettau thrust and the Rhine (Fig. 3-1b, App. 5-1). The quality of reflection seismics in this zone is poor and a reliable correlation between cover and basement is difficult to establish. However, based on the fault pattern to the north of the Rhine (Vorwald and Dinkelberg blocks), it can be stated that Hercynian- (WNW) and Eggen-striking faults (NNW) prevail to the east of Laufenburg. While the Rhenish trend (N-NNE) still dominates in the west (Fricktal block), to the east of a line Wölflinswil Graben (App. 5-3) - Kaisten it is no longer dominant and, further to the east, only very few Rhenish faults have been observed.

In the eastern Tabular Jura between Waldshut and the Randen fault zone, the fault pattern is dominated by Hercynian-striking features. The young horst and graben tectonics of the SE Black Forest in some cases appear to extend to the ESE into the Molasse Basin (1st and 2nd order faults, cf. Tab. 5-1, Fig. 5-8). In addition, there is a varied spectrum of higher order faults which are difficult to summarize into statistically significant fault families. As only scarce seismic information is available here (Fig. 2-1a), the data are based mainly on surface geology.

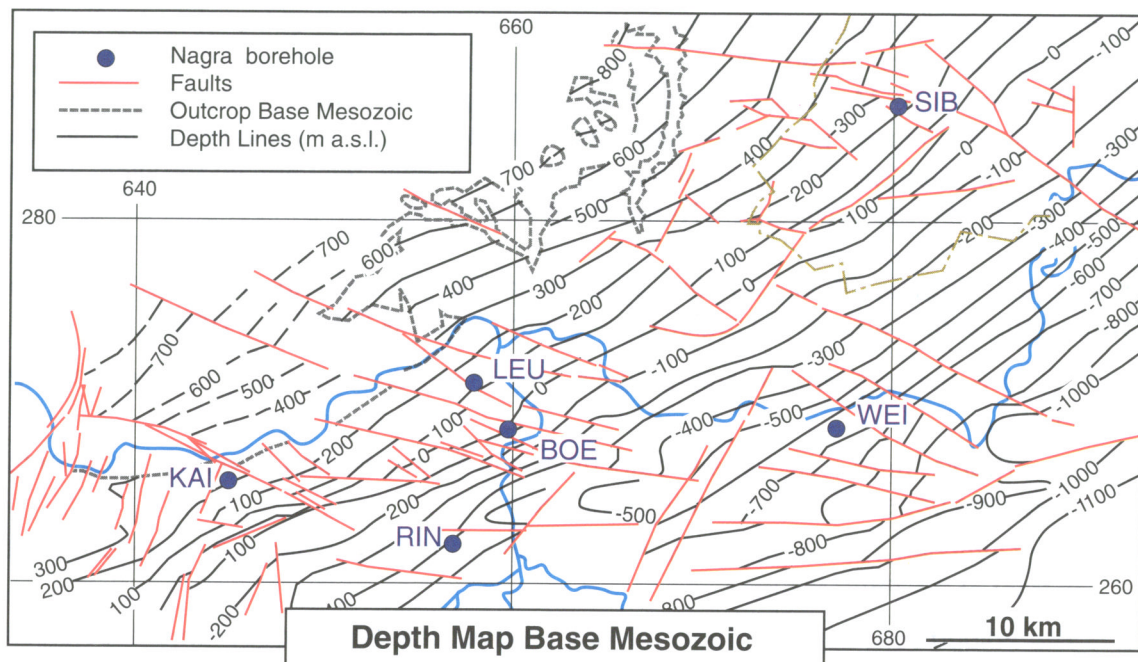


**Fig. 5-2 :** Simplified depth map of the seismic marker "Base Mesozoic" showing identified faults that were active during the Tertiary.

In the area overlying the PCT, to the south-east of a line Beznau - Siblingen, several flexures (Siblingen, Rekingen, Rheinfelden, Rüdlingen flexures), and both thetic and antithetic faults are known. These have a trend parallel to the PCT and provide evidence for extensional tectonics (e.g. line 84-NF-65, cf. App. 5-1). At the northern boundary of the Molasse deposits, the facies pattern, the depositional edges and the isopachs of individual Molasse formations (mainly USM and OMM) show an alignment along these PCT-parallel flexures. They are therefore identified as external marginal flexures of the Molasse Basin and are presumed to be an expression of syn-depositional extensional tectonics during the Oligo-Miocene. The Permo-Carboniferous Trough of Northern Switzerland therefore acted as hinge zone between meso-Europe to the north and the Alpine foreland to the south ("Molasse Basin").

### **The Detached Tabular Jura and the eastern end of the Jura décollement thrust**

The southern Tabular Jura is characterized by a series of compressive structures which evolved beyond the front of the Folded Jura. Morphologically this zone forms part of the Tabular Jura but, from the point of view of tectonics, it belongs to the sheared-off overburden. For this reason it is treated as an independent tectonic unit and called the "Detached Tabular Jura" (cf. Fig. 3-1).

To the west of the Aare river, the Detached Tabular Jura is clearly delimited to the north by the frontal Mandach thrust fault and to the south by the main Jura décollement overthrust. To the east of the Aare, clear dividing lines disappear and the Detached Tabular Jura peters out - similarly to the Folded Jura - beneath the eastern Molasse.

The area north of the Lägeren is particularly interesting; it is well-documented by numerous geological maps, seismic lines and the Weiach borehole, the latter having cored the most complete sedimentary sequence in the area. Flexures and anticlines strike mainly parallel to the underlying PCT - similar to the situation in the Tabular Jura s.str. to the north. However, in this area surface structures in the Mesozoic sediments are the expression of a late Miocene Alpine compressive tectonic event which is superimposed on older extension lineaments (marginal flexures) in the underlying basement. This relationship between extensional structures in the basement and compression features in the detached overburden has been illustrated in a set of structure maps for the marker horizons Base Mesozoic - Top Liassic - Base Tertiary (cf. DIEBOLD et al. 1991: App. 33 - 35; NAGRA 1988b: App. 7 - 8; LAUBSCHER 1985; profile in App. 5-1).

A concordant deformation of Mesozoic as well as all Tertiary (Molasse) sediments indicates that the compressive overprinting of the Detached Tabular Jura is an event that occurred after Molasse sedimentation. Early Pleistocene gravels (Deckenschotter) which overlie the Molasse on an erosional unconformity are not affected by this deformation, i.e. there is no perceptible post-Early Pleistocene tectonic activity.

The structural configuration of the sedimentary cover in the area between the Black Forest crystalline basement and the Jura décollement front - i.e. the Tabular Jura s.str. and the Detached Tabular Jura - must both be considered as key areas for the reconstruction of Neogene tectonics in the basement of Northern Switzerland.

### **Folded Jura and sheared-off Molasse**

The thrust and folded sediments of the Folded Jura are of minor importance for understanding the basement structures of Northern Switzerland. To a very limited extent, the relief at basement level can be reconstructed from surface geology data. However, seismic data indicate a close relationship between extension structures in the basement and the orientation of the Jura chains. From the tectonic sketch map of the eastern Folded Jura (based on seismics), it is apparent that Hercynian-striking and PCT (and Jura)-parallel directions dominate (Fig. 5-3; DIEBOLD et al. 1991: Fig. 29). These directions must therefore be considered as prevailing trends for the basement structures of Northern Switzerland, also below the Folded Jura, with Rhenish elements being of secondary importance.

### 5.2.3 The Permo-Carboniferous Trough of Northern Switzerland (PCT)

The three-dimensional basement structure of the Southern Black Forest and of Northern Switzerland can be traced only locally on the basis of a few available artificial (boreholes, tunnels) and natural exposures.

Reflection seismics have been shown to give no interpretable results from within the crystalline basement (SPRECHER & MÜLLER 1986, DIEBOLD et al. 1991, cf. also Fig. 5-6). Therefore, any regional reconstruction must remain hypothetical in character.

However, in this respect the seismic mapping and interpretation of the PCT has been helpful for the development of a three-dimensional structural concept of the crystalline basement. Owing to the very good reflectivity of coal series, the complex structure of this Late Paleozoic graben system is known in broad outline, and in some cases in considerable detail (Weiach borehole). It can safely be assumed that the tectonic processes which formed and altered the PCT in several phases also affected the surrounding crystalline basement. This is illustrated by the Vorwald fault zone along which the Variscan Albtal granite (320 Ma) has been dextrally displaced by some 5 km, probably in pre-Upper Permian times (App. 5-3). The structural inventory of the northern margin of the PCT (Fig. 3-3) can, in general, be expected to be present, albeit in a weaker form, in the neighboring crystalline basement.

Appendix 5-2 gives an idea of the complex conditions which have been reconstructed using reflection seismics data (cf. also Fig. 3-3 and 5-4). Based on LAUBSCHER's (1987) approach, a multiphase evolution of the PCT with several typical structural trends is postulated. Wherever possible an attempt was made to correlate these findings with the most recent data from other Central European Permo-Carboniferous regions (cf. section 3.1 and, for more detail, DIEBOLD et al. 1991).

To summarize, four key structural elements can be defined in the PCT (1st and 2nd order faults):

- early, approximately ENE - WSW (60°)-striking normal faults mark the subsidence of the Upper Carboniferous-Lower Permian Trough. Some of these structures were reactivated as normal faults in the Late Permian and/or the Tertiary ("1" in App. 5-2). These faults were partly reactivated during the Saalian tectonic phase as steeply dipping, transpressive reverse faults ("2" in App. 5-2).
- younger, Hercynian-striking wrench fault zones, along which the PCT was sheared dextrally during the Saalian phase in the Early Permian ("3" in App. 5-2; cf. section 3.1). During the post-Saalian phase up to the Early Triassic, and then during the Oligo-Miocene, some of these zones were reactivated as normal faults ("4" in App. 5-2).

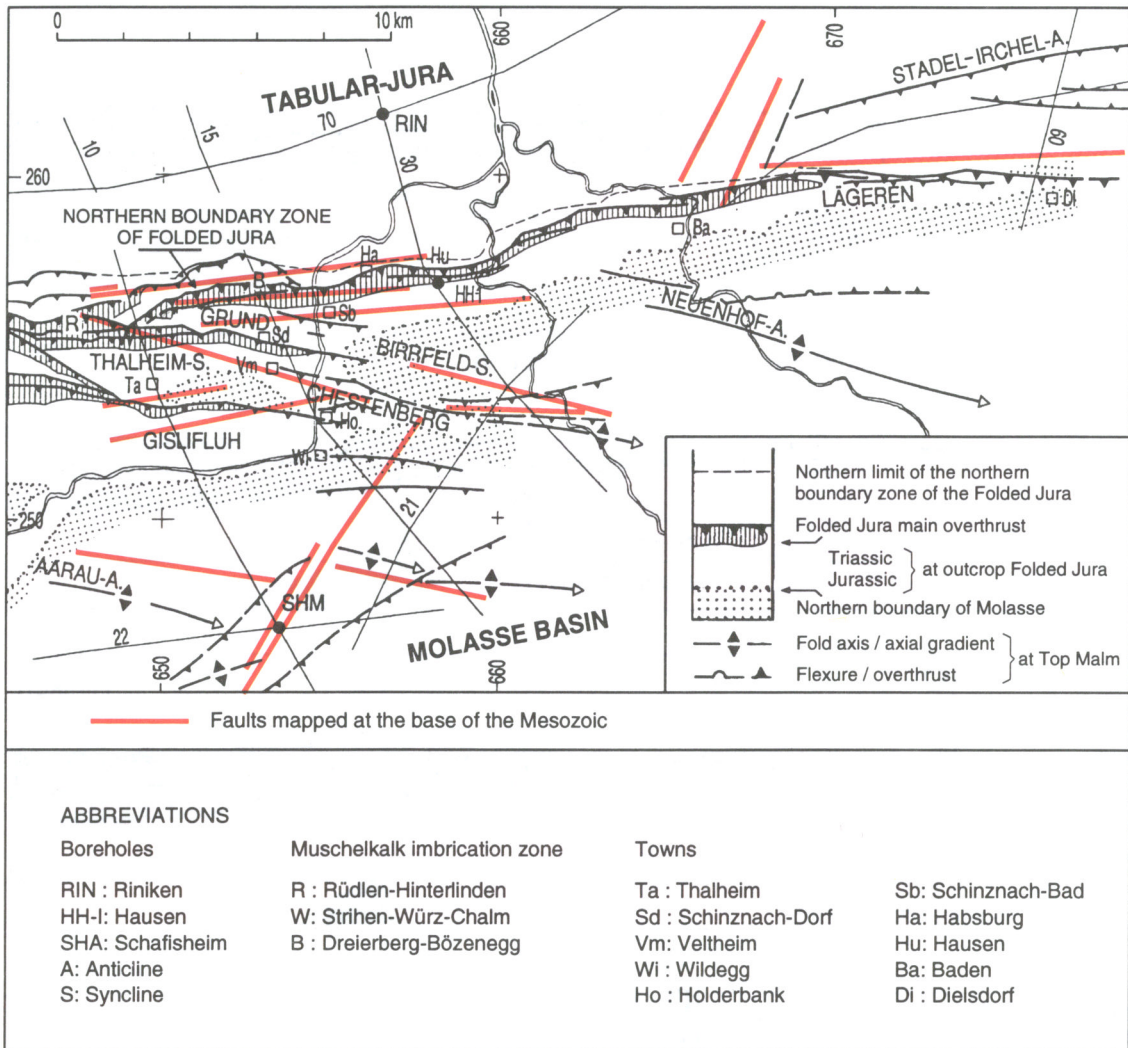


**Fig. 5-3 :** Tectonic sketch map of the eastern end of the Folded Jura. The Hercynian (WNW-ESE), "Jurassic" (WSW-ENE) and Rhenish (NNE-SSW) striking fault zones mapped at the base of the Mesozoic acted as a template for the fold trend in the overlying Folded Jura.

**5.2.4 Structural elements in the Southern Black Forest and the crystalline basement of Northern Switzerland**

The crystalline basement of the Southern Black Forest and Northern Switzerland forms part of the Central European crust which was consolidated around 250 Ma. After a long phase of relative tectonic inactivity during the Mesozoic, this Central European crust was again subjected to tectonic activity as the foreland of the Alpine orogeny since the Cretaceous. During various phases with differently oriented stress fields,

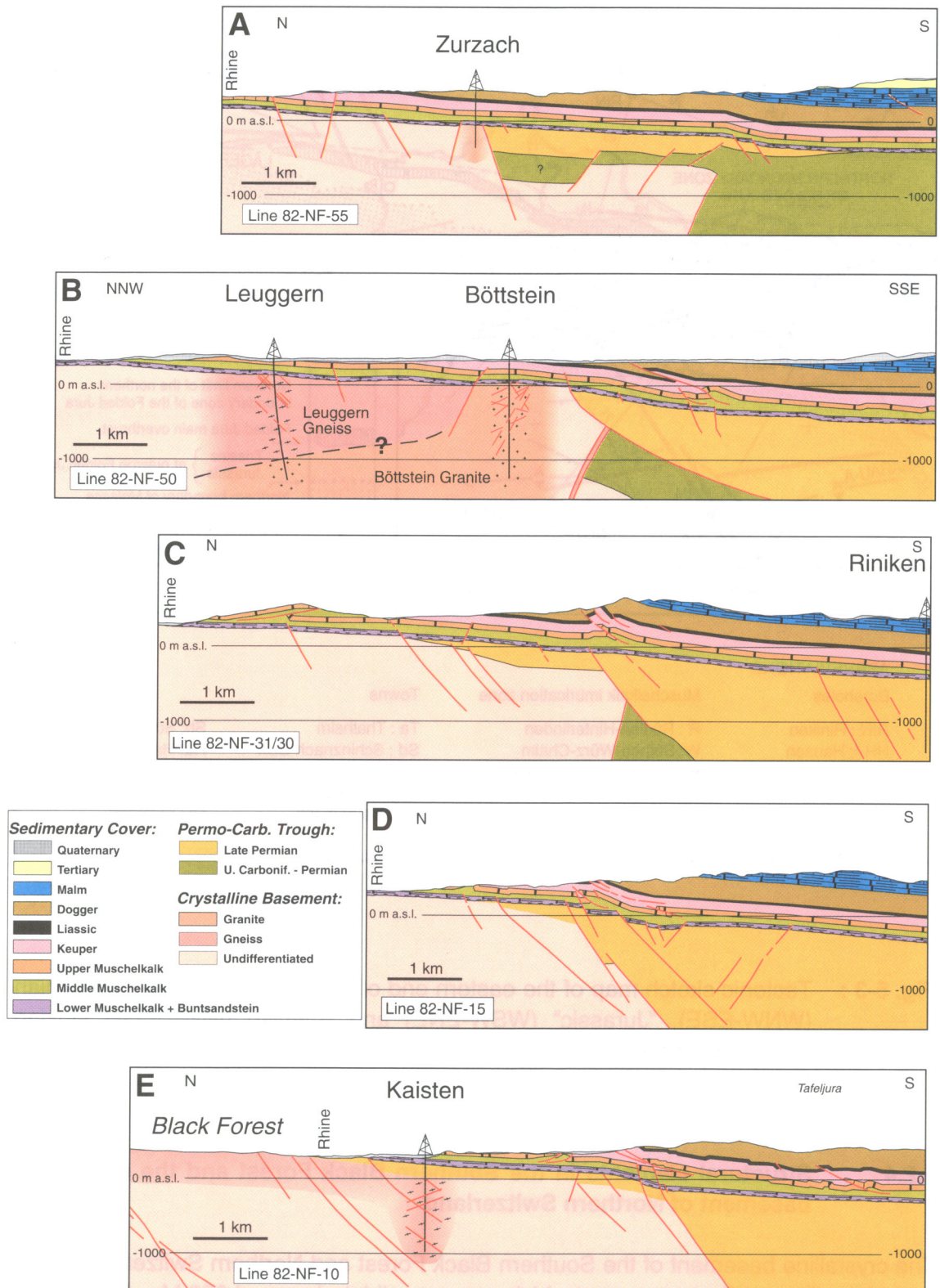
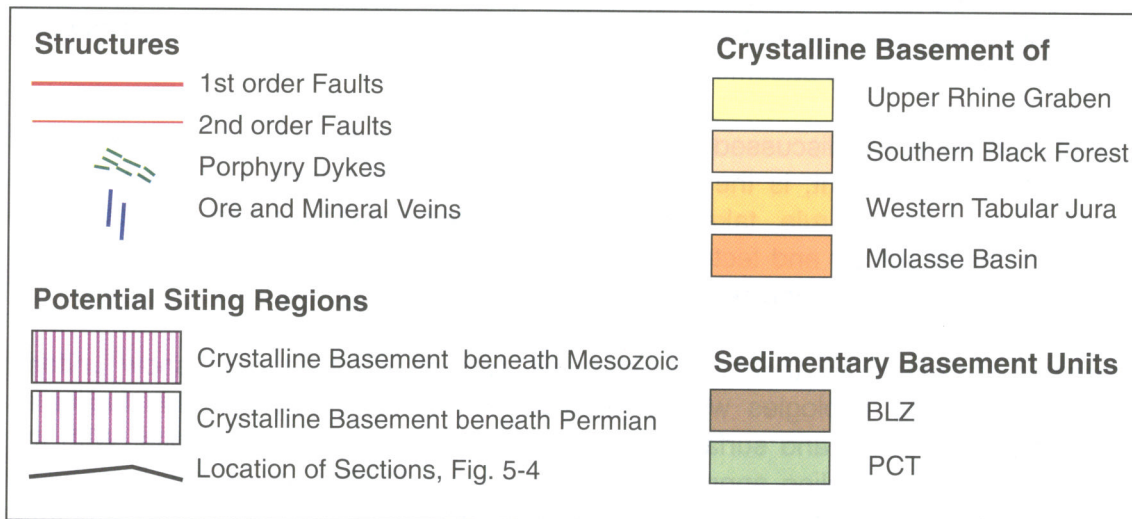
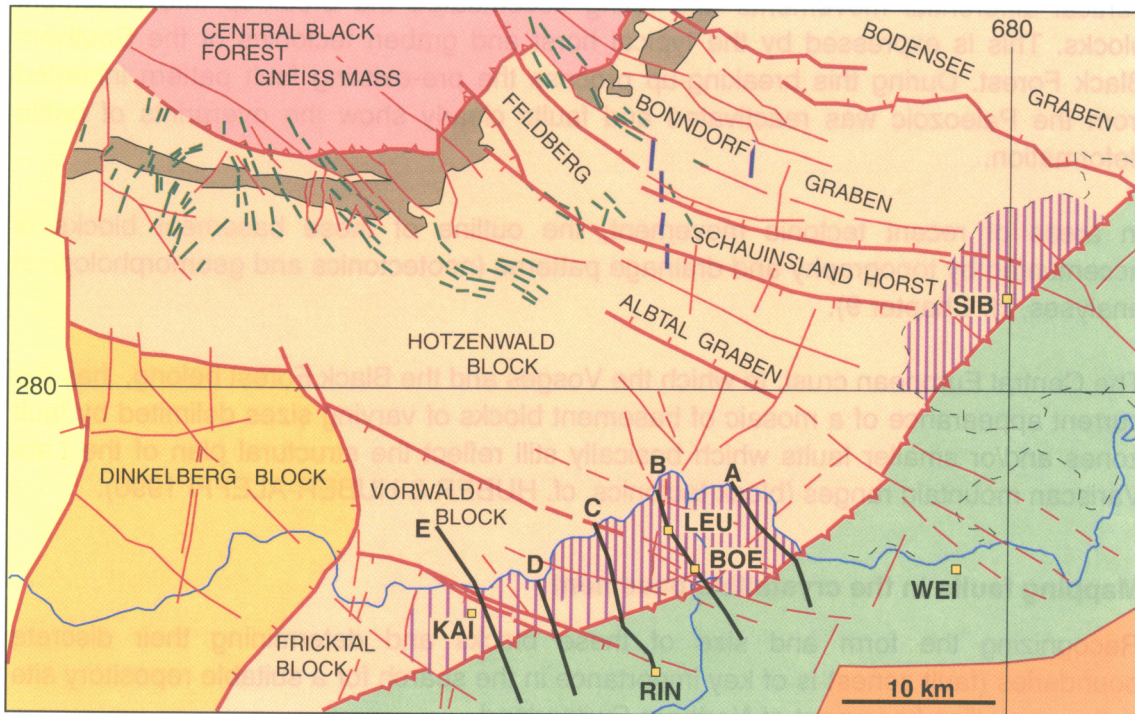


Fig. 5-4 : Geological profiles through the potential siting area West based on seismic and well data. For location of lines cf. Fig. 5-5.



**Fig. 5-5 :** Overview of the basement of the Black Forest - Northern Switzerland and adjacent units; Mesozoic/Tertiary uncovered.

vertical differential movements and rifting accentuated the break-up into basement blocks. This is expressed by the typical horst and graben tectonics of the Southern Black Forest. During this breaking-up process the pre-existing fault pattern inherited from the Paleozoic was reactivated and faults clearly show the overprints of brittle deformation.

In areas of recent tectonic movement, the outline of these basement blocks is accentuated by topography and drainage patterns (neotectonics and geomorphological analyses, cf. Chapter 9).

The Central European crust, to which the Vosges and the Black Forest belong, has the current appearance of a mosaic of basement blocks of varying sizes delimited by fault zones and/or smaller faults which basically still reflect the structural plan of the Late Variscan mountain ranges (block tectonics, cf. HUBER & HUBER-ALEFFI 1990).

### **Mapping faults in the crystalline basement**

Recognizing the form and size of these blocks and determining their discrete boundaries (fault zones) is of key importance in the search for a suitable repository site in the crystalline basement of Northern Switzerland.

Figure 5-4 shows a set of geological profiles crossing the potential siting area West. These profiles are based on a compilation of data from surface geology, seismics and boreholes. They clearly demonstrate actual exploration problems: there is a striking difference in the resolving power of available mapping tools between the sedimentary cover and the crystalline basement.

Common to the faults discussed in sections 5.2.2 to 5.2.4, both in the sediments and the crystalline basement, is the fact that all show at least some brittle deformation (cataclasis) and, as a rule, take the form of discrete, narrow zones. However, the evolution, the character and tectonic setting of faults in the crystalline basement differ significantly from those in the sedimentary cover.

Mesozoic sediments by their very nature as epicontinental deposits show uniform laterally extending lithologies with a pronounced vertical variability. This facilitates detection, by seismics and surface geology, even of relatively small faults. With the help of accepted modeling approaches and analogue studies, even very incomplete datasets can be used to reconstruct the tectonic development and general structural plan of a larger area (cf. e.g. MANDL 1988).

With Tertiary and/or neotectonic reactivation, block boundaries (faults) can also be traced from the basement into the overlying sediments and mapped to a certain extent at the surface. In the area of the Folded Jura, reflection seismics proved invaluable for mapping the structure of the autochthonous cover (tegument, cf. Fig. 3-1) under the detached and folded sediments.

In contrast to the situation in the sedimentary cover, basement faults are significantly more varied and more difficult to interpret. This is due partly to their long and complex

history characterized by phases of both ductile and brittle deformation as well as metamorphic and hydrothermal overprinting (Fig. 3-2; cf. Chapter 4). In addition, the stratification characteristics of sedimentary rocks are largely absent in the spatial disposition of the different crystalline lithologies. The general lack of features correlatable across faults makes an assessment of fault displacement virtually impossible. As a consequence it is very difficult to assign discontinuities in crystalline rocks (e.g. cataclastic zones, fault gouge, etc.) observed locally in artificial and/or natural exposures to given fault categories (Tab. 5-1).

Therefore, it has to be assumed that some fault zones, even large ones, remain unidentified to date. It is also not surprising that correlation of structures from artificial exposures (drifts, boreholes) with those identified at the surface is rarely satisfactory (cf. HUBER & HUBER-ALEFFI 1990, AMMANN et al. 1992).

Exploration using reflection seismics is fraught with similar problems: correlation and extrapolation are impossible even over short distances. Although a large number of generally diffuse reflections can often be identified in the crystalline basement, their conclusive interpretation is impossible without additional information (cf. Fig. 5-6).

Lineament studies and morphostructural analyses are valuable tools for reconstructing the regional structure pattern. Work in the South-east Black Forest has already made a significant contribution to the understanding of block geometry and neotectonic activity (summaries in HALDIMANN et al. 1984, HUBER & HUBER-ALEFFI 1990, cf. also App. 5-3).

Attempts to reconstruct and correlate regional structural features in the South-eastern Black Forest by analyzing small-scale structures, particularly joints and fractures, have been of limited success so far. The results are generally only of local significance because the lithological anisotropies and existing discontinuities in the rock are still insufficiently understood on a regional scale (e.g. WIRTH 1984).

All of the above limitations have to be borne in mind when preparing an inventory of fault zones for the crystalline basement. Basically the following applies: basement faults active during Tertiary to recent are more likely to be detected by exploration than older faults which remained inactive after the Variscan orogeny. This in turn means that the structural plan with which we are familiar today for the crystalline basement of the Southern Black Forest and Northern Switzerland focuses on the younger fault pattern and thus on the post-Variscan break-up (into blocks) of the basement.

### **5.2.5 Description of the key structures**

Using information obtained from boreholes, geological mapping and, in particular, from reflection seismics a structural map has been drawn for the Base Mesozoic in the region (Fig. 5-2). Such a map illustrates both the pattern of faults which have been active in the basement during the post-Permian and the extent of vertical movements along these faults (cf. DIEBOLD et al. 1991, App. 35).

Definition		Example	Geological Identification		Character / Modeling
Discontinuity	Features		Surface	Borehole	
Deep-reaching tectonic lines (lineaments, geosutures)	Displacement: > 1 km (vertical and/or lateral) length > 10 km width: 100 m - > 1 km	Boundary faults PCT, Rhine Graben flexure, Thrust planes BLZ	Regional mapping, aerial photography, geophysical surveys	Identification requires additional information from surface mapping and/or seismics	Supraregional structures only as boundary conditions for model, delimiting of large blocks; consists of a network of 1st and 2nd order faults.
1st order fault (or fault zone)	Displacement: > 100 m (vertical and lateral) length: > 10 km width: 100 m - 1 km (generally in several fault branches)	Hercynian-striking block boundaries of SE Black Forest: e.g. Vorwald fault (cf. Fig. 5-8).	Geophysical methods (mainly seismic), morphostructural analysis (mapping)		Important dominant structures, location well-known, character very heterogeneous, multiphase etc.
2nd order fault (or fault zone)	Displacement: 10 - 100 m (vertical and lateral) length: several km - ca. 10 km width: several m - 100 m	Rhenish fault family in the area West.	Seismics, mapping, morphostructural analysis		Very varied element. Modeled as fault family of regional extent and partly as accompanying elements of 1st order faults. Boundaries of sub-blocks.
3rd order fault	Displacement: 1 -10 m length: several dm - few km width: several dm - several m	The majority of the so-called disturbed core sections in the Nagra deep boreholes.	Geological mapping	Cores + logs	Not taken into account in the model since the regional systematics are not well-known. Only local modeling in the vicinity of boreholes possible.
Small fault	Displacement: < 1 m length: dam-range width: up to a few dm		Geological mapping, mainly in outcrops	Cores + logs	Regional modeling not possible. Secondary systems of larger fault zones.
Joints, fissures	No displacement length: dm - dam width: mm- to cm-range	Locally significant fracture systems in deep boreholes of Northern Switzerland.	Detailed outcrop mapping	Cores, logs + thin sections	Different fracture generations accompanying faults or as spatially extensive systems. Restricted regional (not local) modeling possible.
Dyke, ore vein	Thickness > 2 dm (ore veins > 3 dm) length: dam - a few km, mostly with distinct joint pattern, often regular trend	Dyke swarms of Leuggern, ore and mineral veins of the SE Black Forest.	Geological field work with mapping, geophysical methods (magnetic etc.)	Cores, logs + thin sections	± planar structures with constant orientation, of local and sometimes regional significance, restricted modeling possible.
Vein	Thickness: < 2 dm length: cm - few m no distinct joint pattern, generally irregular trend		Detailed outcrop mapping	Cores, logs + thin sections	Secondary significance. Regional modeling not possible.
Mobilisation, injection, schlieren	Thickness: cm- and dm-range length: cm - few m often associated with material deposits, unclear contacts	Migmatites in the Kaisten gneiss.	Detailed outcrop mapping	Cores, logs + thin sections	Lithological discontinuity. Only important if overprinted by a fault.

Tab. 5-1 : Systematics of faults and lithological discontinuities in the basement  
(AMMANN et al. 1992).

The important fault zones strike primarily WNW-ESE to NW-SE (Hercynian) and, to a lesser degree, also NNE-SSW (Rhenish). They have dip slips of up to several decameters and can thus be mapped seismically in the sedimentary cover. In the marginal zone of the PCT, trough-parallel structures have been mapped in the strike direction ENE-WSW (strike of Folded Jura). Additionally, faults striking around NNW-SSE (Eggian), particularly in the Vorwald and Hotzenwald blocks, can be recognized.

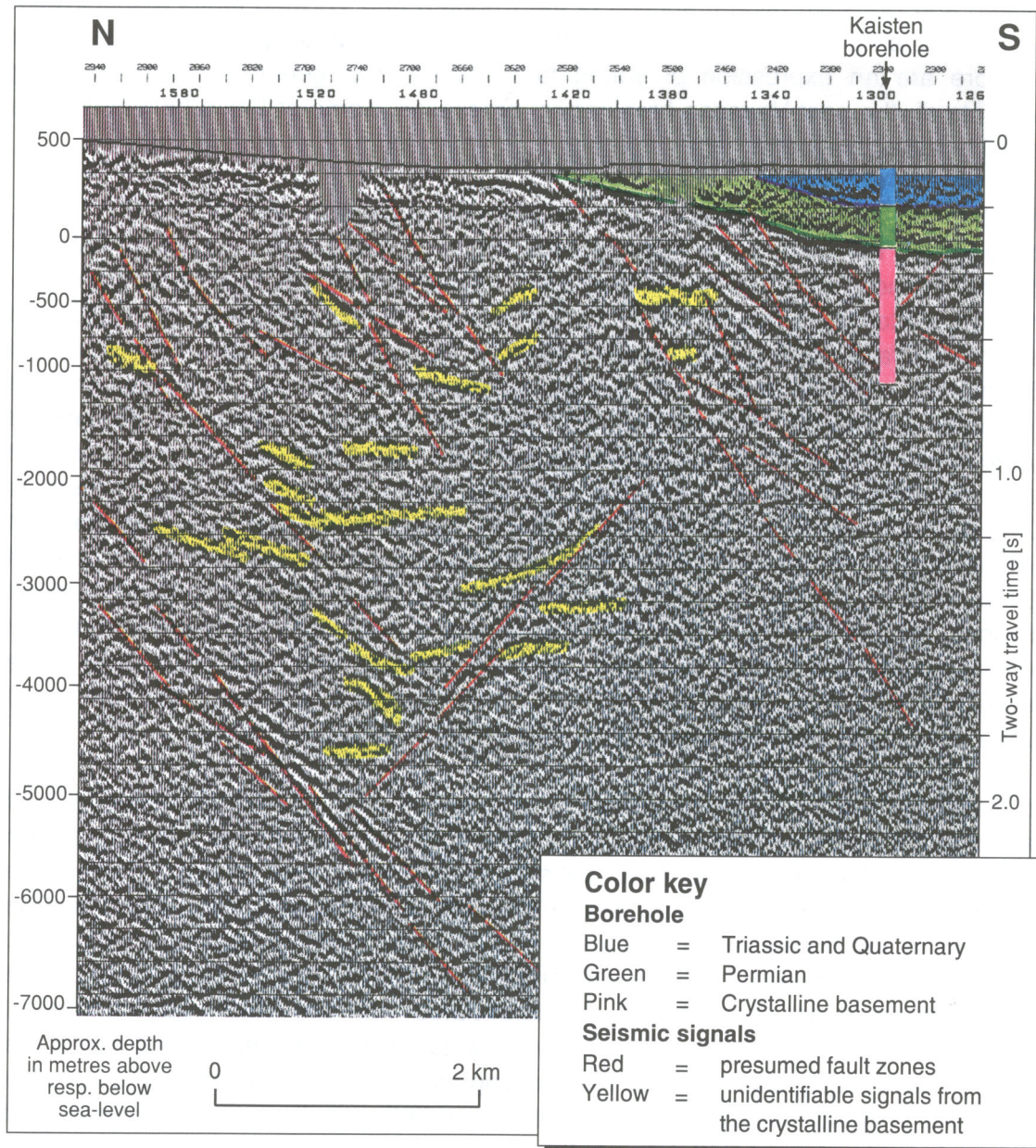


**Fig. 5-6 :** Fault zones in the crystalline basement as mapped on reflection seismic line 82-NF-10 (Geological profile cf. Fig. 5-4E).

### 1st order faults as block boundaries

The basement blocks of the Southern Black Forest are bounded by large 1st order faults (cf. Fig. 5-5 and App. 5-3). According to the definition in Table 5-1, these include the Vorwald, the Eggberg and the Wehr-Zeiningen fault zones, the northern border of the PCT and the NW-SE-striking faults associated with horsts and grabens in the South-eastern Black Forest (cf. Fig. 5-5).

1st order faults were possibly encountered in only two of the Nagra boreholes, i.e. in Kaisten and Böttstein (side-branches of the Eggberg and Vorwald faults respectively). It is to be noted that the fault zones, which are also geomorphologically manifested and therefore are an expression of young fault movements, generally represent older elements of the post-Variscan breaking-up processes. Some of these fault zones are probably still active today.

The **Vorwald fault zone** (App. 5-3) is probably a pre-Variscan feature (WIRTH 1984). Following the intrusion of the Albtal granite, this fault was active as a steep, NW-SE-oriented transcurrent fault, which resulted in dextral shearing of the Albtal granite by around 4.5 kilometers (METZ 1980). In the Tertiary, the Vorwald fault was reactivated as a normal fault. ERB (1948) believes that the Tertiary vertical movement of around 160 meters occurred during the Eocene-Oligocene. Quaternary moraines are not displaced. According to PFANNENSTIEL (1957), the vertical separation, as determined by the displacements of the Buntsandstein, is more than 100 m over long sections but never exceeds 150 m. In the east, near the Rhine, the vertical displacement is 40-50 m, from which PFANNENSTIEL (1957) has deduced that the Vorwald fault terminates (as a normal fault) towards the east. The fault zone, which is of the order of 100 m wide, is clearly recognizable in the terrain as a morphostructural element (stepping, valley incisions). It is not directly exposed but was encountered in a tunnel for the underground hydro-power plant at Wehr (western end of Vorwald fault). Here extensively fractured, friable rock penetrated by argillated fault branches was found over a distance of 100 m (HUBER & HUBER-ALEFFI 1990).

To the NE of Wehr, the Vorwald fault is accompanied by an important parallel fault (fault at Wolfristkopf, cf. App. 5-3, VOGT 1983, REST 1977) and in the area some 5 km to the N of Laufenburg several minor subsidiary faults are known to exist. These strike at 10-50° obliquely to the Vorwald fault. Faults with a similar orientation could also be observed in the boreholes at Leuggern and Böttstein (pole diagrams in App. 5-3). Some of these subsidiary faults on both sides of the Rhine show a displacement in the overburden. It is not clear if they are associated with the much older horizontal displacement at the Vorwald fault and to what extent they were reactivated during the Tertiary. The interpretation of these faults acting as a conjugate system to the dextrally transverse Vorwald fault appears plausible. Towards the south-east, the Vorwald fault presumably extends past Böttstein into the PCT (App. 5-2, 5-3).

The **Eggberg fault zone** runs roughly NW-SE, parallel to the Vorwald fault, and consists of a large number of subparallel faults, some of which can be mapped at the surface. The majority of fault planes dip with ca. 50° towards the SSW (Fig. 23 in HUBER-ALEFFI & HUBER-ALEFFI 1984). This information is derived from outcrops

seismics (Fig. 5-6) and underground exposures (Säckingen cavern and Nagra borehole at Kaisten). The overall width of the entire fault zone is estimated at 3 km.

The Eggberg fault zone was reactivated during the Tertiary/Quaternary as a normal fault with a max. vertical displacement of 200 m (cf. PETERS et al. 1989b). The Tertiary fault zone is probably a rejuvenated older feature, namely a dextral strike-slip fault, similar to the Vorwald fault. The nearby northern margin of the PCT is also displaced dextrally by the Eggberg fault (Fig. 5-5, App. 5-3). Two phases of movement could be identified in the Kaisten borehole (depth 1240-1265 m) along what is presumed to be a branch of the Eggberg fault (PETERS et al. 1989b).

The **Wehr-Zeiningen fault zone** forms the boundary between the South-east Black Forest (Vorwald block) and the Dinkelberg block (Fig. 5-5). To the north of the Rhine it strikes approximately N-S (Rhenish). Across the Rhine to the south, the main branch turns towards the SW and disperses in the Tabular Jura. In addition, Rhenish-striking subsidiary branches also cross the Rhine and pass into the Tabular Jura (Fricktal block, cf. App. 5-3). The fault zone in the vicinity of Wehr-Säckingen is described in detail in LUTZ (1964). Fault activity during the Permian is evident, since Permian deposits of significant thickness have been identified practically only to the west of it (cf. GONZALEZ 1990) and a Tertiary reactivation of the fault zone has been demonstrated by LAUBSCHER (1982). The Wehr-Zeiningen fault zone apparently lies along an old weak zone (ductile shear zone?) which, as the western boundary of the Albtal granite intrusion (and continuation to the north of the Vorwald fault along the Wehra valley), already trended in a N-S direction. The schistosity of the gneiss anatexites east of the Wehr and Carboniferous intrusive dykes also strike parallel to this Rhenish-striking zone (LUTZ 1964).

The border faults of **WNW-ESE-trending horst and grabens in the Southern Black Forest** (northern border fault of the Hotzenwald block, boundary of the Feldberg-Schauinsland horst towards the Münstertal-Albtal graben and the Bonndorf graben zone, App. 5-3, Fig. 5-5) are basement structures which strike into Northern Switzerland beneath the eastern Tabular Jura. They can be identified by means of seismics or field geology (e.g. Randen fault). The maximum post-Mesozoic vertical displacement of individual faults may reach 200-300 m, but is usually significantly less. These fault zones are poorly exposed in the area to the south-east of the Badenweiler-Lenzkirch Zone and can generally be recognized only by accumulations of dyke rocks, as quartzose zones or as marked boundary zones of intrusive bodies. Near to the actual fault zone, the country rock has often been affected by tectonics. When investigating the northern margin of the Albtal graben, WIRTH (1984) encountered tectonically displaced fracture zones up to a distance of 2 km away from the main fault. He explains that these fracture zones were displaced as a result of the rotation of basement blocks caused by the graben border faults. This fault zone also marked the intrusion boundary between the Bärhalde granite and the granite of St. Blasien and thus represents an older discontinuity in the crystalline basement.

The ENE-WSW-trending northern **border faults of the PCT** presumably displace the crystalline basement by several kilometers (seismic evidence, DIEBOLD et al. 1991).

These faults have been involved in the Saalian shearing of the PCT and were reactivated during the Paleogene as normal faults and flexures (cf. section 5.2.4, App. 5-2).

### **Fault blocks and higher order faults in the basement to the north of the PCT (App. 5-3)**

The 1st order fault zones discussed above, which underwent post-Saalian reactivation, form the boundaries of approx. rectangular basement blocks which have a size of the order of 5-15 km in the Southern Black Forest/Northern Switzerland region. These blocks have an internal fault pattern (2nd and higher order faults, Tab. 5-1) which at present is hardly known.

Seismic investigations have provided only restricted data on second order faults as the line spacing is not sufficiently dense and, in any event, only faults with a vertical throw > 20 m can be traced at the Base Mesozoic and extrapolated into the basement. Seismic mapping of fault zones in the crystalline basement proved to be contentious as illustrated by Figure 5-6.

It can be presumed that the internal structure of the crystalline basement is directly comparable with the conditions in the neighboring Southern Black Forest.

Numerous higher order faults were encountered in the Nagra boreholes; these have been analyzed, described in detail and documented comprehensively (cf. Chapters 4 and 6 of this report). The spatial orientation of these fault zones is presented in Appendix 5-3 in pole diagrams.

The following basement blocks in the investigation area will be reviewed below: the Fricktal block, the Vorwald block, the Hotzenwald block and the continuation of the Münstertal-Albtal graben, the Feldberg-Schauinsland horst and the Bonndorf graben zone (App. 5-3).

Relatively little is known about the fault zones in the crystalline basement of the **Fricktal block** (boundaries: Wehr-Zeiningen fault zone, Eggberg fault, northern margin of PCT). Nagra has only one seismic line which passes through this area (83-NS-81). According to the presentation in Appendix 3-1, which is based largely on surface mapping, Rhenish-striking fault zones dominate this area. These form an actual block-faulted area mainly in the south-west.

In the Kaisten borehole (PETERS et al. 1989b), the observed fault zones are generally narrow (10-50 cm) and dip at various angles towards the S to SW and gently towards the west. These data do not contradict the above interpretation, but suggest that in addition to the dominant Hercynian directions, which can be explained by the proximity of the Eggberg fault, there are also discontinuities which trend N-S.

The **Vorwald block** is bounded by the Wehr fault zone, the Eggberg fault, the Vorwald fault and the northern margin of the PCT. According to the literature, in addition to the

few elements which are perpendicular to the Vorwald fault, the western section of the block is presumably dominated by WSW-ENE- to WNW-ESE-striking elements. Morphological analyses have also indicated the existence of NW-SE- to NNW-SSE-striking faults (DIEBOLD et al. 1991: Fig. 16 & 18).

According to surface mapping, a dense fault network dominated by Hercynian and WSW-ENE-striking zones can be recognized and compiled in the north-west section of the block, in the region of the Southern Black Forest.

To the south of the Rhine, several faults can be identified on the seismic lines (marker Base Mesozoic). Unfortunately, their strike is often ambiguous. Presumably Hercynian-striking features dominate here, possibly also with PCT-parallel ones (e.g. direction of the Mettau thrust). In the Böttstein borehole, which is located near the SE edge of the Vorwald block, cataclastic zones (kikirites) (HEITZMANN 1985) are frequent (around 3 per 100 meters) (PETERS et al. 1986), often extending over several meters in the drillcore. The dip is 50-75° towards the SSW to W, the azimuth generally turning from SSW to W with increasing depth. To some extent, the kikirites have a Hercynian strike, corresponding to the direction of the Vorwald fault, the SE extension of which probably passes to the SW of the Böttstein borehole (App. 5-2). Both the absence of cataclastic zones in the Buntsandstein as well as the measured illite ages (hydrothermal infills of cataclastic zones: Permian-Triassic) appear to rule out the possibility that younger movements occurred at the cataclastic zones in the Böttstein borehole (Tab. 4-6).

The conditions in the **Hotzenwald block** (bounded by the Vorwald fault, the PCT northern margin and the border faults of the NW-SE-trending Münstertal-Albtal graben) are presented in Appendix 5-3. According to surface geology studies, the area between Albrück and Waldshut is dominated by NNW-SSE directions (cf. Fig. 5.12 in HUBER & HUBER-ALEFFI 1990). To a lesser extent Hercynian and more or less PCT-parallel faults are also recognized.

In the Leuggern borehole (PETERS et al. 1989a), the few fault surfaces identified in the gneiss section dip, for the most part, gently towards the E, whereas in the granite section they dip steeply towards SW to WSW and NE to ENE.

According to the geochemical investigations of EMMERMANN (1970), the St. Blasien granite consists of several blocks. Those to the west are more strongly uplifted than those to the east (KLEINE BORNHORST et al. 1984). There are also kikirites (cataclastic zones) which strike NNW-SSE to N-S, as identified in the Leuggern borehole. This trend can be correlated with faults mapped in the area along the Rhine between Albrück and Waldshut that have been recognized on the basis of displacements in the overlying Triassic sediments. According to VON BUBNOFF (1928), break-up into blocks along NW-SE- to NNW-SSE-striking lines applies to the entire South-west Black Forest (particularly for the Bärhalde granite, lines NW-SE to N-S). Somewhat to the north, GROSCHOPF & SAWATZKI (1989: Fig. 6) mapped N-S trending faults.

Hercynian-striking fault zones dominate in the region of the **NW-SE-trending grabens in the south-east Black forest**; the Siblingen borehole lies in the eastern continuation

of these graben structures. The map of this area (App. 5-3) contains morphostructural elements whose significance is not always clear (cf. discussion in HUBER & HUBER-ALEFFI 1990). The semiquantitative presentation on that map is intended to show the potential density of the fault network. Based on the structures which can be identified morphostructurally, break-up of the granite by 2nd & 3rd order faults into blocks of the order of one km<sup>2</sup> would appear to be a realistic estimate.

This regional fault pattern in the investigation area of Northern Switzerland with 1st and 2nd order faults is accompanied by smaller structures which cannot be localized geophysically. This was done for isolated locations in deep boreholes. However, the structural information from deep boreholes provides very local datasets; interpolation between the few boreholes and regional extrapolation of smaller structures is therefore unrealistic at present.

In summary: Meaningful correlation between surface data (mapping) and reflection seismics is possible on a regional scale but only to a minor extent on a local scale. Furthermore linking this regional information (Chapters 3, 5 and 9) with structural borehole data from the crystalline basement (Chapters 4 and 6) is hardly possible at present.

## **5.3 Schematic fault models**

### **5.3.1 Introduction**

The aim of our analysis of available regional structural data is the compilation of a comprehensive and plausible picture of the extent, the characteristics and the spatial arrangement of the faults within the crystalline basement of Northern Switzerland. However, it is obvious that the heterogeneous and incomplete set of data, as outlined in section 5.2, is quite insufficient for a realistic representation. It was therefore necessary to resort to a simplified approach by constructing schematic fault models for the areas of interest.

The two schematic fault models which are outlined below are considered to represent an acceptable compromise. They deal exclusively with tectonic aspects; hydrological and hydrodynamic properties of the modeled fault pattern are the subject of Chapter 8.

The two schematic fault models served as input for both the local hydrodynamic model (cf. Chapter 8) as well as the explorability study presented in Chapter 11.

- After classification and definition of the observed faults (in section 5.3.2),
- schematic fault networks and schematic fault models are derived (in section 5.3.3 and
- schematic models for both the areas West and East are presented (in section 5.3.4 and 5.3.5 respectively).

### 5.3.2 Classification and description of relevant structural features

#### Classification

Table 5-1 defines the different classes of faults and discontinuities as used for the modeling (cf. AMMANN et al. 1992).

Based on present knowledge, and with regard to practical application, i.e. modeling, four categories of relevant features have been identified (cf. Tab. 5-1, section 5.1):

- a) Large fault zones of regional significance (1st and 2nd order)
- b) Small, higher order fault zones, generally of local significance and often associated with 1st and 2nd order faults
- c) Extensional discontinuities without infill: open joints
- d) Extensional discontinuities with infill: dykes and ore veins.

Higher order faults and extensional discontinuities of categories b) and c) above, although important, cannot be included explicitly in the modeling due to a lack of consistent data. These features have to be accounted for as contributing to the bulk properties of the rock matrix. Ore veins, on the other hand, are partly planar elements with a constant spatial orientation and can be directly included in the model. Ore veins in particular are important water flow paths and should, wherever possible, be explicitly included (cf. Chapter 6).

#### 1st and 2nd order fault zones

Although often shown as simple lines on maps and profiles, fault zones of every size have a specific thickness and a complex internal structure. Some general remarks on geometry and origin which are important in connection with the internal structure of fault zones are described below:

##### 1. *Geometry*

Fault zones in the crystalline basement consist of a set of shear planes which make up a braided network and which contain between them lenses of more or less unaffected rock. In terms of volume, these lenses are generally more dominant than the deformed zones.

This geometry of a braided network of shear planes occurs on every scale (it is self similar); it applies for example for the Eggberg fault (width = 100 m - 1 km), a fault at outcrop or in tunnel profiles (m to 10 m range), in drillcores (cm range) or in a thin section (mm range). A "large" fault zone ("lower order" fault) can be considered as a particularly dense accumulation of branches of "smaller" faults ("higher order" faults, cf. Fig. 4-3, Fig. 5-7).

##### 2. *Kinematics*

In this braided network only a few individual shear planes are active simultaneously, i.e. at any time, shear strain is concentrated at a few zones of variable thickness.

### 3. *Dynamics*

The formation and character of a fault zone can only be determined within the framework of a regional analysis. The majority of all the fault zones in the basement of Northern Switzerland have been activated several times under various geodynamic conditions and therefore cannot simply be assigned to one single regime.

#### Discussion:

In an isolated borehole, it may be impossible to recognize even a large fault zone as such because generally there is no spatial correlation in crystalline rocks. In addition, the deep boreholes drilled in Northern Switzerland were more or less vertical and thus rarely intersected steeply-dipping fault zones. For these reasons, it is still difficult today to correlate any large fault zone of the crystalline basement encountered in the Nagra boreholes with those mapped in the Black Forest.

In the Southern Black Forest, 1st order WNW-ESE-trending fault zones can be followed at the surface over distances of up to 15-20 km. How far these fault zones could possibly continue into the sediment-covered basement of Northern Switzerland is shown, for example, in Figures 5-7 and 5-8. From the exposed length of the fault zones, certain regularities in their trace can be identified. This allows three basic types of lateral continuity to be distinguished (cf. App. 5-3):

- uniformly linear faults (example: Vorwald fault, central segment)
- faults which are broken up into short, step-like offset segments (example: Vorwald fault, western segment, northern margin of PCT)
- branching faults (example: Eggberg fault, Randen fault zone, cf. App. 5-1).

The formation of a particular fault type probably depends on prevailing lithological and structural conditions.

Based on general observations, by comparing the near-surface fault patterns particularly at strike-slip faults with the form of the same fault at depth, it is to be expected that complex, wide fault zones will generally narrow with depth (e.g. WALLACE & MORRIS 1979). This is not necessarily associated with a reduction in the number of fault branches; they may simply be concentrated in a narrow zone (cf. Fig. 4-3). Although the overall width of the fault zone may decrease drastically due to convergence of individual branches, the main branch may increase considerably in thickness as the individual sub-branches converge. The depth at which there is a significant reduction of the overall width of the fault zone probably varies from fault to fault (for more detail cf. HUBER & HUBER-ALEFFI 1990). A similar phenomenon has been observed for fault zones in the sedimentary overburden. Here faults which are clearly defined as discontinuities at the Base Mesozoic disperse towards the surface, forming flexure zones at shallow levels (cf. App. 5-1, section along seismic profile).

Within a fault zone, various degrees of rock disintegration can be observed. For the purpose of the present discussion three intensities of brittle deformation are distinguished (e.g. WALLACE & MORRIS 1979):

- zone A with strong fracturing
- zone B with strong faulting
- zone C with total crushing (fault gouge).

These three zones each show a characteristic deformation intensity which can be defined by its lithological rock type. Zone A, with strong fracturing, is characterized as fractured country rock, while zone B, with strong faulting, is made up of (tectonic) breccias and kakirites. In zone C, with total crushing, the typical products of tectonic deformation are clay-like fault gouge or rock flour.

Within a fault, the degree of rock disintegration increases gradually from fresh rock which is loosened only in the immediate vicinity of fractures, through the breccia-type zone where lenses of more or less intact rock float in a matrix of finely-ground material, to the strongly tectonized zone where the rock has lost cohesion. The amount of friction products increases with increasing fault displacement; this is also true for the content of clay minerals which is negligible in zone A, but is very high in zone C where the rock shows plastic flow properties when wet. In addition to this purely mechanical crushing (cataclasis), the effects of mineral alterations are brought about mainly by circulating mineralized water (hydrothermal solution and cementation, e.g. ore and mineral veins, cf. sections 4.5.7 and 6.5.1).

### 5.3.3 Modeling faults

Based on data known to be incomplete, two schematic fault networks and corresponding schematic fault models have been constructed for the crystalline basement (cf. AMMANN et al. 1992), one each for the area West (Böttstein - Kaisten - Leuggern - Zurzach) and for the area East (greater Siblingen area).

These constructions involved the following four-step procedure:

- Compilation of an inventory of known faults in the region, integrating data from boreholes and the results of reflection seismics. At this stage a decision also had to be made on data to be excluded from modeling (e.g. faults of higher orders, fractures, basement lithologies, etc.). One of the results of this compilation was a map of the network of known 1st and 2nd order faults (cf. Figs. 5-7a and 5-8a).
- Based on this inventory, the fault families were determined. This was done on the map resulting from the previous step.

The schematic model considers fault surfaces to be represented by geometric planes of uniform strike and dip, which project as straight fault traces on a map. Fault families were constructed by fitting straight lines to the fault traces as actually mapped, discriminating between the distinctly different strike direction characteristic for the fault families.

As each fault family is considered to consist of a set of parallel and regularly spaced faults, the fault spacing had to be determined as well. The fault spacing could be based either on direct field observation, if data are available, or otherwise a conservative educated guess was necessary.

- Once the fault families were defined they had to be tied geographically into the framework of the Southern Black Forest and Northern Switzerland, thus creating a schematic fault network, cf. Fig. 5-7b and 5-8b where these ties are indicated. It is obvious that only a few major faults used in this model can actually be related to their true geographic location.
- The step from this schematic fault network to a (three-dimensional) schematic fault model is made by including information on the dip of the fault zones (cf. Fig. 11-2).

#### 5.3.4 Schematic fault model in area West (Fig. 5-7)

Using the depth map of the Top Crystalline Basement (DIEBOLD et al. 1991) and tectonic surface maps, the inventory of known regional faults is presented in Figure 5-7a. The complex structural conditions in the region of the PCT northern margin and its basement shoulders (e.g. Kaisten) are shown in Figures 3-3, 5-4 and Appendix 5-2. The fault model West (Fig. 5-7b) was generated from these data, including the evaluation of structural data from the deep boreholes.

The following 5 steeply-dipping fault families and a set of regionally important ore and mineral veins were distinguished.

*Fault family W1: strike 110°-290° (ESE-WNW, "Hercynian")*

From interpreted seismic data and surface observations, this family appears to be the dominant element in the fault network. Known dips of the fault planes vary between 55° towards the SSW (Eggberg fault) and 80° towards the NNE. The spacing of the parallel faults of this set was taken to be 7 km for the first order (distance between Eggberg and Vorwald faults) and 1 km for the 2nd order faults and was kept constant over the whole area. Each of the 1st order fault zones is considered to be about 1 km wide.

The Hercynian-striking fault family W1 could be tied geographically to the two well-documented 1st order Vorwald and Eggberg fault zones.

*Fault family W2: strike 000°-180° (ca. N-S, "Rhenish")*

The assumed N-S orientation of this fault family which includes ore veins is schematic. Based on observations in the field, a sub-vertical dip was assumed for both the faults and the ore/mineral veins. The distance between known individual elements is variable; spacing of 1.5 km for 2nd order faults in the western part of the area was increased to 2 km in the east. In this way, the diminishing influence of the Upper Rhine Graben

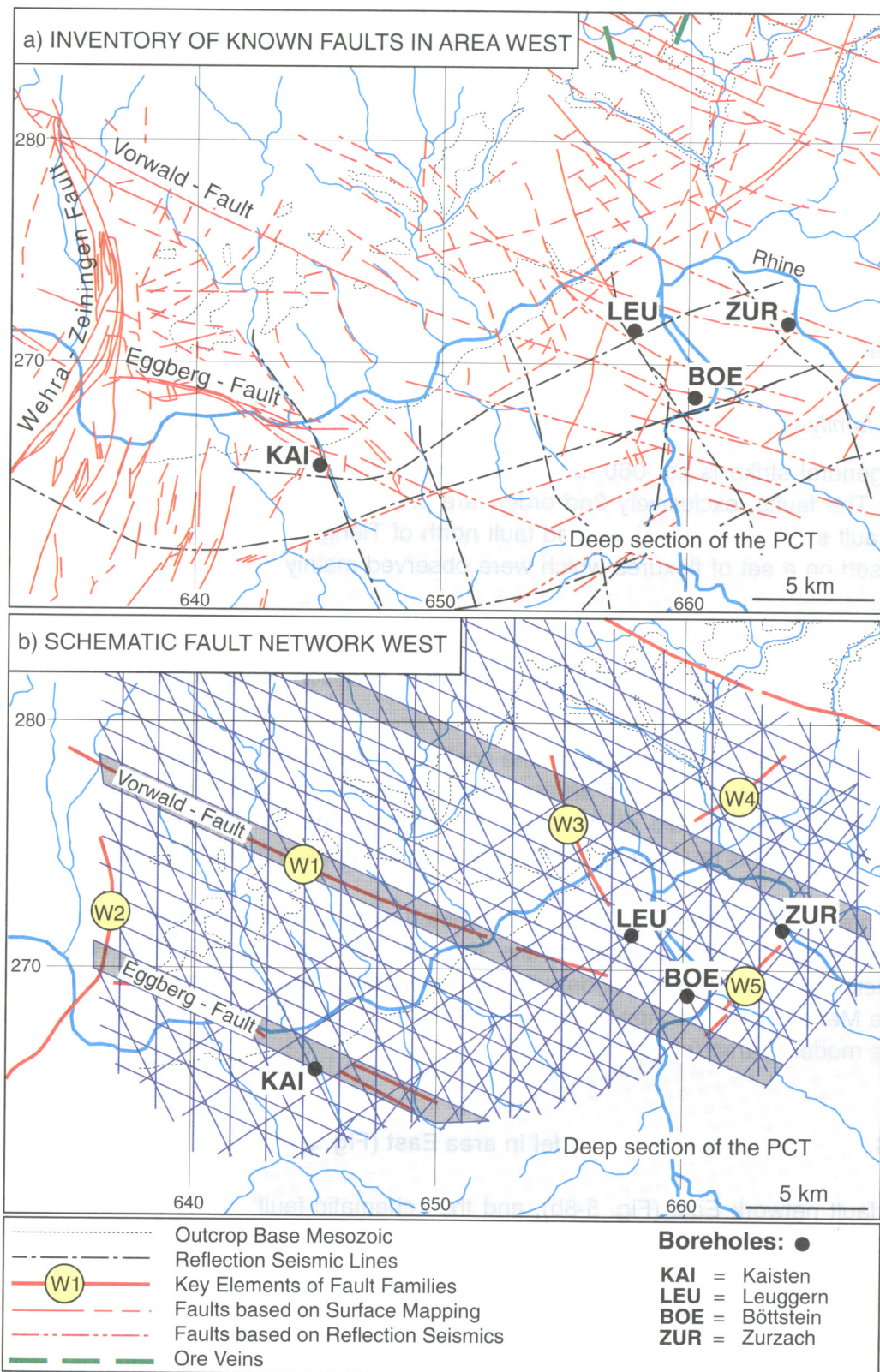


**Fig. 5-7a :** Inventory of structures in the area West. Seismically mapped faults and depth lines of the Top Basement in black, structures mapped by surface geology in red (incomplete!).

**Fig. 5-7b :** Schematic fault network of the area West.

towards the east is taken into account. This fault set was fixed geographically at the tectonically significant (1st order) fault zone of Wehr-Zeiningen at the western edge of the area West.

*Fault family W3: strike 150° - 330° (ca. SSE-NNW, "Eggian")*

Only 2nd order fault zones were observed for this family. The elements strike approximately 150°-330° and dip mostly with about 70° towards the WSW, and in isolated cases about 70° to the ENE. Even fault spacings of 1.5 km were assumed. The fault set was fixed geographically at a documented fault at Dogern (4 km NW of Leuggern).

*Fault family W4: strike 060°-240° (ca. ENE-WSW, parallel to Folded Jura and PCT)*

The general strike is ca. 060°-240° and the dip varies between 70° and 80° towards SSE. The faults, exclusively 2nd order, are plotted with a constant spacing of 2 km. The fault set was tied to a mapped fault north of Tiengen near Waldshut (Fig. 5-8b); it is based on a set of flexures which were observed mainly in the southern Hotzenwald block.

*Fault family W5: strike 040°-220° (ca. NE-SW, a direction conspicuously parallel to the Wutach river)*

This fault set, which is restricted to the southern area of the modeled domain, consists of 2nd order fault planes with an assumed constant spacing of 1 km. The strike is ca. 040°-220°, while the dip is generally 80° towards the SE (less frequently ca. 80° towards NW). This fault family is influenced by the northern margin of the PCT.

The three fault families W1 - W3 are distributed over the entire modeled domain; this is not assumed to be the case for the two families W4 and W5. The W4 family is restricted to the northern boundary line corresponding more or less to the outcrop trace of the Mettau thrust (cf. App. 5-1), while W5 is restricted to the remaining southern part of the modeled area (cf. App. 5-3).

### **5.3.5 Schematic fault model in area East (Fig. 5-8)**

The fault network East (Fig. 5-8b), and the schematic fault model derived therefrom, are based on the structural inventory presented in Figure 5-8a and Appendix 5-3.

The area East is difficult to model due to lack of data. The crystalline basement is exposed only in a few valleys and, within the area to be modeled south-east of the Wutach, there are no basement exposures whatsoever. Little information is available from two reflection seismics lines, and from the crystalline basement only small-scale structures are accessible in the Siblingen borehole.

*Fault family E1: strike 095°-275° to 105°-285° (ca. ESE-WNW, "Hercynian")*

As in area West, the Hercynian features appear to be the most significant elements of the fault network in the model area East. The margins of the horst and graben structures in the South-east Black Forest are considered to be 1st order faults. With the exception of the Randen fault zone, these have only been mapped to the west of the area East (cf. App. 5-1). Nevertheless, it is likely that they continue into the model area East. Since they are not clearly mapped in the central region of the fault network East and do not fit directly into the mapped faults of the Bonndorf graben zone, they are modeled in an idealized manner. The strike of these 1st order faults presumably deviates from ca. 285° to ca. 275° in the Wutach - Siblingen area.

This so-called flat-Hercynian strike, which appears to deviate back to the 285° strike in the east (cf. Randen fault zone), is confirmed by faults/fractures in the Siblingen borehole. If the 1st order faults are considered in a regional context, they can be assigned to the broad southern rim of the Bonndorf graben zone ("Freiburg-Bodensee graben"); these faults dip steeply towards the north. At several locations the elements of the E1 fault family can be tied geographically to the observed fault.

In the East, the PCT's northern margin, although not well-known, must be considered to represent a 1st order fault zone of the E1 family (cf. Fig. 5-5).

*Fault family E2: strike 010°-190° (ca. N-S, "Rhenish", includes ore and mineral veins)*

In the model area East, there are no indications for 1st order faults with a Rhenish strike. Locally the Rhenish direction is well-represented in surface exposures and in the Hegau to the east of the region which is a central part of the "Bodensee graben".

Nonetheless, since the Rhenish direction is also represented in the Southern Black Forest, it appeared reasonable to integrate this family into the schematic fault network in the form of 2nd order faults. However, the basement is not accessible to direct observation; for this reason the strike direction is taken as being 010°-190°, which corresponds to the strike of dominant structures in the Danube - Alb region to the north of the area East. The dip of the faults can be taken as very steep to sub-vertical. The family is fixed at fault branches to the west of Siblingen. The Rhenish direction is assumed here to comprise ore and mineral veins, as a "worst case" scenario (not corroborated by field observations); this is in analogy to the area West where Rhenish striking ore veins do occur.

*Fault family E3: strike 140°-320° (ca. SE-NW)*

The fault family E3 is regionally very well-documented (Southern Black Forest - Danube). 1st order fault zones are represented in this family. In the north-east of the fault network and in the area of the Randen fault zone, E3 fault branches which displace Hercynian faults are frequently observed. This observation gives the Randen fault the appearance of a wrench fault! As described above (E1), regional observations show some deviations in the Hercynian strike direction. The fault family E3 may be a somewhat rotated subfamily of E1. The values for dips in the model are 60° towards NE through vertical to 60° towards the SW. Additional faults of the E3 family are rotated

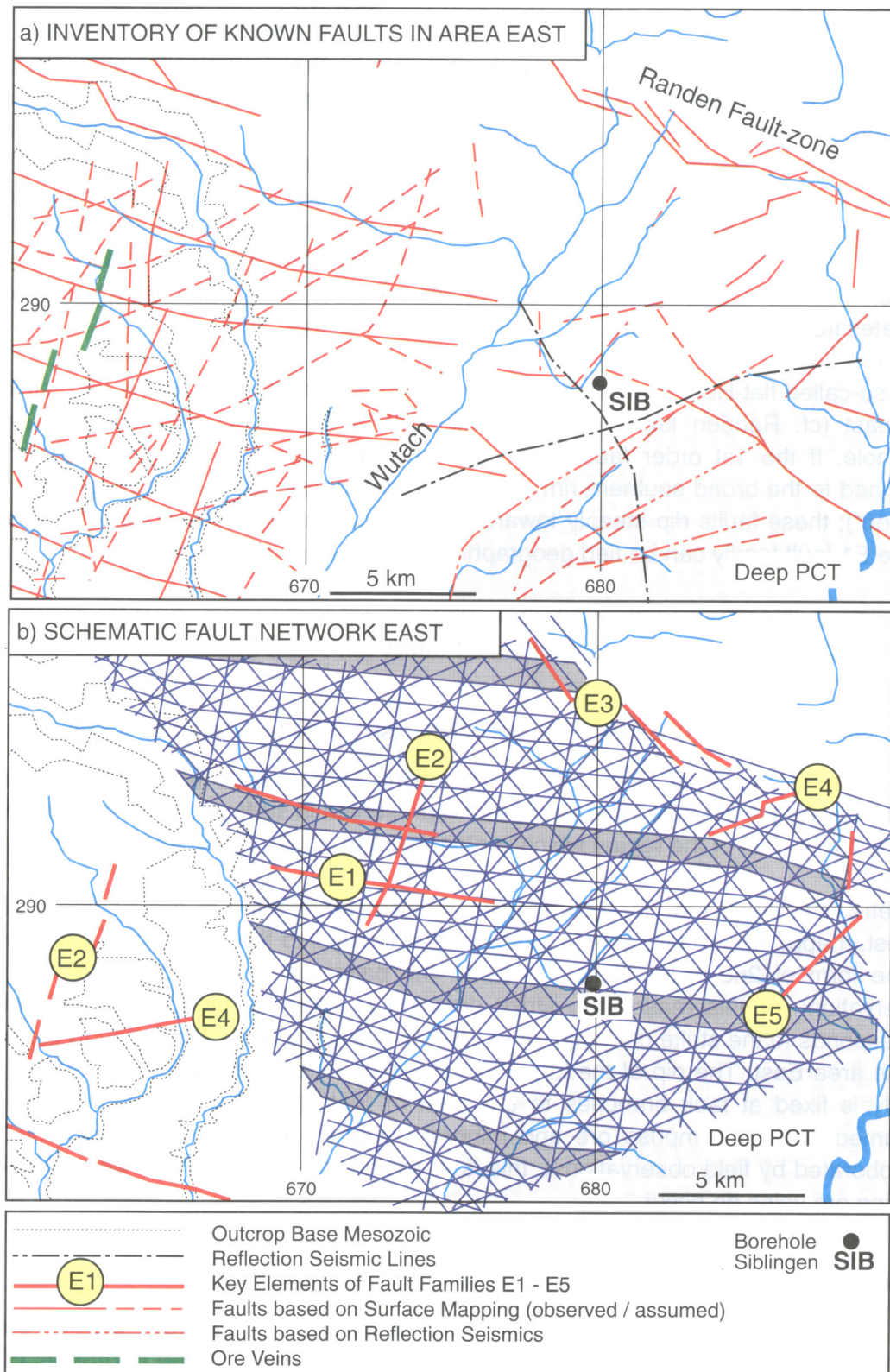


**Fig. 5-8a:** Inventory of structures in the area East around Siblingen. Seismically mapped faults and depth lines of the Top Basement in black, structures mapped by surface geology in red.

**Fig. 5-8b:** Schematic fault network in the area East.

by up to 30° towards the N (local mapping, exposures, Siblingen borehole). Correlation of direction is possible with some splay faults of the Randen fault zone and also with presumed faults to the north-west of the Wutach valley.

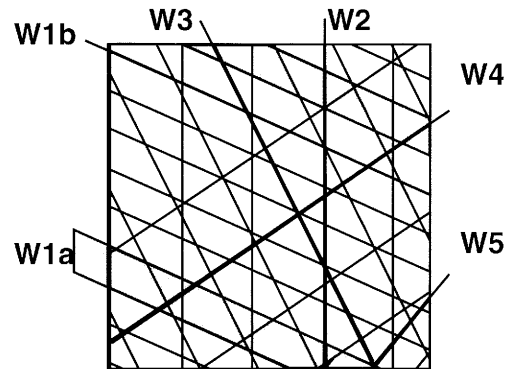
*Fault family E4: strike 065°-245° (ENE-WSW)*

The ENE-WSW-trending Siblingen flexure (1 km S of the Siblingen borehole) is a prominent representative of this fault family, causing a moderate steepening of the strata to the south-east (App. 5-1). In the Southern Black Forest, the direction is not particularly well-documented regionally, but it does occur in Northern Switzerland, e.g. as the Rekingen flexure and the Mandach structure. To some extent, the contours of the PCT in the area West also follow this direction. The direction can also be identified by geological surface mapping and is also clearly represented by microstructures in the Siblingen borehole. The dip is steep (60° to sub-vertical) and preferentially to the SSE.

*Fault family E5: strike 040°-220° (ca. NE-SW)*

The E5 strike direction is well-documented in the Black Forest, the Danube and the Hegau region (e.g. eastern section of the Badenweiler-Lenzkirch Zone). The direction is well-represented by microstructures observed both in exposures and in the Siblingen borehole. It is possible to fit this fault family geographically to the structural inventory along faults mapped in the Wutach-SE-Black Forest area. The dip is steep and preferentially towards the SE.

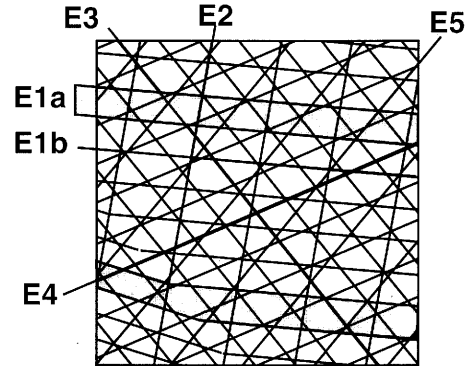
**Schematic Fault Network West :**



**Schematic Fault Model West :**

Fault families	Strike	Dip	Interval of faults
<b>W1</b> a) 1st and b) 2nd order faults	Hercynian 290 ± 10	Varies between 55 degrees towards SSW and 80 degrees towards NNE	1st order = ca. 7 km 2nd order = ca. 1km
<b>W2</b> 2nd order faults, ore and mineral veins	Rhenish 180 ± 10	Very steep to vertical	Western part = 1.5 km Eastern part = 2 km
<b>W3</b> 2nd order faults	NNW - SSE 330 ± 10	predominantly 70 degrees towards WSW, occasionally 70 degrees towards ENE	entire area = ca. 1.5 km
<b>W4</b> 2nd order faults	WSW - ENE 240	70 to 80 degrees towards SSE	entire area = ca. 2 km
<b>W5</b> 2nd order faults	SW - NE 220	predominantly 80 degrees towards SE, (occasionally 80 degrees towards NW)	South of Wutach only = 1 km

**Schematic Fault Network East:**



**Schematic Fault Model East:**

Fault families	Strike	Dip	Interval of faults
<b>E1</b> a) 1st and b) 2nd order faults	Hercynian a) 285 ± 10 b) 275 ± 10	1st order faults: steeply towards N 2nd order faults: steeply towards N and S	1st order = ca. 5.5 km 2nd order = ca. 1km
<b>E2</b> 2nd order faults, ore and mineral veins	Rhenish 190 ± 10	Very steep to vertical	= 2 km
<b>E3</b> 2nd order faults	NW - SE 320 ± 10	60 degrees towards NE / vertical to 80 degrees towards SW	= ca. 1 km
<b>E4</b> 2nd order faults	WSW - ENE 245 ± 10	Steep (60 degrees to subvertical), predominantly towards SSE	= ca. 1 km
<b>E5</b> 2nd order faults	SW - NE 220	Steep, predominantly towards SE	= ca. 1.5 km

**Fig. 5-9 :** Schematic fault models of the areas West (Kaisten - Leuggern - Böttstein) and East (Siblingen).

## 6 GEOLOGICAL CHARACTERIZATION OF WATER-CONDUCTING FEATURES IN THE CRYSTALLINE BASEMENT

Advective groundwater flow through the crystalline basement occurs mainly through discrete permeable structures that were subjected to brittle deformation (such as faults), which are termed **water-conducting features** in the following. One of the major aims of this Chapter is to provide a geometric/structural and a mineralogical/geochemical characterization of all types of water-conducting features that were identified in the boreholes. Geometric/structural parameters such as fracture aperture, fracture length, heterogeneity of the fracture surface and the wallrock porosity provide the basis for the characterization of the flow field (including Darcy fluxes through single water-conducting features), of the connectedness of water-conducting features and of diffusive transport of solutes from fractures to the microporous wallrock matrix. Mineralogical/geochemical parameters, such as mineralogy of fracture infills and of wallrocks, determine the sorption properties of rock surfaces exposed to flowing groundwater. These parameters form part of the geological database for the safety assessment of a potential radioactive waste repository, and this database is discussed in Chapter 10 in more detail.

### 6.1 Comments on the scale of observation

Surface-based methods such as seismics and geological mapping at outcrops provide structural and geometric information on the crystalline rocks (cf. Chapter 5). However, these methods do not provide any of the hydraulic parameters necessary to define groundwater flow. Some qualitative geometric information on groundwater flow paths may be gained from tunnels in the Black Forest, but permeable zones in the tunnels often have a concrete lining. Therefore, deep boreholes are the most important source of data with respect to small-scale geometric and mineralogical description of zones that are actually water-conducting, particularly with respect to the quantitative hydrogeological aspects.

Faults are potentially important for groundwater flow. While large-scale faults have been described in detail in Chapter 5, in the present Chapter the scale of observation is much smaller and limited by the geometry of the boreholes. In order to create a link between the different scales of observation, it is important to address the internal structure of large-scale faults and their manifestation in boreholes. Geometric features of faults are addressed in general terms in section 5.3.3. Points relevant for the characterization of groundwater flow are the following:

- A fault consists of an interconnected system of individual shear zones where differential movement has occurred. The individual shear zones are separated by isolated bodies of more or less undeformed rock. Every shear zone contains a fairly large proportion of rock that has not been affected by deformation.
- Faults occur on a variety of scales (mm-scale: microcrack seen in thin-section; 100 km scale: mappable features, such as the Rhine Graben or the San Andreas fault in California).

- The geometry of a large fault can be conceived as a combination of a system of smaller faults. This relation is valid on all scales considered.

The complex internal structure of faults must be accounted for when core logs are subjected to structural and hydrogeological interpretation. In practice, a regional fault as described in Chapter 5 may be observed as an enhanced frequency of smaller shear zones separated by intact rock portions. Therefore, it is often difficult to decide whether shear zones identified in the core material make up part of a large, regional fault system or represent small, local features.

## **6.2 Identification of water inflow points in Nagra's deep boreholes: definitions and methodology**

The approach to the characterization of water-conducting features, as presented in this Chapter, is specific to fractured crystalline rocks. Permeable borehole sections are identified by hydraulic testing and fluid logging techniques. Intervals of hydraulic packer tests are typically 10 - 25 m long and are defined as *permeable* if their hydraulic conductivity (K) exceeds 1E-9 m/s. Such intervals may contain at least one discrete *inflow point (water-conducting feature)*, which may be detected by fluid logging techniques (conductivity, temperature and flowmeter logs).

Based on information from cores and geophysical data, a much larger number of *potential inflow points* is identified compared to the number of inflow points actually identified by the hydraulic tools. One possible interpretation is that flow within fractures is heterogeneous (channeling, cf. section 6.13) and that many of the open structures in the core do not have a hydraulic link to large-scale flow paths (major faults) in the rock.

This Chapter deals only with structures that are actually hydraulically active in the boreholes. However, there is no systematic difference in geological or geophysical parameters between these water-conducting features and similar features that do not carry water in the borehole.

### **6.2.1 Sources and treatment of hydraulic data**

The raw data for fluid logging and packer tests in the Nagra deep boreholes are extensively documented elsewhere (NAGRA 1988a and NAGRA 1992a, cf. also Figs. 2-2a-g). To ensure some uniformity in investigating the different boreholes, despite marked differences in the quality of fluid logging and packer tests, a systematic approach was adopted for the detection of permeable zones and inflow points:

1. *Fluid logging*: Temperature and electrical conductivity logs are the most useful tools and are complemented by spinner flowmeter logs in many borehole sections. For the first boreholes (Böttstein, Weiach, Schafisheim), logging techniques were still in an early stage of development and results are relatively poor. Uncertainties

in the depth location of the individual inflow points are of the order of several meters. In the subsequent boreholes (Kaisten, Leuggern, Siblingen), the logging campaigns were modified on the basis of experience acquired, and the quality of data was significantly improved (cf. BLÜMLING & HUFSCHMIED 1989). Uncertainties in the inflow location were reduced to 1 m, which generally allows unambiguous correlation with geological features in the cores (cf. KELLEY et al. 1991). Conductivity logs were also used for the calculation of the transmissivities of the inflow points in some borehole sections (HALE & TSANG 1988; illustration in Fig. 6-1).

Under favorable conditions, fluid logging detects inflow points whose transmissivity is greater than  $1E-9$  m<sup>2</sup>/s. Detection limits may be much higher in borehole sections with poor logging quality. Features with transmissivities below the detection limit of fluid logging are, in most cases, excluded from the discussion.

2. *Hydraulic packer tests:* In all boreholes except Siblingen, a standardized procedure for the determination of hydraulic conductivities in packer intervals of 25 m was applied (the so-called H-logs). In addition, some tests with shorter and longer intervals were conducted. Figure 8-2 gives an overview of all hydraulic packer tests performed in the deep boreholes. The full data are reported in VOBORNY et al. (1993a).

In some borehole sections, permeable ( $K > 1E-9$  m/s) intervals have been detected by hydraulic testing, while no discrete inflow points could be identified in fluid logs over the same intervals. This apparent inconsistency is due to poor quality (high response threshold) of fluid logs. In addition, permeable intervals exist where fluid logs are not available. In such locations, inflow points were determined from core inspection, assuming that each permeable interval must contain at least one inflow point. Ambiguities remain in cases where more than one potential inflow point was identified in the core material of the permeable interval. In order to reduce these ambiguities, only packer tests with intervals  $\leq 25$  m were taken into consideration; uncertainties are too high in longer intervals to allow any meaningful interpretation of results.

## 6.2.2 Results

A total of 138 inflow points have been identified in the crystalline basement sections of the six deep boreholes in Northern Switzerland using fluid logging and hydraulic packer tests. A list of all inflow points is given in Table 6-1; further details are in MAZUREK (1994).

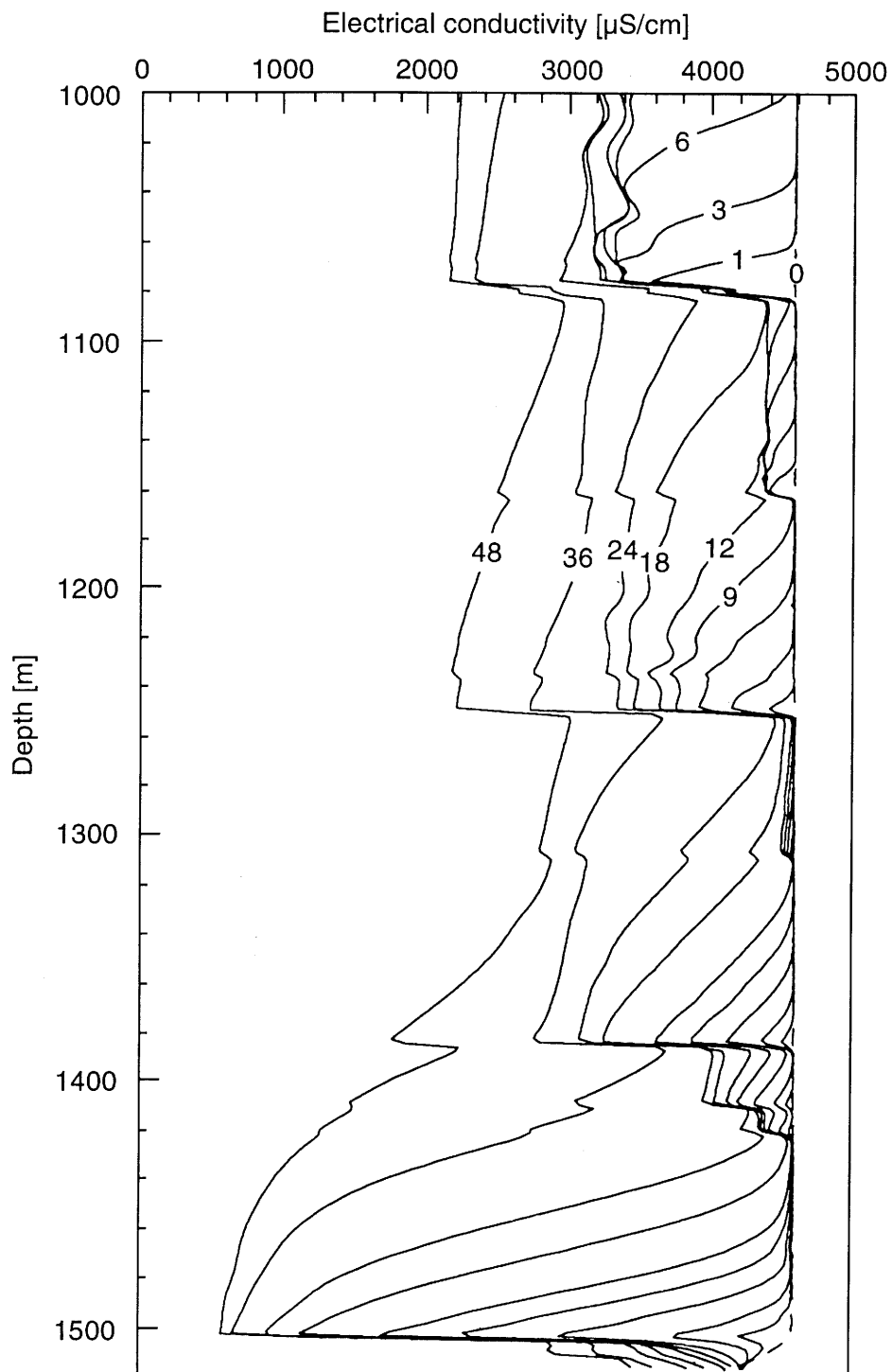


**Fig. 6-1 :** Identification of inflow points in the Siblingen borehole by fluid logging: electrical conductivity vs depth profile, following exchange of drilling-fluid with a salt solution ( $4600 \mu\text{S/cm}$ ) and continuous pumping. The measuring times 0, 1, 3 ... 48 h after fluid exchange are given on the curves. Water-conducting fractures appear as jumps in the electrical conductivity, for example at 1078.5 m, 1251.5 m, 1385.5 m and 1503 m. Taken from BLÜMLING & HUFSCHMIED (1989).

BÖTTSTEIN		SIBLINGEN		SCHAFISHEIM		LEUGGERN		KAISTEN		WEIACH	
inflow point, [m] below surface	type of water-conducting feature	inflow point, [m] below surface	type of water-conducting feature	inflow point, [m] below surface	type of water-conducting feature	inflow point, [m] below surface	type of water-conducting feature	inflow point, [m] below surface	type of water-conducting feature	inflow point, [m] below surface	type of water-conducting feature
376 - 389	2	420	2	1493	1	256	1	302.5	2	2066	3
401.5	3	691	2	1512	1	275	1	310.5	2	2077	1
466	1	781.5	2	1568 - 1590	1	319.5	3	328	1	2160	1
477	1 or 2	842.5	2	1701	1	458.5	2	355	1	2192	2
563 - 564.5	1	857	1	1741	1	479	2	382	2	2222	2
621	3	878	1	1750	1	540	1 or 3	423	1	2271	3
638	3	887	2	1753	3	543	3	433	1	2358	n.d.
650.5 - 654.5	2	926	2	1771	1	547	3	488	1	2426	n.d.
758 - 766	1	932	1	1794	1	684	1	503	1	2452	3
771 - 778	1	942	2	1820	3	705	*	523	2		
791	1	955.5	2	1835.5	1 or 3	707	3	542	2		
844	2	967	2	1893	3	728.5	1	575	2		
970	1	1013.5 - 1016	2	1904 - 1928	3	765	3	620.5	2		
1158	3	1078.5	2	1930	3	777	2	647.5	1		
1245	n.d.	1083.5	1	1968	3	823	2	649.5	1		
1302	n.d.	1163	2			835	2	656	1		
1321	2	1236.5	1			844.5	1	665.5	1		
1328	n.d.	1251.5	1			856.5	1	673.5	1		
1442	2	1308	2			895	3	688.5	1		
		1385.5	1			918	1	692	1		
		1410	2			923.5	1	698.5	1		
		1419.5	1			1042	1	820.5	2		
		1473.5 - 1476	2			1046.5	1	950	2		
		1493 - 1499	1			1084	1	1041	3		
		1503	3			1187.5	3	1045	2		
		1512	2			1200	3	1051.5	1		
						1215	2	1088.5	2		
						1223	1	1092.5	3		
						1248.5	2	1099	2		
						1271	2	1144.5	3		
						1301	3	1176	3		
						1328	2 or 3	1193	3		
						1439.5	1	1206	3		
						1519	1				
						1638 - 1662	*				
						1662 - 1689	*				

**Tab. 6-1 :** Depths of all inflow points identified in deep boreholes penetrating the crystalline basement of Northern Switzerland and classification according to type of water-conducting features. "n.d." = no data, "\*" = inflow points not fitting the classification scheme (potential hydrothermal mineral veins in Leugger). Types of water-conducting features: 1 = Cataclastic zone, 2 = Jointed zone, 3 = Fractured aplite/pegmatite dyke or aplitic gneiss layer.

## 6.3 Geological classification of inflow points

### 6.3.1 Concept

As described in Chapters 3 to 6, the basement of Northern Switzerland experienced several phases of magmatic intrusion, brittle deformation and hydrothermal alteration. Each of these phases left a structural and mineralogical imprint in the basement rocks on a regional scale. Each phase also played a role in the development of fracture permeability (by cataclastic deformation or jointing) or, on the contrary, in the sealing of existing fractures by precipitation of hydrothermal minerals. Present-day permeability of the crystalline basement is the end-product of the competition between such processes.

The effects of intrusion, deformation and alteration are characterized by a set of *structural elements*<sup>1)</sup> that are observed in the core material. The formation of structural elements in more recent phases of deformation/alteration is influenced by the existence of mechanical discontinuities from earlier phases (pre-existing geometry). Thus, cataclasis may be concentrated in primary-magmatic discontinuities, such as contacts of aplite dykes with the embedding wallrock. Vug/channel formation always follows pre-existing structures, such as joints or cataclastic matrices.

### 6.3.2 Structural elements and their regional correlation

The core material at all 138 identified inflow points was investigated in detail. A systematic description of each is given in MAZUREK (1994) and is not repeated here. A comparison of the descriptions for all the boreholes leads to the conclusion that, according to petrographic and structural criteria, the inventory of structural elements is common to the granites and gneisses of Northern Switzerland. With the exception of Schafisheim (cf. below), 7 types of structural elements are found in all the boreholes and are likely to represent features occurring over the whole region of interest. The terminology refers to the description given in Chapter 4, summarized in Table 4-5:

1. Type of primary rock (e.g. granite, metapelitic gneiss, aplite dyke);
2. Cataclastic zones of the high-temperature phase;
3. Joints of the high-temperature phase;
4. Cataclastic zones of the low-temperature phase;
5. Joints of the low-temperature phase;
6. Vugs/channels;
7. Mineral veins.

---

1) A structural element is the product of a specific primary (rock-forming) or secondary (overprinting) process that affected the structure of the rock. It is a genetic term because it refers to regional geological events whose relative ages and physical conditions are reasonably well-constrained. For the purpose of this Chapter, only those structural elements are discussed in detail that are also relevant for present-day permeability. Other structural elements exist but do not significantly affect hydraulic properties of the rock (e.g. schistosity in gneisses).

All of these structural elements are illustrated in Figure 6-2. The schistosity in the gneisses is not a structural element enhancing water flow. Water-conducting structures are always oblique to the schistosity, which presumably has a sealing effect due to the presence of abundant sheet silicates.

The Schafisheim borehole fails to fit the pattern of the above-mentioned structural elements. The tectono-hydrothermal<sup>1)</sup> history is apparently different in this case, which means that the structural elements are different from those of the other boreholes (cf. Chapter 4). This difference is due, presumably, to the location of the Schafisheim borehole on a local horst-like structure in the Permo-Carboniferous Trough system, which led to very extensive cataclasis and a unique type of alteration.

As discussed in Chapter 4, the crystalline basement of Northern Switzerland was subjected to at least 2 phases of argillic alteration, namely the "low-temperature phase" and the "kaolinitic phase" (Tab. 4-5). While the low-temperature phase was associated with intense cataclasis and jointing, the younger kaolinitic alteration mostly reactivated pre-existing structures (often those of the low-temperature phase). For the purposes of the present Chapter, the kaolinitic phase is treated together with the low-temperature phase, because the petrographic expressions of both phases are comparable. Alterations of both phases are thus referred to as "argillic alteration".

### **Type of primary rock**

In certain cases, the nature of the primary rock type is relevant for present-day water flow through the basement. Different rock types have different mineralogical compositions and textures, which lead to variable mechanical behavior during deformation, variable types and extent of alteration and therefore different permeabilities. The most important rock types (presented in detail in Chapter 4) are:

- Gneisses;
- Granites (+ basic intrusives in Schafisheim);
- Dykes.

#### *Gneisses and granites*

The most common types of gneiss are metapelites and biotite-plagioclase gneisses. In spite of the somewhat different mineralogies and textures, no systematic difference in the development of structural elements could be detected between these types of gneiss and the granites. The same is true for hydraulic conductivities and frequencies of inflow points.

---

1) The term "tectono-hydrothermal" refers to postmagmatic/postmetamorphic events that involved brittle deformation (cataclasis, jointing) and subsequent hydrothermal alteration due to interactions with waters circulating in the cataclastic zones and joints. Tectono-hydrothermal events (e.g. the high- and low-temperature phases described in Chapter 4) are characterized by an interplay between more or less coeval processes of deformation and alteration.

In the boreholes of Kaisten and Leuggern, other types of gneiss are interlayered with metapelites and biotite-plagioclase gneisses (cf. section 4.4.1) and show a markedly different deformational behavior. Permeability in these inhomogeneous gneisses mainly depends on 1) the tendency of the rock to undergo fracturing (brittle vs ductile behavior) and 2) the potential of the rock to seal existing fractures by hydrothermal alteration products. Both of these factors are mainly a function of mineralogy and texture. Mica-rich rocks such as the metapelites are less affected by brittle deformation than the almost mica-free aplitic gneisses, in which fractures tend to concentrate. In addition, metapelites are rich in plagioclase, cordierite and biotite, which are mostly altered adjacent to fractures (e.g. to chlorite and clay minerals), thus providing abundant material that may coat and/or seal open structures. In contrast, aplitic gneisses (containing albite, K-feldspar and quartz but only minor amounts of micas) produce very little alteration products, and fractures therefore tend to stay open.

Table 6-2 compares the relative abundances of the rock types in the gneiss series with the numbers of inflow points observed in these rock types. The last two columns of Table 6-2 give the average spacing of inflow points in various rock types as calculated from these data. Even though the database is meagre from a statistical point of view, some trends can be recognized. In Leuggern, inflow points are strongly concentrated in aplitic gneisses.

**Fig. 6-2 :** Illustrations of structural elements in the crystalline basement.

- a. *Aplite dyke* with open fractures. Sample KAI 1091.70 from the Kaisten borehole, width of photograph 9 cm.
- b. *Cataclastic zone of the high-temperature phase*: Rounded fragments of granite are embedded in a dark, quartz-hematite-rich cataclastic matrix. Sample BOE 764.80 from the Böttstein borehole, width of photograph 10 cm.
- c. *Steeply-dipping joint of the high-temperature phase*. Fracture coating comprises quartz and sericitic muscovite but no clay minerals. Sample SIB 439.95 from the Siblingen borehole, width of photograph 10 cm.
- d. *Cataclastic zone of the low-temperature phase*: Gneiss fragments are embedded in a clay-rich cataclastic matrix. Sample LEU 257.50 from the Leuggern borehole, width of photograph 8 cm.
- e. *Joint of the low-temperature phase*: Fracture coating comprises mainly clay minerals, and feldspars in the adjacent wallrock are altered to clay minerals. Sample SIB 886.59 from the Siblingen borehole, sample width 6 cm.
- f. *Large vugs/channels* in a pre-existing cataclastic zone. Sample BOE 789.90 from the Böttstein borehole, width of photograph 10 cm.
- g. Large calcite crystals from a *mineralized, drusy vein*. Sample LEU 704.44 from the Leuggern borehole, width of photograph 5 cm.

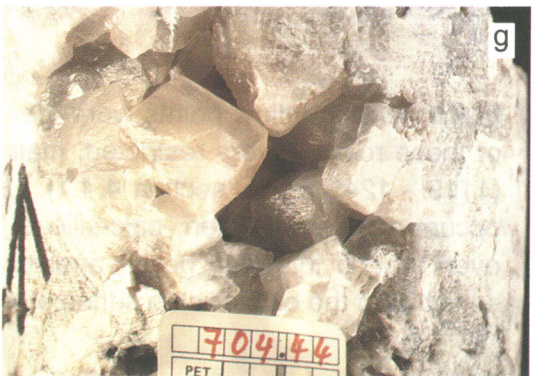
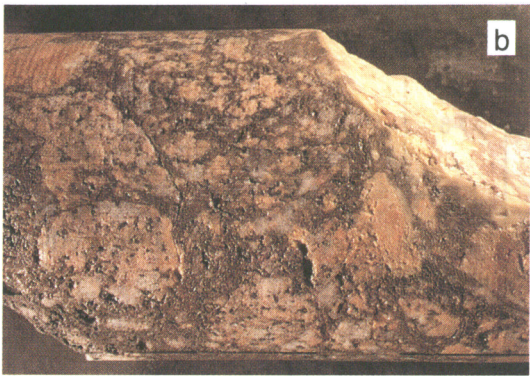


Fig. 6-2

	profile length along hole [m]		number of identified inflow points		average spacing of inflow points, [m]	
	LEU	KAI	LEU	KAI	LEU	KAI
metapelites and biotite-plagioclase gneisses	933	773	18	21-22	52	36
rocks from the banded series, including pegmatites	58	131	2	4	29	33
calc-silicate rocks	6	50	0	3	data insufficient	17
aplitic gneisses	58	18	7-8	0	8	data insufficient
aplite dykes	27	8	4	0	7	data insufficient
pegmatite dykes outside banded series	3	9	0-1	2	data insufficient	5
lamprophyre dykes	79	20	0	0-1	data insufficient	data insufficient
total	1164	1009	32	33	36	31

**Tab. 6-2 :** Dependence of inflow point frequency on rock type within the gneiss series of Leuggern and Kaisten. Calculated average spacings of inflow points (in the last two columns) give a rough idea of the relations but suffer, in many cases, from the scarcity of data.

In Kaisten, no inflow points were identified in aplitic gneisses because the occurrence of these rocks is very restricted, mainly to thin beds (< 1 m) within the banded series (1119 - 1246 m, cf. section 4.4.1). Unlike Leuggern, there are not many meter-thick occurrences. In Kaisten, calc-silicate rocks seem to contain abundant inflow points, even though this may be an analytical artefact because fluid logging was extremely sensitive in the calc-silicate series of Kaisten due to very favorable testing conditions.

### *Dykes*

The following types of dykes were identified in the crystalline basement of Northern Switzerland (more detailed characterization in Chapter 4):

- Aplites;
- Pegmatites;
- Lamprophyres;
- Granite porphyries (less common);
- Rhyolite porphyries (less common).

The relevance of the dykes for present water flow is very variable. While only 4 % of the crystalline borehole sections are aplites and pegmatites, these rocks are of prime importance for groundwater flow. Together with the aplitic gneisses, they contain 22 % of all inflow points in the deep boreholes, while lamprophyres appear to be irrelevant. Because of their low abundance, little information is available on granite and rhyolite porphyries. Reasons for such contrasting properties among different types of dykes are the same as in the case of the gneisses, as discussed above:

The relative insignificance of *lamprophyres* for water flow is explained by their mineralogy. The lamprophyres are fine-grained basic rocks and are significantly altered in most cases. Primary minerals such as amphibole, pyroxene and Ca-rich plagioclase are sources for the hydrothermal formation of large amounts of clay minerals that seal most of the fractures opened by brittle deformation.

*Aplite and pegmatite dykes* are preferred sites of brittle deformation because they are very rich in quartz and feldspars but poor in sheet silicates. Once fractures have been generated, the self-healing potential of these dykes is very limited due to the lack of primary minerals that could be hydrothermally altered and act as a source for argillic fracture coatings. Plagioclase, the most important reactant in all phases of hydrothermal alteration, is very rich in the Na (albitic) component and therefore much less altered under the geochemical conditions that prevailed during the various phases of alteration<sup>1)</sup>. In spite of their different genesis, aplite and pegmatite dykes are comparable to the aplitic gneisses with respect to hydraulic and transport parameters. In Leuggern, these rock types make up only 7 % of the profile length but contain about one third of the identified inflow points.

Aplite and pegmatite dykes were identified in all deep boreholes, cross-cutting both gneisses and granites. Thick dykes are less common than thin ones (cf. Fig. 6-3 for the boreholes north of the Permo-Carboniferous Trough). On the other hand, the thicker the dyke, the more likely it is to contain an inflow point. Only 8 % of thin dykes (0.2 - 0.4 m) are water-conducting, while 3 out of 4 dykes (75 %) thicker than 6.4 m contain inflow points. The concentration of inflow points in dykes is also seen in Table 6-2.

---

1) In general, Ca-rich plagioclase is unstable during hydrothermal or low-temperature water/rock interactions and is altered, while Na-plagioclase (albite) is only weakly affected or even stable. Albite, unlike Ca-rich plagioclase, is also a common hydrothermal product.

### **Cataclastic zones of the high-temperature phase**

Cataclastic deformation and hydrothermal alteration at elevated temperatures (300 - 400 °C; cf. section 4.5.6) were identified in granites, gneisses and dykes. Cataclastic zones have a very variable thickness (between 1 dm and several m) and are characterized by intense fracturing of the core material, which often is completely disaggregated. The regional correlation of the "high-temperature phase", comprising deformation and alteration, is based on petrographic evidence and is discussed in section 4.5.6.

### **Joints of the high-temperature phase**

Many inflow points are characterized by sets of more or less parallel joints with alteration features typical of the high-temperature phase. The frequency of joints is greater in the vicinity of cataclastic zones; however, joints occur independently of cataclastic zones in many cases.

### **Cataclastic zones of the low-temperature phase**

While the mineralogy of fracture coatings and altered wallrocks is significantly different from cataclastic zones of the high-temperature phase, no systematic variation of geometric parameters (thickness, number of fractures, orientation) could be identified (possibly due to the limited scale of observation in boreholes).

### **Joints of the low-temperature phase**

The only known difference between joints of the high-temperature phase and those of the low-temperature phase is the mineralogy of the alteration products. In Siblingen, systematically different joint orientations of the two phases could be documented; this was not possible in any of the other boreholes.

### **Vugs/channels**

Vugs/channels are open spaces in rocks, often lined with idiomorphic crystals of calcite or other phases precipitated from groundwater. Their formation is due to chemical dissolution of pre-existing fracture infills and cataclastic matrices, while no deformation is involved. Vugs/channels are small-scale features (typical cross-sections: 1 - 5 cm x 0.1 - 0.5 cm) which may significantly increase the flow porosity and, where interconnected, also the hydraulic conductivity. Measured hydraulic conductivities are high wherever vugs/channels abound in fractures. This suggests that the degree of interconnection with the groundwater flow system is high.

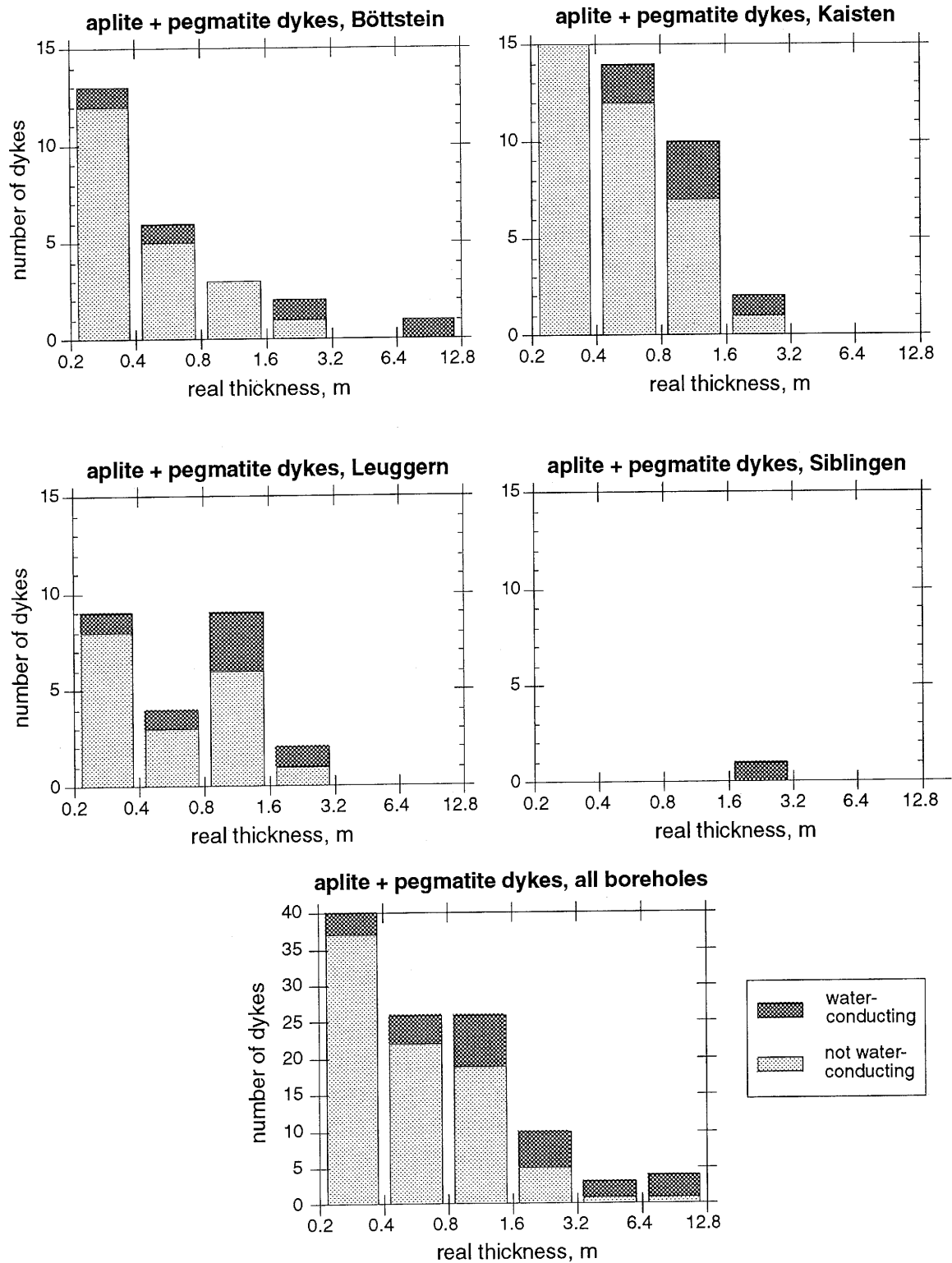


**Fig. 6-3 :** Occurrence of aplite and pegmatite dykes in borehole sections north of the Permo-Carboniferous Trough: relations between dyke frequency, dyke thickness (real thickness, i.e. corrected for dip angle) and inflow point frequency.

## Mineral veins

Structures similar to mineral veins have only been observed in Leuggern, where these elements are of major hydrogeological significance. These veins occur only in pre-existing cataclastic zones that were subjected to extreme chemical alteration (dissolution of fracture infills and cataclastic matrices) and that contain abundant vugs/channels. Subsequently, these highly permeable channels were partially mineralized by barite, calcite and minor metal ores. The mineralization was incomplete, leaving an interconnected and open system of vugs/channels. Mineral veins, as observed in the Black Forest, can be conceived as extreme cases of vugs/ channels and potentially extend over several hundred meters or more (cf. section 4.5.7 and Fig. 4-4). The high permeabilities measured in the lowest section of the Leuggern borehole (Fig. 8-2) could be due to this type of mineralization.

The mineral veins of Leuggern are probably comparable to mineralized ore veins known from the Black Forest and in fact may represent such veins in *statu nascendi*. Ore veins, described in section 4.5.7, are known to be major aquifers in the Black Forest.

## 6.4 Types of water-conducting features in the basement of Northern Switzerland

Permeable zones identified in the boreholes are mostly characterized by the superposition of several structural elements generated in the course of geological history. Preferential flow paths, such as aplite dykes, are permeable today because they were fractured during one or several phases of brittle deformation, and their flow channels (vugs) were generated by interaction between groundwater in fractures with the wallrock. In other words, the present-day *water-conducting features* are the result of the superposition of several geological events that have affected the rock body since the intrusion of the Variscan granites some 300 Ma ago.

In detail, the patterns in which structural elements were superposed on each other are highly complex and variable over the region. MAZUREK (1994) defines types of water-conducting features in each of the Nagra deep boreholes, which results in sets of 3 - 7 types per borehole. Good regional cross-correlations of these very site-specific types of water-conducting features are possible to the following extent:

1. Types of water-conducting features are analogous in the gneisses of the Kaisten and Leuggern boreholes.
2. Fractured aplite/pegmatite dykes are a type of water-conducting feature that is encountered throughout the region.

For all other types of water-conducting features defined for each borehole, correlations across the region on a *genetic* basis are difficult and often impossible. A genetic correlation would mean that the same structural element (e.g. a high-temperature cataclastic zone) was reactivated *in the same way* by the same younger elements (e.g. joints of the low-temperature phase and vugs/channels) in all boreholes across the

region. However, even when the inventory of structural elements involved is identical, the reactivation patterns may be different. For example, in Siblingen, high-temperature joints are cross-cut perpendicularly by joints of the low-temperature phase, and several inflow points were identified in zones where the two fracture systems intersect. On the other hand, in many of the other boreholes, low-temperature joints do not create a new fracture system with a different orientation but rather reactivate the pre-existing fractures. Whether old fractures are reactivated or simply cross-cut by a new system is a function of the orientations of the old fractures in relation to the stress field that prevailed during the reactivating phase.

Due to the variability of structural elements and their association patterns in all boreholes, a regional representation of water-conducting features must remain on a purely geometric basis. For example, cataclastic zones both of the high- and low-temperature phase produce comparable patterns of interconnected fracture systems, irrespective of the phase during which the shear deformation occurred. Even though cataclasis (and also jointing) occurred during at least 2 distinct geological events (i. e. high- and low-temperature phase), cataclastic zones (and jointed zones) are grouped together on a geometric basis. No significant differences in the length, thickness or hydraulic properties are identified between cataclastic zones (or jointed zones) of the high-temperature and low-temperature phases. This is due to the fact that the same deformation process (e.g. cataclasis) produces similar geometries irrespective of the age of the deformation.

Based on principal similarities and analogies, the following 3 types of water-conducting features are derived that represent the structural relations in the whole region:

**Type 1: Cataclastic zones;**

**Type 2: Jointed zones (with open joints);**

**Type 3: Fractured aplite/pegmatite dykes and aplitic gneisses.**

Significant and well-characterized differences exist between the mineralogical properties and wallrock porosities of cataclastic zones (and jointed zones) of the high-temperature and the low-temperature phases. Because of the importance of these parameters for solute transport modeling (safety assessment), water-conducting features of types 1 and 2 are each characterized by 2 sets of mineralogical and porosimetric data, referring to the 2 main phases of alteration.

A detailed characterization of all inflow points encountered in the deep boreholes, including borehole-specific structural elements and water-conducting features, is given by MAZUREK (1994). Table 6-1 gives an integrated view of the relations in all boreholes, characterizing inflow points in terms of the 3 types of water-conducting features defined above. 42 % of all inflow points are in cataclastic zones, 33 % are in jointed zones and 22 % are within aplite/pegmatite dykes and aplitic gneisses. Three inflow points in Leuggern are associated with small mineral veins (cf. section 6.5.1).

#### **6.4.1 Comments on fractured aplite/pegmatite dykes and aplitic gneisses**

Aplitic gneisses form layers within the gneiss series of the Kaisten and Leuggern boreholes, and they are also known from the Black Forest. As a part of the pre-Variscan basement, they were subjected to ductile deformation, namely large-scale folding. Their thickness varies between 1 dm and several meters, and their lateral extent could, in principle, be several hundreds of meters or more. As an approximation, the aplitic gneiss layers thus have a slab-like geometry and are, in this respect, quite similar to aplite/pegmatite dykes. In addition, the intense fracturing and the scarcity of hydrothermal neoformations in fractures are characteristic both of the aplite/pegmatite dykes and of the aplitic gneiss layers. Even though dykes and gneiss layers are quite different from a genetic point of view, they are very similar in their effects on present-day groundwater flow and potential for radionuclide retardation. For these reasons, they are grouped together in one type of model water-conducting feature.

#### **6.4.2 Distinction between plutonites and gneisses**

As discussed above, the crystalline basement of Northern Switzerland consists of approximately equal components of gneisses and plutonic rocks, particularly granites. Prediction of their spatial distribution in the basement is not currently feasible. Differences between gneisses and granites that are potentially relevant for water flow paths comprise:

1. Generally, granites are homogeneous, isotropic bodies (on a scale of decimeters and larger), while gneisses are mechanically anisotropic and inhomogeneous due to their schistosity and sedimentary or metamorphic layering. Compared to granites, the mineralogy of gneisses is characterized by a higher content of micas and a lower content of feldspars.
2. The gneisses are older than the plutonic rocks and, therefore, have undergone a longer tectono-hydrothermal evolution. Even before the intrusion of the plutonites, they were possibly subjected to several phases of ductile and cataclastic deformation.

No systematic differences in structural elements, water-conducting features, hydraulic parameters and inflow point frequencies could be observed between granites and gneisses (cf. also Chapter 6.5.2). For the purposes of hydrodynamic modeling and safety assessment, the geometric aspects of the water-conducting features are assumed to be largely identical. Geochemical and petrophysical parameters, such as mineralogy and porosity, are systematically different, and separate datasets are reported for gneisses and granites (cf. Chapter 10).

## 6.5 How representative are the borehole observations ? Comparison with geological and hydrological evidence from the Black Forest

The Nagra deep boreholes yielded about 6 km of core material from the basement of Northern Switzerland. Geological and hydrogeological parameters were derived from core analysis and hydraulic testing. It is assumed, implicitly, that the borehole information is representative of the whole region. The validity of this assumption can be checked by comparison with the Black Forest. Information from the Black Forest is, in part, a consistency check for the borehole data but also yields additional information on parameters which cannot be derived from boreholes (e.g. lateral extensions of cataclastic zones or dykes). Because topographical relief and outcrop size are limited in the Black Forest, the best exposures are found in roadcuts or quarries. Additional geological and hydrogeological data are available from numerous boreholes, tunnels and caverns built by hydropower or mining companies.

Based on these field data, the metamorphic, magmatic and tectono-hydrothermal evolution derived from the boreholes is fully corroborated by field evidence from the Black Forest. The latter also contains some additional information over and above that derived from the boreholes:

- Identification of *hydrothermal ore and mineral veins* as potentially permeable features;
- Improved hydrogeological characterization of the uppermost few hundreds of meters of crystalline rock;
- Improved geometric and hydrogeological characterization of *dykes*.

### 6.5.1 Ore and mineral veins in the Black Forest

#### Possible occurrence in the target area

Ore and mineral veins are well-known Late Variscan structures in the Black Forest and are described in section 4.5.7. In the deepest part of the Leuggern borehole (1640 - 1689 m), the granite is highly fractured and contains many vugs/channels with abundant barite and very minor amounts of ore minerals. This borehole section may represent an early stage in the development of a vein system, but it is a minor feature compared with ore and mineral veins in the Black Forest.

#### Geometry of ore and mineral veins

As described in section 4.5.7, ore veins are not evenly distributed over the entire Black Forest but rather occur in well-defined districts (Fig. 4-1). They are always associated with steeply-dipping cataclastic shear zones whose orientation generally is N-S. The vertical extent of the mineralized zones is at least several hundred meters (Grube Clara: > 350 m (HUCK 1984); Menzenschwand: > 400 m (HOFMANN 1989, cf. Fig. 4-3), and lateral extents are as much as several kilometers (Fig. 4-5). Single veins range between decimeters and meters in thickness.

### Hydraulic conductivity of ore and mineral veins

Ore veins in the Black Forest (and elsewhere) are highly permeable features because of the presence of abundant large vugs/channels. The hydraulic conductivity of the "Hermann" ore vein system, which was cross-cut by a tunnel through Albtal granite in the Southern Black Forest, is estimated to be  $4E-5$  m/s at a depth of 300 m below surface (HIMMELSBACH 1993).

Hydraulic conductivities are large ( $K > 1E-7$  m/s) in the deepest part of the Leuggern borehole (1640 - 1689 m), where features similar to ore veins (abundant vugs/channels) occur.

### 6.5.2 Hydrogeological parameters derived from boreholes in the Black Forest

A large number of boreholes, mainly aimed at supplying mineral-, drinking- or thermal water, have been drilled in the Black Forest. For many of them, hydraulic data exist and are discussed in detail by STOBER (in prep.). Most of these boreholes only penetrated the uppermost 100 - 500 m of crystalline rock exposed in the Black Forest. In contrast, several hundreds of meters of sediments cover the crystalline basement in Northern Switzerland, such that the majority of the test results reported by STOBER refers to a depth range above the top of the crystalline basement in Northern Switzerland. Thus the deepest tests from the Black Forest correspond to the uppermost sections of crystalline basement in Northern Switzerland, and the limited comparability of the data must be considered in the discussion of hydraulic parameters. STOBER (in prep.) draws the following relevant conclusions from her systematic study:

- Most inflow points are located in cataclastic zones, in dykes (aplites, pegmatites, granite porphyries, but not in lamprophyres) and in hydrothermal ore and mineral veins.
- Hydraulic conductivity varies within very wide limits (over 5 orders of magnitude) and is distributed log-normally. Conductivities of different rock types show wide overlaps in their distribution. In spite of the natural spread, the mean value for granites ( $9.6E-7$  m/s) is about 20 times (or 1.3 log units) higher than that for gneisses ( $5E-8$  m/s).

STOBER's (in prep.) findings concerning the geological characterization of inflow points (water-conducting features) are identical to those reported in sections 6.3 to 6.4 for Northern Switzerland, which increases confidence in the data. On the other hand, a systematic difference in the hydraulic conductivity of granites and gneisses was not identified in Northern Switzerland (VOBORNY et al. 1993a), which is probably due to the limited amount of data available (in contrast, STOBER's conclusion is based on about 400 tests). Different mean values for the hydraulic conductivity of granites and gneisses may well occur in Northern Switzerland, but more data would be needed for conclusive interpretation. However, the *absolute values* for hydraulic conductivity measured in the Black Forest cannot simply be transferred to Switzerland, where the crystalline basement is covered by several hundreds of meters of sediments (which increases confining pressure and protects the crystalline basement from post-Triassic

weathering effects). In addition, borehole locations in the Black Forest are not randomly distributed but rather biased. Most drilling campaigns were aimed at locating water, and boreholes were preferentially sited in areas where high permeabilities were expected, based on surface geology.

### 6.5.3 Geometric and hydrogeological characterization of dykes

*Aplite and pegmatite dykes* account for a significant proportion of the identified inflow points (cf. section 6.3.2), while lamprophyres do not have a large hydraulic conductivity in the Nagra boreholes. Only a few *granite and rhyolite porphyries* were penetrated by the Nagra boreholes and do not contain inflow points. In this Chapter, the findings from the boreholes are compared with evidence from the Black Forest outcrops and mines.

Even though the majority of all investigation efforts in the Black Forest published in the open literature is aimed at defining the geochemical characteristics of dykes, some recent studies address structural and hydrogeological aspects. The following list of observations is based on detailed studies in the Southern Black Forest by DANECK (in prep.) on the geometric properties, and by BIEHLER (in prep.) and STOBER (in prep.) on the hydraulic properties of dykes. The observations are compared to evidence from Northern Switzerland:

#### Geometric properties

1. Granite porphyries, lamprophyres and aplites are common in Southern Black Forest, while pegmatites are rare. Granite porphyries and lamprophyres are frequently concentrated in dyke swarms.

*Comparison with Northern Switzerland:* Aplites, pegmatites and lamprophyres are common in the borehole sections, while porphyries are very subordinate. One small swarm of 6 granite porphyry dykes was identified in Schafisheim.

2. Granite porphyries and lamprophyres strike about NW-SE and dip approximately vertically. In contrast, the spatial orientation of aplites is rather irregular.

*Comparison with Northern Switzerland:* Aplites and one of two pegmatite generations in the borehole sections have systematic orientations with strike directions NW-SE and steep dips (cf. section 6.8.3), i.e. very similar to the orientations of porphyries and lamprophyres in the Southern Black Forest. This is not consistent with the irregular orientation of aplites in the Black Forest. However, it was also stated in section 4.4.4 that more than one sequence of aplites intruded in Northern Switzerland (and presumably also in the Black Forest), and observations in both regions may refer to different generations.

3. Systematic cross-cutting relationships show that aplitite dykes are older than the granite porphyries and the lamprophyres. DANECK (in prep.) shows an example where an aplitite is dissected by a series of shear zones and cross-cut by a later lamprophyre. These relationships suggest that at least one phase of cataclastic deformation occurred between the intrusion of the aplitites and the lamprophyres (even though the type of shear deformation is not easily recognized in the outcrop).

*Comparison with Northern Switzerland:* Data from boreholes are unsuitable for the derivation of large-scale geometric information and relative ages based on structural criteria.

4. Observed lateral extents of outcropping dykes are less than 500-700 m; however, the significance of these numbers is somewhat reduced by the limited size of the surface exposures. In principle, some dykes could also be much longer.

*Comparison with Northern Switzerland:* Data from boreholes are unsuitable for the derivation of large-scale geometric information.

5. Granite porphyries tend to be very thick (up to 40 m), while lamprophyres do not exceed a thickness of a few m. All aplites observed are thinner than 12 m.

*Comparison with Northern Switzerland:* These data are fully consistent with evidence from the boreholes (e.g. Fig. 6-3).

6. Aplite contacts are often diffuse and gradual in granites, indicating a high wallrock temperature at the time of dyke intrusion. Aplites form complex dyke networks and presumably intruded shortly after the crystallization of the granites. In contrast, the contacts between aplites and gneisses are rather sharp.

*Comparison with Northern Switzerland:* The relations in the boreholes are different. Both in granites and gneisses, aplite contacts are sharp, indicating brittle wallrock behavior during dyke intrusion. Aplites observed in the Southern Black Forest and in the boreholes probably have no genetic relation and may belong to different generations. Diffuse contacts and irregular orientations in the Southern Black Forest are indicative of dyke intrusion under ductile wallrock behavior (BRISBIN 1986), i.e. shortly after the intrusion of the Variscan granites. In contrast, aplites in Northern Switzerland have systematic, mostly steep orientations (similar to those of the porphyries and the lamprophyres in the Black Forest) and sharp contacts, which is indicative of intrusions at shallower crustal levels (in the brittle domain).

7. Average fracture spacings in dykes range from 10 cm (aplites, lamprophyres) to 50 cm (granite porphyries). Aplites and lamprophyres, in particular, are more strongly fractured than the adjacent wallrocks; joints in aplites often end at the dyke/wallrock contacts.

*Comparison with Northern Switzerland:* These data are consistent with the borehole observations.

### **Hydraulic significance**

As stated above, the comparison of hydraulic properties in basement rocks of the Black Forest and of Northern Switzerland can only be made for the uppermost few hundreds of meters of crystalline rock because data referring to deeper parts of the crystalline basement are very scarce and of limited quality in the Black Forest (STOBER in prep.).

1. Granite porphyries that cross-cut drifts are often correlated with water inflow points. Both the contacts to the wallrock and the dykes themselves seem to be permeable.

*Comparison with Northern Switzerland:* The boreholes do not yield much evidence on the hydraulic conductivity of the dykes, because only a few granite porphyries are penetrated.

2. Lamprophyres that cross-cut drifts are often very permeable and sometimes account for a large part of all formation water inflow (BIEHLER in prep.). In most cases, the contacts to the wallrock are fractured and permeable, while internal deformation of the lamprophyre is less relevant for water flow. In addition to the evidence from drifts, examples exist from large quarries where water discharges out of lamprophyres. However, lamprophyres are not preferential water flow paths in boreholes (STOBER in prep.).

*Comparison with Northern Switzerland:* With the possible exception of a single shallow-level inflow point at Kaisten, lamprophyre dykes are not permeable in the borehole sections in Northern Switzerland. This is probably not a regional characteristic but rather a function of depth below ground. All permeable lamprophyres in the Black Forest are at shallow levels (0 - 200 m below ground), while the Northern Switzerland crystalline basement is covered by thick sedimentary sections. Due to their generally extensive degree of alteration, most lamprophyres are rich in clay minerals, and their mechanical properties show some analogy to sedimentary shale formations. The latter are commonly fractured and permeable in the upper tens of meters while they are highly impermeable under greater lithostatic pressures (e.g. Opalinus Clay, NAGRA 1991d, MAZUREK 1990c).

## Conclusions

The comparison of geological and hydrogeological properties of the crystalline rocks in Northern Switzerland and in the Black Forest shows a general agreement of observations in both regions. No major differences or contradictions could be identified in the geological evolution or in the relevance of specific structures for groundwater flow. Minor differences (such as the occurrence of ore veins and the hydraulic significance of certain types of dykes) have also been identified, but are probably related to the different scales and methods of observation in surface outcrops and in boreholes.

Due to the inability of borehole observations to identify regional patterns of large-scale structures (e.g. faults, dyke swarms, ore and mineral vein systems), the Black Forest data are used as additional information for the derivation of geological concepts related to groundwater flow and solute transport.

## 6.6 Mineralogy of water-conducting features

Knowledge of the mineralogy of permeable zones is essential for reliable solute transport modeling (safety assessment), because mineralogy is a key factor determining the sorption capacity of the flow path. Sorption of radionuclides on mineral surfaces of the flow and interconnected matrix porosity is an important process

retarding radionuclide transport. From the mineralogical rock composition, an element-specific sorption database was compiled, based primarily on empirical data for specific minerals (STENHOUSE 1994). The uncertainties involved in this process are such that a more detailed mineralogical database is not needed for this purpose.

The mineralogy of the *primary rock types* is well-characterized and is presented in section 4.4 and Table 4-4. The mineralogy of the fracture materials and of the altered wallrocks depends on the primary rock type and on the type and extent of hydrothermal alteration or mineralization that the water-conducting feature has undergone. However, the mineralogy is independent of deformation type, i.e. no mineralogical distinctions exist between cataclastic and jointed zones that were generated during the same geological event. Although the mineralogy of a water-conducting feature varies significantly on a small scale (range of dm - m), the variation is much less pronounced on a larger scale. Geosphere transport of radionuclides from a repository will involve path-lengths of several hundred meters before reaching accessible aquifers. Therefore, it is justified to use mean values for the whole crystalline basement, because local variations average out.

### **6.6.1 Mineralogy of cataclastic and jointed zones**

Even though the genesis of cataclastic zones is quite different from that of jointed zones, the small-scale structure and mineralogy is basically similar and comprises the following mineralogical domains:

- Unaltered wallrock;
- Altered wallrock within permeable cataclastic/jointed zones;
- Fracture infill (i.e. cataclastic matrix or joint infill).

#### **Unaltered wallrock embedding permeable cataclastic/jointed zones**

The unaltered wallrock embedding the permeable structures comprises mainly granites and gneisses, and separate sets of mineralogical data are reported for these rocks. While the mineralogy of fresh granites of Northern Switzerland is rather uniform, a significant variability is typical of the heterogeneous gneiss series. More than 90 % of the gneisses encountered in Northern Switzerland are metapelites and biotite-plagioclase gneisses, which are therefore chosen as representative of the whole gneiss series.

In addition to the primary mineralogical variability of the unaltered wallrock, further variations occur due to selective hydrothermal alteration. In fact, even some sections within the so-called "unaltered wallrock" have experienced hydrothermal alteration, even in zones that do not contain water-conducting features today. Fluid pathways through the formations have changed with time, and many zones that were permeable during Paleozoic alteration events were subsequently sealed by hydrothermal alteration products. Specifically, the upper 350 - 650 m of the crystalline basement in all borehole sections contain numerous zones that were significantly affected by hydrothermal alterations, and totally fresh rock only occurs at deeper levels. However,

altered zones of limited spatial extent occur even in some sections of the lower parts of the core profiles.

Petrographic evidence suggests that at least 20 % of the rock mass in the uppermost 350 - 650 m of the crystalline basement is significantly altered. This 20 % comprises high-temperature and argillic alteration in about equal amounts. The average mineralogy of this *partially altered upper part of the crystalline basement* is derived by combining the mineralogies of 10 % wallrock altered in the high-temperature phase (cf. next section), 10 % wallrock altered in the low-temperature phase (cf. next Chapter) and 80 % fresh rock; results are shown in Table 6-3. The altered wallrock mineralogies used for this calculation are equated to those of altered wallrock adjacent to fractures, as derived below in detail.

### Altered wallrock within permeable cataclastic/jointed zones

The mineralogy of the altered wallrock depends both on primary rock type and the type of hydrothermal alteration. Starting with the primary (fresh rock) mineralogies from Table 6-3, the most important effects of alteration are the following (simplified data derived from petrographic evidence, referring to volume fractions):

#### *high-temperature alteration:*

1 biotite	⇒	0.75	chlorite
		0.2	sericitic muscovite
		0.05	titanium oxides
1 plagioclase	⇒	0.9	albite
		0.1	sericitic muscovite

According to petrographic evidence, high-temperature alteration affects all biotite and plagioclase present in the altered wallrock. Alteration of other phases, such as cordierite, hornblende and pyroxene, is of minor quantitative importance.

#### *argillic alteration (i.e. low-temperature and kaolinite phases):*

plagioclase	⇒	0.5	illite
		0.25	illite/smectite mixed-layer
		0.25	kaolinite

According to petrographic observations, about 50 % of all plagioclase present in the rock is altered.

Based on these data, a mineralogy of the altered wallrock was calculated which is consistent with direct field observations. The resulting mineralogies are listed in Table 6-3.

## **Fracture infill**

Very different types of fracture infills result from different types of hydrothermal alteration and are, therefore, treated separately. High-temperature infills generally are rich in quartz and very fine-grained muscovite (= sericite), which is a high-temperature alteration product of plagioclase. Minor accessories comprise feldspars and chlorite. Fracture infills associated with argillic alteration are dominated by quartz and clay minerals, with accessory feldspars and often traces of hematite. Regardless of the type of tectono-hydrothermal event that produced the permeable structure, the majority of all fractures has been reactivated by younger events, which results in reopening of the fractures and precipitation of calcite (and minor barite, fluorite, siderite) in the fracture infills. Based on these observations, the average mineralogy of the fracture infills is estimated as listed in Table 6-3.

### **6.6.2 Mineralogy of fractured aplite/pegmatite dykes and aplitic gneisses**

#### **Country rock outside the dyke or aplitic gneiss layer**

The country rock consists of granite and gneiss whose mineralogies are discussed in the previous section.

#### **Unaltered dyke or aplitic gneiss**

Similar to granites, the mineralogy of unaltered dykes and aplitic gneisses comprises quartz, feldspars, biotite and muscovite. Micas are less abundant than in the granites. Representative values are listed in Table 6-4.

#### **Altered dyke or aplitic gneiss layer adjacent to fractures**

Hydrothermal alterations in aplite/pegmatite dykes and aplitic gneisses are less strongly developed than in all other rock types. Nevertheless, a detailed study (MAZUREK 1991) showed that a small amount of wallrock alteration is virtually ubiquitous and penetrates a few cm into the wallrock. The alteration involves the decomposition of biotite, minor alterations in plagioclase and minor production of clay minerals and chlorite. Representative data are listed in Table 6-4. No distinction is made between the two types of alteration (i.e. high- and low-temperature phases) because, in general, both occur in the rock near fractures.

#### **Fracture infill (i.e. cataclastic matrix or joint infill)**

Fracture infills generally are very thin and dominated by quartz and calcite with minor feldspars, muscovite and clay minerals. Mean values are given in Table 6-4.

data in [vol.-%]	rock matrix outside permeable zones			
	granite		gneiss	
	fresh rock	partially altered rock	fresh rock	partially altered rock
quartz	30	30	25	25
plagioclase	30	24	30	24
K-feldspar	30	30	10	10
biotite	8	7.2	15	13.5
muscovite	2	2.5	15	15.6
sillimanite	-	-	5	5
chlorite	-	0.6	-	1.1
Ti oxides	-	0.05	-	0.1
albite	-	2.7	-	2.7
illite	-	1.5	-	1.5
illite/smectite ML	-	0.8	-	0.8
kaolinite	-	0.8	-	0.8

data in [vol.-%]	altered wallrock adjacent to fractures			
	granite		gneiss	
	affected by high-T alteration	affected by argillic alteration	affected by high-T alteration	affected by argillic alteration
quartz	30	30	25	25
plagioclase	-	15	-	15
K-feldspar	30	30	10	10
biotite	-	8	-	15
muscovite	6.6	2	21	15
sillimanite	-	-	5	5
chlorite	6	-	11.3	-
Ti oxides	0.4	-	0.8	-
albite	27	-	27	-
illite	-	7.5	-	7.5
illite/smectite ML	-	3.8	-	3.8
kaolinite	-	3.8	-	3.8

fracture infills in cataclastic and jointed zones			
cataclastic and jointed zones associated with high- temperature alteration	quartz	42	[vol.-%]
	muscovite	28	
	calcite	30	
cataclastic and jointed zones associated with argillic alteration	quartz	35	
	illite	17	
	illite/smectite ML	9	
	kaolinite	9	
	calcite	30	

**Tab. 6-3 :** Average mineralogy of water-conducting feature types 1 and 2 (cataclastic and jointed zones). ML = mixed-layer.

data in [vol.-%]	rock matrix outside the dyke or aplitic gneiss layer			
	granite		gneiss	
	fresh rock	partially altered rock	fresh rock	partially altered rock
quartz	30	30	25	25
plagioclase	30	24	30	24
K-feldspar	30	30	10	10
biotite	8	7.2	15	13.5
muscovite	2	2.5	15	15.6
sillimanite	-	-	5	5
chlorite	-	0.6	-	1.1
Ti oxides	-	0.05	-	0.1
albite	-	2.7	-	2.7
illite	-	1.5	-	1.5
illite/smectite ML	-	0.8	-	0.8
kaolinite	-	0.8	-	0.8

data in [vol.-%]	unaltered dyke or aplitic gneiss layer	altered dyke or aplitic gneiss layer adjacent to fractures	fracture infill
quartz	32	32	56
plagioclase	32	26	3
K-feldspar	31	31	2
biotite	3	0.5	-
muscovite	2	5	5.5
chlorite	-	2	-
illite	-	1.5	1.5
illite/smectite ML	-	1	1
kaolinite	-	1	1
calcite	-	-	30

**Tab. 6-4:** Average mineralogy of water-conducting feature type 3 (fractured aplite/pegmatite dykes and aplitic gneisses). ML = mixed-layer.

## 6.7 Porosity of water-conducting features

### 6.7.1 Microscopic pore-space geometry

The microscopic distribution of pore-spaces in wallrocks adjacent to fractures was studied in thin-sections that were impregnated with a fluorescent dye under vacuum conditions (MAZUREK 1994). Microscopic observations suggest that all rocks, both fresh or altered, contain an interconnected network of micropores. Even though part of this porosity may have been produced during drilling or sample preparation, some

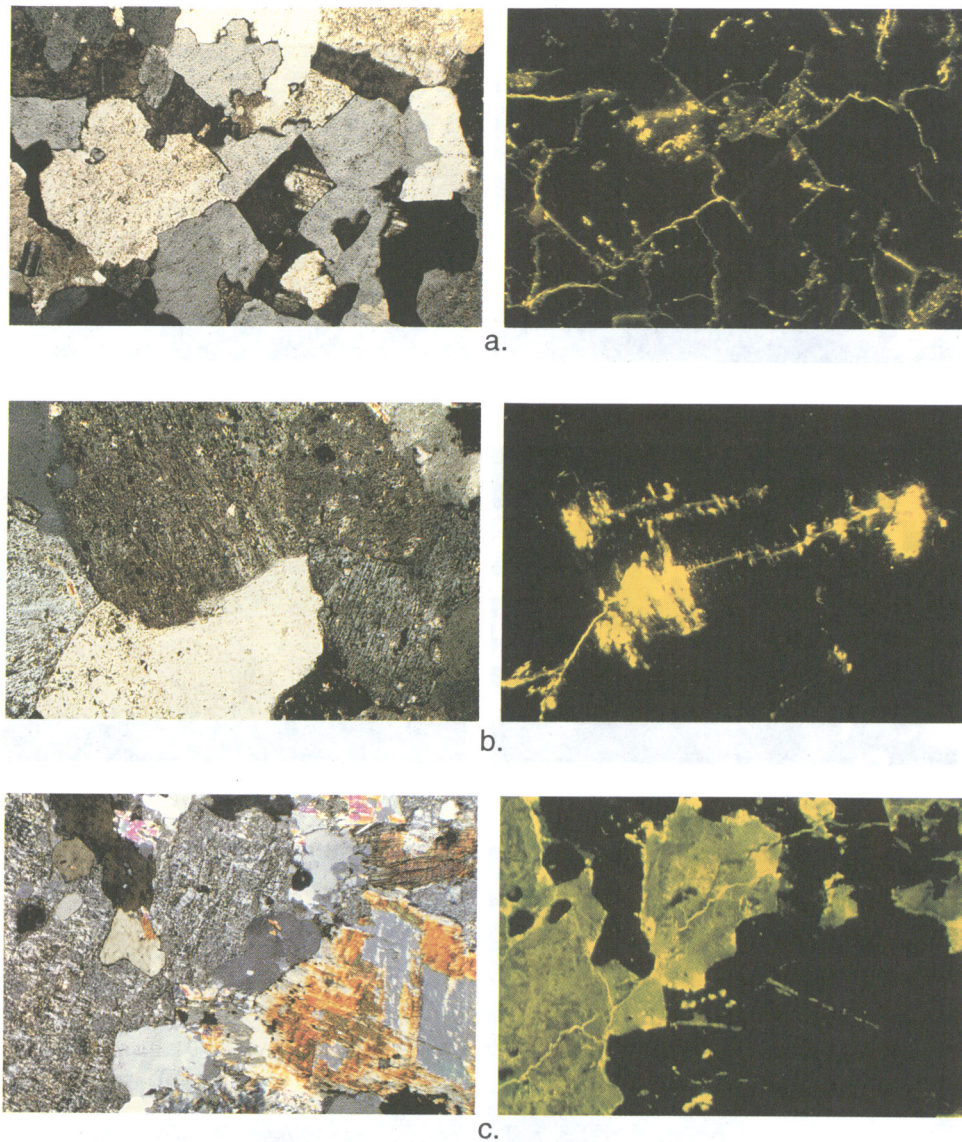


**Fig. 6-4 :** Types of pore-spaces in crystalline rocks in transmitted (left) and fluorescent (right) light. Photographs are from impregnated thin-sections; fluorescent regions represent porosity.

- a. Grain boundary and transgranular micropore network in an aplite/pegmatite dyke. Sample BOE 618.85, width of photographs 2.5 mm.
- b. Bright, cloudy arrays represent solution porosity (etching features) in feldspars, emanating from grain boundary and transgranular pores. Sample from aplitic gneiss LEU 319.21, width of photographs 1 mm.
- c. Clay mineral porosity in altered feldspars: Large plagioclase grains are completely replaced by clay minerals, resulting in a microporosity of 20 - 40 vol.-% in the pseudomorphs. Connections to other pore types are provided by transgranular pores and microcracks. Sample from granite SIB 1083.23, width of photographs 6 mm.

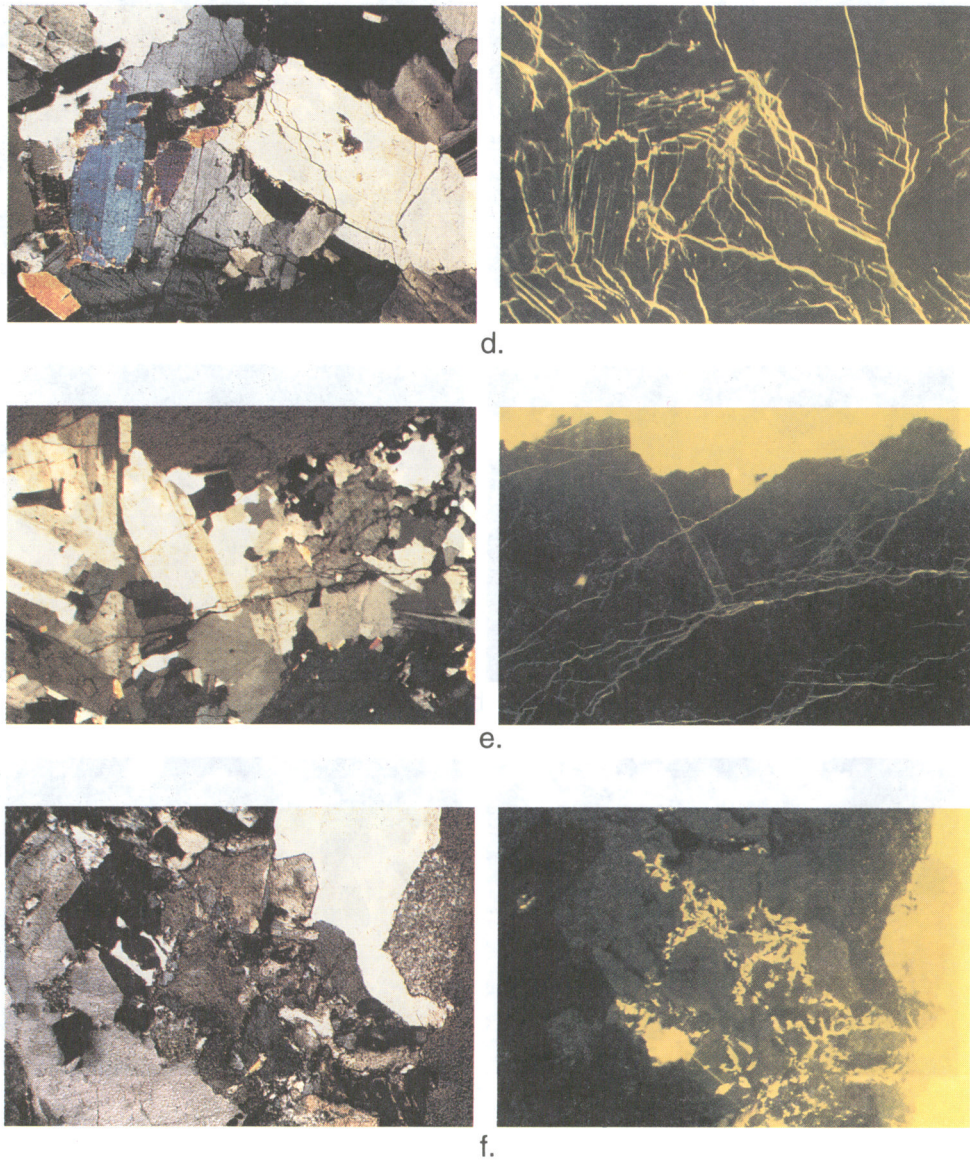


**Fig. 6-4 :**

- d. Interconnected microcrack network in wallrock adjacent to a cataclastic zone, generated during brittle shear deformation. Sample from pegmatite dyke KAI 1091.71, width of photographs 2.5 mm.
- e. Uncoated fracture surface (top) with good interconnection to the wallrock porosity via microcracks and transgranular pores. Sample from pegmatite dyke KAI 1091.71, width of photographs 2.5 mm.
- f. Open fracture partially coated by sericite (right edge) and adjacent wallrock with porosity decreasing with distance from the fracture. This porosity gradient is due to variable degrees of hydrothermal alteration, the latter being most strongly developed near the wallrock/fracture interface. Sample from pegmatite dyke KAI 1174.38, width of photographs 4 mm.

pore-spaces always remain that are clearly natural (e.g. because they contain microcrystalline, idiomorphic quartz). Porosity in all rock types is significantly increased by hydrothermal alterations. Several types of pore-spaces are distinguished, as shown in Figure 6-4:

- *Grain boundary and transgranular pores:* These planar pore-spaces have typical apertures of 0.5 - 2  $\mu\text{m}$  and follow grain boundaries of quartz and feldspars or cross-cut these minerals. Because their orientation is generally random, they constitute a well-interconnected network of pore-spaces and are often the dominant pore types observed in thin-section. Part of these pores may represent artefacts of sample preparation (see comment above).
- *Solution pores in plagioclase ( $\pm K$ -feldspar):* Magmatic and metamorphic feldspars were unstable during retrograde cooling and during the hydrothermal alteration phases. This led to the development of abundant etching features and therefore enhanced microporosity, even though this feature is commonly not very conspicuous in hand-specimens. Typically, solution pores emanate from transgranular cracks through feldspar grains. These pores have a complex, non-planar geometry and can be seen under the microscope as porous zones or clusters. The pore-space apertures are very small, with estimated mean apertures of 0.01 - 0.05  $\mu\text{m}$ .
- *Clay mineral pores:* This type of pore-space developed during the low-temperature argillic alterations of the rocks and mainly affects plagioclase and cordierite. Plagioclase that has altered to clay minerals forms a major pore-space reservoir which consists of uncompacted and unoriented clay platelets with interstitial pores constituting 20 - 40 vol.-% of the whole structure. Pore-space apertures are similar to those of solution pores, with an estimated mean aperture of 0.01 - 0.05  $\mu\text{m}$ . In thin-section, the altered, porous plagioclase grains are connected with open macroscopic fractures via the transgranular and grain boundary pore network.

Adjacent to cataclastic zones, the wallrock is generally dissected by numerous large microcracks (apertures of several tens of  $\mu\text{m}$ ) in addition to the pore types described above, which leads to an additional increase of the pore volume. Hydrothermal alteration is often most strongly developed in wallrock portions that are immediately adjacent to fractures, which results in very high porosities that decrease with distance from the fracture (example in Fig. 6-5a).

Hydrothermal cementation (e.g. by microcrystalline quartz) may partially seal the wallrock porosity from the open macroscopic fractures. However, even in strongly sealed samples, the mean distance between two fracture/wallrock connections via microcracks or grain boundary pores is 10 mm at the maximum and often much less.

The presence of interconnected micropores in wallrocks adjacent to fractures is also corroborated by the isotopic analysis of natural decay series of U and Th in PEARSON et al. (1991). Identified radioactive disequilibria between mother and daughter isotopes (such as  $^{234}\text{U}/^{238}\text{U}$ ,  $^{230}\text{Th}/^{234}\text{U}$ ) indicate rock/water interactions that took place within the last ca. 1 Ma. Such rock/water interactions were identified in wallrocks up to 4 cm away from open fractures (cf. Fig. 6-5c), which is proof of diffusion-accessible (interconnected) matrix porosity in these wallrocks.

## 6.7.2 Quantitative porosimetry

### Terminology

An estimate of the porosity of the advective water flow paths (i.e. the flow porosity for modeling purposes) was made from core inspection (e.g. geometry of open joints and vugs/channels). The present Chapter deals mainly with the *open porosities* of the fracture fillings and the wallrock materials adjacent to the macroscopic flow channels. Open porosities were determined using the Hg injection technique with maximum injection pressures of 2 kbars, which corresponds to a pore size limit accessible to Hg of 4 nm. Because this technique gives a measure of the interconnected network of pores in the rock but does not include isolated pore-spaces, the open porosity determined by Hg injection probably represents the pore volume that is interconnected and accessible to diffusion. By definition, pores with radii  $< 7.5 \mu\text{m}$  are called *open micropores*, those  $> 7.5 \mu\text{m}$  are called *open macropores*.

In addition to the open porosities, total porosities were determined on the same samples by measuring the *rock density* (i.e. density of a compact piece of rock) and *grain density* (i.e. density of the finely ground rock powder). Total porosity is not directly relevant to safety assessment because it includes isolated pore-spaces that are inaccessible to matrix diffusion. The terminology of types of pore-spaces as used in this report can be summarized as follows:

open macroporosity + open microporosity	= open porosity	} pore-spaces in wallrocks and fracture infills
	= diffusion-accessible porosity	
open porosity + isolated pores	= total porosity	
flow porosity		} fracture porosity/ channels

For technical reasons, Hg injection analyses cannot be conducted on cohesionless structures such as argillic fracture coatings. Therefore, the analytical data have to be complemented by information gained from impregnated thin-sections of the cohesionless material. In addition, porosimetric analyses are performed on quite small samples ( $\sim \text{cm}^3$ ), and some degree of averaging is needed to obtain representative values of wallrock porosity. A more detailed discussion of the methodology, error estimation and of possible artefacts is given at the end of this section and in MAZUREK (1994).

### Results and discussion

About 160 porosimetric determinations were conducted on samples of the crystalline basement of Northern Switzerland. The results of both the densitometric and Hg injection analyses are reported in Tables 6-5 to 6-7. Because of the large analytical errors associated with densitometric porosity measurements, the discussion mainly deals with the Hg injection results.

Analytical results are grouped according to primary rock types and states of hydrothermal alteration. Mean values and standard deviations are calculated in Tables 6-5 to 6-7 and graphical representations are given in Figures 6-5 and 6-6.

Variation with rock type (Fig. 6-6, Tab. 6-6): All rock types occupy quite large, widely overlapping fields in Figure 6-6. The scatter of the data is mainly due to variable degrees of hydrothermal alteration. The mean open porosity of dykes is slightly smaller than that of other rock types (cf. Tab. 6-6), because dykes are less affected by alteration (see below). The averaged values of open porosity (Hg injection) and total porosity (densitometry) are very similar, indicating that most of the pore-space in the rock is interconnected. This agrees well with qualitative observations made from impregnated thin-sections.

Variation with state of hydrothermal alteration (Fig. 6-6, Tab. 6-7): A good distinction exists between fresh and altered rocks, regardless of the primary rock type (granite, gneiss, dyke, etc.). The open porosity of fresh rocks mostly is between 0.1 and 2 vol.-%, with mean values of 0.9 vol.-%. The macro- and, much more pronounced, the microporosity increase with high-temperature alteration ( $\phi = 2.5$  vol.-%). Much of this microporosity is due to the partial alteration of primary feldspars to albite and mica, leaving microporous etching features in the dissolving feldspars. The increase of microporosity is even stronger in rocks affected by argillic alteration ( $\phi = 6.9$  vol.-%). In these rocks, feldspars and micas have been partially altered to highly porous aggregates of  $\mu\text{m}$ -sized clay minerals. On the other hand, the increase of the macroporosity is insignificant. Figure 6-6 also shows that, while the grain density is largely independent of hydrothermal alteration, the rock density decreases significantly due to the increased porosity of the rocks.

*Porosity of intrusive rocks excluding dykes* (Fig. 6-6, Tab. 6-5): The open porosity of fresh granites is very low ( $\phi = 0.27$  vol.-%) and does not overlap with that of altered granites at all. Irrespective of the type of alteration, altered granites have open porosities between 1 and 10 vol.-%. Fresh basic rocks (all from the Schafisheim borehole) have open porosities at about 1.5 vol.-%, probably due to the presence of abundant biotite with its sheet silicate porosity. Porosities of altered basic intrusives fully overlap with the fields of altered granites.

*Porosity of dykes* (Tab. 6-5): Open porosities of fresh aplite/pegmatite dykes partly overlap with those of fresh granites but have a higher average value of about 0.9 vol.-%. Hydrothermal effects may slightly increase the microporosity, but this increase is much less pronounced than in granites. This minor effect is because primary plagioclase in aplite/pegmatite dykes is very rich in albite and therefore much less affected by both types of hydrothermal alterations. Porosities of fresh lamprophyres overlap with those of fresh aplites/pegmatites, whereas much higher porosities occur in altered lamprophyres.

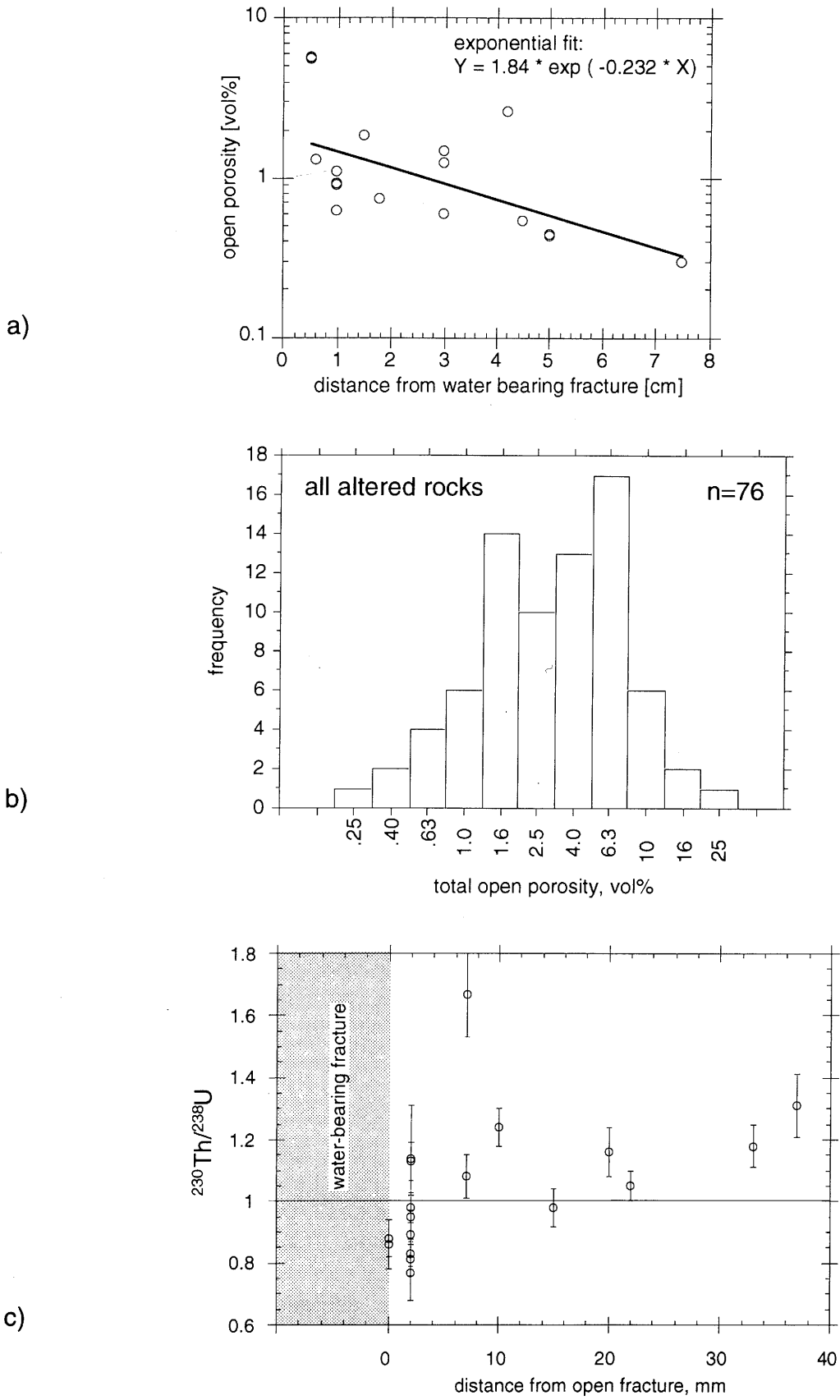


Fig. 6-5

**Fig. 6-5 :** Quantification of wallrock porosity by Hg injection and U/Th disequilibrium measurements.

- a. Open porosity (as determined by Hg injection) as a function of distance from a macroscopic fracture. Example from an aplite dyke (LEU 319.21).
- b. Frequency distribution of total open porosity of altered rocks.
- c. Example of U/Th radioactive disequilibrium measurements from fractured aplite dykes. Disequilibrium was identified in most rock matrix samples up to 37 mm away from the nearest open fracture.

rock type	no. of analyses	rock density	grain density	total porosity	open macroporosity	open microporosity	total open porosity
		[g/cm <sup>3</sup> ]	[g/cm <sup>3</sup> ]	[vol.-%]	[vol.-%]	[vol.-%]	[vol.-%]
		mean	mean	mean	mean	mean	mean
fresh granite	12	2.63 ± 0.01	2.66 ± 0.02	0.83 ± 0.45	0.14 ± 0.07	0.14 ± 0.12	0.27 ± 0.15
granite, high-T alteration	10	2.52 ± 0.05	2.64 ± 0.03	4.44 ± 2.55	0.58 ± 0.42	3.73 ± 1.89	4.31 ± 2.14
granite, argillic alteration	10	2.41 ± 0.09	2.62 ± 0.03	8.10 ± 3.67	0.50 ± 0.20	5.30 ± 1.95	5.80 ± 2.07
granite, altered (unspecified)	18	2.55 ± 0.06	2.65 ± 0.05	3.77 ± 1.86	0.32 ± 0.17	2.72 ± 1.47	3.04 ± 1.56
fresh basic intrusives	7	2.77 ± 0.05	2.81 ± 0.04	1.42 ± 0.37	0.53 ± 0.05	0.95 ± 0.43	1.48 ± 0.42
basic intrusives, altered (unspecified)	3	2.63 ± 0.02	2.70 ± 0.02	2.35 ± 0.23	0.43 ± 0.42	3.00 ± 0.78	3.43 ± 0.60
fresh aplitic/pegmatitic dyke	16	2.61 ± 0.04	2.66 ± 0.04	1.92 ± 1.31	0.26 ± 0.11	0.59 ± 0.36	0.85 ± 0.43
aplitic/pegmatitic dyke, altered (unspecified)	11	2.62 ± 0.04	2.65 ± 0.04	1.25 ± 0.93	0.19 ± 0.08	1.66 ± 1.92	1.85 ± 1.97
fresh lamprophyre	3	2.76 ± 0.02	2.79 ± 0.02	1.31 ± 1.15	0.29 ± 0.06	0.49 ± 0.31	0.78 ± 0.35
lamprophyre, argillic alteration	1	2.58	2.68	3.73	0.45	5.00	5.45
fresh metapelite	9	2.76 ± 0.04	2.80 ± 0.02	1.39 ± 0.69	0.41 ± 0.07	0.90 ± 0.64	1.32 ± 0.66
metapelite, high-T alteration	2	2.70 ± 0.05	2.76 ± 0.02	2.17 ± 2.55	0.71 ± 0.23	0.56 ± 0.51	1.27 ± 0.74
metapelite, argillic alteration	5	2.57 ± 0.18	2.75 ± 0.07	6.70 ± 5.99	0.51 ± 0.30	5.81 ± 4.32	6.32 ± 4.52
fresh biotite-plagioclase gneiss	8	2.69 ± 0.04	2.72 ± 0.03	0.96 ± 0.55	0.27 ± 0.11	0.67 ± 0.55	0.94 ± 0.64
biotite-plagioclase gneiss, high-T alteration	3	2.56 ± 0.11	2.71 ± 0.04	5.72 ± 5.45	0.34 ± 0.12	2.85 ± 2.33	3.19 ± 2.37
biotite-plagioclase gneiss, argillic alteration	8	2.46 ± 0.11	2.74 ± 0.05	10.18 ± 3.95	0.58 ± 0.33	9.19 ± 4.41	9.77 ± 4.52
fresh aplitic gneiss	6	2.65 ± 0.05	2.68 ± 0.05	1.17 ± 1.26	0.23 ± 0.06	0.66 ± 0.84	0.89 ± 0.85
aplitic gneiss, high-T alteration	3	2.62 ± 0.04	2.64 ± 0.01	0.76 ± 1.01	0.63 ± 0.57	0.25 ± 0.26	0.88 ± 0.83
fresh calc-silicate rock	1	2.91	2.95	1.36	0.16	0.12	0.28
calc-silicate rock, argillic alteration	3	2.68 ± 0.07	2.75 ± 0.06	3.63 ± 0.95	0.52 ± 0.53	9.64 ± 14.32	10.17 ± 14.86
amphibolite, high-T alteration	1	2.77	2.98	7.05	0.48	0.50	0.98
cataclastic matrix	21	2.60 ± 0.118	2.71 ± 0.05	4.21 ± 3.37	0.37 ± 0.18	3.34 ± 2.69	3.71 ± 2.76

**Tab. 6-5 :** Summary of porosimetric data from the crystalline basement of Northern Switzerland.

general groups of rocks	no. of analyses	rock density [g/cm <sup>3</sup> ]	grain density [g/cm <sup>3</sup> ]	total porosity [vol.-%]	open macroporosity [vol.-%]	open microporosity [vol.-%]	total open porosity [vol.-%]
		mean	mean	mean	mean	mean	mean
gneisses	49	2.64 ± 0.13	2.74 ± 0.07	3.78 ± 4.43	0.42 ± 0.27	3.14 ± 5.11	3.57 ± 5.26
granites	49	2.54 ± 0.10	2.64 ± 0.04	4.08 ± 3.34	0.36 ± 0.28	2.77 ± 2.28	3.13 ± 2.47
basic intrusives	10	2.73 ± 0.08	2.78 ± 0.07	1.70 ± 0.55	0.50 ± 0.22	1.63 ± 1.15	2.13 ± 1.07
dykes	31	2.63 ± 0.06	2.67 ± 0.05	1.67 ± 1.21	0.25 ± 0.11	1.10 ± 1.45	1.35 ± 1.49
cataclastic matrices	21	2.60 ± 0.11	2.71 ± 0.05	4.21 ± 3.37	0.37 ± 0.18	3.34 ± 2.69	3.71 ± 2.76

**Tab. 6-6 :** Porosimetric data grouped according to rock types.

state of alteration	no. of analyses	rock density [g/cm <sup>3</sup> ]	grain density [g/cm <sup>3</sup> ]	total porosity [vol.-%]	open macroporosity [vol.-%]	open microporosity [vol.-%]	total open porosity [vol.-%]
		mean	mean	mean	mean	mean	mean
fresh rocks	61	2.68 ± 0.08	2.72 ± 0.08	1.33 ± 0.94	0.28 ± 0.14	0.59 ± 0.53	0.87 ± 0.62
rocks affected by high-T alteration	27	2.59 ± 0.08	2.67 ± 0.08	3.12 ± 3.02	0.45 ± 0.36	2.06 ± 2.00	2.50 ± 2.16
rocks affected by argillic alteration	29	2.50 ± 0.14	2.69 ± 0.07	7.51 ± 4.52	0.51 ± 0.28	6.88 ± 5.29	7.39 ± 5.48
altered rocks (unspecified)	22	2.57 ± 0.06	2.66 ± 0.05	3.43 ± 1.81	0.32 ± 0.21	2.65 ± 1.45	2.97 ± 1.54
cataclastic matrices	21	2.60 ± 0.11	2.71 ± 0.05	4.21 ± 3.37	0.37 ± 0.18	3.34 ± 2.69	3.71 ± 2.76

**Tab. 6-7 :** Porosimetric data grouped according to state of alteration.

*Porosity of gneisses* (Tab. 6-5): Metapelites and biotite-plagioclase gneisses are by far the most common types of gneisses in the basement of Northern Switzerland. The open porosity of fresh types of these gneisses (mean values about 0.9 - 1.3 vol.-%) is significantly higher than that of fresh granites, which is due to the occurrence of abundant mica in these gneisses. The effects of high-temperature alteration are not well-established, due to the low number of analyses, but an increase occurs at least in the biotite-plagioclase gneisses. Argillic alteration causes a large increase in microporosity (means between 5 - 10 vol.-%), which is even greater than the porosity of altered granites. Gneisses also have significant contents of minerals such as cordierite and sillimanite that are susceptible to argillic alteration.

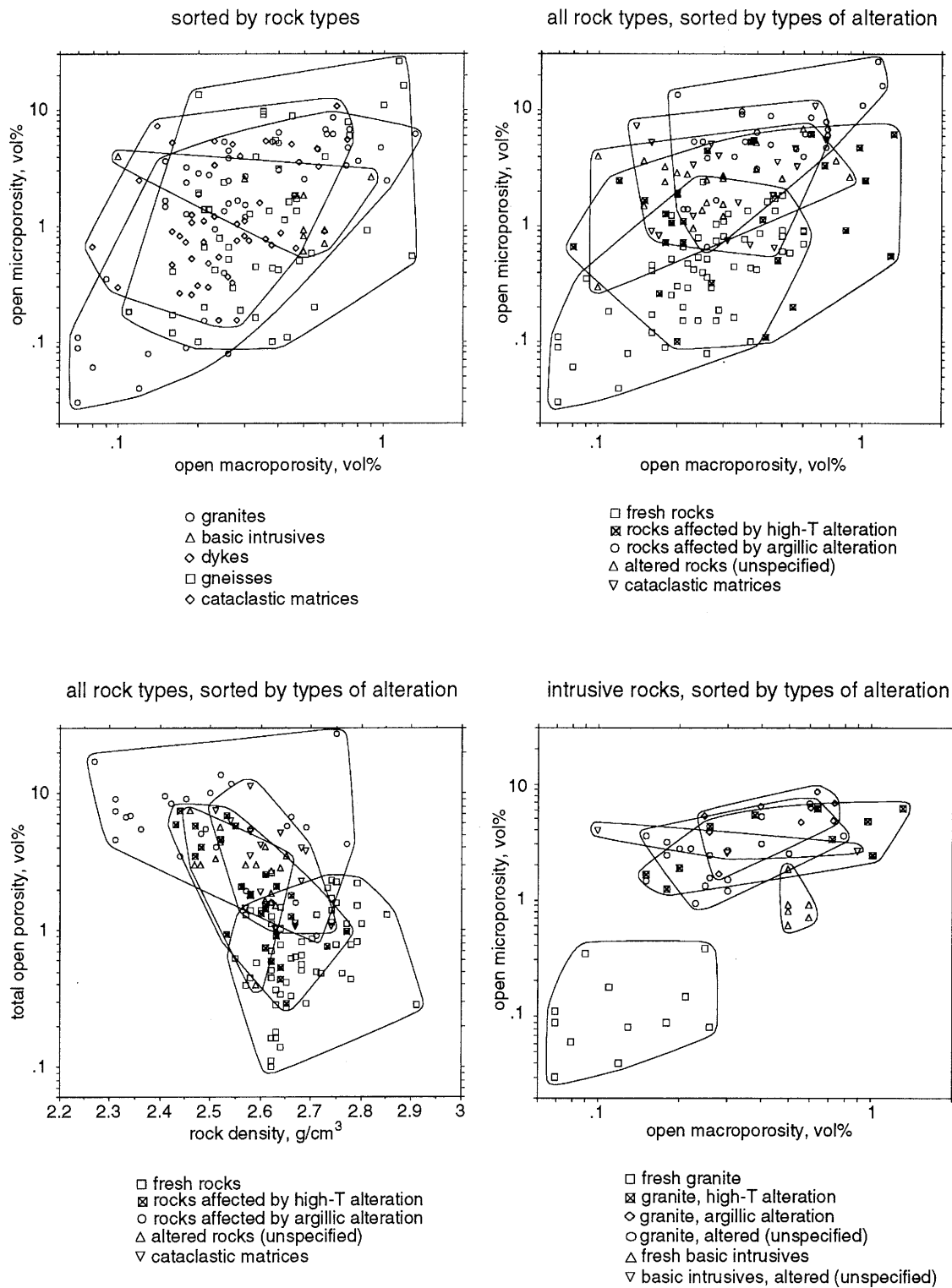


**Fig. 6-6 :** Open porosities of wallrocks as a function of rock types and type of alteration as determined from Hg injection measurements.

Although the proportion of aplitic gneiss is relatively small in volume, this rock type contains a significant number of inflow points (see above). The porosity of fresh aplitic gneisses is very similar to that of fresh aplite/pegmatite dykes. Total open porosity is small in the 3 altered samples. Like the dykes, this type of gneiss lacks minerals that are susceptible to hydrothermal effects.

Because of the small number of analyses, porosities of calc-silicate and amphibolite layers in the gneiss series are very uncertain. Due to the minor abundance and isolated occurrence of these rocks in the gneiss series, they are not considered safety-relevant in any case.

*Porosity of cataclastic matrices* (Tab. 6-5): All samples analyzed have a porosity > 1 vol.-% (mostly microporosity). Typical values are 3 - 4 vol.-%, which approximately corresponds to the porosities of the altered wallrocks.

### Summary and critique

Although the analytical error of Hg injection porosimetry is small, uncertainties arise due to sampling effects that are not easily quantifiable:

1. Decompression to atmospheric conditions during sampling.
2. Drilling and sawing may have caused mechanical damage to the microscopic structure of the rock.
3. Using 2,000 bars as the maximum Hg injection pressure, only pores with equivalent radii > 4 nm will be detected. It has previously been shown that, in microporous rocks, the Hg injection measurements typically yield lower values than data derived from mass-transfer measurements (such as diffusive access of  $^3\text{H}$  to the pore-space). This discrepancy has been attributed to the presence of pore-spaces with equivalent radii < 4 nm which were not intruded by Hg.
4. The representativity of the 10 - 20 g samples for a larger rock body is questionable.

Points 1 and 2 lead to an overestimation of the open porosity. Point 3, however, leads to an underestimation. Therefore, the systematic errors in our measurements may, at least partially, cancel each other out. Problems with representativity of small samples (point 4) should be overcome by the large number of data points, because small-scale variations average out.

Porosities of crystalline rocks of Northern Switzerland vary greatly. While the nature of the primary rock type is only of secondary importance, the type and extent of hydrothermal alteration is the major factor governing porosity. Fresh granites have mean porosities about 0.25 vol.-%, while the major types of fresh gneisses have about 1 vol.-%. High-temperature alteration is associated with a significant increase of open microporosity (a typical value is 3 vol.-%) in both granites and gneisses. Even more pronounced is the increase of microporosity in rocks that underwent argillic alteration. Here, gneisses (5 - 10 vol.-%) appear to be more porous than granites (5 - 6 vol.-%).

The porosities of cataclastic matrices in deformed rock portions are well within the range of values for the altered wallrocks.

The porosity of fresh aplite/pegmatite dykes is slightly less than 1 vol.-% and increases only slightly with hydrothermal alteration. The pore-space characteristics of aplitic gneisses are very similar to those of the dykes.

## **6.8 Spatial orientation of water-conducting features**

### **6.8.1 Orientation of cataclastic zones**

The spatial orientation of cataclastic zones is difficult to derive from borehole data, because of the small-scale variability of individual fracture plane orientations that is typical of cataclastic shear zones in general. Due to this variability, a large scatter of the data results when fracture orientations are measured in boreholes. Even though preferential orientations of cataclastic features are observed in data from some boreholes, no regional correlation is possible among the boreholes. In general, cataclastic zones have an angle of dip between  $45^\circ$  -  $90^\circ$  and the strike direction is variable. This pattern is consistent with the large-scale structural model of Northern Switzerland, presented in Chapter 5, where all families of faults dip steeply but are distinguished by variable strike directions.

### **6.8.2 Orientation of joints**

Joint orientations tend to be randomly distributed and have even less systematics than orientations of cataclastic zones. Joint formation was a multiphase process, and several sets of joints have formed since the Variscan orogeny. A systematic distribution of joint orientations and a good correlation with phases of deformation was observed only in Siblingen (MAZUREK 1990a). Relations vary between boreholes, and no regional correlation exists. As in the case of cataclastic zones, steeply-dipping joints dominate over flat-lying structures.

### **6.8.3 Orientation of aplite/pegmatite dykes**

In the Schafisheim borehole, no orientation data are available at all; in Weiach, dyke orientations are randomly distributed; in Siblingen, only one dyke was observed. This section is therefore restricted to the discussion of the Böttstein, Leuggern and Kaisten data, where some degree of regional consistency in the orientation of aplite/pegmatite dykes exists. Available data are presented in Figure 6-7 in equal-area stereographic projections. These include all measurements regardless of the thickness of the dykes.

*Aplite dykes* have similar orientations in all 3 boreholes. The mean value is 75/65<sup>1)</sup>, i.e. many aplites dip steeply in an ENE direction. However, considerable scatter exists in the data, and the use of a single mean value may not be appropriate. Dip directions vary between NNE and ESE, while the dip angle of most aplites is greater than 45°. Because the probability of drilling across steeply-dipping dykes is low in a vertical borehole when compared with flat-lying structures, the proportion of very steeply-dipping aplites is in reality expected to be even greater than suggested by Figure 6-7.

The orientation of *pegmatite dykes* has a bimodal distribution (Fig. 6-7): One generation has a mean orientation of 40/60, which is very similar to the orientation of the aplites. Another generation has a more scattered orientation, with a mean value of 270/30, and is mainly concentrated in the banded series of Kaisten (cf. section 4.4.1). The contrasting orientation patterns were correlated with petrographic evidence, which also suggests the presence of 2 pegmatite types:

1. *Pegmatites from the banded series*: Contacts with the wallrocks are often gradational and rugged, suggesting that the surrounding wallrock deformed in a plastic manner during pegmatite intrusion. Pegmatite orientation is approximately parallel to the schistosity of the gneisses, i.e. 270/30 on average.
2. *Most other pegmatites in granites and gneisses*: Contacts with the wallrock are sharp and generally discordant to schistosity, suggesting brittle deformation behavior of the wallrock during pegmatite emplacement and therefore a shallower crustal level of intrusion. The same is true of all aplites, whose mean orientation is very similar.

Mechanical aspects of dyke intrusion in general and the dependence of dyke orientation on the regional stress field are discussed by BRISBIN (1986). Dykes tend to be vertical in the brittle domain of the basement if horizontal stresses or major mechanical anisotropies are absent. This probably is the case for most aplites and pegmatites of the basement of Northern Switzerland. In the ductile domain, orientations are irregular and partly governed by wallrock anisotropies, such as schistosity. This pattern generally fits the pegmatites in the banded series, where the complex contacts with the wallrock indicate a deeper crustal level of intrusion.

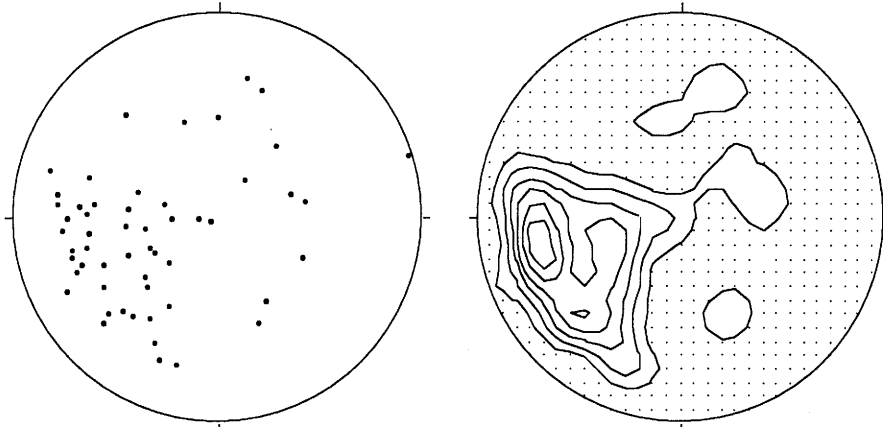
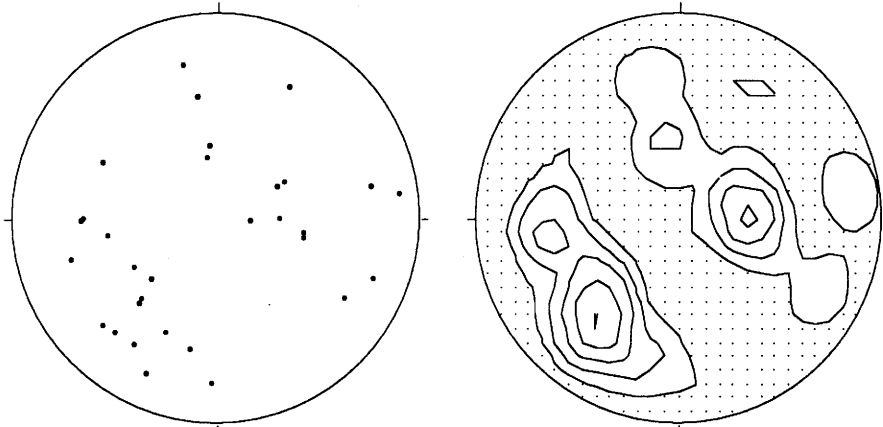
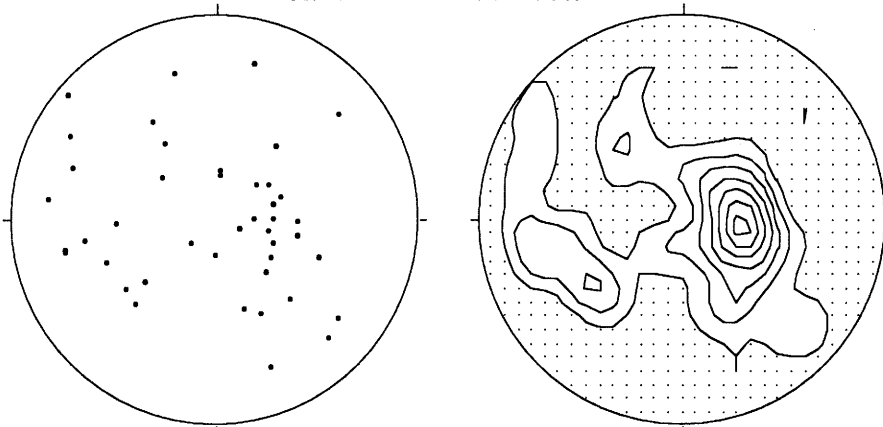
#### 6.8.4 Orientation of aplitic gneiss layers

Aplitic gneisses occur as layers in the gneiss series of Leuggern and Kaisten and are parallel to schistosity, the orientation of which is fairly constant and well-known. In Leuggern, schistosity in the upper part of the profile (where aplitic gneisses occur) dips 30° - 40° to S-W. In Kaisten, dip directions are similar to those in Leuggern (i.e. S-W) but angles of dip tend to be flatter (0° - 30°). By analogy with evidence from the Black Forest, the orientation of schistosity (and therefore of the aplitic gneiss layers) probably varies on a scale of km due to large-scale folding.

---

1) Notation of orientation measurements: First number = dip azimuth measured clockwise from north; second number = dip angle.

## aplite dykes Böttstein, Kaisten, Leuggern

pegmatite dykes Böttstein, Kaisten, Leuggern  
(without banded series at Kaisten)pegmatite dykes from the  
banded series at Kaisten

**Fig. 6-7 :** Spatial orientation of aplite/pegmatite dykes in the boreholes of Böttstein, Kaisten and Leuggern. Equal-area stereographic projections of the lower hemisphere. Contours indicate 2x, 3x, 4x, ... average point density.

Aplite/pegmatite dykes and aplitic gneisses have similar mineralogies and similar mechanical behavior during deformation. In addition, both are largely 2-dimensional structures. The main difference between dykes and aplitic gneisses is their spatial orientation, which is mostly steep for the dykes and rather flat for the aplitic gneisses.

## 6.9 Depth dependence of water-conducting features, geological and hydraulic parameters

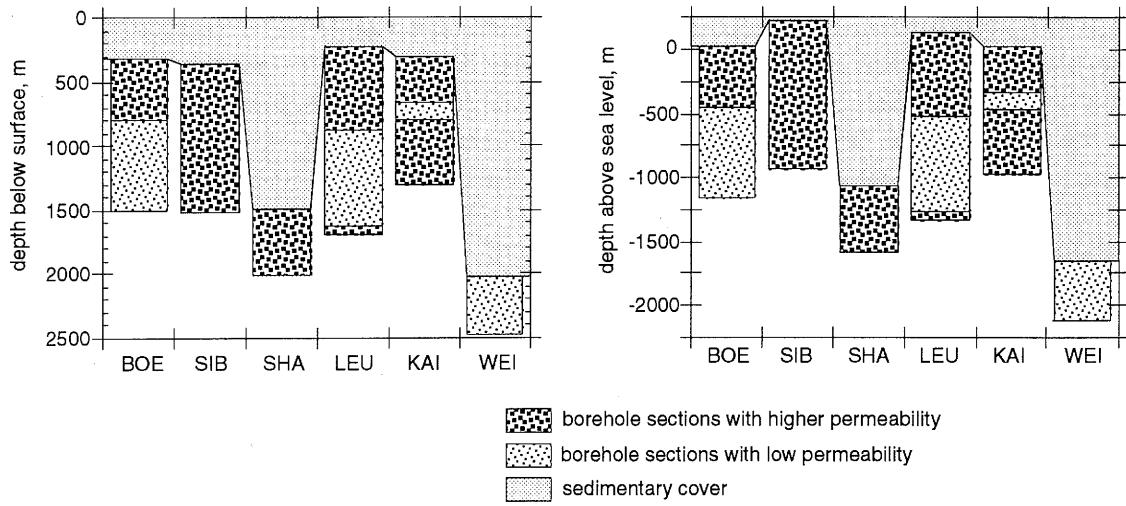
Some of the observed depth zonations of geological, hydrological and geophysical parameters are unique in each borehole and do not justify a regional correlation. No systematic depth variation was observed for primary rock types (gneisses - granites - dykes) or the relative abundances of the types of water-conducting features. However, some degree of systematic distribution was recognized in the depth dependence of hydraulic conductivity (cf. Fig. 8-3): in some of the boreholes, conductivity substantially decreases with depth (e.g. Böttstein, Leuggern), while no depth dependence was observed in others (e.g. Kaisten). Test intervals of low hydraulic conductivity ( $< 1E-9$  m/s) are preferentially situated in the deeper sections of the boreholes, while the upper parts tend to have higher conductivities. Based on hydraulic data, the crystalline basement sections drilled in the boreholes are divided into 2 units:

1. Borehole sections with *higher permeability* (hydraulic conductivity of test intervals predominantly  $> 1E-9$  m/s);
2. Borehole sections with *low permeability* (hydraulic conductivity of test intervals generally  $< 1E-9$  m/s).

All shallow occurrences of crystalline basement in the boreholes have higher permeability, while deeper parts of the basement contain higher-permeability sections in some boreholes and low-permeability sections in others (Fig. 6-8). In boreholes where a section with low permeability is present, its upper boundary is at about 700 - 900 m below surface or 350 - 550 m below sea level. Above this level, a basement "layer" of 350 - 650 m thickness is more permeable in all boreholes (except Weiach, where the crystalline basement is covered by 2000 m of sediments), while at lower levels both sections with higher and low permeability occur. The occurrence of sections with higher permeability in the deeper parts of the crystalline basement is possibly due to large-scale faults (see below).

The systematics of this hydraulic division are also reflected in some geological parameters:

*Sections with higher permeability* are strongly affected by both major phases of deformation and alteration (i.e. the high-temperature and the low-temperature phase), and zones with compact fresh rock are small or absent. While in the upper few hundreds of meters the effects of the low-temperature phase are very strong, the deeper occurrences of higher-permeability sections are more strongly affected by the



meters below surface	BOE	SIB	SHA	LEU	KAI	WEI
higher-permeability borehole sections	315 to 801	349 to 1522	1490 to 2006	223 to 881, 1640 to 1689	297 to 666, 790 to 1306	-
low-permeability borehole sections	801 to 1501	-	-	881 to 1640	666 to 790	2020 to 2482

meters above sea level	BOE	SIB	SHA	LEU	KAI	WEI
higher-permeability borehole sections	+33 to -453	+225 to -948	-1069 to -1585	+136 to -522, -1281 to -1330	+23 to -346, -470 to -986	-
low-permeability borehole sections	-453 to -1153	-	-	-522 to -1281	-346 to -470	-1651 to -2113

**Fig. 6-8 :** Borehole sections with higher and low permeability in the crystalline basement of Northern Switzerland.

high-temperature phase. Exceptions to this scheme are Kaisten and Leuggern, where the effects of the low-temperature phase are significant over the whole profile. Apart from the depth dependence of the tectono-hydrothermal phases, there is no geological or hydrogeological distinction between the properties of the sections with higher permeability in the shallower and in the deeper parts of the boreholes. Except for minor variations in the mineralogy, the geometric and petrophysical properties of water-conducting features are not depth-dependent within the sections with higher permeability.

*Sections with low permeability:* In the corresponding core material, tectono-hydrothermal effects are markedly less developed when compared with the higher-permeability sections (namely Böttstein and Leuggern). The primary rock types are often very fresh and undeformed over several tens of meters.

The relative proportions of the types of water-conducting features do not differ systematically between the higher-permeability and the low-permeability sections, but the frequencies of inflow points are different. In the sections with higher permeability, the average distance between inflow points is 37 m along hole, while in sections with low permeability this distance is 55 m. In addition to the wider spacing, water-conducting features in sections with low permeability have a lower transmissivity (cf. Fig. 8-5).

### **6.10 3-dimensional spatial arrangement of higher- and low-permeability crystalline basement**

The discussion in this Chapter deals with the large-scale structure of the crystalline basement and provides input for the construction of a conceptual model for hydrodynamic modeling (cf. Chapter 8) and for repository layout studies.

Based on the borehole data from Northern Switzerland, the uppermost 350 - 650 m of the crystalline basement are assumed to be strongly deformed, altered and permeable throughout the region. This assumption is consistent with evidence from the Black Forest, where outcrops of fresh and undeformed basement rocks are rare. Even in the numerous granite quarries, the extent of relatively weakly affected rock is limited to only about 100 m in both horizontal dimensions, and cataclastic and jointed zones with associated alterations occur even in these rocks. The same conclusions are deduced from roadcuts.

The relative proportions and the geometric arrangement of the higher and the low-permeability sections in the deeper parts of the boreholes are more difficult to document and not fully understood. In the deep boreholes, the relative proportions of the sections with higher and low permeability are roughly equal, but 6 boreholes are insufficient to provide a statistically relevant number. Even less is known about the absolute and relative sizes of the higher-permeability and the low-permeability "blocks" and their spacings.

A fault model of the crystalline basement in Northern Switzerland was presented in section 5.3 on the basis of evidence from the Black Forest, complemented by seismic and borehole data from Northern Switzerland. This pattern consists of 4 - 5 families of large-scale fault zones, where each family consists of parallel faults with characteristic thicknesses and spacings and generally occurs throughout the region of interest. While the strike directions of the fault families vary widely, the dips generally are steep in all of them. Applying this structural pattern to the geometric concept for Northern Switzerland, fault zones (consisting of sections with higher permeability in the boreholes) with several strike directions are hypothesized to dissect the crystalline basement and leave isolated, near-vertically-sided prisms of low-permeability crystalline rock bodies between the fault zones. If low-angle normal faults (cf. Fig. 3-3) exist in the crystalline basement, these prisms may also have a base. However, such faults have not been observed in the deep boreholes. Under this scheme, the deeper parts of the crystalline basement consist of an interconnected higher-permeability network with isolated "islands" of low-permeability crystalline blocks. In contrast, it would be difficult to provide a genetic explanation for isolated higher-permeability blocks embedded in a low-permeability matrix.

In the cases of the Kaisten and Schafisheim boreholes (both of which contain sections with higher permeability even at great depths), core evidence indicates that faults penetrate deeply into the basement. On the basis of geometric considerations, the Kaisten borehole possibly represents the subsurface continuation of the Eggberg fault, known from the Black Forest. The Schafisheim borehole is located on a small horst structure within the Permo-Carboniferous Trough, where major fault movements have occurred. Thus, the proximity of regional-scale faults is a plausible explanation for the presence of sections with higher permeability, even in the deeper parts of these boreholes.

### **6.11 Water-conducting features in large-scale faults**

Taking the crystalline profiles drilled at Schafisheim and Kaisten as possible examples of large-scale faults, it is worth noting that there are no significant differences in the geometry and mineralogy of water-conducting features inside and outside faults (or, in other words, large faults consist of a number of small ones, cf. section 6.1). Also, the frequencies of inflow points at Schafisheim and Kaisten are not significantly higher than in any of the other boreholes. This can, in part, be due to the strong dependence of the detection limit of fluid logging tools on transmissivity. In low-permeability sections, even small inflow points can be detected because the drilling-fluid is virtually stagnant. On the other hand, in more permeable sections, the presence of very transmissive inflow points precludes detection of smaller inflows because of interferences and due to vertical water flow in the borehole.

However, even taking some influence of analytical artefacts into account, inflow point frequencies are not high enough to explain the enhanced hydraulic conductivities observed in the faults. It appears that higher hydraulic conductivities must be explained by a higher degree of interconnection of water-conducting features, or, in other words,

a larger lateral extent of each water-conducting feature in faults. Given the complex fault geometries, lengths of water-conducting features (especially cataclastic zones) of several hundreds of meters seem reasonable. At least in the case of cataclastic zones, the average spatial orientation is expected to be parallel to the trend of the large faults, even though undulations occur on a small scale.

## 6.12 Relative abundances of water-conducting features

All 3 types of water-conducting features, as defined in section 6.4, occur both in the higher-permeability and in the low-permeability borehole sections, and their relative abundances are shown in Table 6-8. Table 6-8 also shows that no substantial differences occur among the 4 boreholes north of the Permo-Carboniferous Trough (Böttstein, Kaisten, Leuggern, Siblingen) and those within or south of the Permo-Carboniferous Trough of Northern Switzerland (Schafisheim, Weiach).

	total sections		higher-permeability sections		low-permeability sections	
	all 6 boreholes	boreholes north of Permo-Carbonif. Trough	all 6 boreholes	boreholes north of Permo-Carbonif. Trough	all 6 boreholes	boreholes north of Permo-Carbonif. Trough
cataclastic zones	43 %	42 %	42 %	38 %	46 %	52 %
jointed zones	34 %	39 %	36 %	43 %	27 %	26 %
fractured aplite/ pegmatite dykes, aplitic gneisses	23 %	19 %	22 %	19 %	27 %	22 %

**Tab. 6-8 :** Relative abundances of water-conducting features. Inflow points not fitting the classification scheme (cf. Tab. 6-1) are disregarded in the calculation.

## **6.13 Spatial heterogeneity of water-conducting features: fracture apertures and channeling**

### **6.13.1 Conceptual models of natural fractures**

Water-conducting features (e.g. shear zones, joints) in rocks are mostly planar structures. For this reason, several authors have used a parallel-plate model for the computation of flow and transport properties of fractures in rocks (e.g. WITHERSPOON et al. 1980, SNOW 1968, 1970). However, fracture apertures computed from hydraulic tests and tracer transport experiments are different in many cases (e.g. SILLIMAN 1989). Field and laboratory experiments (including crosshole tests) performed in the last decade have shown that a parallel-plate model is not always appropriate, because of identified heterogeneities of the fracture surfaces and, hence, variable apertures (RASMUSON & NERETNIEKS 1986, NERETNIEKS et al. 1982, HEATH 1985, SHAPIRO & NICHOLAS 1989, KIKUCHI et al. 1989). These experiments indicate that flow and solute transport within a fracture plane are concentrated in regions with large apertures, surrounded by low-aperture regions where fluid is nearly stagnant and diffusive processes quantitatively dominate over advective transport. In order to include these findings in conceptual models, the parallel-plate model was replaced by various models that assume the presence of variable fracture apertures (BROWN 1987, JOHNS & ROBERTS 1991, TSANG et al. 1988).

However, the assumption of fast-flowing channels in water-conducting features accounting for all advective flow is still a severe simplification of reality. The transmissivity distribution in natural fractures is heterogeneous due to surface roughness and the distribution and porosity of infill materials, and a wide range of transmissivities exists rather than simply "permeable" and "impermeable" regions (Fig. 6-9). The transmissivity cut-off between "permeable" and "impermeable" regions is artificial and also depends on flow rate (i.e. slow advection takes place even in smaller-aperture regions) or, equivalently, the imposed hydraulic gradient. The estimation of the surface fraction of a water-conducting feature in which significant advective flow occurs is difficult and often obliterated by experimental artefacts or biased by personal preferences (cf. much of the literature cited above).

More solid information on channeling is provided by the migration experiment at the Grimsel Test Site (FRICK et al. 1992). 7 out of 8 boreholes cross-cutting the migration shear zone are water-conducting, and a transmissivity distribution across the fracture plane was inferred on the basis of pressure responses in the boreholes during hydraulic packer tests (FRICK et al. 1988). The results show that water flow in the migration fracture is much less focused in channels than suggested previously, and tracer migration tests can be modeled well using averaged hydraulic parameters if the scale of the experiment exceeds 1 m.

### 6.13.2 Possible channeling in water-conducting features in the crystalline basement in Northern Switzerland

All information presented above is site-specific and cannot easily be extrapolated into areas that were subjected to different tectono-hydrothermal histories, such as the crystalline basement of Northern Switzerland. In the latter, channeling might well be more important than in Grimsel due to frequent intersection patterns of fracture systems and the presence of visible vugs/channels (cf. section 6.3).

Due to the lack of crosshole tests and the small-scale nature of fracture intersections in the cores, no site-specific data on channeling are available for the crystalline basement of Northern Switzerland. In spite of the inability to describe the size and geometry of the channels, some relevant observations can be made:

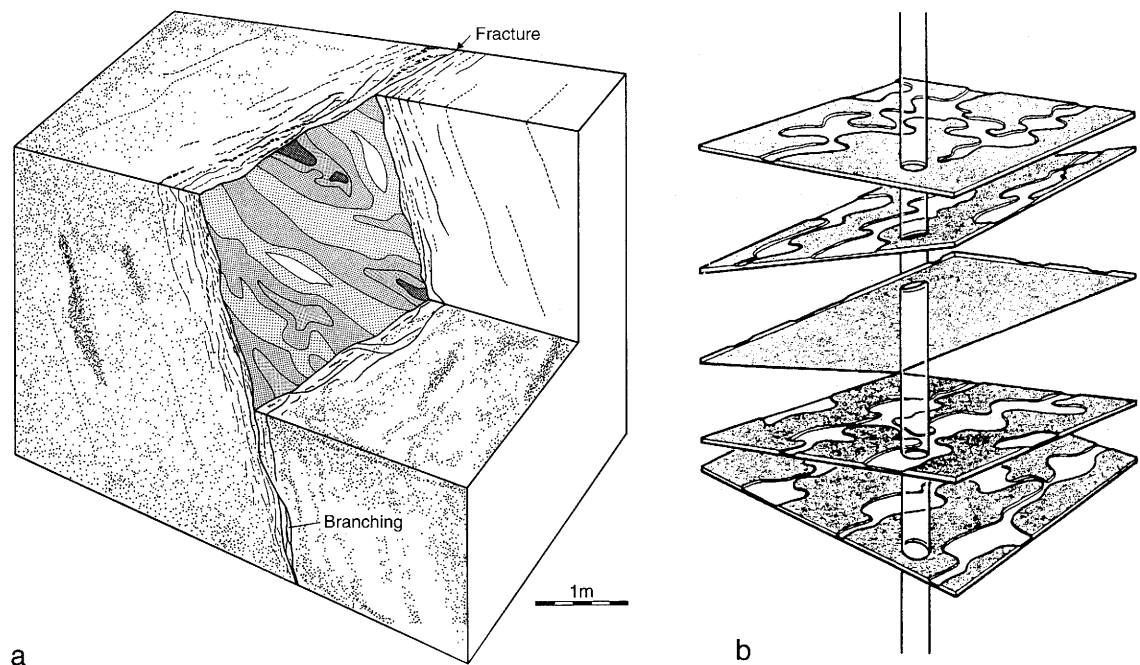


**Fig. 6-9 :** Concepts representing channel flow through fractures.

- Schematic sketch of the migration shear zone at the Grimsel Test Site with contours for transmissivity (white = highly transmissive). Taken from FRICK et al. (1988).
- Intersections of a borehole with fractures containing permeable channels (white) and small-aperture, impermeable regions (grey). Only one of the five fractures would be identified as water-conducting in hydraulic borehole tests. Taken from RASMUSON & NERETNIEKS (1986).

1. The number of open fractures in the boreholes exceeds the number of inflow points by at least one order of magnitude. Abundant fractures occur in the core material which, according to fluid logging, carry no water but look exactly the same as water-conducting fractures. Therefore, the core logging data are not in contradiction with the presence of spatial heterogeneity.
2. Due to the multiphase history of deformation and alteration, relations are much more complex in Northern Switzerland when compared to relatively simple structures at Stripa in Sweden or in the granites of Cornwall, where most of the channeling investigations cited above were performed. Inflow points (i.e. the intersections of the borehole with water-conducting features) in the basement of Northern Switzerland are not single fractures but rather fractured zones sometimes several meters in length, containing numerous single fracture planes of variable orientation, length, aperture and persistence. Given such complex relations, it is difficult to obtain quantitative data on channel proportions (even if better exposures were available), because of the unclear definition of an inflow point.
3. Heterogeneity on the scale of centimeters is easily observed in the cores. Fracture apertures are largely controlled by the presence or absence of hydrothermal fracture coatings. Where coatings are lacking, vugs/channels generally exist that represent channels for groundwater flow. These small-scale findings are directly incorporated into the geological database for safety assessment in Chapter 10.

## 6.14 Summary

Groundwater flow in the crystalline basement of Northern Switzerland takes place in discrete zones (water-conducting features). In the deep boreholes, 138 such features were identified by fluid logging techniques. Inspection of the corresponding core material showed that water flow concentrates in rock portions that have suffered repeated brittle deformations in the course of the Late and post-Variscan tectono-hydrothermal evolution. Typically, pre-existing mechanical discontinuities were reactivated by younger deformations, resulting in complex structural and mineralogical relations. A common set of 3 types of water-conducting features occurs throughout the entire region studied:

- Cataclastic zones;
- Jointed zones (with open joints);
- Fractured aplite/pegmatite dykes and aplitic gneisses.

This classification is consistent with evidence from surface outcrops and tunnels in the Black Forest. Large ore vein systems, which are major aquifers in parts of the Black Forest, have not been identified in Northern Switzerland, but their existence cannot be fully excluded on the basis of present knowledge.

Based on the variable orientations of the water-conducting features and the uniform chemical compositions of the groundwaters (Chapter 7), all types of water-conducting features are assumed to be interconnected. Their macroscopic structure, mineralogy and porosity are discussed in detail.

Based on an integrated interpretation of hydrogeological and geological data, higher- and low-permeability sections are penetrated in all boreholes. Sections with higher permeability preferentially contain highly fractured and altered rocks, and water-conducting features are more densely spaced. In contrast, low-permeability sections may contain zones of fresh and unfractured rocks. While the uppermost 350 - 650 m of the basement invariably consist of sections with higher permeability that contain more densely spaced water-conducting features, the deeper parts of the basement contain both sections with higher and low permeability. The presence of higher-permeability sections in the deep crystalline basement is attributed to the occurrence of major faults. The synthesis of the borehole evidence and geological data from surface outcrops in the Black Forest provides input for the development of a conceptual structural model for hydrodynamic modeling.

## **7 CHEMISTRY, ORIGIN AND RESIDENCE TIME OF GROUND-WATER IN THE CRYSTALLINE BASEMENT**

### **7.1 Scope of investigations and data presented**

The chemical and isotopic character of groundwater in the crystalline basement reflects the conditions of the water's origin and the water-rock reactions that have occurred during its flow. As part of the Nagra hydrochemical programme (section 2.5), samples of water were taken from springs and shallow boreholes where the basement is exposed at the surface in the Black Forest and from deeper boreholes where the basement is under sedimentary cover in Northern Switzerland. Borehole samples from the Buntsandstein (BST) and Permian (P) sediments directly overlying the crystalline basement or adjacent to it in the Permo-Carboniferous Trough of Northern Switzerland were also taken into consideration, because these waters are similar to, or have an influence on, waters in the basement in some locations. Hydrochemical analyses were also carried out on waters collected from aquifers of the Mesozoic and Tertiary sedimentary cover, and from Buntsandstein and Permian sediments and the crystalline basement outside the region of interest for this synthesis. The locations of the water sampling sites considered in this section are shown in Figure 7-1 in the context of the major tectonic units of Northern Switzerland.

This Chapter is a summary of data and detailed interpretations more fully reported in the Nagra Technical Report series. All water chemical and isotopic data collected as part of the Nagra programme are included in the Nagra hydrochemical database (GEOL. INST. UNIV. BERN 1989). Chemical data from all Nagra boreholes except Siblingen were evaluated and documented by WITTWER (1986) and PEARSON et al. (1989). Isotopic data and detailed interpretations of samples from the regional programme and all boreholes except Siblingen are given by PEARSON et al. (1991). Chemical and isotopic data for Siblingen are presented and evaluated by BLASER & SCHOLTIS (1991). SCHMASSMANN et al. (1992) give an exhaustive discussion of the chemistry of groundwater from the crystalline basement and adjacent water-bearing units.

The reference groundwater chemistry for potential repository sites, which is defined as the best estimate of in situ hydrochemical conditions in the host rock, is based on analyses of samples from the Zurzach, Böttstein, Leuggern and Kaisten boreholes for the area West, and from the Siblingen borehole in the area East. The reference waters are discussed in section 10.4.1.

Additional chemical data were obtained as part of a recent study of colloids in water from the Zurzach and Leuggern boreholes (DEGUELDRE 1994). They are summarized in section 10.4.2 of this report.

The water chemistry will be described using one or both of two types of units. The masses of constituents per volume solution will be expressed as milligrams per liter (mg/l), which is equivalent to  $\text{mg}/\text{dm}^3$  in strict SI units. These are the units in which much of the analytical data were reported and which are used in some of the previous reports on water chemistry (e.g. WITTWER 1986, PEARSON 1985, PEARSON et al. 1989, PEARSON & SCHOLTIS 1993). When referring to the amounts of substances

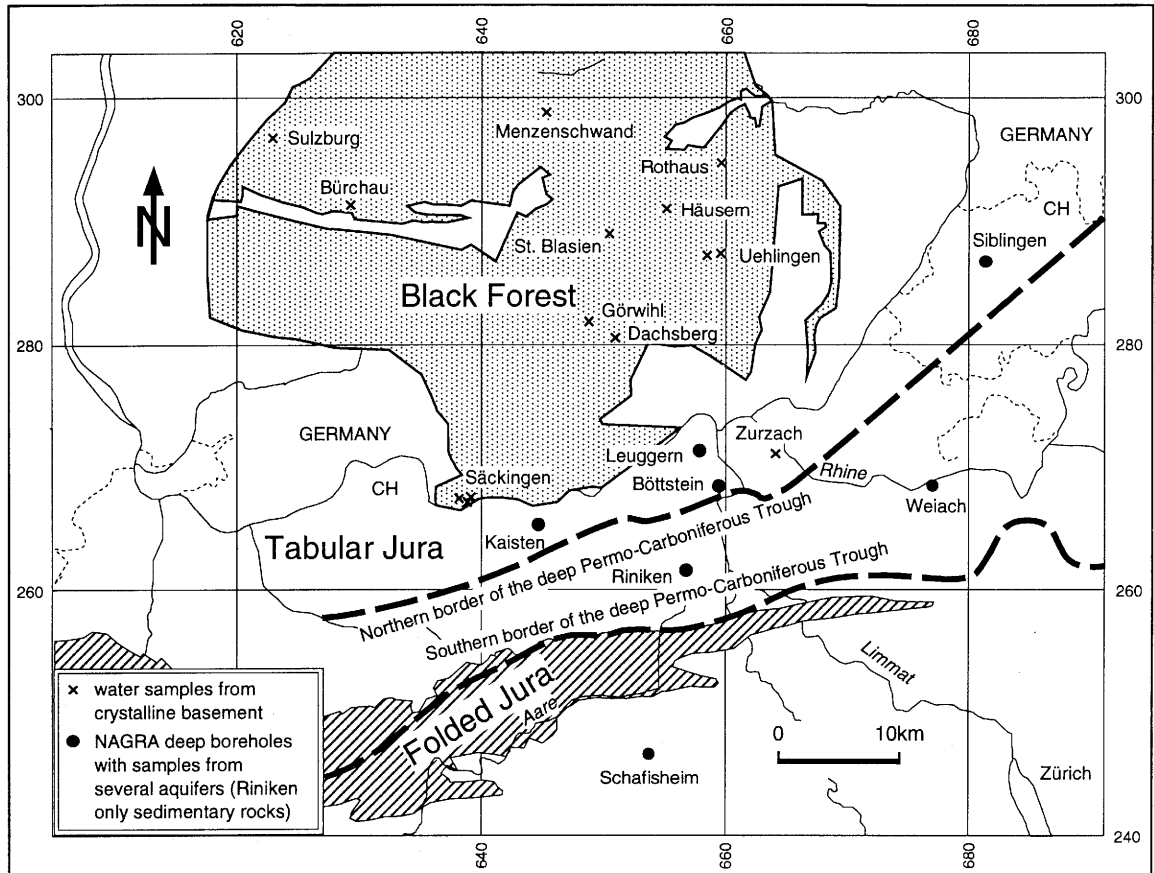


**Fig. 7-1 :** Map showing major tectonic units of Northern Switzerland with locations of Nagra boreholes and of springs and other boreholes from which groundwater samples were taken from the crystalline basement and from the overlying or adjacent sediments of the Permo-Carboniferous Trough.

potentially involved in reactions, molality (M; mol/kg H<sub>2</sub>O) or millimol equivalents per kg H<sub>2</sub>O (meq/kg H<sub>2</sub>O) will be used.

In other previous reports, chemical data were reported as mol equivalents per cubic meter (mol(eq)/m<sup>3</sup>) (e.g. SCHMASSMANN et al. 1992). Even for the most saline waters discussed here, concentrations expressed per mass H<sub>2</sub>O differ by less than one percent from those expressed per volume solution at room temperature. Conversion among concentration units is described in detail by PEARSON et al. (1989: section 1.2).

Water Group	Geographic Area	Sampling Points and Geologic Units	Representative Samples Text and Figure Code: Name or Depth: Location/Sample number(s)	Chemical Character and Salinity as Total Dissolved Solids and Total Ions	Sources of Detailed Descriptions and Analyses
Recharge	Central and South-eastern Black Forest	Existing springs and boreholes in the crystalline basement sampled as part of the Regional Programme: KRI	ROT: Rothaus: 150/1 HÄU: Häusern Sägtobel: 191/101,102 STO: Uehlingen Stollennund: 192/101-103 GIE: Uehlingen Giessbach: 193/101 GÖH: Göhrwil Bohrlöch 30: 167/1 DBH: Dachsbach Hierbach: 194/101,102 ME1: Menzenschwand 1: 162/1 ME2: Menzenschwand 2: 163/1 ME3: Menzenschwand 2b: 164/1 BLA: St. Blasien Erzgrube: 165/1 BUR: Büschau: 110/2,4 SULa: Sulzburg Waldhotel: 166/1 SULb: Sulzburg ob. Waldhotel: 189/101 SULc: Bad Sulzburg: 190/101	Alkaline Earth - HCO <sub>3</sub> < 0.2 g/l; < 10 meq/kg	SCHMASSMANN et al. (1992) Sections 4.1.1.1; 5.3.1
	Eastern	North-eastern Switzerland and adjacent parts of Germany; Siblingen Area	Siblingen Borehole: BST and KRI SIB2: 337-345 m: 307/2b (BST) SIB4c: 490-564 m: 307/4b corrected SIB6: 1154-1164 m: 307/6b SIB7: 1493-1499 m: 307/7b	Na-HCO <sub>3</sub> -SO <sub>4</sub> 0.5 g/l; 17 meq/kg	SCHMASSMANN et al. (1992) Sections 4.1.1.2; 5.3.2  BLASER & SCHOLTIS (1991)
Western	Central Northern Switzerland north of Permo-Carboniferous Trough	Zurzach thermal water boreholes: KRI Böttstein Borehole: KRI Leuggern Borehole: KRI Kaisten Borehole: P and KRI	ZU1: Zurzach 1: 131/1-18 ZU2: Zurzach 2: 132/1-18  BÖT9: 394-405 m: 301/8c,9 BÖT13: 618-624 m: 301/12b,13 BÖT17: 608-629 m: 301/16,17 BÖT18: 782-803 m: 301/18  LEU4: 235-268 m: 306/4 LEU6: 440-448 m: 306/5,6 LEU8: 507-569 m: 306/7,8 LEU10: 702-710 m: 306/9,10 LEU19: 834-860 m: 306/17-19 LEU21: 1179-1227 m: 306/20,21 LEU16: 1637-1649 m: 306/16 LEU23: 1642-1689 m: 306/23  KAI3: 276-292 m: 305/2,3 (P) KAI5: 299-322 m: 305/4,5 KAI7: 476-490 m: 305/6,7 KAI11: 816-823 m: 305/9-11 KAI13: 1021-1041 m: 305/12,13 KAI15: 1141-1166 m: 305/14,15 KAI17: 1238-1306 m: 305/16,17	Na-SO <sub>4</sub> 0.9 g/l; 28 meq/kg  Na-SO <sub>4</sub> 1.0-1.1 g/l; 33-36 meq/mkg  Na-SO <sub>4</sub> 0.9-1.3 g/l; 28-35 meq/kg  Na-SO <sub>4</sub> 1.3-1.4 g/l; 38-44 meq/kg	SCHMASSMANN et al. (1992) Sections 4.1.1.3; 5.3.3  WITTWER (1986)  PEARSON et al. (1989)
	Saline	In and adjacent to Permo-Carboniferous Trough; Isolated occurrences in crystalline basement	Leuggern Borehole: KRI Säckingen: KRI Böttstein Borehole: KRI Weiach Borehole: P Weiach Borehole: KRI Riniken Borehole: BST-P and P Schafisheim Borehole: BST-KRI Schafisheim Borehole: KRI	LEU13c: 916-930 m: 306/11b-13 corr  LEU26: 1427-1439 m: 306/26  SÄS: Säckingen Stammelhof: 161/1  BÖT22c: 1321-1331 m: 301/19-22 corr  WEI19: 1109-1124 m: 302/19 WEI18: 1401-1416 m: 302/17,18  WEI16: 2212-2225 m: 302/16 WEI14c: 2260-2274 m: 302/14 corr  RIN3: 793-820 m: 303/3 (BST-P) RIN5: 958-972 m: 303/5b RIN9: 977-1010 m: 303/6,8,9 RIN20c: 1354-1369 m: 303/20 corr  SHA6: 1476-1500 m: 304/4,6  SHA9: 1564-1578 m: 304/8,9 SHA11: 1884-1892 m: 304/10,11	Na-SO <sub>4</sub> 5.0 g/l; 140 meq/kg  Na-Cl 1.3 g/l; 43 meq/kg  Na-Cl 7.2 g/l; 240 meq/kg  Na-Cl 13 g/l; 440 meq/kg  Na-Cl 36-120 g/l; 1200-3400 meq/kg  Na-Cl 6.4-8.4 g/l; 210-270 meq/kg  Na-Cl 10-44 g/l; 320-1400 meq/kg  Na-Cl 16 g/l; 520 meq/kg  Na-Cl 7.7-8.0 g/l; 250-260 meq/kg

Tab. 7-1 : Summary of location, sampling points and chemical character of water types in the crystalline basement and adjacent units. KRI: crystalline basement; P: Permian; BST: Buntsandstein.

## 7.2 Hydrochemistry of groundwater in the crystalline basement and adjacent units

### 7.2.1 Description of water chemistry

Based on their geographic locations, water chemistry and isotopic properties, the groundwaters from the crystalline basement and adjacent units fall into four groups: Recharge, Eastern, Western and Saline.

Table 7-1 provides a summary description of each of the four water groups and includes a column listing the individual water samples that make up each group. The samples are identified by three- to six-character codes that are also used to identify the sample in the text or figures. The code is followed by the name of the sampling point for samples collected as part of the regional programme, or by the depth interval represented by the sample for samples collected from the Nagra deep boreholes. The final numbers are the location number and sample number(s) at that location. The codes, names, depths, and location/sample numbers correspond to those used in the Nagra database (GEOL INST. UNIV. BERN 1989) and in the chemical data tables of SCHMASSMANN et al. (1992). The location/sample numbers also correspond to those used in the isotope data tables of PEARSON et al. (1991).

Figures 7-2a through 7-2g include Schoeller diagrams that illustrate the chemistry and salinity of samples composing the four groups. Each group is described in more detail in the remainder of this section.

#### Recharge Group - Black Forest

Recharge to the crystalline basement of Northern Switzerland occurs on the south-eastern slope of the Black Forest. As shown in Table 7-1 and Figure 7-2a, waters here and elsewhere in the Black Forest are of the alkaline earth (Ca, Mg, Sr and Ba)-hydrogen carbonate ( $\text{HCO}_3$ ) type, with total dissolved solids contents (salinities) of less than 75 milligrams per liter (mg/l) and total ion contents of 1.9 milliequivalents/kg  $\text{H}_2\text{O}$  (meq/kg). Such low dissolved solids contents indicate that the water has undergone minimal water-rock interaction and, thus, has been very recently recharged. This is supported by other chemical and isotopic characteristics including tritium ( $^3\text{H}$ ) values characteristic of precipitation in the last several decades, dissolved helium (He) contents below detection, dissolved oxygen contents and platinum electrode (Eh) potentials characteristic of water recently in contact with the atmosphere, and dissolved carbonate species chemistry and stable and radio-carbon isotopic contents indicating a modern soil-air source for the dissolved carbonate.

In parts of the Black Forest north and west of the region recharging the crystalline basement of Northern Switzerland, waters with higher total dissolved solids contents occur. These waters, such as were sampled at Bürchau and Sulzburg, are still of the alkaline earth- $\text{HCO}_3$  type, but have total dissolved solids contents up to 200 mg/l (6.4 meq/kg) and isotopic characteristics suggesting greater residence times. They represent the type of early evolution of water chemistry expected in the recharge to the

crystalline basement of Northern Switzerland, but not sampled in the part of the Black Forest through which that recharge flows.

### **Eastern Group - Siblingen area**

Samples from the Siblingen borehole show virtually uniform water chemistry from the zone at 337 to 345 m depth, comprising the Buntsandstein and weathered crystalline basement, to the maximum depth interval sampled (1493 / 1499 m). As shown in Table 7-1 and Figure 7-2b, these waters are of the sodium - hydrogen carbonate - sulphate ( $\text{Na-HCO}_3\text{-SO}_4$ ) type with total dissolved solids contents between 510 and 540 mg/l and total ion contents of 17 meq/kg. This higher salinity is consistent with a longer period of water-rock interaction than is characteristic of groundwater in the Black Forest. As discussed in section 7.3, the isotopic characteristics of this water indicate that it was recharged under lower temperatures than presently prevail in the Black Forest and that it has a model  $^{14}\text{C}$  age of greater than 17 thousand years (ka). Such conditions are consistent with recharge during the last glaciation. The area over which water of the type sampled at Siblingen occurs is unknown. Because the same water chemistry was found over a depth interval of more than one kilometer, it seems likely that it should have a significant horizontal extent as well. Therefore, the reference water chemistry for use in safety assessment calculations for a potential repository in north-eastern Switzerland was based on the Siblingen samples. The discussion of the eastern reference water in section 10.4.1 gives more details about the chemistry of this water.

### **Western Group - Zurzach, Böttstein, Leuggern, Kaisten area**

Waters of similar chemistry are found over a considerable area and range of depths in the crystalline basement of Central Northern Switzerland, as summarized in Table 7-1. These waters are of a sodium-sulphate ( $\text{Na-SO}_4$ ) type, with total dissolved solids contents from 0.9 to 1.4 grams per liter (g/l), and total ion contents from 28 to 44 meq/kg. The easternmost samples of these waters are from the thermal water boreholes at Zurzach at depths from 402 to 469 m. These are shown in Figure in 7-2c, along with virtually identical waters that occur within the basement at Böttstein between 394 and 803 m. Figure 7-2d shows that waters from most of the basement at Leuggern from 235 to 1689 m are of the same type. Two Leuggern samples, from zones of restricted water yield at depths of 916 to 930 m and 1427 to 1439 m, have higher dissolved solids contents and are considered among the saline water types discussed in the next section. Samples from the Kaisten borehole are shown in Figure 7-2e. They are not identical with the Zurzach - Böttstein - Leuggern waters in that they have slightly higher alkaline earth and sulphate and lower chloride contents, and have generally higher total dissolved solids of 1.3 to 1.4 g/l and total ion contents of 38 to 44 meq/kg. However, their similarity is sufficient to include them as members of the same water group. Waters in Permian sediments from 276 to 293 m overlying the crystalline basement and from intervals within the basement from 299 to 1306 m in the Kaisten borehole have similar chemistry.

Figure 7-2a

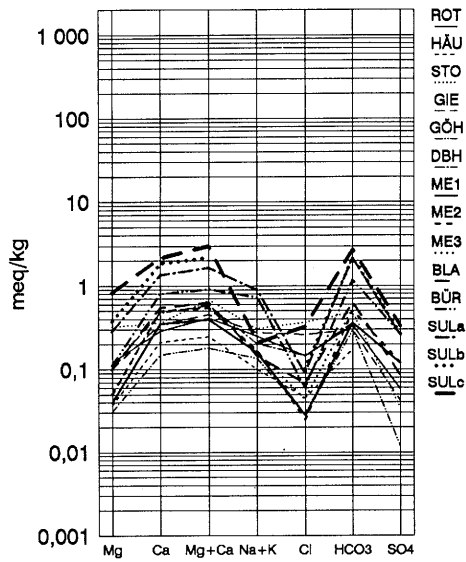


Figure 7-2b

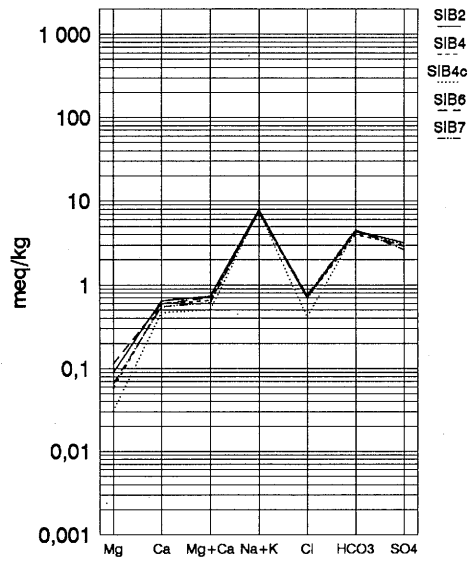


Figure 7-2c

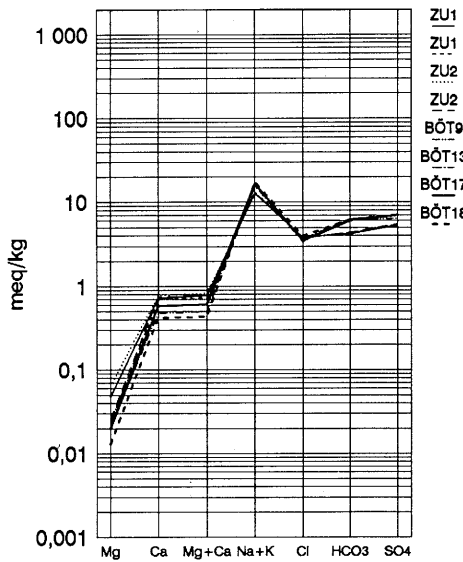
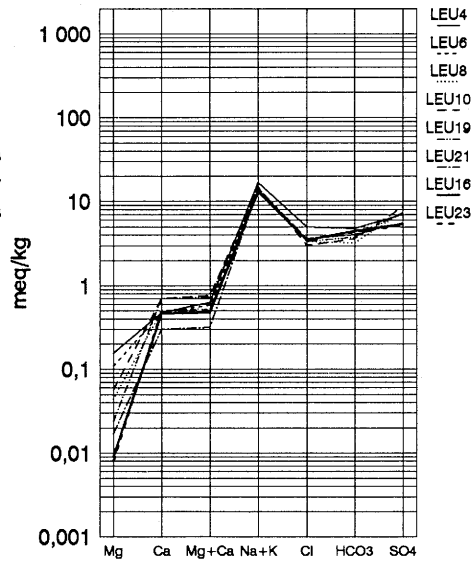


Figure 7-2d



**Fig. 7-2a :** Schoeller diagram of waters of the alkaline earth-HCO<sub>3</sub> chemical type from the crystalline basement of the Black Forest representing the Recharge Group.

**Fig. 7-2b :** Schoeller diagram of waters of the Na-HCO<sub>3</sub>-SO<sub>4</sub> chemical type from the crystalline basement of the Siblingen borehole representing the Eastern Group.

**Fig. 7-2c :** Schoeller diagram of waters of the Na-SO<sub>4</sub> chemical type from the thermal boreholes at Zurzach and the upper crystalline basement of the Böttstein borehole representing members of the Western Group.

**Fig. 7-2d :** Schoeller diagram of waters of the Na-SO<sub>4</sub> chemical type from the crystalline basement at Leuggern (except 916 to 930 and 1427 to 1439 m), representing members of the Western Group.

Figure 7-2e

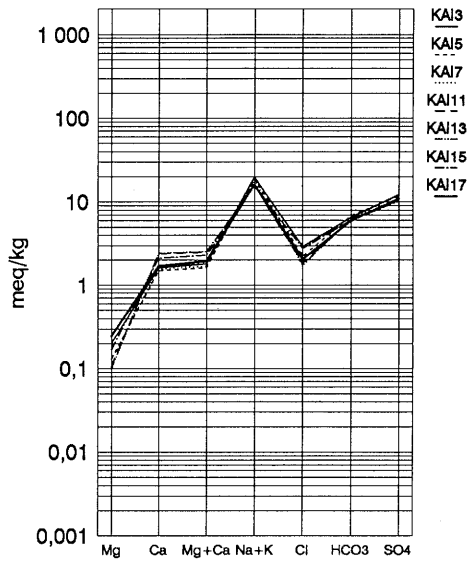


Figure 7-2f

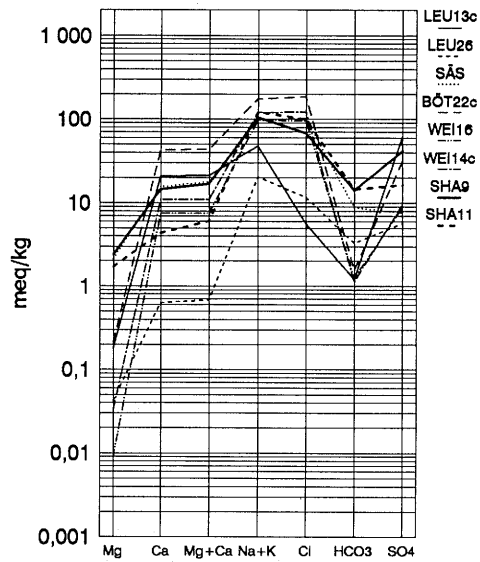
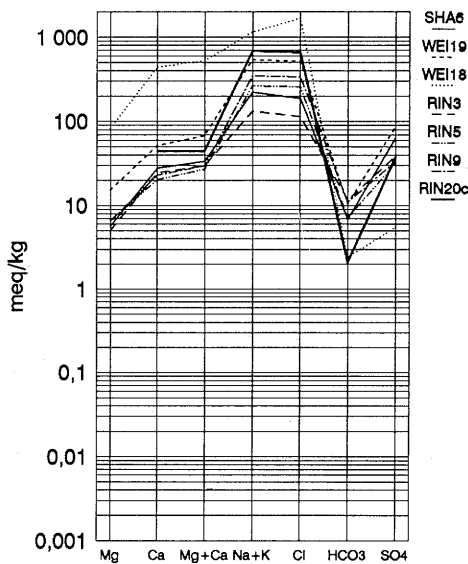


Figure 7-2g



**Fig. 7-2e :** Schoeller diagram of waters of the Na-SO<sub>4</sub> chemical type from the Permian and crystalline basement of the Kaisten borehole representing members of the Western Group.

**Fig. 7-2f :** Schoeller diagram of waters of Na-SO<sub>4</sub> and Na-Cl chemical types from the crystalline basement at Leuggern, Böttstein, Schafisheim, Weiach and Säkingen representing members of the Saline Group.

**Fig. 7-2g :** Schoeller diagram of waters of Na-Cl chemical types from the Buntsandstein and Permian of the Weiach, Riniken, and Schafisheim boreholes representing members of the Saline Group.

The isotopic compositions of waters in this group and their solutes wherever sampled are virtually identical, as discussed in section 7.3, indicating recharge under climatic conditions similar to, or slightly cooler than, those of the present but at a time before the water now present at Siblingen was recharged. The higher salinity of this water is consistent with its greater residence time.

Because this water type is found over such a large area, it was chosen as the basis of the reference water to be used for safety assessment calculations for a potential repository located in Central Northern Switzerland. The discussion of the western reference water in section 10.4.1 includes more details about its chemistry.

### **Saline Group - Permo-Carboniferous Trough and isolated zones in the crystalline basement**

Water of higher salinity and different chemical type than those of the other groups were sampled from sediments of the Permo-Carboniferous Trough in the Riniken, Schafisheim and Weiach boreholes, and from the crystalline basement in the Säckingen, Leuggern, Böttstein, Weiach and Schafisheim boreholes. The general character of the saline waters and the points from which they were sampled are given in Table 7-1. Figures 7-2f and 7-2g are Schoeller diagrams of the saline waters from the crystalline basement and from the sediments of the Permo-Carboniferous Trough, respectively.

Sediments of Triassic and Permian age (Buntsandstein and Rotliegendes, respectively) of the Permo-Carboniferous Trough yield water of an Na-Cl type with dissolved solids contents of 10 to 120 g/l and total ion contents of 320 to 3400 meq/kg. Although these waters are not from the crystalline basement itself, their properties are important because they are similar to certain of the saline waters that are found in the crystalline basement. Thus, they are included in the remaining discussions of this Chapter. The sources of the water and dissolved salts in these sedimentary rocks are not known. They may be marine or continental saline waters associated with the deposition of the sediments, since modified by water-rock reactions, or they could be waters of younger age that developed their salinity by water-rock reactions.

The saline waters from the crystalline basement can be differentiated on the basis of the source of their salinity. Some of these waters have a component derived from saline sedimentary water, while others have developed their salinity during chemical evolution entirely within the crystalline basement itself. The Böttstein, Weiach, Schafisheim and Säckingen boreholes, which are adjacent to or within Permo-Carboniferous Trough (cf. Fig. 2-1b), yield Na-Cl waters of high salinity from the crystalline basement. These samples are described in Table 7-1 and shown in Figure 7-2f.

Two samples from the crystalline basement of the Schafisheim borehole from between 1565 and 1892 m (SHA9 and SHA11) have total dissolved solids of about 7.8 g/l and total ion contents of 250 to 260 meq/kg. Water from a zone comprising the Buntsandstein and uppermost crystalline basement (SHA 6) has a salinity of about

16 g/l, or 520 meq/kg. As discussed in the following section, the water from the deeper crystalline basement of Schafisheim includes a component derived from the adjacent sediments.

A saline sample from Böttstein (BÖT22c) was collected from a zone of very low permeability between 1321 and 1331 m. It is the most saline water found in the crystalline basement and has total dissolved solids of about 13 g/l or 1440 meq/kg. As discussed in the following section, it is not possible to state unequivocally whether this water evolved entirely within the basement or includes a component derived from sediments of the deep Permo-Carboniferous Trough of Northern Switzerland.

Two samples from the crystalline basement of the Weiach borehole between 2212 and 2274 m (WEI16 and WEI14c) have total dissolved solids of 6.4 and 8.4 g/l corresponding to total ion contents of 210 and 270 meq/kg. These salinities are below those of waters found in the overlying Permian section (WEI18 and WEI19), which approach 120 g/l (3400 meq/kg) in salinity. For reasons discussed in the following section, the waters from the basement at Weiach appear to have evolved entirely within the crystalline basement.

Saline water is also present in the crystalline basement in several locations distant from the highly saline, sedimentary water of the Permo-Carboniferous Trough. Within the Leuggern borehole there were two zones of very low permeability that yielded water more saline or of a different type than found in the more highly permeable zones of the borehole. A zone between 916 and 930 m (LEU13c) contained an Na-SO<sub>4</sub> water with a total dissolved solids content of 5.0 g/l, or about 140 meq/kg. A second zone from 1427 to 1439 m (LEU26) yielded an Na-Cl water with 1.3 g/l or 43 meq/kg total solids. The former water is of the same chemical type as most of the waters from Leuggern and the other boreholes in this vicinity, but is considerably more saline. The latter water is about the same salinity as water from the Kaisten borehole, but it is of the Na-Cl chemical type.

The thermal water boreholes at Säckinggen also produce Na-Cl waters. All of them have at least some component of local tritium-bearing water, but the low tritium content of water from one of them, Bohrung Stammelhof (SÄS), suggests that it represents reasonably well undiluted water from deeper in the crystalline basement (PEARSON et al. 1991). This sample has a total dissolved solids content of 7.2 g/l or 240 meq/kg. As discussed in the following section, the Säckinggen Stammelhof groundwater includes a component derived from Permo-Carboniferous sediments. The saline waters from Böttstein (BÖT22c) and Leuggern (LEU13c) are also included in the discussion of reference waters in section 10.4.1.

### 7.2.2 Chemical evolution

The preceding section addressed the occurrence of several types of water and described their general characteristics. This section discusses in more detail certain patterns among the concentrations of selected dissolved constituents and relates them to the chemical evolution of water in the crystalline basement of Northern Switzerland.

Water entering a geological unit as recharge is not in chemical equilibrium with the minerals of that unit. However, as soon as recharge occurs, the water begins to react towards chemical equilibrium with the minerals. The water will reach equilibrium with various minerals after different times depending on the amount of each mineral available to the water and the rate at which the reaction takes place. Minerals such as calcite, siderite, barite and fluorite react rapidly enough that they are commonly in chemical equilibrium with groundwater. They comprise only a small proportion of the rock mass of the crystalline basement but, because of their reactivity, they control many features of groundwater chemistry.

Primary silicate minerals such as the feldspars, micas and quartz, which compose the bulk of the rock mass of the crystalline basement, are commonly in equilibrium with fluids only under hydrothermal conditions. Reactions with silicate minerals at lower temperatures are so slow that water can reach equilibrium with them only after residence times of  $10^4$  to  $10^6$  years, if at all. Thus, many waters with long residence times in silicate aquifers have not reached equilibrium with rock-forming silicate minerals. Conversely, if equilibrium does exist between water and these minerals at a low or moderate temperature, it is evidence that the water has been present within the rock for a considerable period of time. Unfortunately, the state of knowledge of geochemical kinetics is not advanced enough to permit residence time estimates from the state of equilibrium, or disequilibrium, of water-rock reactions (BRANTLEY 1992).

Even though primary silicate minerals may not be in equilibrium with groundwater, they react with the groundwater towards equilibrium and, in the process, form other minerals such as clays and secondary silica precipitates. Because the primary minerals make up the bulk of the rock mass, the alteration of only a small proportion of them can have a major influence on groundwater geochemistry. MICHARD (1987, 1990b) discusses the chemical characteristics of groundwater in equilibrium with its host rock under various conditions, with particular reference to rock-forming silicates. On theoretical grounds, he shows that the concentrations of dissolved constituents depend on the minerals present, the temperature and the concentration of mobile solutes. Mobile solutes are constituents such as chloride that are not controlled by mineral equilibria. The mobile anion content of water in a single water-bearing unit increases with the extent of water-rock interaction, and so is a useful indicator of water chemical evolution.

Sulphate is also a mobile constituent of all waters from the crystalline basement and in waters from adjacent sedimentary rock, except some of those of high salinity (RIN 20c, WEI19, RIN9 and RIN5) which are saturated with respect to celestite ( $\text{SrSO}_4$ ) (PEARSON et al. 1989 Tab. 3.1, 4.1 and 4.3). Many of the waters from the crystalline basement are saturated with respect to barite ( $\text{BaSO}_4$ ). This is reflected by decreasing barium concentrations with increasing sulphate (SCHMASSMANN et al. 1992: Fig. 4.3.7a), and so does not contradict the attribution of mobility to sulphate.

Figure 7-3 is a graph of the molality of sodium in these waters against their mobile anion ( $\text{Cl}+\text{SO}_4$ ) molality. This figure illustrates the correspondence between the evolution of these waters, as measured by their mobile anion contents, and the water chemical types described in the previous section.

## Origin of solutes

Solutes have their origin in both reactive minerals, which are generally not silicates, and less reactive rock-forming silicate minerals. Mobile solutes are derived in large part from fluid inclusions which are exposed as their containing minerals react or are broken up. Some members of the Saline Group also contain solutes derived from more saline water in adjacent sedimentary units.

Except among members of the Recharge Group, water in the crystalline basement is generally in equilibrium with fluorite, barite and calcite. The first two control the fluoride and barium contents of the waters, while the third, along with the pH of the water, influences the total dissolved carbonate.

There is little correlation between the dissolved calcium and fluoride contents of members of the Recharge Group, but there is a strong correlation among members of the Eastern and Western Groups, as well as among members of the Saline Group (SCHMASSMANN et al. 1992: Fig. 4.4.1c). The highest fluoride contents occur in members of the Western and Eastern Groups and can be accounted for by the dissolution of fluorite during their evolution from waters of the Recharge type. Fluorite is abundant in parts of the crystalline basement, such as in the upper section of the Siblingen borehole (MAZUREK 1989). The fact that the fluorite at Siblingen shows no evidence of corrosion suggests that fluorite dissolution occurs during flow prior to Siblingen.

There is an increase in the sulphate content of crystalline basement water from the Recharge through the Eastern and Western to the Saline Groups. Sulphate in the Eastern Group waters could have its origin in part from the oxidation of pyrite or other sulphide minerals under conditions of temperature and water isotopic composition similar to those of the present. The oxidants required cannot be entirely identified, but could be dissolved oxygen from the recharge water itself and(or) the reduction of ferric iron from hematite to ferrous iron in siderite. Both minerals are found in the crystalline basement.

The origin of the remainder of the sulphate dissolved in the Eastern Group waters and virtually all of that in the Western Group waters is not definitely known. Figure 7-4 shows that the sulphate and chloride concentrations of the water of the Recharge, Western and Eastern Groups increase sympathetically. This suggests that both ions may have the same origin. The saline waters generally have a lower sulphate/chloride ratio than waters of lower salinity from the crystalline basement.

The origin of the increasing dissolved chloride in the basement waters is of particular interest. There is strong correlation between dissolved chloride and both dissolved  $^4\text{He}$  and  $^{36}\text{Cl}$  as well as between dissolved  $^{40}\text{Ar}$  and dissolved potassium (PEARSON et al. 1991: Fig. 6.4.4, 6.2.1, and 6.5.4). These three isotopes are produced in the rock matrix by in situ nuclear reactions and enter the groundwater as the matrix is leached. Their correlation with total dissolved chloride and potassium suggests that presence of these elements in solution is also a result of matrix leaching.

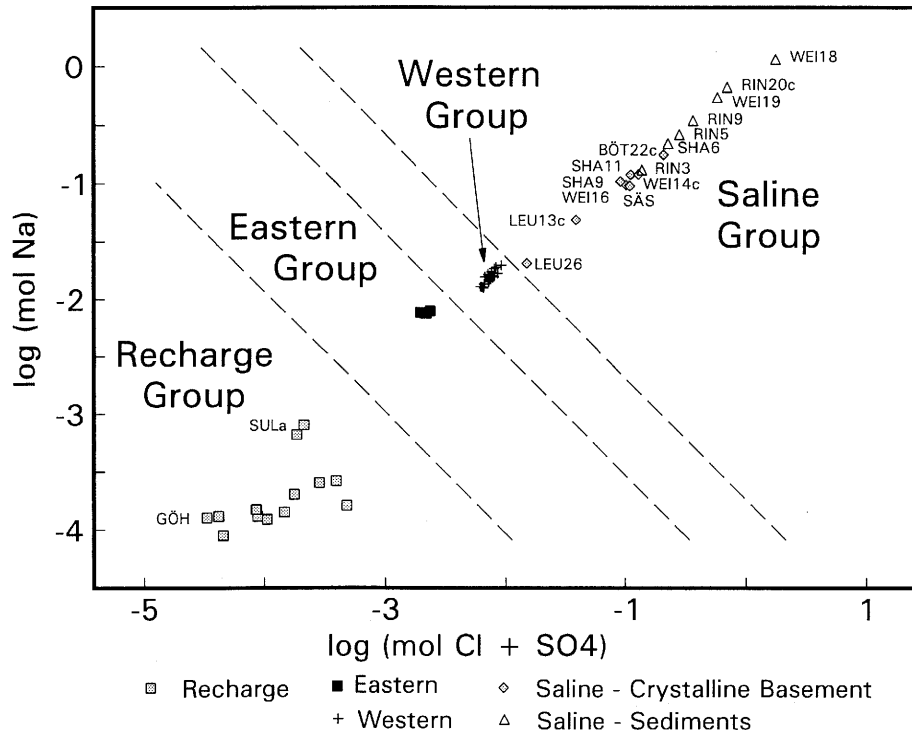


**Fig. 7-3 :** Graph of sodium concentration against mobile anion ( $\text{Cl} + \text{SO}_4$ ) concentrations illustrating the chemical evolution of water in the crystalline basement and the evolutionary stage of the four water groups.

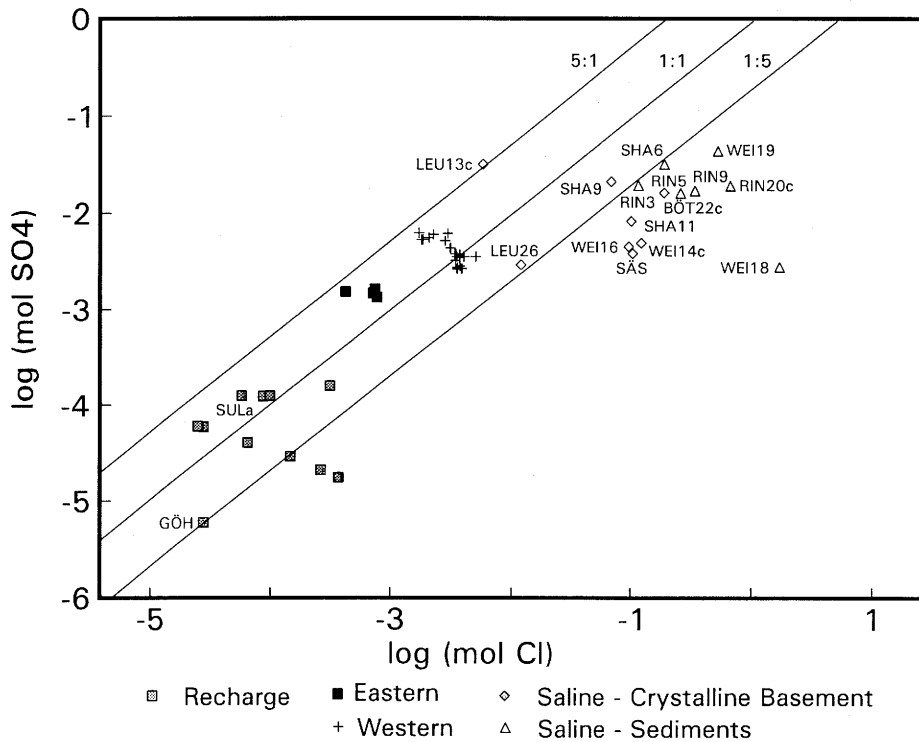


**Fig. 7-4 :** Graph of sulphate and chloride contents of water from the crystalline basement and adjacent sedimentary units illustrating the relatively lower  $\text{SO}_4/\text{Cl}$  ratios in waters of the Saline Group.

The dissolved helium data collected as part of the chemical programme are plotted against chloride in Figure 7-5. The chemical helium data probably are not as precise as the data collected as part of the isotope programme and given in Table 6.4.1 of PEARSON et al. (1991). However, many more helium analyses are available from the chemical programme, and these show the same correlation with chloride.

Laboratory studies have been made to determine the total amount of chloride that could be leached from granite of the crystalline basement (PETERS 1986). Granite crushed finely enough to have broken the fluid inclusions ( $< 5 \mu\text{m}$ ) yielded 160 g of water-leachable chloride per  $\text{m}^3$ . Less than 10 per cent of this was from residual pore water in the granite before crushing to the fine grain size. This indicates that virtually all of the water-leachable chloride is present in fluid inclusions. The total water-leachable chloride content corresponds to possible maximum dissolved groundwater chloride contents of 32 g/l and 8 g/l for porosities of 0.5 and 2 %, respectively. The crystalline basement waters of highest chloride content are the deep Böttstein sample (BÖT22c) and a sample from Weiach (WEI14c), with concentrations of 6.6 and 4.3 g Cl/l respectively (Fig. 7-2f).

The dissolved  $^4\text{He}$ ,  $^{36}\text{Cl}$  and  $^{40}\text{Ar}$  isotopes show that the source of dissolved chloride and potassium in waters sampled from the crystalline basement could have been the rock itself, while rock analyses show that the rock contains more than enough leachable chloride to produce even the most saline waters sampled, provided that not more than a few pore volumes of water have passed through the rock. Thus, there is no need to invoke an external source of chloride to explain even the most saline water from the crystalline basement.

Waters of high salinity from the crystalline basement of the Säcking, Weiach, Schafisheim and Böttstein boreholes, which are near sediments of Permo-Carboniferous troughs, could have a significant component of water from these sediments. As Figures 7-2g and 7-3 show, a number of samples from the sediments of the Weiach, Riniken and Schafisheim boreholes are more saline than any of the crystalline basement waters and fall along the same trend line.

Several aspects of the water chemistry, namely the magnesium/calcium and bromide/chloride ratios, suggest that waters from the crystalline basement at Weiach are distinct from the waters of the sediments, but also indicate that waters from the crystalline basement of Schafisheim, and probably those from Säcking and deep Böttstein (BÖT22c) as well, have a component of sedimentary water. The stable sulphur and oxygen isotopic compositions of dissolved sulphate also provide information about sources of solutes, as discussed in section 7.3.4.

Figure 7-6 shows the magnesium vs calcium contents of water from the crystalline basement and adjacent sediments. Three regions can be distinguished, corresponding to waters of different chemical types or source formations. The first region, with low magnesium and calcium contents, includes waters of the Recharge, Eastern and Western Groups from the crystalline basement. The second region, with similar magnesium but higher calcium contents, includes the saline waters from the crystalline basement of the Weiach borehole.

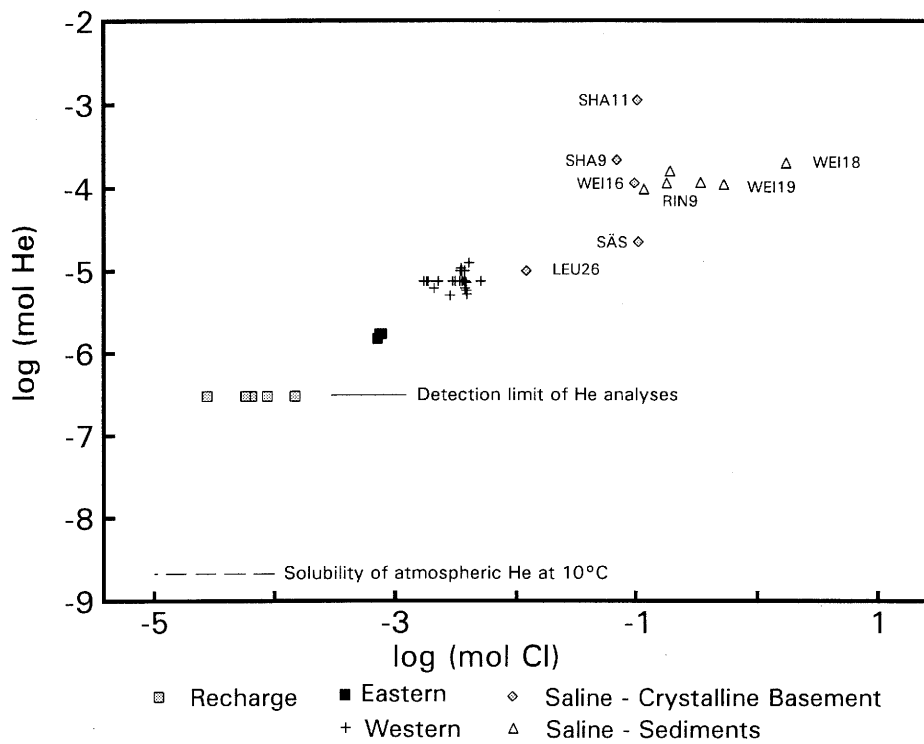


**Fig. 7-5 :** Graph of dissolved helium and dissolved chloride contents illustrating the increase of dissolved helium with salinity.

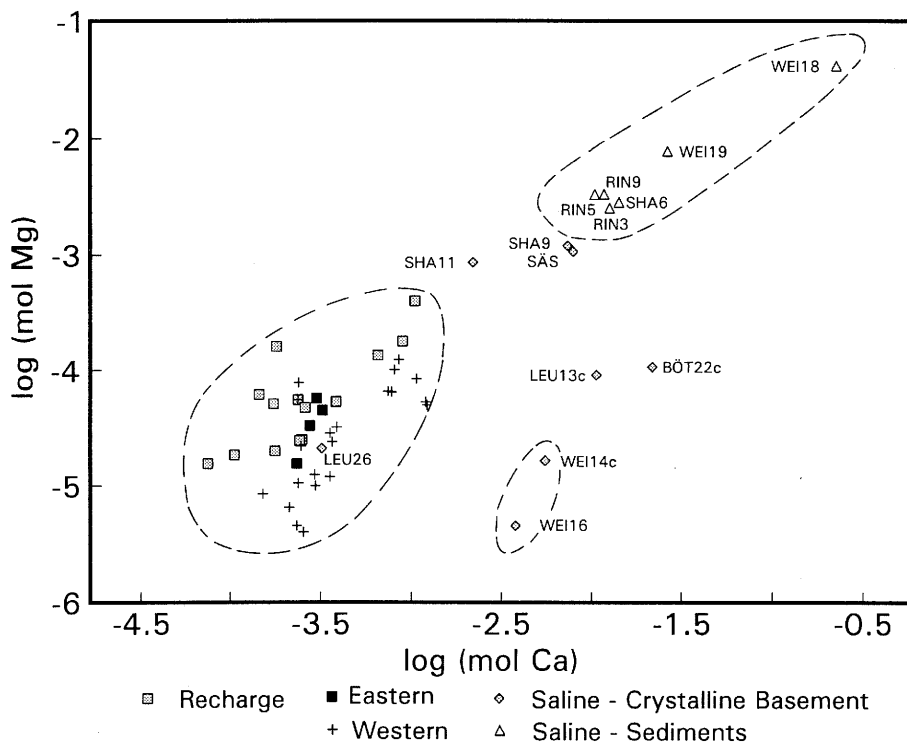


**Fig. 7-6 :** Graph of magnesium and calcium contents illustrating the differences in concentrations in waters of various types from the crystalline basement and from adjacent sedimentary units.

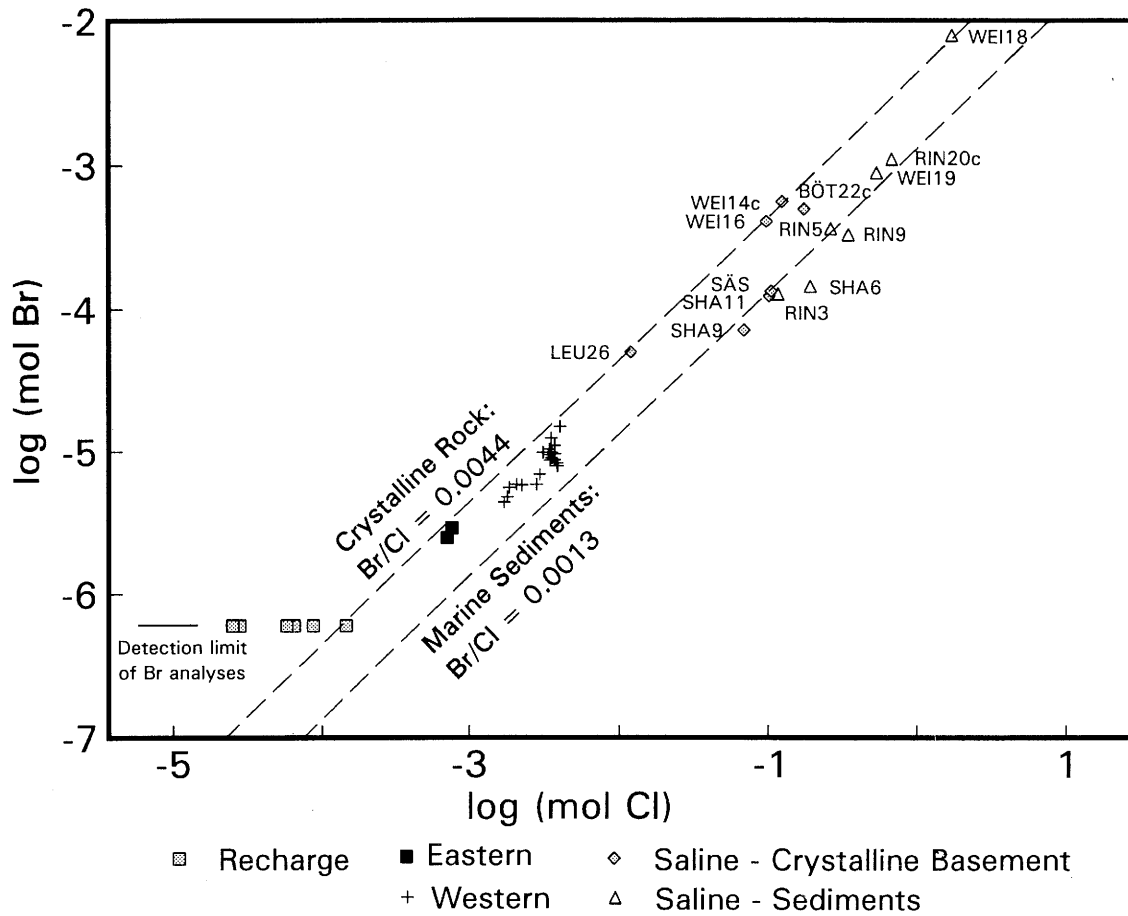


**Fig. 7-7 :** Graph of bromide and chloride contents illustrating the distinction between the Br/Cl ratios of waters from the crystalline basement and from adjacent sedimentary units.

The third group, with highest magnesium and calcium contents, includes saline waters from the sediments of the Permo-Carboniferous Trough. The saline samples from the crystalline basement at Schafisheim (SHA9 and SHA11) and Säckingen (SÄS) and from the crystalline basement at Böttstein (BÖT22c) and Leuggern (LEU13c) are intermediate between the regions. This suggests that their salinity could result in part from admixtures of water of sedimentary origin rather than continuing evolution in the crystalline basement. One sample from the sediments, RIN20c, is not shown in Figure 7-6. The calcium concentration of this sample is similar to that of other saline waters, but it has a very low magnesium concentration. The chemistry of this water is based on extrapolation from analyses of contaminated samples. The analyzed magnesium values are so low that there is significant uncertainty in the extrapolated value (PEARSON et al. 1989: section 4.3.4).

Figure 7-7 shows that the bromide/chloride ratios of waters from the crystalline basement are distinct from those of the sediments. Most of the waters from the basement, including those of high salinity from Weiach, have bromide/chloride mol ratios close to 0.0044. This is the ratio of leachate from crystalline basement rocks of Northern Switzerland (PETERS pers. comm.) and of leachate and groundwater from granites elsewhere in the world (e.g. FRAPE & FRITZ 1987, NORDSTROM et al. 1985, 1989a, 1989b). The samples from the sediments have bromide/chloride mol ratios of about that of sea water, namely 0.0013. The samples from the crystalline basement of Schafisheim (SHA9 and SHA11) and Säckingen Stammelhof (SÄS) have sedimentary bromide/chloride ratios. One sample from the Permian sediments of Weiach (WEI18) has a bromide/chloride ratio typical of water from crystalline rock. However, it is in the region of the magnesium-calcium diagram that is typical of other waters from sedimentary rock.

The magnesium/calcium and bromide/chloride data show that the salinity of water from the crystalline basement at Schafisheim (SHA9 and SHA11) and Säckingen (SÄS) is derived in part from water of sedimentary origin. These data also suggest, but less conclusively, that the saline water from the crystalline basement at Böttstein (BÖT22c) also has a sedimentary component. The remaining waters from the crystalline basement, including those of high salinity from Weiach (WEI14c and WEI16), have no detectable sedimentary component. Thus the composition of some of the waters in the crystalline basement can be treated as a product of evolution entirely within the crystalline rock itself.

### **Evolution and mineral controls on water chemistry**

Geochemical modeling of groundwater samples from the crystalline basement shows that many are saturated with respect to the reactive minerals barite, fluorite and calcite (PEARSON et al. 1989). These equilibria control the dissolved barium, fluoride and, with the pH, the carbonate contents of the waters. The overall evolution of the water including the concentration of its dominant mobile anions chloride and sulphate is determined by slower reactions with rock-forming silicate minerals (MICHARD 1990b), and is discussed in this section.

Temperature and mobile anion content are factors determining the composition of water at equilibrium with its host rock. A number of geochemical indicators of subsurface temperature are in common use in studies of geothermal systems. The formation temperatures of the intervals from which the Nagra borehole samples were taken are known from the borehole logs (WITTEWER 1986: Chapter 6, BLASER & SCHOLTIS 1991: Beil. 5). Comparing formation temperature with calculated geochemical equilibrium temperatures suggests possible additional mineral controls on water chemistry and the extent to which these waters are in equilibrium with the host rock.

Two widely used geothermometers are based on the dissolved silica content of a water and on the ratio of dissolved sodium to potassium (Na/K). The silica geothermometer is based on the well-known solubility of solid silica phases such as quartz and chalcedony, and the fact that silica solids precipitate relatively slowly, particularly at temperatures below ca. 100 °C. Thus, the silica content of a water cooled rapidly

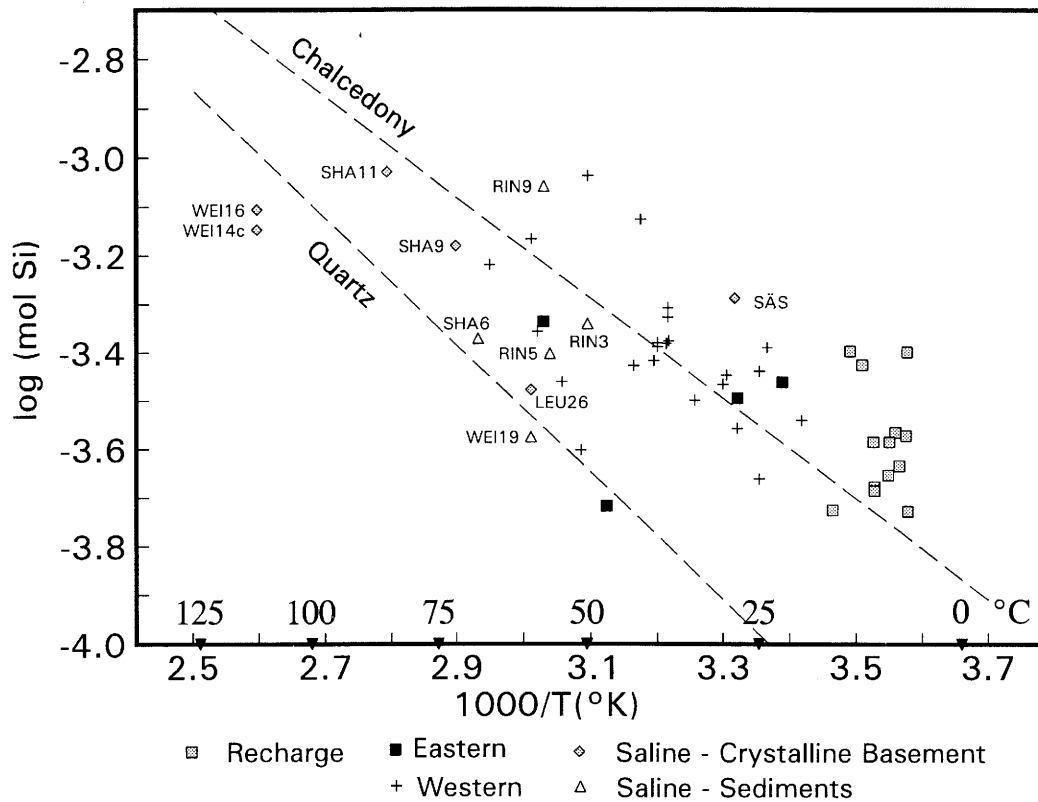


**Fig. 7-8 :** Graph showing dissolved silica concentrations and formation temperatures of waters, and the solubilities of quartz and chalcedony, illustrating possible mineral controls on dissolved silica.

during its ascent to the surface for sampling will still represent a higher subsurface temperature. The variation of Na/K with temperature in many groundwaters was treated empirically when it was initially observed, but is now interpreted as indicating equilibrium between Na- and K-feldspars, at least at temperatures above 150 or 200 °C (GIGGENBACH 1988, MICHAARD 1990a).

Figure 7-8 shows the silica content of the waters sampled plotted against  $10^3/T$  (formation temperature in Kelvin; solubilities are straight lines on this temperature scale, °C are also given in the Figure). Although there is considerable scatter in the data, most points appear to fall closer to chalcedony solubility than to quartz solubility. The samples with the highest formation temperatures, WEI14c and WEI16, have silica concentrations below those of quartz solubility. This could be a result of silica loss on cooling during sampling or storage before analysis.

Some samples have silica concentrations above chalcedony saturation. Most of these are members of the Recharge Group. The residence times of these waters may be too low for silica mineral precipitation to keep up with the silica brought into solution during the relatively rapid hydrolysis of silicate minerals in the recharge area. Samples of the Eastern and Western Groups also have silica concentrations above silica saturation. These can be attributed principally to the difficulty in completely eliminating silica-containing particulates from samples taken during drilling.

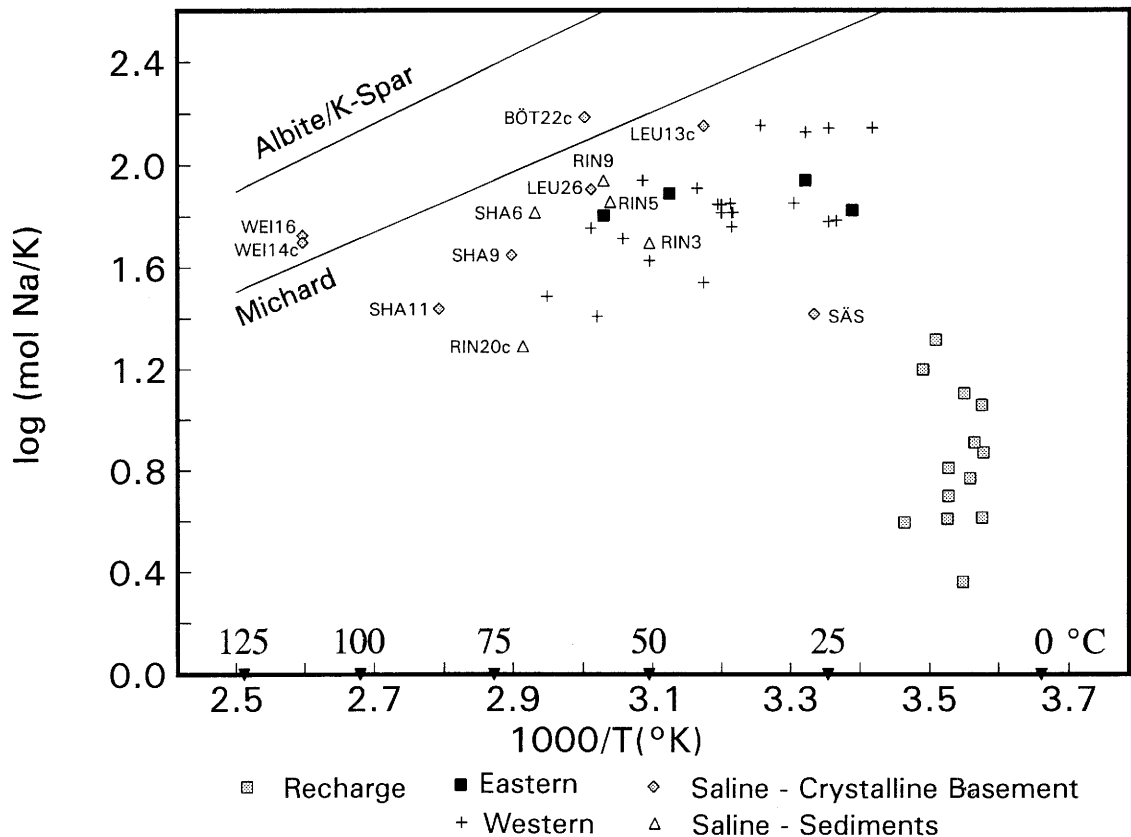


**Fig. 7-9 :** Graph showing Na/K ratios and formation temperatures of waters, and two Na/K geothermometer equations, illustrating approach to equilibrium control of Na/K ratio in saline waters.

Figure 7-9 shows the Na/K ratios vs formation temperatures and includes lines based on two Na/K geothermometer equations. The upper line is based on equilibrium between albite and K-feldspar using recent thermodynamic data (SUPCRT92; JOHNSON et al. 1992). The lower line represents an equation developed by MICHARD (1990a) from thermal spring data. The Na/K ratio of water during the initial stage of water-rock reaction will be that of the bulk rock, which is about 1 for this system. As water-rock reactions proceed, this ratio will change towards a value determined by equilibrium with solid phases. As Figure 7-9 shows, waters of the Recharge Group have Na/K ratios ranging from about 2 ( $10^{0.3}$ ) to about 15 ( $10^{1.2}$ ), while all other samples are above 15. Three saline samples from the crystalline basement, WEI16, WEI14c and BÖT22c, have Na/K ratios that fall between the lines representing the geothermometer equations. The remaining samples, including the other members of the Saline Group, have Na/K ratios between those of the recharge water and those predicted by the geothermometer equations. This suggests that while the Na/K ratios of the Weiach and Böttstein samples are consistent with water-rock equilibrium at present formation temperatures, the remaining samples have not reached this stage, presumably because of insufficient time and (or) temperature.

The magnesium/calcium and bromide/chloride ratios of samples WEI16 and WEI14c suggest that their chemistry is not influenced by water from adjacent sedimentary units, and that they evolved entirely within the crystalline basement. They have the highest mobile anion contents of such water and so are the most evolved. Their formation temperature (112 °C) is also the highest of any water sampled. To explore how closely these waters represent rock-water equilibrium, a geochemical computer program (EQ3; WOLERY 1992) was used to calculate the equilibrium composition of a water under two sets of constraints. Both sets included equilibrium with the minerals albite ( $\text{NaAlSi}_3\text{O}_8$ ), K-feldspar ( $\text{KAlSi}_3\text{O}_8$ ), kaolinite ( $\text{Al}_2\text{Si}_2\text{O}_5(\text{OH})_4$ ), calcite ( $\text{CaCO}_3$ ), illite ( $\text{K}_{0.6}\text{Mg}_{0.25}\text{Al}_{2.3}\text{Si}_{3.5}\text{O}_{10}(\text{OH})_2$ ) and quartz ( $\text{SiO}_2$ ). These minerals occur in the water-bearing fractures of the crystalline basement. Both sets of constraints also used the analyzed concentrations of sulphate and chloride and a temperature of 112 °C. One set included equilibrium with the mineral prehnite ( $\text{Ca}_2\text{Al}_2\text{Si}_3\text{O}_{10}(\text{OH})_2$ ), which is present in small amounts in the Weiach core. The other set included the partial pressure of  $\text{CO}_2$ ,  $P_{\text{CO}_2}$ , fixed at the measured value. The program calculated the concentrations of all solutes and the pH of the solution for each set of constraints.

Table 7-2 compares the model results with the analyzed values for all constituents except Al. The analyzed value for Al is thought to be uncertain (cf. section 10.4.1) (PEARSON et al. 1989). The modeled and measured concentrations of all constituents except Mg agree within factors of three or less. The modeled Mg content is more than ten times the measured value. This would probably improve if thermodynamic data were available on other phases more likely to be influencing Mg contents in these waters, such as (Mg+Fe)-bearing chlorites. The model including prehnite predicts about twice the measured calcium concentration and about one-third the measured total dissolved carbonate. The model with a fixed  $P_{\text{CO}_2}$  leads to a better agreement with the concentrations of both substances. Given the uncertainty in the identity of the actual controlling mineral phases and in the thermodynamic data for silicate minerals at these temperatures, the modeled and analyzed compositions can be considered to be in agreement and to support the conclusion that water in the crystalline basement at Weiach is close to equilibrium with its host rock.

Volume changes accompanying the evolution of water in the crystalline basement have been calculated. They are based on the amounts of mass transfer during reactions that can plausibly account for observed changes in water chemistry and are expressed per liter of water. As an illustration, a schematic mass balance has been constructed by which water of the type found at Görwihl (sample GÖH) in the recharge area could evolve to Eastern Group water as found at Siblingen. The Görwihl water analysis used for the mass balance was first adjusted for electrical neutrality. The Eastern Group water is the eastern reference water (section 10.4.1). The water chemistry and mass balance are given in Table 7-3.

The principal changes accompanying the evolution of Recharge to Eastern Group water are increases in sulphate, total dissolved carbonate and sodium. The sulphate increase is modeled as the oxidation of an iron sulphide mineral (pyrite) with the accompanying iron precipitated as a ferric hydroxide mineral (goethite). Dissolved oxygen in the recharge water is insufficient to oxidize pyrite to produce all the sulphate required, so it is likely that oxidation occurs in the unsaturated zone where a free



for inclusion in Table 7-3 because it minimizes the increase in pore volume accompanying the increase in dissolved sulphate, and the object of this table is to illustrate that the net result of whatever reactions are chosen to account for water chemical evolution, they lead to a porosity increase.

The carbonate increase is attributed to the dissolution of calcite, which is accompanied by a calcium increase. The isotopic composition of dissolved Sr suggests its source may be plagioclase dissolution (section 7.3.4). The Sr increase is attributed to the dissolution of calcic plagioclase with an arbitrarily chosen composition of  $(Ca_{0.99}Sr_{0.01})Al_2Si_2O_8$ . The total calcium increase from mineral dissolution is greater than its increase in the water so a sink for calcium is required. This is taken to be exchange on clays derived from plagioclase alteration in the crystalline basement, which releases an equivalent amount of sodium. Secondary calcite is present in the core from Siblingen and the other boreholes, which appears to contradict Table 7-3. Because the reactions in the table summarize reactions occurring over the entire flow path from recharge to the Siblingen region, calcite dissolution occurring at the beginning of the flow system could easily compensate for precipitation later.

Reactions influencing several of the minor dissolved constituents are also included. The chloride increase is attributed to the breakdown of fluid inclusions and is accompanied by an equivalent amount of sodium. It is probable that at least some of the sulphate increase is also of this origin, but this is not included in the model. The decreasing barium concentration is attributed to barite precipitation which accompanies the increase in dissolved sulphate. Fluoride increases as fluorite dissolves. The increases in the potassium and magnesium contents and the amount of sodium not generated by the fluid inclusions and exchange for calcium are accounted for by the dissolution of K-feldspar, illite and albite. To maintain the low dissolved aluminium and silica contents of the water, kaolinite and quartz precipitate.

The number of mols of each mineral precipitating or dissolving are given in Table 7-3 and are used with their molar volumes to calculate the volume changes. The net effect of this set of reactions is to increase the pore volume by  $0.125 \text{ cm}^3$  per kg  $H_2O$  that has reacted.

It is possible to model the chemical change between Recharge and Eastern Group waters using many other combinations of minerals, so the specifics of Table 7-3 must be taken as no more than a plausible hypothesis. However, the volume changes accompanying other hypothetical reaction schemes are not very different from that of this set of reactions, indicating that the overall net effect of the chemical evolution of water in this region will be to increase pore space. This would increase the ease with which succeeding volumes of water will be able to flow through the rock.

Tab. 7-3 : Possible mineral dissolution and precipitation by which Recharge Group water could evolve to the Eastern Group (cf. text).

				Na <sup>+</sup>	K <sup>+</sup>	Mg <sup>++</sup>	Ca <sup>++</sup>	Sr <sup>++</sup>	Ba <sup>++</sup>	Al <sup>+++</sup>	Alkalinity (HCO <sub>3</sub> <sup>-</sup> )	SO <sub>4</sub> <sup>--</sup>	F <sup>-</sup>	Cl <sup>-</sup>	SiO <sub>2</sub> (aq)	Total Carbonate
Recharge Water: GOERWIHL																
Analysed molality				1.26E-04	1.10E-05	1.55E-05	7.50E-05	2.50E-07	3.15E-06	3.00E-07	2.95E-04	6.00E-06	1.50E-05	5.70E-05	2.68E-04	1.74E-03
Balanced <sup>1)</sup> molality				1.36E-04	1.18E-05	1.67E-05	8.07E-05	2.69E-07	3.39E-06	3.23E-07	2.73E-04	5.55E-06	1.39E-05	5.27E-05	2.68E-04	1.74E-03
Eastern Group: REFERENCE WATER																
Analysed molality				7.70E-03	1.07E-04	4.53E-05	2.87E-04	3.99E-06	5.48E-07	4.35E-07	4.39E-03	1.41E-03	6.21E-04	7.36E-04	5.93E-04	4.52E-03
Balanced <sup>1)</sup> molality				7.74E-03	1.08E-04	4.55E-05	2.88E-04	4.01E-06	5.51E-07	4.37E-07	4.37E-03	4.40E-03	6.18E-04	7.32E-04	5.93E-04	4.52E-03
Composition Difference: molality				7.60E-03	9.57E-05	2.89E-05	2.08E-04	3.74E-06	-2.84E-06	1.15E-07	4.10E-03	1.40E-03	6.04E-04	6.79E-04	3.25E-04	2.78E-03
REACTING MINERALS																
Name	Composition	Quantity Precipitated (-) or Dissolved (+) per kg water														
		cm <sup>3</sup>	mols													
Barite	BaSO <sub>4</sub>	-0.000	-2.84E-06						-2.84E-06							
Pyrite	FeS <sub>2</sub>	0.017	7.00E-04									-2.84E-06 1.40E-03				
Geothite	FeOOH	-0.015	-7.00E-04													
Fluorite	CaF <sub>2</sub>	0.007	3.02E-04				3.02E-04									
Albite	NaAlSi <sub>3</sub> O <sub>8</sub>	0.044	4.34E-04	4.34E-04												
Plagioclase	see below <sup>2)</sup>	0.038	3.74E-04							4.34E-04					1.30E-03	
K-Feldspar	KAlSi <sub>3</sub> O <sub>8</sub>	0.010	9.57E-05			9.57E-05	3.70E-04	3.74E-06		7.48E-04					7.48E-04	
Chlorite	see below <sup>3)</sup>	0.001	5.77E-06							9.57E-05					2.87E-04	
Kaolinite	Al <sub>2</sub> Si <sub>2</sub> O <sub>5</sub> (OH) <sub>4</sub>	-0.064	-6.45E-04			2.89E-05				1.15E-05					1.73E-05	
Calcite	CaCO <sub>3</sub>	0.103	2.78E-03				2.78E-03			-1.29E-03					-1.29E-03	
Exchange	2 Na <sup>+</sup> = Ca <sup>++</sup>	0.000	6.49E-03	6.49E-03							4.10E-03					
Quartz	SiO <sub>2</sub>	-0.017	-7.41E-04				-3.24E-03								-7.41E-04	
Fluid Incl.	NaCl	0.000	6.79E-04	6.79E-04										6.79E-04		
Sums of Reactions:		0.124	9.77E-03	7.60E-03	9.57E-05	2.89E-05	2.08E-04	3.74E-06	-2.84E-06	1.15E-07	4.10E-03	1.40E-03	6.04E-04	6.79E-04	3.25E-04	2.78E-03

<sup>1)</sup> Calculated by distributing charge imbalance of analysis proportionally among all dissolved substances.

<sup>2)</sup> (Ca<sub>0.99</sub> Sr<sub>0.01</sub>) Al<sub>2</sub>Si<sub>2</sub>O<sub>8</sub>

<sup>3)</sup> Mg<sub>3</sub>Al<sub>2</sub>Si<sub>3</sub>O<sub>10</sub>(OH)<sub>8</sub>

## **7.3 Isotope hydrogeology**

### **7.3.1 Scope and objectives of isotope studies**

Measurements of the isotopic composition of water and solutes in most borehole and many regional samples were part of the Nagra hydrochemical programme. The isotope hydrogeology programme was one of the most extensive ever undertaken and provided information on the origin and residence time of groundwaters and their solutes in the crystalline basement of Northern Switzerland and, in addition, led to scientific conclusions of general importance in the field of isotope hydrogeology.

The remainder of this section summarizes the results of the isotope studies. It is organized on the basis of the conclusions drawn rather than by isotope. Thus, some isotopes may be mentioned more than once when they are relevant to more than one aspect of the hydrogeology of the system.

The isotope data themselves, detailed discussions of their interpretation, and the conclusions to be drawn from them are given by PEARSON et al. (1991) for the first six boreholes and the regional programme, and by BLASER & SCHOLTIS (1991) for the Siblingen borehole. Data and discussion of some isotope results also appear in SCHMASSMANN et al. (1992). This section draws extensively from those reports.

### **7.3.2 Groundwater mixing and sample contamination**

Analyses of the short-lived isotopes tritium ( $^3\text{H}$ , half-life 12.3 a) and  $^{85}\text{Kr}$  (half-life 10.8 a) were useful in detecting the presence of young waters (less than a few decades old) in a sample.

Tritium measurements were made on virtually all borehole and regional programme samples. This isotope was first introduced into the atmosphere in significant quantities in the early 1950s by thermonuclear weapons testing. The Black Forest samples have tritium contents consistent with their being virtually all young water. This is in keeping with their position in the recharge area, low salinity (section 7.2.1), stable H and O isotope ratios and noble gas contents (section 7.3.3), and long-lived radioisotope contents (section 7.3.5). The tritium contents of the remaining regional samples are near or below the detection limit, except for two of the three locations sampled at Säckingen. The high tritium in these two samples is consistent with their chemistry in indicating that they are mixtures of young and old waters, and they are not included in the discussions of this Chapter.

By itself, the tritium content of even a young water cannot provide an unambiguous estimate of groundwater residence time.  $^{85}\text{Kr}$  is another isotope introduced into the atmosphere since the early 1950s by nuclear activities. Together, tritium and  $^{85}\text{Kr}$  can provide unambiguous estimates of model residence times (PEARSON et al. 1991: section 4.3). Collection of  $^{85}\text{Kr}$  samples for this study required on-site degassing of ca. 10000 l of water, but with recently developed analytical techniques the gas from only 500 l of water is necessary. This isotope was measured in a few samples from Nagra deep boreholes, but not from any other sampling points in the crystalline basement.

Samples collected during the deep borehole programme were particularly susceptible to contamination from drilling-fluid. The drilling-fluids used contained tracers that were analyzed in samples as they were collected to assess the extent of contamination. Tritium contents near or below the detection limit indicated that samples contained less than a few per cent of drilling-fluid, and so could be interpreted with some confidence. In a few contaminated intervals (BÖT22c, LEU13c, WEI14c, SIB4c), the change in tritium with volume extracted provided assistance with the drilling-fluid tracers in correcting the measured sample composition to that of the in situ groundwater.

### 7.3.3 Recharge areas and conditions

The concentrations of the stable  $^2\text{H}$  and  $^{18}\text{O}$  isotopes were measured in virtually all water samples taken. The results are expressed as  $\delta^2\text{H}$  and  $\delta^{18}\text{O}$  values, which represent the per mil deviation of the  $^2\text{H}/^1\text{H}$  and  $^{18}\text{O}/^{16}\text{O}$  ratios in the samples from those in a standard, Standard Mean Ocean Water (SMOW). Isotope ratios in atmospheric precipitation vary with climate, altitude and location. Thus, differences in the  $\delta^2\text{H}$  and  $\delta^{18}\text{O}$  values of groundwaters can indicate changing climate in the recharge area, or changing locations or elevation of the recharge area. Conventions for reporting stable isotope ratios and the systematics of the H and O isotopic composition of modern recharge in Switzerland are discussed in section 1.4 and Chapter 3 of PEARSON et al. (1991).

The  $^2\text{H}$  and  $^{18}\text{O}$  concentrations of groundwaters from Northern Switzerland and of surface waters from the Alps are illustrated in Figure 7-10. The line represents the trend of values in meteoric water in Switzerland (PEARSON et al. 1991: section 3.1.2). More negative values correspond to meteoric waters infiltrated in regions of cooler temperature or higher altitude. The Recharge Group (Black Forest) samples and the Western Group samples fall in a cluster centered at about -10.2 per mil  $\delta^{18}\text{O}$  and -72.5 per mil  $\delta^2\text{H}$ . Waters of more negative  $\delta^2\text{H}$  and  $\delta^{18}\text{O}$  values are found at Siblingen (the Eastern Group), and in the Alpine waters. The saline waters of the crystalline basement at Böttstein (BÖT22c), Weiach and Schafisheim, and the saline waters from the sedimentary units, have more positive  $\delta^2\text{H}$  and  $\delta^{18}\text{O}$  values.

The dissolved concentrations of the noble gases Ne, Ar, Kr and Xe were measured in several of the borehole and regional programme samples. The temperature coefficients of the solubilities of these gases are quite different, so their concentrations in groundwater can be interpreted to yield recharge temperatures corresponding to known or assumed recharge elevations (PEARSON et al. 1991: section 3.3).

Considered together, the stable H and O isotope data and noble gas concentrations lead to four principal observations.

Young (tritium-bearing) waters from the Black Forest (Recharge Group) have noble gas recharge temperatures from 4 to 8 °C and  $\delta^2\text{H}$  values from about -64 to -75 per mil.

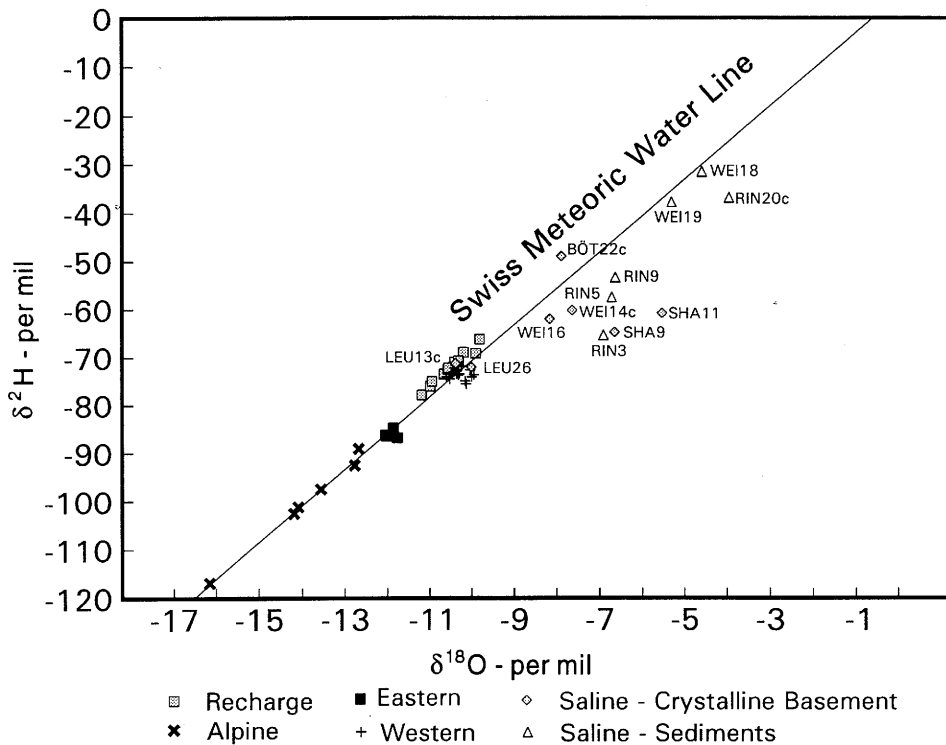


**Fig. 7-10 :** Graph of the  $\delta^2\text{H}$  and  $\delta^{18}\text{O}$  values of water from the crystalline basement and adjacent and sedimentary units and the meteoric water line for Switzerland illustrating differences among the several groups that result from differences in recharge conditions and extent of water-rock reactions. (PEARSON et al. 1991: section 3.1.2).

Second, the samples from Siblingen (Eastern Group) have noble gas temperatures of about 2 °C and relatively negative  $\delta^2\text{H}$  and  $\delta^{18}\text{O}$  values (BLASER & SCHOLTIS 1991). Such low recharge temperatures and  $\delta^2\text{H}$  and  $\delta^{18}\text{O}$  values are consistent with present-day recharge only in an area such as the Alps (Fig. 7-10), and would have occurred in the Black Forest, where the maximum elevation is 1400 m, only during a time of glaciation. The salinities and He contents of the Siblingen waters are considerably higher than those of the Black Forest samples (Fig. 7-3 and 7-5), consistent with a much greater residence time. As discussed below, the  $^{14}\text{C}$  data after adjustment for dilution with mineral carbonate cannot be interpreted more precisely than to conclude that the model ages of these waters are greater than about 17 ka (BLASER & SCHOLTIS 1991).

Third, samples from the Böttstein, Kaisten and Leuggern boreholes (Western Group) have noble gas recharge temperatures of 2 to 5 °C and  $\delta^2\text{H}$  and  $\delta^{18}\text{O}$  values similar to those of young water in the Black Forest (Fig. 7-10). This indicates that these waters were recharged under climatic conditions similar to, or slightly cooler than, those of the

present, but not as cool as the recharge conditions for the Eastern Group waters.  $^{14}\text{C}$  adjusted for the effects of mineral carbonate shows that these waters have model ages greater than about 10 ka (PEARSON et al. 1991, Chapter 5). Thus, the climatic conditions under which the water was recharged cannot be those of the present, but must be those of a previous warmer period, the most recent of which ended approximately 70 ka ago (SCHREINER 1992: Fig. 94). The salinities and He contents of the Western Group waters are higher by factors of about 2 and 10, respectively, than those of the Eastern Group (Fig. 7-3 and 7-5). This is consistent with a greater residence time.

Fourth, the samples from the Weiach, Riniken and Schafisheim boreholes (Saline Group), as well as sample BÖT22c, are enriched in both  $^2\text{H}$  and  $^{18}\text{O}$  with respect to the other groups (Fig. 7-10). This enrichment results from a combination of recharge under different conditions (the samples that fall along the meteoric water line), or evaporation prior to recharge or water-rock reactions occurring at high temperature and(or) with very long residence times (samples that fall significantly away from the meteoric water line). The high salinities and He contents of these waters are also consistent with long residence times.

#### 7.3.4 Isotopic composition, geochemistry and origin of solutes

The stable and radioisotopic composition of a number of substances dissolved in the groundwaters were used to develop an understanding of the origin of the solutes, and the geochemical reactions affecting them. Knowledge of solute origin is important for understanding the history and movement of the groundwater. Once the geochemistry of certain solutes is understood, it is possible to use the radioisotope content of the solutes to model groundwater ages.

##### *Carbon and oxygen isotopes of carbonates*

The stable oxygen ( $^{18}\text{O}/^{16}\text{O}$ ) and carbon ( $^{13}\text{C}/^{12}\text{C}$ ) isotope ratios, and the radioactive carbon ( $^{14}\text{C}$ ) contents of the total dissolved carbonate ( $\text{CO}_{2(\text{aq})} + \text{HCO}_3^- + \text{CO}_3^{2-}$ ), of many water samples were measured. Carbonate stable isotope ratios are reported in the  $\delta$ -notation as  $\delta^{18}\text{O}$  and  $\delta^{13}\text{C}$  values relative to the PDB standard, while  $^{14}\text{C}$  is reported in per cent of the  $^{14}\text{C}$  content of an idealized modern (1900 AD) plant carbon (pmc) (PEARSON et al. 1991: section 1.4, 2.1). In addition, the  $\delta^{13}\text{C}$  and  $\delta^{18}\text{O}$  values of a number of mineral carbonate samples from core were determined.

The stable oxygen and carbon isotope ratios of calcite precipitating from a solution depend on the isotope ratios of the water and dissolved carbonate, the water chemistry (pH, particularly), and the temperature. Figure 7-11 compares the oxygen isotopic composition of the calcite found in water-bearing fractures in the crystalline basement of the Kaisten borehole with compositions of calcite calculated at isotopic equilibrium with water presently in the fractures at temperatures corresponding to their depths (PEARSON et al. 1991: section 5.3). The dashed lines represent the effects of differences of  $\pm 5^\circ\text{C}$  on the calculated compositions. The measured  $\delta^{18}\text{O}$  values of many of the fracture calcites are near or within the  $5^\circ\text{C}$  band. This indicates that they could have formed from waters isotopically like those now present at temperatures not

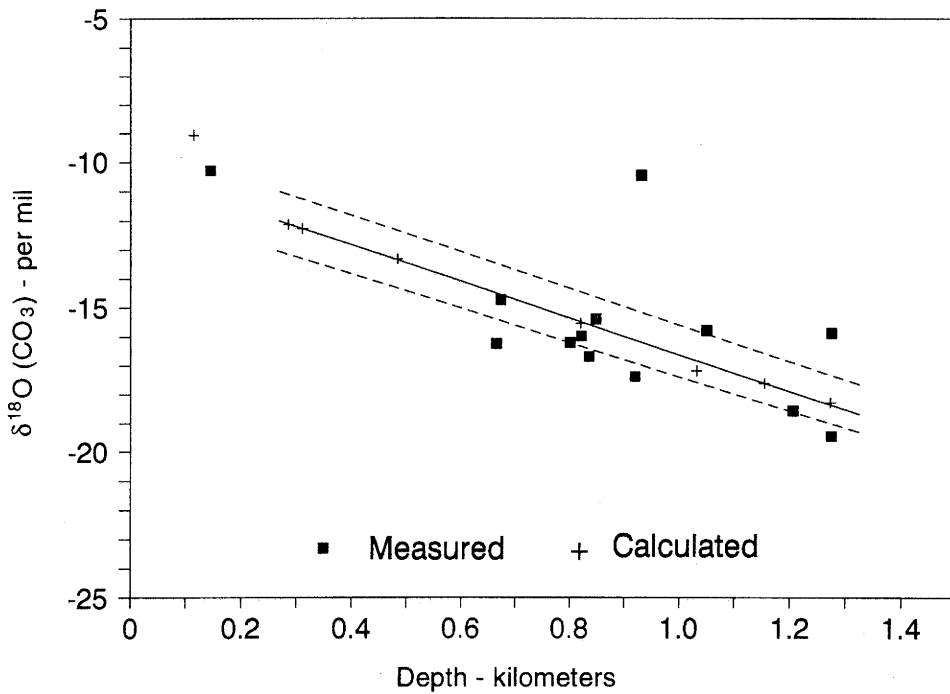


**Fig. 7-11 :** Graphs illustrating the correspondence between the measured  $\delta^{18}O$  values of calcite sampled from core of the crystalline basement from the Kaisten borehole, and calculated  $\delta^{18}O$  values for calcite at equilibrium with waters sampled (PEARSON et al. 1991: Fig. 5.3.4).

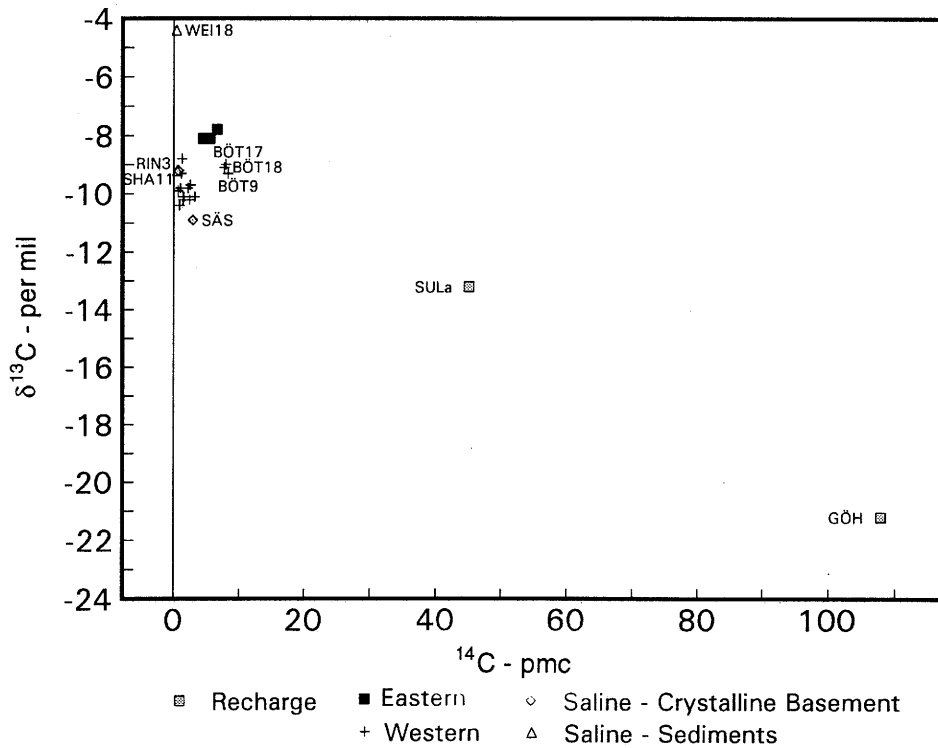


**Fig. 7-12 :** Graph of  $\delta^{13}C$  values and  $^{14}C$  contents of waters illustrating the relatively low values that make possible interpretation only of limiting  $^{14}C$  model ages, except for Recharge Group samples.

more than ca. 5 °C different from those now prevailing. Similar relations are found between dissolved carbonate and at least some of the fracture calcite in the crystalline basement in all Nagra boreholes.

The  $^{13}\text{C}$  contents of members of the Western Group are similar (Fig. 7-12), and suggest similar infiltration conditions and chemical evolution for all samples. The  $\delta^{13}\text{C}$  values of the Eastern Group samples are more negative, suggesting different recharge conditions or less carbonate chemical evolution than the Western Group waters. The  $^{14}\text{C}$  contents of these samples are discussed in the following section.

#### *Sulphur and oxygen isotopes of sulphates*

The stable oxygen and sulphur ( $^{34}\text{S}/^{32}\text{S}$ ) isotope ratios of dissolved sulphate from a number of water samples and of sulphate minerals from core samples were measured with results shown in Figure 7-13. Three types of sulphate minerals can be distinguished: gypsum or anhydrite found in the sedimentary rocks of the Permo-Carboniferous Trough and Triassic formations overlying the crystalline basement, and two mineralogically distinct generations of barite found in the fractures of the crystalline rock itself. Virtually all basement waters beyond the Recharge Group are saturated with barite.

The  $\delta^{34}\text{S}$  values of the dissolved sulphate (expressed relative to the CD standard) (PEARSON et al. 1991: section 1.4) are in the same range as those of pyrite from relatively unaltered gneiss from the Kaisten and Leuggern boreholes. At least from the standpoint of the sulphur isotopes, dissolved sulphate could have resulted from the oxidation of such pyrite.

The older generation of barite in the crystalline basement has relatively high  $\delta^{18}\text{O}$  values that are similar to sedimentary sulphates of the age of the immediately overlying and adjacent sedimentary formations.

Dissolved sulphates in Eastern Group waters and from the saline waters of the Böttstein and Leuggern boreholes have the same range of  $\delta^{18}\text{O}$  values. Dissolved sulphates from the Western Group of waters have a wider range of  $\delta^{18}\text{O}$  values, from negative  $\delta^{18}\text{O}$  values to values nearly as positive as are found in the Eastern Group of waters. The  $\delta^{18}\text{O}$  values in the younger barite of the crystalline basement is included in the range of water  $\delta^{18}\text{O}$  values.

Differences between the oxygen isotopic compositions of sulphates and the waters in which they are found have been used as geochemical thermometers in geothermal systems (TRUEDELL & HULSTON 1980) and waters from sediments in Northern Switzerland (WEXSTEEN & MATTER 1989).

These differences between the Eastern Group waters and their dissolved sulphate correspond to isotopic equilibrium at temperatures of 50 to 70 °C. Temperatures at the bottom of the Siblingen borehole approach 60 °C, so the  $\delta^{18}\text{O}$  values of the sulphate from this borehole could result from isotopic exchange with the water.

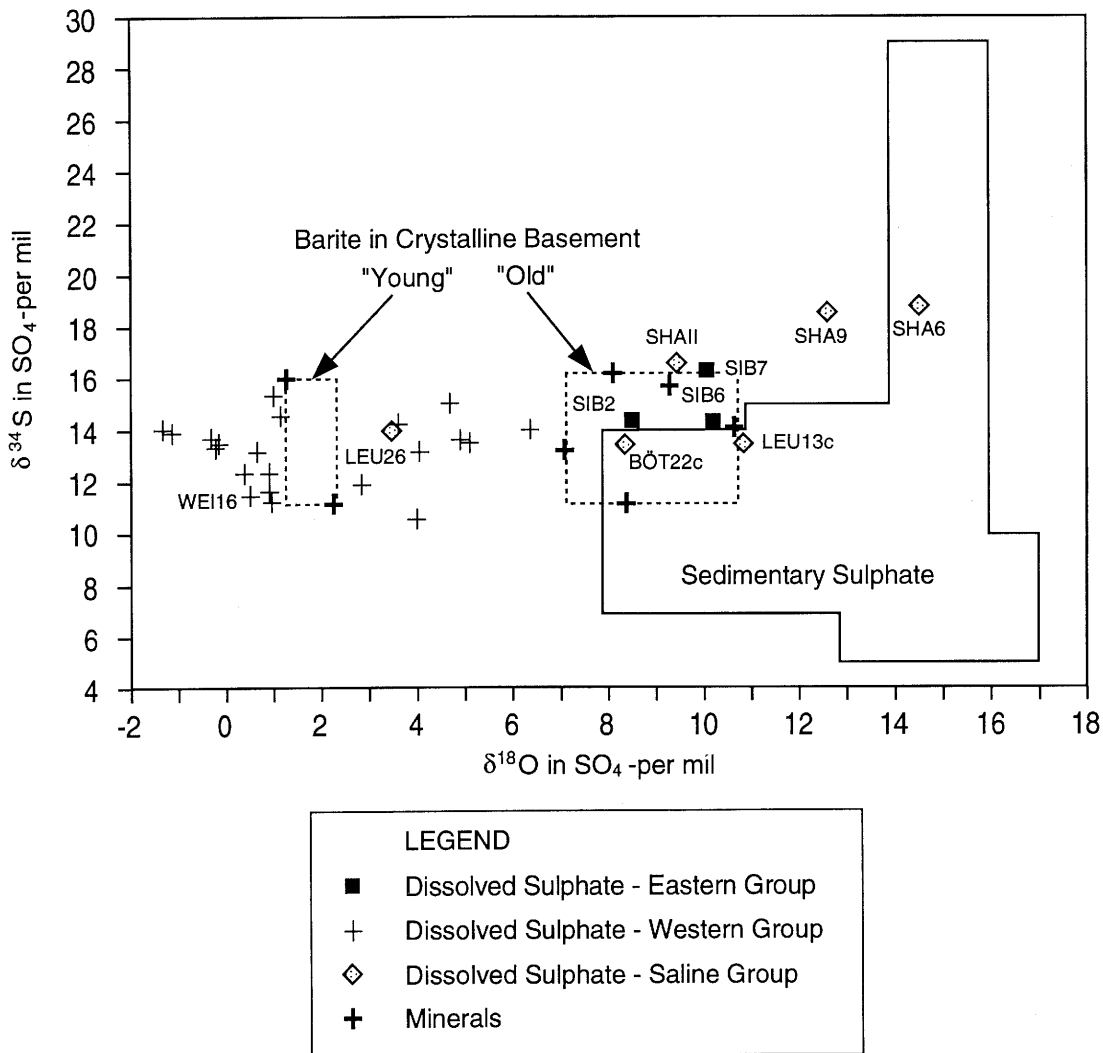


**Fig. 7-13 :** Graph of  $\delta^{34}\text{S}$  and  $\delta^{18}\text{O}$  of sulphate minerals and dissolved sulphate illustrating the differences between sedimentary sulphate minerals and water and sulphate in "Young" barite, and water of the Western Group from the crystalline basement.

Sulphate oxygen isotope exchange occurs so slowly at temperatures below ca. 100 °C that such exchange is unlikely, however. More probably, the isotopic composition of this sulphate indicates a sedimentary source or pyrite oxidation by atmospheric oxygen.

Differences in the  $\delta^{18}\text{O}$  values of Western Group waters and their dissolved sulphate correspond to temperatures of 100 to 200 °C, far above the temperatures of any of the borehole intervals from which they were sampled. This sulphate could have a hydrothermal origin and, perhaps, enter the water accompanying chloride from fluid inclusions.

Sulphate in saline water from the crystalline basement at Schafisheim and from the more saline intervals at Leuggern (LEU13c) and Böttstein (BÖT22c) resembles that of sedimentary sulphate or older generation barite. The Böttstein and Schafisheim boreholes are in or adjacent to the Permo-Carboniferous Trough, and their dissolved sulphate could well be of sedimentary origin. The distance of the Leuggern borehole from the Trough is such that it is unlikely to contain sedimentary sulphate. The difference between the  $\delta^{18}\text{O}$  values of dissolved sulphate and water of the LEU13c sample corresponds to a temperature of 63 °C, considerably below those for other Western Group samples. The sulphate in this sample may be approaching isotopic equilibrium with the water, implying a greater residence time. This would also be consistent with the development of high salinity in this sample.

In summary, the sulphate isotope data indicate that there are several possible sources for the sulphate in waters from the crystalline basement. This conclusion is similar to that of a study of the sulphate isotopes in waters from the Canadian Shield (FRITZ et al. 1994).

#### *Strontium isotope ratios*

The  $^{87}\text{Sr}/^{86}\text{Sr}$  ratios of whole crystalline rock samples from the Böttstein, Leuggern and Kaisten boreholes are between 0.724 and 0.824, significantly higher than those of associated groundwaters, which range from 0.716 to 0.718. This indicates that most of the strontium dissolved in the waters results from the dissolution of Rb-poor minerals such as plagioclase. This is consistent with the interpretation that the chemical evolution of these waters includes considerable plagioclase hydrolysis (section 7.2.2 above).

The  $^{87}\text{Sr}/^{86}\text{Sr}$  ratios of two barite crystals from the Leuggern and Kaisten boreholes match those of the associated groundwaters, confirming their precipitation from these waters. Barite precipitation results principally from the increasing sulphate content of the waters. Plagioclase hydrolysis is probably a source of small amounts of additional barium. The  $^{87}\text{Sr}/^{86}\text{Sr}$  ratios of water from the crystalline basement at Schafisheim were lower than those of any other samples of water from the crystalline basement and resembled that of water from the Buntsandstein. This provides additional confirmation that water from the crystalline basement at Schafisheim has a significant sedimentary origin (PEARSON et al. 1991: section 7.2).

#### *Radioactive Cl and Ar isotopes*

The concentrations of several radioisotopes and stable products of radioactive decay provide additional information on water-rock reactions.  $^{36}\text{Cl}$  (half-life 300 ka) and  $^{39}\text{Ar}$  (half-life 269 a) are useful for dating groundwaters in some environments. However, the levels found in these waters are a result of in situ production in the crystalline rock itself and are not useful for dating. The rate of in situ production of these isotopes depends on the neutron flux. This, in turn, depends on the concentration of actinide elements, which produce neutrons, and of certain trace elements in the rock, which moderate them. The aqueous concentrations of the nuclides depend, in addition, on the rate at which they escape from the rock matrix, where they are produced, to the liquid phase.

$^{39}\text{Ar}$  levels correspond to production rates calculated for the rock, with release to the water of 0.5 to 4 % of the total produced. A few measurements of  $^{37}\text{Ar}$  (half-life 35 d) were available, and led to similar estimates of release fractions, confirming the conclusion that  $^{39}\text{Ar}$  in water from the crystalline basement is produced in situ (PEARSON et al. 1991: section 6.3).

There is a strong linear relationship between the  $^{36}\text{Cl}$  and chloride contents of the waters from the crystalline basement. Further, the  $^{36}\text{Cl}/\text{Cl}$  ratios in waters from the crystalline basement correspond, within the analyzed uncertainties, to those calculated for in situ production in the intervals from which the samples were taken. This is added evidence that the chloride dissolved in these waters results from reactions with the crystalline rock itself. The principle exceptions are the Schafisheim samples (SHA9 and SHA11) which have lower measured than calculated  $^{36}\text{Cl}$  contents. These samples are interpreted as having a strong sedimentary influence (section 7.2.2 above). Their lower  $^{36}\text{Cl}$  contents suggest that they may have migrated into the crystalline basement from their sedimentary source less than ca.  $10^5$  years ago, and that their dissolved chloride has not yet had time to reach equilibrium with the neutron flux in the crystalline rock. (PEARSON et al. 1991: section 6.2).

#### *He concentrations and He isotope ratios*

$^3\text{He}/^4\text{He}$  ratios and  $^4\text{He}$  concentrations were measured. Both isotopes are also formed by in situ production. The  $^3\text{He}/^4\text{He}$  ratios in waters from the crystalline basement correspond to the calculated production ratio in crystalline rock and indicate that the contribution of either atmospheric or mantle-derived He to waters in the crystalline basement is negligible.  $^4\text{He}$  represents  $\alpha$ -particles from decay of actinide elements disseminated through the rock matrix. Because of the long half-life of actinides, the rate of  $^4\text{He}$  production is virtually constant with time, and the concentrations in a groundwater will roughly correspond to residence time. Unfortunately, the volume of rock yielding He to a given volume of water is not known, so no absolute ages can be determined. The fact that  $^4\text{He}$  and Cl increase sympathetically (Fig. 7-5) suggests that increasing Cl concentrations also depend on residence time, and supports the qualitative correlation between salinity and residence time implicit in this discussion.

### **7.3.5 Groundwater residence and travel times**

A number of radioactive isotopes and radioactively produced stable isotopes were measured. Although several of these isotopes are often used in hydrogeological studies to model groundwater ages, this was possible only to a very limited extent in waters from the crystalline basement of Northern Switzerland. As pointed out, the  $^{39}\text{Ar}$  and  $^{36}\text{Cl}$  concentrations correspond to levels produced in situ, and so do not yield water ages. The  $^4\text{He}$  concentration is related to residence time, but cannot be interpreted quantitatively.

The  $^{14}\text{C}$  content of a groundwater depends on the evolution of its carbonate chemistry as well as on its residence time and mixing among waters. With  $^{13}\text{C}$  and carbonate chemical data, the chemical factors affecting  $^{14}\text{C}$  can be corrected and model groundwater ages calculated (PEARSON et al. 1991: section 5.1).

The measured  $^{14}\text{C}$  and  $^{13}\text{C}$  values are compared in Figure 7-12. The two samples with  $^{14}\text{C}$  contents above 20 pmc are from the Black Forest. Both represent young (less than one or two centuries) water, and differ only in the extent of reaction diluting the initial  $^{14}\text{C}$  with  $^{14}\text{C}$ -free aquifer carbonate.

The remaining samples have  $\delta^{13}\text{C}$  values from ca. -8 to -11 per mil, and  $^{14}\text{C}$  contents below 10 pmc. Most samples are below ca. 2 or 3 pmc. Drilling-fluid contamination and difficulties in collecting dissolved carbonate from groundwater for  $^{14}\text{C}$  analyses can introduce a few pmc. Thus, only limiting ages were calculated for samples with low  $^{14}\text{C}$  contents. Samples BÖT17, 18 and 9 have  $^{14}\text{C}$  contents above detection, but they are likely to be contaminated relative to BÖT13, which has a  $^{14}\text{C}$  content below detection. The Siblingen samples also could well be contaminated because of the difficulties of sampling in this borehole, and so limiting ages were calculated for them as well.

The limiting  $^{14}\text{C}$  model ages, combined with inferences about the recharge climate from the  $^2\text{H}$ ,  $^{18}\text{O}$  and noble gas concentrations of the waters, provide water residence time bands.  $^{14}\text{C}$  and  $^3\text{H}$  indicate that the Recharge Group waters from the Black Forest are young. The Eastern Group of waters from the crystalline basement have  $^{14}\text{C}$  model ages of greater than 17 ka, and were recharged under conditions much colder than those of the present. Their age is not likely to be greater than the main phase of the last glaciation, or 70 ka (SCHREINER 1992: Fig. 94). The Western Group waters were recharged under climatic conditions similar to or slightly cooler than the present, but all have model ages greater than 10 ka. The fact that they have one order of magnitude higher  $^4\text{He}$  contents and higher salinities than the Eastern Group waters suggests that they are older, so their age is at least greater than the end of the previous warm period (Early Würm interstadials), which means at least 70 ka. No direct age information is available for the Weiach, Schafisheim, LEU13c and BÖT22c samples, but their high  $^4\text{He}$  contents, salinities and  $^2\text{H}$  and  $^{18}\text{O}$  concentrations indicate that they are considerably older than the other samples from the crystalline basement.

#### **7.4 Hydrochemical and isotopic evidence of cross-formational flow between the pre-Mesozoic basement and overlying sedimentary aquifers**

As part of the Nagra hydrochemical programme, a number of samples were taken for chemical and isotopic analyses from aquifers in sedimentary rocks overlying the pre-Mesozoic basement (i.e. crystalline basement and Permo-Carboniferous) in Northern Switzerland and adjacent regions. Results of this sampling are given by BIEHLER et al. (1993). The chemical and isotopic compositions of these waters were examined for any anomalies that might indicate the presence of water or solutes that had their origin in the crystalline basement or in the Permo-Carboniferous and, by their existence in waters of overlying sedimentary rocks, would provide evidence of upward cross-formational flow.

$^{39}\text{Ar}$  is produced *in situ* in the crystalline rocks and in the Permo-Carboniferous at far higher concentrations than in any of the overlying sedimentary formations. Very high

$^{39}\text{Ar}$  levels are found in waters from the Muschelkalk at Pratteln, in the western part of the Tabular Jura where faulting of the Rhine Graben type (cf. Rhenish faults, Chapter 5) occurs. They are also found in the thermal springs of Baden and Ennetbaden along the main Jura thrust, which corresponds with the southern margin of the Permo-Carboniferous Trough of Northern Switzerland. This is an unequivocal indication of communication between the basement and the Muschelkalk at those locations. However, all these locations are outside the potential siting area for a radioactive waste repository (cf. Chapter 12).

BIEHLER et al. (1993) also point out anomalies in the ratios of dissolved ions in Muschelkalk water that indicate possible cross-formational flow from the basement. Water from Baden and Ennetbaden has chemical as well as  $^{39}\text{Ar}$  anomalies indicating a basement component. The waters at Birmenstorf and Schinznach Bad along the main Jura overthrust also have chemical anomalies suggesting basement components. There are some chemical anomalies in samples from the Muschelkalk at Beznau, Böttstein and Frick that could be caused by an upward component of flow from the basement along the Mandach overthrust, which coincides with the northern border of the deep Permo-Carboniferous Trough of Northern Switzerland. The Frick sample could also be associated with cross-formational flow along faults of the Rhine Graben type in the western Tabular Jura, like the flow influencing the water at Pratteln. However, very low  $^{39}\text{Ar}$  contents in the Böttstein and Beznau samples exclude strong or rapid, direct cross-formational flow at these locations.

There is no hydrochemical or isotopic evidence of cross-formational flow between the basement and the Malm or Tertiary aquifers.

## 7.5 Summary of conclusions

The following conclusions about the origin and history of waters in the crystalline basement can be drawn from their chemical and isotopic composition.

Recharge occurs in the Black Forest where the crystalline basement is at the surface. Flow takes place from the Black Forest through the Siblingen area, where Eastern Group waters are found, and continues through the Zurzach - Böttstein - Leuggern - Kaisten area where Western Group waters occur.

Eastern Group waters were recharged under a colder climate than the present, and so are of the age of the main phase of the last glaciation, namely 10 to 70 ka.

Western Group waters were recharged under conditions similar to the present, but are chemically more evolved and thus older than Eastern Group waters. Western Group waters date at least from the previous warmer period and are a minimum of 70 ka old.

Saline waters are found in the crystalline basement and in overlying or adjacent sedimentary units. The saline waters from isolated intervals of the crystalline basement at Leuggern and at Weiach evolved entirely within the crystalline basement and

represent zones of restricted circulation and great age. Saline waters from the crystalline basement at Säckingen and Schafisheim include components characteristic of waters from sedimentary units. The origin of the saline waters from the deeper part of the Böttstein borehole is ambiguous (evolution entirely within the crystalline basement or admixture of a sedimentary component?).

## **8 HYDROGEOLOGY OF THE CRYSTALLINE BASEMENT**

The most probable scenarios leading to release of radionuclides from a repository all involve groundwater as the active agent for degradation of engineered barriers and transport of radionuclides to the biosphere. Thus, knowledge of the hydrogeology of the crystalline rocks of Northern Switzerland is needed in order to describe the expected groundwater flux, flow paths and travel times for safety analyses. Included in this Chapter are analyses of hydraulic data from Nagra boreholes, a summary of the hydrogeological conceptual model and results of numerical modeling of groundwater flow in the period 1987 - 1993.

The general approach that was taken is illustrated in Figure 8-1. Geological, structural and flow path information presented in the preceding Chapters, as well as hydraulic data from boreholes (this Chapter), were utilized to define hydrogeological conceptual models. These descriptions were used to help design and develop numerical models of groundwater flow at various scales. These models serve as tools to synthesize descriptions of the groundwater flow system, test concepts, improve understanding and define parameter values. The process was an iterative one, in which conceptual and numerical models were periodically modified on the basis of feedback and input obtained from each step along the way; hydrochemical interpretations served as a check on the reasonableness of descriptions of flow that were developed on the basis of hydraulic data.

The general area of hydrogeological interest is bounded to the south by the deep Permo-Carboniferous Trough, to the east by the Randen fault zone and to the west by an extension of the Zeiningen-Wehr fault zone (cf. Appendices 4-1, 5-1 and 5-3); in the north, the area extends to the Black Forest. For this area, regional-scale studies were performed to define regional flow patterns. Two smaller areas were further defined within this region, namely an area West and an area East; in these areas, detailed hydrogeological studies were performed to evaluate hydrogeological conditions that would be expected in the vicinity of a repository. Finally, at the scale of emplacement tunnels, studies were performed to evaluate detailed groundwater flow characteristics in typical blocks of crystalline rock in areas West and East.

### **8.1 Hydraulic data from boreholes**

The principal hydrogeological database includes (1) information about the general geology and structural geology of the region, and (2) hydraulic and hydrogeological data from boreholes. Geological and structural knowledge is derived principally from numerous regional and local geological, tectonic and geophysical studies, from the study of borehole cores and from analyses of borehole geophysical logs. Hydraulic and hydrogeological information is derived almost entirely from testing and monitoring in the Nagra boreholes. Included are results of in-situ hydraulic tests, laboratory analyses of cores, geophysical borehole logs, hydrochemical analyses of water samples and monitoring of hydraulic pressures.

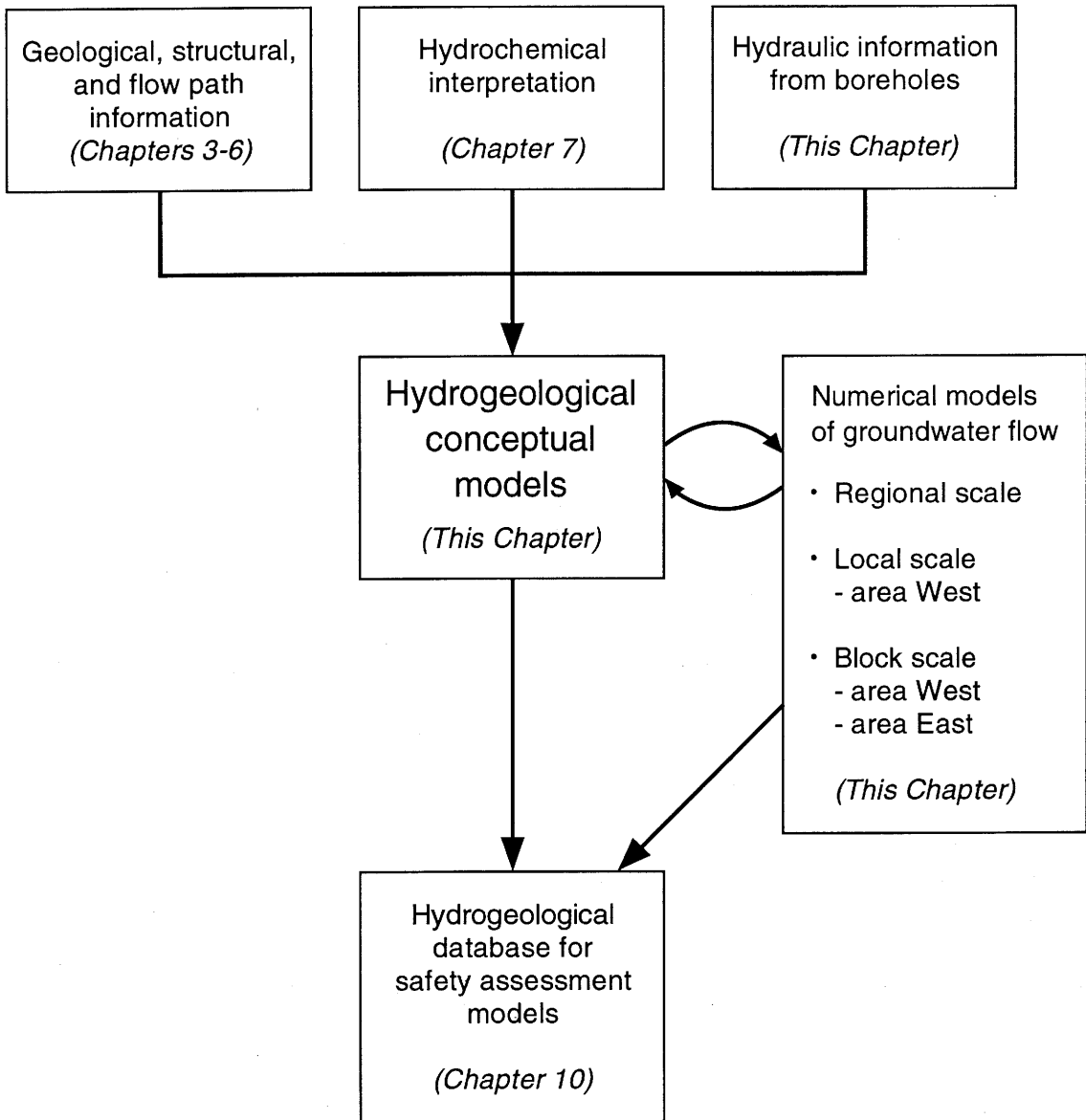


**Fig. 8-1 :** Approach to the evaluation of the hydrogeology of the crystalline basement.

Much of this information is presented in numerous technical reports and is summarized in the preceding Chapters of this report. This section summarizes data on hydraulic properties and hydraulic heads that were obtained from the Nagra boreholes. Further interpretation of the hydraulic property data for the purpose of defining and characterizing components of the hydrogeological framework is given in section 8.2, which describes the hydrogeological conceptual model.

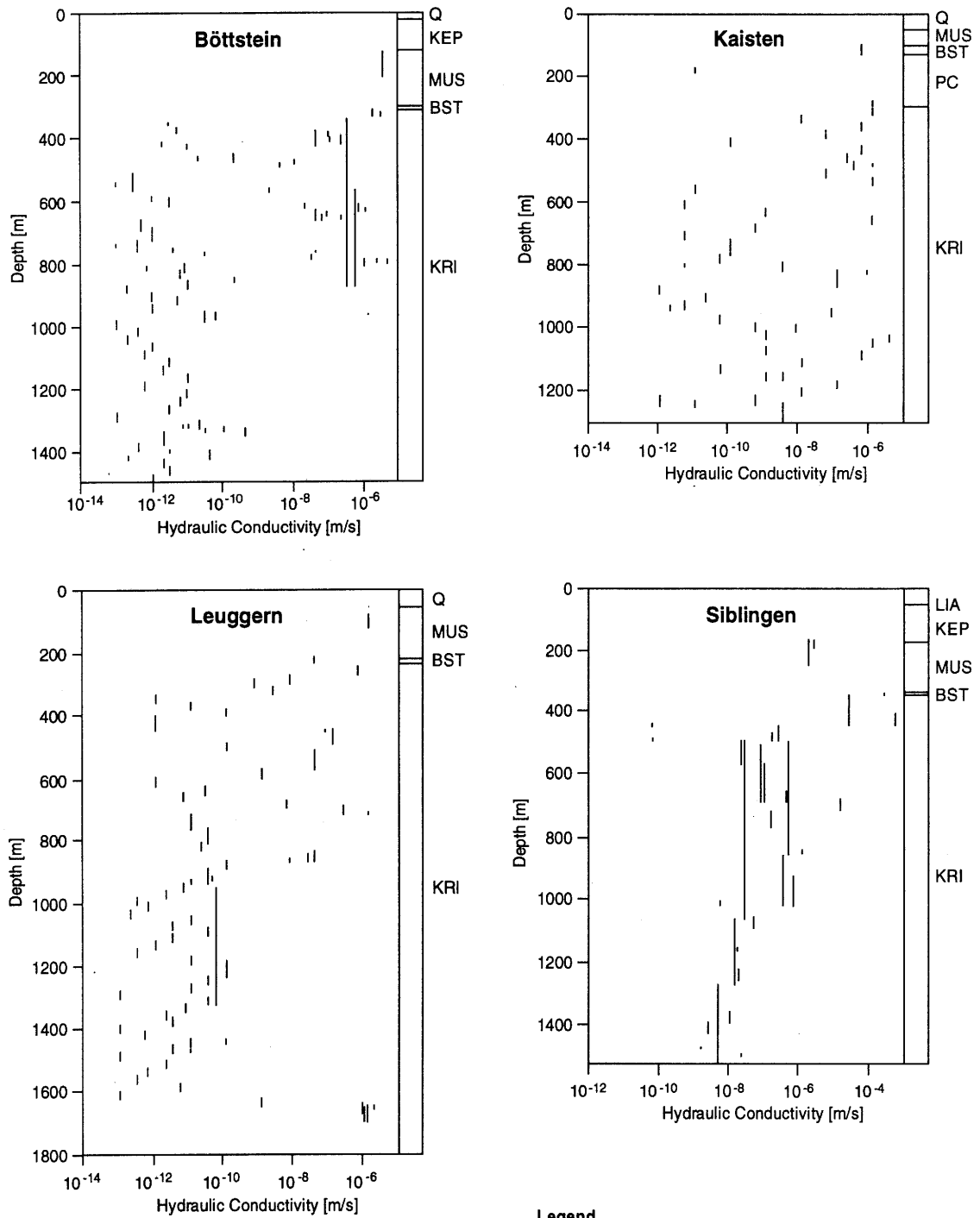
### 8.1.1 Hydraulic properties

*Approach to data analysis* - Nagra's crystalline rock drilling and testing programme is summarized in sections 2.2 and 2.4; the identification and geological characterization of water-conducting features is described in section 6.2.

The principal field testing methods used to obtain hydraulic data are single- and double-packer tests, fluid logging and long-term monitoring of selected intervals. The testing methods, notably the fluid logging technique, evolved during the course of the drilling programme, and the six Nagra boreholes that penetrate the crystalline basement have varying degrees of quality and types of hydraulic data.

The identification of the Permo-Carboniferous Trough - considered to be a major hydraulic barrier to regional-scale groundwater flow (cf. section 8.3) - served to restrict the area of principal hydrogeological interest for characterizing the crystalline rocks to the area north of the Trough. Therefore, hydraulic property analysis focuses on test results from the following four Nagra boreholes in that area (including length of drilled section in crystalline rock): Böttstein (1186 m), Kaisten (1009 m), Leuggern (1466 m) and Siblingen (1173 m). Data from these four boreholes form the basis for defining hydrogeological units and developing the initial conceptual model of the groundwater flow system.

Various simplifying assumptions must be made in order to justify the analysis of field test data to determine formation hydraulic parameters. These assumptions and their justification for the analysis of test data from fractured crystalline rock are discussed by GRISAK et al. (1985). The authors conclude that the assumptions which, in general, relate to the conceptualization of the flow regime in these rocks as being analogous to radial flow in a confined porous medium are appropriate if test intervals are several meters to tens of meters long. Generally, only test intervals within this approximate range are considered in the analysis of data from the boreholes in Northern Switzerland, where the typical interval length was 25 m, except for the Siblingen borehole (and the upper part of Böttstein, where typical interval lengths of 12.5 m were used). The average hydraulic conductivity of the rocks in each tested section was determined from the packer test results. Preliminary results are presented in field reports, and a final report was prepared for each borehole (cf. section 2.2 for references). Conductivity profiles for the six boreholes that penetrate the crystalline basement are shown in Figure 8-2.



**Legend**

Q	Quaternary	KEP	Keuper
MOL	Molasse	MUS	Muschelkalk
MAL	"Malm"	BST	Buntsandstein
DOG	"Dogger"	PC	"Permo-Carboniferous"
LIA	"Lias"	KRI	Crystalline basement

Lithostratigraphic division according to NTB 84-02

**Fig. 8-2 :** Hydraulic conductivity, as determined from packer tests, versus depth below ground surface for the 6 Nagra boreholes that penetrate the crystalline basement (KÜPFER et al. 1989).

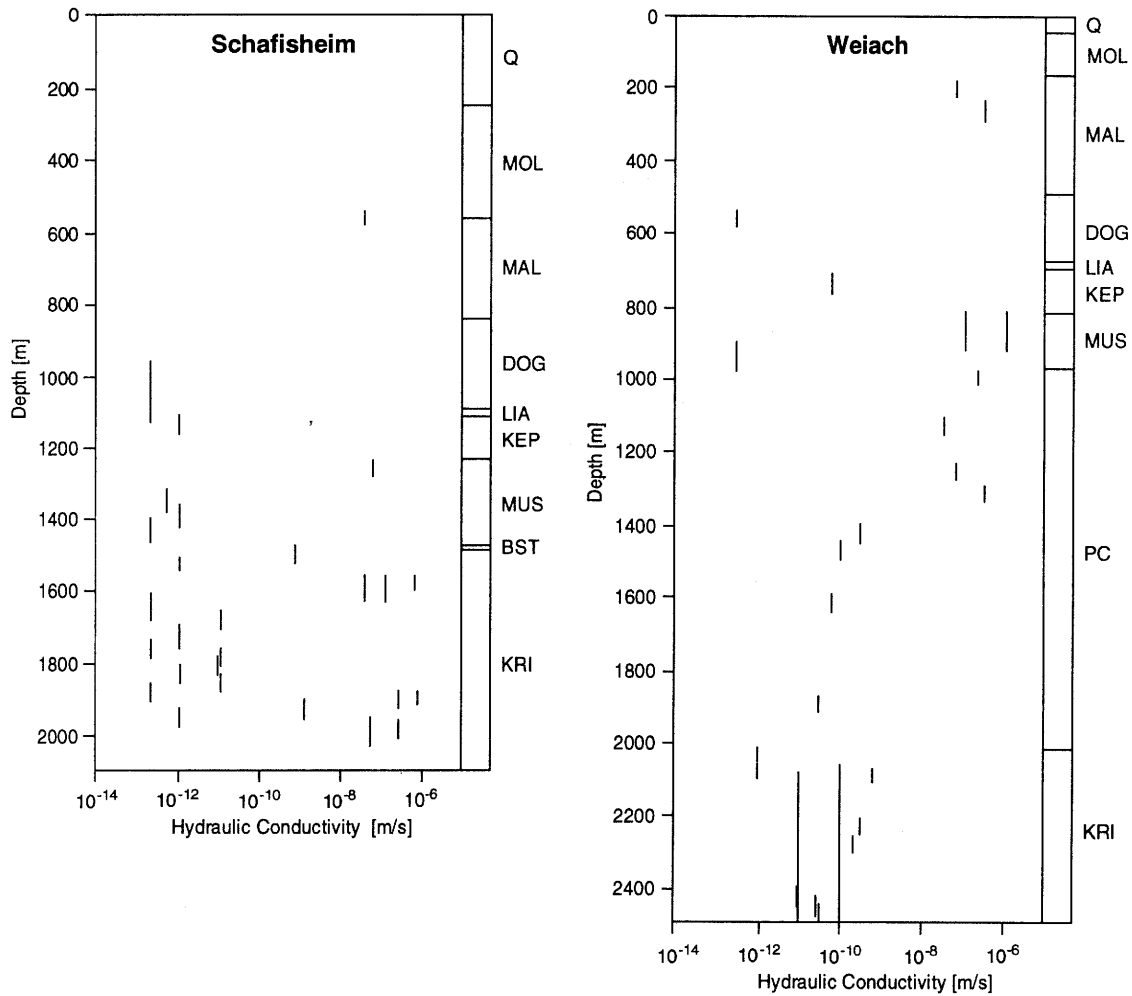


**Fig. 8-2 :** (Continued) Hydraulic conductivity, as determined from packer tests, versus depth below ground surface for the 6 Nagra boreholes that penetrate the crystalline basement (KÜPFER et al. 1989).

The transmissivity<sup>1)</sup> and location of individual inflow points along each borehole were principally determined from fluid logging results. Each inflow point represents the intersection of an individual water-conducting feature with the borehole. The detection limit of these discrete features depends upon the contrast in hydraulic properties between the feature and the background rock. For fractured crystalline rock, the smallest fracture transmissivity that can be detected with fluid logging is generally

1) Transmissivity [ $\text{m}^2/\text{s}$ ] = hydraulic conductivity [ $\text{m}/\text{s}$ ] x thickness [ $\text{m}$ ].

about  $1\text{E-}9\text{ m}^2/\text{s}$ . In borehole sections containing crystalline matrix with very low permeability, fluid logs of very good quality allow a further extension of the lower detection limit to about  $1\text{E-}10\text{ m}^2/\text{s}$  (e.g. Leuggern below 700 m from ground surface). Finally, in borehole sections where relatively permeable intervals (hydraulic conductivity  $K > \text{E-}9\text{ m/s}$ ) were detected from packer testing, but no discrete points were identified in fluid logs (because of poor quality or lack of such logs), the location of water-conducting features was determined from core inspection (cf. section 6.2).

A systematic analysis of packer test and fluid logging data was performed in order to characterize the properties of water-conducting features and of the relatively low-permeability rock matrix. In a first step, the overlapping packer test results (cf. Fig. 8-2) were subjected to a deconvolution procedure (described in BLACK et al. 1987), in order to obtain a continuous conductivity profile. In the next step, the fluid logging results were used to separate the packer test intervals into two groups: one that includes one or more inflow points and one that includes none (designated as "matrix" intervals). The hydraulic characteristics of a discrete inflow point are described by its transmissivity, which is derived directly from fluid logging or from the observed transmissivity of the packer interval. The assumption is that, within a relatively short interval (25 m), the transmissivity of the water-conducting feature dominates the total interval transmissivity; therefore, the contribution of the matrix portion to the flow can be neglected. Packer intervals without inflow points are characterized by the mean hydraulic conductivity of that section.

Final definitions of the inflow point locations used in the hydrogeological synthesis and their hydraulic properties were made by KLEMENZ (1991) and KLEMENZ & GUYONNET (1992). The final set of the water-conducting features thus identified includes almost all inflow points used in Chapter 6 (Tab. 6-1) for the geological characterization of the water-conducting features. A small number, 9, was not included in the final set due to the very low hydraulic conductivity of the borehole intervals as estimated from packer tests. This choice is a conservative one, since it does not shift the transmissivity distribution towards lower values; the set was augmented by a few additional points identified from hydraulic test interpretations. Additional statistical analyses were performed by JAQUET (1991) in an effort to identify a basis for defining hydrogeological units.

*Results* - Hydraulic property data for crystalline rocks penetrated by the four Nagra boreholes north of the Permo-Carboniferous Trough that are within the area of hydrological interest are compiled in VOBORNY et al. (1993a). Included are transmissivity values for 136 hydraulically defined water-conducting features (see comments above) and hydraulic conductivity values for 100 intervals of crystalline rock matrix. These data are plotted in Figure 8-3.

Figure 8-3 shows the relationship between the transmissivity of the hydraulically defined water-conducting features and depth below the top of the crystalline basement for all data points; each data point is identified by the borehole from which it was obtained. The data show that transmissivity of water-conducting features ranges widely, from about  $1\text{E-}10\text{ m}^2/\text{s}$  to about  $1\text{E-}3\text{ m}^2/\text{s}$ , and that, in general, transmissivity

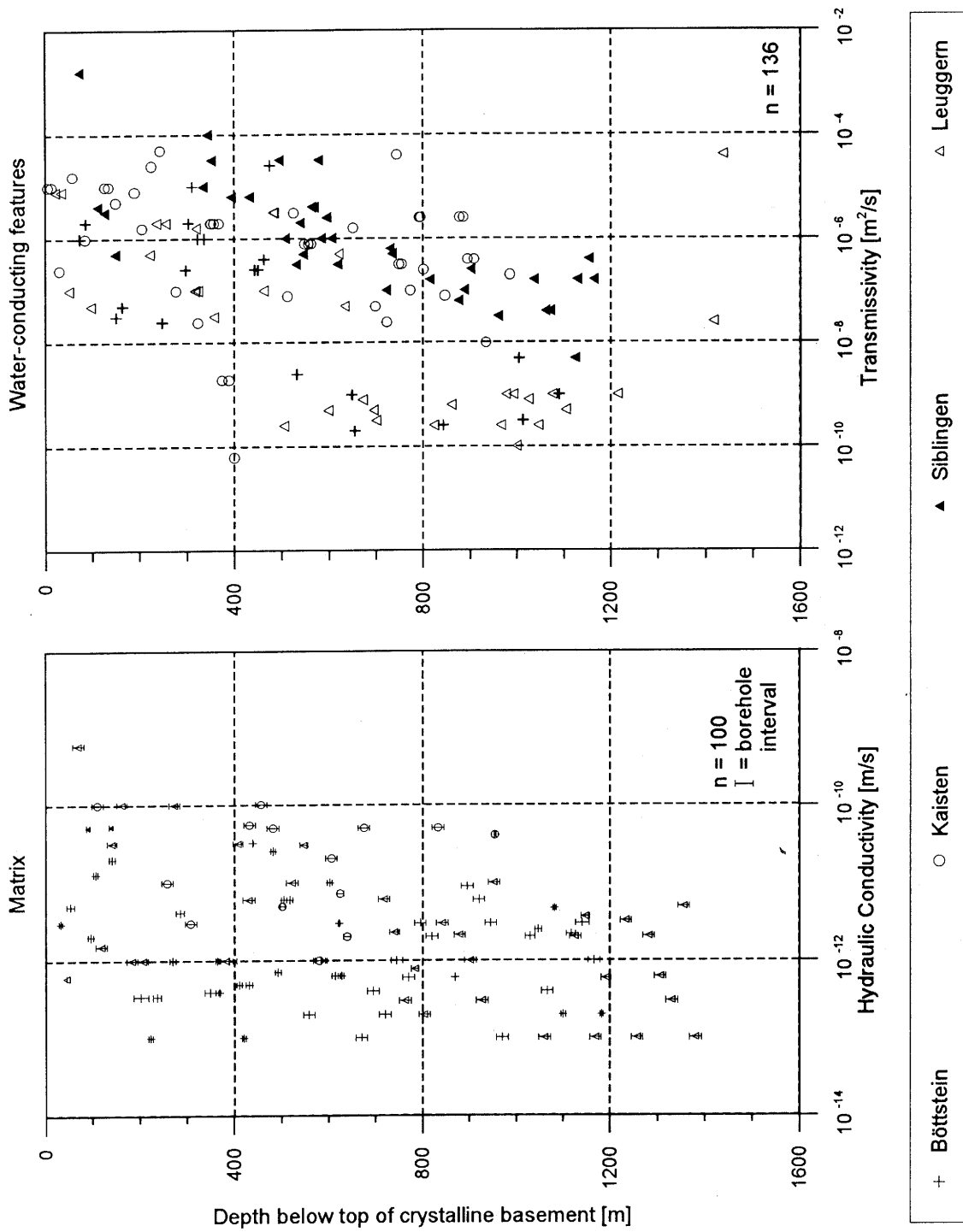


**Fig. 8-3 :** Log transmissivity of the water-conducting features (top) and log hydraulic conductivity of the matrix (bottom) versus depth below the top of the crystalline basement (VOBORNY et al. 1993a).

decreases with depth. Figure 8-3 also shows the relationship between the hydraulic conductivity of the crystalline rock matrix and depth below the top of the crystalline basement. Average hydraulic conductivity of the matrix is about  $2\text{E-}12$  m/s. The data indicate that there is a slight trend of decreasing conductivity with depth.

### 8.1.2 Hydraulic head

Hydraulic pressures or depths to water level have been monitored in the Nagra boreholes since their completion. These data, in combination with other borehole site information, were used by PASQUIER et al. (1993) to calculate a "reference set" of hydraulic heads for various depth intervals of the boreholes. This set is considered to be consistent for all boreholes with respect to the definitions and parameters used in the analysis. Results for the four boreholes that occur in the area of interest (plus Weiach) are summarized in Table 8-1.

Knowledge of hydraulic head distribution aids in estimating hydraulic gradients and in checking the accuracy of numerical models of groundwater flow. Two expressions of head were calculated by PASQUIER et al. (1993): freshwater head and environmental head. Freshwater head is useful in evaluations of horizontal components of hydraulic gradients. In the calculations of freshwater head, the density profile of the fluid in the piezometer was estimated and converted to an equivalent column with a uniform density of  $1000 \text{ kg/m}^3$ , approximately equal to that of freshwater; constant values for gravity ( $9.81 \text{ m}^2/\text{s}$ ) and atmospheric pressure (102 kPa) were applied.

Environmental head most appropriately applies to analyses of vertical flow, because this expression of head accounts for the distribution of fluid density in the geological section ("environment"). In the calculations of environmental head, the fluid in the piezometer was assumed to have the same density distribution as that of the groundwater in the environment; similarly, the estimated gravity profile of the environment was used. Estimates of environmental profiles of density and gravity are based on interpretations of geological units, temperature profiles, Bouguer anomalies, rock densities, mineralization of groundwater and monitoring-line history and conditions.

The accuracy of the values for freshwater and environmental head in Table 8-1 is variable among boreholes and generally decreases with depth. Errors due to instrument uncertainties are estimated to be less than a meter (BELANGER et al. 1990). Added to these are errors resulting principally from uncertainties in estimates of density profiles in the piezometer lines and (for environmental heads) in the geological section. For most crystalline rock intervals, total errors in the estimated head values are less than 5 m. Exceptions are interval Z8 in Böttstein and intervals Z5, Z6 and Z7 in Weiach, where errors are up to 10 m for freshwater head and about 15 - 25 m for environmental head (PASQUIER et al. 1993).

Monitored interval	Depth <sup>1</sup>	Geological unit <sup>2</sup>	Hydraulic head, m a.s.l.	
			Freshwater	Environmental <sup>3</sup>
<b>Böttstein</b> (Ground elevation = 347.5 m a.s.l.)				
Z1	313.0	BST	364.9	363.5
Z2	429.2	KRI	365.3	363.9
Z3	742.5		363.7	363.3
Z4	972.4		364.7	365.1
Z5	1150.9		406.0	406.6
Z6	1329.0		405.2	405.8
Z7	1368.8		406.3	406.9
Z8	1408.5		407.0	407.7
<b>Kaisten</b> (Ground elevation = 320.4 m a.s.l.)				
Z1	103.05	MZ	294.6	294.8
Z2	180.15	PC	298.7	298.2
Z3	549.30	KRI	323.0	322.2
Z4	649.80		343.5	342.9
Z5	743.50		350.3	349.9
Z6	1008.30		349.2	350.0
Z7	1266.70		347.2	350.0
<b>Leuggern</b> (Ground elevation = 358.8 m a.s.l.)				
Z1	708.0	KRI	362.4	362.2
Z2	923.2		361.4	361.8
Z3	1176.7		359.9	361.6
Z4	1472.1		357.0	361.5
Z5	1606.5		355.8	361.9
<b>Siblingen</b> (Ground elevation = 574.4 m a.s.l.)				
Top <sup>4</sup>	489.98	KRI	440.7	440.0
Bottom	1502.50		437.6	439.8
<b>Weiach</b> (Ground elevation = 369.7 m a.s.l.)				
Z1	826.7	MZ	355.6	352.7
Z2	987.5	BST	418.7	416.3
Z3	1116.1	PC	441.1	437.8
Z4	1408.2		441.1	431.6
Z5	2134.7	KRI	402.6	414.4
Z6	2215.0		391.4	405.9
Z7	2350.6		384.9	404.1

<sup>1</sup> Depth of center of monitored interval, in m below land surface; intervals shown in Fig. 2-2

<sup>2</sup> Geological unit that is open to the monitored interval:

BST Buntsandstein aquifer; MZ Sediments of Mesozoic age, younger than BST  
KRI Crystalline rocks; PC Sediments of Permo-Carboniferous age

<sup>3</sup> "Most plausible value"; cf. PASQUIER et al. (1993) for explanation and for max./min. values

<sup>4</sup> No isolated monitored intervals; the long-term monitored data are water level measurements in the open borehole, corresponding to the crystalline rock groundwater pressures below the casing shoe at 490.4 m depth. The values in the table reflect a small downward gradient observed during testing.

**Tab. 8-1:** Hydraulic heads in long-term monitored zones of Nagra boreholes (PASQUIER et al. 1993).

A comparison of the most plausible environmental head values indicates that, within the crystalline rocks, an increase in head occurs with depth in Böttstein and Kaisten, little change with depth exists in Leuggern and Siblingen, and a decrease with depth exists in Weiach (Tab. 8-1). For most monitored intervals, little difference exists between freshwater and environmental heads, although environmental heads generally are slightly greater than freshwater heads in the deeper intervals, because temperature generally increases with depth; the maximum difference between most plausible values of environmental and freshwater heads is about 19 m, in the deepest interval in the Weiach borehole.

The generalized potentiometric surface of the upper part of the crystalline basement is shown in the contour map of Figure 8-4. The map is based principally on head data from the Nagra boreholes and a few other deep boreholes, as well as on topographic information in areas of exposed basement. In these outcrop areas, it is assumed that the groundwater table is controlled primarily by the elevations of river valleys. The potentiometric data from the Nagra boreholes are reasonably reliable, though irregularly spaced; only few additional reliable head data from other boreholes are available in the region. Consequently, the positions of the contour lines are very approximate, and the map is useful principally for showing generalized directions of flow; it was used to develop initial conceptual models of groundwater flow and to derive fixed head conditions for open boundaries of the regional-scale model.

At Zurzach, thermal wells discharge a long-term (about 30 a) average of approximately 10 l/s; the elevation of the free outflow is about 337 m a.s.l., but the radial extent of the corresponding cone of depression and the elevation of the undisturbed pre-pumping level are uncertain.

East of the investigation area, in the region of Lake Constance, a pronounced potentiometric depression was observed within the deep regional aquifer of Upper Muschelkalk (STOBER & VILLINGER 1993). Elevations of heads in the axis of this depression are consistently 300 m a.s.l. or lower, which is below the elevation of the regional discharge into the Rhine River. The depression opens to the north, but its westward extent is unknown. For the base case of the regional model, it was assumed that the heads in the crystalline basement in the eastern part of the region of interest are influenced by this depression. This condition is plausible, because in this area the crystalline rocks are probably in hydraulic communication with the sedimentary aquifer across one or several major faults with large vertical offset (e.g. the Randen fault). To test this concept, various alternative head conditions were considered in the regional-scale model, as described in section 8.4.

## **8.2 Conceptual hydrogeological model**

*Development of the conceptual model* - The conceptual model of the hydrogeology of Northern Switzerland is defined as a comprehensive and internally consistent description of those hydrogeological aspects of the region that are pertinent to the waste disposal issue. Emphasis, therefore, is on the proposed host rock, the crystalline

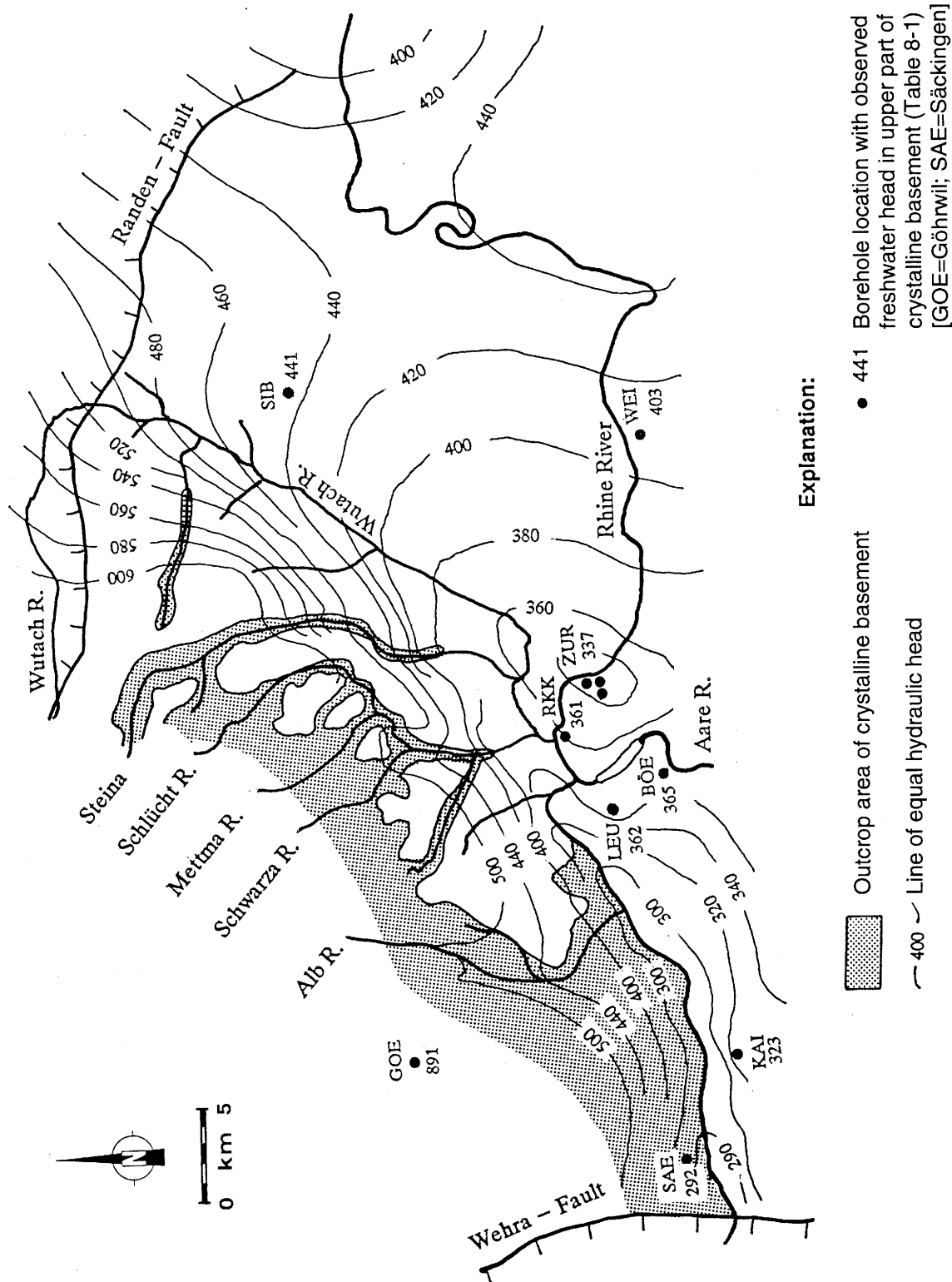


**Fig. 8-4 :** Potentiometric surface in the upper part of the crystalline basement (VOBORNY et al. 1993b); interpretation in the eastern part assumes an influence, through the Randen fault, from the hydraulic heads in the Muschelkalk of the Lake Constance region.

basement. Various geological disciplines, including structural geology, hydrogeology and hydrogeochemistry, contribute to the understanding of the system and to the description. The model incorporates interpretations of regional geology and data from Nagra boreholes, including results of hydraulic tests, hydrochemical analyses of water samples and examinations of cores; it also reflects results from preliminary numerical modeling of groundwater flow, performed for the purpose of discriminating among alternative hypotheses for the conceptual model components (cf. Fig. 8-1, iterative loop).

The conceptual model serves to quantify groundwater flow. Preliminary concepts of the flow system are based on general hydrogeological knowledge, such as distributions of hydraulic heads and locations of groundwater recharge and discharge. Much of the final description of groundwater flow is based on the results of numerical models. In these models, the simulated flow is a consequence of the imposed framework and boundary conditions. An improved understanding of the flow system results principally from the iterative process of simulation of groundwater flow and refinement of concepts.

At any stage of conceptual model development, varying degrees of uncertainty are associated with the level of understanding about particular elements of the hydrogeological system. The degrees of uncertainty can range from virtually none (established facts) to very high (multiple hypotheses). A complete expression of the conceptual model would ideally include the known facts, definitions of currently preferred hypotheses and plausible alternative hypotheses, presentations of supporting and seemingly conflicting data and expressions of the degrees of uncertainty in the interpretations. A conceptual model is expected to evolve with time, as new data are obtained and new understanding is gained. As the model evolves, both the number of alternative interpretations and the levels of their uncertainty are expected to be reduced, until in the final description they reach a level that is satisfactory in terms of the requirements of the investigation.

The description presented in this section is not a complete expression of the conceptual model, but is, rather, a compilation of pertinent facts and currently preferred hypotheses. As a result, the descriptions are mostly expressed as if they were all statements of fact; details concerning the large range of the degree of uncertainty are not discussed in this report. However, assumptions that are made with little or no supporting evidence are so acknowledged. Supporting data and degrees of uncertainty are more fully described in the sections that follow; the technical documents that are cited in these sections should be consulted for background information and more detailed discussion.

*Hydrogeological framework* - Groundwater flow in the crystalline basement is controlled principally by the hydrogeological framework, which is the combination of units and structural features that constitutes the geological medium for transmitting and storing groundwater. At various scales of interest, each of these elements is distinctive and each is homogeneous with respect to the distribution of its hydraulic properties. Thus, the framework is described by the properties and geometric relationships of these elements.

In Northern Switzerland, the hydrogeological framework comprises sedimentary rock components and crystalline rock components. This is illustrated in the sketches of Figure 12-2. The figure is schematic and is intended to illustrate the main elements and their geometric relationships. The upper part of Figure 12-2 approximates a north-south geological section in the area West, but the geometric relationships apply throughout the region. The sedimentary rock components include Quaternary deposits, i.e. glacial deposits and alluvium in the river valleys, Molasse sediments of Tertiary age (in the area East only), sediments of Mesozoic age and sediments of the Permo-Carboniferous Trough and its shoulder. Principal crystalline rock components are major water-conducting faults, blocks of relatively undisturbed rock and small-scale water-conducting features (or transmissive elements) embedded both in major water-conducting faults and in blocks of relatively undisturbed rock. These components are discussed in the following sections.

### 8.2.1 Sedimentary rock components

Sedimentary rock hydrogeological units in contact with the crystalline basement in Northern Switzerland consist principally of the Mesozoic sedimentary cover and sediments of the Permo-Carboniferous Trough. The Mesozoic cover consists of a heterogeneous sedimentary sequence of variable thickness that overlies the crystalline basement in Northern Switzerland. The strata are subhorizontal and relatively undisturbed tectonically. The basal unit is the Buntsandstein aquifer, consisting of red conglomerates, sandstones and mudstones. The average thickness of this layer is about 15 m and the mean hydraulic conductivity is about  $1\text{E-}6$  m/s. Because of its small thickness and large conductivity, this aquifer is treated in numerical flow models as a two-dimensional element characterized by transmissivity. North of the Permo-Carboniferous Trough shoulder, the Buntsandstein aquifer was deposited directly on the weathered crystalline rocks.

The Buntsandstein aquifer is overlain by a very low-permeability sequence of evaporites and argillaceous marine sediments of Triassic age (NAGRA 1988b). These layers act as a hydraulic barrier that confines groundwater in the underlying Buntsandstein/crystalline rock aquifer. Based on hydrochemical evidence (SCHMASSMANN et al. 1992), it is assumed that no significant exchange of groundwater occurs between the crystalline rock flow system and the stratigraphically higher Muschelkalk aquifer north of the Permo-Carboniferous Trough. Therefore, the top of the Buntsandstein layer is treated as a no-flow boundary in numerical models and the overlying Mesozoic sequence is not included in the models.

Sediments that infill the Permo-Carboniferous Trough have variable but generally relatively low permeabilities, with distinct vertical anisotropy. Those deposits that are within the deep part of the Permo-Carboniferous Trough do not contribute significantly to the groundwater flow system in the crystalline basement. Hence, the deep Trough forms a natural flow boundary and the Trough sediments are not explicitly included in the numerical models. The Permian deposits of the Trough shoulder are treated as a single hydrogeological unit.

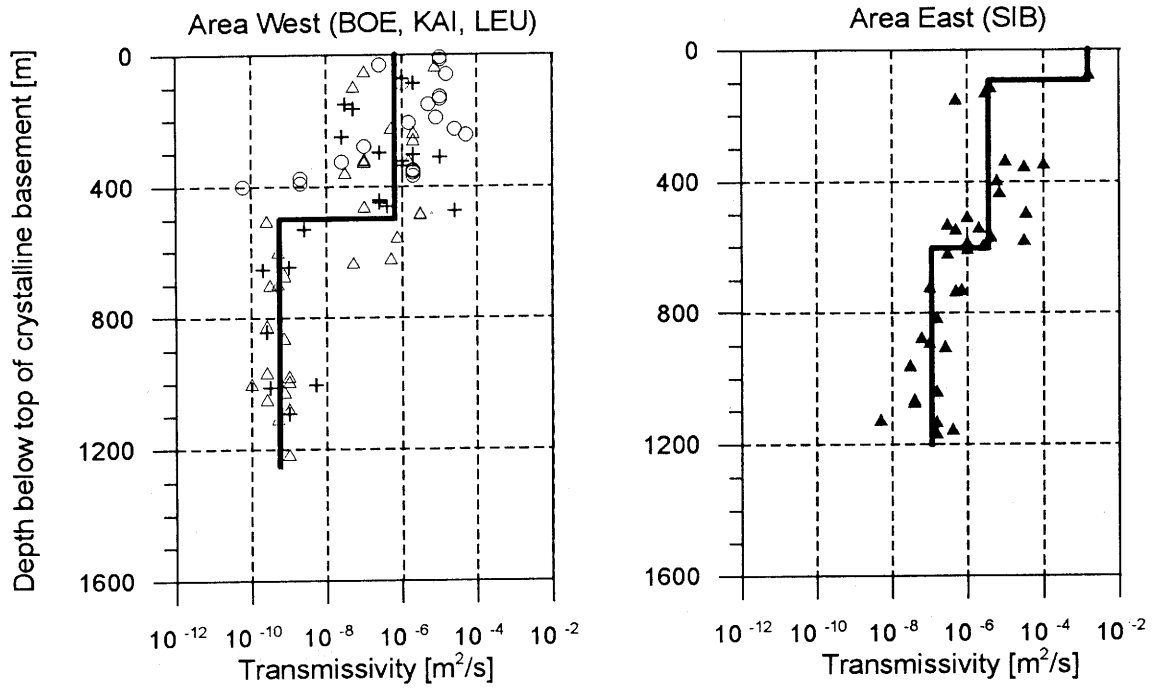
## 8.2.2 Crystalline rock components

*Water-conducting features / Transmissive elements* - Water-conducting features are small-scale mostly planar discontinuities in fractured rocks that control, if they are interconnected, the advective groundwater flow through the rock (Chapter 6; idealized in Fig. 12-2, bottom); they are identified as inflow points when intersected by a borehole. The transmissivity, frequency and interconnectedness of these features define the effective hydraulic conductivity of a volume of crystalline rock (cf. section 8.6). Accordingly, the classification of the crystalline basement into hydrogeological components is based on analysis of the transmissivity distribution (Fig. 8-5) and frequency of water-conducting features, combined with geological and structural knowledge. For the purposes of describing the advective groundwater flow through crystalline basement, no distinction is made among the different types of water-conducting features. This simplification is justified because no correlation was found between the principal types of water-conducting features and their transmissive properties, nor between their occurrence in granite or gneiss and their hydraulic properties (VOBORNY et al. 1993a). For modeling purposes they are designated, therefore, as transmissive elements (TEs).

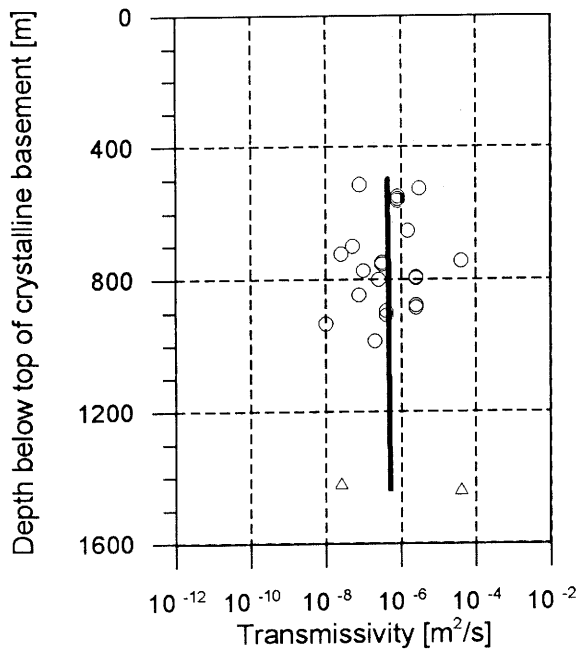
Figure 8-5 shows the depth distribution of the transmissivity of water-conducting features in two geographic areas, West and East, and in major water-conducting faults. The graphs are re-plots of the database shown in Figure 8-3 (top). Also shown are the trend lines that were used to divide the crystalline rock into hydrogeological units in areas West and East. Mean log transmissivity values for each unit are summarized in Table 8-2. These are input parameters for deriving effective hydraulic properties, as discussed below in sections 8.4 to 8.6.

*Major water-conducting faults* - First and second order faults in the region that act as regional-scale conduits for groundwater flow are designated as major water-conducting faults (MWCF; Figs. 8-6 and 12-2). As described in section 5.2.5, first and second order faults are distinguished by their dimensions and amount of displacement. First order faults are major structural elements that dissect the region into tectonic blocks; second order faults are smaller but are also of regional scale. Both are expected to be identifiable features if encountered in surface or underground exploration (cf. Tab. 5-1 and Chapter 11). Like all faults, both types consist principally of cataclastic zones (cf. section 6.3). Both types are also assumed to have similar hydraulic properties, expressed by effective hydraulic conductivity, because the same tectonic processes were responsible for the formation of large-scale faults and small-scale cataclastic zones. The principal hydraulic difference between the two types of major water-conducting faults is the resulting transmissivity, which is greater in first order faults because they are thicker than second order faults. A major tectonically disturbed zone with characteristics similar to the ones of first order major water-conducting faults is also assumed to occur along the northern margin of the deep Permo-Carboniferous Trough (App. 5-2 and Fig. 12-2).

Water-conducting features not within major water-conducting faults



Water-conducting features within major water-conducting faults



EXPLANATION

- ┌ Estimated trend line
- Nagra boreholes:
- + Böttstein
- o Kaisten
- ▲ Siblingen
- Δ Leuggern

Fig. 8-5 : Transmissivity of water-conducting features versus depth below top of crystalline basement (VOBORNY et al. 1993a); the values are classified into three groups based on geographic and structural criteria.

Ore veins are conceptually considered part of this domain, because of their presumed dimensions (length up to a few km; cf. Tab. 5-1 and Fig. 5-7). Although ore veins were not penetrated by the Nagra boreholes in Northern Switzerland, their likely occurrence in this region is inferred from analogy with the Southern Black Forest (section 6.5.2), where they are associated with second order faults.

As indicated in Figure 8-5 and Table 8-2, the mean transmissivity of water-conducting features associated with major water-conducting faults is  $4.1E-6 \text{ m}^2/\text{s}$ . However, the hydraulic characterization of this domain is derived from a very sparse and uncertain database. The only data are the transmissivity values of water-conducting features observed in the lower parts of the sections penetrated by the Kaisten and Leuggern boreholes. Structural and geometric relationships in the vicinity of Kaisten suggest that among the cataclastic zones observed below 830 m, some are parts of the Eggberg fault zone (first order) (AMMANN et al. 1992; section 6.9). The mineralization and abundant vugs/channels observed in the Leuggern cores at 1640 - 1689 m below ground surface (1417 - 1466 m below top of crystalline basement) may represent an early stage in the development of ore vein mineralization (section 6.5.2). No direct field evidence exists of the hydraulic properties of second order faults, although some of the observed water-conducting features probably are associated with second order faults. Due to the one-dimensional aspect of borehole observations, the identified water-conducting features cannot be assigned to a specific fault dimension (section 6.5.4), without additional information (e.g. geophysical surveys).

The occurrence of large transmissivities of water-conducting features at considerable depths in the crystalline basement suggests that at least some permeable faults penetrate deeply into the basement and act as significant conduits for groundwater flow. Simulation results (described in later sections) suggest that not all first and second order faults in the fault models defined in sections 5.3.4 and 5.3.5 are, in fact, major water-conducting faults. It is reasonable to expect that these large tectonic features would have highly variable hydraulic properties. Some probably act principally as barriers to flow, others may have little influence on the flow system, and the effects of a fault on groundwater flow probably vary substantially along a single fault zone, laterally and with depth.

*Crystalline rock domain between major water-conducting faults* - This domain corresponds to the volume of crystalline rock that consists of the crystalline matrix and the numerous small-scale discontinuities that dissect it. It is delimited by major water-conducting faults (first and second order). The discrete discontinuities associated with this domain range in size from microfractures to third order faults (cf. section 5.2) and comprise all three types of water-conducting features.

Since the crystalline rock matrix has a very low hydraulic conductivity (cf. Tab. 8-2), the bulk hydraulic properties of this domain are determined by the transmissivity of the constituent water-conducting features.

		Parameter			
		LogT or logK <sup>1</sup>		T or K <sup>1</sup>	
		Mean	Standard Deviation	Mean	Standard Deviation
<b>A. Water-conducting features<sup>2</sup> (T [m<sup>2</sup>/s])</b>					
Within major water-conducting faults (MCWF)		-6.32	0.9	4.1E-6	1.1E-5
In crystalline basement but not within MWCF					
Area West (BOE, KAI, LEU)	Upper Domain <sup>3</sup>	-6.17	1.1	4.4E-6	8.5E-6
	Lower Domain <sup>4</sup>	-9.24	0.4	9.4E-10	1.1E-9
Area East (SIB)	Upper Domain	-5.42	0.7	1.3E-5	2.3E-5
	Lower Domain	-6.94	0.5	2.0E-7	1.9E-7
<b>B. Matrix<sup>5</sup> (K [m/s])</b>		-11.6	0.9	1.7E-10	6.3E-11

<sup>1</sup> T transmissivity of water-conducting features [m<sup>2</sup>/s]  
K hydraulic conductivity of crystalline rock matrix [m/s];

<sup>2</sup> cf. Fig. 8-5

<sup>3</sup> Designated "higher-permeability domain";

<sup>4</sup> Designated "low-permeability domain";

<sup>5</sup> cf. Fig. 8-3

**Tab. 8-2 :** Hydraulic parameters of crystalline rock components, derived from borehole data (VOBORNY et al. 1993b).

Hydraulic characteristics of the crystalline rock domain between major water-conducting faults differ according to geographic area and depth. Hydrogeological subdivision of the region of Northern Switzerland into an area West and an area East is warranted on the basis of both tectonics and hydraulic properties. According to section 5.3, area West has been subjected mainly to compressive stress deformation with strike-slip faulting, whereas area East is characterized by a tensile regime with predominantly normal faulting. As mentioned above, the hydraulic nature of this domain is controlled by the properties (in particular the transmissivity) of the constituent water-conducting features. Figure 8-5 indicates that a rather abrupt decrease in observed transmissivities of these features occurs consistently at about 400 - 600 m below the

top of the crystalline basement. This change is the basis for subdividing the domain in both area West and East into upper and lower domains. Mean transmissivity values for water-conducting features in the two domains in area West are substantially smaller than for the corresponding units in area East (cf. Tab. 8-2).

In area West, observed transmissivity values of the water-conducting features are similar in the three boreholes that occur in that area (Böttstein, Kaisten and Leuggern). Therefore, these conditions are assumed to be representative of the area West as a whole, and the two units are designated the low-permeability domain (LPD) and the higher-permeability domain (HPD). The mean transmissivity of the water-conducting features in the low-permeability domain is  $9.4\text{E-}10$  m<sup>2</sup>/s (cf. Tab. 8-2). In this area, blocks of the low-permeability domain form near-vertical prisms bounded by major water-conducting faults. A water-conducting feature occurs in a borehole in this domain about every 66 m (VOBORNY et al. 1993b). This average spacing is larger than the one given in section 6.9 (55 m); this difference is because in section 6.9 no differentiation between areas East and West is made and Weiach is also included in the set of inflow points used for the geological characterization of water-conducting features.

The mean transmissivity of water-conducting features in the higher-permeability domain in area West is  $4.4\text{E-}6$  m<sup>2</sup>/s (cf. Tab. 8-2), very similar to the value derived for major water-conducting faults. Thus, in area West, the higher-permeability domain is hydraulically indistinguishable from major water-conducting faults. On average, a water-conducting feature occurs about every 29 m in a vertical borehole in the higher-permeability domain (VOBORNY et al. 1993b). For similar reasons as mentioned above, this number is different from the average spacing of 37 m calculated in section 6.9, where i) Siblingen and Schafisheim are also included in the analysis, and ii) higher-permeability domain and major water-conducting faults are combined in the high-permeability sections used for the estimation of spacing.

The effective hydraulic conductivities of these two domains are further discussed in sections 8.5 and 8.6. Here it suffices to define formally, within the context of the hydrogeological conceptual model of Northern Switzerland, the two domains as follows: i) the low-permeability domain designates the crystalline rock domain that occurs between major water-conducting faults and that has an effective hydraulic conductivity of about  $1.0\text{E-}10$  m/s, and ii) the higher-permeability domain similarly designates crystalline rock with an effective hydraulic conductivity of about  $1.0\text{E-}7$  m/s. In both domains the hydraulic properties are a consequence of the constituent water-conducting features described above.

Hydraulic properties of the crystalline rock domain between major water-conducting faults in area East are based on data from Siblingen. As shown in Table 8-2, at Siblingen the mean transmissivity of water-conducting features in the upper domain is  $1.3\text{E-}5$  m<sup>2</sup>/s; in the lower domain, mean transmissivity is  $2.0\text{E-}7$  m<sup>2</sup>/s. On average, water-conducting features occur in the vertical dimension at Siblingen with about the same frequency as in the upper domain in area West, although a slight decrease in frequency occurs with depth (about every 27 m in the first 500 m and about every 35 m in the lower 550 m; VOBORNY et al. 1993b).

Because Siblingen is the only Nagra borehole in area East, the degree to which the borehole data are representative for the entire eastern part of the region is unknown. Because of this uncertainty, the rocks at Siblingen are designated simply as "upper" and "lower" domain, rather than as higher-permeability and low-permeability domains. Based on geological considerations, one plausible hypothesis is that the data **are** representative, and that in general the rocks in area East are much more transmissive than in area West. Under this hypothesis, the low-permeability domain, such as observed in area West, does not occur extensively in area East at depths down to 1500 m.

An equally plausible alternative hypothesis is that the hydrogeological properties observed at Siblingen **are not** representative. Instead, they indicate a local anomaly, perhaps strongly influenced by the presence of a nearby major water-conducting fault. Under this hypothesis, crystalline rocks in area East have hydraulic properties that are similar to those in area West, that is the low-permeability domain as well as the higher-permeability domain occur extensively.

### 8.3 Approach to the quantification of groundwater flow

The conceptual model described in section 8.2 provides the basis for simulations of groundwater flow at various scales. Figure 8-6 summarizes the basic relationship between the conceptual model and the numerical representations.

Groundwater flow was modeled at three successively finer scales: regional (1000 km<sup>2</sup>), local (50 km<sup>2</sup>) and block (0.25 km<sup>2</sup>). As described below, each model has specific objectives, but the models are all interrelated. At each successively finer scale, additional elements of the hydrogeological framework were explicitly examined for their influence on flow, and each model contributed to the development of the next.

The principal objectives of the regional-scale studies were to define regional flow patterns and to provide the basis for establishing boundary conditions for local-scale models.

At the regional scale, each component of the hydrogeological framework was described as an equivalent porous medium (EPM). In the base case, the crystalline basement was simplified into two units; their hydraulic properties also accounted for the major water-conducting faults not explicitly modeled (cf. section 8.4). Sensitivity analyses were conducted in which boundary conditions and hydraulic properties were varied; in addition, the effect of a few major structural features was also examined with simulations incorporating these features into the model as 3-dimensional elements.

The local model developed for area West (section 8.5) had as its principal objective the evaluation of the hydrogeological conditions that would be expected in the vicinity of a repository. Emphasis was placed on testing the impact of having various patterns of structural features acting as major water-conducting faults. No local scale model was developed for the area East, because the spatial distribution of hydraulic properties in this area is poorly known.

At the local scale, a representation was chosen that explicitly includes numerous large-scale structural features and simultaneously describes the intervening crystalline rock and other units as equivalent porous media; this model was thus termed a "hybrid" model. The structural features correspond to the major water-conducting faults described in the previous section and patterned after the schematic structural model developed in section 5.3. For area West, the intervening crystalline rock, which includes the water-conducting features (section 8.2), is divided into an upper domain with effective properties similar to the higher-permeability domain and a lower domain with effective hydraulic properties similar to the low-permeability domain.

The principal objectives of the block-scale models were to assess the effective hydraulic properties of the low-permeability domain and to provide various geometric and hydraulic characteristics of water-conducting features in the vicinity of emplacement tunnels.

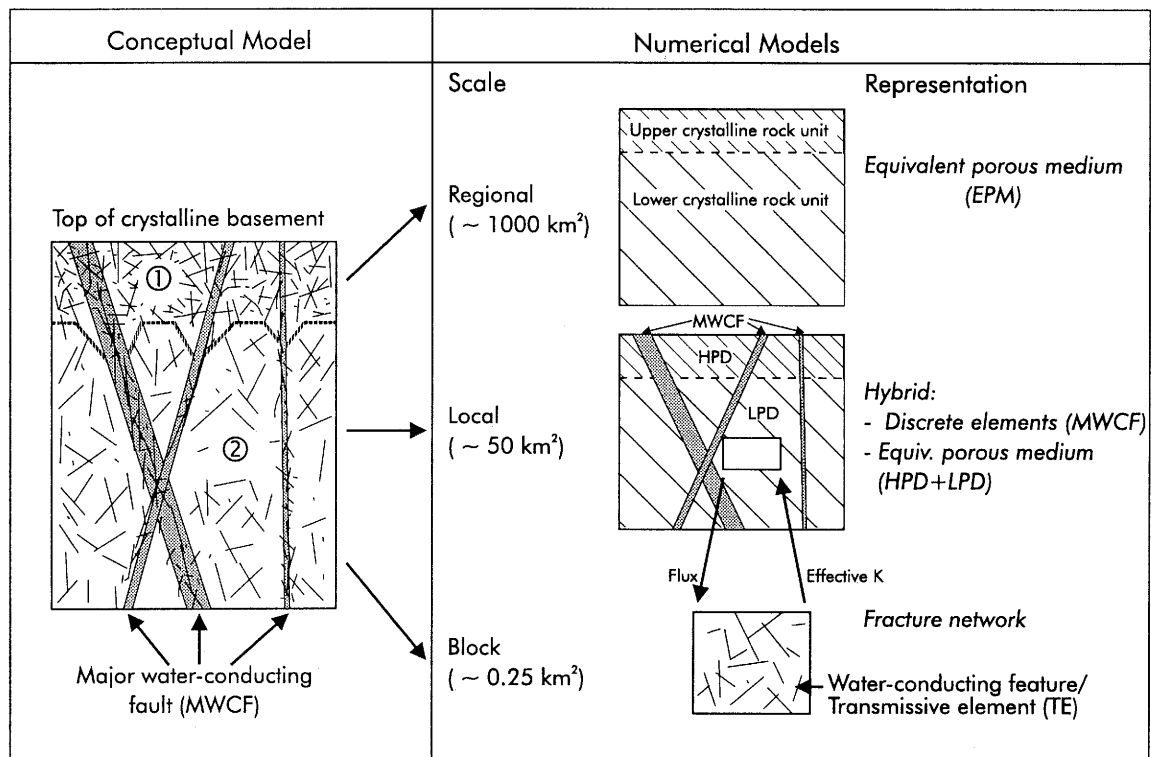
At the block scale, flow near hypothetical emplacement tunnels was studied. At this scale, the water-conducting features are explicitly simulated in networks of fractures that transect typical blocks of crystalline rock in areas West and East. For modeling purposes, no hydraulic or geometric distinction was made among the three types of water-conducting features (section 8.6 and 8.7.2); the term transmissive element (TE) was introduced to describe the numerical representation of any water-conducting feature. Advective flow predominantly takes place in the transmissive elements and the crystalline rock matrix is not explicitly modeled. Discrete fracture networks were generated on the basis of borehole testing results and the occurrence of inflow points in boreholes.

Results from the numerical models at various scales were further combined to provide hydrogeological input for the performance-assessment analysis (Figures 10-2 and 10-6). The methodology developed for this derivation, together with the resulting hydrogeological database, is described in Chapter 10.

## **8.4 Regional groundwater flow system**

An evaluation of the groundwater flow system at a regional scale was made in order to improve understanding of the general flow system and to provide a basis for defining hydraulic boundary conditions for models of flow at smaller scales. Regional-scale modeling of Northern Switzerland was performed in three dimensions using the finite-element code FEM 301 (KIRALY 1985). In the regional-scale model, each hydrogeological unit is described as an equivalent porous medium (EPM).

In the following discussion, sections 8.4.1 to 8.4.3 present the conditions and results of the base-case model run; section 8.4.4 describes sensitivity analyses; section 8.4.5 presents special flux analyses that were conducted to assess origins of groundwater in the area West; section 8.4.6 examines the potential effects of including some major structural features as separate components in the model and section 8.4.7 discusses implications of model results for assessment of groundwater flow in the crystalline



- ① Upper crystalline rock domain; designated as higher-permeability domain (HPD) in area West  
 ② Lower crystalline rock domain; designated as low-permeability domain (LPD) in area West

**Fig. 8-6 :** Conceptual model of the crystalline basement and its representation for numerical modeling of groundwater flow at various scales.

basement. All regional-scale modeling studies are described in greater detail by VOBORNY et al. (1993b).

The regional-scale model covers about  $1300 \text{ km}^2$  in Northern Switzerland and Southern Germany. The southern boundary is approximately the northern margin of the deep Permo-Carboniferous Trough (cf. App. 4-1). The northern boundary transects the Southern Black Forest. The western and eastern boundaries are fault zones, namely a branch of the Zeiningen-Wehr fault zone and the Randen fault zone (App. 5-1 and 5-3). In the vertical dimension, elevations of the model range from  $1000 \text{ m a.s.l.}$  to  $3000 \text{ m b.s.l.}$  Hydraulic descriptions of these boundaries are given in section 8.4.1.

The model area was selected on the basis of the following considerations: 1) model boundaries either coincided with natural flow or no-flow boundaries, or they could be reasonably well defined hydraulically; 2) the area was large enough to incorporate a major part of the regional flow system; 3) the area was small enough to be tractable

with the available computer capabilities; and 4) the scale was such that the hydrogeological units could be appropriately represented as equivalent porous media.

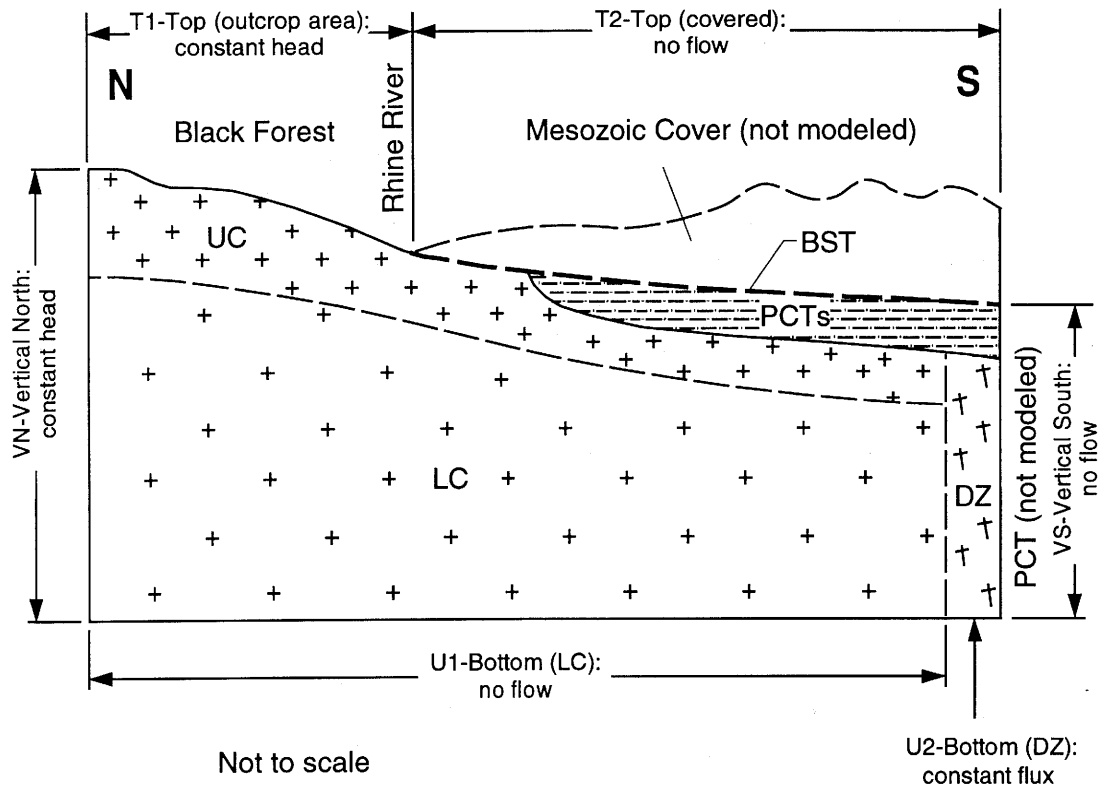
The boundary conditions and hydraulic properties for the regional-scale base case represent the conditions currently considered to be most plausible, on the basis of the iterative development of the conceptual and numerical model. In the sensitivity analyses, a wide range of alternative conditions was considered, in order to test the sensitivity of model results to the full spectrum of plausible hypotheses. Hydraulic boundary conditions, geometric relationships of hydrogeological units and parameter values for the base case are illustrated in the schematic section and explanation of Figure 8-7; the numerical model, including a 3-dimensional view and typical vertical sections in the western and eastern parts, is shown in Figure 8-8 (VOBORNY et al. 1993b).

#### 8.4.1 Hydraulic boundary conditions

*Vertical boundaries* - As shown in Figure 8-7, constant-head boundary conditions are defined along the northern boundary and the upper part of the eastern and western vertical boundaries. The Black Forest is expected to be the principal recharge area for groundwater in the crystalline rocks of Northern Switzerland (Fig. 8-4). The northern model boundary is positioned about 20 km south of the regional groundwater divide in the Black Forest. At that location, flow lines in the deep part of the flow system are assumed to be approximately horizontal; the shallow part consists of local recharge areas (topographic divides) and local discharge areas (rivers). These hydraulic conditions were accommodated in the model by assigning external constant heads to all nodes along the northern boundary. Head values were assigned on the basis of topographic elevations and by assuming a zero vertical gradient over the boundary face.

The western boundary is positioned along a branch of the Zeiningen-Wehr fault and the eastern boundary is positioned along the Randen fault, shown in Appendix 5-3. Constant-head conditions allow free flow across these boundaries. In the west, groundwater discharges through the Zeiningen-Wehr fault into the Rhine River. In the east, recharge into the model occurs across the northern section of the Randen fault; in the south-east corner, a lateral discharge across the fault into the adjacent Muschelkalk aquifer is assumed. For the base case, the elevation of the south-eastern corner is about 400 m.

A no-flow boundary is assigned to the southern model boundary, which corresponds approximately to the northern boundary of the deep Permo-Carboniferous Trough (PCT). This major structural feature generally contains low-permeability sediments with mostly stagnant, highly mineralized groundwater. Some of the saline water that is observed in the crystalline rocks north of the Trough could come from the sediments in the PCT. However, hydrochemical and isotopic evidence suggests that the composition of most groundwater in the basement is a product of chemical evolution of water entirely within the crystalline rock itself (cf. Chapter 7). On the basis of these conditions, the assumption is made that, at the regional scale, no significant lateral



Hydrogeological unit	/ Effective hydraulic property (T=transmissivity; K=hydraulic conductivity)
BST: Buntsandstein aquifer	/ $T=1.5 \times 10^{-5} \text{ m}^2/\text{s}$
UC: Upper crystalline rock unit	/ $K=1.0 \times 10^{-7} \text{ m/s}$
LC: Lower crystalline rock unit	/ $K=1.0 \times 10^{-9} \text{ m/s}$
DZ: Tectonically disturbed zone	/ $K=1.0 \times 10^{-7} \text{ m/s}$
PCT: Permo-Carboniferous Trough	/ Not modeled
PCTs: Permo-Carboniferous Trough (shoulder)	/ $K=1.0 \times 10^{-9} \text{ m/s}$

**Additional boundary conditions (not shown above):**

VW-Vertical West : constant head in UC; no flow in LC  
 VE-Vertical East : constant head in UC; no flow in LC

**Fig. 8-7 :** Boundary conditions and hydraulic properties, regional-scale model, base case (VOBORNY et al. 1993b).

migration of deep groundwater occurs from the PCT into the adjacent crystalline basement. Therefore, a no-flow condition is warranted along the southern boundary of the regional-scale model. This boundary condition was further tested, as described in section 8.4.5.

*Bottom boundary* - Along the model bottom, two hydraulic conditions are assigned (Fig. 8-7). A no-flow boundary is assumed as the general condition, on the basis of the probably very low hydraulic conductivity of the rocks at the depth of 3000 m b.s.l. The major tectonically disturbed zone (DZ), which is assumed to occur along the northern margin of the deep PCT (section 8.2), i.e. along the southern model boundary, is explicitly modeled as a zone of 500 m width. A non-zero flux through the bottom was prescribed in the western part of this zone (from approximately south-east of Zurzach to the western boundary; VOBORNY 1993b), in order to match the value of ascending volumetric flow that has been hypothesized to help explain the occurrence of a geothermal anomaly in the area (RYBACH et al. 1987). The volumetric flow they proposed is equivalent to  $1\text{E-}07 \text{ m}^3/\text{s}$  per linear meter of axial length of the DZ, or a Darcy flux of  $2\text{E-}10 \text{ m/s}$  per unit area. This fixed Darcy flux corresponds to an imposed vertical gradient (upward) of 0.002 in the DZ.

*Top boundary* - Two hydraulic conditions also occur along the model top. Where the Buntsandstein layer representing the model top is overlain by the Mesozoic cover, a no-flow boundary is assigned, due to the very low permeability of the overlying clayey and evaporitic Lower and Middle Muschelkalk deposits. An exception is along the lower section of the Wutach River valley, where the Mesozoic cover beneath the river bed is relatively thin, generally about 40 - 50 m. Although the units have low permeability, they are transected by numerous faults (Fig. 5-10). It is assumed that these faults provide a hydraulic connection between the crystalline rocks and the river (VOBORNY et al. 1993b). Therefore, constant-head values corresponding to river elevations are assigned.

In the outcrop areas of crystalline rocks, such as in the southern part of the Black Forest, prescribed constant heads are assigned as a boundary condition that approximates the position of the groundwater table. The head values approximate the topography, i.e. the river elevations are reproduced exactly, whereas the heads beneath the hills between the valleys are somewhat "smoothed" (VOBORNY et al. 1993b). This model simplification assumes that the groundwater table in crystalline rocks approximately follows the topography.

*Other boundary conditions* - The thermal wells at Zurzach have discharged an average of 10 l/s for several decades. In order to incorporate this condition into the model, a constant-head boundary (337 m) was assigned to the node that represents the well site. This value corresponds to a drawdown of a few tens of meters from estimated undeveloped conditions.

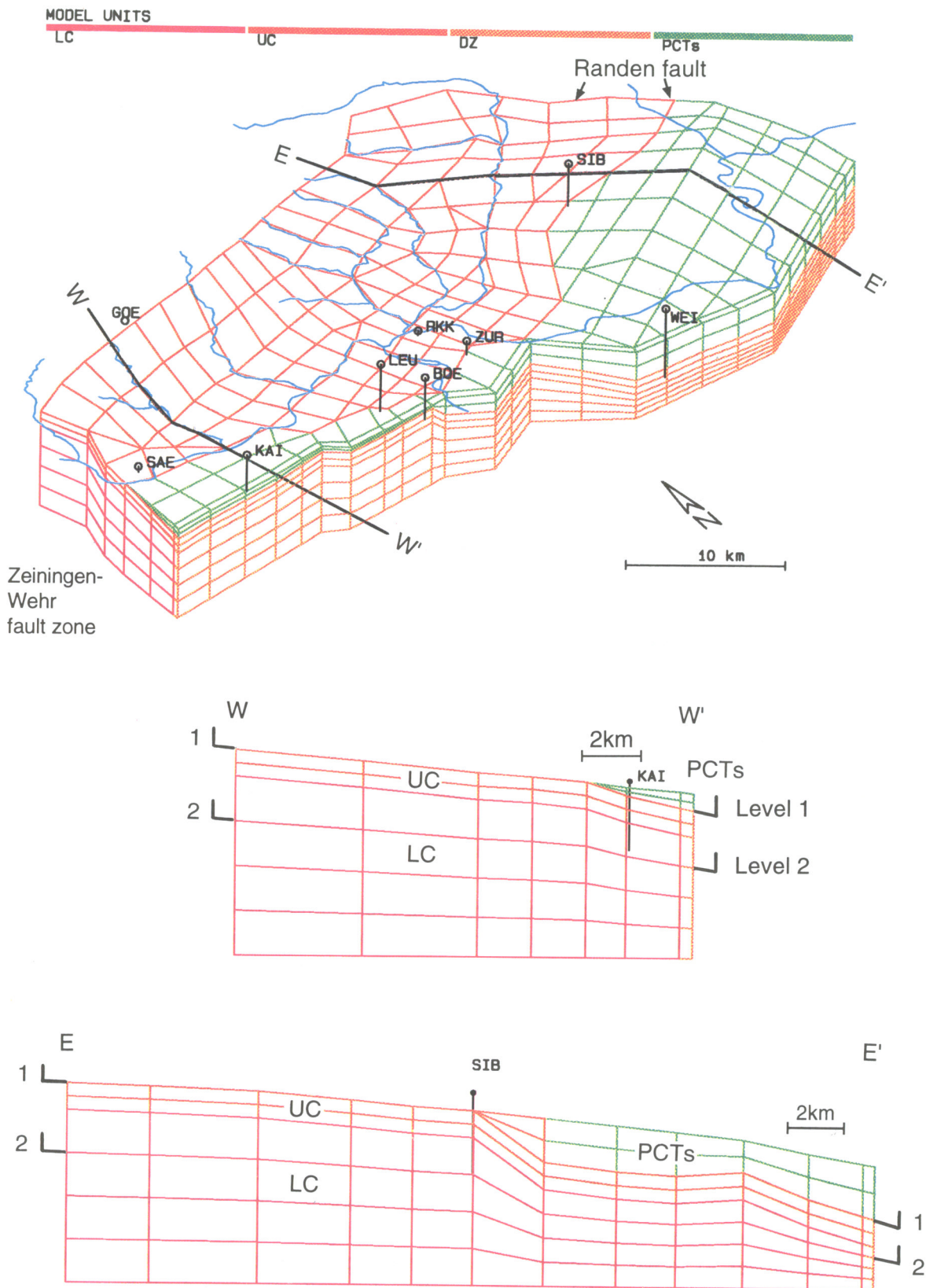


**Fig. 8-8 :** Structure of the regional-scale model, base case (VOBORNY et al. 1993b); vertical scale exaggeration by a factor 2.

### 8.4.2 Hydraulic properties

*Crystalline rock units* - As shown in Figures 8-7 and 8-8, two crystalline rock units are defined for the base case of the regional-scale model, an upper unit (UC) and a lower unit (LC). In order to provide input to the regional-scale model, average values for transmissivity of water-conducting features in area West were used to estimate values of average effective hydraulic conductivity, reported in VOBORNY et al. (1993a). The analysis provided a first estimate of the equivalent conductivities of the crystalline rock domain between major water-conducting faults (separated into upper and lower units), and of major water-conducting faults, based on experimental data obtained from the Böttstein, Kaisten and Leuggern boreholes. However, the regional-scale model approximates the crystalline rocks as a homogeneous equivalent porous medium (EPM); i.e. the crystalline rock domain and major water-conducting faults form a continuum with average properties. Hence, the effective hydraulic conductivity of the modeled EPM units implicitly accounts for the presence of major water-conducting faults in the region.

For the base case, the assumption was made that the Siblingen data **are not** representative. Thus, the low-permeability domain is assumed to occur extensively in the area East, and the area West values for effective conductivity are applied throughout the region as a whole. The regional-scale model was later modified to test the hypothesis that Siblingen data **are** representative, as described in section 8.7.2.

As indicated by Figure 8-5 and Table 8-2, the mean transmissivity of water-conducting features within major water-conducting faults is very similar to the transmissive properties of the features that characterize the upper unit of the crystalline rock domain. Also, the resulting estimate of effective conductivity is similar for both components ( $K_{\text{eff}} = 1\text{E-}7$  m/s). Consequently, no adjustment is required for deriving the effective properties of the upper EPM unit.

In contrast, within the lower unit of the crystalline rock domain between MWCFs, both the mean transmissivity of water-conducting features (Fig. 8-5) and the resulting analytical value for effective conductivity ( $K_{\text{eff}} = 9\text{E-}11$  m/s) are significantly smaller than the corresponding values for major water-conducting faults. Thus, the permeable faults that transect the lower unit probably have a significant impact on its bulk effective properties. Consequently, the effective value given above was scaled up by approximately a factor of 10 to obtain an estimate of the effective conductivity of the lower EPM unit ( $1\text{E-}9$  m/s).

The regional-scale EPM model includes the explicitly modeled tectonically disturbed zone (DZ) alongside the boundary of the Permo-Carboniferous Trough. Although this structure has not been directly observed and investigated, it is assumed to have properties similar to those of major water-conducting faults, because of its tectonic origin. Consequently, this model unit was assigned an effective conductivity equal to that of major faults which, in turn, is equal to that of the upper EPM unit ( $1\text{E-}7$  m/s).

*Sedimentary rock units* - Two sedimentary rock hydrogeological units are included in the model: 1) the shoulder of the Permo-Carboniferous Trough (PCTs), and 2) the Buntsandstein aquifer (BST) (Fig. 8-7). Testing of Permian sedimentary units in the PCTs indicates highly variable hydraulic properties. Figure 8-2 shows estimated hydraulic conductivities of about  $1\text{E-}10$  m/s or lower in the section penetrated by Kaisten and in the lower part of the PCTs in Weiach; locally, some higher values were measured (K of  $1\text{E-}8$  to  $1\text{E-}7$  m/s). However, the PCTs contains substantial amounts of mudstones and siltstones that probably have very low conductivity, particularly in the vertical direction. Therefore, the unit is treated in the model as a low-permeability unit; the assumed effective hydraulic conductivity is  $1\text{E-}9$  m/s.

The Buntsandstein aquifer has an average hydraulic conductivity of about  $1\text{E-}6$  m/s and an average thickness of 15 m, based on observations in Nagra boreholes. Because this unit is highly conductive and very thin, it is treated in the model as a two-dimensional unit with a transmissivity (equal to conductivity times thickness) of  $1.5\text{E-}5$  m<sup>2</sup>/s.

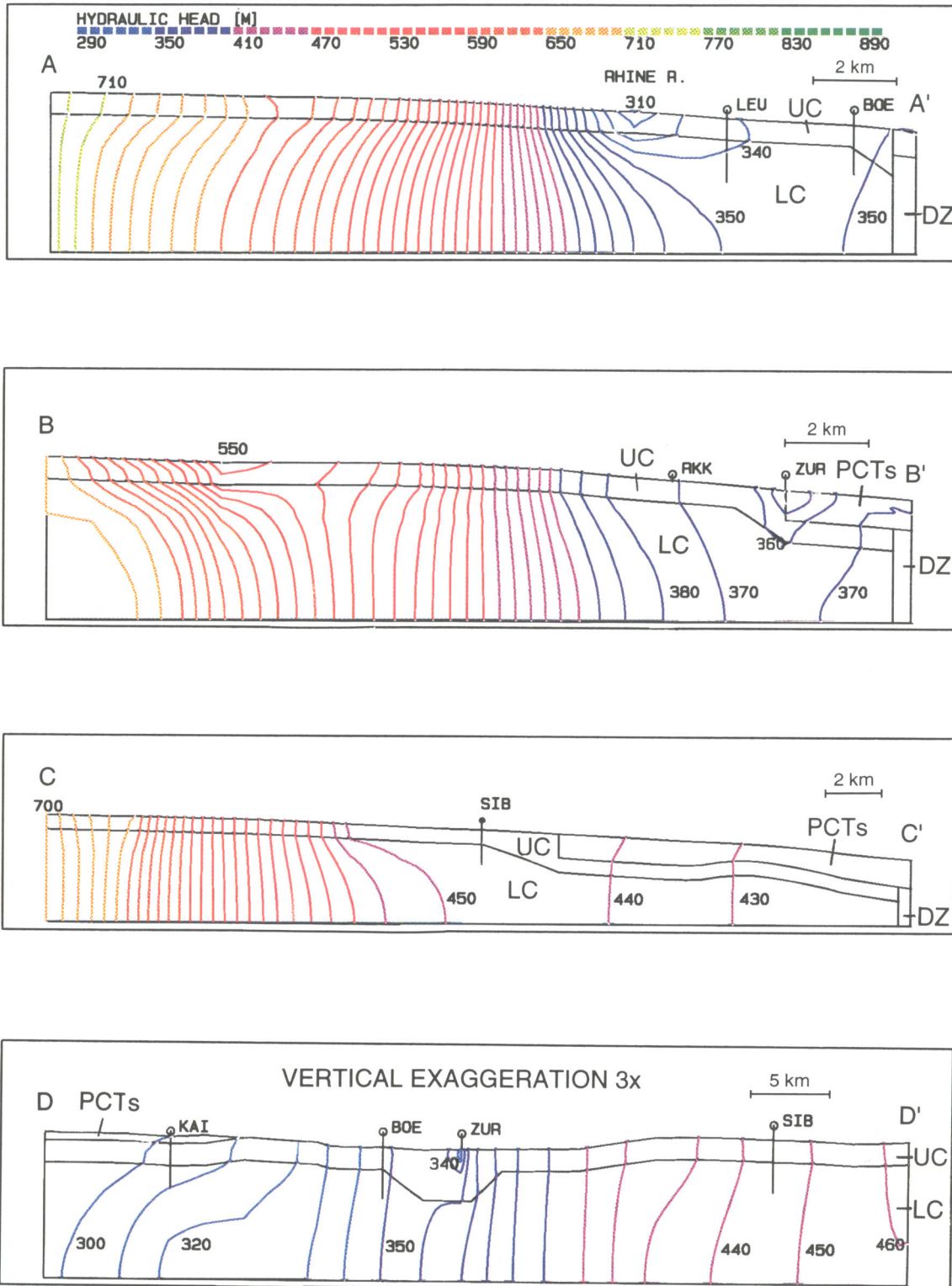
#### **8.4.3 Model results (base case)**

Figure 8-9 shows the areal distribution of simulated head in the upper EPM unit for the base-case condition. General flow patterns can be interpreted from the map. In the Black Forest area, the configuration of the groundwater surface reflects in detail the topography; the tributary river valleys act as discharge areas for local flow systems. Major discharge areas are the Rhine and Wutach Rivers. In the eastern part of the area, a broad groundwater divide occurs, with some groundwater leaving the area towards the south-east and some flowing towards the south-west. Flow parallels the southern no-flow boundary of the Permo-Carboniferous Trough and moves under small gradients towards the Rhine River and across the western boundary.

Head distributions are also illustrated in the vertical sections of Figure 8-10. The sections indicate that generally horizontal gradients are simulated except for the area of the DZ beneath the discharge zone of the Rhine River, and in the vicinity of the drawdown of the open Zurzach wells; in these areas, flow is upwards.

Some measure of the plausibility of the simulations is obtained by comparing simulated and observed heads in specific boreholes, as shown in Table 8-3. For the base case, simulated and observed heads in the EPM crystalline rock units match reasonably well for Siblingen and Weiach, but simulated heads are substantially lower than observed in these units for the three boreholes in the western part of the area. Furthermore, the model is inherently unable to reproduce the upward vertical gradient that is indicated between the two EPM crystalline rock units by the observed heads in Böttstein and Kaisten.





**Fig. 8-10 :** Distribution of simulated hydraulic head in selected vertical sections, regional-scale model, base case (VOBORNY et al. 1993b); section locations shown in Fig. 8-9; contour interval 10 m.

Nagra borehole	Hydro-geological unit <sup>1</sup>	Hydraulic head, [m] a.s.l.		
		Observed <sup>2</sup>	Simulated, regional-scale model <sup>3</sup>	
			Base case (faults are not modeled explicitly)	With faults modeled explicitly
Böttstein	UC	364-365	347	363
	LC	405-407	348-349	364
Kaisten	BST	295	300	301
	PCTs	299	301	302
	UC	323	302	304
	LC	344-350	312	308
Leuggern	UC	361-362	338	351
	LC	356-360	345	358
Siblingen	UC	441	445	452
	LC	438-440	446	453
Weiach	BST	419	412	423
	PCTs	441	412	423
	UC	403	412	423
	LC	385-391	412	423

- <sup>1</sup> Hydrogeological units:  
 BST Buntsandstein aquifer  
 PCTs Permo-Carboniferous Trough shoulder  
 UC Upper crystalline rock unit  
 LC Lower crystalline rock unit

- <sup>2</sup> Freshwater head estimated from observed hydraulic pressures (PASQUIER et al. 1993); cf. also Table 8-1;

- <sup>3</sup> From VOBORNY et al. (1992).

**Tab. 8-3 :** Observed and simulated hydraulic heads in Nagra boreholes.

#### 8.4.4 Sensitivity analyses

Various modifications of parameter values and boundary conditions were made to test the sensitivity of the flow system to the conditions which represent the perceived range of plausible alternative hydrogeological conditions (VOBORNY et al. 1993b).

In separate model runs, the Buntsandstein unit was assigned a hydraulic conductivity tensor horizontal anisotropy to test the effect on the north-west component of the hydraulic gradients in the UC, an additional segment of the PCT was included in the

model geometry to test the effect of a deep PCT in the eastern part of the model, various changes to hydraulic conductivity of EPM crystalline rock units were made, including a gradually decreasing conductivity with depth in the lower EPM unit, and the disturbed zone (DZ) was made inactive or assigned a reduced conductivity.

While maintaining the base case for parameter values, separate runs were made to test each of the following plausible alternative boundary conditions: no-flow conditions at the western or northern boundaries; various constant-head conditions or a no-flow condition at the eastern boundary; no-flow at the Wutach valley; a no-flow boundary at the base of the DZ; replacement of the vertical flux along the DZ by lateral flux from the PCT or by downward leakage from the Mesozoic cover; and no-flow conditions instead of fixed head at the thermal wells at Zurzach.

Results of sensitivity analyses are shown in Table 8-4. The Table summarizes, for various parameter values and boundary and geometric conditions, the changes in simulated head (compared to the base case) that were modeled in the area West (represented by Böttstein, Kaisten, and Leuggern boreholes) and in the area East (Siblingen borehole; including the south-eastern part represented by Weiach borehole).

Table 8-4 shows that the simulated flow system was relatively insensitive to most model modifications, i.e. simulated head changes at the sites of the five boreholes generally were less than 3 m compared to the base case. Some modifications resulted in head changes that actually increased the differential between simulated and observed heads, as compared to the base case. In the south-eastern area, further improvements in the match resulted only when the constant head at the eastern boundary was set at a very low value (Tab. 8-4: B6).

In the area West, the match improved (i.e. simulated heads at the borehole sites increased) when:

- 1) Zurzach wells were closed (B9);
- 2) flux entered from the south (B13);
- 3) a large downward leakage was introduced (B12);
- 4) effective properties of the crystalline rock units were substantially modified (A5);  
and
- 5) the effective conductivity of the DZ was reduced (A7).

In the base case, the simulated long-term steady-state discharge at Zurzach is 3.8 l/s, or one third of the average measured discharge (10 l/s) during the few decades of operation. By increasing the effective conductivity of the upper unit by three times (A4), the simulated discharge (11.2 l/s) more closely matches the observed value.

The observed upward hydraulic gradient in the western part of the region is simulated only when flow is introduced into the lower unit from the south (PCT); in this run, simulated heads in the lower EPM unit increase more than in the upper EPM unit (Tab. 8-4: B13), thereby creating a vertical gradient.

Modified value or condition in model	General effects on heads in crystalline rock units (compared to base case) <sup>1</sup>	
	Area West (BOE, KAI, LEU)	Area East (SIB) and SE (WEI) area
<b>A. Geometry or parameter value</b>		
1. Anisotropy in BST	–	–
2. Inclusion of northern segment of PCT	–	–
3. Depth-dependent decrease in K of LC	UC: – LC: ↓ (KAI, LEU)	–
4. Small increase in K of UC (3x)	UC: – LC: ↓	–
5. Large increase in K of UC, LC, and DZ <sup>2</sup>	↑ (BOE, LEU)	↑ (WEI)
6. Omit DZ; no basal flux <sup>2</sup>	–	↑ (WEI)
7. Reduce K of DZ <sup>2</sup>	↑ (BOE, LEU)	↑ (WEI)
<b>B. Boundary conditions</b>		
1. Close <sup>3</sup> Vertical West (VW)	–	–
2. Close Vertical East (VE)	–	↑ (WEI)
3. Close Vertical North (VN)	–	–
4. High head at VW	–	–
5. High head at VE (500 m)	–	↑
6. Very low head at VE (300 m)	–	↓
7. Close Wutach valley	–	↑
8. Close Wutach and VE	–	↑
9. Zurzach wells off	↑ (BOE, LEU)	↑ (WEI)
10. Close U2 (zero basal flux)	↓	–
11. Small local downward leakage from Mesozoic cover (between BOE and KAI)	–	–
12. Large local downward leakage; increase in K of sediments in PCTs (10x)	↑	–
13. Open <sup>4</sup> Vertical South (VS), no DZ <sup>2</sup>	UC: ↑ (BOE, LEU) LC: ↑	–

<sup>1</sup> – Head change is small (generally less than a few meters), or occurs only near a boundary  
 ↑, ↓ Heads increase (↑) or decrease (↓), generally by 3 - 10 m; maximum is 50 m;

<sup>2</sup> Also, Zurzach wells are closed;

<sup>3</sup> Close, make a no-flow boundary;

<sup>4</sup> Open, allow flux to cross boundary.

**Tab. 8-4 :** Results of sensitivity analyses, regional-scale model (for further explanations of the abbreviations cf. Fig. 8-7).

Although some modifications of model parameters resulted in an improved match between simulated and observed conditions, these modifications generally contradicted hydrogeological reasoning or other (e.g. hydrochemical) observations. Therefore, in the final analysis, such modifications were not applied to the base case, which represents the most likely scenario with the most plausible parameters.

#### 8.4.5 Flux analyses

A special study was conducted with the regional-scale model in order to evaluate the following two plausible assumptions: 1) deep ascending groundwater or basal flux occurs along the disturbed zone at the northern margin of the PCT, and 2) no flow occurs through the PCT itself (VOBORNY et al. 1993b). The mineralization that is observed in crystalline rock groundwater in the upper crystalline domain at the Böttstein and Leuggern boreholes was used as the criterion for the evaluation.

As discussed in Chapter 7, hydrochemical evidence suggests that the composition of most groundwater in the upper and lower units of the crystalline basement is the result of chemical evolution of water entirely within the crystalline rock itself. However, some of the saline groundwater that occurs in isolated zones of the lower unit in the area West (e.g. at Böttstein) could contain a component with chemical characteristics that are similar to those of groundwater from sedimentary formations, e.g. the sediments of the Permo-Carboniferous Trough (section 7.2). This occurrence implies that some saline groundwater could flow from the Trough and mix with the crystalline rock groundwater. Water in the upper unit has been interpreted by SCHMASSMANN et al. (1992) as being principally crystalline rock water that was mostly recharged in the Southern Black Forest but that could contain small amounts of saline water. Based on the chloride content of these water (e.g. Böttstein), a contribution of less than 1 % of saline waters from the PCT can be estimated.

For the purposes of this study, a submodel, or small element box, was incorporated within the regional-scale model in the vicinity of the Böttstein, Leuggern and Kaisten boreholes (Fig. 8-11). Various runs of the model were made, each with different boundary conditions at the PCT boundary and at the base of the DZ. In some runs, an external flux was applied at one or both of these boundaries, which allowed groundwater to enter the flow system from the PCT or from below the base of the DZ; in other runs, no-flow conditions were assigned to these boundaries, which cut off flow from these sources.

For each run, flow paths entering the box were traced back to their origins (VOBORNY et al. 1993b). The fluxes entering the box from various sources were calculated and balanced against fluxes leaving the box, and the proportions of low-mineralized water and saline water were estimated for the water within the box. Water that originated as recharge in the Black Forest and that followed relatively short flow paths to the box was assumed to be low-mineralized groundwater (termed here "Black Forest water"). Potential sources of "saline" water were assumed to be (1) water from the Black Forest that followed relatively long flow paths and was thus chemically evolved; (2) basal flux introduced from below along the DZ and (3) water entering from the PCT, also via the DZ (Fig. 8-11).

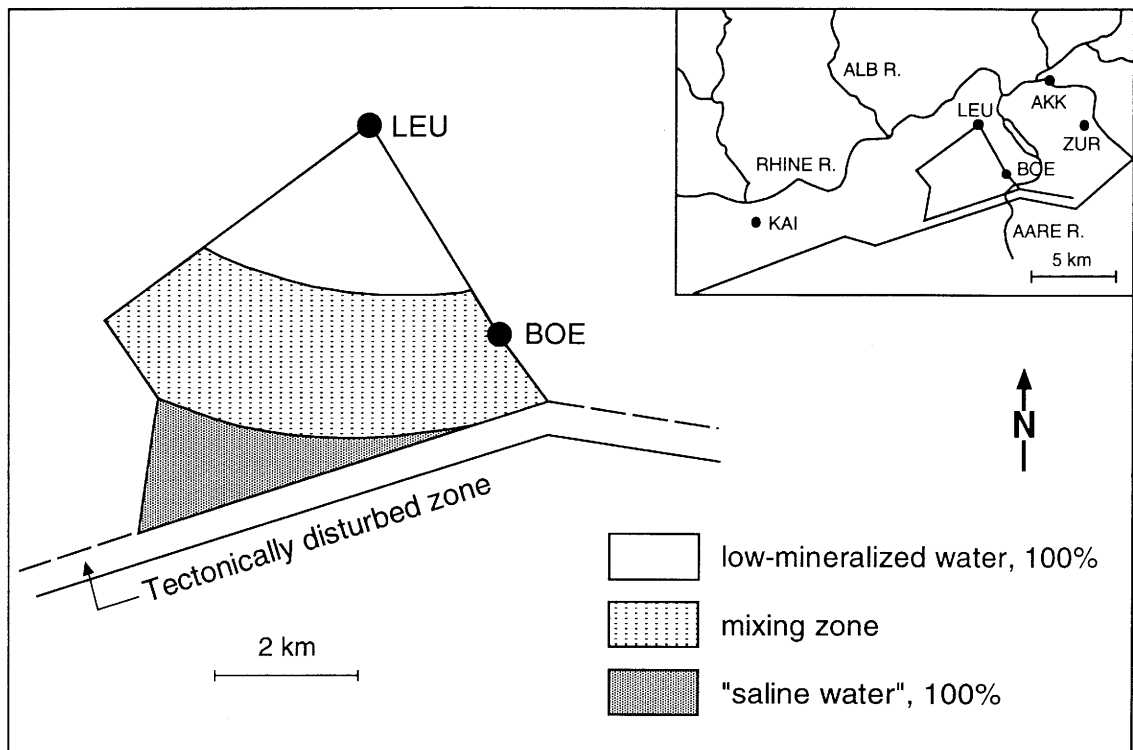


**Fig. 8-11 :** Selected box for the evaluation of rising deep groundwater along the northern boundary of the PCT and the no-flow boundary condition for the PCT (VOBORNY et al. 1993b).

The flux calculations indicate that more than 95 percent of the water entering and leaving the box did so through the upper unit. Thus, the estimates of proportions of saline and low-mineralized water are for water in this unit and do not apply to the lower unit.

Results indicate that, for runs in which external fluxes were imposed as boundary conditions (i.e. basal flux or PCT water), groundwater in the box contains a large percentage (up to 64 %) of "saline" groundwater, derived from the three potential sources mentioned above (VOBORNY et al. 1993b). In these runs, most of the "saline" water in the box occurs in the vicinity of Böttstein. For the same runs, the water in the box near Leuggern is estimated to be entirely Black Forest water (i.e. no saline water from any of the three sources). Figure 8-11 shows schematically the composition of groundwater in the upper unit (as defined above) in the base case. In runs that had no externally imposed fluxes, much smaller proportions (less than 9 %) of "saline" water are simulated in the box, consisting entirely of chemically evolved crystalline rock

water. Hence, only these model results are consistent with the hydrochemical evidence (Fig. 7-3, Western Group waters), which shows that only low-mineralized groundwater has been encountered in the upper crystalline rock unit in the Leuggern and Böttstein boreholes. Thus, the simulation results argue against the existence of basal flux or a lateral inflow from the south. The former conclusion implies that the basal flux estimated in RYBACH et al. (1987) is rather high; the latter justifies the assumption of the deep PCT acting as a no-flow boundary for the investigated region.

#### 8.4.6 Addition of first order faults

The potential effects of major water-conducting faults were examined by explicitly including seven first order faults in the regional-scale model as three-dimensional features with relatively large hydraulic conductivities. Included are representations of the Eggberg and Vorwald faults in the western part of the region, and five faults in the eastern part. Locations and orientations are based on the fault models described in Chapter 5 and are shown in Figure 8-12. The modeled thickness of each fault is 500 m as a mean value derived from the possible range given in Chapter 5.

The hydraulic conductivities of the faults are the same as for the upper unit ( $1\text{E-}7$  m/s). Otherwise, the properties and conditions of the base case are maintained, except that the effective conductivity of the lower unit is reduced by a factor of 5 (to  $2\text{E-}10$  m/s), in order to offset the "removal" of the high-permeability faults from the EPM unit. An additional run was made in which one of the faults (representing the Vorwald fault) is assumed to be a barrier to flow in the upper unit, in order to evaluate such effects on the regional flow field. The conductivity of this fault is reduced to  $1\text{E-}9$  m/s.

Figure 8-12 shows the simulated areal distribution of head in the lower unit (level 2 in Fig. 8-8) when major water-conducting faults are included explicitly. The result is an overall flow anisotropy in the NW-SE direction.

In general, the introduction of permeable faults into the regional model results in a locally enhanced impact of the surface topography on the deep groundwater flow: slightly higher heads occur in the recharge areas and slightly lower ones in the discharge areas, compared to base-case conditions. The presence of a low-permeability fault zone results in a slight increase in heads upstream and near that fault. The impact is more significant for regional flow patterns (VOBORNY et al. 1993b); if all seven faults were continuous and permeable, as is assumed in the sensitivity runs, they would also capture almost all flow originating upstream. This pattern contradicts the large residence times inferred from geochemical analysis (Chapter 7), which implies that not all modeled faults are highly permeable along their whole extent.

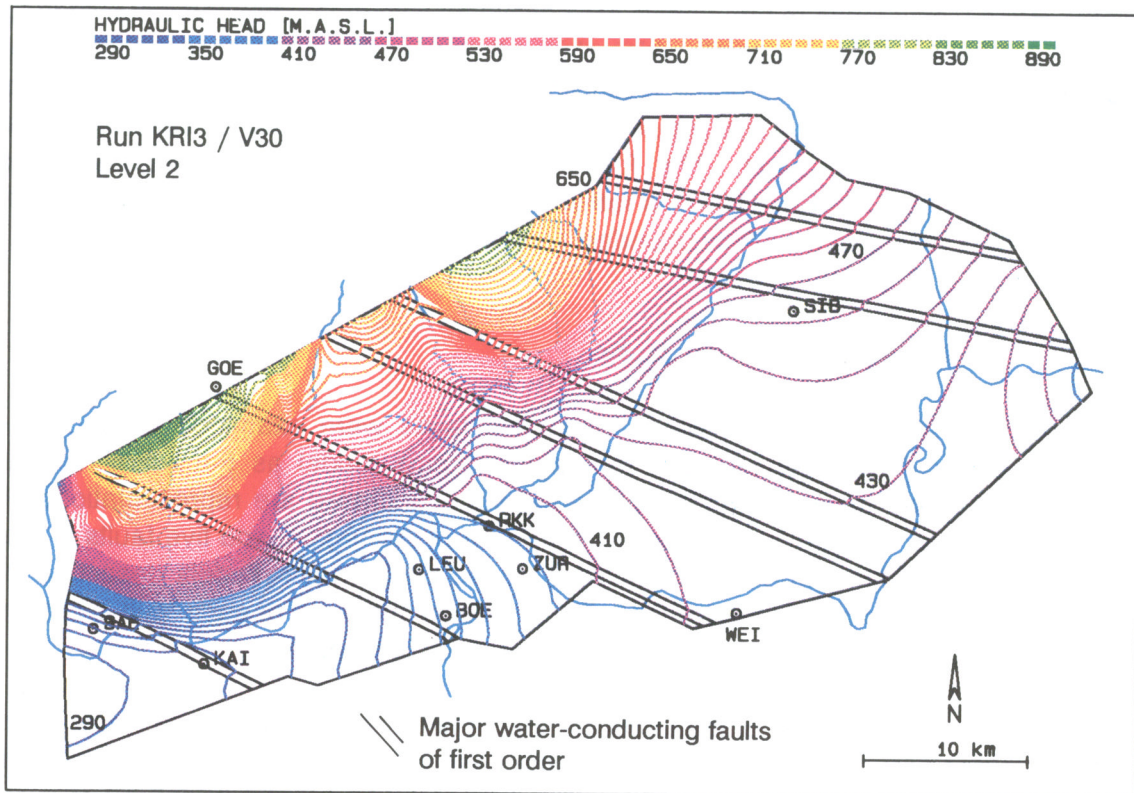


**Fig. 8-12 :** Effect of permeable major water-conducting faults of first order on the regional-scale groundwater flow system (VOBORNY et al. 1993b); simulated hydraulic head in level 2 (Fig. 8-8).

#### 8.4.7 Evaluation of regional flow

Results of the regional-scale EPM model, in combination with hydraulic and hydrogeological observations, provide insights into regional groundwater flow and are considered a satisfactory basis for development of smaller-scale models. Model results are consistent with hydrochemical and hydraulic evidence of regional flow from recharge areas in the Southern Black Forest towards discharge areas along the Rhine River. In general, simulated flow directions, horizontal gradients and fluxes seem reasonable.

Borehole data presented in section 8.1.1 indicate that a decrease in conductivity occurs with depth in the crystalline rocks. In the regional-scale model, this decrease is described as a step change at a uniform depth of 500 m below the top of crystalline rock. An alternative approach, a uniform depth-dependent decrease in conductivity within the lower EPM unit, has little impact on simulated heads. In reality, the upper,

more permeable zone probably varies greatly in thickness throughout the modeled area, and this variability could have a greater impact on flow conditions than the precise manner in which the depth-dependency of conductivity is described.

In the eastern part of the region, simulated and observed heads are best matched by including the Wutach River as a discharge area and by assigning relatively low heads along the eastern boundary. The Wutach River condition is justified by the presence of a faulted, relatively thin Mesozoic cover in the river valley. The assigned low heads at the eastern boundary reflect westward extension of the observed potentiometric depression in the Muschelkalk aquifer in the Lake Constance area. An even lower head (300 m) in the south-eastern corner of the model would further improve model results, but this would entail extending the deep part of the depression much farther west, an unlikely condition (VOBORNY et al. 1993b).

One consequence of these model conditions in the eastern part of the region is the possible occurrence of a groundwater divide. In the base case, the simulated divide is slightly east of the Siblingen borehole (cf. Fig. 8-9). A further reduction of the assigned heads along the eastern boundary results in a westward shift of the divide in the crystalline basement; under these conditions, groundwater flows from the Siblingen site towards the eastern boundary. As discussed above, such a very low value of head along the eastern boundary probably is not realistic; however, data do not exist that would confirm or contradict either the occurrence or the location of such a groundwater divide. Thus, the question of whether groundwater from Siblingen leaves the region to the east is unresolved.

In the western part of the region, the simulated flow system is relatively insensitive to modifications in the model and, therefore, assessment of the reasonableness of the base-case assumptions is difficult. The insensitivity is due in part to the large capacity of the upper unit and the Buntsandstein aquifer to absorb changes. Because of the relatively large conductivity of the upper unit, changes in flux resulting from most model modifications tend to occur principally in this unit, without significant head changes, and hardly affect the lower unit. A reasonable conclusion is that general flow patterns in the lower unit in the area West probably are relatively unaffected by a wide range of plausible hydrogeological conditions, both in the model and in reality. Exceptions would be associated with substantially larger conductivity occurring in the lower unit and with substantial fluxes entering the unit from the DZ.

The insensitivity in the western part of the region is also due in part to the close proximity of several no-flow model boundaries in the area. To some extent, this problem is addressed by the development of a local-scale model that describes the area in greater detail, as discussed in the next section.

Additional uncertainties about the flow system arise because various model modifications that tend to improve the match between simulated and observed heads also tend to simulate flow conditions that are contradicted by hydrochemical observations.

For example, several of the modifications that were made in the sensitivity analyses were designed to increase the flux entering the crystalline rock units in the western part of the region, in an effort to increase the heads and to simulate the general upward vertical gradient that is observed in the area. These efforts were only partly successful, and many resulted in the simulated introduction of saline water in amounts that generally exceed estimates that are based on observations. Thus, the occurrence of a substantial basal flux or lateral inflow from the PCT remains unlikely. The occurrence of widespread downward leakage from the Mesozoic cover into the crystalline units is also unlikely, on the basis of hydrogeological and hydrochemical evidence (cf. e.g. Tab. 8-4).

Some uncertainty also exists about the spatial distribution, magnitude and direction of the vertical gradient in the crystalline rocks in the western part of the region. An upward gradient would be expected directly beneath the Rhine River discharge area, and this condition is simulated by the model. The observed head distributions in the Böttstein and Kaisten boreholes suggest that a large upward gradient may exist elsewhere in the area West. In contrast, the observed heads in Leuggern, which is actually nearer than Böttstein to the discharge area, do not indicate an upward gradient at that site. The model, on the other hand, simulates an upward gradient at Leuggern and Kaisten but not at Böttstein. The marked change in observed head in Böttstein (intervals Z4, Z5, Table 8-1) does not correspond with a change in hydraulic properties, but rather occurs within the low-permeability domain. The conditions at both Böttstein and Leuggern probably reflect, in fact, local conditions that are not representative for the entire modeled area and, hence, can not be reproduced by a regional-scale model.

The open Zurzach boreholes were simulated in the numerical model as a sink with a fixed head, in accordance with the observed conditions at this site. The boreholes have been open for about 30 years, and whether a steady-state condition exists (as assumed in the model) is not known. Furthermore, an EPM model is not a realistic way to represent local conditions (faults) that probably control flow at Zurzach. Closing of the boreholes in the (steady-state) model generally improved model results in the vicinity, and thus in many of the sensitivity runs the boreholes remained closed (cf. footnote 2, Tab. 8-4). This improvement implies that the actual radius of influence of Zurzach discharge is smaller than the radius of influence simulated in the steady-state EPM model.

The explicit inclusion of permeable first order faults in the model introduced some flow anisotropy but did not significantly affect head distribution. This outcome supports the conclusion that the numerical model generally is insensitive to parameter variations. In addition, flow probably is influenced by the full spectrum of sizes, orientations and types of structural features, and the inclusion of a few major faults was insufficient to adequately represent this influence. Particle-tracking studies accompanying the modeling of fault inclusions suggest that the modeled faults are not highly permeable along their full lateral extent (VOBORNY et al. 1993b).

In conclusion, the regional-scale model provides a basis for estimating hydraulic gradients and groundwater fluxes that are required as boundary conditions for smaller-scale models (sect. 8.3). However, the EPM model was neither intended nor expected

to simulate in detail a flow system that probably is controlled by structural features. For this reason, and because of the sparse database, no predictive capability was planned and no formal calibration was conducted. As expected, following regional-scale modeling, numerous uncertainties remained concerning various detailed features of the system. Many of these features were further tested in the smaller-scale models that were subsequently developed, as described in the following section.

## **8.5 Local groundwater flow system - area West**

An evaluation of the groundwater flow system at a local scale - in the order of tens of square kilometers - was conducted in the western part of Northern Switzerland in order to (1) improve understanding of hydrogeological conditions that might be encountered in the development of a repository, and (2) contribute to an analysis of the expected safety of such a repository and its environment. The model approach, input and results are described in greater detail by VOBORNY et al. (1993b) and VOMVORIS et al. (1992).

A "hybrid" modeling approach was utilized to simulate local groundwater flow. In this approach, each of the principal hydrogeological units is treated as an equivalent porous medium, and major water-conducting faults are described explicitly. The general approach is the same as when major water-conducting faults were added to the regional-scale model (section 8.4.6). The principal difference between the two scales of modeling is that the regional-scale model includes only one family of first order faults with uniform geometry, whereas the local-scale model includes multiple sets of first and second order faults with their various dips and orientations explicitly simulated.

In this local-scale model, hydraulic boundaries, fault geometries, unit contacts and the distributions of hydraulic properties are considered to be representative of those that occur in the western part of Northern Switzerland, in the vicinity of the Böttstein, Leuggern and Kaisten boreholes. These features are represented in an idealized manner (cf. Chapter 5) and their positions in the model do not necessarily represent actual locations in the field.

### **8.5.1 Input to the local-scale model**

The evaluation of area West focused on the impacts of four alternative scenarios of occurrences of major water-conducting faults. Multiple scenarios were tested because the frequency of hydraulically active faults within the schematic pattern as defined in section 5.3 is unknown. The scenarios are intended to cover the range of plausible conditions, from one in which all first and second order faults are assumed to be hydraulically active (full scenario), to one in which only a few are (sparse scenario).

Figure 8-13 shows plan views of the hybrid model of area West for the two bounding scenarios. The model covers about 50 km<sup>2</sup>. It is bounded to the north by a river (representing the Rhine River) and to the south by a deep structural trough

(representing the PCT). The base of the model was set at a depth of 2000 m b.s.l. to limit the number of finite elements and because observations from the deepest borehole are available to a depth of approximately -1300 m a.s.l. A shoulder of the PCT extends northwards from the Trough boundary.

All faults are inclined in accordance with the geometric model of Figure 5-7. Not explicitly included is the fifth set of faults, which is a variation of the fourth set with reduced spacing, and it occurs in only part of the area in place of the fourth set (Fig. 5-7 and 5-8). This approach is justified on the basis of the model results (cf. section 8.5.2 and 8.5.3, below), which suggest that an MWCF frequency lower than the one in the full scenario may better represent groundwater flow characteristics observed in area West. The local-scale model was run with the same finite-element code (FEM 301) as was used for the regional-scale model.

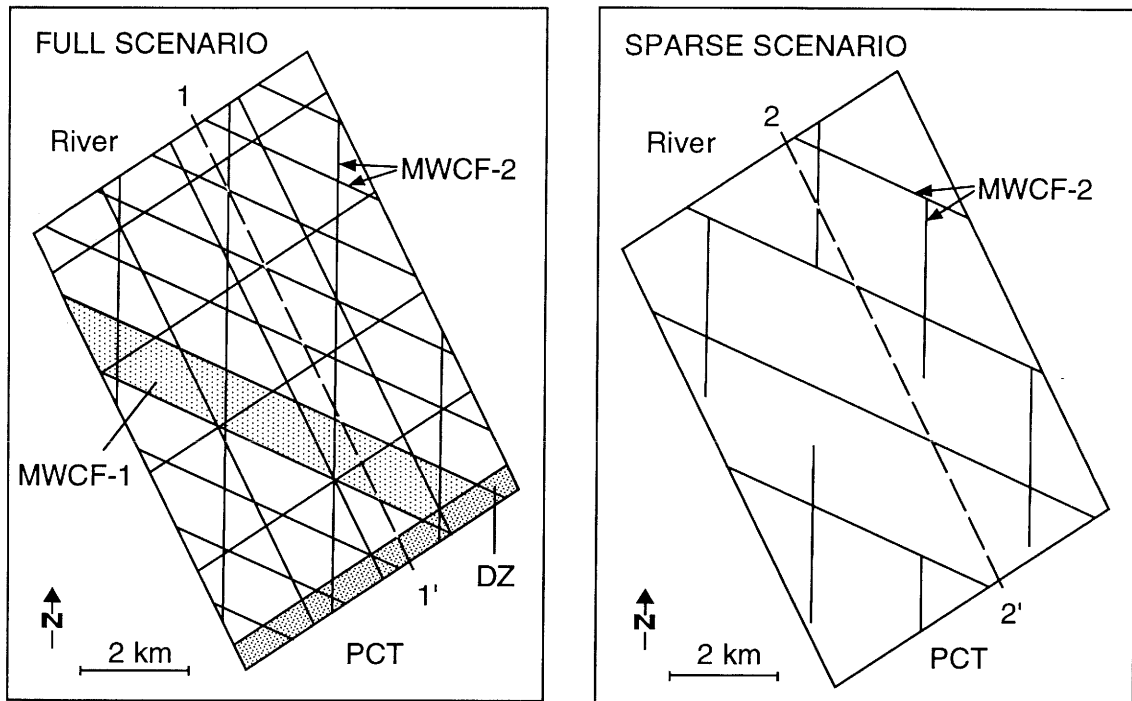
Included as MWCFs in the full scenario (Fig. 8-13, left) are a first order fault (MWCF-1), a tectonically disturbed zone (DZ) (with hydraulic properties equivalent to a first order fault), and four sets of second order faults (MWCF-2). MWCF-1 and the DZ have thicknesses of 1,000 m and 500 m, respectively, and are simulated by 3-dimensional elements, characterized by hydraulic conductivity. Each MWCF-2 is modeled as a 2-dimensional element, characterized by transmissivity.

Figure 8-13 (right) illustrates the geometry of faults for the most restricted case, the sparse scenario. In this scenario, no first order faults and only two sets of second order faults (with reduced frequency) are shown as major water-conducting faults. One of these sets has a double spacing (thereby increasing the size of the intervening blocks), and the other occurs intermittently. The intermittent north-south (Rhenish) faults represent the possible occurrence of permeable ore veins of limited lateral extent.

Boundary conditions, geometric relationships and hydraulic properties for the local-scale model are shown in Figure 8-14. The figure indicates that the units and their geometries are approximately the same as for the regional-scale model, except for the inclusion of both first and second order MWCFs in the local-scale model. Some parameter values are different (for example LPD values), because the values are specific for area West and not the entire region.

Hydraulic properties of major water-conducting faults were assigned on the basis of water-conducting feature values observed in the lower sections penetrated by the Kaisten and Leuggern boreholes (cf. Fig. 8-5). An average thickness of 20 m was assumed in assigning transmissivities to the 2-dimensional second order faults. Ore veins are assumed to occur along segments of second order faults and to have the same conductivity as those faults (cf. Fig. 5-7).

No-flow hydraulic boundary conditions were assigned to the top, south and north boundaries. Constant heads were assigned to the river at the north boundary and to the Buntsandstein aquifer at the south boundary. The remaining boundaries (east, west and bottom) have prescribed fluxes. These fluxes are based on the combination



#### EXPLANATION

- 1-1',2-2' Lines of section shown in Fig. 8-18  
 MWCF-1 First order major water-conducting faults  
 MWCF-2 Second order major water-conducting faults  
 DZ Tectonically disturbed zone  
 PCT Permo-Carboniferous Trough

**Fig. 8-13 :** Local-scale model, area West, level B (Fig. 8-14); summary of main components and definition of the two bounding scenarios - full and sparse (VOBORNY et al. 1993b).

of hydraulic gradients and conductances<sup>1)</sup> at the boundary faces. Regional gradients were assessed from the regional-scale model and from head observations at boreholes and rivers. Vertical gradients across the bottom boundary are assumed to be 0.05 for the low-permeability domain and 0.003 for the major water-conducting faults, in accordance with observed conditions in the Böttstein and Leuggern boreholes, respectively. The assigned gradients were constant in the simulations; however, the imposed volumetric flux across each boundary varied from run to run, according to the varying conductance of the boundary face as function of the fault density. The resulting total inflow into the model (across the eastern and bottom boundary) ranged from 24 l/s for the full scenario to 10 l/s for the sparse scenario (VOBORNY et al. 1993b).

The local-scale models were used directly to evaluate the general distributions of hydraulic head, hydraulic gradient and groundwater flux. In addition, modifications were made to the modeling procedure in order to generate model output that is a suitable basis for safety analysis calculations. This output includes statistical analyses of the distributions of hydraulic gradients and Darcy flux within the low-permeability domain.

### 8.5.2 Model results

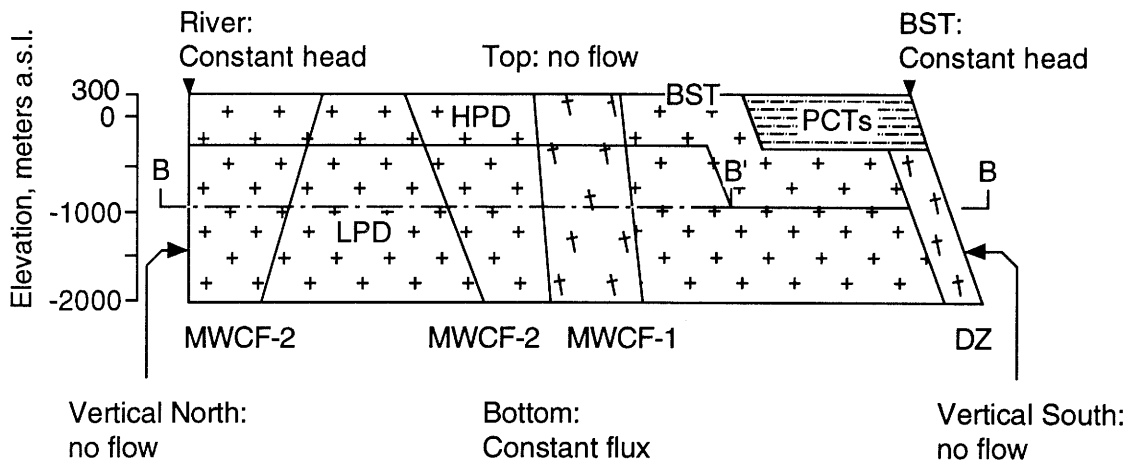
Model results are presented for the full scenario and the sparse scenario; results for the intermediate scenarios differ little from those for the full scenario (VOBORNY et al. 1993b).

*Hydraulic head* - Vertical head profiles were simulated at 16 hypothetical borehole sites in the model. These hypothetical borehole sites were chosen to give a range of conditions likely to be encountered in boreholes in the crystalline rock, namely intersection of a major water-conducting fault or varying degrees of proximity to such a fault. The simulated vertical head profiles for the full and sparse scenarios are compared to profiles observed in the Nagra boreholes. The amount of change in head with depth is compared rather than absolute values for head, because the model does not describe a specific geographic area and, therefore, the positions of faults are not location-specific.

The profiles of simulated head (VOBORNY et al. 1993b) indicate that, in the well-interconnected full scenario, only a small increase in head occurs with depth. The flow through the system is controlled by the relatively small gradients that exist within the interconnected network of permeable faults. In the sparse scenario, with relatively large blocks of intact rock, large vertical gradients are simulated in those boreholes located within these blocks. Boreholes that are at or near the perimeter of blocks or that are intersected by an inclined fault are dominated by small vertical gradients, which are typical for the fault system in the sparse scenario. The introduction of hypothetical

---

1) Conductance [ $\text{m}^3/\text{s}$ ] is equivalent to the hydraulic conductivity times the area (for EPM), or transmissivity times length in case of 2-D elements; conductance multiplied by a gradient gives the total flux through a given area (for an EPM) or a 2-D element of a given length.



**Hydrogeological unit**

- BST: Buntsandstein aquifer
- PCTs: Permo-Carboniferous Trough (shoulder)
- HPD: Higher-permeability domain
- LPD: Low-permeability domain
- DZ: Tectonically disturbed zone (=MWCF-1)

**/ Effective hydraulic property**  
(T=transmissivity; K=hydraulic conductivity)

- /  $T=1.5 \times 10^{-5} \text{m}^2/\text{s}$
- /  $K=1.0 \times 10^{-9} \text{m/s}$
- /  $K=2.8 \times 10^{-7} \text{m/s}$
- /  $K=4.2 \times 10^{-11} \text{m/s}$
- /  $K=3.2 \times 10^{-5} \text{m/s}$

**Major water-conducting faults**

- MWCF-1: First-order /  $K=3.2 \times 10^{-7} \text{m/s}$
- MWCF-2: Second-order /  $T=6.4 \times 10^{-6} \text{m}^2/\text{s}$

**Additional boundary conditions** (not shown above):

- VW-Vertical West : Constant flux
- VE-Vertical East : Constant flux

**Fig. 8-14 :** Simplified section showing boundary conditions, geometric relationships and hydraulic properties, local-scale model, area West (VOBORNY et al. 1993b).

boreholes into the model helps to illustrate the impact of permeable faults on vertical head distribution. Based on the better match of the sparse scenario head profiles with the observations, it is concluded that not all of the major faults that are proposed by the structural model (and simulated in the full scenario) are water-conducting (VOBORNY et al. 1993b).

*Hydraulic gradient* - The distributions of simulated gradients are shown in the histograms of Figure 8-15. Results are given for the horizontal and vertical components and the absolute value, for the full scenario (left) and the sparse scenario (right). The histograms reflect the gradient distribution at all nodes in LPD located along a single horizontal plane at the depth of a hypothetical repository (500 m below the top of the low-permeability domain; cf. level B-B' in Fig. 8-14). To eliminate boundary effects in the analysis, nodes near the lateral model boundaries are excluded. The histograms indicate that the gradients generally are larger for the sparse scenario than for the full scenario, because of differences in the hydraulic interconnectedness of the two systems.

*Groundwater flux* - The distribution of the horizontal component of simulated groundwater flux in the modeled area is shown in Figure 8-16 for the 500 m-level (level B-B' in Fig. 8-14). In the full scenario, the horizontal component of flux is in the general direction of the regional hydraulic gradient, principally from south-east to north-west. Fluxes in the first order faults are substantially larger than fluxes in the blocks of low-permeability domain.

In the sparse scenario, the horizontal component of flux generally is radial from the centers of the large blocks of low-permeability domain and toward the adjacent faults. In places, the horizontal flow direction is counter to the regional flow regime.

The distribution of the vertical component (upward) of simulated groundwater flux is shown by the contours of Figure 8-17, also at the 500-m level B-B' (Fig. 8-14). In the full scenario, the vertical component of flux in the LPD is relatively small (i.e. maximum  $q_z$  is about  $6E-13$  m/s). In the sparse scenario, the vertical component in the LPD is larger (i.e. maximum  $q_z$  is about  $2E-12$  m/s). In both scenarios, the vertical component of flux generally is larger within the centers of the blocks of low-permeability domain than it is near the margins of the blocks. The vertical component of the flux in the MWCF-1 (only full scenario) is nearly constant (about  $1E-9$  m/s).

The combined effects of the vertical and horizontal components of simulated flux are indicated by the projections of the vectors in the sections of Figure 8-18. The representation is quasi - 3-dimensional; the color of the vectors corresponds to the absolute value, whereas the length corresponds to the projected value. In both scenarios, flow is predominantly horizontal in the higher-permeability domain. In the full scenario (Fig. 8-18, top), vertical flow is simulated only beneath the discharge area and, as a boundary effect, near the bottom of the model. In most of the low-permeability domain, flow is uniformly towards the north-west, reflecting the regional trend in this area. Fluxes in the first order faults are several orders of magnitude larger than those in the low-permeability domain between the faults.

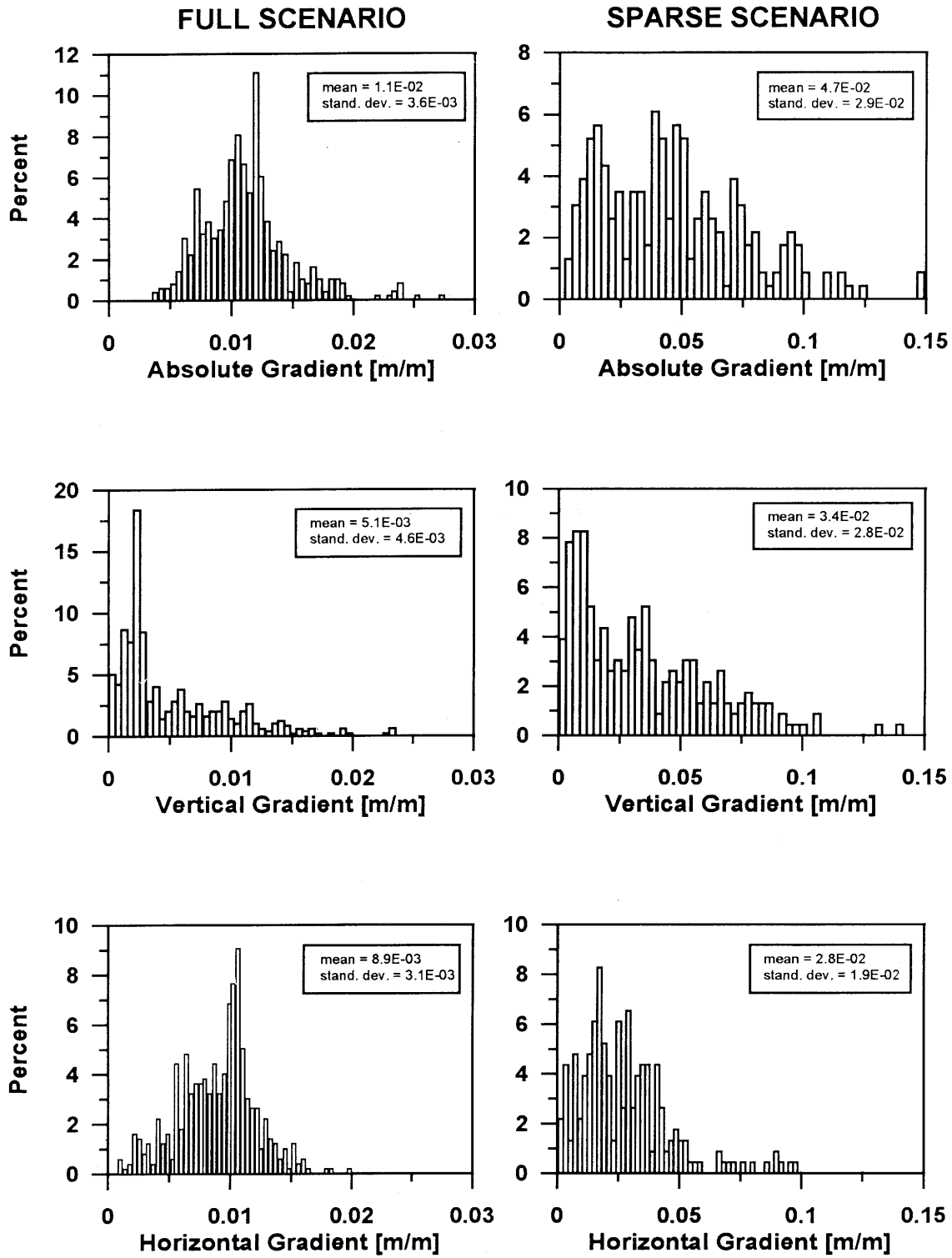
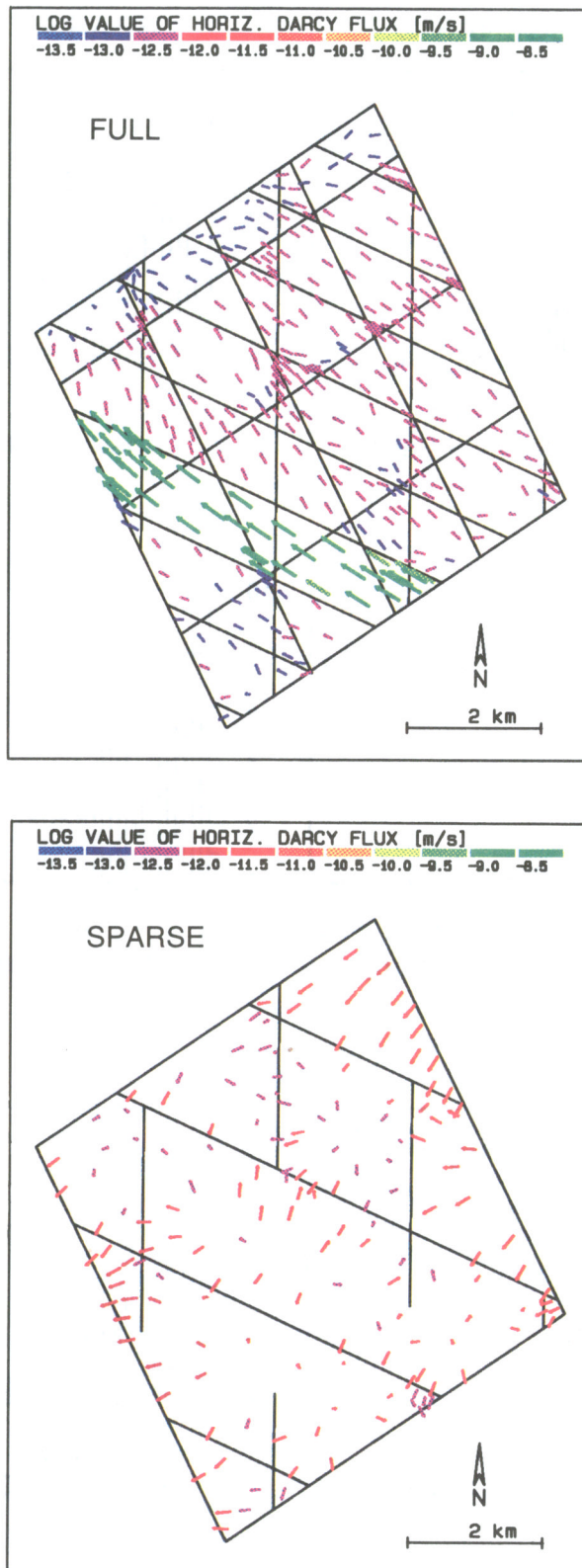
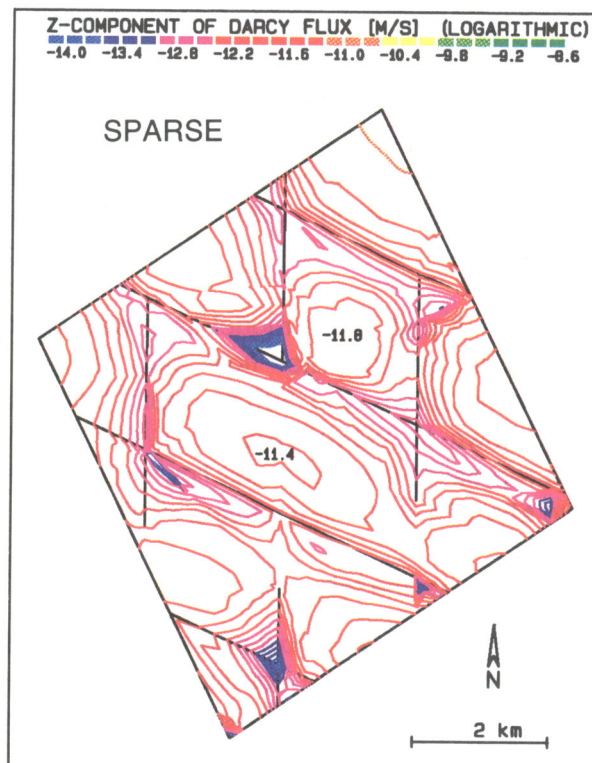
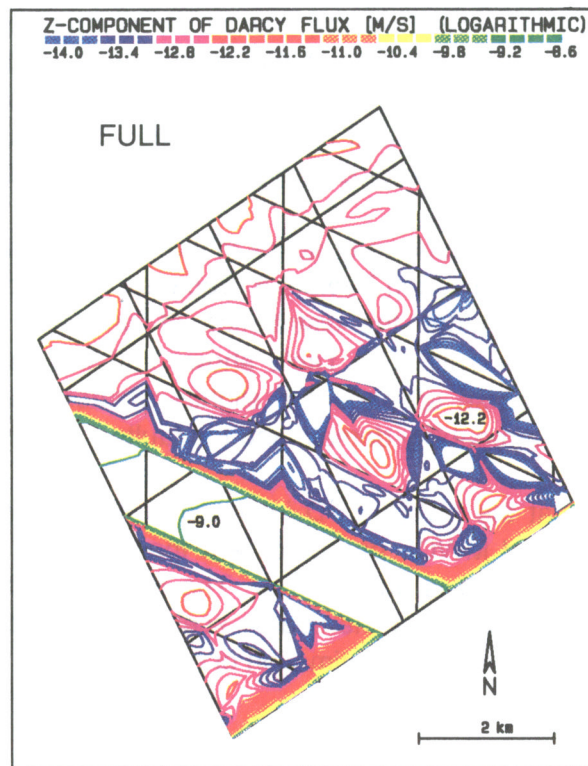


Fig. 8-15 : Distributions of simulated hydraulic gradient in the low-permeability domain (level B-B', Fig. 8-14), local-scale model, area West: full scenario (left), sparse scenario (right) (VOBORNY et al. 1993b).



**Fig. 8-16 :** Horizontal component (logarithmic scale) of simulated Darcy flux in the low-permeability domain and major water-conducting faults (level B-B', Fig. 8-14), local-scale model, area West - full scenario (top) and sparse scenario (bottom) (VOBORNY et al. 1993b).



**Fig. 8-17 :** Contours of vertical component (logarithm) of simulated Darcy flux in the low-permeability domain and major water-conducting faults (level B-B', Fig. 8-14), local-scale model, area West - full scenario (top) and sparse scenario (bottom) (VOBORNY et al. 1993b).

In the sparse scenario (Fig. 8-18, bottom), flow in the central portions of the larger blocks is predominantly vertical throughout the depth range of the low-permeability domain. Near the block margins, flow is towards the bounding faults. In this section, the short arrows indicate flow directions that are oblique or perpendicular to the plane of section. The magnitude of the full vector is designated by the color scale.

The distributions of simulated groundwater fluxes in the low-permeability domain and in second order faults are summarized in Table 8-5. Because the conductivity of each unit is constant throughout the model, the distribution of simulated Darcy flux directly reflects the variability of gradients. The Table shows that the mean values and the ranges of fluxes for the sparse scenario are slightly greater than those for the full scenario, in both the low-permeability domain and the faults.

The Darcy flux ratio,  $D$ , at the MWCF-LPD interface is also shown in Table 8-5. As expected, because LPD and MWCF properties are the same for the full and sparse scenarios, the mean value of  $D$  is quite similar. The range, which is affected by the variability of the gradient, is wider for the sparse scenario. The accompanying sketch explains the approach followed for the estimation of dilution factors from LPD to MWCF (VOMVORIS et al. 1992 and sect. 10.2).

The calculation of the Darcy fluxes in the LPD and MWCF required a further development of the hybrid modeling approach (VOBORNY et al. 1993b). A model box was generated with dimensions 1000 m x 1000 m x 50 m (height), in the upper part of the LPD domain. The MWCFs within this box were modeled as 3-D structures, to allow estimations of the detailed Darcy flux variations within MWCFs. The boundary conditions at the nodes in the surface of the box were taken directly from the hybrid model nodes. By moving the box within the hybrid model, analysis of the flux in the LPD and the MWCFs could be performed in a detailed and systematic manner.

*Groundwater flow path length* - A part of the model area was selected to illustrate the impact of spacing of faults on groundwater flow path lengths. Contour maps of simulated flow path lengths at 250 m and 500 m depth below the top of the low-permeability domain are shown in VOMVORIS et al. (1992) and VOBORNY et al. (1993b); the contour lines represent lines of equal flow path length from points within the blocks of LPD either to MWCFs or to the overlying HPD.

Analysis of the contour maps shows the following

- i) in both scenarios, within the blocks of low-permeability domain, narrow marginal zones occur alongside the major water-conducting faults; in these zones, flow is directly to the adjoining faults and flow path lengths are relatively short;
- ii) in the full scenario, relatively long flow paths occur where particles start either (1) near and downstream from a fault, or (2) in the central parts of large blocks where vertical flow predominates. In the first situation, particles move laterally to another permeable fault that is farther downgradient. In the second situation, particles move diagonally upwards, towards a downgradient fault;

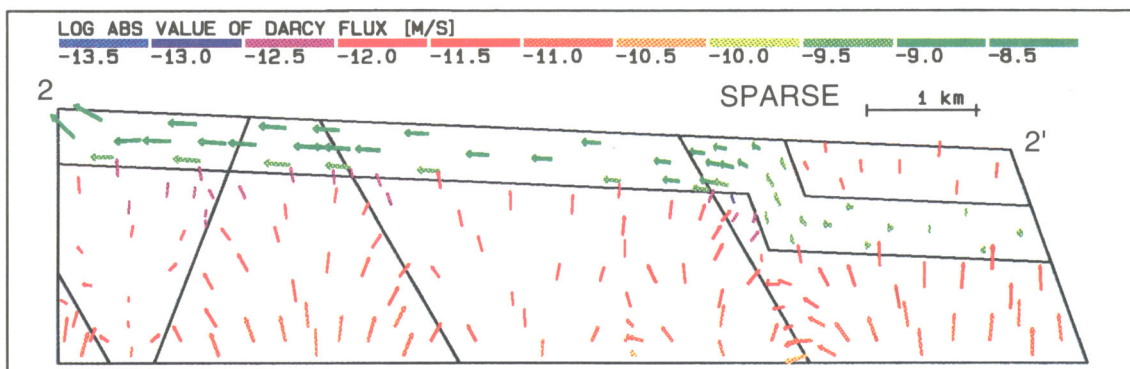
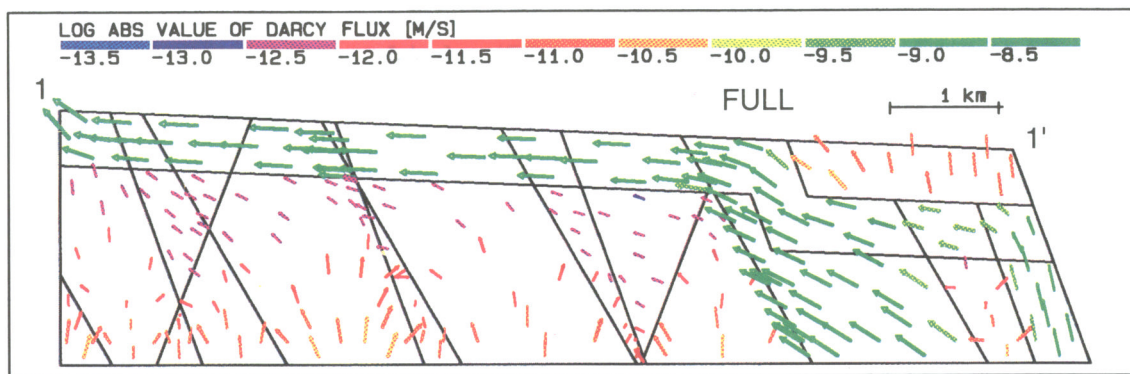
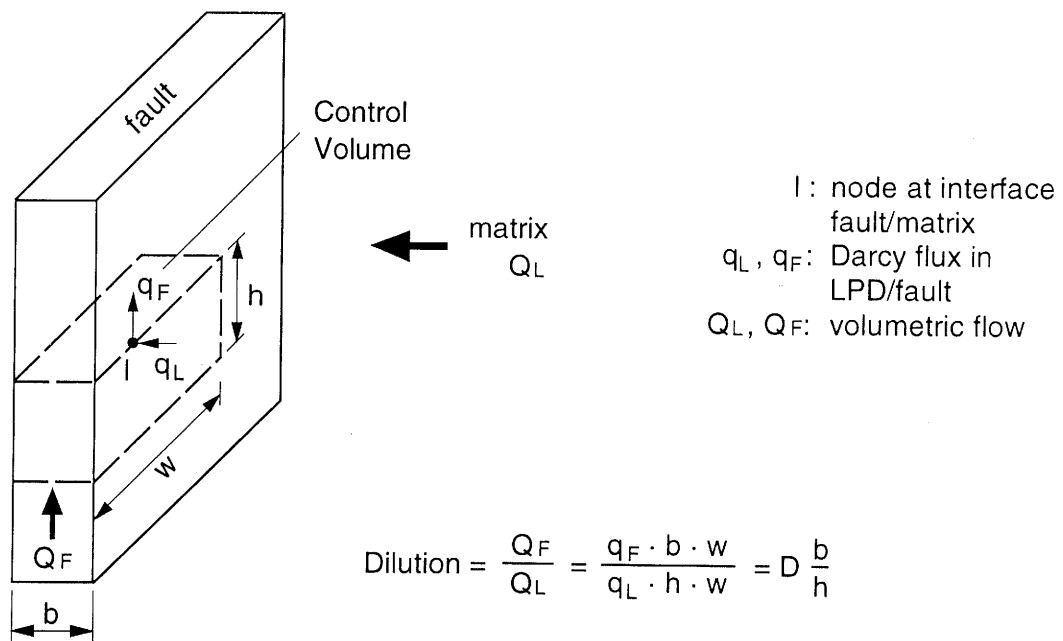


**Fig. 8-18 :** Projection of simulated Darcy flux vectors in selected vertical sections (Fig. 8-13), local-scale model, area West - Full scenario (top) and sparse scenario (bottom) (VOBORNY et al. 1993b). Color scale corresponds to the magnitude of the full vector (logarithmic scale).

Parameter	Full scenario	Sparse scenario
<b>1. Darcy flux in second order major water-conducting faults (MWCF), <math>q_f</math>[m/s]</b>		
Mean	$1.9 \times 10^{-9}$	$6.7 \times 10^{-9}$
Range (approx.)	$3.5 \times 10^{-10} - 6.1 \times 10^{-9}$	$9.0 \times 10^{-11} - 5.0 \times 10^{-8}$
<b>2. Darcy flux in low-permeability domain (LPD), <math>q_L</math>[m/s]</b>		
Mean	$1.0 \times 10^{-12}$	$3.2 \times 10^{-12}$
Range (approx.)	$4.0 \times 10^{-13} - 3.0 \times 10^{-12}$	$5.0 \times 10^{-14} - 3.0 \times 10^{-11}$
<b>3. Flux ratio at MWCF-LPD interface, D [-]</b>		
Mean	1920	1950
Range (approx.)	400 - 5000	100 - 9000



**Tab. 8-5 :** Distributions of simulated Darcy fluxes in second order faults and in low-permeability domain, local-scale model, area West - Full scenario and sparse scenario. Sketch shows definition of control volume used for the estimation of dilution from low-permeability domain to major water-conducting faults (VOMVORIS et al. 1992).

- iii) in the sparse scenario, larger blocks occur and vertical gradients predominate within them. Thus, away from the marginal zones, most contour lines represent the distances that particles travel upwards to the overlying higher-permeability domain rather than laterally to downgradient faults. In these blocks, flow path lengths are controlled by the depth below the base of the higher-permeability domain. The lengths for the sparse scenario (where vertical flow predominates) can be shorter than the lengths in block centers at comparable depths of the full scenario (where horizontal flow toward MWCFs predominates).

### 8.5.3 Evaluation of local groundwater flow

The results of the local-scale model of area West provide insights into the influences of networks of MWCFs - or, equivalently, of the sizes of LPD blocks - on groundwater flow. The results are not location-specific, but rather apply to crystalline rock that has properties and conditions that are similar to those of the crystalline rock in area West of Northern Switzerland.

Groundwater-flow characteristics at the local scale depend significantly on the frequency of major water-conducting faults. These faults act as the principal flow conduits, and their frequency determines the size of the intervening blocks of low-permeability domain. In three of the four scenarios that were tested with different fault frequencies, most blocks of low-permeability domain are small enough that the distributions of hydraulic head within the blocks are controlled by the distributions of head in the adjoining faults. Only in the sparse scenario do blocks occur that are large enough to significantly affect local flow conditions.

If the full scenario (or other high-frequency fault scenarios) applies to the crystalline rocks in the area West of Northern Switzerland, then the following groundwater flow conditions probably occur:

1. Horizontal flow towards the north-west predominates, except in the deep part of the flow system and near the discharge area, where upward flow predominates;
2. Most flow from points within blocks of LPD is lateral towards MWCFs;
3. Some flow from the central parts of larger blocks is vertical towards the HPD;
4. Relatively short flow paths occur from narrow marginal zones, where flow is directly to the adjoining fault; and
5. Relatively long flow paths occur from points near and downgradient from MWCFs, and from deep points in the central parts of blocks.

If the sparse scenario applies, the following flow conditions probably occur:

1. In the MWCFs and HPD domain, horizontal flow components predominate;
2. In the LPD, vertical flow components predominate, and flow in the blocks is generally upwards towards the overlying HPD; only near the MWCFs is the flow radial towards bounding faults;

3. Generally, flow path lengths that originate in areas away from the MWCFs are determined by the proximity of the point of origin to the HPD; and
4. Groundwater fluxes are slightly larger than in the full scenario (up to a factor of about 3), due to slightly higher gradients.

Considerable uncertainty exists as to which is the correct scenario for area West because little information exists concerning the frequency of faults that are classified as major water-conducting faults and their transmissivities. A comparison of model results showing head distributions in hypothetical boreholes with observations indicates that actual conditions are better represented by reduced fault frequencies that approach those of the sparse scenario.

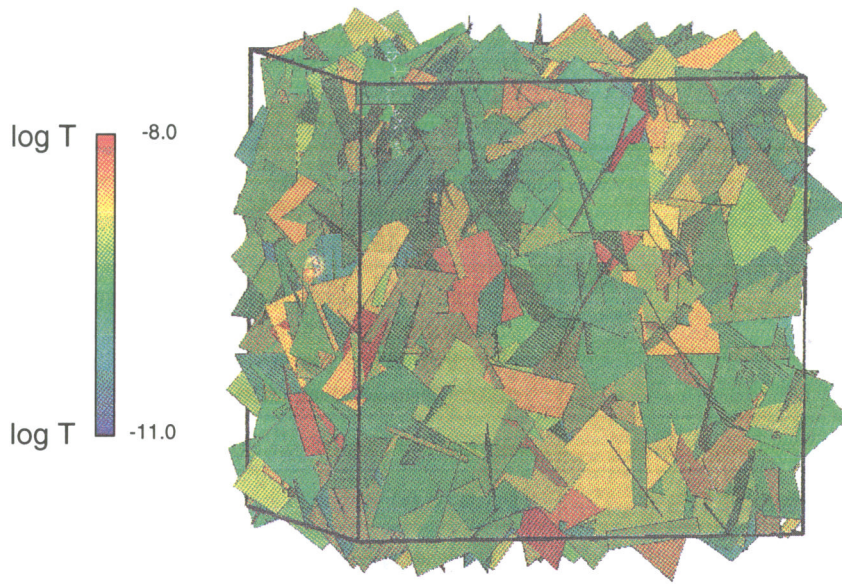
## **8.6 Flow within blocks of low-permeability domain - area West**

Distribution of the rates and directions of groundwater flow in the low-permeability domain is controlled principally by the geometry, locations and hydraulic properties of small-scale water-conducting features. Thus, in order to understand flow in the immediate vicinity of a repository, knowledge of these characteristics is required. At the block scale, the continuum (EPM) approximation is no longer valid, and discontinuum (fracture network) models are used as tools to evaluate flow and, if required, advective transport through a complex network of discrete fractures that transect a block of rock matrix.

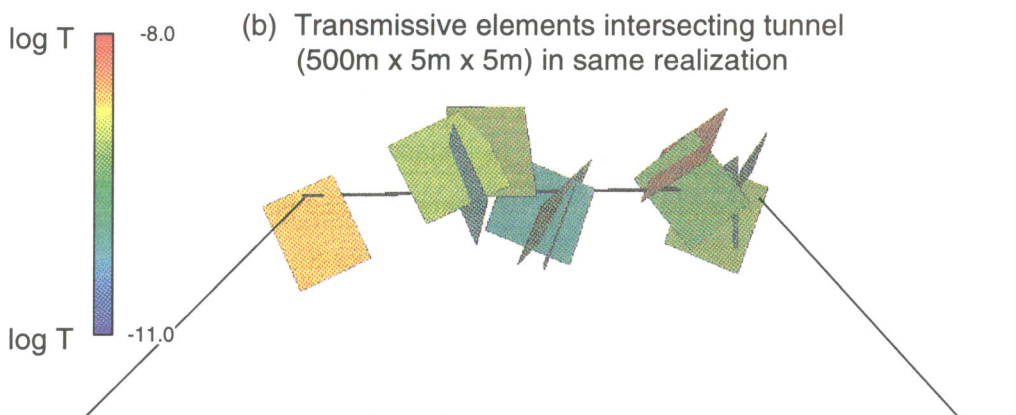
At the repository (block) scale, the computer code NAPSAC (GRINDROD et al. 1991) was used to simulate flow in generic blocks of low-permeability domain. Generic designates, in this study, that the hydrogeological characteristics of the blocks are representative for the low-permeability domain in area West, but a block does not have specific geographic coordinates. The objectives of the analysis were to (1) evaluate the effects of two parameters that have large degrees of uncertainty (fracture length and channeling factor) on the simulated effective hydraulic conductivity; (2) estimate the geometric and hydraulic properties of water-conducting features that would intersect an emplacement tunnel of a repository; and (3) evaluate the characteristics of flow paths that lead away from an emplacement tunnel.

The NAPSAC code describes a discrete fracture network within an impermeable matrix. In the model, the fractures (representing all types of water-conducting features) are described as transmissive elements with highly idealized hydraulic and geometric characteristics. A typical network realization generated by NAPSAC is illustrated in Figure 8-19. Because the fracture parameters, such as the position, orientation, length and transmissivity cannot be determined explicitly, statistical distributions are used as input to these models. The required input for the statistical framework is derived from borehole measurements and/or is inferred from general geological knowledge. In the analysis of a typical block of low-permeability crystalline rock in Northern Switzerland, the transmissivity, frequency and orientation of water-conducting features (fractures) were derived from borehole testing and core analysis (Tab. 8-6).

(a) Typical fracture network in a 500m x 500m x 500m volume



(b) Transmissive elements intersecting tunnel (500m x 5m x 5m) in same realization



(c) Trace length map along tunnel

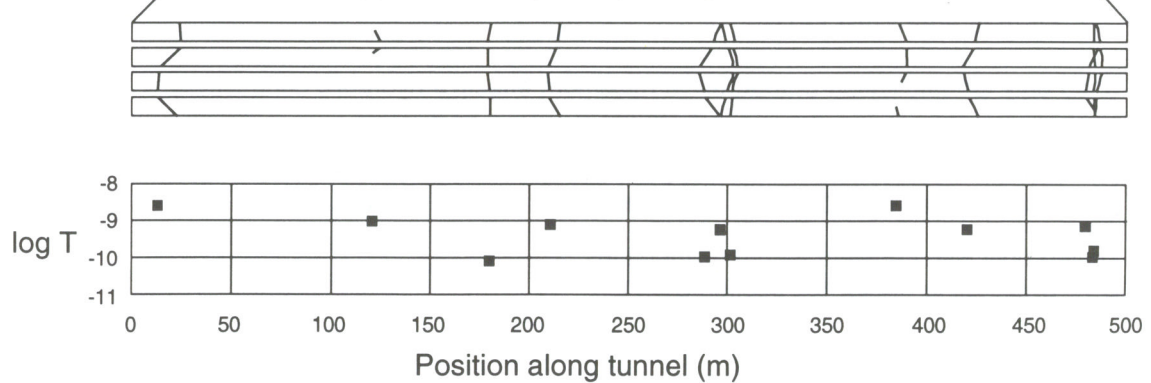


**Fig. 8-19 :** Typical fracture network in the low-permeability domain of area West, generated by NAPSAC (LANYON 1992). (a) Full network of transmissive elements (TEs) in a 500 x 500 x 500 m volume; (b) TEs intersecting a fictitious 500 x 5 x 5 m tunnel; (c) trace lengths and log transmissivities of the TEs.

Characteristic	Description
Transmissivity [m <sup>2</sup> /s]	Distribution: Log normal Mean log T: -9.24 Standard deviation: 0.4
Strike, dip	Uniform distribution: – azimuth, 0 - 360° (isotropic) – dip, 45 - 90°
Aperture	Constant (parallel-plate model); transmissivity varies among TEs, but within a TE is constant over the whole plane - exception: the channeling studies (see below and in text)
Shape	Square
Surface-area density of TEs (P <sub>32</sub> ) <sup>1</sup>	P <sub>32</sub> = 0.04 m <sup>-1</sup>
Length distribution	Infinite lengths <sup>2</sup>
	Constant lengths (20, 40, 100, 200 m)
	Variable lengths – Bimodal (20 m, 200 m) <sup>3</sup> – Continuous: Log-normal (Mean = 100 m; stand. dev. = 0.25, 0.75, 1.25)
Channeling <sup>4</sup>	Unchanneled TEs (C = 1)
	Channeled TEs (C = 5) – "Stripe" model – "Cross" model

<sup>1</sup> P<sub>32</sub> Defined as the total surface area of TEs contained in a unit volume of rock; this determination is based on intersections along a borehole (e.g. spacing of approximately 66 m in area West LPD).

<sup>2</sup> Used only for calculation of theoretical maximum effective hydraulic conductivity.

<sup>3</sup> Two models tested:

- (1) Surface area of 200-m TEs is 5 percent of total TE surface area, and
- (2) Surface area of 200-m TEs is 20 percent of total TE surface area.

<sup>4</sup> Tested only with constant length distribution;

C Channeling factor (cf. section 8.6.1).

**Tab. 8-6 :** Input characteristics of transmissive elements (TEs) for evaluation of effective hydraulic conductivity - area West, low-permeability domain (LANYON 1992a and HERBERT & LANYON 1992a).

The features are assumed to be planar, with an isotropic strike and with a steep dip ranging from 45° to 90°. No direct observations are available on the size of the features and degree of channeling of flow along the fracture planes. Appropriate parameter studies were performed to address these uncertainties.

Modeling transmissivity values with a continuous distribution (Tab. 8-6), rather than introducing cut-offs, may result in extreme values in the generated fracture network that have not been observed in the boreholes. This conservative inconsistency is accounted for in the estimation of the range of parameters affected by transmissivity; for example, flux through individual transmissive elements or flux through tunnel segments. As shown in section 10.2, the range for these parameters corresponds to the 2.5 % and 97.5 % values in their cumulative distribution.

Principal model output consists of (1) effective hydraulic conductivity of the modeled block; (2) number, spacing and conductances (for definition, cf. sect. 8.5.1) of transmissive elements that intersect a hypothetical tunnel within the block; and (3) tortuosity and composition of flow pathways that lead from the hypothetical tunnel. In addition, analytical calculations were made of the theoretical maximum effective hydraulic conductivity of a block.

Details of the analyses for the area West are reported in LANYON (1992a), HERBERT & LANYON (1992a, b) and VOBORNY et al. (1993a); results are summarized in VOBORNY et al. (1993b).

### **8.6.1 Effective hydraulic conductivity**

*Approach* - Effective hydraulic conductivity was estimated by analytical means for the regional-scale and local-scale models (cf. sections 8.4.2 and 8.5.1). For this purpose, the fractures were described as parallel plates of infinite extent. Assuming no interaction among the fractures, the effective hydraulic conductivity of a block of crystalline rock is proportional to the sum of the transmissivities of the constituent transmissive elements. The resulting conductivity values are considered to represent plausible upper bounds for networks of intersecting fractures in the crystalline rocks of Northern Switzerland (VOBORNY et al. 1993a).

The use of a fracture network model provides a basis for checking the reasonableness of the analytical results and for testing alternative concepts concerning fracture properties. As shown in Table 8-6, both constant length and variable length distributions were tested (in this context, "length" is the length of the side of a square transmissive element). In the former, lengths were held constant at 20, 40, 100 and 200 m (LANYON 1992a). Both bimodal and continuous length distributions were tested (HERBERT & LANYON 1992a). In the bimodal analysis, third order faults were assumed to be 200 m in length and all other elements (representing smaller faults and joints) were assumed to be 20 m in length. In the analysis of continuous length distributions, a log-normal distribution of sizes of transmissive elements was assumed on the basis of fracture-trace distributions that have been observed in trace mapping in crystalline rocks (GALE et al. 1991). The arithmetic mean length was 100 m and runs were made with standard deviations of 0.25, 0.75 and 1.25 (natural log).

Channeling refers to the degree to which flow in a transmissive element is constrained to occur only along certain parts of its surface, or channels (cf. Chapter 6). In the models that simulate channeled transmissive elements, the large spatial heterogeneity of the transmissive properties of an individual element is highly idealized - parts of the transmissive element are assigned either a single finite value of transmissivity or zero transmissivity. In such a model, an unchanneled element (channeling factor of 1) has flow occurring over the entire element surface. If an element has a channeling factor of 5, flow occurs only along about 20 per cent of the fracture surface.

To evaluate the potential effects of channeling on effective hydraulic conductivity, each constant length distribution was tested with no channeling and with "stripe" and "cross" channeling models (i.e. two parallel "channels" or two intersecting "channels"). The two channels transect a hypothetical fracture plane; no special properties were assigned to the intersections of fracture planes, i.e. channels in two different planes were interconnected only if they intersected each other directly. In the channeled models, a channeling factor of 5 was assumed, on the basis of results of various field investigations (e.g., BOURKE 1987). The channeled models thus had 5 times the number of fracture planes (permeable along 20 % of their area) than the unchanneled models. This arrangement ensured that the total surface area of transmissive elements was constant in all network realizations, in order to be consistent with borehole observations.

For most runs, the model describes crystalline blocks that are 500 m on a side. Because of computational constraints, smaller blocks (200 m on a side) were used to analyze channeling effects with networks of 40 m transmissive elements.

*Results and conclusions* - The results of the model runs serve principally to provide (1) insights into concepts concerning the effects of fracture network properties on effective hydraulic conductivity, and (2) a basis for checking plausibility of analytically derived values. The results are not intended to provide firm values of conductivity to be used in further analyses. Therefore, only general results and conclusions are provided herein.

In models with constant length transmissive elements, the values of simulated effective conductivity in both the unchanneled and channeled systems increase with increasing length. All values are less than the theoretical maximum, which corresponds to conductivity of infinite non-interacting fractures and gradient along their plane. In runs with constant length 40 m transmissive elements, the network was unconnected. As expected, the vertical component of conductivity is always slightly greater than the horizontal component, reflecting the assumed sub-vertical dip of the elements.

The results indicate that, in the simulations, the channeled networks have smaller values of effective conductivity (by about a factor of 2) than unchanneled networks with comparable lengths of transmissive elements. Only small differences exist between conductivity values of the "stripe" channel model and those of the "cross" model.

In models that contain variable length distributions of unchanneled transmissive elements, the resulting effective conductivity is controlled by the presence of large

fractures within the network. Thus, in networks with continuous distribution and a constant mean value, conductivity increases slightly with increasing log standard deviation. For networks with mean transmissive element lengths of 100 m, those with variable length distributions have a larger effective conductivity than those with constant lengths.

The results further suggest that, for LPD in area West (which is not densely fractured), fracture networks that include even just a few large fractures (100 - 200 m) are well connected; the effective conductivity of such networks approaches the analytically derived theoretical maximum value. Thus, the numerical results support the use of the analytically derived values of maximum effective hydraulic conductivity in larger-scale models as being appropriate and conservative.

### 8.6.2 Properties of transmissive elements

The NAPSAC code was used to simulate transmissive element networks, in order to predict the geometric and hydraulic properties of elements that intersect a hypothetical repository tunnel. These results contribute to an evaluation of the potential total flux from the tunnel into the network, and of the spacing between discrete flow locations within the tunnel.

*Input to the block-scale model* - Most of the characteristics of transmissive elements that were used in the analysis of their geometric and hydraulic properties are the same as those used in the analysis of effective hydraulic conductivity (Tab. 8-6). The transmissive element size was maintained at a single constant value (100 m), and only an unchanneled network was considered. On the basis of the available data, a more complex model is unjustified.

For this analysis, networks of transmissive elements were generated in blocks of low-permeability domain. Each block surrounds a prismatic tunnel segment 500 m long and 5 m x 5 m in cross-section. This cross-section is selected to represent a tunnel with a diameter of 3.5 m, plus an excavation disturbed zone. Network characteristics were simulated with 20 realizations.

*Model results* - For each transmissive element that intersects the tunnel, the following were calculated: position in the tunnel, trace length on the tunnel faces, spacing and conductance. Details and assumptions of the calculations are described by HERBERT & LANYON (1992b).

Figure 8-20 shows distributions describing characteristics of transmissive elements that intersect the tunnel segment. For the 20 realizations considered, the number of transmissive elements per tunnel segment ranges from 6 - 20; the mean is 13.7. On average, a transmissive element intersects the tunnel segment about every 35 m, but a clustering occurs at the lower end of graph, indicating that the spacing of most transmissive elements is less than the mean. In contrast, some elements are spaced more than 100 m apart.

The mean trace length of individual transmissive elements that intersect the tunnel segment is about 22 m, and most values are 20 - 30 m. Values that are less than 20 m are indicative of elements that do not fully transect the tunnel. A few values are several tens of meters (maximum is 72 m); these represent elements that intersect the tunnel with a strike that is more closely parallel to the tunnel axis.

The distributions of conductances of transmissive elements that intersect the tunnel segment are also shown in Figure 8-20. "Conductance", as used here, is the product of transmissivity and one-half the trace length. This conductance corresponds to the cross-tunnel conductivity that is due to the presence of the intersecting transmissive element. On average, flow enters the tunnel through one half of the rectangular perimeter and leaves the tunnel through the other half. The conductance distribution generally reflects the transmissivity distribution, because transmissivity has a much greater spread than trace length. Some values of conductance are large, however, because they represent transmissive elements that have large trace lengths. Mean conductance is  $5E-9 \text{ m}^3/\text{s}$ .

### 8.6.3 Characteristics of flow paths

In the low-permeability crystalline domain, a flow path consists of either (1) all or part of a single water-conducting feature, or (2) segments of multiple intersecting water-conducting features. The NAPSAC code was used to characterize flow paths that lead from a hypothetical tunnel segment to the model boundaries.

Flow path tortuosity is the principal output from the simulations that is of value to quantifying solute transport in crystalline rocks of Northern Switzerland. Tortuosity as used by HERBERT & LANYON (1992b) in this analysis is the total flow path length divided by the straight-line distance between the starting and ending points.

*Input to the block-scale model* - Several realizations of blocks 1,000 m on a side were used for the analysis of flow paths. Input characteristics of the transmissive elements are the same as for the analysis of geometric properties (cf. Tab. 8-6). Each realization contains about 4,000 transmissive elements and incorporates a one-dimensional element 200 m long that represents a tunnel segment. A larger block was chosen for this study to allow for a flow path distance of a few 100 m to the boundary (MWCF or HPD). Two cases of tunnel conductivity were considered: 1) small conductivity case ( $K_T = 1E-10 \text{ m/s}$ ), and 2) large conductivity case ( $K_T = 1E-6 \text{ m/s}$ ). In the latter case, the tunnel acts as a short-circuit, by diverting flow along the tunnel between the transmissive elements; it can thus be assessed whether flow will be carried by a small percentage of the transmissive elements due to short-circuiting through the tunnel.

Uniform linear pressure gradients of 1 Pa/m were applied to the model block, simulating gradients in two horizontal directions (x, y) and the vertical direction (z). Unit gradients were applied because the blocks are generic and do not represent any particular location; results can be adjusted by applying actual gradients that occur at a site.

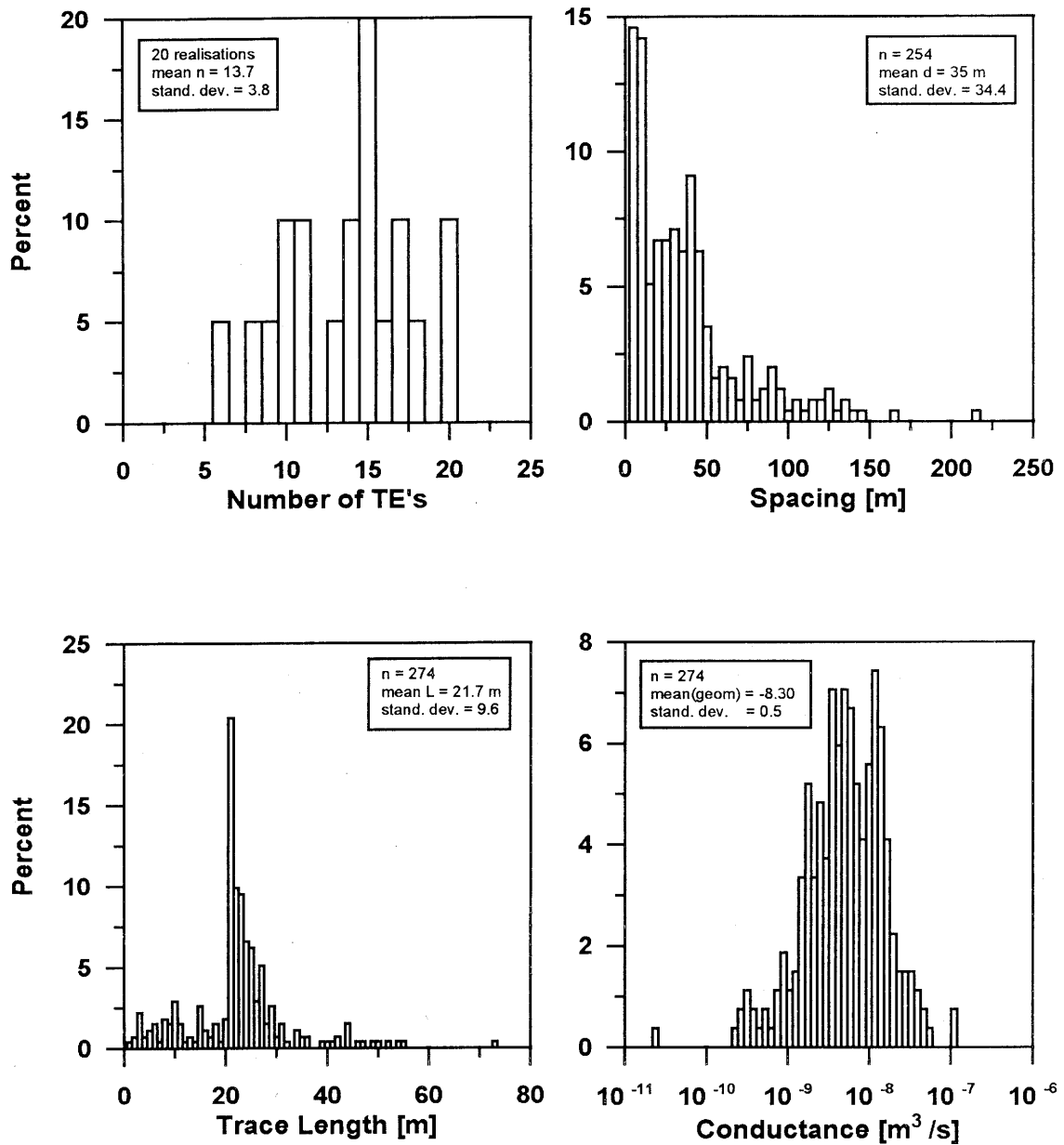


**Fig. 8-20 :** Distributions of number, spacing, trace lengths and conductances of transmissive elements intersecting a tunnel segment 500 meters long with a cross-section 5 x 5 m (VOMVORIS et al. 1992).

*Model results* - All simulated tortuosity values are between 1.15 and 2.96. Median tortuosity values are smaller for the high conductivity case and when the gradient is in the vertical direction. Thus, some pathways are nearly equal to a straight-line distance, and some are nearly 3 times longer than a straight-line distance.

#### **8.6.4 Evaluation of flow in blocks**

Results of block-scale analyses of groundwater flow in the low-permeability domain provide insights into (1) the effective hydraulic properties of this domain, and (2) the characteristics of networks of transmissive elements that would be expected to intersect repository tunnels and act as flow paths. The results form the basis for assessing expected flow conditions in individual transmissive elements and in tunnel segments; the methodology and the resulting database are described in Chapter 10.

At the block scale, flow in the low-permeability domain is appropriately described as occurring in networks of water-conducting features that dissect an impermeable matrix.

In numerical models, these features are described as planar transmissive elements. Proper evaluations of the properties of this domain depend to a large extent on the appropriateness and accuracy of descriptions of transmissive elements and on the validity of the code used to describe the networks. A set of input parameters (cf. Tab. 8-6) was used to calculate and simulate effective conductivity and geometric and hydraulic properties. Most of these parameters were derived from borehole testing and are considered to be reasonably representative. However, major uncertainties do exist concerning knowledge of the length distribution of transmissive elements and the degree of heterogeneity (channeling); in some simulations, these characteristics were varied to test their effects on geometry and hydraulics.

The NAPSAC modeling results indicate that the following conditions lead to relatively large effective conductivities of a block of low-permeability domain: no channeling, continuously variable length distribution of water-conducting features, large mean length and large log standard deviation of length. The actual conditions are unknown, but geological considerations suggest that networks with water-conducting features that are channeled have continuously variable lengths and mean lengths of about 100 m are plausible. According to the model results, such a network would have an effective conductivity that is about one order of magnitude less than the theoretical maximum value. However, the inclusion of some 200 m (or larger) water-conducting features probably would substantially increase the effective conductivity of the block. Therefore, one can consider the theoretical maximum value of effective conductivity to be a conservative upper bound for representing the low-permeability domain in local-scale groundwater flow models.

Results of block-scale modeling (cf. Fig. 8-20) indicate that the number and spacing of transmissive elements that would intersect a tunnel is likely to be quite variable - clusters of these features can be expected, as well as some tunnel lengths of 100 m or more with no intersecting features. In the simulations, most transmissive elements intersected the tunnel approximately perpendicular to the tunnel length; most trace lengths, therefore, would approximate, within 50 %, the perimeter of the tunnel.

The small tortuosity values that were simulated by the model indicate that flow pathways in the case of no channeling are not greatly different from direct-line paths; on average, simulated flow paths are less than twice as long as direct-line paths, indicating that the input data used generate a reasonably well-connected network.

## 8.7 Groundwater flow conditions in area East

In area East, borehole hydrogeological data are available only from Siblingen. The transmissive properties of the crystalline basement at this site are substantially greater than those that are characteristic of the low-permeability domain in area West. Thus, a large degree of uncertainty exists concerning the representativeness of the Siblingen data for area East as a whole. As a result, analyses for this area are limited to scoping calculations that are designed to provide general indications of flow conditions.

Because of the very limited database, development of a local-scale model was deemed unwarranted. Instead, the regional-scale model was modified as a check on the reasonableness of assigning large conductivities to area East and to obtain distributions of hydraulic gradients for the area. At the block scale, two equally plausible hypotheses were considered:

- 1) Siblingen data **are** representative; and
- 2) Siblingen data **are not** representative.

General procedures and some results are summarized herein; details and complete results are described in VOBORNY et al. (1993b).

### 8.7.1 Modification of the regional-scale model

In the regional-scale model, a single value of effective hydraulic conductivity was assigned to each unit throughout the region, on the basis of data from boreholes in area West (section 8.4.2). However, the average transmissivities of water-conducting features in the upper and lower domains at Siblingen are substantially greater than transmissivities in the corresponding domains in Böttstein, Kaisten and Leuggern (cf. Fig. 8-5). In the upper domain, the difference is about one order of magnitude; in the lower domain, the difference is about two orders of magnitude. Moreover, the frequency of the water-conducting features is substantially greater at Siblingen. The result is a substantially larger effective hydraulic conductivity of crystalline rocks at Siblingen in comparison with the corresponding EPM domains in the area West. Therefore, in order to test the hypothesis that Siblingen data are representative, the regional-scale model was modified to account for this hydraulic heterogeneity (VOBORNY et al. 1993b).

The impact of different values of effective conductivity in area East on the flow system in that area was tested by several model runs. Fluid-particle-tracking techniques were applied as a plausibility check to compare simulation results with available

hydrochemical evidence at the Siblingen borehole. The best match was obtained when the value of effective conductivity in the lower crystalline rock unit in area East is about  $1\text{E-}8$  m/s, or intermediate between that of area West and that which results directly from Siblingen data.

Model results were also used to obtain estimates of the distributions of hydraulic gradient in area East. The mean absolute gradient is about 0.003, or about a factor of 6 smaller than in area West.

### **8.7.2 Properties of transmissive elements in blocks of crystalline rock**

Two sets of data were utilized in order to estimate hydraulic and geometric properties of water-conducting features that would intersect a repository tunnel segment in a block of crystalline rock in area East. The resulting two sets of properties provide the basis for estimating the plausible ranges of fluxes in the lower unit that are needed for safety analysis of area East (Chapter 10).

For the high end of the range, data from Siblingen were input into a fracture network model using the NAPSAC code, similar to the approach taken for area West (section 8.5) but focused more on geometric properties. In this scenario, it is assumed that Siblingen data **are** representative of conditions in area East and that, therefore, blocks in the crystalline domain within the major water-conducting faults with transmissive properties that are similar to (but not greater than) those of the lower unit at Siblingen could be expected throughout much of the area.

For the low end of the range, results from the block-scale modeling in area West were adopted directly in the analysis of area East. In this scenario, it is assumed that Siblingen data **are not** representative, and that blocks in the crystalline domain within the major water-conducting faults with transmissive properties that are similar to (but not smaller than) those of the low-permeability domain in area West also occur extensively in area East.

Distributions of the following properties were obtained from these analyses: 1) number and spacing of transmissive elements that intersect a 500 m tunnel segment; 2) trace lengths of individual transmissive elements that intersect a tunnel segment; 3) transmissivities of transmissive elements; and 4) conductances of transmissive elements. The application of these parameters (Tab. 10-2), in combination with gradient distributions, to obtain distributions of fluxes is described in Chapter 10.

## **8.8 Underground constructions in the crystalline basement: hydrogeological effects**

Underground constructions, such as shafts and tunnels associated with a potential repository, will affect the hydraulic head and hence the groundwater flow regime in their

vicinity. The extent of these effects depends on the local structural and hydrogeological conditions, as well as the ability to seal permeable sections in the shaft or tunnels. Some of the required information will be collected during the exploration steps, e.g. seismic surveys and inclined boreholes (cf. also Chapter 11), once a location for a potential repository has been selected. Some initial considerations are documented in this section. Further evaluation of these effects will be part of the next phase of investigations.

The relevant issues include effects on the constructions, e.g. water inflows, and effects of the constructions on wells or aquifers in the vicinity of the repository. The effects are either short term, i.e., during construction and operation, or long-term, i.e. post-closure.

In the area West, the predominant groundwater flow is expected to be in a south-east - north-west direction towards the discharge area in the Rhine valley. Thus, with respect to a potential repository one should also distinguish between "upstream" effects, i.e. how far against the gradient such an effect would propagate, and "downstream" effects.

*Construction and operation - effects on the constructions:* Questions related to operational issues, such as water inflows, are addressed in NAGRA (1985b). It is expected that with careful advancement of the construction: i) large water inflows can be anticipated and, if necessary, avoided, and ii) successful sealing of fault zones can be undertaken.

*Construction and operation - effects on the groundwater flow system:* The magnitude, spatial extent and propagation rate of the tunnel's influence on the hydraulic head depends on the hydraulic diffusivity, defined as the ratio of hydraulic conductivity to the storativity of the rock. The lower the hydraulic diffusivity, the more localized are these effects and the slower is their propagation speed.

Crystalline rocks at the Grimsel Test Site have hydraulic properties similar to LPD, and therefore some observations from the Test Site provide a basis for a first estimate of the expected effects. Observed flux in the main access tunnel to the Grimsel Test Site (tunnel meter 700 to tunnel meter 2314) is about 18 l/min (VOBORNY et al. 1991); measured hydraulic head in the matrix about 100 m away from the tunnels is about 25 bars (CHALMERS & CORREA 1993).

Based on the modeling studies of VOBORNY et al. (1991), this condition implies a decrease of about 10 to 15 bars (100 to 150 m) compared to the situation without the tunnel. The same studies show that inclusion of two families of continuously permeable faults results in decreases - compared to the no-tunnel situation - in hydraulic heads of up to 20 m about 1.5 km away from the tunnel.

With respect to the effects of shaft and tunnels on wells away from the repository, two bounding conceptual models are considered. In the first model, no direct connection is assumed between the shaft or tunnels and the major-water conducting fault where a

well is situated; in the second conceptualization, such a direct connection exists. The assumption that in both cases the wells penetrate major water-conducting faults is supported by hydrogeological and geothermal evidence in existing deep wells in the crystalline basement. In the Zurzach boreholes, for example, the hydraulic conductivity of the producing sections - located in the Buntsandstein and in the first few decameters of the crystalline basement (top crystalline basement at 415 to 425 m below surface) - is about  $1\text{E-}4$  m/s (compared to about  $1\text{E-}7$  m/s for HPD and less than  $1\text{E-}10$  m/s for LPD); the reservoir temperature of the groundwaters is estimated to be around  $44$  °C (VUATAZ 1982). Taking into account a geothermal gradient of  $3.5$  to  $4.5$  °C/100 m (RYBACH et al. 1987), these observations imply rising waters from a depth of  $900$  -  $1000$  m below surface, which would require the presence of a major water-conducting fault.

On the basis of simple analytical expressions (Cooper-Jacob method; cf. e.g. FREEZE & CHERRY 1979) with a  $500$  m-thick HPD and a hydraulic conductivity of  $1\text{E-}7$  m/s, total inflow to an unsealed shaft would be less than  $0.1$  m<sup>3</sup>/s. Drawdowns to a well in the HPD,  $5$  km from the shaft, would be a few tens of meters. The influence is expected to be much smaller if the wells were located in a major water-conducting fault, which would act as a constant head boundary, or if the effective hydraulic conductivity of the HPD were greater.

In the case of a direct connection to the well through a major-water conducting fault, the drawdown would be smaller but the water inflow would be greater. Because of the presence of the sedimentary cover, which is a few hundred meters thick in area West, and the low permeability of the Lower and Middle Muschelkalk sediments, groundwater in the crystalline basement is under confined conditions. In many cases, artesian conditions have been observed. Thus, construction of the shaft and tunnels, even if it has some effect on wells, is not expected to lower the hydraulic head below the top of the crystalline basement; hence, the possibility exists of achieving the original well yield through increased pumping rates.

*Post-closure:* Closure and resaturation of the repository and the shafts are expected to re-establish the original groundwater flow system after a time period that is about the same length as the operation and construction one. The exact behavior depends on the local structural, geological and hydrogeological characteristics, which will be investigated once a potential repository location has been selected.

## 8.9 Conclusions

The investigation of groundwater flow conditions in Northern Switzerland included a comprehensive synthesis of hydrogeological data, development of a conceptual hydrogeological model and numerical modeling of groundwater flow at various scales.

Input data were obtained principally from five Nagra boreholes, supplemented by geological, hydrogeological, geophysical and hydrochemical information from the

region. Although the conceptual model is based on numerous simplifying assumptions, it was developed from the integrated analysis of a variety of field observations and modeling results. Thus, the conceptual model represents the currently most plausible description of the hydrogeological system.

Because of the sparseness and irregular spacing of the data, considerable uncertainty is associated with the parameters used and, consequently, with the results of the investigation. For example, the locations, frequency, extent and properties of regional faults in the region can be described only on a statistical basis derived principally from observations in Southern Black Forest. Similarly, on a much smaller scale, flow through low-permeability fractured rock is characterized by a statistical analysis of single conductive features. Sensitivity studies were performed with the numerical models to address the significance of the underlying major conceptual uncertainties.

Despite the uncertainties, the investigation did lead to improved understanding and increased confidence concerning many aspects of the groundwater flow system. The general flow patterns seem well-defined, with principal recharge in the Black Forest and discharge along the Rhine River and potentially along the Wutach River. Leakage to or from overlying sediments probably is a minor factor in the flow system. A groundwater divide could exist in the eastern area crystalline basement, with some groundwater flow occurring towards the south-east. The hydraulic conductivity of the crystalline rocks investigated shows consistently an inverse correlation with depth. The crystalline basement is dissected by multiple sets of regional faults into irregular blocks. Probably only a few of the faults are major water-conducting features, but these are the principal conductors of flow in the region. Flow in them is predominantly horizontal, governed by regional gradients, except beneath discharge areas where flow is upward.

Upper and lower domains of crystalline rock are distinguished throughout the region, based on a contrast in hydraulic properties. In area West, the lower domain, identified as the low-permeability domain, is under consideration as a potential host rock. The effective hydraulic conductivity of this domain averages about  $4E-11$  m/s. A network of major water-conducting faults transects the low-permeability domain, resulting in isolated blocks of variable size and shape. The local flow conditions within such a block are controlled by the block size and the relative position of any internal point to a bounding fault. Flow from a repository located in the interior of a block would be either upwards to the overlying higher-permeability domain or laterally to a major water-conducting fault.

The advective flow through the blocks of low-permeability domain is dominated by a network of small-scale water-conducting features. Use of a fracture network model provided insight into the influences of channeling and different distributions of lengths of these features on the effective hydraulic conductivity of a block of low-permeability domain. Based on a particular set of input data, distributions were derived of geometric and hydraulic characteristics of water-conducting features that would intersect a repository tunnel in area West.

In area East, borehole data are available only from Siblingen, where the transmissive properties of the upper and lower domains are up to two orders of magnitude larger

than in boreholes in area West. The representativeness of the Siblingen data for area East is unknown; thus, whether or not the low-permeability domain occurs extensively in area East is also unknown. Analyses were performed to provide data for safety analysis that cover these two alternative possibilities in area East.

## 9 NEOTECTONICS AND SCENARIOS OF GEOLOGICAL PROCESSES

### 9.1 Introduction

When considering the long-term safety of a repository located in the crystalline basement of Northern Switzerland, realistic concepts of future geological processes and groundwater flow conditions have to be developed.

Because of the very long half-lives of some high-level waste nuclides, these predictions have to cover a timespan of around 1 Ma.

Such a geological timespan is far beyond the conventional forecasting timescales for any other social or technical projects. It cannot therefore be the intention to make singular quantitative predictions but rather to develop plausible scenarios whose extreme variants represent the boundaries to which geological and hydrogeological evolution may lead in future (cf. section 9.3). These extreme scenarios will be defined as bounding scenarios and quantified as far as possible (cf. section 9.4).

The development of geological scenarios is based on two interrelated sets of data:

- A first dataset which describes the present state of geological structures in Northern Switzerland (e.g. the fault inventory) as a result of the geological evolution in the past (geological history). These data, which are summarized in Chapters 3 to 6, are essentially historic in nature and end with the Upper Miocene (end of Molasse deposition). From these data, a set of geological processes can be gleaned that has shaped the geological evolution in the past. These processes can be defined by type (e.g. uplift) and their rate of action (e.g. m/Ma, cf. NAEF et al. 1985).
- The second dataset is the result of neotectonic investigations. It pertains mainly to the geological processes which are active either at present or have been ongoing in the recent past. This dataset is reviewed in the next section.

By comparing the types, evolutionary directions and rates of geological processes which were active in the past (first dataset) with those observed to be active today (second dataset) trends of the geological evolution in the future can be inferred. These trends have provided the perspective on which the extrapolation of the geology into the long-term future (scenarios) has been based.

The geodynamic context required for the development of realistic scenarios reaches far beyond the geographic limits of Northern Switzerland. Therefore, the regional geological datasets taken into account extend from the Upper Rhine Graben and the Black Forest to the Alps.

## **9.2 Neotectonics**

### **9.2.1 General aspects**

Neotectonic studies investigate geological processes in the earth's crust that have made an imprint on the recent past and/or can be identified as actually active today. If generally accepted rules and models are taken into account, the information from these studies can be used to develop scenarios for geological processes active in future.

Selecting the time interval to be considered depends on the timespan required for the forecasts and on the available information. Long-term processes which occur slowly and continuously (e.g. regional uplift) can only be interpolated reliably over long periods of time. Rapid events (e.g. earthquakes) can be observed and even measured today with high precision.

Appendix 9-1 provides an overview of neotectonic indications in Northern Switzerland and surrounding areas. The acquisition technique for the different datasets, i.e. how they were obtained, is shown with a color code; a distinction can be made between the following datasets:

- a) Geology, geomorphology and analysis of drainage patterns (green)
- b) Measurements of the recent stress field (brown)
- c) Regional geodesy, i.e. precision leveling surveys (beige)
- d) Seismicity and seismotectonics (blue).

The interpretation and integration of these data into the regional geological framework leads to the postulation of a series of neotectonically active structures and of ongoing processes which form input for scenarios of long-term geological evolution.

Section 3.4 provided an overview of the geological history of Northern Switzerland for the Tertiary that can be traced chronologically up to the end of the Molasse sedimentation some 12 Ma ago. Between the Late Miocene and the Pleistocene, there was a period of several Ma for which no sedimentary record is preserved (cf. Fig. 3-4) and events during this time interval are largely unknown.

The sediments deposited during the Quaternary, namely detritus, gravel, moraines and lacustrine deposits, can generally be related to glaciations and can be dated accurately if organic residues are found ( $^{14}\text{C}$  method). Nevertheless we are still quite far from achieving a uniform Quaternary chronostratigraphy. Because of the generally erosive regime during the Pleistocene glaciations, Quaternary sediments have been partly removed and transported further into the foreland. Their sequence is often incomplete and therefore of limited use for a chronological timescale. Nevertheless, the relative sequence and the erosion forms of these deposits, particularly the development of the drainage patterns, give numerous indications of very young movements of the earth's crust.

### 9.2.2 Geology, geomorphology and analysis of drainage patterns

The analysis of young and recent exogenous dynamics is based largely on geomorphology and yields important data on climate evolution, the sequence and intensity of glaciations and the erosion processes which have marked the recent past. These processes are also expected to be active in the immediate future.

Information that can be derived from this geomorphological dataset includes uplift and subsidence, regional and local tilt movements, arching, etc. However, the chronology and/or absolute dating of these young movements in Northern Switzerland is still unclear. It is therefore difficult to obtain accurate data both on magnitudes and rates of uplift/subsidence and correspondingly on erosion.

Discrete neotectonically active structures such as faults and flexures have not been identified as yet in Quaternary sediments of Northern Switzerland exposed in numerous gravel pits. This is in contrast with the situation in the Upper Rhine Graben where MONNINGER (1985) found such indications at several locations.

Observations of subtle displacements of river terraces and river courses, however, imply the existence of such recently active structures underground; Appendix 9-1 summarizes the relevant geological-geomorphological information (in green).

- a) In the southern part of the Upper Rhine Graben, tilting, uplift and displacement of Plio- and Pleistocene alluvial plains are evidence of various block movements (MONNINGER 1985, THEOBALD et al. 1977).
- b) Analyzing the gravel terraces along the Rhine valley between Basel and Laufenburg, SCHMASSMANN (in HALDIMANN et al. 1984) concludes from displacements of the deepest channel of the Rhine that several Rhenish-striking faults were active during the Quaternary; this implies continuing extensional tectonics in the area Dinkelberg - western Tabular Jura.
- c) Further to the east, in the Rhine valley between Laufenburg and Eglisau, there are several indications of young movements at faults and flexures with Hercynian and Jura-parallel strike (HALDIMANN et al. 1984).

Both b) and c) indicate neotectonic activity of fault families which have been defined for modeling purposes in sections 5.4 and 5.5.

- d) Divergent gravel terraces in the lowermost Aare valley between Brugg and the Rhine indicate young Quaternary tilting of the eastern Tabular Jura approx. to the NW (HALDIMANN et al. 1984).

Important methods used in neotectonic studies are the linear analysis of stream profiles and regional investigations of drainage patterns. For the region South-east Black Forest - Lake Constance, studies of this type give numerous indications of ongoing uplift in the Black Forest and a corresponding S to SE tilt of basement blocks, at least to the north of the Rhine. This uplift is associated with active block tectonics which can be identified in the area by river course drifts and marked nickpoints in their profiles (mainly at Hercynian-striking fault systems).

Figure 9-1 shows a schematic profile of the Alb river SE slope of the Southern Black Forest, presenting important geomorphological information:

- The gradient of the Alb, which is a uniform 10 ‰ over a distance of some 20 km, shows a pronounced nickpoint and oversteepening in its lower course. This can be interpreted as the result of young displacements, i.e. uplift of the Black Forest relative to the Rhine valley. The updoming caused a 5-7 km wide flexure zone, where all the consequent stream courses of the Southern Black Forest are oversteepened as compared with their upper courses.
- The Alb profile also allows an estimate of the rate of uplift for the Southern Black Forest: the level of the Sundgau Gravels (approx. 1.5 Ma), extrapolated from the W, is at ca. 600 m a.s.l., or approx. 300 m above the present-day valley level. The extrapolated level of the plateau gravels ("Deckenschotter"), which are around half as old, is still around 150 m higher than the recent valley floor. This is interpreted to mean that the region of the Rhine valley was uplifted here by around 200 m in 1 Ma during the Quaternary in relation to a reference point in the Sundgau area (west of Basel).

A young uplift and tilt of basement blocks in the South-eastern Black Forest with respect to Northern Switzerland is also confirmed by the systematic shift of river courses and the long-term trend of the axial drainage channel of the Rhine shifting towards the SSE (cf. Fig. 9-2, position of the Rhine between Schaffhausen and Waldshut in 9-2b and c).

### 9.2.3 Geodetic and geophysical data

Geodetic measurements provide indications of ongoing neotectonic activity. They represent a kind of geodynamic "snapshot", covering a time period of the order of 100 years, but have no historical dimension in the geological sense and cannot, therefore, simply be extrapolated into the geological future (1 Ma).

#### Precision leveling surveys

The precision leveling measurements carried out by the Federal Office of Topography have provided an important framework for studying recent vertical crustal movements in Switzerland. To enhance reliability, the leveling network was recalculated and the geological setting of the individual benchmarks was verified in the field; as a consequence, benchmarks of doubtful stability were not included in the geodynamic interpretation (GUBLER et al. 1984). DIEBOLD & MÜLLER (1985) have summarized this work and provided a geological interpretation of the results. The data shown in Figure 9-3 (latest revision including new data, 1991) basically still confirm this interpretation.

In the meantime, results from part of the precision leveling network of Southern Germany have also become available (Fig. 9-4, MÄLZER et al. 1988). These data include the area of the Rhine valley from Basel to Lake Constance and the Southern Black Forest. Calculations are based on a reference benchmark located in gneiss at Laufenburg (Switzerland). This latter point is also included in the Swiss precision

leveling network. Values for rates of uplift and subsidence derived from these networks have to be interpreted in relation to their relevant reference points whose own vertical movement can be determined only in comparison with the other (overlapping) network.

Although the two adjacent leveling networks are based on different reference points located at Aarburg (Fig. 9-3) and Laufenburg (Switzerland, Fig. 9-4) for the Swiss and the South German networks respectively, there is now a neotectonically relevant set of leveling data available that extends from the Black Forest to the Alps.

The following summarizes salient results from precision leveling data:

- To the west of a line Basel - Biel - Payerne there is a consistent tendency for subsidence (as compared to the reference point at Aarburg) that could be interpreted as recent subsidence in the southern extension of the Rhine Graben (former Rauracian Depression).
- Figure 9-3 shows the prominent zone of recent uplift in the Central Alps with maximum values of 2 mm/year.
- In the adjacent northern zone (Prealpes and Molasse plateau) north of a line Aigle Thun - Lucerne - Altstätten, no clear tendencies can be observed.
- The uplift tendencies in the region of the eastern Jura are confirmed, also including the new data from Southern Germany. The most recent data from leveling surveys in the Hauenstein railway tunnel (Olten - Liestal, Fig. 9-3) indicate that the southern portal is rising at a rate of 0.3 mm/year as compared to the northern one. This could support the idea of ongoing compressional tectonics in the Folded Jura (SCHNEIDER et al. 1992).

The observed relative vertical movements in Northern Switzerland and the adjacent Southern Black Forest, including also the German data (cf. Fig. 9-4), do not show the simple picture which had been expected from geological and geomorphological data.

- The Rhine valley from Basel to Stein am Rhein (for locations cf. Fig. 9-3) appears to mark a contiguous zone of subsidence, with significant values particularly in the area SW of Waldshut. However, this zone of subsidence coincides largely with the occurrence of Triassic salt deposits. The interpretation of subsidence as being the result of natural and/or artificial salt withdrawal is supported by the fact that no significant subsidence is observed in the Laufenburg area, where salt is known to be absent (note the vicinity of the grid reference point).
- Geodetic measurements seem to contradict a recent uplift of the Southern Black Forest relative to the Rhine valley (Basel - Schaffhausen). However, the observed non-uniform tendencies of vertical movements in the Black Forest could possibly be seen as a consequence of block tectonics at a scale that cannot be resolved by the data available, e.g. the single N-S leveling line from Waldshut to Neustadt (Fig. 9-4).



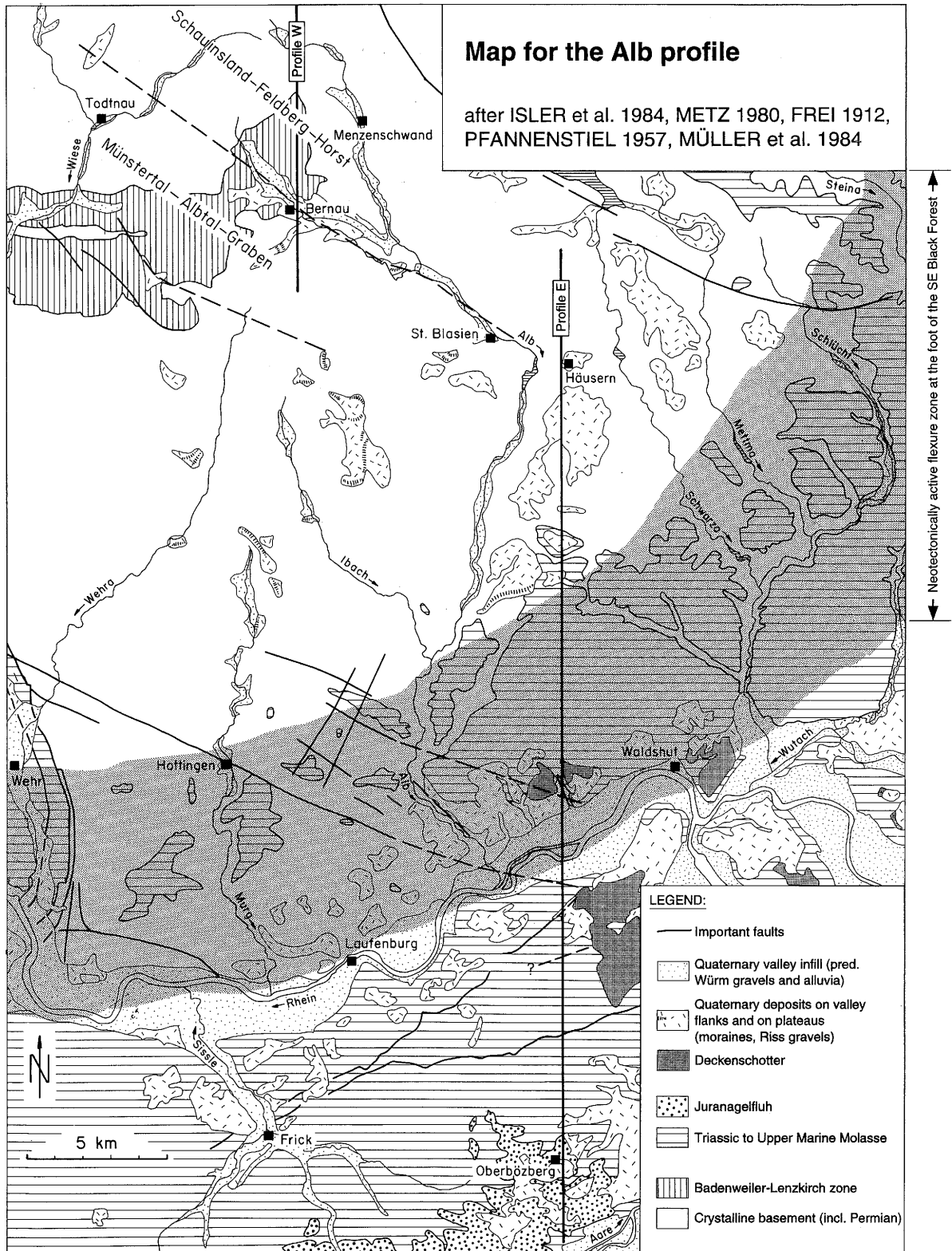
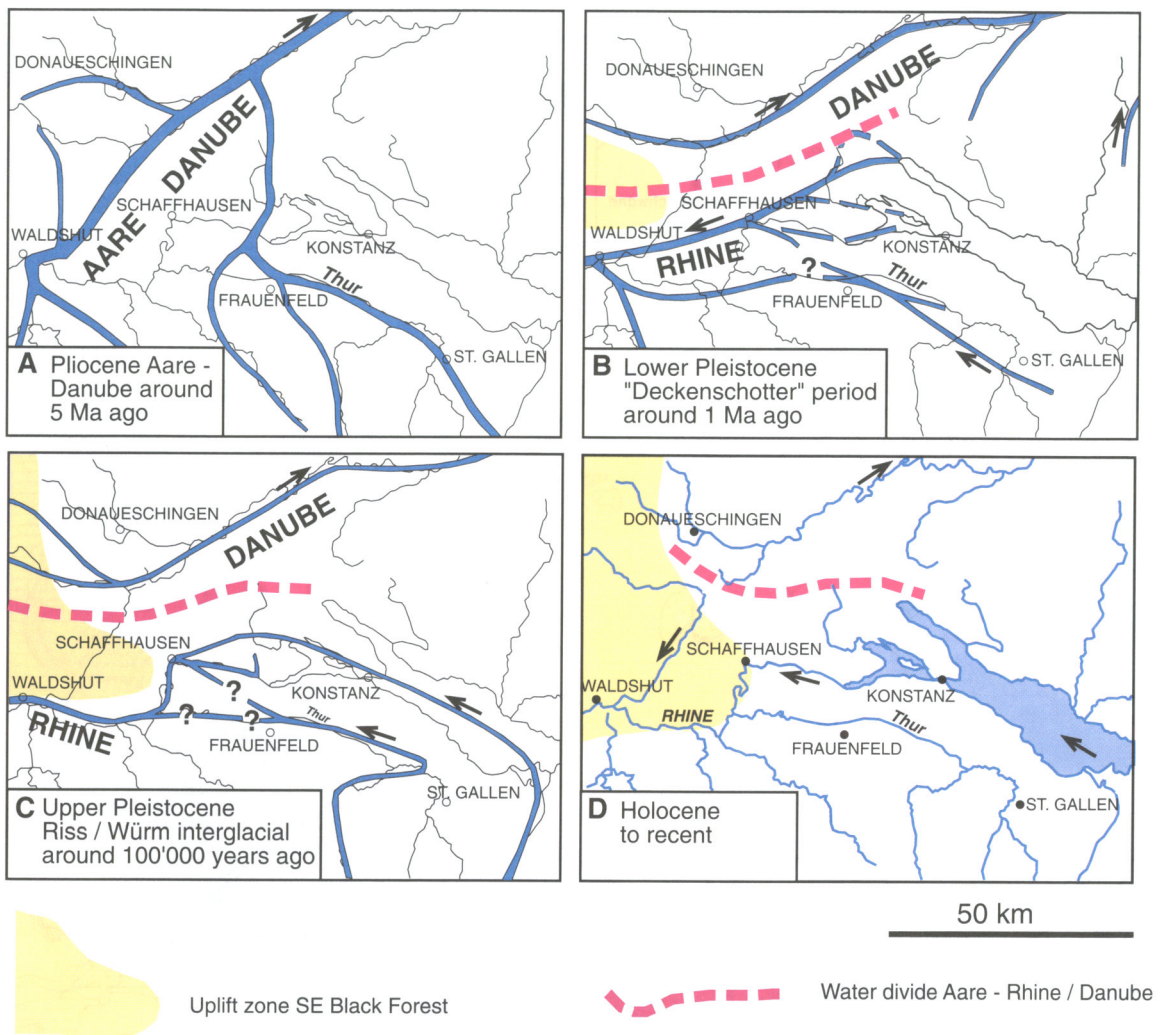


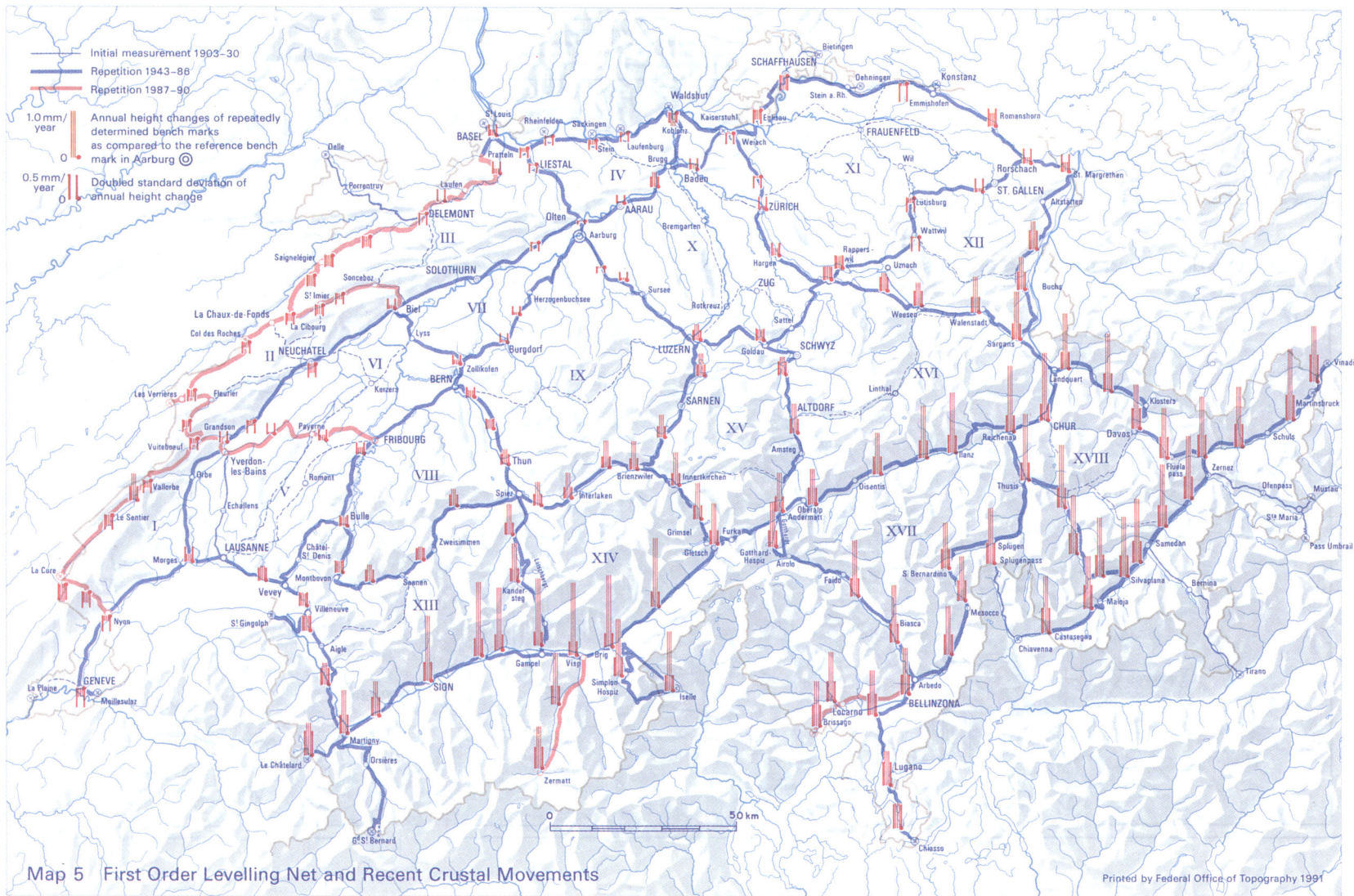
Fig. 9-1 : (continued)



**Fig. 9-2 :** Uplift of the South-eastern Black Forest and the evolution of the Plio-Pleistocene drainage pattern in the region of Northern Switzerland.

- Evidence of active block tectonics at Hercynian-striking faults in the Black Forest can be found further to the north. Repeated measurements on a line through the Hohenzollern Graben (App. 9-1) confirm that this structure is neotectonically active (MÄLZER 1988, VAN MIERLO et al. 1992, JLLIES 1983).
- The W-E line along the Danube through Tuttlingen to Lake Constance (location: Fig. 9-4) again shows a tendency of increasing subsidence towards the E (Molasse Basin), indicating that the eastern part of this line is no longer within the zone of active uplift around the Black Forest dome (Figs. 9-2, 9-4).

**Fig. 9-3 :** First order leveling network and recent crustal movements in Switzerland relative to a reference point at Aarburg based on data from 1903 to 1990 (published 1991 by the Federal Office of Topography).



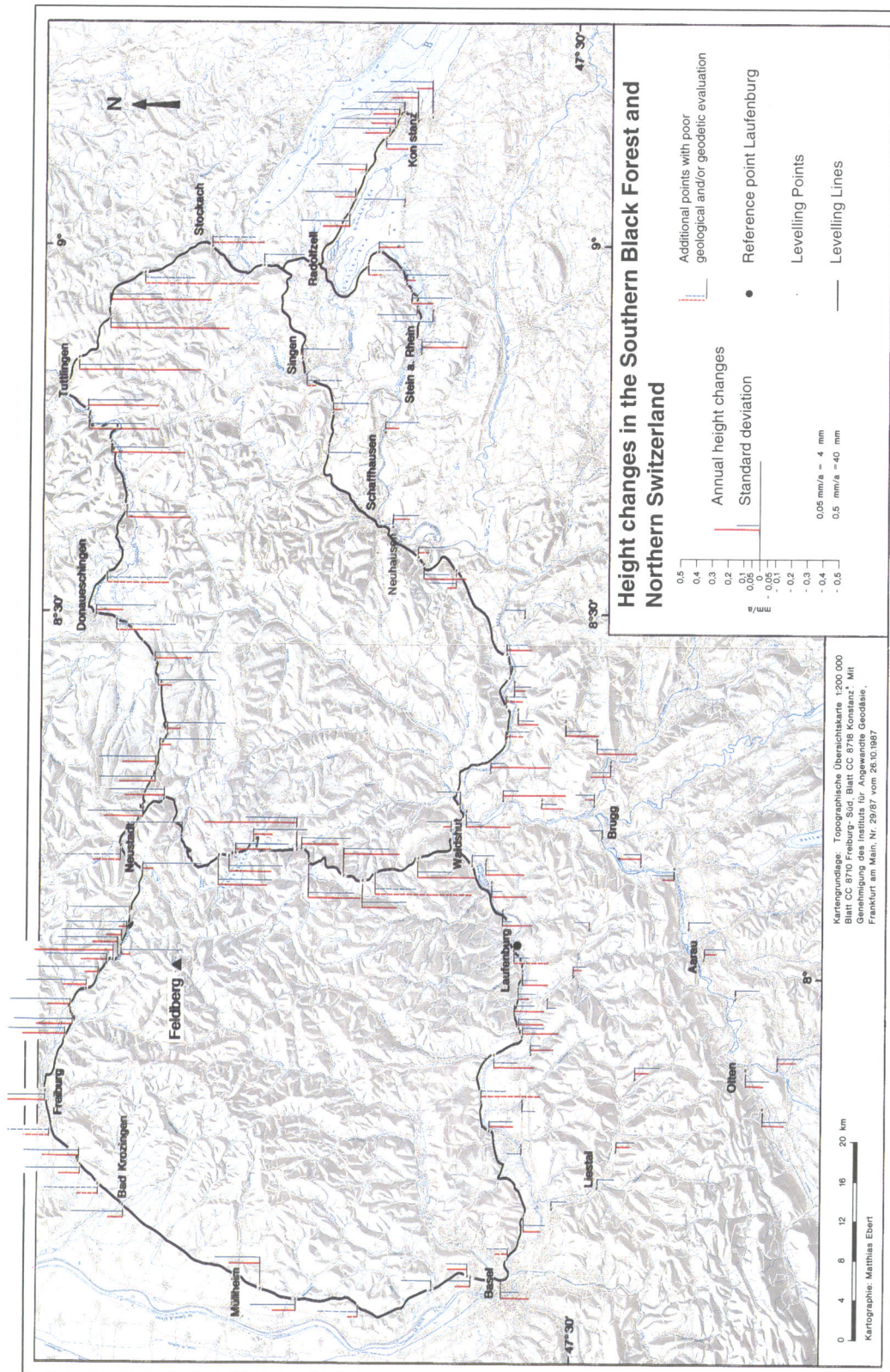


Fig. 9-4 : Precision leveling in the Southern Black Forest and adjacent N Switzerland according to the German leveling programme, calculated for a common reference point at Laufenburg (CH) (from MÄLZER et al. 1988).

The interpretation of vertical crustal movements may leave considerable ambiguities as to related horizontal crustal displacements (e.g. compressional tectonics).

In order to directly investigate possible differential horizontal movements, a GPS network was installed in Northern Switzerland by the Federal Office of Topography in 1988. A first set of measurements was taken in 1988. Repeated later surveys can thus be used to identify horizontal and vertical movements. A second set of measurements is planned for 1995. However, significant results are only expected after a third measurement which will be made several years later.

## Seismicity

Earthquakes provide direct information on the location and intensity of recent endogenous processes (e.g. faulting, stress distribution, etc.) in those sections of the crust where brittle deformation mechanisms dominate. Stresses build up over time in these sections of the crust and are released episodically in the form of earthquakes. If conditions are favorable, not only the location and intensity of (micro)earthquakes can be recorded, but the focal mechanism may be determined and the principal stress directions derived therefrom (seismotectonics). In favorable situations where a local earthquake series (swarm) can be registered, relative localization allows the calculation of the fault plane orientation; sometimes even the direction of displacement can be determined. This is demonstrated in Figure 9-6 for an earthquake series near Läuelfingen (10. - 17.04.1987).

Seismicity therefore provides important information about active tectonic processes in the crust. The knowledge of the actual stress regime and related strain releases shows directly which fault families are most likely to be activated.

The seismicity of Northern Switzerland has been the subject of a long-term Nagra investigation programme (technical background is provided in section 2.8). A series of Technical Reports provides information on methodology and procedures, the results to date and their seismotectonic interpretation (MAYER-ROSA et al. 1983, DEICHMANN & RENGGLI 1984, PAVONI 1984, DEICHMANN 1987, 1990). Today these data are central to a discussion of geodynamics in the investigation area, particularly in connection with the analysis of the recent stress field.

DEICHMANN (1990) summarizes the results on the seismicity of Northern Switzerland (earthquakes of 1977 - 1989) and provides a geological interpretation of these data (cf. Figs. 9-5 and 9-6):

In the few years since detailed earthquake monitoring of Northern Switzerland began, seismicity has been concentrated mainly in two separate zones (cf. Fig. 9-5).

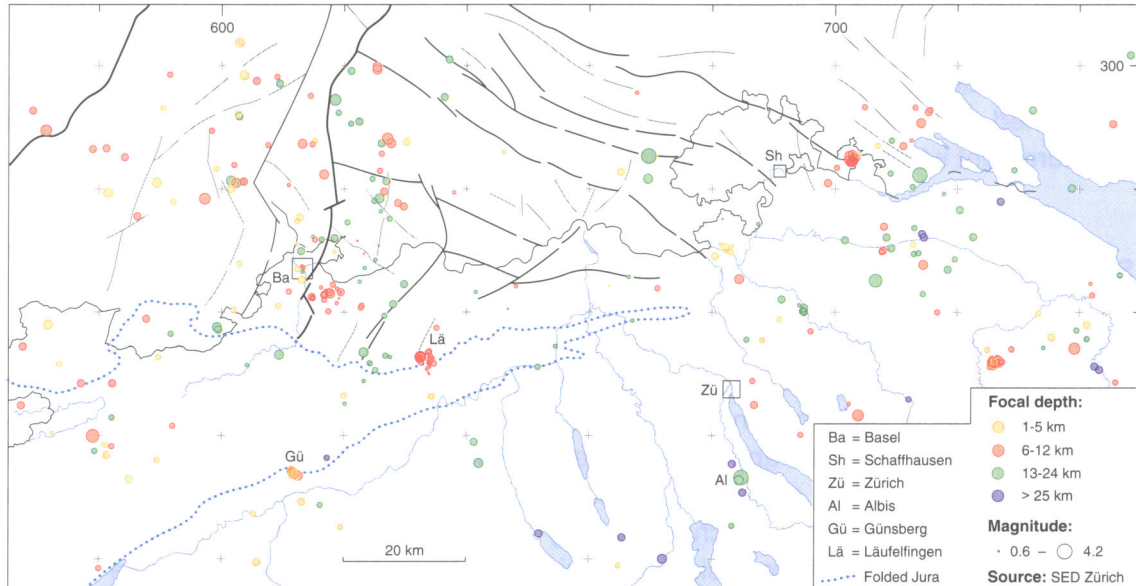


**Fig. 9-5 :** The epicenters of seismicity in Northern Switzerland (1983 - 1993).

The distribution of epicenters in the region of Northern Switzerland clearly shows two areas of elevated seismic activities:

- in the north-west, the region around Basel (Ba) includes the neotectonically active Rhine Graben that extends into the eastward adjacent areas of the Dinkelberg and the Tabular Jura, reaching as far east as Läuelfingen (Lä).
- To the east of a line Schaffhausen - Zurich, in the Molasse Basin, a zone of higher seismic activity extends from the Swabian Alb (Eastern Black Forest) southward to the Alps.

Inbetween is the seismically quiet zone of Central North Switzerland.

The first lies to the north-west of Nagra's investigation area and corresponds to the continuation of the seismically active southern Rhine Graben and the faults beneath the Tabular and Folded Jura in the area to the east of the Rhine Graben (Dinkelberg block, cf. Fig. 5-5).

The second zone comprises north-eastern Switzerland, with a wide field of epicenters which extends from the north-west of Lake Constance into the Zürcher Oberland and further to the south.

In the central part of Northern Switzerland between the two seismically active zones where the station density and thus the detection sensitivity is highest, only isolated and weak events (magnitude < 2) have been observed (Fig. 9-5).

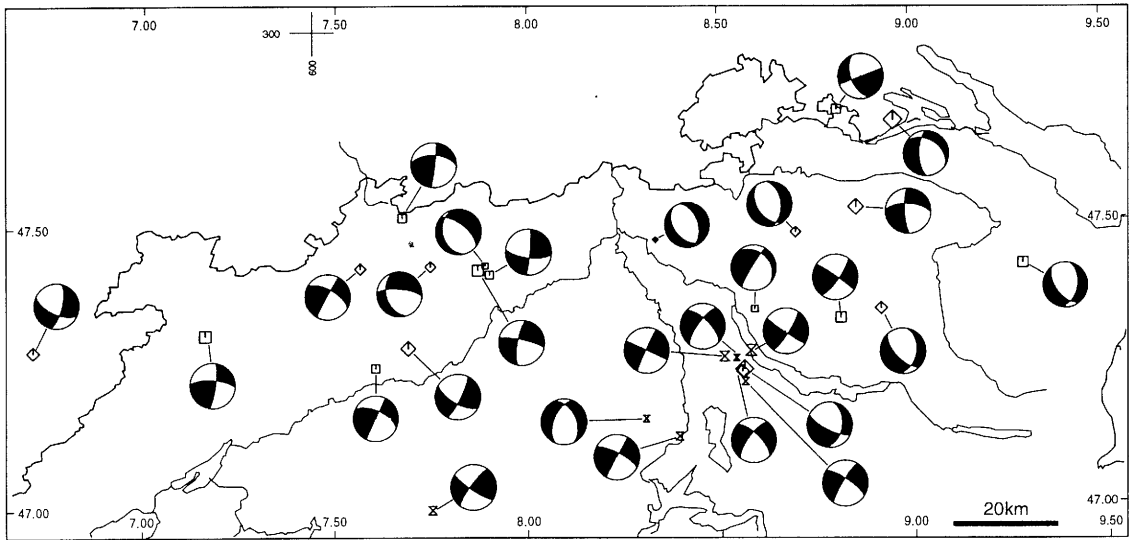
Based on earthquake swarms beneath the Jura south of Basel it has been shown directly that both sinistral N-S ("Rhenish")-striking and dextral WNW-ESE ("Hercynian")-striking faults are active in the crystalline basement of Northern Switzerland (Figs. 9-6). The former are also a prominent structural feature in the sedimentary cover, especially around the Rhine Graben, while the latter can be recognized in the trend of folds and thrusts of the northern Folded Jura (cf. App. 3-1, App. 9-1). Both fault mechanisms are in agreement with the recent NNW-SSE-oriented maximum stress generally observed in Northern Switzerland (e.g. BECKER et al. 1984) and correspond to a WSW-ESE extension (App. 9-1).

A comparison of results obtained in Northern Switzerland with those from south-west Germany provides some interesting information (e.g. BONJER 1992, BONJER et al. 1989):

- Recent microearthquake activity in the Upper Rhine Graben is concentrated in the central part (Karlsruhe region) and in the southern part, the latter including both the Dinkelberg block (with western Tabular Jura) and the Central Black Forest.
- Hypocenter distribution shows clear trends:
  1. Seismicity occurs frequently in the lower crust (from around 10 km to greater depths)
  2. The maximum focal depths beneath the Upper Rhine Graben are significantly shallower than beneath the Black Forest, but in turn, the latter do not reach the depths of the quakes of Northern Switzerland. There is a trend of increasing maximum focal depth from the Upper Rhine Graben via the Dinkelberg-Black Forest into Northern Switzerland.
- The earthquake magnitudes in Germany are of the same order as those in Switzerland.
- The fault plane solutions show similar characteristics in the two regions: wrench faults dominate in the Tabular Jura, the Dinkelberg and in the Upper Rhine Graben, while the Central Black Forest shows an increasing frequency of dilatational fault planes of a "Hercynian", i.e. a WNW-ESE-strike (cf. Hohenzollern Graben, App. 9-1).

### **Measuring the recent stress field**

Possibilities and problems associated with direct measurements of the recent stress field in the upper crust (in exposures and boreholes) are discussed in detail in BECKER et al. (1984) and DIEBOLD & MÜLLER (1985). As the database has not expanded significantly since then, the conclusions in these reports are still valid today.



	Type of displacement	Fault plane solution T: T-axis P: P-axis	Principal stress direction $\sigma_1 > \sigma_2 > \sigma_3$
Thrust fault			
Normal fault			
Strike-slip fault			
Oblique reverse fault			

**Fig. 9-6a:** Fault plane solutions for earthquakes (1977 - 1989) in Northern Switzerland (DEICHMANN 1990).

Different methods for direct measurement of the recent horizontal stress field (overcoring techniques, borehole wall breakouts, horizontal stylolites, hydrofractures, dilatometers etc.) have provided reproducible, consistent results (cf. App. 9-1, in brown colors). However, in order to obtain reliable results, a large number of single measurements has to be made using independent techniques (cf. e.g. MÜLLER et al. 1987, BECKER & PALADINI 1990).

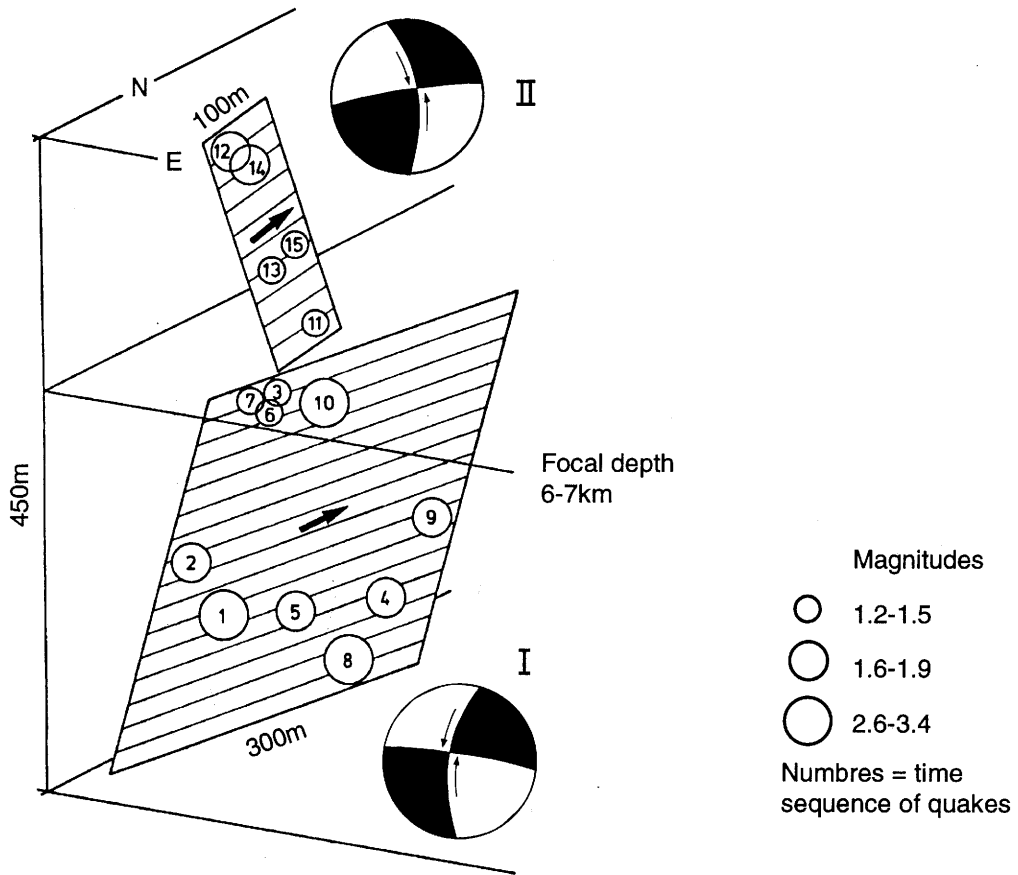


**Fig. 9-6b:** The fault planes of the Läuelfingen earthquakes series (10.04 - 17.04.1987, location: Fig. 9-5).

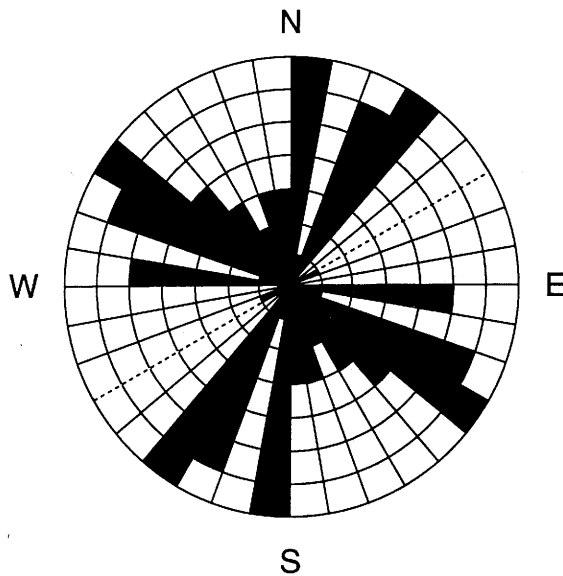


**Fig. 9-6c :** Rose diagram compiling the orientation of fault plane solutions for 28 earthquakes in Northern Switzerland. Clearly the Hercynian (WNW-ESE) and Rhenish (NNE-SSW) strikes dominate.

Analyses of borehole wall breakouts play a key role as they provide not only isolated point values but also a continuous series of measurements over a vertical crustal section - depending on drilling depth and quality of the log. This allows stress distribution to be determined in three dimensions.

There is a direct correlation between lithological anisotropy and local stress deviations. This is particularly apparent in boreholes with alternating rock sequences. The uppermost ca. 300 m of crust are strongly influenced by local stress conditions and show a different fracture mechanism (predominantly surface parallel and less shear fractures). This zone is therefore unsuitable for analyzing the regional stress regime by the breakout method.

Large-scale anisotropies also cause a deviation in the regional stress field; this is shown, for example, by measurements carried out in the Weiach borehole in the PCT. Fault zones also appear to be able to cause a deviation in the stress field (cf. CLAUSS 1987, BECKER & PALADINI 1992).

The supraregional stress distribution in the north-west Alpine foreland shows a maximum horizontal principal stress ( $\sigma_1$ ) trending about NW-SE; a similar situation was also observed in the basement of Northern Switzerland ( $135^\circ \pm 10^\circ$ , PAVONI 1984, 1987).

On a smaller scale, the stress distribution in Northern Switzerland and the surrounding areas is not uniform and individual zones with differing behavior can be identified. These zones correspond more or less to the individual tectonic units. The apparent decoupling of the regional stress field in the basement from that in the sedimentary cover, as observed in the Schafisheim borehole (NAGRA 1987), should be noted. This observation provided the first direct evidence of the long-postulated theory of active décollement of the overburden as a result of distant push (JORDAN & NÜESCH 1989).

#### **9.2.4 Conclusion**

The data available on neotectonics, outlined in the foregoing pages and summarized in App. 9-1, not only indicate for Northern Switzerland and the surrounding areas a setting of ongoing (moderate) tectonic activity but also show a gratifying conformity between different, independently acquired datasets:

- The regional stress fields in the crystalline basement derived from seismotectonics and from in situ measurements show the same orientation, namely a NW - SE direction for (the horizontal component of) the principal stress ( $\sigma_1$ ).  
The decoupling of the stress field in the basement from the one in the sedimentary cover has been noted for the Schafisheim borehole.
- Uplift tendencies as calculated from precision leveling are compatible with the results of the geomorphological analysis.

- In the Southern Black Forest and possibly also in Northern Switzerland young and recent faulting along Hercynian lineaments is indicated by both geomorphology and seismotectonics and fits meaningfully into the recent stress field. Precision leveling data are compatible with these results.

Recalling the geological evolution of Northern Switzerland during the Tertiary (Chapter 3, Fig. 3-5 and 3-6), it becomes apparent that the present day neotectonic setting is generally similar to the tectonic regime of the Middle to Late Miocene some 15 - 10 Ma ago. This conclusion can be taken to indicate a continuing geological evolution for the crystalline basement of Northern Switzerland since the Miocene. Superimposed, but not affecting this basement evolution, is the tectonic event of the Jura folding.

### 9.3 Long-term scenarios of geological development

To allow long-term repository safety to be evaluated meaningfully, it was necessary to formulate so-called bounding scenarios as guidelines. It is probable that the geological future will evolve within the limits set by these extreme scenarios. They were formulated in DIEBOLD & MÜLLER (1985) and are, in principle, still valid for present purposes.

Based on an improved understanding of the dynamics and kinetics of tectonic processes, and in the light of new data available, these scenarios were revised and updated

Two categories of scenarios have been distinguished:

- *Endogenous scenarios (9.3.1)* that deal with the forecast of movements driven by forces emanating from the earth's interior/crust (e.g. faulting, folding and thrusting, regional uplift and subsidence; earthquakes and thermal-magmatic aspects).
- *Exogenous scenarios (9.3.2)* that focus on predicting events and processes at the earth's surface mainly caused by climatic conditions or extraterrestrial forces (e.g. weathering, erosion and sedimentation, meteorite impact).

After the endogenous and exogenous bounding scenarios have been defined, worst case studies are presented: these provide an evaluation of safety-relevant aspects and their quantification in the light of the most pessimistic scenarios.

#### 9.3.1 Endogenous scenarios (Tab. 9-1 and App. 9-2)

Table 9-1 summarizes the key features of bounding endogenous scenarios A and B:

- Scenario A basically assumes that the Alpine orogeny is largely complete and that active crustal shortening is no longer to be expected in Northern Switzerland. The only major processes occurring would be decreasing crustal movements in the form of isostatic uplift.

Tab. 9-1 : Summary of endogenous (tectonic) bounding scenarios A and B.

	<b>Bounding Scenario A</b>	<b>Bounding Scenario B</b>
Alpine orogeny	The Alpine orogeny is complete and active crustal shortening no longer occurs. Driving forces between the Alps and the Upper Rhine Graben are subcrustal and thermal processes: rifting and isostatic movements. The regional uplift of the Alps: continuing isostatic compensation for the pronounced Tertiary thickening of light crustal material beneath the Alps. Uplift fading in time; max. amount ca. 5 - 7 km in 10 Ma. No further décollement in the foreland.	Crustal convergence and compression is continuing in the Alps and the foreland. Advance of the Alpine front, narrowing of the Molasse Plateau by ca. 30 km/10 Ma. Uplifting: central massifs > 10 km, Molasse wedge and Jura 1 - 3 km/10 Ma. Compression and continued shear in European crust along transcurrent faults and thrusts (crystalline basement wedges, future massifs). Inversion of the Permo-Carboniferous Troughs, possibly including the PCT. Décollement of the foreland sedimentary cover and Jura folding continue; dislocation approx. 500 m in 1 Ma. Accelerated erosion in uplift areas.
Upper Rhine Graben and uplift of the Black Forest	The continuing updoming of the Southern Black Forest associated with rifting in the Upper Rhine Graben and is primarily of thermal origin (Mantle diapir). Although a long-term continuing process, the uplift will slowly die out; max. expected uplift ca. 2 km. Uplift in the potential siting regions of the order of max. 200 m (West) to max. 500 m (East) in 1 Ma.	The thermal anomaly around the Upper Rhine Graben (thin crust, rifting) ensures continuing uplift in the region. The Graben itself undergoes transpressive shearing, which causes some segments to be uplifted and others to subside (seismic activity). Thermal and compressive updoming of the Black Forest and the Upper Rhine Graben marginal segments of up to several km in 10 Ma. Regional uplift for next 1 Ma similar to scenario A.
Stress field	The present-day stress field is not an expression of active compressive tectonics, but rather a residual stress which will decrease with time.	The regional stress field is a result of continuing orogenic activity and will prevail in the future.
Regional structures in the crystalline basement of Northern Switzerland	Reactivation of existing fault zones as extensional structures: jointing and normal faulting (kakirites). Preferred strike: Hercynian, in the W also Rhenish.	Reactivation of existing fault zones 1.) as normal faults around the Black Forest dome (horst and graben structures). 2.) as ca. NW-SE-striking dextral and ca. NNE-SSW-striking sinistral shears ( $\pm$ transpressive).
Local structures in potential repository regions	Moderate reactivation of small-scale structures with no formation of new systems. Undisturbed blocks remain stable.	Continuing slight displacements at faults. Movements oriented along existing structures.

- Scenario B assumes that Alpine tectonics are continuing, with corresponding stresses in the crust of Northern Switzerland. This causes active movements at fault zones and further folding of the Folded Jura. The basement will become increasingly involved in the compressive tectonic regime.

Appendix 9-2 attempts to give a schematic overview of scenario B along a profile from the Alps to the Upper Rhine Graben for the time horizons of 1 Ma and 10 Ma. Tectonic activity in the Alps and the northern foreland is expressed by continuing thrusting and folding of an upper crustal slab (shaded red). Its northern edge, which today is marked by the Jura décollement front, will presumably prograde further to the NNW (e.g. also involving the PCT). Below and in front of this thrustured crust, the European foreland is continuously being sheared along pre-existing fault planes. In the area of the southern Upper Rhine Graben, transpressive deformation is expected to prevail.

Seismic activity due to shearing and thrusting will continue in a similar way to today (shaded in violet). The extreme assumption is made that the present-day relief will remain more or less unchanged, i.e. future uplift (green) will be continually compensated by erosion (yellow).

### 9.3.2 Exogenous scenarios

*Future climatic conditions* play the dominating role in the exogenous scenarios for Northern Switzerland.

In recent years topics related to climate have seen a considerable world-wide research effort and a corresponding plethora of relevant publications is now available. Although a number of interrelated factors have been recognized to influence or control the climate, there is as yet no viable global or local model available that would allow a reliable forecast to be made of future climates and also for a time horizon of one Ma, as required for our scenarios. Predicting future climatic evolution still proves to be highly elusive.

The Quaternary, i.e. the last 1.8 Ma of the geological record, in areas at high latitude (incl. Northern Switzerland) is characterized by a quasi cyclic alternation of cold, glacial and interglacial periods, the latter with a temperate climate. During cold, glacial periods glacier ice extended far into the lowlands, with tundra vegetation in periglacial areas.

These climatic cycles have been confirmed as being world-wide by high-resolution measurements of stable oxygen isotopes on (Quaternary) carbonate shells collected from ocean bottom cores and on water samples from ice cores from both polar ice-caps. These data show a consistent pattern of global cyclic temperature changes (CRAYMO et al. 1990). The cycles show the saw-tooth pattern of  $\delta^{18}\text{O}$  concentrations with three prominent isotope cycles which correlate with the model of five primary periods postulated by MILANKOVITCH (1930). This model is based on MILANKOVITCH's premises that principal climate forcing is due to variations in global insolation which in turn is the result of predictably changing orbital parameters.

Based on the model calculations by MILANKOVITCH (1930), we could expect that a new cold period would begin within the next 20000 years and that the next maximum glaciation could occur within 80000 years.

A further unknown quantity in all predictions is the impact of anthropogenic greenhouse gases (CO<sub>2</sub>, CH<sub>4</sub>, etc.).

The general consensus is that anthropogenically induced climate forcing will not be able to delay the next ice age. The last interglacial some 125000 years ago (so-called Riss-Würm "superinterglacial") had higher natural CO<sub>2</sub> values than any pre-industrial measurements, the sea-level was several meters higher, the temperatures were around 1 °C higher than the highest in the Holocene and there were increased precipitation levels in the Sahara. Despite all this, the transition to the Würm glaciation did occur.

A conservative scenario with several future glaciations has to be taken into account for our purposes, but it is impossible to predict the timing of these next glaciations in Switzerland more accurately. If the climatic system does not move into another state, it is highly probable that a cold period will prevail again in Switzerland within 20000 years.

On a local scale, glaciation raises the questions of how intensive the cold periods will be and what erosive effects glaciers will have. Information available in this respect is provided by sediments of the Würm and possibly also the Riss glaciation.

There appears to be a consensus that the pattern of Quaternary ice-ages, i.e. the cyclic alternation of cold and temperate periods, is likely to continue over the next one Ma. One bounding scenario is therefore based on the assumption of further repeated glaciations in Northern Switzerland. Possible consequences of this scenario are outlined in Table 9-2 (Erosion scenario 1) and Table 9-3.

The alternative, i.e. that the present warm period is not just another inter glacial episode but signals the end of the Quaternary ice ages (either due to greenhouse effects or natural causes) has been accounted for by a second set of bounding exogenous scenarios. Three variations in possible climatic conditions have been taken into account, namely the cases of continuing humid, seasonally humid or arid conditions (Erosion scenario 2 cf. Tab. 9-2).

It should be noted that unlikely massive events (major meteorite impact, massive volcanic eruptions, nuclear winter) could, apart from other detrimental effects, trigger a change in the global weather pattern (most likely in the direction of the ice age scenario).

Tab. 9-2 : Principal erosion scenarios.

	<b>EROSION SCENARIO 1</b> Alternating cold and warm periods	<b>EROSION SCENARIO 2</b> Greenhouse effect and no future glaciation		
	<b>Glacials and interglacials</b>	<b>Humid</b>	<b>Seasonally humid</b>	<b>Arid</b>
General climate	Marked long-term alternation between cold periods with permafrost/tundra/cold deserts/ice cover and warm periods with close vegetation cover and a humid-temperate climate.	Humid-temperate to warm-wet climate with permanent close vegetation cover.	Short-term alternating rainy and dry periods. Disperse vegetation.	Dry climate with episodic precipitation. Vegetation minimal to absent.
Hydrology	Glacial: Separation of surface and groundwater in permafrost areas, braided streams with high bedload. Interglacial transition: meltwater streams with high discharge and high bedload. Interglacial (cf. seasonally humid).	Fixed drainage network, high discharge, low bedload. Steady groundwater table, infiltration of meteoric waters.	Shifting drainage network, seasonally dry, floods with high bedload. Strongly fluctuating groundwater tables, episodic infiltration.	Shifting rudimentary drainage pattern of wadi type, sheet floods with extremely high bedloads. Evaporation dominates groundwater regime.
Erosion type	Glacial abrasion and deep scouring during ice ages; marked fluvial erosion at cold/warm period transition (glacial meltwater). Average erosion and moderate denudation during warm periods.	Average fluvial erosion. Intensive deep weathering. Moderate denudation.	Seasonally marked erosion effects, both linear and denudative. No overdeepening; dynamic groundwater regime with strongly fluctuating water tables.	Denudation (uniform erosion) due to aeolian erosion and episodic rainfalls (sheet floods). Ascending water circulation (evaporation).
Erosion effects	Large weathering and erosion potential. Glacial scouring up to several 100 m deep, in places to below erosion base level. Fluvial erosion rate can greatly exceed the rate of regional uplift. Denudation (uniform erosion) max. 100 m/Ma.	Low to average denudation rates < 50 m/Ma. Uplift could be compensated by erosion only in high mountain areas.	Seasonally high; denudation rate < 100 m/Ma. Fluvial erosion continually compensates uplift.	Marked denudation, but generally less than regional uplift. Fluvial erosion along existing valleys.

## 9.4 Safety-relevant aspects

### 9.4.1 Overview

The different endogenous and exogenous scenarios can be combined at random - depending on the weight attached to individual arguments - to provide somewhat incomplete predictions of the future. However, when considering the long-term safety of a waste repository, certain processes which degrade repository performance have to be considered in the most pessimistic manner. Decisive is a scenario which is still plausible and has the most detrimental impact on repository safety; this does not necessarily have to be the most likely scenario (DIEBOLD & MÜLLER 1985).

With respect to the release of radioactive substances to the biosphere from a repository at a depth of around 1000 m, the following processes are likely to affect future repository performance:

- near-field geosphere: perturbation by tectonic/seismic/thermal events;
- far-field geosphere: alteration of hydrodynamic and hydrochemical conditions as a result of erosion and climate;
- near-surface bio-/hydrosphere: changes in hydrological conditions, e.g. drainage pattern, river discharge, in- and exfiltration zones.

These three repository-related zones are affected to a differing degree by the safety-relevant processes/events.

These processes/events are discussed for Northern Switzerland in more detail in the following section and are also quantified wherever possible. Conservative or pessimistic scenarios are emphasized. Tables 9-1, 9-2 and 9-3 demonstrate that the combination of bounding scenario B and the continuation of the ice ages (exogenous scenario 1) will have the most significant impact on the long-term safety of a potential repository in the crystalline basement of Northern Switzerland (giving maximum erosion of overburden and strong perturbation of hydrology).

### 9.4.2 Safety-relevant aspects of the endogenous scenarios

Two bounding endogenous scenarios have been outlined in section 9.3.2. Here, safety-relevant thermal-magmatic and tectonic-mechanical processes will be discussed.

#### *Thermal-magmatic aspects*

Conditions and consequences of **magmatic activity** in the form of intrusions or volcanic activity have already been discussed in detail by DIEBOLD & MÜLLER (1985).

A reactivation of the alkaline volcanism which was active in Kaiserstuhl and Hegau 10 to 20 Ma ago is considered highly unlikely. This continental volcanic activity is associated with weak zones in the crust which allow low-viscosity mantle material to rise directly to the surface. Assuming that rifting continues in the Upper Rhine Graben,

Repository Zone		Near-field geosphere	Far-field geosphere	Hydro-/ biosphere	
Scenario	Safety-relevant aspects	Direct perturbation of repository zone	Changes in hydrodynamic and/or hydrochemical conditions	Erosion and shortening of migration pathways, change of dilution potential	
Endogenous scenarios A & B	Thermal	Plutonism	(XX)	(XX)	
		Volcanism	(XX)	(XX)	(XX)
		Hydrothermal activity, diagenesis	X	X	—
	Mechanical-tectonic	Regional vertical movements	—	X	XX
		Regional horizontal movements in overburden	—		(X)
		Movements along large fault zones	XX	0	(X)
		Movements along small fault zones	X	0	—
		Seismicity	(X)	(0)	0
	Exogenous scenarios	1	Glacial/ interglacial	—	X
Warm - wet			—	0	0
2		Alternating - wet	—	X	X
		Arid	—	XX	X
		Meteorite impact	(XX)	(XX)	(XX)

**Legend:**

- insignificant
- 0 minimal significance or effect
- X important effect
- XX very important effect
- ( ) possibility of occurrence very low

**Tab. 9-3 :** Safety-relevant aspects of the endogenous and exogenous scenarios.

the conditions required for further volcanic activity in this region would at least theoretically be present (e.g. Quaternary volcanism in the Eifel).

Plutonic and/or volcanic activity in the immediate vicinity of a repository could have serious deleterious effects. However, intrusion or extrusion of magma is extremely unlikely in Northern Switzerland for the time period being considered.

The **geothermal anomalies** in Northern Switzerland can be reconsidered in the light of new research results. A relationship between the abnormally high geothermal gradient and the Permo-Carboniferous Trough of Northern Switzerland (PCT) has been postulated repeatedly (DIEBOLD & MÜLLER 1985, RYBACH et al. 1987, KANZ 1987, NAGRA 1988b). The fault systems at the margins of the deep PCT (DIEBOLD et al. 1991), which were partly identified using reflection seismics, appear to promote the rise of deep groundwaters (Fig. 9-7 and Fig. 3-7).

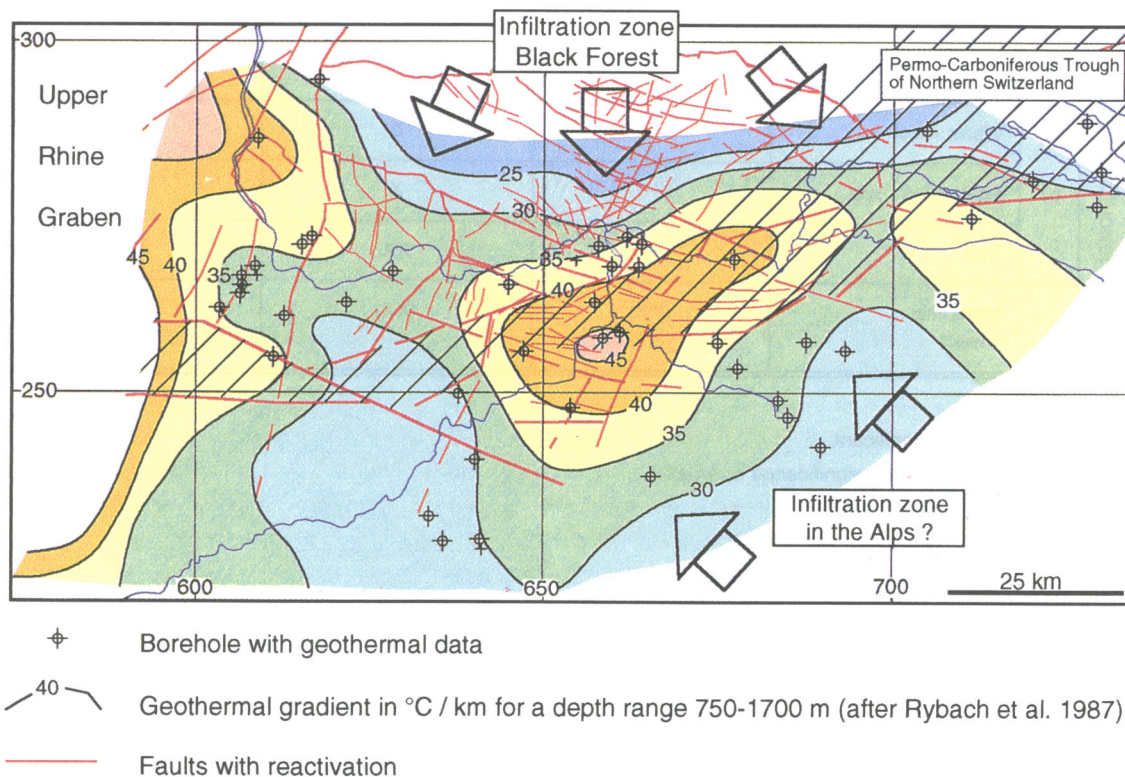


**Fig. 9-7:** Relationship between young reactivated fault pattern and geothermal gradient in Northern Switzerland and the Permo-Carboniferous Trough.

The thermal waters cause an overprinting of the conductive heat flux by convective and possibly also by advective heat transport. Particularly clear examples of these phenomena are seen in the thermal springs to the north and south of the PCT.

Although the geothermal dataset is still tenuous, particularly in the eastern part of the area of interest, the positive geothermal anomaly observed in Central Northern Switzerland appears to correlate, as a first approximation, with the pattern of those faults which form the margins of the PCT and have been reactivated during the Tertiary as normal faults (DIEBOLD et al. 1991: Encl. 28, cf. also Chapters 3 and 5). This implies a relationship between the young fault pattern, reactivated in the Tertiary, and ascending deep groundwaters from the basement (HAUBER 1993). In detail, the local map of heat flow values appears to be modified, however, by the admixture of shallower groundwaters. In Figure 9-7 an attempt has been made to illustrate this situation.

Analogous cases for the relationship between fault zones and locally increased geothermal heat flows have also been demonstrated for certain local areas of the Upper Rhine Graben (e.g. DÖBL 1970).

The results of modeling the maturity of organic material in sedimentary rocks of Northern Switzerland indicate that, in the geological past, an elevated paleo-heatflow existed and that it was mainly due to convective heat transport along fractured (fault) zones (TODOROV et al. 1993). These data lead to the conclusion that the observed thermal anomaly is not a recent phenomenon but one that probably started sometime during the Tertiary.

Based on the above models for the heat flow anomaly of Central Northern Switzerland the following "**geothermal**" **scenario** can be formulated:

- The geothermal anomaly and the related elevated geothermal gradients are expected to persist in principle for the next one Ma and to remain geographically stable.
- The convective and advective components of the heat flow that are controlled by deep and shallow groundwater flow could be affected by fault reactivation and by possible climatic changes (glacial and interglacial periods) as foreseen by the exogenous scenario 1.

#### *Tectonic-mechanical aspects*

The fault pattern and, in particular, its future changes are relevant to safety in three respects (Tab. 9-3):

1. The possibility of direct disruption of the repository by movements along faults. This case requires concrete criteria to allow the extent and the likelihood of such events to be quantified.

2. Structural and lithological discontinuities in the basement represent preferential water flow paths which will act as conduits of groundwater to the repository and from there to the earth's surface. Knowledge of these discontinuities, their dynamics and potential alterations is therefore of key importance both for the near-field of the potential repository and for the regional geosphere.
3. In the form of uplift and subsidence, the regional deformation of the crust influences surface hydrology, e.g. river gradient, shifts in river courses and erosion, but also hydraulic heads, i.e. factors which concern the far-field and the biosphere. These indirect effects of endogenous processes are dealt with in section 9.4.3.

The objective of a longer-term prognosis must be to predict and quantify the dynamics of the overall fault pattern in order to be able to draw conclusions about the future development of the hydrodynamics of the fault systems.

The following general comments can be made about possible future movements at fault zones:

- On a regional scale, the two potential repository sites in Northern Switzerland, particularly the area East, are located in a region of the domal uplift of the Black Forest with horst and graben structures. This results in a tectonic setting with an uplift tendency and overall extension. Normal faulting is expected mainly at discrete pre-existing fault zones. For bounding scenario B there will be additional overprinting by a marked shear component.
- A high density of structural discontinuities, although actually mapped only locally, is expected to prevail in the basement of the entire region. Future crustal deformations will therefore be accommodated by the fault pattern already in existence and new faults or fault zones are most unlikely to develop over the next one Ma.
- Young tectonic dislocations, in accordance with the existing stress field, have been oriented generally along existing faults of "Hercynian" and "Rhenish" strike. The orientation of the regional stress field is expected to remain unchanged within the time horizon of the scenarios. Therefore, future tectonic movements on faults are likely to follow the same predetermined strike directions.
- The future reactivation of existing faults in the uppermost few kilometers of the crust has only a limited geometric relationship with the overall regional stress field. Although active directions can be discerned, neotectonic activity, particularly in near-surface locations, will be determined by local stress conditions which are only known in isolated cases. Lithological discontinuities also play an important role (e.g. PCT).
- It is unlikely that all the fault families contained in the schematic fault model (cf. Fig. 5-7b, Fig. 5-8b) will be reactivated in future.

### Seismicity

Seismicity is low in the area of interest in Northern Switzerland (Figs. 9-5 and 9-8) where the corresponding safety risk is considered to be negligible. Direct disturbance of a sealed repository by seismically active faults can practically be ruled out. In addition, Figures 9-8 and 9-9 indicate that earthquakes to be expected in Switzerland will never exceed a magnitude that could cause serious damage to an underground tunnel system during the operational phase (cf. DIEBOLD & MÜLLER 1985, BERGER 1987).

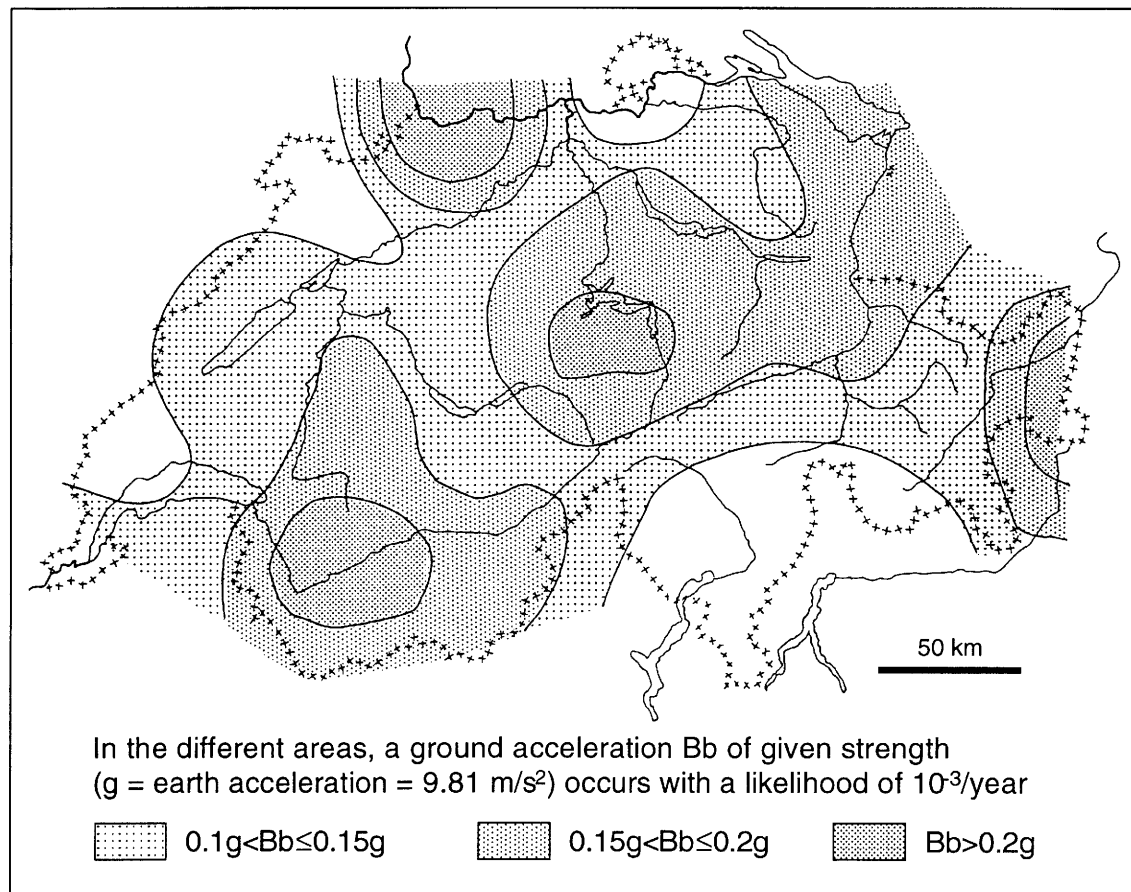


**Fig. 9-8 :** Potential ground acceleration values as expected from earthquakes in Switzerland. In Central Northern Switzerland these values are less than  $0.1 \text{ g}$  (Compiled by MAYER-ROSA in GÜNTENSPERGER 1987).

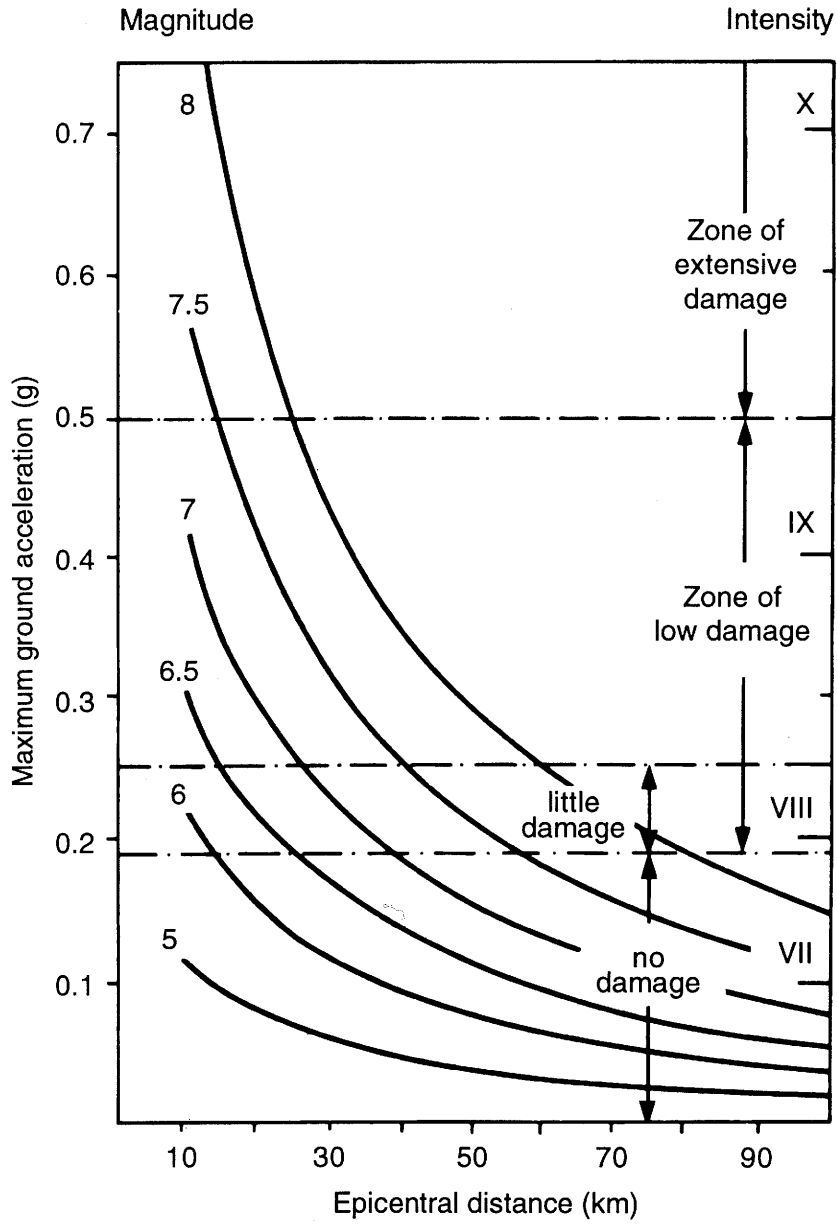


**Fig. 9-9 :** Damage in underground tunnels in relation to earthquake magnitude (from BERGER 1987). Magnitude: Richter Magnitude  
Intensity: MSK Intensity scale.

### *Endogenous scenario - possible quantifications*

Currently available knowledge allows safety-relevant tectonic-mechanical aspects to be roughly quantified for the next approx. 1 Ma. Table 9-4 summarizes the most important conclusions for areas East and West.

The important reference frame required for regional vertical movements can be derived mainly from geomorphological data. Gravel relicts of the Aare - Danube system (Fig. 9-2a), which drained the Swiss Plateau towards the east a few Ma ago, are now located at an altitude of approx. 700 m a.s.l. (Blumberg, HANTKE 1978), as compared to a mean level of the drainage channel of approx. 200 m a.s.l. The age of these gravels is not known exactly but, even if an extreme age of 5 Ma was assumed, this would still give an average uplift of approx. 100 m per Ma. Using fission-track dating, MICHALSKI (1987) obtained average uplift rates for the South-east Black Forest of up to 70 m per Ma for the last 20 Ma. However, we do know from stratigraphic evidence that the uplift in the Black Forest was not in fact uniform over such a long period of time, but accelerated in more recent times (cf. Figure 9-10).

There is also evidence to support the view that the updoming of the Southern Black Forest was, and is not, uniform over the entire area (cf. App. 9-1). The opposing movements at different points of the leveling network in the Black Forest (Fig. 9-4) are probably an indication of active fault block tectonics.

This would indicate that the Southern Black Forest is now being uplifted and that active block faulting is occurring simultaneously. The potential siting regions in Northern Switzerland are located on the edge of this uplift zone (cf. Fig. 3-6). These marginal zones are characterized by flexuring.

Table 9-4 summarizes tectonic displacements for the scenarios A and B. Whereas values for the vertical displacements can be based on field observations, horizontal displacements are merely estimates which are compatible with the two scenarios.

Dislocation in 1 Ma			SCENARIO A		SCENARIO B	
			West	East	West	East
<b>Regional vertical movements</b> <sup>1)</sup>			up to 200 m	up to 500 m	up to 200 m	up to 500 m
<b>Regional horizontal displacement</b>	in overburden		< 100 m		up to 500 m (Jura overthrust)	
	in basement		< 100 m		< 100 m	
<b>Displacement at faults</b>	1st/2nd order faults	horizontal	~ 0		0 - 100 m	
		vertical	1 - 100 m		1 - 100 m	
	higher order faults	horizontal	~ 0		0 - 1 m	
		vertical	0 - 1 m		0 - 1 m	

<sup>1)</sup> only relative uplift considered

**Tab. 9-4 :** Endogenous scenarios (time horizon 1 Ma): quantitative estimates of total displacements.

Scenario B (App. 9-2, Tab. 9-1) is taken first: bounding scenario B assumes continuing horizontal compressive strain which necessarily implies corresponding shear, i.e. the horizontal movements are a consequence of this scenario. Indirect evidence for neotectonic wrench faulting at shallow crustal levels is provided only by seismotectonic data (e.g. Fig. 9-6). However, the total displacement is thought to be distributed over a large number of higher order faults so that no discrete neotectonically active wrench fault zones can be singled out.

The assumption of horizontal displacement rates of up to 100 m/Ma at active major fault zones appears to be justified under scenario B.

Scenario A (Tab. 9-1): for vertical and horizontal movements, the values indicated in Table 9-4 are the same as for scenario B. This conservative assumption is based on the premise that a future accelerated uplift of the (Southern) Black Forest would induce lateral displacements between adjacent basement blocks (radial gravitation from the uplift center outwards).

#### **9.4.3 The safety-relevant aspects of exogenous scenarios**

Exogenous processes deal mainly with the effects of erosion and weathering at the earth's surface and the shallow geosphere. These effects are reflected in changes in the hydrodynamic conditions in the far-field of a repository and of the hydrology in the biosphere (drainage pattern, river discharge, etc. cf. Tab. 9-3).

Exogenous processes, apart from extraterrestrial impact, are controlled by the prevailing climate. Therefore, in order to quantify the future effects of such processes, two bounding scenarios for possible future climates have been presented in section 9.3.2 above: under bounding scenario 1, the Quaternary ice ages will continue into the future and under bounding scenario 2 an end has come to ice ages and future climates will remain temperate to warm.

The following discussion emphasizes the effects under the ice age scenario, which is more conservative than bounding scenario 2 as far as repository safety is concerned. Results and quantifications are summarized in Tables 9-3 and 9-5, respectively.

##### *Morphological effects of future ice ages*

A future ice age will be the most decisive event in terms of bringing about morphological changes within a relatively short time period. Generally speaking, the erosion events of a continental glaciation comprise scouring by glacier ice, subglacial meltwater erosion as well as fluvio-glacial erosion and increased soil removal in non-glaciated areas (increased precipitation, desert formation, etc.) and the effects of local outbreaks of glacier lakes. The potential effects of glacial erosion in Switzerland can be estimated using examples from the Holocene and the Pleistocene.

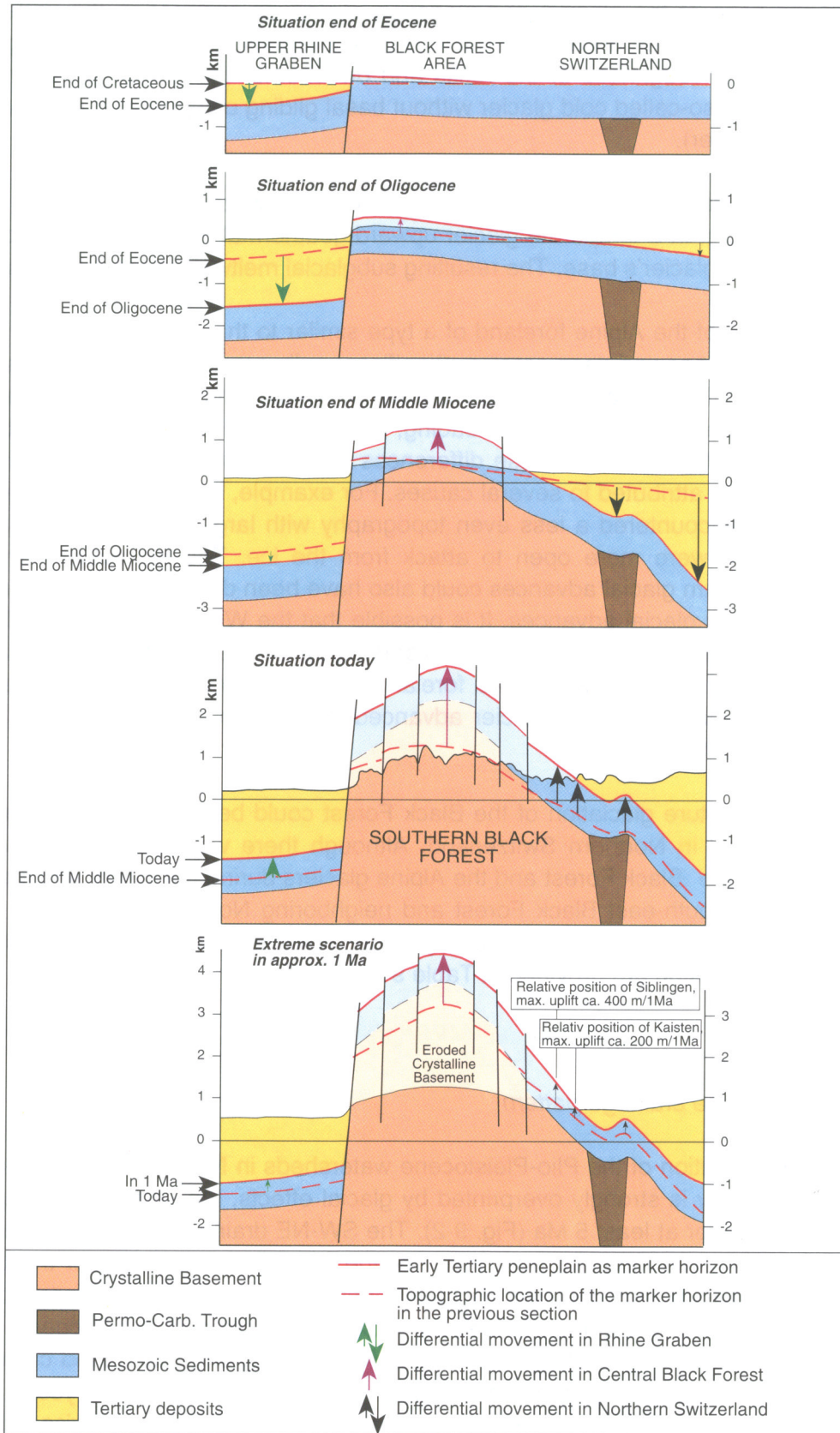


Fig. 9-10 : Erosion history for a NW-SE section through the Black Forest.

Deep erosion by glaciers consists of a combination of grinding (by rock material carried along at the base of the glacier) and planation of uneven surfaces in the underlying rock. The form of erosion depends in each case on the geology of the underlying rock, the fracturing and roughness of the rocks and on whether the glacier is frozen right down to its base (so-called cold glacier without basal gliding components) or not (warm or temperate glacier).

During past glaciations, the foreland ice in Northern Switzerland was made up of temperate glaciers. In a temperate glacier upward geothermal heat flow is balanced by ice melting at the glacier's base. The resulting subglacial meltwaters activate erosion.

Future glaciation of the Alpine foreland of a type similar to that of past ice ages would certainly result in renewed deep erosion. Significant gully erosion is generally assigned to the Riss (penultimate) and older glaciations. In Switzerland, most interglacial lake deposits have been subject to glacial loading, i.e. they have been passed over by the Würm glacier (last glaciation). These differences in the erosion behavior of individual glaciations can be attributed to several causes. For example, it is possible that the pre-Würm glaciers encountered a less even topography with large unconsolidated zones (fractures) which were more open to attack from the ice. The ice volume and the number of maximum glacial advances could also have been different, since ice erosion only occurs during glacial advances. It is possible that the Würm glacier had only one real maximum advance (around 200000 years ago), whereas the older glaciations advanced several times well into the foreland with full erosion potential. It is also assumed that, when the Würm glacier advanced, some lake basins were only partly filled with sediments.

The extent of a future glaciation of the Black Forest could be of key importance for a repository located in Northern Switzerland. Although there was probably an ice-free zone between the Black Forest and the Alpine glaciers during the Würm and the Riss glaciations, the South-east Black Forest and neighboring Northern Switzerland could conceivably also be affected by erosion by future Black Forest glaciers. Estimates of relevant glacial erosion are provided in Table 9-5.

#### *Development of the drainage pattern*

Although the evolution of the Plio-Pleistocene watersheds in Northern Switzerland and Southern Germany is strongly overprinted by glacial effects, the same basic drainage pattern persisted for at least 5 Ma (Fig. 9-2). The SW-NE drainage axis Rhine-Danube, Fig. 9-2a), which was inherited from the Miocene (mica sand channels of the Upper Freshwater Molasse), has retained its basic orientation (basin-axial drainage of the Alpine foreland). The most important event was the disruption of the Pliocene Aare-Danube river system (Fig. 9-2b,c). A new Late Pliocene regional watershed came into existence at the SE foot of the Black Forest clearly as a result of a young uplift extending to the ESE (Fig. 9-2b-d). Subsequently drainage of the Swiss Plateau remained oriented towards the NW, initially via the Bresse to the Mediterranean (Late Pliocene Sundgau gravels) and later via the Upper Rhine Graben to the North Sea.



vegetation-free landscape. Lateral meltwater courses can develop, within a fairly short time, into major drainage channels and thus have a lasting influence on the drainage pattern.

Subsequent (tangential) water courses on the southern and south-eastern slopes of the Black Forest show a displacement trend towards the S and SE. This is caused by the ongoing domal uplifting of the Black Forest that is likely to continue into the future. In the (potential repository) area West, the course of the Rhine could also be affected by this southward shift which is estimated at some 2 km in one Ma. Linear river erosion will deepen the Rhine valley, exposing a large surface of the gently S to SE dipping basement surface. The hydrodynamic implications of this scenario have been investigated by modeling. Results are shown in Figure 9-11a, where the "Old" and "New" (future) position of the river Rhine are indicated; the "New" course of the Rhine is close to the present position of the Leuggern borehole.

#### *Fluvial erosion and denudation*

Over long periods of time, fluvial erosion and denudation result in peneplanation of a landscape. A significant topographic relief will only remain intact if endogenous processes are simultaneously active. Figure 9-10 illustrates a very conservative scenario in which the Central Black Forest is uplifted by around 1 km in 1 Ma relative to Basel. The prediction of a maximum **fluvial erosion** assumes that removal keeps pace with uplift, i.e. there are no new nickpoints in river courses or oversteepening of the relief. However, examples from the South-east Black Forest indicate that nickpoints and oversteepened river courses did form as a result of neotectonic activity (Fig. 9-1; cf. HALDIMANN et al. 1984, HUBER & HUBER-ALEFFI 1990, DIEBOLD & MÜLLER 1985). It is therefore safe to assume that fluvial erosion for a given constant erosional base level will not exceed the maximum expected amount of uplift.

The extreme values for erosion to be expected in the siting areas of Northern Switzerland are listed in Table 9-5. A direct one-to-one correlation with the endogenous scenario is made such that the maximum amount of erosion is equated with the values in Table 9-4 for maximum uplift.

**Denudation**, vaguely defined as the diffuse and spatially extensive leveling (by erosion) of the land surface, is less effective than (linear) river erosion in degrading an existing relief. The quantification of a general denudation rate for Northern Switzerland, that depends on such factors as climate, vegetation cover, relief and subsoil lithology, etc., proves to be quite elusive. The denudation rates, i.e. 50 to 100 m/Ma given in Table 9-5, have been taken from DIEBOLD & MÜLLER (1985, p. 95). Their estimate is based on a comparison with denudation rates actually measured in the Swiss Alps.

## 9.5 Evaluation of potential changes in groundwater flow conditions in the crystalline basement

As a result of continuing action of geological processes, the future surface geology of Northern Switzerland will be different from the present one. The influence of these changes, after 1 Ma, on the regional flow pattern of deep groundwaters in the crystalline basement was investigated using simulations with an appropriately modified version of the regional groundwater flow model described in Chapter 8. A detailed discussion of the modeling results can be found in VOBORNY et al. (1993b).

The following geological conditions (cf. above long-term scenarios) were considered for the investigation of possible influences on the groundwater flow conditions in the crystalline basement:

- 1) Regional uplift of the Black Forest (continuing domal uplift): the center of the uplift is located in the Feldberg massif, while the PCT approximately represents the southern edge of the uplift area and is considered to remain stable.
- 2) River pattern: a change in the river network is associated with the uplift. The Rhine and Wutach rivers are generally displaced towards the south. For the Rhine this S-shift will amount to 2 km. It is assumed for modeling purposes that fluvial erosion keeps pace with uplift, so that the valley floors of the larger rivers (e.g. Rhine) remain at their present level.
- 3) Erosion: a ribbon of the Mesozoic basement cover, corresponding in width to the S-shift of the Rhine or Wutach river, will be eroded. Simultaneously, the outcrop line of the crystalline basement migrates towards the south and the area of "open" crystalline basement in the model thus becomes larger.

The effect of other erosion processes, such as removal of the Quaternary valley fills or denudation (max. 100 m), are not expected to be hydraulically relevant for the groundwater flow in the crystalline basement.

The regional hydrodynamic model (section 8.4) was appropriately modified to accommodate the above changes in topography and geological conditions. The changes correspond to the values in Table 9-5.

The results of the hydrodynamic model simulation are presented below and the general effects on the flow regime in areas East and West are highlighted.

### **Area West (Böttstein - Leuggern - Kaisten)**

The amount of uplift in the area between the northern margin of the PCT and the present-day Rhine valley is very slight. However, the outcrop line of the crystalline basement is displaced some 2 km towards the south and new drainage conditions will be created. The groundwater in the crystalline basement, which is currently confined

beneath the Mesozoic of the Tabular Jura, will exfiltrate along the deepest free surface (roughly between present Leuggern and Kaisten). With the shift of the regional drainage channel (Rhine) towards the south and its simultaneous deepening relative to the basement surface, the exfiltration conditions prevailing in the area West will generally be enhanced, i.e. the upward vertical gradients will become more marked as compared to values observed presently in Böttstein, Leuggern and Kaisten. These conditions are illustrated for a N-S section from the Black Forest to Böttstein (section A-A' in Fig. 9-11; as compared to section A-A' in Fig. 8-10).

Thus, the possible influence of the assumed geological changes on the flow pattern are not significant; no fundamental changes are expected, but vertical gradients will be enhanced.

### **Area East (Siblingen)**

As a result of uplifting and south-vergent tilting of the crystalline basement, the area around Siblingen takes the form of a high with an infiltration regime prevailing. The outcrop line of the crystalline basement will migrate southwards. The Wutach river will then flow over its whole length on crystalline basement and will act as regional drainage for the South-east Black Forest. Possible hydrodynamic conditions in area East are shown on section C-C' in Figure 9-11 (cf. section C-C' in Fig. 8-10).

In the model the water divide between the Wutach river and the Rhine in the region of Schaffhausen is located to the north of Siblingen so that this area will drain towards the SW into the Rhine. However, the alternative not taken into account is a possible lateral displacement of the Wutach towards the south, which would fundamentally change flow conditions. Such a displacement would bring Siblingen into the catchment area of the Wutach river and into the immediate vicinity of the exfiltration zone. As a consequence a potential repository site might better be located as far south as possible.

To summarize, it can be stated that significant changes in the flow regime could occur in area East; under certain future conditions this could result in extremely short flow paths and large hydraulic gradients.

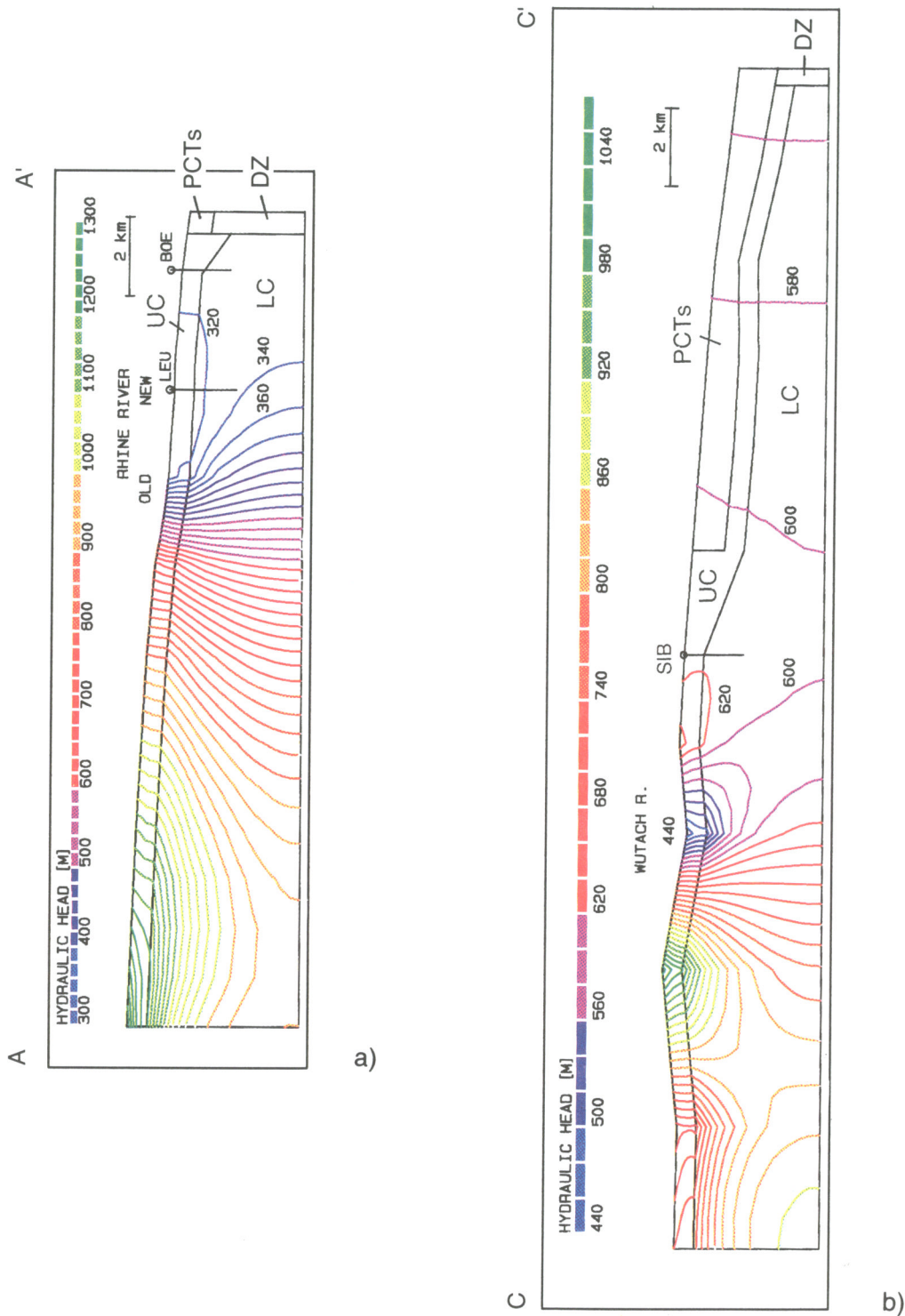


**Fig. 9-11 :** The effects of future changes in surface geology on hydraulic heads in area West (a) and area East (b):

Distribution of simulated hydraulic head in two sections; regional hydrodynamic model modified according to scenario B (VOBORNY et al. 1993b); section locations are shown in Figure 8-10 where hydraulic gradients are given based on present geological conditions.



## 10 GEOLOGICAL DATABASE FOR SAFETY ASSESSMENT MODELS AND REPOSITORY DESIGN

### 10.1 Overview of geological data requirements

The Swiss repository system for high-level radioactive waste consists of a deep mined repository in which the waste packages (massive steel canisters containing vitrified waste) are horizontally emplaced in tunnels backfilled with highly compacted bentonite (cf. e.g. NAGRA 1994a). For the expected evolution of the repository system, the steel canisters will slowly degrade and, after a period of time, radionuclides will be released into deep groundwater by diffusion through the bentonite backfill. Quantitative evaluation of the extent and consequences of such releases utilizes a chain of models which evaluate the flux of water through the repository, the corrosion/alteration/erosion of the engineered barrier system<sup>1)</sup>, the release of radionuclides from the near-field<sup>2)</sup>, their transport through the geosphere to the biosphere and the consequent radiological doses to man. All of these models require site-specific geological input (NAGRA 1994a).

#### 10.1.1 Geological input for near-field modeling

Nuclide release from the engineered barriers is constrained by the hydraulic conditions at the bentonite / rock interface and by the prevailing geochemical conditions.

Nuclide transport through the bentonite backfill occurs predominantly by diffusion due to the very low permeability of the backfill. The rate of such transport is, however, influenced by the rate of nuclide transfer at the outer surface of the bentonite, which, in turn, depends on the water flux through the surrounding rock. This emphasizes the importance of low hydraulic conductivities in combination with low hydraulic gradients in the repository environment. In addition to total groundwater flux, the possibility of localized zones of high water velocity needs to be considered in order to evaluate the potential for erosion of the bentonite barrier.

Groundwater chemistry (predominantly Eh, pH, ionic strength, concentration of organic and inorganic complexing ligands, colloids) plays an important role in establishing the near-field chemistry which, in turn, defines the solubility and sorption properties of radionuclides which are used directly in the safety assessment model chain. This chemistry also constrains the stability of the bentonite and the longevity of the steel canister.

---

1) glass matrix, steel canister and bentonite backfill

2) engineered barrier system plus the near-repository host rock

### 10.1.2 Data for geosphere transport models and biosphere modeling

The choice of models for geosphere flow and transport modeling depends on the features and processes that are considered to be significant at the potential repository site. After the choice of the model, a reference database must be defined to provide input for the model. The database contains data from geology (geometry of water-conducting features, mineralogy, porosity), hydrogeology (flow rates, flow vectors) and geochemistry (reference hydrochemical compositions and redox states, sorption).

In certain cases, averaging of natural variability is justified. For example, small-scale variability of the mineralogies of fracture infills averages out because the flow path is very long with respect to mineralogical heterogeneity. In other cases, ranges or more than one single dataset are specified.

Figure 10-1 gives an overview of the processes that are taken into account in the geosphere transport model and also indicates what kinds of geological, hydrogeological and hydrochemical data are needed to quantify these processes. Advective transport is thought to occur in open fractures or channels within water-conducting features. Hydraulic input data determine flow velocity through the fractures/channels and the length of the flow path between the repository and the groundwater discharge area. In order to quantify retardation processes (such as sorption and matrix diffusion) in fracture infills and wallrocks, the mineralogies and open (i.e. diffusion-accessible) porosities of all rock domains must be specified. Hydrochemical data<sup>1)</sup> are used to calculate maximum concentrations of solubility-limited radionuclides in the groundwater. Groundwater chemistry also constrains the sorption properties of radionuclides on wallrock minerals.

As radionuclides are transported from a low-permeability host rock into aquifers or surface waters, dilution will occur. The extent of dilution is dependent on the contrast in fluxes involved and can be many orders of magnitude - resulting in an equivalent reduction in nuclide concentrations. Therefore, quantitative hydrogeological information is also needed on the exfiltration region and on aquifers along the flow paths from the repository to the exfiltration region.

Finally, the geography and human lifestyle in the exfiltration zone must be characterized. These factors are based on present-day conditions, but variations take into consideration the effects of potential climatic and geomorphological changes.

---

1) These data are not used directly in the safety assessment model chain, but are used to check if precipitation or colloid formation could occur at the near-field/far-field interface.

### 10.1.3 Data for repository design and construction

Rock mechanical data are needed for shaft and tunnel design and to evaluate constraints on how closely together emplacement tunnels can be constructed, which, together with temperatures, defines the waste emplacement density. Other physical rock properties of importance are those used to model the thermal transient, which results from the radiogenic heat output of the waste, i.e. local geothermal gradient, thermal conductivities and heat capacities of the host rock.

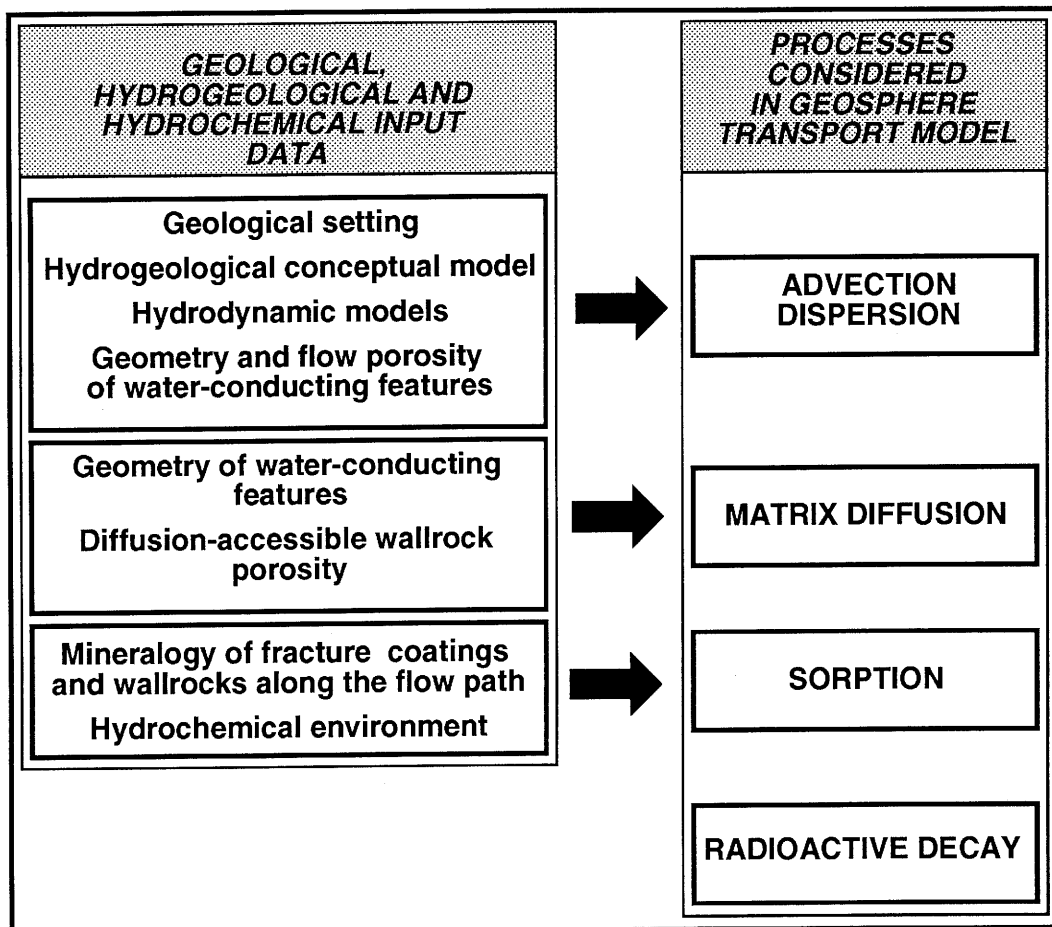


**Fig. 10-1 :** Processes taken into account in the safety assessment of geosphere transport and the relation to input data from geological, hydrogeological and hydrochemical investigations.

## 10.2 Groundwater flow

The principal hydrogeological data requirements for the safety analysis are the descriptions of various hydraulic and geometric parameters in the vicinity of a repository and along pathways to the biosphere. These parameters include 1) the distributions of properties of small-scale water-conducting features that intersect a repository tunnel segment, 2) descriptions of flow pathways leading from a repository, 3) distributions of groundwater fluxes through the water-conducting features, and 4) estimates of total flux through the repository area. In addition, the dilution of groundwater as it flows from the low-permeability domain to domains of higher permeability and eventually to the biosphere is an important parameter for biosphere modeling in terms of evaluating the consequences of any releases from the geosphere.

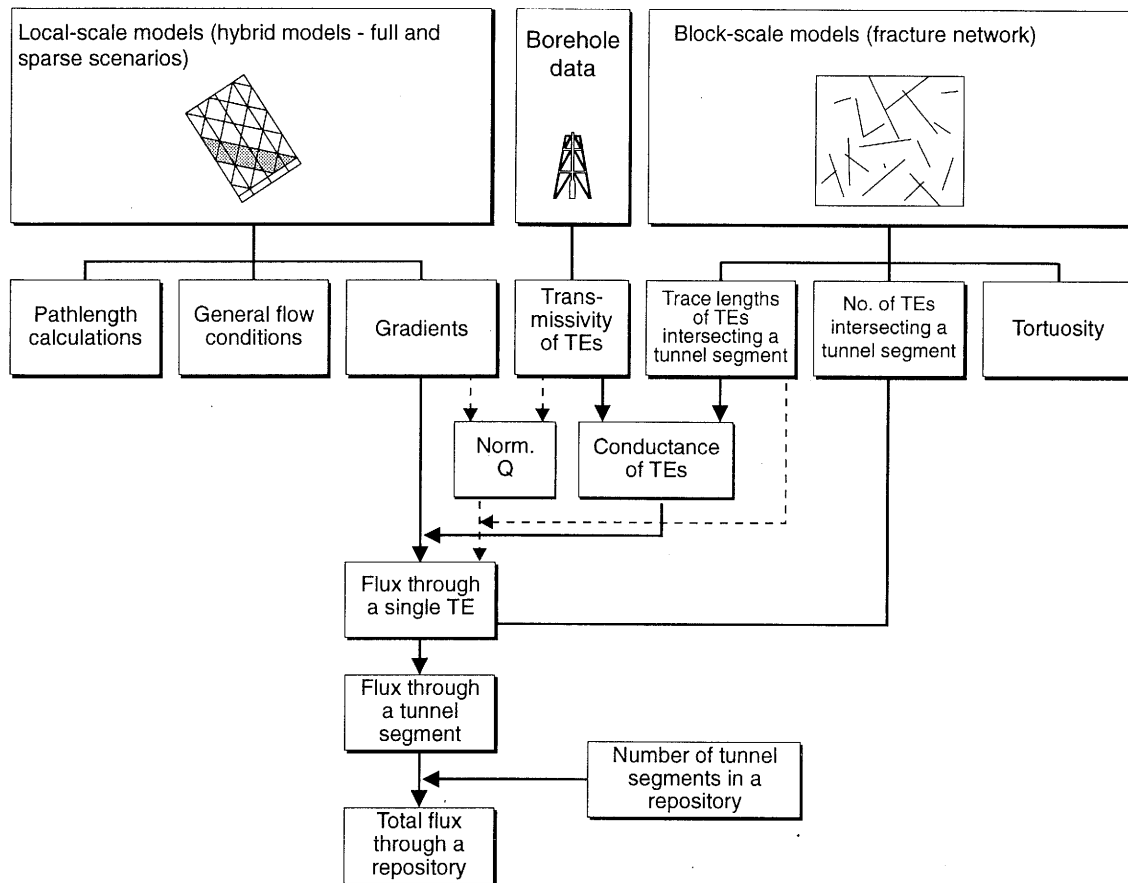
Borehole data and groundwater flow models on various scales were used to estimate the distributions of geometric and hydraulic properties of small-scale water-conducting features, characteristics of flow paths, and distributions of hydraulic gradients, as described in Chapter 8. These serve as the basis for estimating the distributions of groundwater fluxes and the expected dilution, as described below.

From a hydraulic standpoint, as described in section 8.2.3, no systematic differences occur with respect to hydraulic properties (transmissivity, storage coefficient) among the three types of water-conducting features; for flow analyses, they are therefore all treated as transmissive elements with similar geometric and hydraulic properties.

### 10.2.1 Area West

#### Approach and assumptions

The general approach for deriving various hydrogeological inputs for safety analysis for area West is shown in Figure 10-2 and is termed the geometric approach. One key hydrogeological input is the groundwater flow through typical blocks of the low-permeability domain of the crystalline basement. The trace length distributions and number of transmissive elements in tunnel segments 500 m long and with a cross-section of 5 m x 5 m were generated from fracture network models, as described in section 8.6. The hydraulic characteristics, namely the effective transmissivity of transmissive elements, were assigned from distributions of transmissivity of transmissive elements derived from borehole data (section 8.2). The hydraulic gradient applied to flow in a transmissive element was taken from hydraulic gradient distributions in low-permeability blocks from the local-scale model (cf. section 8.5). As shown in Figure 10-2, the distributions of transmissivity of transmissive elements were combined with distributions of trace lengths of individual transmissive elements that intersect the tunnel segment to obtain the distribution of conductances of the individual elements. Conductance ( $\text{m}^3/\text{s}$ ), resulting from the statistical multiplication of transmissivity with trace length, gives the total amount of flow that will be transmitted through the fracture or this volume of rock for a unit gradient. The conductance distribution was combined with the distribution of hydraulic gradients to obtain the distribution of groundwater flux through individual transmissive elements.



TE = transmissive element (numerical representation of water-conducting features)  
 Norm. Q = normalized flux in TEs (per unit length)

**Fig. 10-2 :** Geometric approach for the derivation of the hydrogeological input for safety analysis, area West (VOMVORIS et al. 1992).

This flux distribution was combined with the distributions of the numbers of transmissive elements (from block-scale models) to obtain the distributions of fluxes through a 500 m tunnel segment. Finally, the number of tunnel segments, as expressed in the repository design, was used to obtain an estimate of the distributions of fluxes through the entire repository.

An interim result of the calculations is the normalized flux, which corresponds to the flux per unit length in a transmissive element. For this purpose, length is defined in a direction perpendicular to the direction of the flow. The normalized flux is estimated from a statistical multiplication of the transmissivity and gradient distributions. A further statistical multiplication with the trace length distribution provides the same distribution of groundwater flux through individual transmissive elements, as described above.

This process was carried out for the two scenarios of spacing, or hydraulic significance, of major water-conducting faults (cf. section 8.5), the full scenario and the sparse scenario. In the full scenario, the major water-conducting faults are relatively closely spaced, and intervening blocks of the low-permeability domain of crystalline rock are relatively small. In the sparse scenario, the spacing of hydraulically active faults is greater and relatively large blocks occur. The two scenarios were simulated in different runs of the local-scale model, resulting in two sets of distributions of hydraulic gradient for area West.

Groundwater fluxes through a tunnel segment and through the whole repository are dependent on the direction and magnitude of hydraulic gradient, the size, number and orientation of transmissive elements, the transmissivity distribution within each transmissive element and the number of tunnel segments planned for the repository. Based on the reference waste inventory, the repository is considered to comprise 30 tunnel segments, each 500 m long. The analysis of flux through an emplacement tunnel segment is based on several assumptions that overestimate the flux values (VOMVORIS et al. 1993c). The most important conservative assumptions are:

- In the analysis, the gradient assigned to each transmissive element is independent of its conductance. In reality, the gradient is expected to be inversely proportional to the transmissive properties, due to the flow dynamics. With the geometric approach, highly transmissive fractures may thus be assigned gradient values that are unrealistically large, which leads to overestimated flux values.
- All transmissive elements that intersect an emplacement tunnel segment are assumed to connect to a major water-conducting fault or to the higher-permeability domain; no network effects (e.g. dead-end transmissive elements) are thus considered. Combined with the assumption above, the flux through a tunnel section will be overestimated. A study performed by LANYON & HOCH (1993) indicates that the difference between geometric and "dynamic" calculations of fluxes through individual transmissive elements, when combined with network effects, could be up to a factor of ten. In this study, hydraulic heads were assigned at the face of the LPD blocks and the distribution of flux in transmissive elements intersecting the tunnel was estimated; thus, these flux values better reflect the groundwater flow system in the LPD block.
- Hydraulically, a transmissive element is modeled with a constant value for effective transmissivity; the more realistic case of locally varying transmissivity in a transmissive element plane would enhance the network effects.
- For the estimation of the total flux through a tunnel with this geometric approach, all intersecting transmissive elements are assumed to contribute to both inflow into and outflow from the tunnel, i.e. a transmissive element brings water into the tunnel from half of its elliptical trace length and takes flow out from the tunnel through its other half. In the real system, the effective conductance of a particular intersection will depend on many details including hydraulic head, the TE geometry and hydraulic properties. For most cases, the difference with respect to the total flux is within a factor of 2 (LANYON & HOCH 1993).

Dilution of groundwater was estimated for several stages of flow along the flow path, as groundwater moves from the low-permeability domain to major water-conducting faults or to the overlying higher-permeability domain, and thence to the biosphere, which is assumed to be the alluvium of the Rhine river valley. The dilution ratio in the crystalline basement was estimated by comparing volumetric or Darcy fluxes in each of the domains, as shown in Table 8-5.

### Results for groundwater flux and dilution

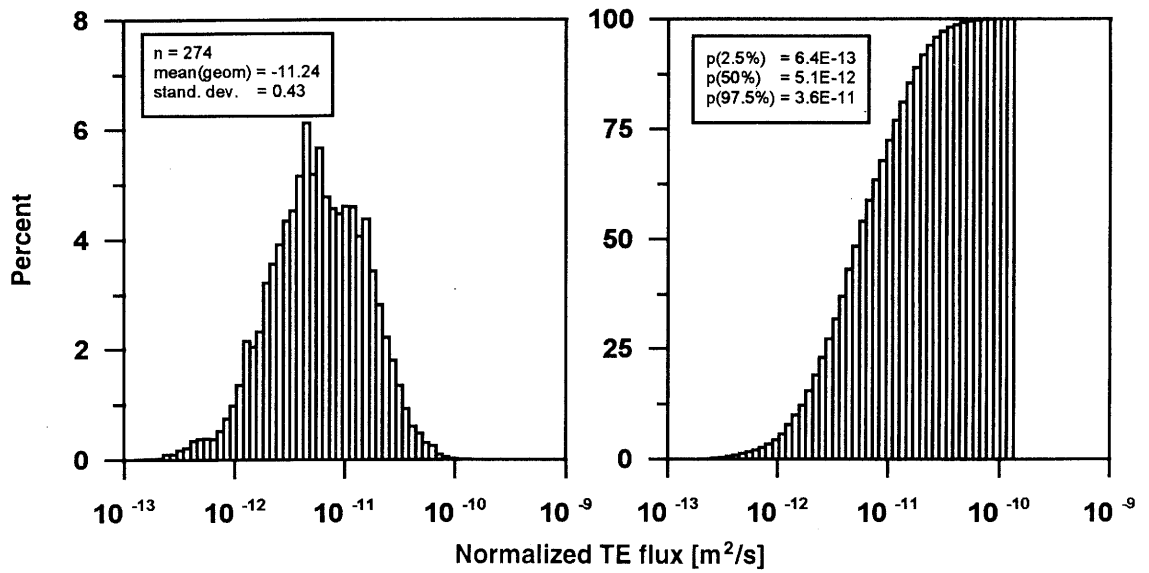
All geometric and hydraulic results relevant to safety analysis for area West are summarized in Table 10-1. For completeness and for convenience of the reader, the table summarizes the results of geometric and hydraulic gradient analyses that are described in sections 8.4 and 8.5. Descriptions of flux and dilution are presented below.

*Flux.* Distributions of groundwater flux (normalized flux, flux through transmissive elements, flux through a tunnel segment) for area West are shown in Figures 10-3, 10-4 and 10-5; results of flux and dilution analyses are summarized in Table 10-1. The input for the derivation of these figures is shown in Figure 8-15 (gradient distribution) and Figure 8-20 (geometric characteristics of transmissive elements intersecting a tunnel). The transmissivity was taken from the distribution observed in the LPD in the boreholes Böttstein, Leuggern and Kaisten (Fig. 8-5), using a log-normal distribution with a mean of  $\log T = -9.24$  and a standard deviation of  $\log T = 0.4$ , as shown in Table 8-6. Table 10-1 shows that the mean flux values for the sparse scenario are all about 3 - 4 times the corresponding mean values for the full scenario, reflecting the larger hydraulic gradients simulated for the sparse scenario (cf. section 8.5).

In Table 10-1, the ranges for flux in the transmissive elements and tunnel segments are based on the distributions shown in Figures 10-3, 10-4 and 10-5. The full range is from the low end (2.5 % in cumulative distribution) of the distribution for the full scenario to the high end (97.5 % in cumulative distribution) of the distribution for the sparse scenario (cf. section 8.6 for range definition). The range and means for flux through the repository are equal to the fluxes through the tunnel segment times the number of tunnel segments (30) that are assumed in the repository design and then converted to  $\text{m}^3/\text{a}$ . The calculated repository flux is, therefore, very approximate and probably overestimates the actual value. The results correspond to a situation with vertical (upward or downward) flow, where all caverns are placed within one block in LPD; flux through the repository would be smaller if flow were horizontal.

Darcy fluxes through second order major water-conducting faults are given in Table 8-5 for the cases of the full and sparse scenarios. A geometric measure required for solute transport modeling is the average trace length of the water-conducting features within a major water-conducting fault,  $\gamma$ , expressed as length per unit cross-section perpendicular to flow. This measure is proportional to  $P_{32} \times \sin(\theta)$ , where  $P_{32}$  is the fracture area density of the water-conducting features within the major water-conducting faults (i.e. how much "fracture surface area" exists in a unit volume of fractured rock), and  $\theta$  is their dip angle from the horizontal. For  $P_{32} = 0.12 \text{ m}^{-1}$  (VOBORNY et al. 1993b) and subvertical water-conducting features with dip angles

**FULL SCENARIO**



**SPARSE SCENARIO**

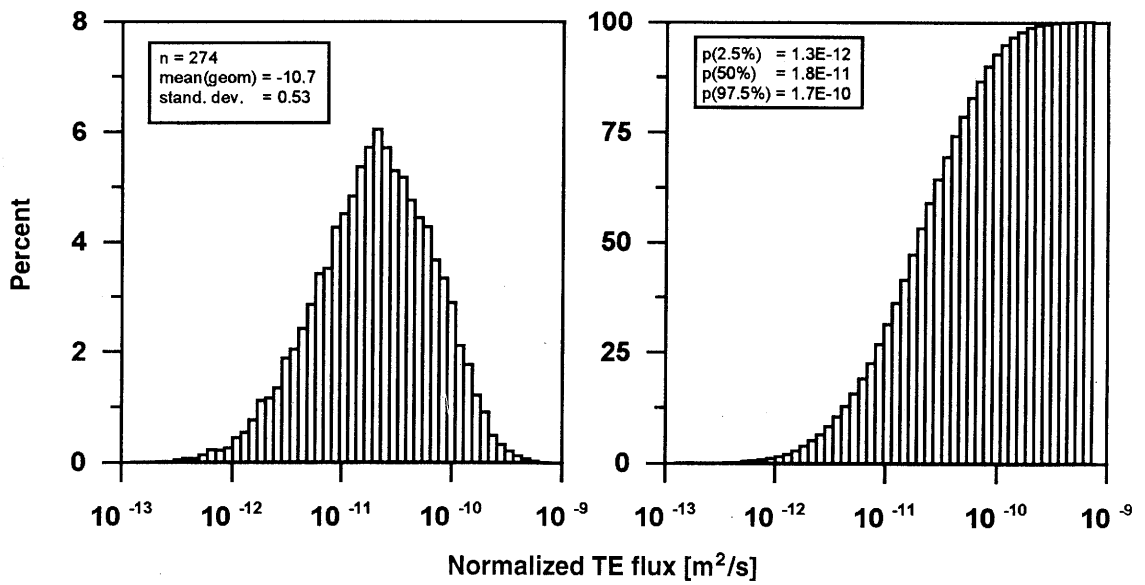
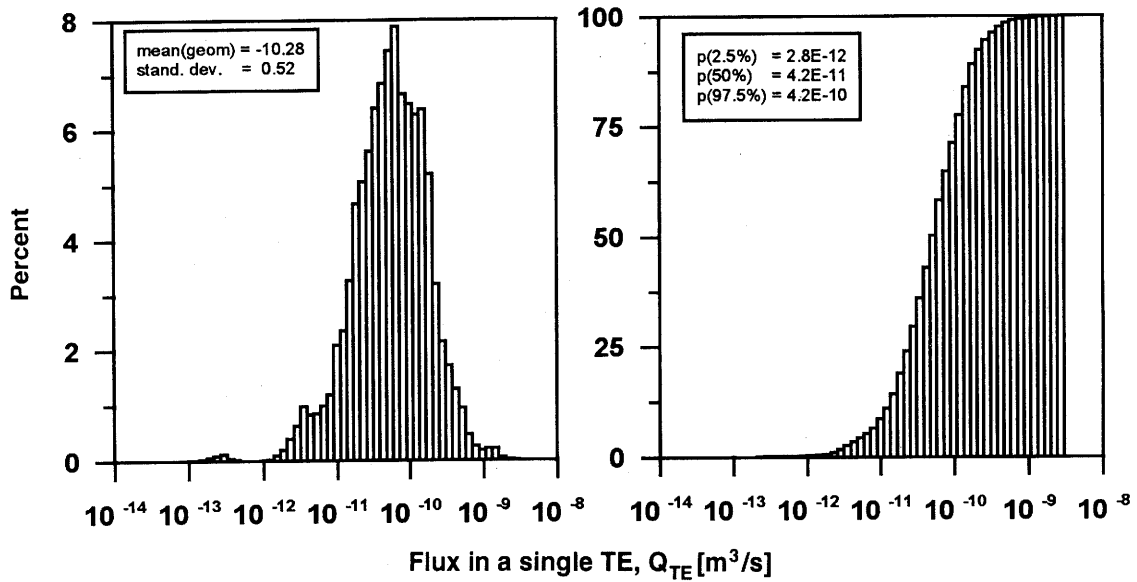


**Fig. 10-3 :** Normalized flux distributions in a single transmissive element (flux per unit length), full and sparse scenarios, area West (VOMVORIS et al. 1992).

**FULL SCENARIO**



**SPARSE SCENARIO**

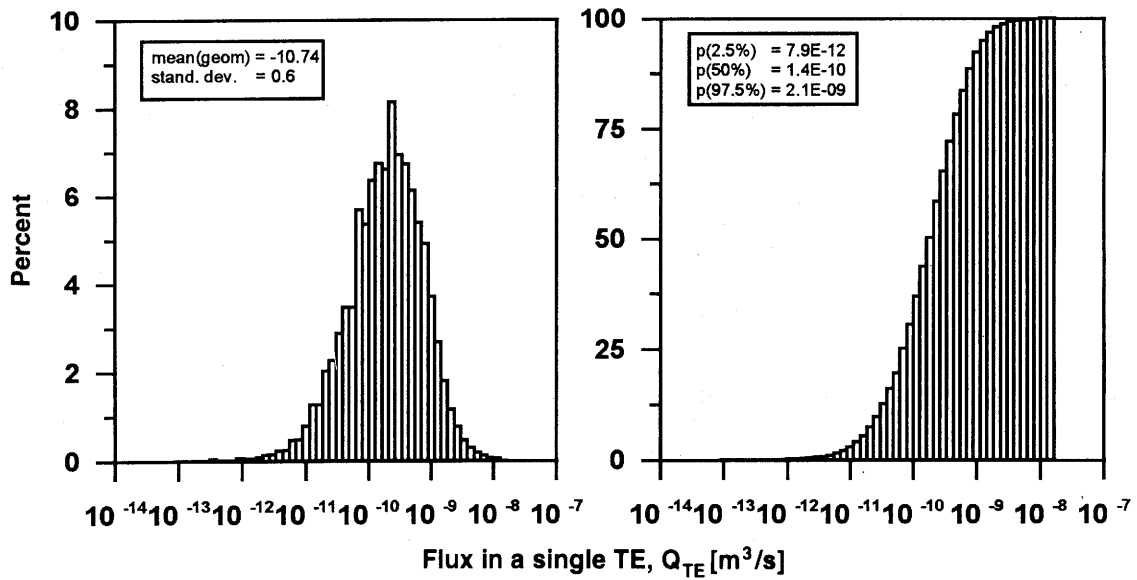
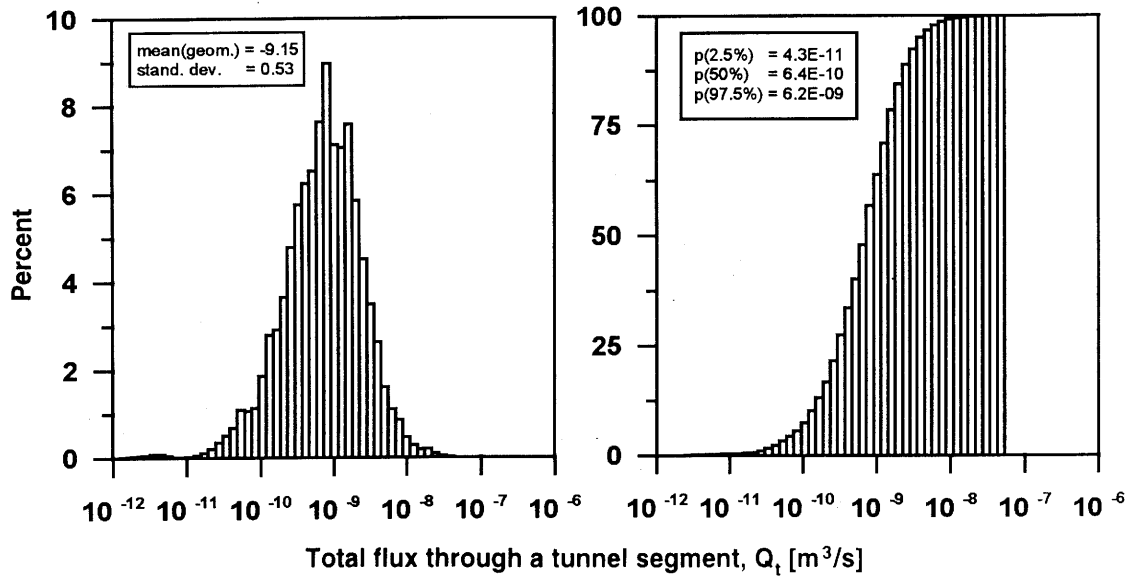


**Fig. 10-4 :** Distributions of flux in a single transmissive element, full and sparse scenarios, area West (VOMVORIS et al. 1992).

**FULL SCENARIO**



**SPARSE SCENARIO**

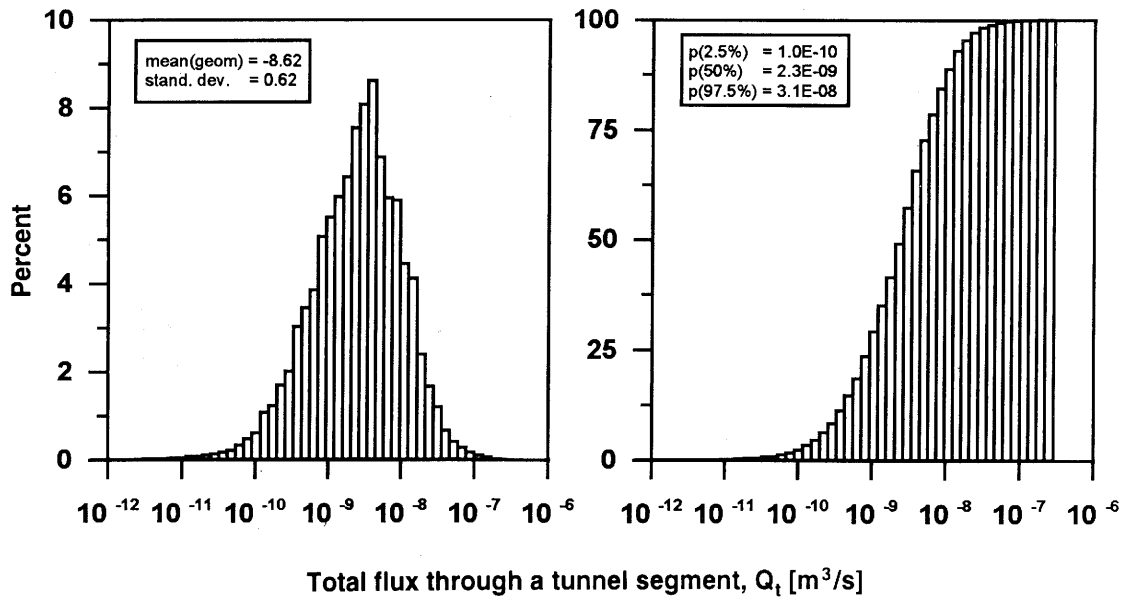


**Fig. 10-5 :** Distributions of total flux through a tunnel segment 500 m long, full and sparse scenarios, area West (VOMVORIS et al. 1992).

between 45 and 90 degrees, the expected values of  $\gamma$  are between 0.08 and 0.12 m<sup>-1</sup>; a value of 0.1 m<sup>-1</sup> for the Performance Assessment Reference Case would be then reasonable.

*Dilution.* The dilution ratio of groundwater entering major water-conducting faults from the low-permeability domain is conservatively estimated to be about 100 - 1000 (Tab. 10-1;  $Q_{MWCF}/Q_{LPD}$ ). This considers ranges of variables that could affect the relevant control volumes (VOMVORIS et al. 1992; cf. Tab. 8-5 for definitions). The dilution ratio of groundwater entering the higher-permeability domain from the underlying low-permeability domain ( $Q_{HPD}/Q_{LPD}$ ) depends on the degree of mixing in the upper unit - the greater the degree of mixing, the larger the dilution ratio. If a small amount of mixing is conservatively assumed, the range of this dilution ratio is also about 100 - 1000 (Tab. 10-1).

In order to assess the dilution in the biosphere, a study was conducted by STÄUBLE (1993) to characterize the surficial aquifer along the Rhine river, where exfiltration is expected to occur. The Rhine river alluvium is a broad aquifer that is in contact with the crystalline bedrock for approximately 20 km between Waldshut and Stein-Säckingen. In the study, this aquifer was characterized at selected sections perpendicular to the main flow, on the basis of compiled data from existing groundwater exploration and production wells. The volumetric flux across each section was determined from the estimated cross-sectional area, the average hydraulic conductivity of the alluvium and the observed hydraulic gradients. The Darcy fluxes in most of this area were estimated to be about 10<sup>-5</sup> m/s; in the Frick valley, larger gradients probably occur, and a Darcy flux of 10<sup>-4</sup> m/s was estimated. Volumetric fluxes were evaluated for three sections between Laufenburg and Säckingen. The values range from 0.05 m<sup>3</sup>/s through the upper narrow section at Laufenburg (0.7 km long) to 0.65 m<sup>3</sup>/s at the downstream section between Laufenburg and Stein (7.3 km long). The latter section, which also includes a large stream of the Frick valley (0.36 m<sup>3</sup>/s) and lateral discharge from the bedrock, was used in combination with the estimated values of flux through the repository to obtain the average dilution ratios for flow directly into the biosphere ( $Q_{BIO}/Q_r$ ), shown in Table 10-1. For comparison, the average volumetric flux in the Rhine river at Rheinfelden is about 1000 m<sup>3</sup>/s.

## 10.2.2 Area East

### Approach and assumptions

As described in section 8.7, the general approach taken in the evaluation of groundwater flow conditions in area East is the same as for area West. However, principally because of the sparse database in area East, certain differences occur in the approach. Also because of the sparse database, analyses for area East are limited to scoping calculations that are designed to obtain general indications of flow conditions and to enable general comparisons with area West. Complete results are described in VOMVORIS et al. (1993a).

Type of input/result	Value/Range	Remarks	Value in P.A. Ref. Case <sup>1</sup>
<b>Selected input parameters and results (local-scale and regional-scale models)</b>			
1. Transmissivity (T) of water-conducting features (WCF) in low-permeability domain (LPD)[m <sup>2</sup> /s]	Arithmetic mean: 9.4E-10 Mean logT: -9.24; Standard deviation logT: 0.4	Table 8-2	-
2. Effective hydraulic conductivity (K-eff) of LPD [m/s]	4.2E-11	Fig. 8-14; locally, over an interval of a few decameters, the value could be up to 5E-10 m/s (see Fig. 8-2).	4E-11
3. T of WCF in higher-permeability domain (HPD) [m <sup>2</sup> /s]	Arithmetic mean: 4.4E-6 Mean logT: -6.17; Standard deviation logT: 1.1	Table 8-2	-
4. K-eff HPD [m/s]	2.8E-7	Fig. 8-14; see comment 2 above; value could be up to 5E-6 m/s (see Fig. 8-2).	-
5. T of WCF in major water-conducting faults (MWCF)[m <sup>2</sup> /s]	Arithmetic mean: 4.1E-6 Mean logT: -6.32; Standard deviation logT: 0.9	Table 8-2	-
6. K-eff of MWCF (first order) [m/s]	3.2E-7	Fig. 8-14	3E-7
7. T-eff of MWCF (second order) [m <sup>2</sup> /s]	6.4E-6	Fig. 8-14	-
8. Transmissive element (TE) length per unit cross-sectional area of MWCF [m <sup>-1</sup> ]	0.08 - 0.12	Section 10.2.1	0.1
9. Darcy flux - LPD [m/s]	Mean <sup>2</sup> : 1E-12 - 3.2E-12 Range <sup>2</sup> : 5E-14 - 3E-11	Table 8-5	-
10. Darcy flux - MWCF [m/s]	Mean <sup>2</sup> : 1.9E-9 - 6.7E-9 Range <sup>2</sup> : 9E-11 - 5E-8	Table 8-5	6.7E-9
11. Darcy flux - Rhine alluvium [m/s]	Eastern part of area West: 1E-5 Frick Valley: 1E-4	Section 10.2.1	-
12. Volumetric flux - Rhine alluvium (Q <sub>bio</sub> ) [m <sup>3</sup> /a]	section in Laufenburg: 0.05 section near Stein: 0.65 section in Frick valley: 0.36	Section 10.2.1	5.5E+6 m <sup>3</sup> /a
13. Volumetric flux - Rhine river [m <sup>3</sup> /s; m <sup>3</sup> /a]	1000; 3.2E+10	Section 10.2.1	3.2E10 m <sup>3</sup> /a
<b>Results from block-scale models: Geometry</b>			
1. Number of TEs that intersect a 500-m tunnel segment	Range: 6 - 20 Mean: 13.7	Section 8.6.2 and Fig. 8-20.	14
2. Trace lengths of single TEs that intersect a 500-m tunnel segment (m)	Range: <1 - 72 Average: 21.7; Most <sup>2</sup> : 20 - 30	Section 8.6.2 and Fig. 8-20. A value of 25 was recommended for P.A. Ref. Case calculations.	25

**Tab. 10-1 :** Geometric and hydraulic results relevant to safety analysis, area West (VOMVORIS et al. 1992).

Type of input/result	Value/Range	Remarks	Value in P.A. Ref. Case <sup>1</sup>
3. Length of direct flow path, LPD to HPD or MWCF	Minimum: defined by SA Maximum: Value depends on position of emplacement caverns and local hydrogeological conditions.	Flow path direction may be predominantly vertical or horizontal.	100 m
4. Ratio, actual flowpath length to direct one	Range: 1.2 - approx. 3 Most: 1.4 - 2.0	For conservatism, assume ratio = 1	2
5. Number of TEs in a flowpath	—	For conservatism, assume 1	1
<b>Results from block-scale models: Hydraulics</b>			
	Range: 2.5%- 97.5%	Geometric mean <sup>2</sup> / Arithmetic mean <sup>2</sup>	
1. Hydraulic gradient/LPD [-]: - Horizontal component - Vertical component - Absolute	0.002 - .09 <E-3 - 0.07 .0055 - .12	N.A. / 0.009 - .03 N.A. / 0.005 - .03 N.A. / .01 - .05	See section 8.5 and Figure 8-15. -
2. Normalized flux [m <sup>2</sup> /s] in TEs in LPD (flux per unit length)	6E-13 - 2E-10	5.7E-12 - 2E-11 / 9.4E-12 - 4E-11	Fig. 10-3 and remark 3, below. 2E-11
3. Conductance of TEs in LPD [m <sup>3</sup> /s]	3E-10 - 3.8E-8	5E-9 / 9E-9	Fig. 8-20 and remark 3, below. -
4. Flux through single TEs intersecting a 500-m tunnel segment in LPD, Q <sub>TE</sub> [m <sup>3</sup> /s]	3E-12 - 2E-9	5.3E-11 - 1.8E-10 / 1.1E-10 - 4.8E-10	Fig. 10-4 and remark 3, below. -
5. Total flux through a 500-m tunnel segment in LPD, Q <sub>t</sub> [m <sup>3</sup> /s]	4E-11 - 3E-8	7E-10 - 2.4E-9 / 1.5E-9 - 6.6E-9	Fig. 10-5 and remark 3, below. -
6. Total flux through repository, Q <sub>r</sub> [m <sup>3</sup> /y] [Q <sub>r</sub> = 30 Q <sub>t</sub> ]	0.04 - 28.4	0.65 - 2.3 / 1.4 - 6.2	Assumes 30 tunnels and vertical flow; cf. remark 3, below, and section 10.2.1 -
7. Dilution ratio, Q <sub>MWCF</sub> /Q <sub>LPD</sub>	E+2 - E+3	—	Section 10.2.1 -
8. Dilution ratio, Q <sub>HPD</sub> /Q <sub>LPD</sub>	E+2 - E+3	—	Section 10.2.1 -
9. Dilution ratio, Q <sub>BI</sub> /Q <sub>r</sub>	7E+5 - 5E+8	9E+6 - 3E+7 / 3.3E+6 - 1.5E+7	Biosphere is Rhine River alluvium at section near Stein; cf. 12, above. -

<sup>1</sup> Explanation for the choice of these values is in NTB 93-22

<sup>2</sup> Mean is mean of full scenario distribution - mean of sparse scenario distribution;  
Range is from lower end of full scenario distribution to upper end of sparse scenario distribution;  
Most is used for the trace length distribution in a qualitative sense, since the distribution is highly skewed.

<sup>3</sup> The study by LANYON & HOCH (1993) indicates that values derived by considering the flow dynamics can be up to 10 times lower than the ones derived from the geometric approach (cf. sect. 10.2.1)

**Tab. 10-1 :** (Continued) Geometric and hydraulic results relevant to safety analysis, area West (VOMVORIS et al. 1992).

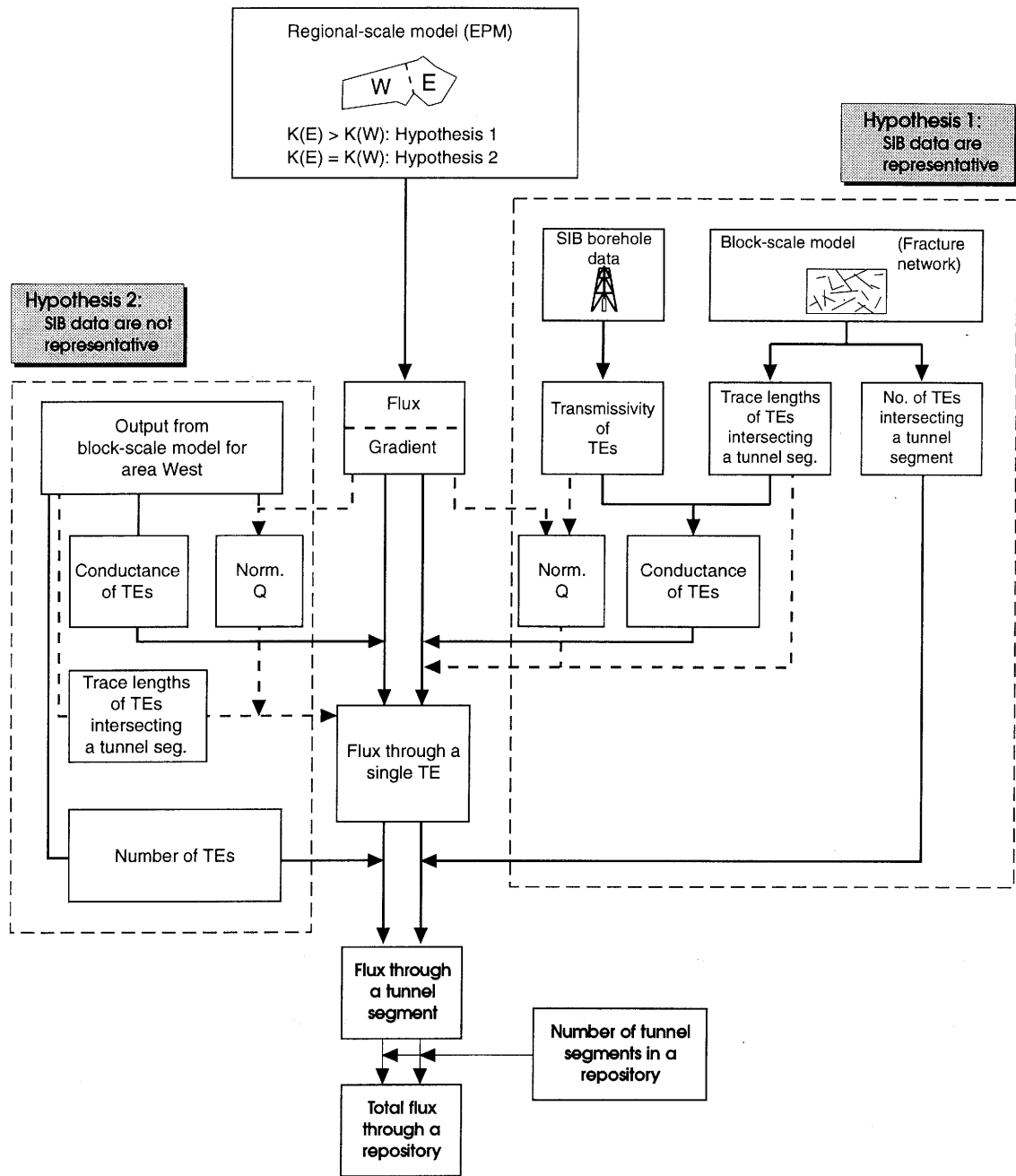
The methodology for analyzing groundwater flux in area East is shown in Figure 10-6. Two equally plausible hypotheses were considered: Hypothesis 1 (right side of diagram), Siblingen data **are** representative of the lower crystalline rock domain in area East; and Hypothesis 2 (left side of diagram), Siblingen data **are not** representative, but instead reflect a local anomaly. Through consideration of these two hypotheses, it is expected that the full spectrum of relevant results would be covered.

For Hypothesis 1, the regional-scale model (equivalent porous medium) was modified by increasing the crystalline rock conductivity in area East to reflect the Siblingen data. Gradient distributions were obtained from the modified regional-scale model, and Siblingen data were used directly as geometric and hydraulic inputs to the fracture network model. Major water-conducting faults were not explicitly considered; they were assumed to have effective properties that are similar to those of the adjoining, relatively permeable crystalline rock domain and, therefore, to have no significant impact on the regional flow system. In this analysis, the system is considered to be well interconnected, because of the relatively large conductivity of the crystalline rock domain. Therefore, the system is equivalent to the full scenario of area West, and no need exists to analyze also a sparse scenario. Furthermore, it is unlikely (based on regional residence times; cf. VOBORNY et al. 1993b) that the actual conductivity of the crystalline rock domain in area East exceeds the value derived from the analysis of the Siblingen data; as a result, the upper ends of the flux distributions that were obtained from the analysis of Hypothesis 1 probably represent the upper bounds of fluxes likely to occur in area East.

Under Hypothesis 2, the crystalline rock domain that is truly representative of area East is assumed to have a much smaller effective conductivity than that observed at the Siblingen site, similar, in fact, to that of area West. On the basis of results from area West, both a full scenario and a sparse scenario were evaluated under this Hypothesis. For the full scenario, the gradient distribution was obtained directly from the original equivalent porous medium model. For the sparse scenario, the gradient distribution was obtained by multiplying the gradient distribution parameters (means and standard deviations) from the equivalent porous medium model by a factor of 5; this scaling factor is based on a comparison of the gradient distribution parameters from the equivalent porous medium model with those of the hybrid model (sparse scenario) for area West (VOMVORIS et al. 1993a).

As indicated by the left side of Figure 10-6, the distributions of hydraulic parameters and numbers of transmissive elements that intersect a tunnel segment were adopted directly from assessments of area West. These distributions reflect a relatively small effective conductivity of the crystalline rock domain in that area. Because under Hypothesis 2 similar properties are assumed for area East, the lower ends of the resulting flux distributions probably represent the lower bounds for fluxes likely to occur in area East.

Dilution of groundwater as it enters the biosphere was estimated as the ratio of flux through the alluvial cross-section of the Rhine river valley,  $Q_{BIO}$ , to flux through the repository,  $Q_r$ . For this analysis, the cross-sectional flow in the alluvium of the Rhine river valley is assumed to be the same as in area West ( $0.65 \text{ m}^3/\text{s}$ ). According to some



K = hydraulic conductivity

TE = transmissive element (numerical representation of water-conducting features)

Norm. Q = normalized flux in TEs (per unit length)

**Fig. 10-6 :** Methodology for the derivation of the hydrogeological input for safety analysis, area East (VOMVORIS et al. 1993a).

of the simulations of groundwater flow (VOBORNY et al. 1993b), groundwater from a repository in the area East could also discharge into the Wutach river, and thus a qualitative judgment was also made of dilution of groundwater as it enters the alluvium of this valley.

### Results for groundwater flow and dilution

All geometric and hydraulic results relevant to safety analysis for area East are summarized in Table 10-2. Complete descriptions are in VOMVORIS et al. (1993a). Values of flux and dilution are presented in Table 10-2 and described below.

*Flux.* Table 10-2 shows that the mean values of flux under Hypothesis 1 generally are 2 - 3 orders of magnitude greater than the comparable values under Hypothesis 2, reflecting principally the substantially larger effective conductivity of the crystalline rock domain assumed under Hypothesis 1 compared to that assumed under Hypothesis 2. As in the area West, values for the sparse scenario are greater than values for the full scenario.

*Dilution ratio.* Dilution ratios for groundwater flow into Rhine river alluvium are shown in Table 10-2. Dilution of flow into the Wutach river alluvium is substantially less than dilution of flow into the Rhine river alluvium, because of the smaller alluvial cross-section of the Wutach river valley. The average volumetric flux of the Wutach river, about 8 m<sup>3</sup>/s, is also much smaller than that in the Rhine river (about 1000 m<sup>3</sup>/s).

#### 10.2.3 Discussion

Hydrogeological input is presented that is relevant to safety analysis of areas West and East, with respect to the disposal of high-level radioactive waste in the crystalline basement of Northern Switzerland. A similar general methodology was followed in the evaluation of both areas (VOMVORIS et al. 1993c). Borehole data, numerical models of groundwater flow at various scales, and analytical approaches were combined to produce geometric and hydraulic results.

A comparison of key parameters in the two areas (results in Tab. 10-1 compared to results in Tab. 10-2) indicates the following:

- 1) The mean number of transmissive elements that intersect a tunnel segment in area East under Hypothesis 1 (based on Siblingen data) is about 3 times the mean number of transmissive elements that intersect a tunnel segment either in area West or in area East under Hypothesis 2 (based on area West borehole data).
- 2) Mean conductances of transmissive elements that intersect a tunnel segment in area East under Hypothesis 1 (based on Siblingen data) are about 2 orders of magnitude greater than mean conductances of transmissive elements that intersect a tunnel segment either in area West or in area East under Hypothesis 2 (based on area West borehole data).

Type of input/result	Value						
	Hypothesis 1 (SIB data are representative)				Hypothesis 2 (SIB data are not representative)		
	Range <sup>3</sup>	Mean		Value in P.A. Ref. Case <sup>1</sup>	Range <sup>2</sup>	Mean <sup>2</sup>	
		Geom.	Arith.			Geom.	Arith.
<b>Selected input parameters</b>							
1. Transmissivity of TEs in LPD [m <sup>2</sup> /s]	Mean of logT = -6.9 Std. deviation of logT = 0.5			-	cf. Table 10-1		
2. Effective hydraulic conductivity of LPD [m/s]	1E-8			-	cf. Table 10-1		
<b>Geometry</b>							
1. Number of TEs intersected in a 500-m tunnel segment	32 - 47	N.A.	40.8	40.8	6-20	N.A.	13.7
2. Trace lengths of single TEs in a 500-m tunnel segment [m]	0.2-136 Most values: 20-25	N.A.	22.8	22.8	0.5 - 72 Most values: 20-30	N.A.	21.7
3. Length of direct flow path within a block in the Lower Unit [m]	Not determined	-	-	200	Not determined	-	-
4. Ratio, actual flow path length to direct flow path length	Not determined: For conservatism, assume ratio = 1.0						
5. Number of TEs along a flow path	Not determined For conservatism, assume number = 1						
<b>Hydraulics</b>							
1. Hydraulic gradient: - Hor. component - Vert. component - Absolute (cf. section 8.7 for gradients)	< 0.0004 - .006 < .0001 - .006 < .0004 - .007	N.A. N.A. N.A.	0.0028 .0013 .0033	-	0.002 - 0.032 0 - .022 .003 - 0.033	N.A.	0.004 - .020 .001 - .007 .004 - .022
2. Normalized flux [m <sup>2</sup> /s] in TEs (flux per unit length)	2E-11 - 5E-9	3.4E-10	8.7E-10	2.8E-10	3E-13 - 7E-11	2E-12 - 1E-11	4E-12 - 2E-11
3. Conductance of TEs [m <sup>3</sup> /s]	5E-8 - 2E-5	1.2E-6	2.7E-6	-	3E-10 - 4E-8	5E-9	9E-9

**Tab. 10-2 :** Geometric and hydraulic results relevant to safety analysis, area East (VOMVORIS et al. 1993a).

Type of input/result	Value						
	Hypothesis 1 (SIB data are representative)				Hypothesis 2 (SIB data are not representative)		
	Range <sup>3</sup>	Mean		Value in P.A. Ref. Case <sup>1</sup>	Range <sup>2</sup>	Mean <sup>2</sup>	
		Geom.	Arith.			Geom.	Arith.
4. Flux through single TEs intersecting a 500-m tunnel segment $Q_{TE}$ [m <sup>3</sup> /s]	1E-10 - 5E-8	3.3E-9	1.1E-8	-	1E-12 - 1E-9	2.1E-11 - 1.1E-10	4.2E-11 - 2.1E-10
5. Total flux through 500-m tunnel segment, $Q_i$ [m <sup>3</sup> /s]	4E-9 - 2E-6	1.3E-7	4.2E-7	-	2E-11 - 1E-8	2.7E-10 - 1.4E-9	5.7E-10 - 2.9E-9
6. Total flux through repository, $Q_r$ [m <sup>3</sup> /a] [ $Q_r = 30 Q_i$ ]	3.8 - 1.9E+3	123	396	-	0.02-9.45	0.25-1.3	0.55 - 2.7
7. Dilution ratio, $Q_{BIO}/Q_r$ ; $Q_{BIO}$ =Rhine river alluvium <sup>4</sup>	1.1E+4 - 5.4E+6	1.7E+5	5.2E+4	-	2.2E+6 - 1E+9	1.6E+7- 8.2E+7	7.6E+6 - 3.7E+7

<sup>1</sup> Explanation for the choice of these values is in NTB 93-22

<sup>2</sup> Mean is mean of full scenario distribution - mean of sparse scenario distribution;  
Range is from lower end of full scenario distribution to upper end of sparse scenario distribution;  
 for hydraulic results, the boundaries of the range correspond to the 2.5% to 97.5% values of the cumulative distributions.

<sup>3</sup> Range for hydraulic results, the boundaries of the range correspond to the 2.5 % to 97.5 % values of the full scenario cumulative distribution.

<sup>4</sup> For Wutach valley alluvium, dilution values are smaller by at least a factor 100.

**Tab. 10-2 :** (Continued) Geometric and hydraulic results relevant to safety analysis, area East (VOMVORIS et al. 1993a).

- 3) Simulated absolute hydraulic gradients in area West generally are a factor of 2 - 3 larger than comparable gradients in area East.
- 4) Based on a combination of the above points, the mean fluxes associated with a repository in area East (i.e. through a single transmissive element that intersects a tunnel segment, through a tunnel segment, and through the repository) are:
  - under Hypothesis 1, more than 2 orders of magnitude greater than in area West (full scenario); and
  - under Hypothesis 2, about a factor of 2 smaller than comparable fluxes in area West.

The hydrogeological characteristics described above provide a basis for preliminary safety analyses. The ranges provided for all quantitative estimates are broad enough to expect that they account for uncertainties as well as natural variability related to the input parameters of the current conceptual geological model. The uncertainties are much larger for area East, where only one deep borehole exists.

The effects of the excavation disturbed zone (EDZ) are not included in the analyses presented above. VOMVORIS et al. (1993b) summarize a preliminary assessment of these effects. It can not be excluded that an excavation disturbed zone will act as a short-cut between transmissive elements and thus increase the flux in an individual transmissive element through accumulation of fluxes from other transmissive elements. A single transmissive element could carry all available flux which would be determined from the hydraulic properties and gradient upstream from the repository. Further investigations of these effects are foreseen for the next phase of the crystalline basement project.

### **10.3 Small-scale characterization of the geosphere: conceptual model of water-conducting features**

This section focuses on geological data that are needed for the quantification of retardation processes (such as sorption and matrix diffusion) of radionuclide transport in the geosphere. These data relate to small-scale properties of the rocks in contact with the radionuclides and are therefore characterized on the basis of drillcore investigations of permeable zones as identified by hydraulic tests. The input data comprise mainly:

- Geometry and interconnectedness of water-conducting features on all scales;
- Mineralogy of the fracture infills and of the wallrock;
- Flow porosity of the fracture and open (diffusion-accessible) porosity of the wallrock.

A regional analysis of permeable zones (inflow points) in the boreholes is derived in Chapter 6, resulting in classification of 3 types of water-conducting features:

1. Cataclastic zones;
2. Jointed zones;
3. Fractured aplite/pegmatite dykes and aplitic gneisses.

Simplified reference data in a form suitable for performance assessment are specified for each of these types of water-conducting features.

Each type of water-conducting feature exhibits variable geometric patterns rather than a single, fixed geometry. Available data on the spatial orientation of the water-conducting features indicate that, in spite of a slight tendency towards steeply-dipping orientations, the variability is very large and all water-conducting features are assumed to be interconnected (cf. section 6.8). This assumption is corroborated by larger-scale observations in surface outcrops in the Black Forest, as well as by the largely

homogeneous water chemistry within the crystalline basement sections of all boreholes.

In the reference concept for high-level waste disposal in Northern Switzerland, a repository will be overlain by about 500 m of crystalline basement rocks. Because of the good interconnection of all types of water-conducting features, it seems unlikely that any radionuclides released from the repository would remain in the same type of water-conducting feature during transit through the crystalline basement. The assumption of flow in one single type of water-conducting feature along the entire flow path within the crystalline basement is a model simplification and serves to test the safety performance of each type of water-conducting feature separately.

### **10.3.1 The need to simplify**

Small-scale natural variability of geological parameters is virtually unlimited. However, transport models are based on simple concepts (e.g. water flow through a set of parallel plates with constant water chemistry, hydraulic gradient, wallrock mineralogy and porosity along the whole flow path). Therefore, natural complexity needs to be reduced, and some degree of averaging is necessary (e.g. hydraulic gradients, water chemistry, mineralogy). Extensive studies of flow and transport through a fracture in granitic rock at the Grimsel Test Site indicated that the relevant fracture properties are homogeneous on a scale of meters (FRICK et al. 1992), and averaging of small-scale properties is therefore possible. A geological reference dataset for solute transport modeling is defined in the following sections. The natural scatter of the data is averaged out, and ranges are given for sensitivity analysis. Data passed to the modelers must be simple enough to fit the models but must still adequately represent the geosphere.

### **10.3.2 Simplified geometry of cataclastic zones**

A cataclastic zone in the deep boreholes has a typical thickness of 50-100 cm, but the lateral extent cannot be determined from core studies. By analogy with basement outcrops in the Black Forest, the length and width of such cataclastic zones is about 100 m or more, which is enough to account for full interconnection with the other types of water-conducting features. Thus if transport processes over 100 m or less are considered, these may take place within one single water-conducting feature. On a scale of several 100 to 1000 m, however, transport is thought to take place in a number of different water-conducting features.

On a smaller scale, a typical cataclastic zone consists of an interconnected network of individual fractures. This pattern is represented in the model abstraction (Fig. 10-7) by a set of parallel plates. In nature, each individual fracture is partially filled by a cataclastic matrix or hydrothermal infill material, but typically contains vuggy portions (represented as open channels) that are responsible for the increased hydraulic conductivity and where advective transport predominantly occurs. These relations are represented in Figure 10-7 by a planar porous fracture infill of constant thickness

# Cataclastic zones

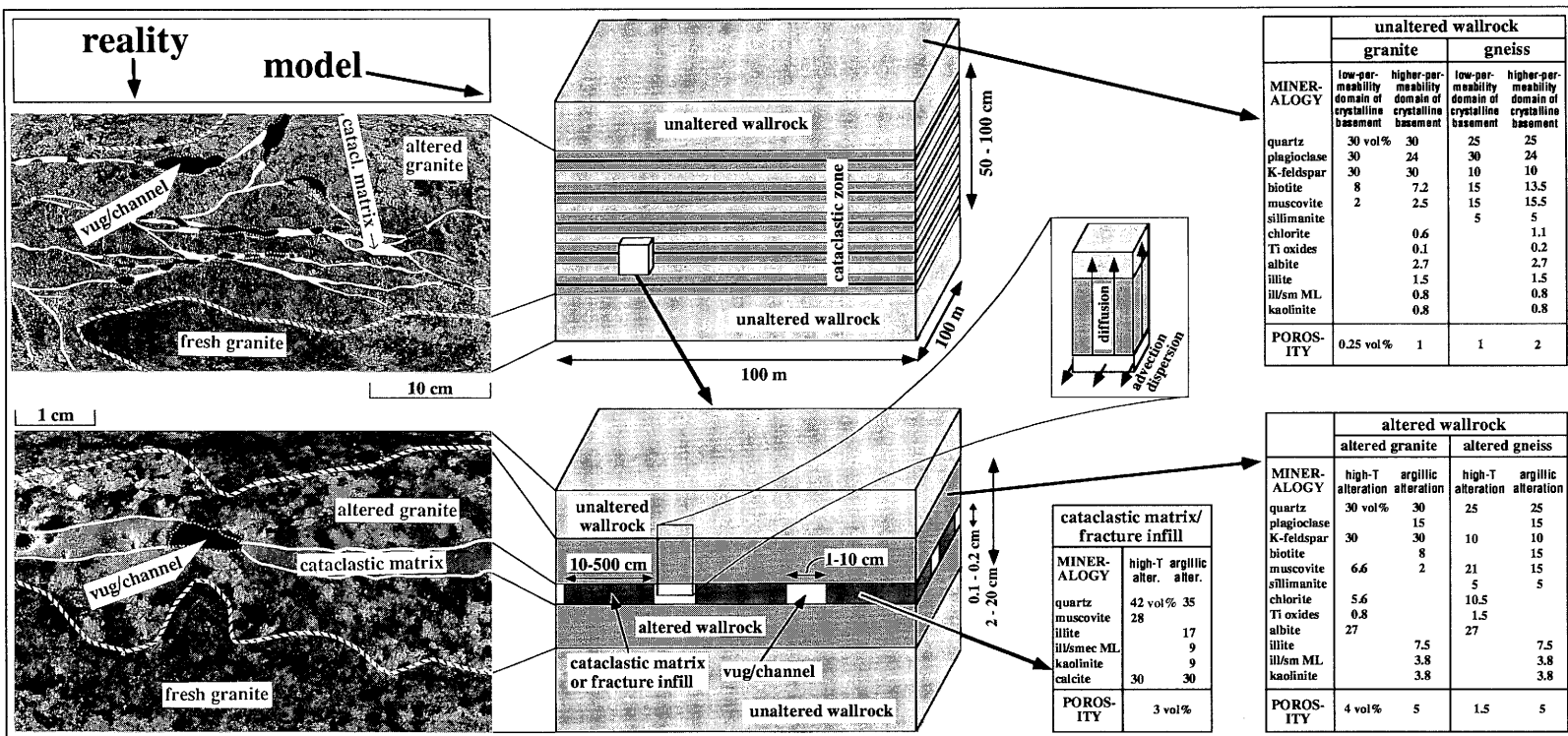


Fig. 10-7 : Small-scale conceptual model of cataclastic zones in the crystalline basement of Northern Switzerland, including geometric, mineralogical and porosimetric data.

(typically 1 - 2 mm), which is interrupted by the vugs/channels. The latter are represented by tubes with rectangular cross-sections, which form a rectangular mesh within the fracture plane. Both the size of the vugs/channels and their spacing within the fracture plane vary widely in natural occurrences. These variations are expressed by the ranges of 1-10 cm for the width and 10 - 500 cm for the spacing of the vugs/channels in Figure 10-7.

Preliminary sensitivity studies of radionuclide transport have indicated that the ratio

$$R = \frac{\text{vug/channel width}}{\text{vug/channel spacing}} \quad \text{i. e.} \quad \frac{1 - 10 \text{ cm}}{10 - 500 \text{ cm}} \quad (10-1)$$

is a sensitive parameter for the prediction of radionuclide transport in the geosphere (MAZUREK et al. 1992a). Observations in core material as well as in outcrops in the Black Forest suggest that the values given for the widths and for the spacings are correlated. Specifically, the vug/channel width would be ~ 10 cm (and not significantly less) in the extreme case of a spacing of 500 cm. It is geologically completely unreasonable to combine a spacing of 500 cm with a width of only 1 cm. Given this restriction, the variation range of R is specified as 0.02 - 0.1.

The wallrock adjacent to each fracture is invariably altered. The thickness of the alteration rims varies widely but always exceeds 1 cm on each side. In many cases, alteration is so extensive that no unaltered wallrock is observed within the cataclastic zones and alterations may penetrate several decimeters into the surrounding undeformed wallrock.

In summary, the conceptual model that is proposed to represent the geometric pattern of cataclastic zones contains the following elements:

1. Cataclastic matrix (fracture infill) in the fracture planes, containing water-conducting channels (representing the flow porosity);
2. Altered wallrock around each fracture;
3. Unaltered wallrock outside the cataclastic zone.

### 10.3.3 Simplified geometry of jointed zones

In spite of the very different genesis and geological significance of joints and cataclastic features, the simplified geometric (and also mineralogical) parameters are very similar at the level of abstraction that is required for modeling purposes. The principal elements again comprise a fracture infill containing vugs/channels, surrounded by altered and unaltered wallrock outside the fractured zone. In permeable zones, joints rarely occur as single structures but rather form subparallel or cross-cutting swarms of joints. As in the case of the cataclastic zones, the lateral extents of joints and jointed zones can only be deduced by analogy with the relations in the Black Forest. While the length of a single joint is a few meters, the lengths of jointed zones as a whole are in the order of tens of meters. In the model representation, a jointed zone is reduced to a

set of parallel single fractures that persist along the whole lateral extent of the jointed zone. This reduction is appropriate because the individual joints are invariably hydraulically interconnected.

The conceptual model representing the geometric relations of jointed zones is sketched in Figure 10-8. This model is almost identical to that of the cataclastic zones, with the exception of a reduced number of parallel fractures. This difference is introduced to account for the fact that the internal structure of cataclastic zones is more complex and contains more individual fractures on average than the jointed zones. Comments made in section 10.3.2 about the correlation of ranges of values (eq. 10-1) also apply to jointed zones.

#### **10.3.4 Simplified geometry of deformed aplite/pegmatite dykes**

Water flow through dykes and aplitic gneiss layers could be particularly important for safety assessment, because mineralogical alterations (producing, for example, highly sorbing clays) are weakly developed and fracture coatings are absent in places. Also, dykes may extend over great distances and might, in the worst case, channel water flow out of a repository directly to aquifers in the overlying sediments with minimal retardation. For these reasons, more effort was invested in evaluating this type of water-conducting feature in order to provide and substantiate a realistic geological dataset replacing the previous, in part overconservative, assumptions of Project Gewähr (NAGRA 1985b).

##### **Host rock: Aplite/pegmatite dykes and aplitic gneiss layers**

Aplite/pegmatite dykes and aplitic gneisses have a distinct chemical and mineralogical composition that has direct consequences for their deformation behavior and alteration type and thus for safety-relevant parameters:

1. The primary mineralogy is dominated by quartz and feldspars, the sum of which may exceed 95 vol.-%. Micas are only minor in abundance. A consequence of this composition is a very brittle deformation behavior at temperatures below 500 °C.
2. Primary plagioclase compositions are very Na-rich, which precludes any significant argillic alteration. In general terms, these rocks produce much less hydrothermal alteration products than gneisses or granites. This means that both the solution porosity is smaller and the abundance of sorbing minerals on fracture coatings and in the altered wallrock is less when compared to the other types of water-conducting features.

*Aplite/pegmatite dykes:* Dykes are intrusive rocks that cross-cut their country rock (gneiss, granite or other intrusives). Their thickness ranges from about 10 cm to several m. Their lengths and widths cannot be determined from borehole data; comparison with analogous structures in the outcrops of the Black Forest and other areas suggests lengths in the order of a few 100 m, in some unusual cases even several kilometers. The spatial orientation of the aplite/pegmatite dykes varies considerably, but steeply-dipping structures are more common than flat ones. While the

# Jointed zones

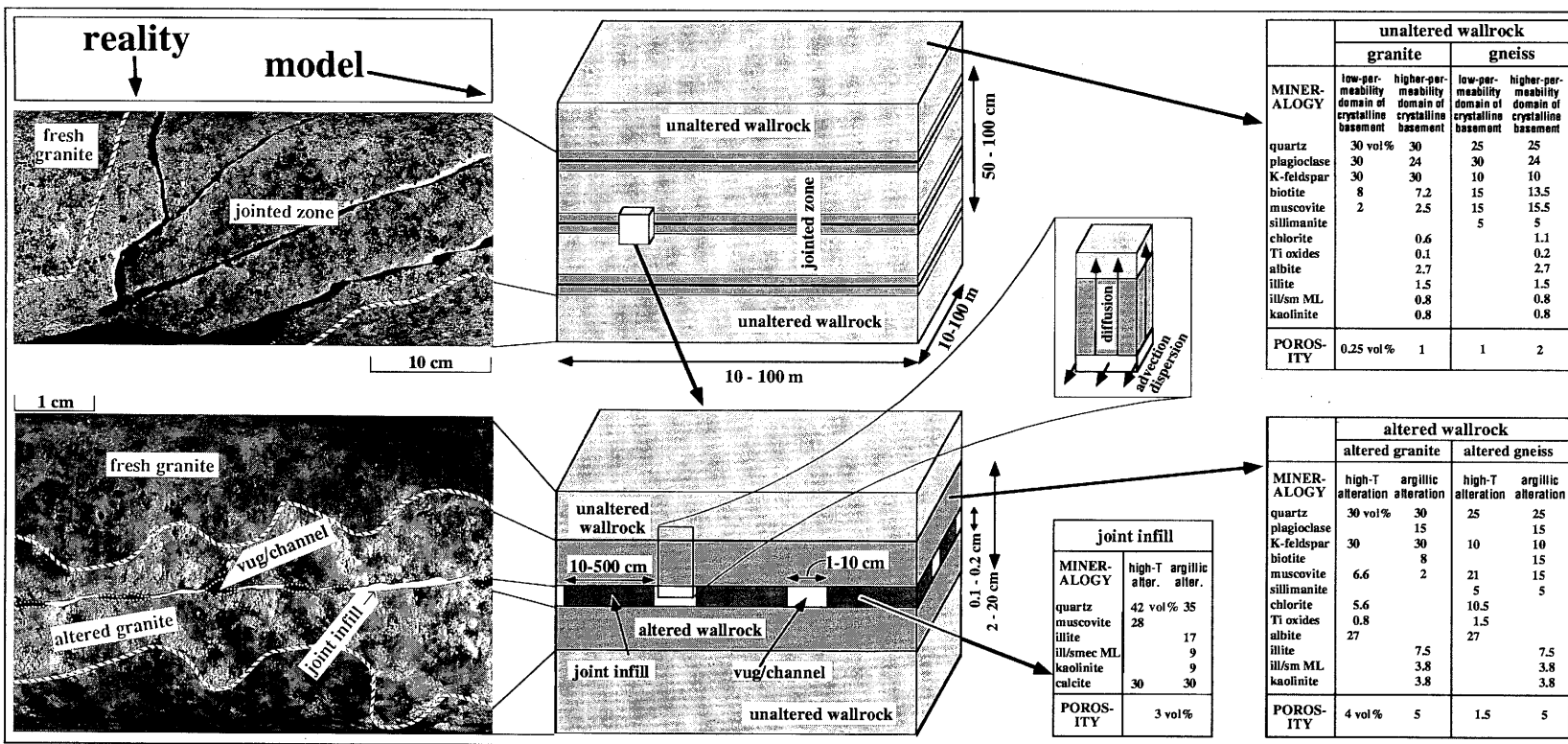


**Fig. 10-8 :** Small-scale conceptual model of jointed zones in the crystalline basement of Northern Switzerland, including geometric, mineralogical and porosity data.

# Fractured aplite/pegmatite dykes and aplitic gneisses

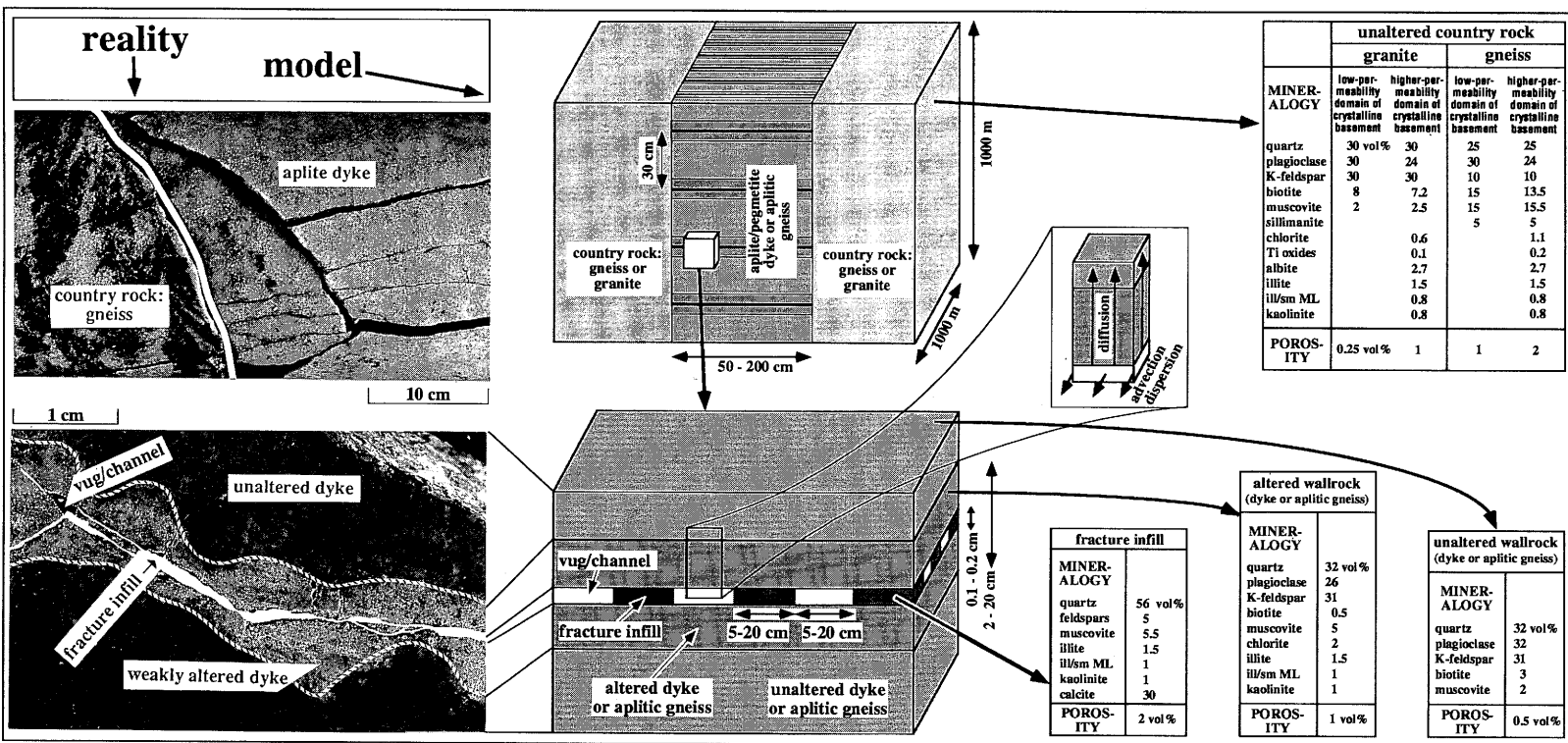


**Fig. 10-9 :** Small-scale conceptual model of fractured aplite/pegmatite dykes and aplitic gneisses in the crystalline basement of Northern Switzerland, including geometric, mineralogical and porosimetric data.

mineralogy is identical, the major difference between aplites and pegmatites is textural: aplites are fine-grained rocks (grain diameters about 1 mm) whereas pegmatites are coarse (grain diameters about 1 cm).

*Aplitic gneiss layers:* These rocks represent the metamorphosed equivalents of rhyolitic sheets, i. e. acid volcanic rocks. In spite of a different genesis, these rocks have a chemical and mineralogical composition that is very similar to that of aplite/pegmatite dykes. In contrast to the dykes, these layers are concordant (parallel) to the schistosity of the gneisses and probably folded on a scale of km. They are generally a few meters thick; the lateral extent is unknown but may be several kilometers. Due to the scarcity of micas and the high-grade metamorphism, aplitic gneisses have little or no schistosity.

### **Fracture geometry**

In permeable zones, dykes or aplitic gneiss layers are highly fractured, which provides a good hydraulic connection between the dykes/aplitic gneiss layers and the country rock (granite or gneiss). In the conceptual model sketched in Figure 10-9, these fractures are represented as perpendicular to the contact to the wallrock, with an average spacing of 30 cm. The average thickness of fracture coatings is about 1 mm. About half of the fracture surfaces are infilled and half contain vugs/channels. The size of uncoated fracture areas varies widely; an estimated mean value is 10 cm. These relations in the individual fractures are simplified in Figure 10-9 to a single plate consisting of an infill that is cross-cut by a mesh of tube-shaped channels (rectangular cross-sections). Comments made in section 10.3.2 about the correlation of ranges of dimensions (eq. 10-1) also apply to fractured aplite/pegmatite dykes and aplitic gneisses.

### **Altered wallrock adjacent to the fractures**

A detailed study of alteration effects in aplite/pegmatite dykes and aplitic gneisses has shown that hydrothermal effects are weak but invariably present, at least within a few cm of the fracture surfaces. In particular, a limited sericitic alteration of plagioclase, associated with the generation of microporosity, is almost ubiquitous.

In half of the samples investigated, the interface between vugs/channels and wallrock has a very low porosity due to sealing effects caused by hydrothermal precipitation (mainly quartz). However, in all cases examined, at least one pore with an aperture greater than 0.5  $\mu\text{m}$  per 10 mm trace length occurs that connects the open fracture and wallrock. Furthermore, the sealing effects vary locally and are often interrupted by zones of good connectivity in the range of cm - dm.

### **10.3.5 Mineralogy and open porosity of water-conducting features**

The mineralogy and open porosity of the fracture materials and of the wallrocks depend on the primary rock type and on the type of hydrothermal alteration or mineralization

that the permeable zone has experienced. However, mineralogy and porosity are largely independent of deformation type, i.e. no major distinctions exist between cataclastic and jointed zones. While mineralogy and porosity commonly vary substantially on a small scale (range of dm - m), the variation is much less pronounced on a larger scale. Because geosphere transport of radionuclides from a repository has a minimum path-length in the order of at least 100 m before reaching the nearest large-scale fault or higher-permeability crystalline basement, use of mean values for the whole crystalline basement is justified, because local variations average out.

In the conceptual models of water-conducting features (Figs. 10-7 to 10-9), average mineralogical compositions and typical values of open porosities are indicated, both based on the derivations described in sections 6.6 and 6.7.

Because cataclastic and jointed zones contain structures of both phases of hydrothermal alteration (high-temperature and low-temperature), two sets of mineralogical and petrophysical parameters are attributed to each in Figures 10-7 and 10-8. Two sets for the mineralogy are probably unnecessary for the "aplite/pegmatite dykes" because alterations of both phases only have minor effects in these rocks. Alternatively, however, different datasets are given for the higher-permeability, strongly altered borehole sections and for the low-permeability, weakly altered sections.

Unimportant by quantity, but potentially relevant for sorption properties of the geosphere, is the presence of penetrative hematite impregnation of the rocks in the uppermost 350 - 650 m of the crystalline basement. This phenomenon is due to the action of oxygenated hydrothermal fluids and occurs in all borehole sections. These fluids circulated in the Late Paleozoic and are unrelated to present groundwater conditions (cf. section 4.5.8).

### **10.3.6 Cation exchange capacities**

Cation exchange between groundwater and minerals, in fracture coatings and on the surfaces of the diffusion-accessible wallrock pores is an important radionuclide retardation mechanism, especially in groundwaters with low ionic strength. In the crystalline basement of Northern Switzerland, minerals with high cation exchange capacities mainly comprise clays (smectite, illite, chlorite, kaolinite, mixed-layer phases), trace amounts of Fe-oxides/oxyhydroxides (such as hematite) and, to a lesser extent, primary sheet silicates such as biotite and muscovite.

68 samples of altered wallrocks adjacent to brittle fractures and containing variable proportions of fracture infill materials were analyzed following the methodology described in PETERS (1991). No analyses are available from pure fracture infills or from unaltered wallrock samples.

## **Results and discussion**

Mean values of cation exchange capacities are shown in Table 10-3, together with determinations of internal and external surfaces (measured by BET [Brunauer, Emmett & Teller method] for external surfaces and glycolation for total surfaces) and the mineralogical compositions of the sheet silicates of the samples. Figure 10-10a shows

that, in spite of a large scatter, a weak positive correlation exists between the sum of exchanged cations and the sheet silicate content of the samples. Because sheet silicates are more abundant in gneisses than in granites or other plutonic rocks (mainly due to the high content of primary micas in gneisses), the sum of exchanged cations is slightly higher (gneisses: mean  $\sim 11$  meq/100 g; granites: mean  $\sim 8$  meq/100 g, cf. Tab. 10-3 and Fig. 10-10).  $\text{Ca}^{++}$  is the dominant cation in all samples, followed by  $\text{K}^+ + \text{Na}^+$ .

### Recommendations for the application of the available cation exchange dataset

All data discussed above refer only to altered wallrocks adjacent to fractures that contain variable proportions of fracture infill materials. Even though pure fracture infills have not been analyzed separately, their cation exchange capacity is assumed to be at least equivalent to that of the wallrock samples, given the mineralogical compositions (Figs. 10-7 to 10-9). No data are available for aplite/pegmatite dykes, aplitic gneisses or any types of fresh wallrocks. Data from the Grimsel granodiorite, a hydrothermally unaltered rock comparable to the granites of Northern Switzerland (BRADBURY 1989), are used by way of analogy. The measurements at Grimsel indicate cation exchange capacities about 0.4 meq/100 g, which is a lower limit for rocks from Northern Switzer-

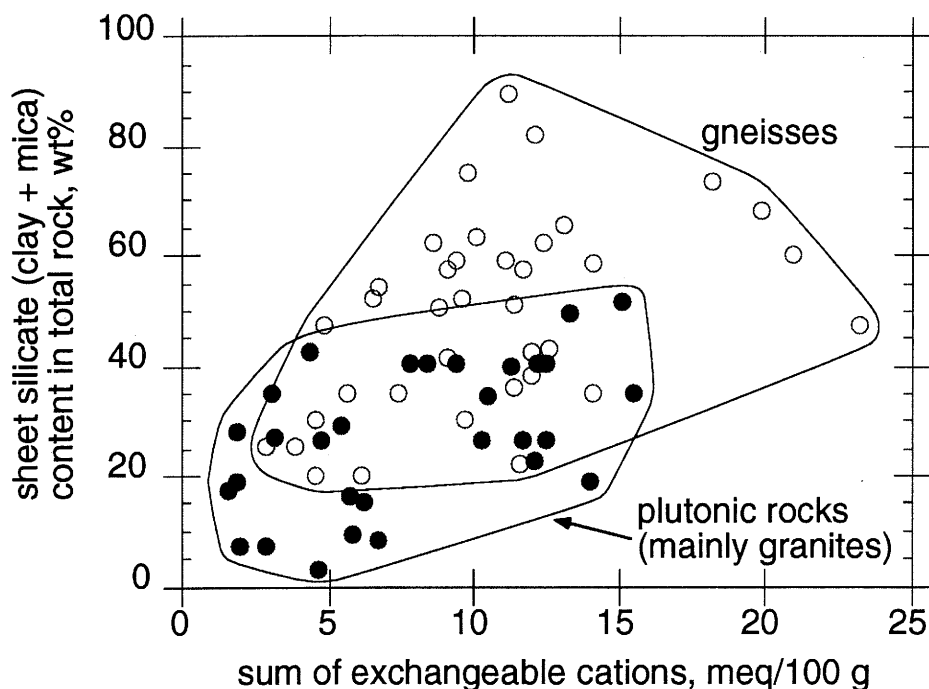


**Fig. 10-10:** Cation exchange capacities of altered wallrock samples. Correlation between cation exchange capacity and the content of clay.

		K [meq/100g]	Na [meq/100g]	Mg [meq/100g]	Ca [meq/100g]	sum of previous columns = exchangeable cations [meq/100 g]	external surface [m <sup>2</sup> /g]	internal surface [m <sup>2</sup> /g]	total surface [m <sup>2</sup> /g]	mica and illite [wt %]	kao- linite [wt %]	smec- tite [wt %]	chlo- rite [wt %]	ill/sm mixed -layer [wt %]	chl/sm mixed -layer [wt %]	total clay content [wt %]
68 datasets, grouped according to rock types	plutonic rocks	1.09	1.21	0.49	5.13	7.93	6.3	67.1	73.4	13	2	0.5	6	3	3	27
	gneisses	1.73	1.95	0.75	6.22	10.65	8.5	49.7	58.2	23	7	0.7	13	4	0	48
68 datasets, grouped according to hydro- geological domains	higher- permeability domain	1.60	1.71	0.61	5.39	9.31	7.8	56.0	63.8	19	5	0.8	7	4	2	37
	low- permeability domain	1.14	1.45	0.70	6.46	9.74	7.0	60.2	67.2	19	4	0.3	17	3	0	43
68 datasets, grouped according to geo- graphic location	Böttstein	1.57	1.79	0.35	8.94	12.65	7.3	61.2	68.5	17	0	0	6	5	3	33
	Weiach	1.32	2.28	0.95	6.47	11.01	6.2	40.0	46.2	15	0	0	27	7	0	49
	Schafisheim	1.90	2.76	1.28	4.18	10.12	8.4	39.2	47.6	7	2	0	15	6	10	40
	Kaisten	2.36	1.72	0.56	4.43	9.07	8.7	33.8	42.5	26	13	1	4	1	0	45
	Leuggern	0.70	1.43	0.73	6.50	9.36	8.1	67.2	75.3	19	0.3	0	13	4	0	36
	Siblingen	0.61	0.12	0.19	2.65	3.56	2.9	127.3	130.3	13	7	2	2	0	0	24

**Tab. 10-3 :** Summary of exchangeable cations, cation exchange capacities, surface areas and mineralogical compositions of altered wallrock samples (mean values). The dataset, comprising 68 analyses, is grouped according to rock type, hydrogeological domain and borehole.

land, because the latter are often affected by hydrothermal effects even in rock portions away from discrete fractures.

A decrease in cation exchange capacity with depth has been identified in some of the boreholes. However, the pattern is not consistent over the whole region and probably reflects local variations.

### **10.3.7 Comments on regional variations of water-conducting features**

Each of the sections penetrated by the six deep boreholes has certain aspects that distinguish it with respect to the development of water-conducting features. For example, jointed zones are frequent in Siblingen while cataclastic zones and fractured dykes are dominant in Schafisheim. However, these variations probably are of local extent and no basis exists for subdividing the region of interest into areas with different geological properties. Therefore, one single geological dataset is given for the entire region, while regional variations of hydrogeological and hydrochemical parameters are significant and require separate sets of parameters for different regions (e.g. area East vs area West).

At present, there is no indication that large ore and mineral veins (section 6.5) occur anywhere in the region; if they do, they are expected to be restricted to specific "ore districts", by analogy with the Black Forest. Investigations related to the presence or absence of ore veins in the siting area will be one of the major tasks of the planned Phase II investigations. In principle, ore and mineral veins could be modeled using the concept of cataclastic zones and some parameter variations (e.g. wider openings, different mineralogy, etc.). In the deepest parts of the Leuggern borehole, high permeabilities of cataclastic zones are due to rock/water interactions that are similar to those that have occurred in ore and mineral veins (even though no major ore concentrations formed, cf. section 6.3.2).

## **10.4 Hydrogeochemical database**

### **10.4.1 Reference waters**

The particular reactions by which repository construction material and backfill may be degraded, canisters corroded and breached, and the waste form leached and dissolved will be constrained by the chemistry of water entering the repository. The reference water chemistry is intended not only as input to the modeling that will assess repository performance but also for planning laboratory experiments to supplement this assessment. It is also used to aid in selecting the values of sorption parameters employed in modeling radionuclide transport.

The chemistry of the water in the environment of an actual repository will be defined based on samples taken during repository construction. To analyze the safety of potential repositories, the probable water chemistry in areas of interest must be deduced from the chemistry of samples taken during surface-based testing.

This section describes the chemistry of reference waters for potential repositories in both areas East and West. It begins with an introduction describing briefly how the reference water chemistries were developed. This is followed by discussions of both the western and eastern reference waters. The section concludes with mention of two other water types found in the crystalline basement that could have a limited effect on a repository. The details of the development of the reference water chemistry from the water analytical data are given by PEARSON & SCHOLTIS (1993).

### Development of reference water chemistries

The water chemistry in the crystalline basement was discussed previously in Chapter 7. With this understanding of regional water chemistry, specific samples and analyses could be chosen that, taken in groups, define the chemistry of water likely to be encountered within the potential repository areas.

The reference water chemistry in area West is defined by samples from the Nagra boreholes at Böttstein, Kaisten and Leuggern, and from the thermal water boreholes at Zurzach. Water in the area East is defined by samples from the Nagra borehole at Siblingen.

Two samples of more saline water of different chemical types were collected from 923 m in the Leuggern borehole and 1326 m in the Böttstein borehole. These waters are also described here. The Böttstein 1326 m water is virtually identical with water used as the reference water for earlier safety assessment calculations for Project Gewähr 1985 (SCHWEINGRUBER 1984; NAGRA 1985b).

Figure 10-11 is a Schoeller diagram illustrating the major ion chemistries of these waters. The eastern reference water is the least saline. It is of the Na-HCO<sub>3</sub>-SO<sub>4</sub>-(Cl) type with total dissolved solids of 0.5 g/l. The western reference water has higher concentrations of all major ions, but particularly of Na, Cl and SO<sub>4</sub>. It is of the Na-SO<sub>4</sub>-(Cl-HCO<sub>3</sub>) type with total dissolved solids of about 1.0 g/l. Both the remaining waters are considerably more saline than the reference waters. Water from the Leuggern borehole at 923 m is of the Na-Ca-SO<sub>4</sub> type and has a total dissolved solids content of 5 g/l after correction for the drilling-fluid content of the original samples. The water from 1326 m at Böttstein is of the Na-(Ca)-Cl-(SO<sub>4</sub>) type and has a total dissolved solids content of 13 g/l after correction for the drilling-fluid content of the original samples. The two reference waters will certainly exert the principal influence on potential repositories in the respective areas. However, it is also possible that at least part of a repository in the area West could be affected by small amounts of the more highly saline waters.

The quality of the samples and analytical data vary among the dissolved constituents and other chemical parameters specified for the reference waters. In the following discussion, it is stated that reference water values for which there is the greatest uncertainty should be used with caution. This means that they should not be used as the sole or principal support for any critical safety assessment conclusion.

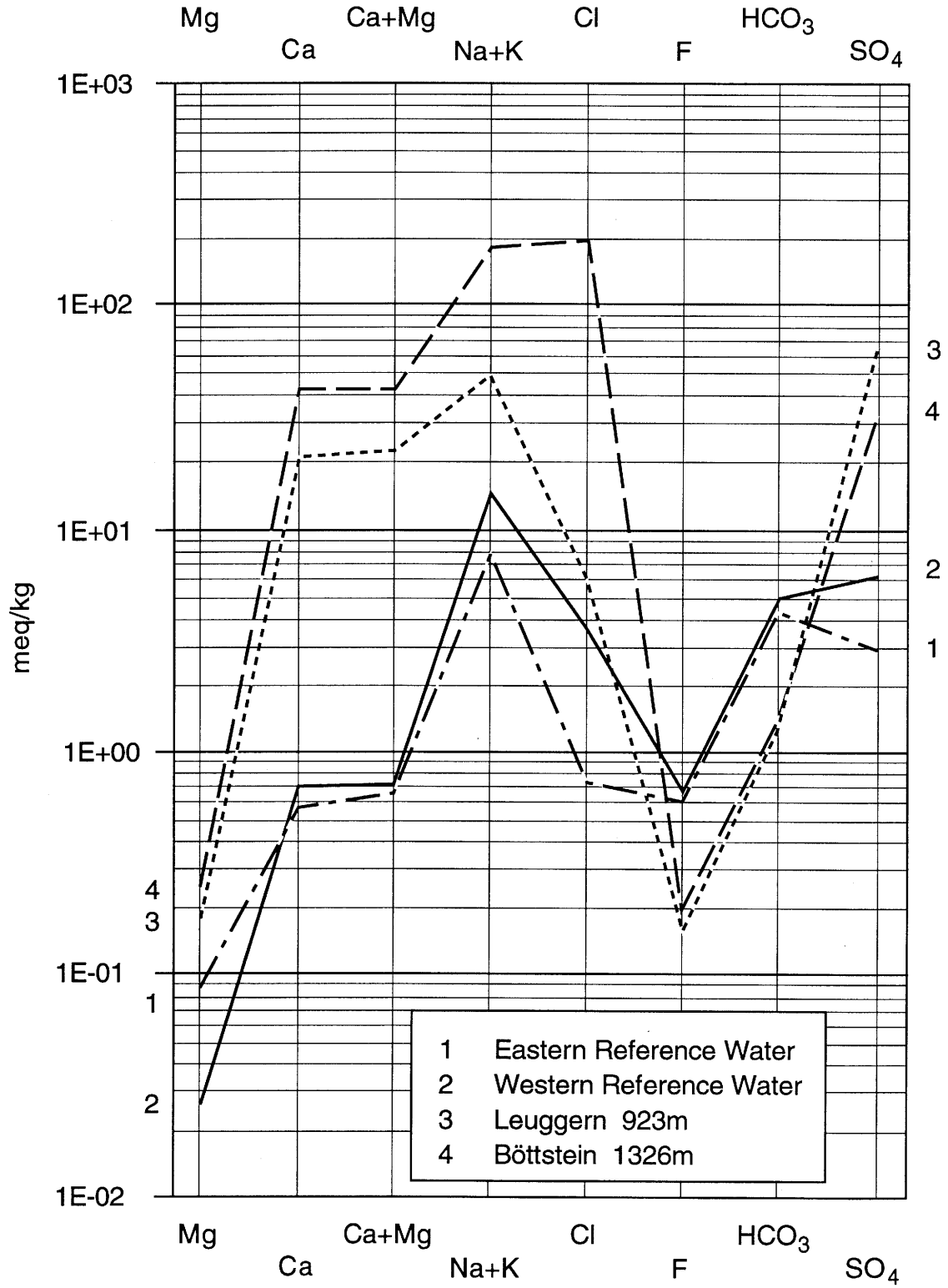


Fig. 10-11 : Schoeller diagram of reference waters and more saline waters from the crystalline basement.

Borehole water samples were filtered through 450 nm membrane filters. ALAUX-NEGREL et al. (1993) recently report that the concentrations of some elements in groundwater samples passed through filters of this size are due to the presence of fine particulate matter as well to material in solution. Of the elements studied by these authors that are included in the reference waters, three, Ba, Th and Zr, appear to be associated with particulate matter, while eight, Ca, Co, Cs, Mo, Na, Rb, Sr and Zn, are present as dissolved species. It is possible that other elements that are present in low concentrations in water from the boreholes, but that were not examined by ALAUX-NEGREL et al. (1993), may also be associated with particulates.

### Western reference water

The western reference water is defined by more than thirty samples taken from the Nagra boreholes at Leuggern, above 800 m depth at Böttstein, and from the thermal water boreholes at Zurzach. These samples all have total dissolved solids contents of 0.9 to 1.1 g/l. Samples from the Kaisten borehole are similar, but have higher SO<sub>4</sub> and lower Cl concentrations and total dissolved solids contents to 1.4 g/l. Because of the number of samples available and their quality, the western reference water can be defined with some confidence. The thermal boreholes at Zurzach have an artesian flow of 600 liters per minute that has had a constant chemical composition for about 30 years, (GEOL. BÜRO DR. H. JÄCKLI AG 1986, GEOL. INST. UNIV. BERN 1989). This indicates the great stability of the geochemical system in this region.

Table 10-4 gives the chemical composition of, and other information on, the western reference water. The first column gives the name of the constituent or parameter. The second and third columns give the most probable concentration (or other parameter value). The constituent concentrations appear both as milligrams per liter (mg/l) and as mols per kilogram H<sub>2</sub>O (molality). The latter values are calculated from the former as described by PEARSON et al. (1989: section 1.2.1), and are displayed to three digits. Note that, as indicated by the mg/l values, the molalities of some of the constituents are significant only to one or two digits.

The remaining columns in Table 10-4 give the ranges of concentrations and other parameters. For the most part, these are based on extreme values found in individual samples from Böttstein, Leuggern and Zurzach. Samples from Kaisten are slightly more saline, but generally fall into the same range. The Kaisten extreme values are given in parentheses when they fall outside the range of the other boreholes.

Geochemical modeling was used in developing the reference water chemistry, as it was in evaluating the water sample data themselves. The modeling was performed using PHREEQE (PARKHURST et al. 1980) with the Nagra thermochemical database (PEARSON & BERNER 1991; PEARSON et al. 1992). Results of the modeling are given in Table 10-4. These include saturation indices (SI)<sup>1)</sup>, which indicate whether a

---

1) The saturation index equals  $\log(IAP/K_T)$ , where IAP is the activity product of the mineral and K<sub>T</sub> is the temperature - corrected equilibrium constant.

water is oversaturated ( $SI > 0$ ), saturated ( $SI = 0$ ), or undersaturated ( $SI < 0$ ) with respect to various minerals and other solids, the partial pressures corresponding to the analyzed concentrations of various dissolved gases and the oxidation potentials corresponding to the concentrations of elements found in the water in more than one oxidation state.

Geochemical modeling of the water samples from the boreholes indicates that they are in equilibrium with several minerals that commonly form at low temperatures. These are barite ( $BaSO_4$ ), fluorite ( $CaF_2$ ), chalcedony ( $SiO_2$ ) and kaolinite ( $Al_2Si_2O_5(OH)_4$ ). As discussed in section 6.6, all of these minerals except chalcedony occur in water-bearing fractures in the crystalline basement. Geochemical modeling was used to adjust the final composition of the reference water for equilibrium with these minerals. Saturation with calcite ( $CaCO_3$ ) was also assumed in deriving the pH values of the reference waters, as discussed below. Because of the assumption of saturation, these minerals all have saturation indices of zero in Table 10-4.

Table 10-4 also gives the saturation indices of the reference water calculated for a number of the other solid phases for which data are available in the Nagra thermochemical database. Many of them have saturation indices more negative than -1, suggesting that they are not active in controlling the concentration of their constituent elements. The concentrations of certain elements may be controlled by solid solutions or other solids not defined well enough to be included in the geochemical model used. Some elements in solution in trace quantities may be present in the rock and minerals of the crystalline basement in concentrations too low for them to reach saturation with possibly controlling solid phases. Some of the solid phases in the thermochemical database may form only at rates that are too slow to influence the chemistry of waters at these temperatures. Such phases certainly include  $NiFe_2O_4$  and  $NiSiO_3$ , but probably quartz, Se,  $SnO_2$  and  $ZrO_2$  as well. Thus, it is necessary to be cautious when drawing conclusions from saturation indices about solid phase controls on the concentrations of dissolved substances.

A brief discussion of the values in Table 10-4 follows. PEARSON & SCHOLTIS (1993: section 2.4) discuss the development of these reference waters in much greater detail.

*Density, Li, K, Rb, Cs,  $NH_4$ , Mg, Ca, Sr, Ra,*

*U, Cl, Br,  $SO_4$ , As(III), Mo, Alkalinity,  $B(OH)_3$ ,  $N_2$ ,  $CH_4$  and Ar*

The reference values and ranges of these constituents are means and extremes of analyzed values for samples from the Böttstein, Leuggern and Zurzach boreholes. Samples from Kaisten typically have higher  $SO_4$  and alkali and alkaline earth concentrations and lower Cl, leading to a higher total dissolved solids content.

The range of uranium concentrations was chosen to be consistent with the range of oxidation potentials chosen, as discussed below.

Sample Source	Base Reference Water		Concentration and Parameter Ranges	
			Minimum	Maximum
pH [units]	7.66		(7.1) 7.6	8.3
pe [units]	- 2.72		- 3.7	- 0.7
Eh [volts, from pe]	- 0.18		- 0.24	- 0.05
Formation Temp. [°C]	55			
Density [g/ml]	0.999			
	[mg/l]	[M]	Minimum [mg/l]	Maximum [mg/l]
Lithium (Li <sup>+</sup> )	1.1	1.59E-04	0.5	3
Sodium (Na <sup>+</sup> )	323.8	1.41E-02	286	393 (432)
Potassium (K <sup>+</sup> )	8.5	2.18E-04	4	16 (34)
Rubidium (Rb <sup>+</sup> )	0.055	6.45E-07	0.025	0.095 (0.15)
Cesium (Cs <sup>+</sup> )	0.043	3.24E-07	(0.01) 0.02	0.07 (0.11)
Ammonium (NH <sub>4</sub> <sup>+</sup> )	0.14	7.78E-06	0	0.39 (0.62)
Beryllium (Be <sup>2+</sup> )	5E-04	5.56E-08	0	5E-04
Magnesium (Mg <sup>2+</sup> )	0.3	1.24E-05	0.0075	2 (3.8)
Calcium (Ca <sup>2+</sup> )	14.0	3.50E-04	6	16 (50)
Strontium (Sr <sup>2+</sup> )	0.46	5.26E-06	0.09	0.6 (1.4)
Barium (Ba <sup>2+</sup> )	0.05	3.65E-07	0.007	0.19
Radium (Ra <sup>2+</sup> )	7E-10	3.10E-15	3E-10	1E-09 (5.2E-09)
Chromium (Cr)	8.5E-04	1.64E-08	0	9E-04
Manganese (Mn <sup>2+</sup> )	0.037	6.75E-07	0.01	0.6 (1.0)
Iron (Fe <sup>2+</sup> )	0.007	1.26E-07	0.004	1.3 (5.9)
Nickel (Ni <sup>2+</sup> )	< 5E-04	8.53E-09	0	0.01 (0.04)
Cobalt (Co <sup>2+</sup> )	1.5E-04	2.55E-09	0	0.002
Copper (Cu <sup>2+</sup> )	< 0.002	3.15E-08	0	0.01
Zinc (Zn <sup>2+</sup> )	0.004	6.13E-08	0.003	1.6
Zirconium (Zr)	1.5E-04	1.65E-09	0	1.5E-04
Palladium (Pd)	< 1E-04	9.42E-10	0	1E-04
Tin (Sn)	6E-04	5.07E-09	0	1E-03
Lead (Pb)	2.5E-04	1.21E-09	0	0.03 (0.07)
Aluminum (Al)	0.012	4.46E-07	0	0.3
Uranium (U)	1.3E-04	5.47E-10	5E-06	1.1E-03
Thorium (Th)	5.0E-04	2.16E-09	5E-05	5E-04
Fluoride (F)	12.2	6.43E-04	(6.6) 10.2	15.5
Chloride (Cl)	128	3.62E-03	(60) 108	178
Bromide (Br)	0.72	9.03E-06	(0.47) 0.04	1.2
Iodide (I)	0.01	7.90E-08	0	0.05 (0.07)
Sulfate (SO <sub>4</sub> <sup>2-</sup> )	296	3.09E-03	(491) 252	426 (598)
Phosphate (as P)	0.04	1.29E-06	0	0.25 (1.14)
Nitrate (NO <sub>3</sub> <sup>-</sup> )	0.1	2.00E-06	0	0.1
Arsenite (As <sup>3+</sup> )	< 0.12	1.60E-06	0.006	1.2
Arsenate (As <sup>5+</sup> )	0.035	4.68E-07	0	0.53
Tot. Arsenic (As)	0.16	2.07E-06		
Selenium (Se)	0.1	7.89E-07	0	0.25
Molybdenum (Mo)	0.005	3.13E-08	0.002	0.008
Tungsten (W)	0.7	2.83E-06	0.07	0.7
Alkalinity as HCO <sub>3</sub> <sup>-</sup>	291	4.78E-03	189	390 (439)
Bicarbonate (HCO <sub>3</sub> <sup>-</sup> )	285	4.67E-03		
Carbonate (CO <sub>3</sub> <sup>2-</sup> )	2.7	4.51E-05		

**Tab. 10-4 :** Reference water chemistry: area West (page 1 of 3)  
(for explanation cf. text).

Molality [M] calculated from mg/l. The number of significant digits is the number of digits in the mg/l values. Values in parentheses are extreme values found in Kaisten samples.

Sample Source	Base Reference Water		Concentration and Parameter Ranges		
	[mg/l]	[M]	Minimum [mg/l]	Maximum [mg/l]	
Tot. Sulfide (H <sub>2</sub> S)	0.005	1.50E-07	0	0.32	
Silica (H <sub>2</sub> SiO <sub>3</sub> )	< 46.1	5.91E-04	11	59	(74)
Borate (B(OH) <sub>3</sub> )	3.4	5.51E-05	1.3	6.4	(7.8)
Total Iron (Fe)	0.026	4.66E-07			
Organic C	0.04	3.34E-06	0	3.6	
Oxygen (O <sub>2</sub> )	5E-04	1.56E-08	0	0.1	(0)
Nitrogen (N <sub>2</sub> )	< 33	1.18E-03	30	39	(48)
Methane (CH <sub>4</sub> )	0.017	1.06E-06	(0) 0.009	0.08	
Hydrogen (H <sub>2</sub> )	5E-04	2.43E-07	0	0.04	
Argon (Ar)	< 0.88	2.21E-05	0.79	0.99	
Carbon dioxide (CO <sub>2</sub> )	7.7	1.75E-04	0	13	(36)
<b>CALCULATED VALUES</b>	<b>[mg/l]</b>	<b>Difference from Sum</b>	<b>[mg/l]</b>	<b>[mg/l]</b>	
Dissolved Solids:					
Sum	969				
Residue (110 C)	957	- 1.2 %	854	1119	(1350)
Residue (180 C)	951	- 1.8 %	822	1114	(1345)
Ionic Strength [M]	1.87E-02				
Carbonate System: pH adjusted for calcite saturation:					
			<b>Minimum</b>	<b>Maximum</b>	
pH [units]	7.66		(7.32) 7.71	7.91	
Total Diss.CO <sub>2</sub> [M]	4.90E-03		4.2E-03	6.3E-03	(6.7E-03)
log P CO <sub>2</sub> [bars]	- 2.02		(- 1.6) - 2.0	- 2.4	
Saturation Indices:					
BARITE	0.00				
BRUCITE	- 5.04				
CALCITE	- 0.00				
CELESTITE	- 1.73				
CHALCEDONY	0.00				
DOLOMITE-DISORD.	- 1.52				
DOLOMITE-ORD.	- 1.08				
Fe(OH) <sub>3</sub> -ALPHA	- 2.50				
Fe(OH) <sub>3</sub> -BETA	- 4.50				
FLUORITE	0.00				
GIBBSITE	-0.79				
GOETHITE	-0.00				
GYPSUM	-1.96				
KAOLINITE	0.04				
MANGANITE	-11.78				
MoO <sub>2</sub>	- 5.58				
MoO <sub>3</sub>	- 11.53				
Ni(OH) <sub>2</sub> S	- 6.29				
Ni <sub>2</sub> SiO <sub>4</sub>	- 9.74				
Ni <sub>2</sub> SiO <sub>4</sub> S	- 11.11				
NiCO <sub>3</sub> S	- 6.95				

Tab. 10-4 : Continued (page 2 of 3).

Sample Source	Base Reference Water		Concentration and Parameter Ranges	
NiFe <sub>2</sub> O <sub>4</sub>		1.58		
NiO		- 5.99		
NiSiO <sub>3</sub>		4.90		
Pd(OH) <sub>2</sub> S		- 3.52		
PdO		- 0.63		
PORTLANDITE		- 9.23		
PYROCHROITE		- 6.57		
PYROLUSITE		- 18.52		
QUARTZ		0.34		
RHODOCHROSITE		- 0.35		
Se		3.51		
SIDERITE		- 1.22		
SnO <sub>2</sub>		1.70		
STRONTIANITE		- 1.15		
Th(OH) <sub>4</sub>		- 7.93		
ThO <sub>2</sub>		0.89		
U <sub>3</sub> O <sub>7</sub> -BETA		- 0.11		
U <sub>4</sub> O <sub>9</sub>		1.76		
UO <sub>2</sub> -AMORPHOUS		- 4.83		
UO <sub>2</sub> -CRYSTALLINE		1.46		
USiO <sub>4</sub>		1.07		
WITHERITE		- 3.13		
ZrO <sub>2</sub>		1.38		
Indicators of Redox State		<b>pe</b>	<b>Eh [volts]</b>	
Used for Modeling:		- 2.72	- 0.18	
Calculated from Redox Couples:				
		<b>pe</b>	<b>Eh [volts]</b>	
As(V) /As(III)		- 2.46	- 0.16	
H <sup>+</sup> /H <sub>2</sub>	>	- 5.92	- 0.39	
HCO <sub>3</sub> /CH <sub>4</sub>		- 5.20	- 0.34	
N <sub>2</sub> /NH <sub>4</sub> <sup>+</sup>		- 4.47	- 0.29	
NO <sub>3</sub> /N <sub>2</sub>	<	8.58	0.56	
O <sub>2</sub> /H <sub>2</sub> O(THEOR)		9.64	0.63	
O <sub>2</sub> /H <sub>2</sub> O(SATO)		- 0.46	- 0.03	
SO <sub>4</sub> <sup>2-</sup> /HS <sup>-</sup>	>	- 4.38	- 0.29	
Gas Partial Pressures: log P (Gas)				
		<b>[bars]</b>		
CH <sub>4</sub> (G)		- 2.94		
CO <sub>2</sub> (G)		- 2.02		
H <sub>2</sub> (G)		- 3.46		
N <sub>2</sub> (G)		0.38		
O <sub>2</sub> (G)		- 4.76		

Tab. 10-4 : Continued (page 3 of 3).

*Be, Cr, Co, Zr, Sn, I, P, As(V) and Se*

These constituents were found in concentrations above the analytical detection limit<sup>1)</sup> only in a few samples analyzed by one laboratory. The reference concentration is the mean of the analyses that were above the detection limit. The maximum is the maximum value reported and the minimum is taken as zero. It is important to note that the meaning of the detection limits given in the original data sources is not clear, so the concentrations of these constituents should be used with caution.

*Mn, Fe, Zn, Pb, Total Fe and Organic C*

There was a very strong possibility that most samples were contaminated with these substances, so the reference and minimum values are the mean and lowest values reported from those samples least likely to have been contaminated. The maximum value was the largest reported for any sample regardless of possible contamination.

Saturation indices for several solids of Mn and Fe are given in the Table. The solubilities of several metals are sensitive to oxidation state. As discussed below, the oxidation potential of the reference solution was chosen for goethite (FeOOH) saturation at the reference Fe concentration. The most common Fe-bearing phase in the crystalline basement is hematite. However, at the temperatures of these waters, hematite is unlikely to form rapidly enough to affect their Fe contents. The less stable but more rapidly formed Fe phase goethite was used instead.

This oxidation potential results in gross undersaturation of the Mn oxide and hydroxide minerals manganite, pyrochroite and pyrolusite, and both forms of Fe(OH)<sub>3</sub>. It also produces undersaturation with respect to the Mn and Fe carbonate minerals rhodochrosite and siderite. The former is undersaturated only by a factor of 0.5 (10<sup>-0.35</sup>), well within the range of Mn concentrations. A Mn concentration somewhat below saturation with rhodochrosite would be consistent with control by Mn in solid solution in another carbonate mineral such as calcite.

There are considerable differences among the results of organic carbon analyses made by different laboratories on samples collected using various techniques. The reference value chosen was measured by PSI as part of the colloid study (DEGUELDRE 1994). Until the reasons for the differing results between the groups are understood, the organic carbon values should be used with caution.

---

1) The detection limit for an element in a groundwater sample is determined not only by the sensitivity of the analytical technique used but also by the background or "blank" concentration introduced from contamination in the sampling equipment, storage vessel and analytical equipment itself. Analytical sensitivities have improved during the project but, for some of the rather exotic trace elements measured, blanks are not well defined. The effort required to determine the extent to which elements at concentrations close to instrumental sensitivity limits could be accurately quantified (and associated errors assigned) was considered not to be cost-effective because, at most, order-of-magnitude estimates of concentration are needed for performance assessment.

*Pd, NO<sub>3</sub>, H<sub>2</sub>S and O<sub>2</sub>*

These concentrations were below detection or had measured values attributable to contamination in the original samples. The reference concentrations are taken as less than the lowest detection limit reported and the minimum concentration as zero. The maximum concentrations are the maximum values reported regardless of possible contamination. Because the meaning of the detection limits in the original data sources is not described, these concentrations should be used with caution.

As the Table shows, the Pd concentration is below saturation with respect to PdO, but only by a factor of 0.2 ( $10^{-0.63}$ ), well within the uncertainty of the analytical and thermodynamic data. Pd metal was included in the thermodynamic database used, but as preliminary modeling showed that this water would be oversaturated by more than 12 orders of magnitude with respect to this phase, it was not included in Table 10-4.

*Ni, Cu and H<sub>2</sub>*

Low but measurable concentrations of these constituents were found in some samples, but concentrations were below detection in others. Both metals are part of most sample collection and analysis apparatus and could represent contamination. H<sub>2</sub> could have formed from corrosion of iron or other metal in the sampling system. The reference concentrations in the Table are given as less than the lower of the minimum measured concentration or the detection limit. The minimum concentration is given as zero. Again, because the meaning of the detection limits is not clear, these concentrations should be used with caution. The maximum concentrations are the maximum of those reported regardless of potential contamination.

*Th, W*

Only one analysis was available for each of these elements. These values are taken as the reference and maximum concentrations. The minimum concentrations are arbitrarily chosen as a factor of ten lower. Because it is based on a single analysis and is unsupported by geochemical considerations, the W value should be used with extreme caution.

The Th concentration is similar to that of U, which is reasonable because both elements are present principally in the IV valence state in these waters. At this concentration, Th is oversaturated by a factor of about ten ( $10^{0.89}$ ) with respect to ThO<sub>2</sub>, but strongly undersaturated with respect to Th(OH)<sub>4</sub>. This is probably within the uncertainty of the analytical and thermochemical data, and does not contradict the concentration given.

*Na*

The Na concentration was adjusted during geochemical modeling so the reference water would be electrically neutral. Its concentration is very close to that of the mean of water typical of the Böttstein, Leuggern and Zurzach samples (322 mg/l).

*Ba, F, H<sub>2</sub>SiO<sub>3</sub> and Al*

The reference concentrations of these constituents were determined by geochemical modeling. The Ba and F concentrations were fixed by equilibrium with the minerals barite (BaSO<sub>4</sub>) and fluorite (CaF<sub>2</sub>), respectively. The modeled concentrations (0.05 mg Ba/l and 12.2 mg F/l) are virtually the same as the mean of the analytical values (0.07 and 12.5 mg/l, respectively). This Ba concentration is also below saturation with witherite (BaCO<sub>3</sub>). The range of values for these constituents represents the range of analytical results.

The concentration of H<sub>2</sub>SiO<sub>3</sub> was determined by modeling equilibrium with respect to a silica (SiO<sub>2</sub>) mineral. Calculations assuming quartz saturation led to 20.6 mg H<sub>2</sub>SiO<sub>3</sub>/l, while chalcedony saturation led to 46.1 mg H<sub>2</sub>SiO<sub>3</sub>/l. The mean measured H<sub>2</sub>SiO<sub>3</sub> concentration was 38 mg/l, closer to chalcedony saturation, so that phase was chosen for the final modeling on which the reference water was based. The spread in the analyzed H<sub>2</sub>SiO<sub>3</sub> values is due in part to the different temperatures of the samples as well as to difficulties in the collection and analysis of samples for this substance.

The reference Al concentration is 0.012 mg/l and is based on saturation with respect to chalcedony and kaolinite (Al<sub>2</sub>Si<sub>2</sub>O<sub>5</sub>(OH)<sub>4</sub>). This value corresponds to undersaturation with gibbsite (Al(OH)<sub>3</sub>). It is within the range of measured Al concentrations, but is higher than the mean value (0.004 mg/l). This could be a result of difficulties in the aluminum analyses themselves, from the fact that these waters are not truly saturated with respect to kaolinite, or of errors in the thermodynamic data for aqueous species or for kaolinite that were used in the geochemical modeling.

*pH, CO<sub>2(aq)</sub>, P<sub>CO2</sub> and Total Dissolved CO<sub>2</sub>*

The values of these properties in the reference water were modeled using the reference Ca and alkalinity values and assuming calcite saturation. The pH value and dissolved CO<sub>2</sub> concentrations are within the range of values measured. The ranges of values given were calculated by adjusting individual samples to calcite saturation.

The bicarbonate (HCO<sub>3</sub>) and carbonate (CO<sub>3</sub>) concentrations, which are components of the alkalinity and which, together with the dissolved CO<sub>2(aq)</sub>, comprise the total dissolved CO<sub>2</sub>, are taken from the geochemical modeling results.

*Oxidation Potential*

The oxidation potential of the reference water (pe = -2.72) was calculated by assuming that the iron concentration of the reference water results from saturation with the mineral goethite (FeOOH). At the reference temperature chosen (55°C), this equals an Eh of -0.18 volts (V). This is the same as the minimum measured Pt electrode potential and close to that corresponding to the As(V)/As(III) ratio in the reference water (-0.16 V).

Determinations of the redox potential of groundwaters by measuring Pt electrode potentials are difficult and unreliable (LINDBERG & RUNNELS 1984). The fact that the

reference redox potential of the water is consistent with the lowest platinum electrode potential measured during both the initial sampling and later long-term monitoring (BRUETSCH et al. 1991) provides support for the value chosen. However, it is not possible to develop a useful range of possible redox values from platinum electrode potential measurements. The range of redox values in Table 10-4 was therefore calculated by choosing saturation with other possible minerals as controls on the concentration of the redox-sensitive elements U and Fe in the water.

The thermodynamic database includes a number of Fe minerals and U-bearing solids. Geochemical calculations were made in which the redox potential was varied, and U concentrations were modeled at equilibrium with various minerals (PEARSON & SCHOLTIS 1993: Tab. 2.4). At the reference redox potential, the reference uranium concentration represents oversaturation with respect to coffinite and uraninite by factors of twelve ( $10^{1.07}$ ) and twenty-four ( $10^{1.38}$ ), respectively. A uranium concentration of  $5 \cdot 10^{-6}$  mg/l corresponds to saturation with respect to uraninite and was chosen as the minimum uranium concentration. The minimum redox potential was arbitrarily chosen as one pe unit lower than the reference pe, or -0.24 V.

Naturally occurring uranium solids such as pitchblende are likely to include more oxidized uranium oxides isostructural with crystalline  $\text{UO}_2$ . The geochemical modeling shows that equilibrium between  $\text{U}_4\text{O}_9$  and  $\text{UO}_2(\text{crystalline})$  occurs at a redox potential of -0.04 V and a uranium concentration of  $2.3 \cdot 10^{-4}$  mg/l. This corresponds closely to the uranium concentration of the reference water. The calculations also show that, at a potential of -0.05 V, the uranium content of the reference water would be in equilibrium with uraninite. Finally, the effective potential (SATO 1960) corresponding to the reference  $\text{O}_2$  concentration (itself a maximum value) is -0.03 V. A potential of -0.05 V (pe = -0.7) was taken as the maximum value.

The reference water composition also includes concentrations of H, C, N and S in different oxidation states from which oxidation potential values can be calculated. Such values are given in the Table. Redox reactions involving more than one or two electrons occur so slowly at low temperatures that, in the absence of bacterial or other catalysts, these values give little or no information about the equilibrium state of the reference water.

### **Eastern reference water**

The eastern reference water is defined by samples taken from the Nagra borehole at Siblingen. Only three useful samples are available, all taken during drilling. Of these, two were virtually pure formation water and yield good concentrations for constituents not affected by the sampling process itself. The third sample required correction for a significant admixture of drilling-fluid and gave concentration values useful principally for establishing possible ranges. PEARSON & SCHOLTIS (1993) describe the development of the eastern reference water chemistry in detail. Because the samples on which it is based were all affected to some extent by the sampling process itself, the eastern reference water is much less completely defined than the western reference water, and contains more uncertainty.

Table 10-5 gives the chemical composition and other information on the eastern reference water. The form of this Table is the same as that showing the western reference water and described in the previous section. A brief discussion of the values in this Table follows. A number of elements included in the western reference water are absent from the eastern reference water because no analyses for them were made on the samples from Siblingen. These include Cr, Co, Zr, Pd, Sn, Th, Se, Mo and W.

*Li, K, Cs, Mg, Ca, Cl, SO<sub>4</sub>, As, Alkalinity, B(OH)<sub>3</sub>, N<sub>2</sub>, CH<sub>4</sub> and Ar*

The reference value of these constituents is the mean of the concentrations of the two good samples, while the range encompasses concentrations reported for all three samples. Some constituents were analyzed on only one sample. For these, the maximum and minimum values were arbitrarily taken as a factor of ten higher or lower than the analyzed value.

*Mn, Fe, NO<sub>3</sub>, O<sub>2</sub>, H<sub>2</sub> and Organic C*

All samples from the Siblingen borehole were probably contaminated to some extent with these constituents. Thus, their reference water concentrations were taken as less than the concentrations measured in the samples in which they were likely to be least contaminated. The minimum values for all but Fe were taken as zero, while the maximum values are the largest in any sample. The minimum Fe concentration is that modeled at equilibrium with goethite at the reference oxidation potential.

Saturation indices for a series of minerals of Fe and Mn at their reference concentrations are given in Table 10-5. All Mn minerals are strongly undersaturated, suggesting that none controls the Mn content of the water. Among the Fe minerals, the more crystalline form of ferrihydrite ( $\alpha$ -Fe(OH)<sub>3</sub>) is within ten percent of saturation ( $10^{-0.04}$ ) at the reference oxidation potential, while goethite is oversaturated by a factor of nearly three hundred ( $10^{2.46}$ ). It is consistent with the pattern of flow in the crystalline basement that Fe in the eastern water could be controlled by ferrihydrite, while that of the western water after additional flow could be controlled by the more stable goethite. Because of uncertainty in the eastern samples, however, the minimum Fe concentration of the eastern reference water is also chosen for goethite saturation.

*Rb, NH<sub>4</sub>, Ni, Zn, Pb, I and P*

The concentrations of these constituents in all samples were below detection. The values in the reference water were taken as less than the detection limits, the minimum value as zero and the maximum value as ten times the reference value.

*Sr and Br*

The concentrations of these constituents were measured in one or two samples, but were below detection in the others. The reference concentrations are taken as the measured values, and the maximum and minimum values represent the detection limit of the analyses made on the other samples.

Sample Source		Base Reference Water		Concentration and Parameter Ranges	
pH	[units]	7.66		7.6	8.1
pe	[units]	- 0.52		- 3.7	- 0.5
Eh	[volts, from pe]	- 0.03		- 0.24	- 0.03
Formation Temp.	[°C]	55			
Density	[g/ml]	1.0005			
		[mg/l]	[M]	Minimum [mg/l]	Maximum [mg/l]
Lithium (Li <sup>+</sup> )		0.64	9.22E-05	0.61	0.66
Sodium (Na <sup>+</sup> )		177	7.70E-03	173	177
Potassium (K <sup>+</sup> )		4.2	1.07E-04	3.4	4.6
Rubidium (Rb <sup>+</sup> )	<	0.05	5.85E-07	0	0.5
Cesium (Cs <sup>+</sup> )		0.05	3.76E-07	0.05	0.05
Ammonium (NH <sub>4</sub> <sup>+</sup> )	<	0.005	2.77E-07	0	0.05
Magnesium (Mg <sup>2+</sup> )		1.1	4.53E-05	0.4	1.4
Calcium (Ca <sup>2+</sup> )		11.5	2.87E-04	9	12
Strontium (Sr <sup>2+</sup> )		0.35	3.99E-06	0.04	0.4
Barium (Ba <sup>2+</sup> )		0.08	5.48E-07	0.01	0.1
Radium (Ra <sup>2+</sup> )		1.7E-07	7.52E-13	2E-08	2E-06
Manganese (Mn <sup>2+</sup> )	<	0.005	9.10E-08	0	0.1
Iron (Fe <sup>2+</sup> )	<	0.01	1.79E-07	3E-05	4.3
Nickel (Ni <sup>2+</sup> )	<	0.01	1.70E-07	0	0.1
Copper (Cu <sup>2+</sup> )		0.01	1.57E-07	0.001	0.1
Zinc (Zn <sup>2+</sup> )	<	0.03	4.59E-07	0	0.3
Lead (Pb)	<	0.005	2.41E-08	0	0.05
Aluminum (Al)		0.012	4.35E-07	0.001	0.03
Uranium (U)		3E-04	1.26E-09	3E-05	3E-03
Fluoride (F <sup>-</sup> )		11.8	6.21E-04	7.6	12
Chloride (Cl <sup>-</sup> )		26	7.33E-04	15	27
Bromide (Br <sup>-</sup> )		0.2	2.50E-06	0.2	0.4
Iodide (I <sup>-</sup> )	<	0.01	7.88E-08	0	0.1
Sulfate (SO <sub>4</sub> <sup>2-</sup> )		135	1.41E-03	128	146
Phosphate (as P)	<	0.02	6.46E-07	0	0.2
Nitrate (NO <sub>3</sub> <sup>-</sup> )	<	0.9	1.45E-05	0	1.5
Tot. Arsenic (As)		0.0065	8.68E-08	0.006	0.007
Alkalinity as HCO <sub>3</sub> <sup>-</sup>		268	4.39E-03	267	281
Bicarbonate (HCO <sub>3</sub> <sup>-</sup> )		262	4.29E-03		
Carbonate (CO <sub>3</sub> <sup>2-</sup> )		2.2	3.67E-05		
Silica (H <sub>2</sub> SiO <sub>3</sub> )		46	5.93E-04	15	36
Borate (B(OH) <sub>3</sub> )		0.9	1.46E-05	0.5	1.3
Organic C	<	6	5.00E-04	0	6
Oxygen (O <sub>2</sub> )	<	0.008	2.50E-07	0	5.85
Nitrogen (N <sub>2</sub> )		31	1.11E-03	23	39
Methane (CH <sub>4</sub> )		0.01	6.24E-07	0	0.01
Hydrogen (H <sub>2</sub> )	<	7E-04	3.40E-07	0	7E-04
Argon (Ar)		1.0	2.50E-05	0.8	1.2
Carbon dioxide (CO <sub>2</sub> )		7	1.59E-04		

**Tab. 10-5 :** Reference water chemistry: area East (page 1 of 3)  
(for explanation cf. text).

Molality [M] calculated from mg/l. The number of significant digits is the number of digits in the mg/l values.

Sample Source	Base Reference Water		Concentration and Parameter Ranges	
<b>CALCULATED VALUES</b>		<b>Difference of Sum</b>		
	<b>[mg/l]</b>			
Dissolved Solids:				
Sum	543			
Residue (110 C)	529	- 2.6 %		
Residue (180 C)	512	- 5.7 %		
Ionic Strength [M]	1.03E-02			
Carbonate System: pH adjusted for calcite saturation:				
			<b>Minimum</b>	<b>Maximum</b>
pH [units]	7.68		7.6	8.1
Total Dissolved CO <sub>2</sub> [M]	4.49E-03		4.33E-03	4.73E-03
log P (CO <sub>2</sub> ) [bars]	- 2.06		- 2.66	- 2.00
Saturation Indices:				
BARITE	0.00			
BRUCITE	- 4.33			
CALCITE	- 0.00			
CELESTITE	-2.23			
CHALCEDONY	0.00			
DOLOMITE-DISORDER	- 0.85			
DOLOMITE-ORDERED	- 0.41			
Fe(OH) <sub>3</sub> -ALPHA	- 0.04			
Fe(OH) <sub>3</sub> -BETA	- 2.04			
FLUORITE	0.00			
GIBBSITE	- 0.81			
GOETHITE	2.46			
GYPSUM	- 2.24			
KAOLINITE	0.00			
MANGANITE	- 10.32			
Ni(OH) <sub>2</sub> S	- 4.91			
Ni <sub>2</sub> SiO <sub>4</sub>	- 6.98			
Ni <sub>2</sub> SiO <sub>4</sub> S	- 8.36			
NiCO <sub>3</sub> S	- 5.62			
NiFe <sub>2</sub> O <sub>4</sub>	7.88			
NiO	- 4.61			
NiSiO <sub>3</sub>	6.28			
PORTLANDITE	- 9.18			
PYROCHROITE	- 7.34			
PYROLUSITE	- 14.84			
QUARTZ	0.34			
RHODOCHROSITE	- 1.16			
SIDERITE	- 1.02			
STRONTIANITE	- 1.36			
U <sub>3</sub> O <sub>7</sub> -BETA	- 0.23			
U <sub>4</sub> O <sub>9</sub>	0.13			
UO <sub>2</sub> -AMORPHOUS	- 6.35			
UO <sub>2</sub> -CRYSTALLINE	- 0.07			
USiO <sub>4</sub>	- 0.46			
WITHERITE	- 2.84			
Indicators of Redox State	<b>pe</b>	<b>Eh [volts]</b>		
Used for Modeling:	- 0.52	- 0.03		

Tab. 10-5 : Continued (page 2 of 3).

Sample Source	Base Reference Water		Concentration and Parameter Ranges
Calculated from Redox Couples:	<b>pe</b>	<b>Eh [volts]</b>	
H <sup>+</sup> /H <sub>2</sub>	- 5.52	- 0.36	
HCO <sub>3</sub> <sup>-</sup> /CH <sub>4</sub>	- 5.20	- 0.34	
N <sub>2</sub> /NH <sub>4</sub> <sup>+</sup>	- 4.03	- 0.26	
NO <sub>3</sub> <sup>-</sup> /N <sub>2</sub>	8.75	0.57	
O <sub>2</sub> /H <sub>2</sub> O(THEOR)	9.92	0.65	
O <sub>2</sub> /H <sub>2</sub> O(SATO)	- 0.19	- 0.01	
Gas Partial Pressures: log P (Gas)			
	<b>[bars]</b>		
CH <sub>4</sub> (G)	- 3.17		
CO <sub>2</sub> (G)	- 2.06		
H <sub>2</sub> (G)	- 4.32		
N <sub>2</sub> (G)	0.35		
O <sub>2</sub> (G)	- 3.56		

Tab. 10-5 : Continued (page 3 of 3).

#### *Ra, Cu and U*

Analyses for these constituents were made on only one sample. Their reference concentrations are taken as the analyzed value, and the maximum and minimum values as factors of ten higher and lower than the reference value.

Saturation indices of several minerals and simple oxides of U are given in the Table. At the reference U concentration and oxidation potential, the water appears within 85 % ( $10^{-0.07}$ ) of saturation with respect to uraninite (UO<sub>2(crystalline)</sub>).

#### *Na*

The Na concentration of the reference water, like that of the western reference water, was adjusted for charge balance. The range is that of the analyzed values.

#### *Ba, F, Al and H<sub>2</sub>SiO<sub>3</sub>*

The concentrations of Ba and F were calculated assuming saturation with respect to barite and fluorite. The assumption of saturation with these minerals is consistent with that made for the western reference water, and the resulting concentrations are consistent with the measured values in these samples. The maximum concentrations for both constituents are the reference water values rounded up to the nearest single digit. The minimum barium concentration is arbitrarily taken as a factor of ten below the reference value, while the minimum fluoride concentration is the minimum value measured in any of the samples.

### *Oxidation Potential*

The reference oxidation potential (-0.03 V) is equivalent to the only Pt electrode potential measured on a Siblingen sample. It also corresponds reasonably well with the SATO potential (SATO 1960) calculated from the reference O<sub>2</sub> content (<-0.01 V), and leads to virtual saturation with respect to UO<sub>2(crySTALLINE)</sub>, and near saturation with respect to U<sub>4</sub>O<sub>9</sub>. At the reference Fe concentration, it also leads to virtual saturation with  $\alpha$ -Fe(OH)<sub>3</sub>.

The minimum oxidation potential is taken as -0.24 V, the same minimum value as chosen for the western reference waters. The maximum value is taken as -0.03 V, the same as the reference value. Potentials calculated from the concentrations of oxidized and reduced forms of H, C and N are also given in the Table. As discussed for the western reference water, these give little or no information about the equilibrium state of this water.

### *pH, CO<sub>2(aq)</sub>, P<sub>CO2</sub> and Total Dissolved CO<sub>2</sub>*

The values of these parameters were determined by geochemical modeling assuming that the reference water was saturated with respect to calcite. The ranges span the values calculated when the individual samples are adjusted for calcite saturation. The CO<sub>2</sub>, bicarbonate (HCO<sub>3</sub>) and carbonate (CO<sub>3</sub>) concentrations, which together comprise the total dissolved CO<sub>2</sub>, are results of geochemical modeling.

### **Other waters in the crystalline basement**

Two samples of water significantly different from the western reference water were taken from the Böttstein and Leuggern boreholes at depths close to that of the reference repository. Both zones yielded very little water, so representative samples were difficult to collect, and their composition cannot be defined with great precision. They are included here as examples of the most extreme water chemistries likely to be encountered. The chemistries of these waters are given in Table 10-6 and are described in more detail by PEARSON & SCHOLTIS (1993).

The first of these samples was taken from a zone centered at 1326 m in the Böttstein borehole. This water has a total dissolved solids content of about 13 g/l and is of the Na-(Ca)-Cl-(SO<sub>4</sub>) type. The chemistry shown in Table 10-6 was developed by correcting analyses made on a number of samples containing varying degrees of drilling-fluid.

The second water is from a zone centered at 923 m in the Leuggern borehole. Its chemistry was also developed by correcting analyses of samples containing varying amounts of drilling-fluid. This water has a total dissolved solids content of about 5 g/l and is of the Na-Ca-SO<sub>4</sub> type.

Sample Source	BÖTTSTEIN 1326 m		LEUGGERN 923 m	
pH (measured)	6.64		7.30	
Formation Temp. [°C]	60		42	
Density [g/ml]	1.008		1.0023	
	[mg/l]	[M]	[mg/l]	[M]
Lithium (Li <sup>+</sup> )			3.09	4.46E-04
Sodium (Na <sup>+</sup> )	4037	1.77E-01	1108	4.83E-02
Potassium (K <sup>+</sup> )	45.0	1.16E-03	13.3	3.41E-04
Ammonium (NH <sub>4</sub> <sup>+</sup> )	0.2	1.11E-05		
Magnesium (Mg <sup>2+</sup> )	2.6	1.08E-04	2.2	9.07E-05
Calcium (Ca <sup>2+</sup> )	870	2.18E-02	424	1.06E-02
Strontium (Sr <sup>2+</sup> )	21	2.41E-04	7.4	8.47E-05
Manganese (Mn <sup>2+</sup> )	3.1	5.67E-05	3.35	6.11E-05
Iron (Fe <sup>2+</sup> )	0.01	1.80E-07		
Aluminum (Al)	0.04	1.49E-06	< 0.006	2.23E-07
Uranium (U)	6E-05	2.53E-10		
Fluoride (F)	3.6	1.90E-04	2.9	1.53E-04
Chloride (Cl)	6621	1.88E-01	203	5.74E-03
Sulfate (SO <sub>4</sub> <sup>2-</sup> )	1560	1.63E-02	3057	3.19E-02
Phosphate (as P)	0.06	1.95E-06	0.013	4.21E-07
Alkalinity as HCO <sub>3</sub> <sup>-</sup>	95	1.57E-03	73	1.20E-03
Tot. Sulfide (H <sub>2</sub> S)			< 0.005	1.47E-07
Silica (H <sub>2</sub> SiO <sub>3</sub> )	21.5	2.77E-04	7.4	9.50E-05
Borate (B(OH) <sub>3</sub> )			5.6	9.08E-05
<b>CALCULATED VALUES</b>	[mg/l]		[mg/l]	<b>Difference from Sum</b>
Dissolved Solids:				
Sum	13277		4871	
Residue (110 C)			4988	2.4 %
Residue (180 C)			4914	0.9 %
Ionic Strength [M]	2.61E-01			1.14E-01
Carbonate System: pH adjusted for calcite saturation:				
pH [units]	6.80		7.34	
Total Diss.CO <sub>2</sub> [M]	1.78E-03		1.25E-03	
log P CO <sub>2</sub> [bars]	- 1.75		- 2.46	

**Tab. 10-6 :** Böttstein 1326 m and Leuggern 923 m waters (page 1 of 2)  
(for explanation cf. text).

Molality [M] calculated from mg/l. The number of significant digits is the number of digits in the mg/l values.

Sample Source	BÖTTSTEIN 1326 m	LEUGGERN 923 m
Saturation Indices:		
BRUCITE	- 5.93	- 5.91
CALCITE	0.00	0.00
CELESTITE	0.12	- 0.14
CHALCEDONY	- 0.34	- 0.65
DOLOMITE-DISORD.	- 2.33	- 2.32
DOLOMITE-ORD.	- 1.91	- 1.84
FE(OH) <sub>3</sub> -ALPHA	- 4.29	
FE(OH) <sub>3</sub> -BETA	- 6.29	
FLUORITE	0.03	- 0.13
GIBBSITE	0.31	- 0.31
GOETHITE	- 1.79	
GYPSUM	- 0.01	- 0.08
KAOLINITE	1.56	- 0.27
MANGANITE	11.84	- 10.13
PORTLANDITE	- 9.21	- 9.56
PYROCHROITE	- 6.61	- 5.42
PYROLUSITE	17.97	- 18.16
QUARTZ	- 0.01	- 0.27
RHODOCHROSITE	- 0.13	0.36
SIDERITE	-2.80	
STRONTIANITE	- 1.26	- 1.37
U <sub>3</sub> O <sub>7</sub> -BETA	- 0.27	
U <sub>3</sub> O <sub>8</sub>	- 7.11	
U <sub>4</sub> O <sub>9</sub>	1.49	
UO <sub>2</sub> -AMORPHOUS	- 5.14	
UO <sub>2</sub> -CRYSTALLINE	1.34	
USIO <sub>4</sub>	0.65	

Tab. 10-6 : Continued (page 2 of 2).

For consistency with the western reference water, the Al and H<sub>2</sub>SiO<sub>3</sub> concentrations of the eastern reference water were adjusted for saturation with respect to chalcedony and kaolinite. Based on the analyzed values of these constituents in the samples, however, dissolved H<sub>2</sub>SiO<sub>3</sub> could be controlled by quartz saturation. If this is the case, the reference water Al and H<sub>2</sub>SiO<sub>3</sub> concentrations would be 0.03 and 21 mg/l, respectively. Both quartz and chalcedony control are encompassed in the ranges given for Al and H<sub>2</sub>SiO<sub>3</sub>. As the Table shows, at the reference Al concentration, gibbsite is undersaturated. At the higher Al concentration corresponding to quartz and kaolinite saturation, however, gibbsite would be oversaturated by a factor of more than one hundred.

## 10.4.2 Colloids

Colloids, in this context, are stable suspensions of solid particles in groundwaters and can be operationally defined to have sizes in the nm to  $\mu\text{m}$  range (e.g. STUMM 1992, McCARTHY & DEGUELDRE 1993). They are ubiquitous in groundwater and could potentially affect radionuclide transport (SMITH 1993). In order to evaluate the impact of colloidal nuclide transport, information on several topics is needed. First, the concentration and size distribution of colloids in water-carrying zones has to be known. Second, their compositions and properties have to be determined, particularly their sorption of relevant radionuclides. Finally, potential transport of radionuclides has to be modeled taking properly into account filtration and adhesion of colloids on the rock surfaces, potential generation of colloids and sorption of radionuclides on colloids. This chapter focuses on the characterization of colloids in groundwaters from the crystalline basement of Northern Switzerland and considers parameters affecting their presence, such as total dissolved solids concentration, redox potential and total organic carbon (TOC).

### Experimental aspects

Effective studies of groundwater colloids require careful sampling of the waters of interest and the colloidal component (DEGUELDRE et al. 1989). Even fairly small sample perturbations (e.g. temperature changes, degassing, etc.) or groundwater interactions with equipment can cause dramatic artefacts. Single-particle analysis was performed with on-line sampling (e.g. filtration) followed by scanning electron microscopy (Fig. 10-12) for colloid counting and energy dispersive X-ray spectroscopy investigations for colloid elemental analysis. From the elemental composition of a single particle, their nature (i.e. organic, inorganic, mineralogical) can be determined. In addition, elemental analysis of the fluid phases (i.e. filtered and/or colloid-concentrated groundwater by tangential filtration) was performed by ICP<sup>1)</sup> techniques (McCARTHY & DEGUELDRE 1993). However, below 1 ppm, quantitative determination of the nature of colloids is difficult by chemical analysis and only qualitative results were obtained. The colloid size distributions are obtained by micrograph analysis using a quantimeter and the code COLIAT (DEGUELDRE 1994).

The observed size distribution of colloids in deep groundwaters shows a characteristic decrease in the number of particles with increasing size; on a log/log plot of number of particles against size, gradients between -2 and -3 are observed (cf. Fig. 10-13). For such distribution (BUFFLE 1988):

- The total number of particles is dominated by the smaller size classes and hence is very sensitive to the lower size cut-off chosen.
- The total surface area of colloidal particles is uniformly distributed over all size classes.

---

1) ICP-AES: Inductively Coupled Plasma Atomic Emission Spectrometry  
ICP-MS: Inductively Coupled Plasma Mass Spectrometry

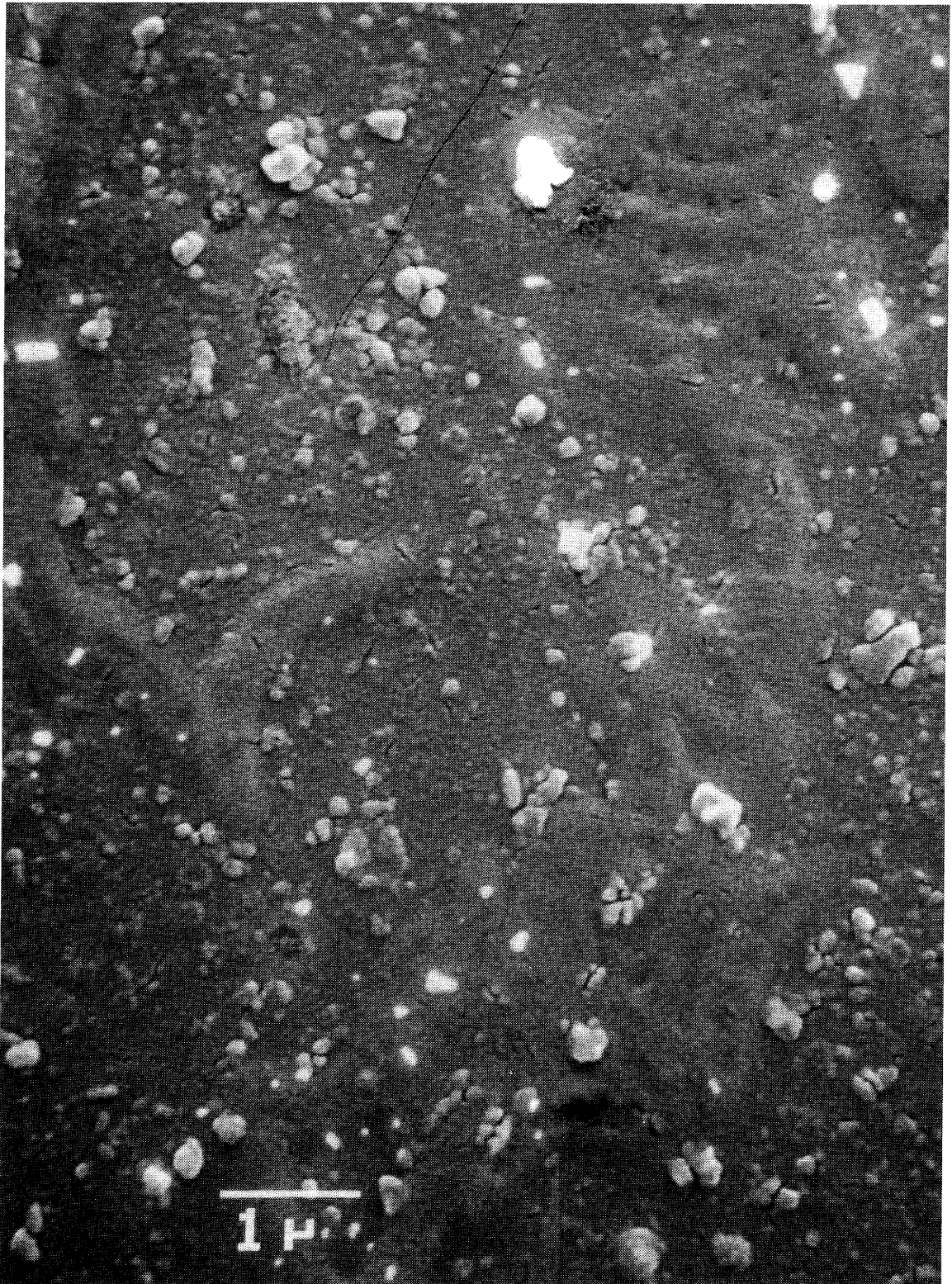


**Fig. 10-12 :** Micrograph of Leuggern groundwater colloids.  
*Conditions:* sampling depth 1635 m below surface, volume filtered 90 ml, membrane Amicon XM50 polyacrylamide, pore size 3 nm, filtration active surface 1.2 cm<sup>2</sup>, sample obtained on-site by pulsed dia-ultrafiltration. Secondary electron imaging.

- The total mass of colloidal material is dominated by the larger size classes and hence is sensitive to the upper size cut-off.

Experimentally, colloid measurements are somewhat uncertain below sizes of about 100 nm but a calculation of the mass of particles in the 100 nm - 1  $\mu$ m range (assuming spherical particles with an average density of 2 g/cm<sup>3</sup>) provides a good estimate of the total mass in the full 1 nm - 1  $\mu$ m size range. In order to calculate the total number of particles or surface area, however, the distribution equation derived from a linear fit to the log/log size distribution plot (e.g. Fig. 10-3) is assumed to be applicable to the entire colloid size range.

### Groundwaters investigated

Six groundwaters of relevance to studies of the crystalline basement of Northern Switzerland were investigated:

- (i) Bad Säckingen; water pumped from the interval 82 - 201 m below the surface is effervescent and of Na-Cl type (DEGUELDRE & WERNLI 1987).
- (ii) Menzenschwand, Black Forest; groundwaters of Ca-Na-HCO<sub>3</sub> type (ALEXANDER et al. 1990) sampled at a depth of 240 m below surface.
- (iii) and (iv) Zurzach; two waters from depths of 430 and 470 m are of Na-SO<sub>4</sub>(-Cl-HCO<sub>3</sub>) type (BRUETSCH et al. 1991).
- (v) and (vi) Leuggern; waters of Na-SO<sub>4</sub>(-Cl-HCO<sub>3</sub>) type (DEGUELDRE et al. 1990) were sampled from depths of 1635 and 1686 m below the surface.

Both Leuggern and Zurzach waters have chemistry comparable to the western reference water (Tab. 10-4).

### Results and discussion

For the 6 selected groundwaters, the colloid concentration ranges from 7 - 400 ppb, which corresponds to 10<sup>7.9</sup> to 10<sup>9.5</sup> pt/l<sup>1)</sup> (DEGUELDRE 1994) (Tab. 10-7). The measured concentration in the deep systems (Zurzach, Leuggern) is 7 to 40 ppb.

For the western reference water, the expected colloid concentration is <100 ppb with a conservative size distribution given by

$$\frac{\Delta [\text{coll}]}{\Delta d} = 10^{12.5} d^{-3}$$

---

1) pt/l: particles per litre

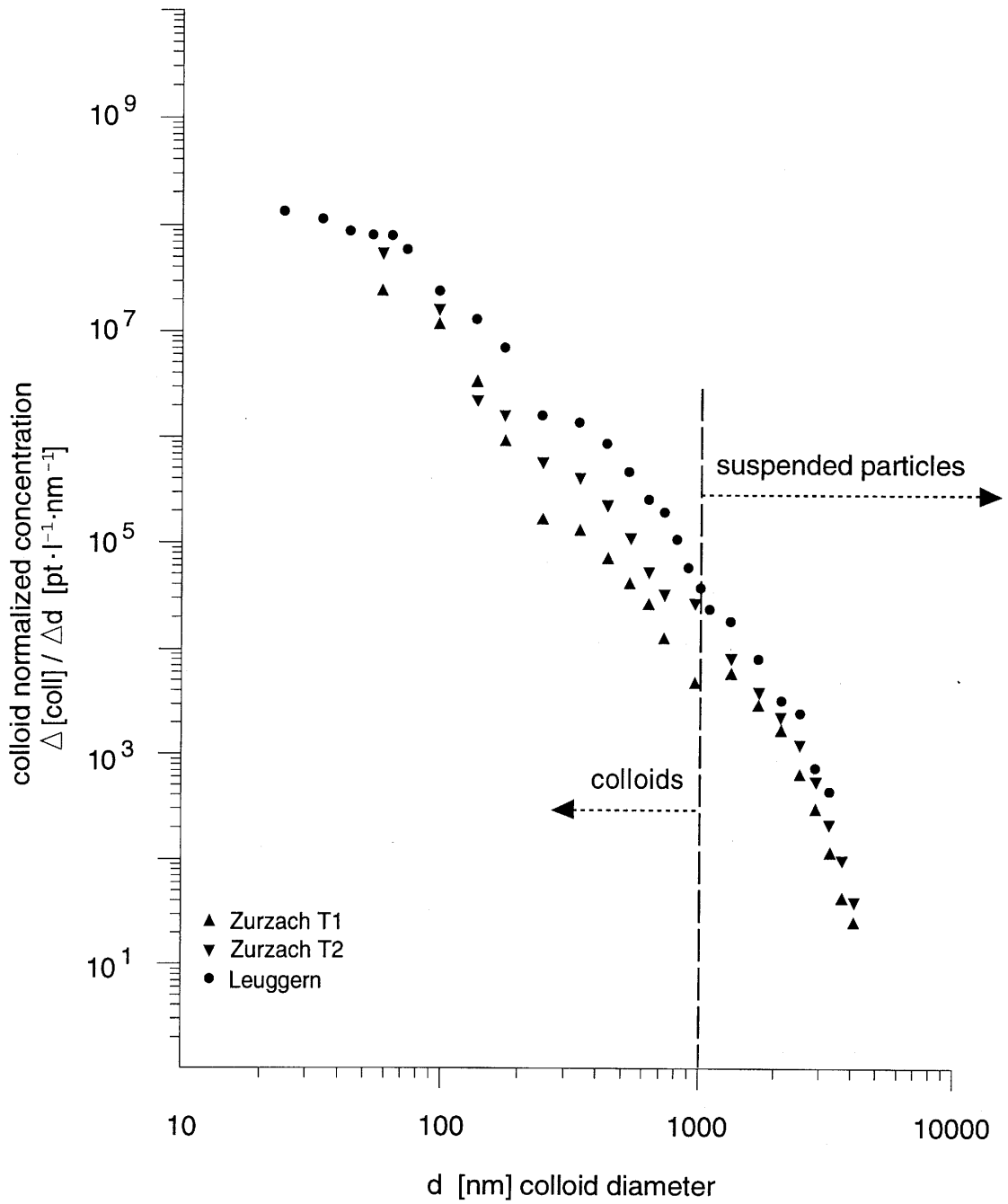


**Fig. 10-13 :** Example of colloid size distributions.

*Conditions:* direct sampling on-line, volume filtered 50 - 500 ml, membrane Amicon XM50 polyacrylamide, pore size 3 nm, scanning electron microscopy of samples obtained on-site by pulsed dia-ultrafiltration, [coll] precision: 25 %  $\Delta [coll] / \Delta d$ : normalized concentration per size unit.

The suggested colloid population is overestimated because:

- the water flow rate in the investigated systems was always several orders of magnitude larger than considered for the safety assessment transport model (NAGRA 1994a);
- the colloids are not spheres but mostly flat particles and their mass is thus overestimated by this procedure;
- for contaminant transport, only smaller colloids may play an important role; larger colloids may well be removed by filtration or sedimentation.

It should be noted that processes which increase pH, changing pe and ionic strength as well as flow rate and temperature variations could considerably increase colloid concentrations (McCARTHY & DEGUELDRE 1993). As the hydrochemistry in the crystalline basement of Northern Switzerland is expected to be relatively constant, such increases are improbable except, possibly, in the vicinity of the engineered barriers.

It is generally observed that a high salinity reduces the stability of the colloid phase and decreases the colloid concentration by mutual attachment (aggregation) or by attachment to colloids sorbed on the rock. A high sodium concentration favors colloid aggregation; calcium is a stronger coagulant which, even at relatively low concentrations ( $10^{-4}$  M), considerably reduces the colloid concentration (DEGUELDRE 1994). Organic carbon, which may stabilize the colloid phase, is present only in very low concentrations in the deep groundwater. The on-line measurements of the total organic carbon (TOC) revealed concentrations of the order of 10 ppb. The Eh of the groundwater is also a relevant parameter concerning colloid generation and stability. For example, redox potential increase could induce iron (III) hydroxide colloid generation. The low colloid concentration measured in groundwaters similar to the wester reference water supports these considerations.

The major elements detected in the colloidal phase are Si, Al and Fe. The main constituents of the colloidal phase are interpreted as being clay and silica. Fe appears to be associated with the colloidal clay phase.

It is difficult to measure sorption on natural colloids since their concentration in deep crystalline basement groundwaters is extremely low. A few measurements have been made for colloids from the Grimsel Test Site (VILKS & DEGUELDRE 1991) and Zurzach (BRUETSCH et al. 1991). The sorption distribution constants determined are comparable to those measured on fine clay particles. Hence, corresponding literature values can be taken (GRAUER 1990). A rough estimate of the upper bound of the sorption capacity can be made by assuming an uptake site density of 3 sites/nm<sup>2</sup> at the surface of spherical colloids (GRAUER 1990, DEGUELDRE 1989). From the colloid distributions measured in the groundwaters from Zurzach and Leuggern, a sorption capacity of the order of the  $10^{-9}$  M can be calculated (BUFFLE 1988).

Location	Water							Colloids		
	depth m	pH	pe	T [°C]	[Na] M	[Ca] M	[TOC] ppb	[coll] ppb*	[coll] pt/l**	composition
Bad Säckingen	80-201	6.5	+6	29	$4.5 \times 10^{-1}$	$3.9 \times 10^{-3}$	(400)	(10-100)	$10^{8-9}$	SiO <sub>2</sub> + clay
Menzenschwand	240	6.5	+6.5	13	$1.2 \times 10^{-4}$	$3.8 \times 10^{-4}$	(350)	400	$10^{9.5}$	clay
Zurzach T1	430	8.0	- 3	37.6	$1.3 \times 10^{-2}$	$3.7 \times 10^{-4}$	33	7	$10^{8.2}$	SiO <sub>2</sub> + clay
Zurzach T2	470	8.0	- 3	39.5	$1.3 \times 10^{-2}$	$3.7 \times 10^{-4}$	35	11	$10^{7.9}$	SiO <sub>2</sub> + clay
Leuggern	1635	7.8	- 3	66	$1.3 \times 10^{-2}$	$2.4 \times 10^{-4}$	41	20	$10^{9.0}$	SiO <sub>2</sub> + clay
Leuggern	1686	7.8	- 3	66	$1.3 \times 10^{-2}$	$2.4 \times 10^{-4}$	45	40	$10^{8.7}$	SiO <sub>2</sub> + clay

\* for size < 1000 nm

\*\* for size > 100 nm

**Tab. 10-7 :** Comparison of groundwater chemistry and colloid data from the Northern Switzerland study.

*Conditions:* pH, pe and T measurements on-line; [TOC]: total organic carbon concentration; [coll]: colloid concentration, error estimate is  $\pm 25\%$ ; for both [TOC] and [coll] the values in parenthesis are off-line measurements; composition: clay and silica colloids. M = mols per kg H<sub>2</sub>O. Source of data: DEGUELDRE (1994), ALEXANDER et al. (1990), BRUETSCH et al. (1991), DEGUELDRE & WERNLI (1987), DEGUELDRE et al. (1990).

## 10.5 Geotechnical data

### 10.5.1 Introduction

In the report series for Project Gewähr, a model dataset for the engineering project, i.e. for the shaft facilities and the disposal zones, was presented (NAGRA 1985b). The data used originated mainly from measurements and laboratory experiments on drillcores from the sedimentary overburden and the basement in the Böttstein borehole. The rock mechanical data from the basement were thus obtained solely for granitic rocks, but the values show a scatter which would certainly include data on the mineralogically similar gneisses. The data from the Böttstein borehole are therefore taken to be representative for the crystalline basement. The Project Gewähr dataset thus remains valid but is supplemented with results of additional investigations which were not available at the time. This applies in particular to:

- the geotechnical properties of 1st and 2nd order faults in the basement and their contribution to water flow;
- information on water flow in ore and mineral veins;
- information on the recent stress field;
- information on the geothermal conditions in the region Böttstein-Leuggern-Kaisten.

Despite these additions to the dataset it is still possible that, when constructing the repository, more difficult sections (from an engineering point of view) will be encountered than those characterized in this report. When a site is identified, however, the geotechnical dataset will be revised and extended to include site-specific data and investigations.

## 10.5.2 Geotechnical properties of the rock

### Overburden

The geotechnical properties of the sedimentary rocks which determine the design of the shaft in the overburden are described in detail in project report NGB 85-03 (NAGRA 1985b) and do not require to be added to at present.

### Basement

When planning a repository, the crystalline basement can be divided into the following units:

#### *Upper higher-permeability domain*

Thickness:	350-650 m (Böttstein, Kaisten, Leuggern boreholes)
Hydraulic conductivity:	in the order of $1E-7$ m/s
Geotechnical properties:	cf. Table 10-8, column 1, if undisturbed.

#### *Deeper low-permeability domain*

Disposal zone	
Hydraulic conductivity:	$< 1E-10$ m/s
Geotechnical properties:	cf. Table 10-8, column 1, if undisturbed.

#### *1st and 2nd order faults*

Faults are made up of one or more strongly deformed zones. These zones may consist of kakirites (tectonic breccias) or pure fault gouge and may be bordered on both sides by strongly fractured rock (damaged zone). The kakirites are made up of broken-up and crushed rock detritus and may contain all fractions up to clay fraction. They are largely non-cohesive and vary in thickness between one and several meters (observations from Nagra's exploratory boreholes in Northern Switzerland). Because of the high component of fine-grained material, the kakirite can actually function as a kind of aquitard and greater water flow might be expected in the damaged rock surrounding the kakirite.

	Rock type		[1]	Crystalline rocks, compact	[2]	Crystalline rocks, strongly fractured	[3]	Kakirite, tectonic breccia, fault gouge	
			Thickness		Elements of a 1st or 2nd order fault				
	Property		dam to several hm		m to several dam		only a few m		
			Quantification	Stage	Quantification	Stage	Quantification	Stage	
Rock	A	Unfavorable components	none	1	none	1	none, partly clayey	1/2	
	B	Compressive strength [N/mm <sup>2</sup> ]	high (150 - 200)	1	average - high (25 - 100)	2	extremely low	4	
	C	Quartz content [%]	low - average (25 - 35)	2/3	low - average (25 - 35)	3	low - average (25 - 35)	3	
	E	Behavior when water-bearing	unchanged	1	unchanged	1	loss of cohesion	2	
Discontinuity of rock	stratigraphic	F	Layering, bedding [m]	none	1	none	1	schistose	3/4
		G	Clayey and micaceous interlayers	none	1	isolated	3	isolated	3
		H	Layer friction [°]	high (> 40)	1	average (30 - 40)	2	very low	4
		I	Cohesion (with sliding friction) [N/mm <sup>2</sup> ]	high (> 2)	1	low (0.02 - 0.2)	3	low - very low	3/4
	tectonic	K	Schistosity, fracture spacing [m]	average (0.1 - 1)	2	high (0.01 - 0.1)	3	very high	4
		L	Type of fracture	continuous	2	continuous, with infill	3	continuous, with infill	3
		M	Aperture [mm]	closed	1	fine (0.1 - 1)	2	narrow	3
		N	Friction within discontinuity [°]	average (30 - 40)	2	low (20 - 30)	3	low 20 - 30	3
		O	Cohesion [N/mm <sup>2</sup> ]	average (0.2 - 2)	2	low (0.02 - 0.1)	3	low - very low	3/4
		P	Form of fracture-bounded bodies	partly cubic	2	partly platy or prismatic	3	partly platy or prismatic	3
Water circulation	Q	Hydraulic conductivity [m/s]	< 10 <sup>-10</sup> - 10 <sup>-7</sup>	2	10 <sup>-9</sup> - 10 <sup>-6</sup>	2/3	10 <sup>-9</sup> - 10 <sup>-6</sup>	1/3	
	R	Type of circulation	joints, fractures	3	joints, fractures	3	fractures, pores	3	

Additional parameters	Density [g/cm <sup>3</sup> ]	2.62 - 2.65	2.35 - 2.65	2.30 - 2.50
	E-modulus [MN/m <sup>2</sup> ]	60 000 - 80 000	20 000 - 60 000	low, no measurement
	Poisson's number	0.2	0.2	no measurement
	Rock strength:			
	c [N/mm <sup>2</sup> ]	35 - 40	30 - 40	very low
	Ø [°]	45 - 50	25 - 40	20 - 30
	δ <sub>2</sub> [N/mm <sup>2</sup> ]	5 - 15	1 - 10	very low
	Swelling pressure [N/mm <sup>2</sup> ]	0	0	0
	Swelling expansion [%]	0	0	0
	Agressivity of water to concrete	negligible	negligible	negligible
	Hydrocarbons	0	0	0
Thermal conductivity [W/m K]	3.2 - 3.4	3.2 - 3.4	2.8 - 3.2	
Heat capacity [MJ/m <sup>3</sup> K]	2.2 - 3.3	2.0 - 2.3	1.9 - 2.2	

**Tab. 10-8 :** Geotechnical properties of the crystalline basement (rock description according to SIA norm 199).

Thickness:	1st order fault zone 100-1000 m 2nd order fault zone 10-100 m
Hydraulic conductivity:	generally in the order of $1E-7$ m/s, but higher local conductivities cannot be ruled out.
Geotechnical properties:	cf. Table 10-8, column 2 for strongly fractured (damaged) rock and column 3 for kakirites.

### *Ore and mineral veins*

Ore and mineral veins present a considerable problem, not because they are less stable but because of their high hydraulic conductivity, which is often associated with high hydrostatic pressures, and their unexpected occurrence during tunnel construction.

Numerous ore and mineral deposits are known from the Black Forest. In Northern Switzerland, on the other hand, none of the Nagra boreholes encountered a significant ore or mineral deposit. Only the highly-permeable zone in the granite of the Leuggern borehole (1648 m to bottom) could be interpreted as an ore or mineral vein in statu nascendi or as the country rock surrounding, and affected by, such a vein.

The transmissivity of this zone is  $7E-7$  m<sup>2</sup>/s, corresponding to a hydraulic conductivity of  $1E-5$  -  $1E-6$  m/s (SPANE 1990). The hydrostatic pressure at a repository depth of 1000 m is approx. 10-12 MPa. However, if an ore or mineral vein is encountered, it is possible that larger water volumes in the order of several m<sup>3</sup>/min may occur temporarily.

### **10.5.3 The recent stress field in the Böttstein - Kaisten - Leuggern area**

The data on the orientation of the recent stress field in the basement of Northern Switzerland are summarized in section 9.2. For the basement of Northern Switzerland there are no measurements which give information on the size of the stress components. In order to be able to make a rough estimate of magnitudes, we draw on measurements made outwith the area of interest, where both the direction and the size of the stress components were determined. The only measurements from deep boreholes which are of use are the "hydrofrac" measurements from the Wellenberg region (NAGRA 1993) and measurements from the Grimsel Test Site (PAHL et al. 1989). The measurements from the Alps can be considered as reference values for the purpose of estimating magnitudes in Northern Switzerland, but they have to be adapted to take account of the tectonic model of recent crustal movement.

Analyses of borehole wall breakouts give a direction for the maximum horizontal stress component of approx.  $135^\circ \pm 10^\circ$  in the crystalline basement section.

Evaluation of local single earthquake events (PAVONI 1984) gave a more or less horizontal trend for the largest principal stress component and a NNW-SSE orientation (azimuth  $145^\circ$ - $150^\circ$ ).

DEICHMANN (1990) comes to a more or less identical conclusion based on his analysis of the earthquake series Läuelfingen, Zegglingen and Günsberg. This gave a maximum compression in a NNW-SSE direction (azimuth  $145^{\circ}$ - $150^{\circ}$ ) and an extension in a WSW-ENE direction.

Based on data from Northern Switzerland and measurements at the Grimsel Test Site and at Wellenberg, the recent stress field for the region Kaisten-Böttstein-Leuggern (target depth 1000 m) can be characterized as follows:

Stress component	Direction	Magnitude
$\sigma_H =$	$135^{\circ} \pm 10^{\circ}$	ca. 30-50 MPa
$\sigma_h =$	$45^{\circ} \pm 10^{\circ}$	ca. 15-25 MPa
$\sigma_v =$		ca. 25 MPa

The orientation of the stress field correlates well with the data obtained from borehole wall breakouts in Northern Switzerland. There is a slight deviation of  $10$ - $15^{\circ}$  compared with the values determined seismotectonically.

The values for magnitude are rough estimates which are based on values from Wellenberg and the Grimsel Test Site. Based on tectonic considerations, it was assumed that the ratio between  $\sigma_v$  and  $\sigma_H$  will be somewhat smaller in Northern Switzerland than in the Alps.

#### 10.5.4 Geothermal conditions

According to RYBACH et al. (1987), when considering geothermal gradient a distinction has to be drawn between the depth intervals 0-500 m and 750-1700 m.

- Mean surface temperature:  $10^{\circ}\text{C}$
- Gradient for depth interval 0-500 m:  $40$ - $45^{\circ}\text{C}/\text{km}$
- Gradient for depth interval 750-1700 m:  $35$ - $40^{\circ}\text{C}/\text{km}$

Based on these high geothermal gradients, the limiting rock temperature for the project of  $\sim 55^{\circ}\text{C}$  will be expected at depths of 1050-1200 m.

## **11 EXPLORABILITY OF THE CRYSTALLINE ROCKS OF NORTHERN SWITZERLAND AND PROPOSED INVESTIGATION CONCEPT**

The Phase I investigations of the Nagra programme (regional investigations) are now complete. The exploration strategy for subsequent Phases II (site-specific, surface-based) and III (site-specific, underground) forms an integral part of the development of a deep repository for high-level radioactive waste. This Chapter describes the investigation concept proposed for a repository in the crystalline basement of Northern Switzerland, as well as the rationale leading to its definition.

Each exploration step is designed to answer specific questions, and progressively increases the level of confidence with which a decision can be made to accept or reject a given location. The key questions to be answered at each step, which are the basis for formulation of an investigation concept, depend on the conceptual geological model assumptions, the requirements for the construction, operation and decommissioning of a repository, and the requirements for the long-term safety of the repository as determined by the performance assessment.

The present Chapter is structured as follows:

- Section 11.1 presents and discusses the main objectives of the exploration programmes. Emphasis is placed on the objectives of the Phase II exploration from the surface.
- Section 11.2 discusses the exploration tools currently available and assesses their contribution to the various phases of the exploration programme (i.e. their ability to provide answers to the key questions).
- Section 11.3 presents and discusses the various steps of the proposed investigation concept. The reader who is interested only in the proposed investigation concept can concentrate on this section and on Table 11-3 and Fig. 11-1.
- Section 11.4 discusses the chances of success of the investigation programme: they depend on the sizes of the low-permeability blocks of crystalline rock which can be expected and the chances of detection of such blocks of suitable size.

The investigation concept presented here is developed for area West, in the sense that the various studies performed to quantify aspects of the exploration programme have been based on parameters representative of the area West. The approach followed, however, is applicable to the crystalline basement of Northern Switzerland in general.

### **11.1 Objectives of the investigation programme**

The conceptual geological model for the crystalline basement of Northern Switzerland incorporates the main geological, hydrogeological and hydrochemical results of the regional investigations. It is summarized in Chapter 12. The hydrogeological aspects (conceptual hydrogeological model) are discussed in Chapter 8. The basic elements of the conceptual geological model that are important for the formulation of an exploration strategy and an investigation programme are:

- a sedimentary cover;
- an upper, higher-permeability domain (HPD) in the crystalline basement with higher average hydraulic conductivity than the underlying crystalline rocks;
- a lower, low-permeability domain (LPD) of the crystalline basement with favorable properties - currently considered as the host rock for a repository;
- steeply-dipping major water-conducting faults (MWCF) of regional or subregional extent, which will determine the layout of the repository. The disposal gallery panels would be placed between these faults. Horizontal major water-conducting faults have not been observed in the boreholes and are therefore not part of the conceptual model;
- small-scale water-conducting features (WCF), which will provide the transport pathways for radionuclides from the emplacement tunnels to the HPD or to a MWCF.

Table 11-1 presents the key questions or key aspects in terms of geology, hydrogeology, hydrochemistry and geomechanics that need to be answered in order to assess the feasibility and safety of a repository and to site repository panels. A detailed description of these questions is presented in VOMVORIS & ANDREWS (1993).

The key aspects listed in Table 11-1 are those that can be addressed with local investigations at a potential siting area. Further questions exist, mainly concerning long-term safety assessment, which will be answered by regional investigations (e.g. earthquake monitoring, regional monitoring of groundwater), by specific studies (e.g. neotectonic investigations), or by field experiments in underground laboratories (Grimsel Test Site or rock laboratories of sister organisations of Nagra in other countries). The investigation programme presented herein is limited, however, to local investigations at a potential siting area.

## **11.2 Overview of potential investigation methods**

Numerous investigation methods may be used to locate and characterize the principal geological and hydrogeological features that are identified in Table 11-1. Nagra has accumulated considerable experience during the Phase I investigations in Northern Switzerland and at the Grimsel Test Site, and this experience can be used to define the advantages and disadvantages of the different investigation methods. Many other countries are also actively investigating crystalline rocks as potential host rocks for the deep disposal of radioactive waste (e.g. Sweden, Finland and Canada), and Nagra closely follows progress in the development of investigation techniques made in these programmes.

Table 11-2 summarizes the applicability of various exploration methods in addressing the key aspects. The purpose and the rationale for the assessment of the chances of success of each of the possible exploration methods is discussed in the following paragraphs.

Purpose	Repository design				Long-term safety assessment				
	Depth of repository	Location of disposal areas	Location of shaft and access galleries	Design of shaft and galleries	Host rock as hydraulic barrier	Radionuclide retention potential of host rock	Dilution of contaminated waters	Regional geological and hydrogeological situation and evolution	
<b>Key aspects of geological and hydro-geological characterization</b>	<b>Sedimentary cover</b>								
	· Lithology, tectonics, hydraulics				X			X	X
	<b>Crystalline basement</b>								
	· Depth of top				X				X
	· Petrography				X		X		
	· Rock mechanics				X				
	· Hydraulics				X	X	X	X	X
	· Water-conducting features (geometry, porosity, mineralogy)						X		
	· Upper boundary of low-permeability domain	X	X		X	X	X	X	X
	· Geothermal gradient	X							
	· Hydrochemistry						X		
	<b>Major water-conducting faults</b>								
	· Existence, orientation		X	X	X	X	X		X
	· Petrography			X	X		X		
	· Rock mechanics			X	X				
	· Hydraulics		X	X	X	X	X	X	X
	· Water-conducting features (geometry, porosity, mineralogy)						X		X
	· Hydrochemistry								X
	<b>Hydraulic Potential Field</b>				X	X			X

**Tab. 11-1 :** Key aspects to be answered for the assessment of feasibility and safety of a repository.

Methods  Key aspects	Reflection Seismics survey	Boreholes (vertical and inclined)						Shaft	Horizontal boreholes from galleries			Pilot Galleries
		Core Observation / Geophysical Logging	Hydrotests / Fluid Logging	Groundwater Sampling	Seismic Tomography	Crosshole Hydrotesting	Long-term Monitoring		Core Obs., Logging, Sampling, Hydrotesting	Crosshole Tomography	Crosshole Hydrotesting	
<b>► Crystalline Basement (HPD and LPD)</b>												
Top of crystalline basement	~	++			+			++				
Petrography		++						++	++			++
Rock mechanical characterization		++			~			++	++	+		++
Characterization of WCF*												
· existence		++	+					++	++	~		++
· orientation		+						++	+	~		++
· extension			+					+		~		+
· geometry, porosity, mineralogy		++						++	++			++
· hydraulics			++					++	++			++
· hydrochemistry				++				++	++			++
Upper boundary of LPD*			++					++				
Geothermal gradient		++										
<b>► Major water-conducting faults</b>												
Existence, location												
· vertical offset <sup>1</sup> > 20 m	++	++						++	++			++
· vertical offset <sup>1</sup> < 20 m		++						++	++			++
Orientation												
· vertical offset <sup>1</sup> > 20 m	+				++	+		++		++		+
· vertical offset <sup>1</sup> < 20 m					++	+		++		++		+
Petrography		++						++	++			++
Rock mechanical characterization		++						++	++	~		++
Geometry, porosity, mineralogy of constituent WCF*		++						++	++			++
Hydraulic characterization			++		~	++		++	++		++	+
Hydrochemistry				++					++			++
<b>► Hydraulic Potential Field</b>												
							++					

\* WCF = Water-Conducting Features  
 LPD = Low-Permeability Domain (= host rock)  
<sup>1</sup> in sedimentary cover

Legend:      blank                      no chance of detecting/characterizing  
 ~                      poor chance of detecting/characterizing  
 +                      moderate chance of detecting/characterizing  
 ++                      good chance of detecting/characterizing

**Tab. 11-2:** Contribution of investigation methods to the characterization of the crystalline basement of Northern Switzerland.

*Reflection seismics surveys* can be used to identify the existence and location of the major faults in the sedimentary cover if these faults have a minimum vertical offset of about 20 m. Faults with a vertical offset of less than about 20 m in sediments and faults in the crystalline basement are not detectable with this method.

*Cored deep boreholes (vertical or angled)* are suitable for the investigation of the lithological/petrographical and mineralogical characteristics of the intersected formations and features. These boreholes provide the fixed points for the structural model for a given area. When combined with seismic tomography or crosshole hydraulic testing, they may provide information about the extent of MWCFs. For the objectives identified in section 11.1, the cored boreholes provide the basic input for the geometry questions, i.e. the thickness of the HPD and the localization of the layout-determining MWCFs.

*Seismic tomography* has the potential to identify the geometry of features between boreholes and between boreholes and the surface. A modeling study was carried out to test the performance of seismic tomography in typical settings of Northern Switzerland (COSMA & STANESCU 1993). The structural elements of the model consisted of horizontal layers, including sediments, crystalline rocks and vertical or steeply-dipping faults (fracture zones). In the model, the seismic velocity of the faults was decreased by 10 % compared to the surrounding intact rock.

The results of the seismic tomography modeling study are summarized as follows:

- tomography between boreholes and from boreholes to the surface provides an adequate approach to locating steeply-dipping faults (fracture zones);
- faults can only be located if they intersect both the source and the receiver array;
- it is expected that tomography can be carried out over distances of several hundred meters.

A reduced seismic-velocity contrast between MWCFs and surrounding rock or strong inhomogeneities in the seismic properties of the crystalline rocks increases the uncertainty in the results of the seismic tomography. However, if conditions similar to the ones assumed in the study exist, the combination of borehole intersection and seismic tomography is expected to increase significantly the ability to interpolate MWCFs between the different boreholes and between boreholes and the ground surface, and thus permit determination of the lateral boundaries of blocks of low-permeability crystalline rock within the area of investigation.

*Crosshole hydraulic testing* allows direct assessment of the hydraulic significance of a structural feature that has been identified with core analysis and interpolated between boreholes with seismic tomography. It is expected that MWCFs detected in the HPD will be more difficult to test than ones detected in the LPD due to the lower contrast to the HPD hydraulic properties. On the other hand, the distance between fault intersections in the lower part of the boreholes (in LPD) is larger. The method is potentially promising, but its successful application depends on the local conditions.

A *shaft* enables confirmation of the findings from the initial vertical boreholes with respect to MWCFs and gives local information on the geometric characteristics of the water-conducting features. With the assumption of a network of monitoring piezometers, direct observations of the local hydrogeological regime are possible. The shaft is essentially a borehole of large diameter from which information on the hydraulic connectivity of the detected MWCFs and water-conducting features may be obtained. With the construction of the shaft, the scale of observations is refined and detailed characterization of the types of WCFs that will be encountered in the emplacement tunnels can be directly performed.

*Horizontal boreholes from underground facilities* are ideally suited for intersection, detection and characterization of subvertical features. Characterization methods include core analysis, geophysical logging, hydraulic testing (single and crosshole), geochemical sampling and crosshole tomography. In addition, these boreholes serve as pilot boreholes for the determination of the location of future potential emplacement tunnels. Rock mechanically problematic zones or strongly water-conducting zones can be detected and characterized.

*Pilot galleries* allow the detailed characterization of local features that may affect the performance of the repository. Through the construction and operation of an in situ rock laboratory, the representative parameters for the geological, hydrogeological, hydrochemical and geomechanical description of local conditions can be directly obtained. The focus of the investigations at that time depends on the updated conceptual model for the geosphere, the description of the near-field and the concept for disposal (e.g. canister material, the role of engineered barriers, etc.).

### **11.3 Proposed investigation concept**

Given the objective of further exploration of the crystalline basement of Northern Switzerland and the available exploration methods with which this objective can be realized, an optimized investigation strategy has been formulated that balances the chances of success against the costs and risks involved. The proposed exploration concept is presented in Table 11-3 and illustrated in Figure 11-1.

The investigation programme for the evaluation of the potential for the development of a high-level radioactive waste repository in the crystalline basement of Northern Switzerland is divided into three phases. Phase I, the regional investigations, is now completed. Phase II includes all surface-based investigations on a subregional or local scale to provide the information required to locate potential repository areas, as well as to site a shaft. Phase III includes all underground investigations. It commences with the activities required for sinking a shaft (possibly including monitoring boreholes) and culminates with the selection of specific locations for the construction of the repository galleries and tunnels.

Tab. 11-3: Exploration concept for the crystalline basement.

Exploration steps		Objectives
<b>Exploration from the surface (Phase II):</b>		
1	<b>Seismic survey</b> (supplementary high-resolution reflection seismics).	Localization of 1st and 2nd order faults with offset in the sedimentary cover.
2	<b>Vertical borehole in a potential repository area.</b>	Demonstration that suitable, low-permeability crystalline rock occurs in the potential repository area at an appropriate depth.
3	From the same drill-site: star of <b>4 inclined boreholes, tomography, crosshole hydraulic tests.</b>	Characterization of the crystalline rock; identification and characterization of <b>some</b> of the faults; identification of the upper boundary of the LPD and preliminary decision on repository depth.
4	<b>Supplementary boreholes</b> in the vicinity of a potential shaft location and possibly in the repository area (inclined/vertical boreholes).	Geological and hydrogeological characterization of the crystalline basement at the <b>shaft site</b> .  If needed, localization and characterization of <b>additional</b> existing faults in the repository zone and identification of sufficiently large, suitable crystalline blocks in which no major water-conducting faults were detected during the investigations.
<b>Underground Exploration (Phase III):</b>		
5	<b>Shaft</b> to repository depth, preceded by boreholes for characterization of undisturbed hydraulic heads and for monitoring the effects of shaft sinking.	Characterization of the hydraulic potential field and baseline measurements of the mineral and thermal springs.  Detailed characterization of crystalline basement. Investigation of the geometry of suitable crystalline blocks by identifying / characterizing <b>all</b> faults in the repository area. Input data for design of repository layout and determination of definitive repository depth(s).
6	<b>Exploration: horizontal boreholes</b> ca. 500 m long, <b>tomography, drift</b> in suitable direction (if the shaft site is outside the potential repository area, preliminary boreholes and drift primarily in direction of potential repository area). Further horizontal boreholes and drifts until a sufficient volume of rock has been identified.	
7	<b>Detailed investigation programme</b> (boreholes, pilot drift, in situ tests) preceding and accompanying repository construction at final repository level(s).	Confirmation of geological predictions and fine-tuning of repository design.

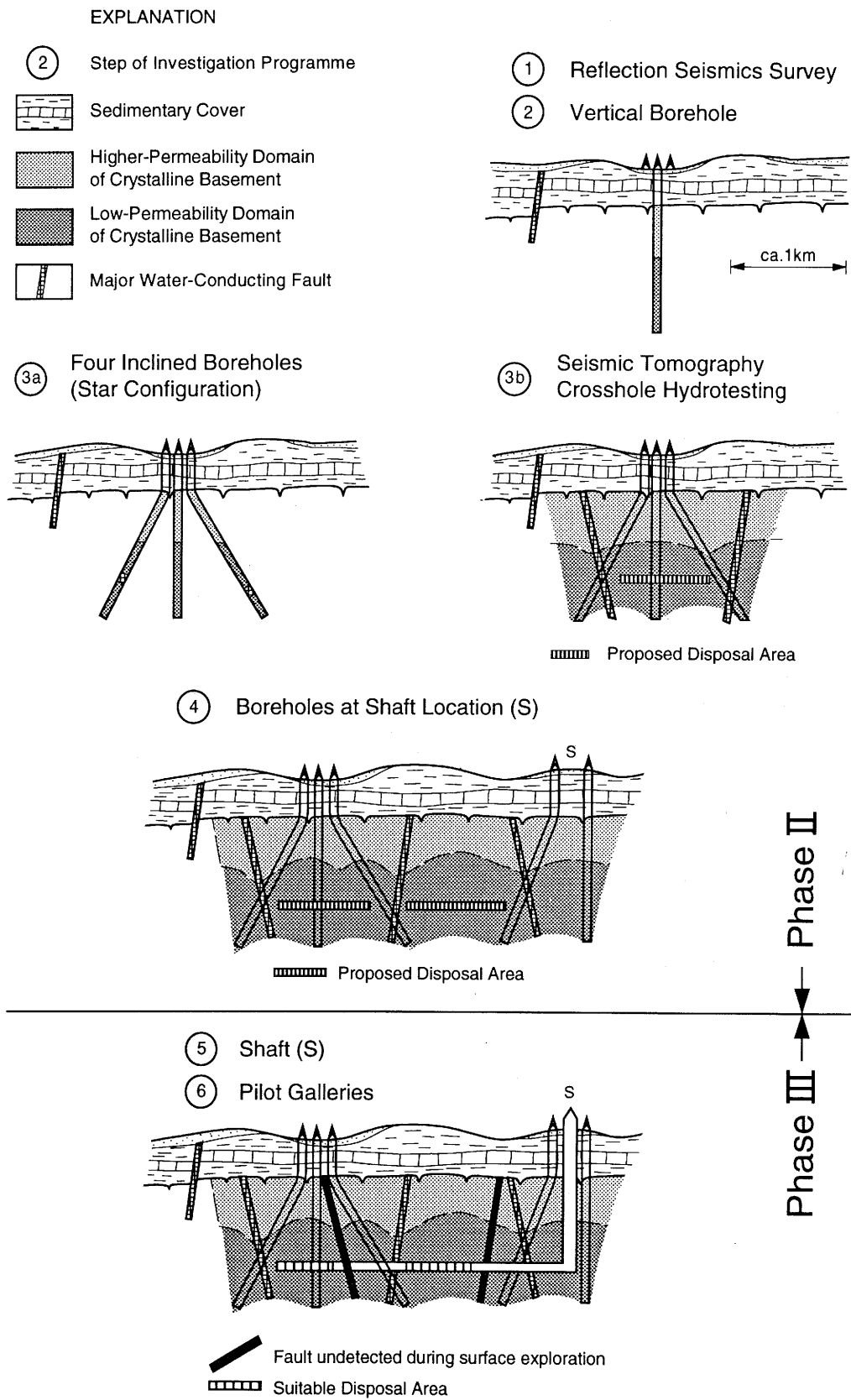


Fig. 11-1: Illustration of the investigation concept.

Based on the key questions identified above, the main objectives of the **Phase II** investigations are to:

- locate major water-conducting faults, which divide the low-permeability domain into different blocks of low-permeability rock;
- identify locations with blocks of low-permeability rock of a sufficient volume at a suitable depth;
- confirm the basic components of the conceptual geological models;
- confirm the feasibility of construction of underground facilities at the target depth;
- identify potential shaft locations and characterize the underlying crystalline rock for shaft sinking.

**Phase III** (underground exploration) focuses on a more local scale with the following main objectives:

- to characterize the local crystalline rock in more detail;
- to locate and characterize all surrounding major water-conducting faults;
- to locate and characterize suitable blocks for disposal tunnels/galleries.

The last objective also includes questions concerning the rock mechanical properties, the in situ stress magnitude and orientation and evaluation of the risk of water inflows.

## **Phase II: Exploration from ground surface**

### Step 1: Reflection seismics survey

Surface seismics will be used in an attempt to identify and locate MWCFs in the vicinity of potential repository and shaft locations. The strikes of faults with offsets of more than 20 m in the sedimentary cover can be identified. Although only a few of the existing MWCFs may be identified, surface seismics may assist in the regional extrapolation of some of the MWCFs that will be detected in the later steps of the investigation.

### Step 2: First vertical borehole

The main objective of the first vertical borehole is to confirm the existence of a low-permeability domain of adequate thickness along the borehole at a suitable depth. Intersection of MWCFs is not, at this stage, a reason to abandon the site, because the area between MWCFs is what is of interest.

### Step 3: Four inclined boreholes

Once the vertical borehole is completed with promising results, four inclined boreholes in a star-like configuration will be drilled from the site of the vertical borehole. The recommended inclination of these boreholes is 30° from vertical in the crystalline basement, which permits conventional logging techniques to be applied. These boreholes will start vertical and they will be deviated within the lower part of the sedimentary cover. The horizontal angle between the boreholes is 90°. The boreholes will be drilled

about 1300 m into the crystalline basement, which permits characterization of a block of crystalline rock with dimensions of about 1 km x1 km x1 km. In addition, seismic tomography studies will be conducted between the boreholes and from the boreholes to the surface, as well as crosshole hydrotesting. The objectives of this step are to:

- characterize crystalline rock domains and their water-conducting features (WCFs);
- identify and characterize the intersected major water-conducting faults (MWCFs);
- identify the upper limit of suitable crystalline rocks and define the preliminary repository depth.

#### Step 4: Additional boreholes (repository area, shaft location)

The aim of the surface-based testing described above is to determine the existence and characteristics of MWCFs, which determine the suitability of any particular site for potential development as a repository. Given the cost of a wrong decision, it may be desirable, following analysis of Step 3 results, to drill additional boreholes from the surface to confirm the existence and location of any such features either directly encountered or inferred on the basis of surface and/or crosshole tomography. If the conceptual geological model is confirmed in Step 3, but an area of suitable size has not yet been identified, it might be decided to drill a second star of boreholes next to the first one. Finally, if the location of the shaft is outside the investigation area, boreholes will be needed to confirm the acceptability of the shaft location and to characterize the area between the shaft and the investigated potential repository area. Additional suitable blocks of crystalline rock could also be identified in this step.

### **Phase III: Underground exploration**

#### Step 5: Shaft to potential repository depth

Once a shaft location has been selected and the target repository area has been identified, additional boreholes will precede the shaft construction. They may be rotary-drilled piezometer boreholes, equipped with a relatively simple pressure observation system to characterize the undisturbed hydraulic potential and to monitor changes of the hydraulic regime during shaft construction. Baseline measurements (e.g. outflow rate, hydrochemistry) of the mineral and thermal springs in the area will also commence before shaft construction. Then the shaft can be sunk. If the shaft is outside the target repository area, access tunnels will additionally be required (cf. Fig. 11-1). Detailed characterization of the hydrogeological, geochemical and geological features of the rock and the faults encountered will be carried out. A in situ rock laboratory could be constructed at or below the shallowest possible repository depth.

#### Step 6: Exploration with horizontal boreholes and pilot galleries

At possible repository depth and within identified repository target areas, exploration will commence with horizontal boreholes in directions identified as potentially favorable. Through direct intersection, hydraulic testing and seismic tomography, it is expected that all subvertical MWCFs in the investigated region can be detected. A pilot gallery would be advanced in a promising direction, to allow direct characterization of

crystalline blocks suitable for construction of emplacement tunnels.

If the shaft is sited outside the potential repository area, then access tunnels will be constructed towards the potential emplacement area. Pilot boreholes will be drilled as required for access tunnel construction. When the access tunnel has reached the potential repository area, the programme will proceed as outlined in the paragraph above, i.e. with horizontal boreholes, identification of all MWCFs through direct intersection, hydraulic testing and seismic tomography, and excavation of a pilot gallery in the promising direction.

The procedure presented above will be repeated until a sufficient volume of rock for repository construction is identified. At the end of Step 6, the layout of the repository will be designed.

#### Step 7: Detailed investigations during repository construction

Through pilot boreholes and observations in pilot galleries, it should be possible to confirm the assumptions required for the repository design and to fine-tune the design with respect to the location of canisters in the individual emplacement galleries. Pilot boreholes (boreholes before tunnel advancement) will also be required for the operational safety of the construction activities. Finally, tests in an in situ rock laboratory will allow estimation of specific location-dependent parameters and long-term experiments will provide input for planning repository closure and completing the corresponding safety analysis calculations on closure.

### **11.4 Chances of success**

A principal conclusion from the Phase I investigations is that low-permeability crystalline rocks suitable for a repository exist in Northern Switzerland.

Two main questions remain:

- do blocks of low-permeability crystalline rock of sufficient size (of at least 100,000 m<sup>2</sup>) exist between major water-conducting faults in the proposed investigation area?
- is it possible to identify such blocks with the investigation programme presented above?

In order to answer these questions, a network of major faults that could be expected in the investigation area was postulated, based on observations in the Black Forest and on the results of the seismic surveys and borehole investigations (Chapter 5). With these data, a statistical analysis was carried out (LANYON 1993) with two aims: to evaluate the distribution of blocks of various sizes that could be expected and to assess the chances of identifying blocks of sufficient sizes by the investigations proposed.

Table 11-4 shows the parameters of the fault network used for this statistical analysis. The parameters were derived from the fault model presented in section 5.3.4. Fault family 5, which replaces family 4 in the southern part of area West, was not used; the fault frequency of family 5, however, was assumed for family 4, which is a conservative assumption. The fault network represents the expected second order faults between the regional first order faults (e.g. Eggberg fault, Vorwald fault), which have an expected spacing of 5-7 km. One hundred realizations of a synthetic fault network were carried out. Fig. 11-2 shows one such realization. With each realization, the size distribution of the blocks between the faults was calculated. Table 11-5 shows the results of these one hundred calculations. Furthermore, the expected block size in a randomly located area of 1 km x 1 km and of 1 km x 2 km was calculated; Table 11-6 shows the results. A third calculation concerns the chance of intersecting a major fault with a vertical and with an inclined borehole; Table 11-7 shows the results.

	Family 1 (Hercynian)	Family 2 (Rhenish)	Family 3	Family 4
Spacing (km)	1.0	1.7	1.7	1.0
Strike (°)	290 ± 10	180 ± 10	330 ± 10	240 ± 10
Dip (°)	90 ± 10	90 ± 5	90 ± 20	75 ± 5
Spacing Variation (m)	50	66	66	50
Thickness (m)	Log-normal distribution of thickness with modal frequency of 20 m; 99 % of all faults with thickness less than 90 m			

Note: Uniform distribution assumed for strike, dip and spacing variations; upper and lower bounds or range as specified for each case.

**Tab. 11-4 :** Parameters of the families of major water-conducting faults (second order faults) used for statistical analysis.

The value of the results of the statistical analysis depends significantly on the reliability of the proposed fault network and of the hydraulic characteristics of the faults. Larger blocks of low-permeability rock can be expected if the frequency of some fault families is smaller or if not all faults are water-conducting. Smaller blocks can be expected if the frequency of the faults of some families is higher or if faults of smaller extent (third order faults, which are not represented in the fault network) are significantly water-conducting and connected with the network of second order faults or the higher-

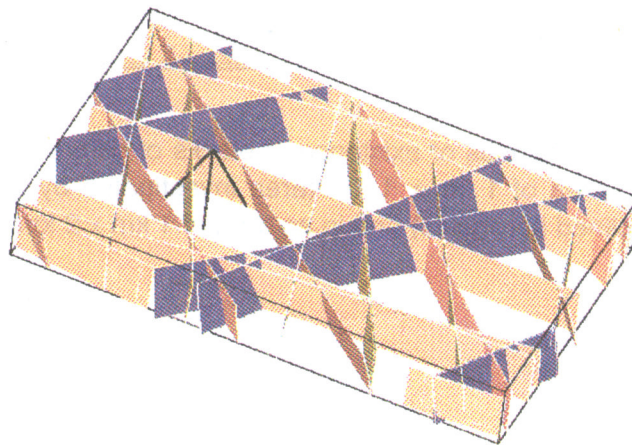
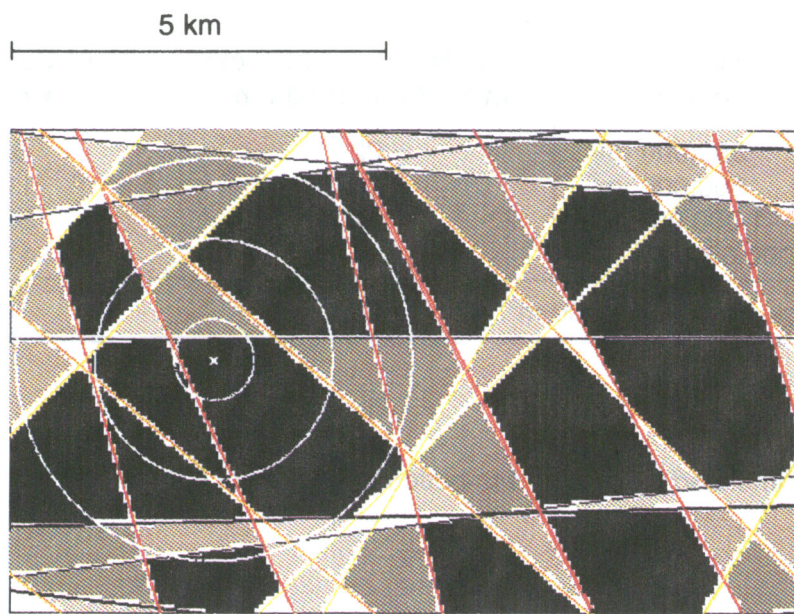


**Fig. 11-2 :** Example of a realization of a synthetic fault network; plan view (above) and three-dimensional view (below). Shaded blocks indicate sizes larger than  $100,000 \text{ m}^2$  (light grey),  $250,000 \text{ m}^2$  (medium grey),  $500,000 \text{ m}^2$  (dark grey) and  $1,000,000 \text{ m}^2$  (black). The concentric circles represent distances of 500, 1500 and 2500 m from a randomly located vertical borehole.

<b>Block Size (horizontal surface area)</b>	<b>Mean Number of Blocks in an Area of 60 km<sup>2</sup></b>	<b>% of Surface of Area *</b>
100,000 - 250,000 m <sup>2</sup>	22	5
250,000 - 500,000 m <sup>2</sup>	18	11
500,000 - 1,000,000 m <sup>2</sup>	17	20
> 1,000,000 m <sup>2</sup>	14	41
Mean block size * : 361,000 m <sup>2</sup>		

\* mean of 100 simulations

**Tab. 11-5 :** Simulated block size distribution in an area of 6 km x 10 km.

<b>Block Size</b>	<b>Chance of existence of at least one block</b>	
	<b>in 1 km x 1 km area</b>	<b>in 1 km x 2 km area</b>
100,000 m <sup>2</sup> or larger	100 %	100 %
250,000 m <sup>2</sup> or larger	94 %	98 %
500,000 m <sup>2</sup> or larger	47 %	72 %

**Tab. 11-6 :** Simulated chances of existence of blocks of different sizes in a randomly located area of 1 km x 1 km (area investigated by the proposed star of four inclined boreholes) and in an area of 1 km x 2 km.

<b>Boreholes</b>	<b>Mean Number of Faults intersected</b>
Vertical borehole that penetrates 1000 m of crystalline basement	0.4
Inclined borehole (30° from vertical) that penetrates 1300 m of crystalline basement	1.0

Note: The mean number of faults (2nd order faults) in an area of 1 km x 1 km, investigated by a star of four inclined boreholes is 3.5.

**Tab. 11-7 :** Mean number of faults intersected by boreholes.

permeability domain that overlies the low-permeability domain. Furthermore, the block size can locally be strongly affected by branching of faults.

Despite all these uncertainties, the results allow some general conclusions to be drawn:

- More than half of the area is expected to consist of suitable blocks of crystalline rock (Table 11-5);
- There is a good chance of finding at least one suitable block of crystalline rock in a randomly located area of 1 km x 1 km that can be investigated with the proposed star of four inclined boreholes (Fig. 11-1) drilled from the same site (Table 11-6);
- In an investigated area of 1 km x 1 km, several major faults can be expected (Table 11-7). These faults can be detected by boreholes that intersect the faults. However, if there is a spacing between the intersection points of the inclined boreholes with the surface of the crystalline basement, faults passing through the area between these intersection points can not be detected (cf. Fig. 11-1). The orientation of the faults is expected to be detected with seismic tomography. The hydraulic characterization of the faults, which is needed to determine whether a fault is significantly water conducting and, therefore, layout-determining, is possible for those faults that are intersected in the low-permeability domain. Faults that are intersected by boreholes in the higher-permeability domain are difficult to characterize hydraulically, and a conservative assumption can be made that such a fault is a major water-conducting fault.
- If the success of seismic tomography is less than expected, there is a greater uncertainty concerning the orientations of the major faults and the sizes of the low-permeability blocks.



## 12 CONCLUSIONS RELEVANT TO A REPOSITORY

This Chapter presents the geological conclusions relevant to a high-level waste repository in the crystalline basement. These conclusions were derived from the final interpretation and synthesis of the regional geological investigation programme in Northern Switzerland.

In many important respects, the detailed investigations carried out have confirmed, substantiated and supplemented the Project Gewähr 1985 conclusions (NAGRA 1985). In particular, it was possible to construct a more complete conceptual model of the small- and large-scale structures of the crystalline basement. Taking this new model into consideration, the regional programme was able to confirm the conclusion in Project Gewähr that crystalline rocks occur in Northern Switzerland that are suitable for hosting a safe repository. In parallel, detailed safety analyses (NAGRA 1994a) have shown that the engineered barriers are capable of making a significantly larger contribution to repository safety than was assumed in Project Gewähr, which means that the demands on geology can be reduced accordingly. In addition, reference waste inventories are smaller. Therefore, smaller blocks of suitable crystalline rock can now be considered as potential repository sites, and the likelihood of finding suitable sites becomes correspondingly higher.

The geological synthesis has indicated that potentially suitable crystalline rocks occur at an appropriate depth in only two areas of Northern Switzerland. The most promising siting possibilities are in a strip a few km wide south of the Rhine river between Kaisten and Koblenz (area West: Kaisten - Leuggern - Böttstein area). A second priority potential siting area is in the Canton of Schaffhausen (area East: Siblingen area); this area is less well-characterized and, based on currently available geological data (section 12.3.2), is not recommended for further investigation at present.

The improved understanding of the crystalline basement and the experience acquired with investigation techniques allow an effective exploration strategy to be designed for further local investigations of the crystalline basement.

Figure 12-1 shows the steps involved in the process of planning a repository and the relationship between geology and the repository project. The present Chapter is organized on the basis of these process steps. It begins by presenting a conceptual geological model of the crystalline basement for the Kaisten - Leuggern - Böttstein area that highlights project-relevant geological aspects (section 12.1). No model is presented for the Siblingen area. A repository design and safety concept adapted to take account of the current understanding of the geological situation are then presented (section 12.2). The siting possibilities in the Kaisten - Leuggern - Böttstein area are discussed in section 12.3, while section 12.4 outlines a concept for further geological investigations related to a repository in the crystalline basement.

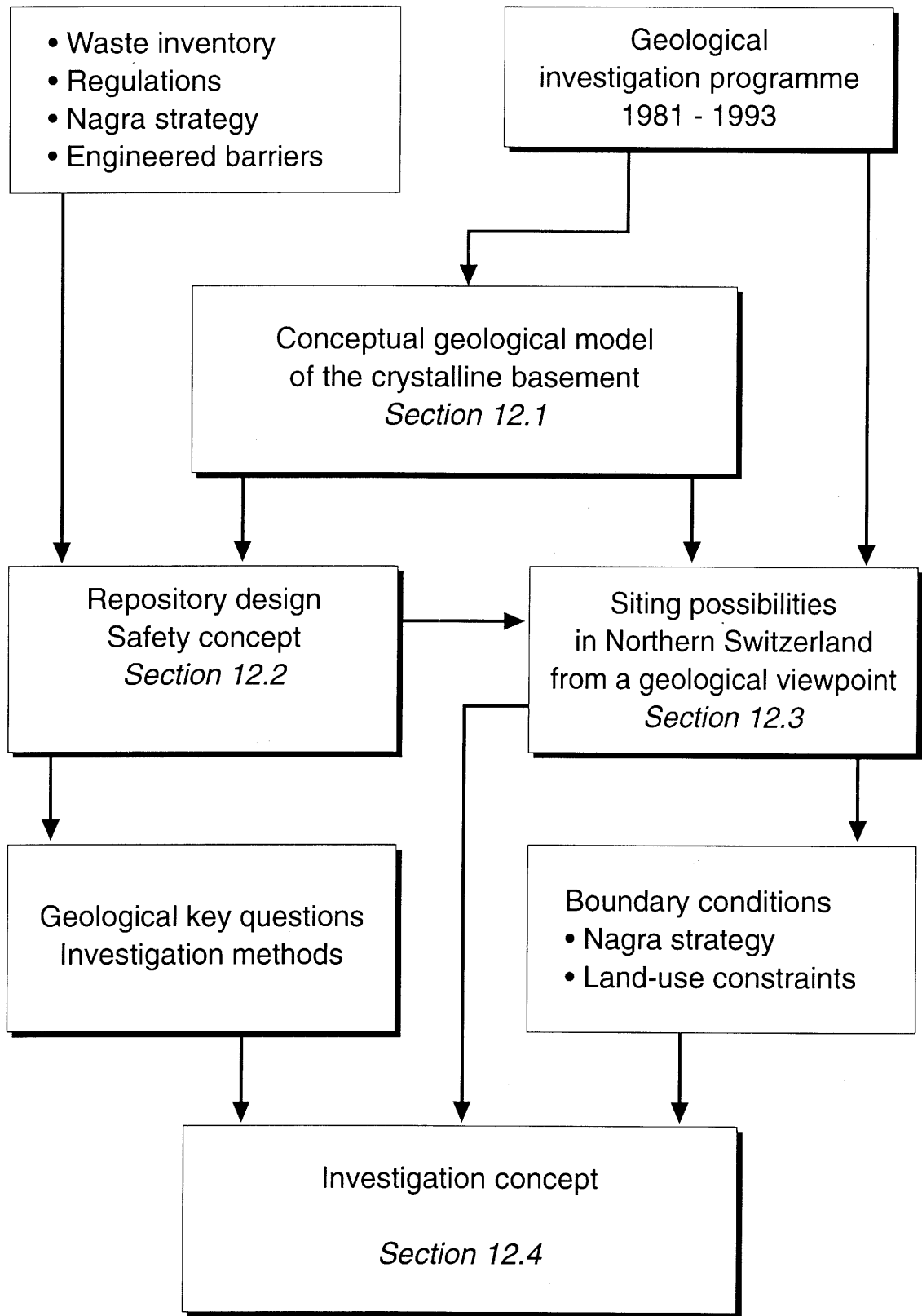


**Fig. 12-1 :** Process steps and relationships involved in planning a repository in the crystalline basement of Northern Switzerland.

## 12.1 Conceptual geological model of the crystalline basement for area West (Kaisten - Leuggern - Böttstein area)

The conceptual geological model for the Kaisten - Leuggern - Böttstein area describes the structure of the crystalline basement, the neighboring sedimentary formations, the groundwater composition and groundwater circulation patterns; potential long-term geological changes are also considered. The model is based on the results presented in Chapters 2 to 10; these results are based on data from several deep boreholes, seismic surveys and studies in the neighboring Black Forest.

### 12.1.1 Structure of the crystalline basement and adjoining sedimentary formations

Figure 12-2 shows the conceptual structure of the crystalline basement and adjoining sedimentary formations. The upper part of the Figure shows a schematic geological north-south profile, while the lower part is a magnified representation of a section of the basement. The section location is indicated with dashed lines on the north-south profile. The elements are described below; the numbering and lettering in the text relate to Figure 12-2.

The crystalline basement is divided into a deeper, low-permeability domain (1), corresponding to the proposed host rock, and an upper, higher-permeability domain (2). Both units are intersected by major water-conducting faults (3). In the south, the basement, which is overlain by Mesozoic (and partly Permian) sediments (4), adjoins the deep Permo-Carboniferous Trough of Northern Switzerland (5). The Quaternary gravels of the Rhine valley (6) (and the Rhine river itself) act as a drainage for the deep groundwater of the crystalline basement.

#### (1) Low-permeability domain of the crystalline basement (proposed repository host rock)

Low-permeability crystalline basement was encountered in the three Nagra boreholes in area West: Böttstein 490 m to 1190 m below the upper boundary of the crystalline basement; Leuggern, 660 m to 1420 m; and Kaisten, 370 m to 490 m. As already demonstrated in Project Gewähr 1985 and confirmed by the recent safety analysis, this low-permeability crystalline basement is suitable for hosting a repository (NAGRA 1985 and NAGRA 1994a). The most important question that was raised within the context of the evaluation of Project Gewähr, namely whether or not a sufficient volume of this potential host rock can be located, is dealt with in Chapter 11.

The low-permeability crystalline domain has an effective hydraulic conductivity (K) of less than 1E-10 m/s. The intact, undisturbed or only slightly disturbed rock itself is practically impermeable (K < 1E-11 m/s). However, water can circulate in interconnected water-conducting features; the following three types have been identified:

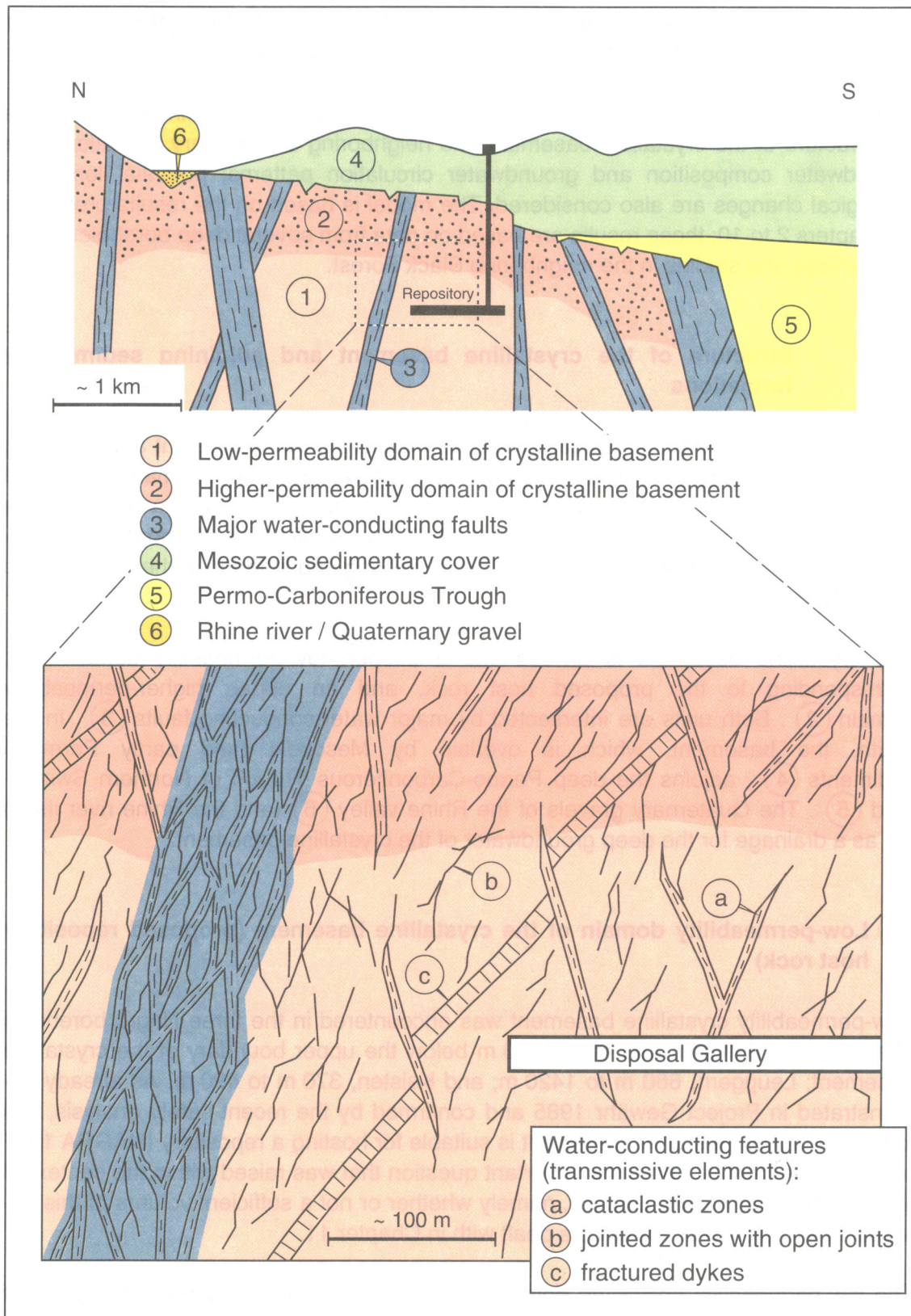


**Fig. 12-2 :** Conceptual geological model of the crystalline basement of Northern Switzerland, area West (Kaisten - Leuggern - Böttstein area).

- *Cataclastic zones* (a) These are minor tectonic faults where blocks of rock have been displaced relative to one another. Direct studies of the lateral extent of these zones were not possible, but it is assumed on the basis of general tectonic information that they extend over decameters to hectometers, and in some cases over several kilometers. They are generally partly infilled with crushed and argillated rock material and often contain open, drusy vugs. In Project Gewähr, the term "kakirite" was used for this type of water-conducting feature. Both permeable and impermeable cataclastic zones were observed in the boreholes. From observations in the Black Forest, it was concluded that water flow is restricted to zones where the vugs are connected to one another. This heterogeneous water flow is termed "channeling" in the literature. Detailed geometric characterization of channeling is not possible on the basis of information obtained from single boreholes alone, and the model of flow distribution has taken into account observations from the Black Forest.
- *Jointed zones with open joints* (b) Open joints are caused by tensile stresses in the rock and are only partly healed with secondary hydrothermal minerals. The lateral extent of the open joints is in the decimeter to decameter range. Water can circulate through these joints only if they are connected with one another or with other water-conducting features. Because of their limited extent, only a small proportion of the open joints carries circulating water. In the Böttstein borehole, this type of water-conducting feature was only identified on the basis of recent studies and was therefore not taken into consideration in Project Gewähr 85. This type was also identified in the Leuggern and Kaisten boreholes.
- *Fractured dykes (and aplitic gneisses)* (c) During a late phase of the Hercynian orogeny, magma penetrated into fractures in the rock and solidified in the form of aplitic (fine-crystalline) and pegmatitic (coarse-crystalline) dykes. This rock contains less mica and is (because of the albite-rich composition of the plagioclase) hydrothermally less altered than the surrounding rock. These dykes, therefore, react in a more brittle fashion to tectonic stresses. The rock is jointed and sheared on a small scale and therefore contains preferential water flow paths. It is assumed on the basis of general geological information that these dykes extend over several hectometers, and, in places, kilometers; in tectonically strongly overprinted rock they are displaced along faults. This type of water-conducting feature was taken into account in Project Gewähr 85. In gneisses, aplitic layers represent a water-bearing system that is equivalent to fractured dykes.

From a hydraulic perspective, no difference exists among the three types of water-conducting features and they are considered as "transmissive elements" in the hydraulic analyses.

The upper boundary of the low-permeability domain in Böttstein, Leuggern and Kaisten is between 350 and 650 m below the upper boundary of the crystalline basement. This database is very limited, and this upper boundary may be locally higher or lower in the vicinity of major faults.

The low-permeability domain of the crystalline basement is subdivided into blocks by major water-conducting faults (cf. (3)), which form the lateral boundaries of the blocks.

## ② Higher-permeability domain of crystalline basement

In all the boreholes north of the Permo-Carboniferous Trough, the uppermost section of the crystalline basement is relatively permeable, with an effective hydraulic conductivity of about  $1\text{E-}7$  m/s in the boreholes Kaisten, Böttstein and Leuggern.

The higher-permeability domain penetrated by the Böttstein and Leuggern boreholes has the same types of water-conducting features as those in the low-permeability domain, but the frequencies and transmissivities of these features are greater in the higher-permeability domain.

The rocks of the higher-permeability domain generally have more significant hydrothermal alteration than those of the low-permeability domain. The alteration has occurred in several phases since the Carboniferous Period at temperatures ranging from 100 to 400 °C. Under the temperature conditions prevailing today, interaction still occurs between groundwater and rock but to a much lesser extent than during the previous high-temperature phases. Hydrothermal alteration has had a marked influence on water flow in the crystalline basement. On the one hand, many fractures that were originally open have been healed by secondary hydrothermal mineralizations (e.g. clay minerals, calcite and quartz); on the other hand, the formation of solution cavities in the cataclastic zones has resulted in locally enhanced transmissivity.

The top of the crystalline basement represents an old land surface that was produced by erosion. Surface weathering phenomena can be recognized only in the uppermost few meters.

It is presently unknown whether the depth zoning of the permeability of the crystalline basement reflects differences in brittle deformation and hydrothermal alteration (stronger alterations in higher-permeability domain) or whether a deep-reaching decompaction of the rock before and during the Buntsandstein.

## ③ Major water-conducting faults

The crystalline basement of the Black Forest and its southern continuation into Northern Switzerland is penetrated by numerous large and small faults. The smaller faults, which are designated as cataclastic zones in the model, have already been discussed. Several families of larger faults, with lengths of 1 km to over 10 km and thicknesses of 10 to 1000 m, penetrate the crystalline basement of Northern Switzerland. The fault traces of one family commonly are subparallel over large areas, but the faults also break up into several branches and then reunite. The spacing of these major faults within a family is several 100 m to a few km. The mean hydraulic conductivity of these faults is about the same order of magnitude as those of the higher-permeability domain. The faults consist of several to numerous cataclastic zones (a) that transect the more-or-less intact rock that is in places penetrated by open joints (b). Studies in the Black Forest have shown that strongly water-conducting ore and mineral veins are associated with these faults in certain areas.

Based on regional tectonic evidence, the strongly water-conducting cataclastic zones of the Kaisten borehole were assigned to the regionally important Eggberg fault, or to a side branch thereof. In the Leuggern borehole, a highly permeable disturbed zone with drusy quartz-barite veins was encountered below 1650 m down to the final depth at 1690 m. This occurrence shows that in Northern Switzerland faults can be permeable to a depth of few km. Whether this is the case for all major faults, or whether some faults or even a whole fault family can be relatively impermeable, cannot be answered as yet on the basis of current information.

Nagra's vertical boreholes did not provide any indication of the existence of horizontal faults.

#### ④ **Mesozoic sedimentary cover**

The crystalline basement south of the Rhine valley is overlain by Mesozoic sedimentary rocks of Triassic and Jurassic age that have retained a tectonically fairly undisturbed subhorizontal stratification with only a few faults (Tabular Jura).

The Middle Triassic section contains thick anhydrite and clay sequences and, where there has been no significant tectonic disturbance, these formations function as an impermeable layer that separates the shallow groundwater from the groundwater circulating in the crystalline basement. This well-known barrier effect of the Middle Triassic rocks was also identified in the Nagra boreholes on the basis of hydrochemical evidence.

#### ⑤ **Permo-Carboniferous Trough of Northern Switzerland**

The Permo-Carboniferous Trough of Northern Switzerland is several kilometers deep and several kilometers wide and dissects the region of Northern Switzerland. In 1983, its discovery in the Nagra deep boreholes caused something of a scientific sensation. The sedimentary infill consists of continental fluvial and limnic deposits and also contains coal and oil shale deposits. The margins of the Trough have been subjected to strong tectonic overprinting along steeply-dipping faults and wrench faults. On average, the Trough infill has a low permeability and forms a hydraulic barrier between the waters which circulate in the crystalline basement of the Swiss Plateau and the crystalline basement to the north of the Trough.

#### ⑥ **Rhine river/Quaternary gravel**

The Rhine river drains area West and the Rhine valley is the discharge area for the groundwaters from the crystalline basement. The Rhine valley contains extensive Quaternary gravels that form significant groundwater reservoirs.

### 12.1.2 Hydrochemical and isotopic characteristics of groundwater

As described in Chapter 7, groundwater in the higher-permeability domain and in the major water-conducting faults of the crystalline basement of area West is a sodium-sulfate type of fairly uniform chemical and isotopic composition; the total dissolved-solids content is 0.9 to 1.4 grams per liter. This groundwater is very similar in composition to the groundwater of the thermal springs of Zurzach. The Zurzach thermal waters, with an artesian outflow of 600 liters per minute, showed a constant hydrochemical composition with a total dissolved solids content of 0.9 grams per liter for about 30 years.

Detailed studies of possible rock-water interactions indicate that the low-mineralized groundwater of area West has evolved entirely within crystalline rocks and that this groundwater has not been in contact with sedimentary formations.

This groundwater is reducing and its pH ranges from 7.6 to 8.3. Its hydrochemical and isotopic characteristics suggest a long mean residence time; infiltration occurred at least as long ago as the last interglacial or during Early Würm interstadials, which means at least 70000 years ago.

In the low-permeability domain of the crystalline basement, in addition to the water types described above, relics of other water types with higher total dissolved solids contents also occur. These types represent zones of restricted circulation and are probably of great age. The higher-mineralized water at Leuggern evolved entirely in crystalline rocks. The saline groundwater of a zone in the lower part of the Böttstein borehole includes components of water that probably represent very old relics of marine water or of water that have infiltrated from the Permo-Carboniferous Trough.

### 12.1.3 Conditions of groundwater circulation

As described in Chapter 8, hydrogeological observations, the results of the regional-scale hydrodynamic modeling and hydrochemical and isotopic composition of groundwaters support the conceptual model of regional flow in the crystalline basement of Northern Switzerland from recharge areas in the southern and South-eastern Black Forest towards discharge areas along the Rhine river west of Koblenz.

In area West, the following geological features are considered to determine the regional groundwater flow directions: i) in the south the deep Permo-Carboniferous Trough which acts as a flow barrier because of its very low hydraulic conductivity; ii) the Rhine river in contact with the crystalline basement which forms a discharge zone; and iii) evaporites of the Middle Muschelkalk sediments which also act as a flow barrier and result in confined flow conditions in the crystalline basement. The overall horizontal flow direction in the region is therefore towards the west, gradually turning north-west as the Rhine is approached. An increasingly vertical (upward) component of the gradient occurs as groundwater approaches the discharge zone.

A significant contrast exists between the flow characteristics of the higher-permeability domain and the low-permeability domain. In the former, the predominant component of

the hydraulic gradient is horizontal; the vertical component becomes significant only near the discharge areas. In the low-permeability domain, flow directions may differ locally from the general characteristics; changes in the hydraulic properties, due, for example, to the existence of major water-conducting faults or the transition to the higher-permeability domain, affect the local gradients.

Most groundwater circulation occurs in the higher-permeability domain and in the major water-conducting faults. The effective hydraulic conductivity of the low-permeability domain is about 1000 times smaller than that of the higher-permeability domain or major water-conducting faults; therefore, even with larger gradients, groundwater fluxes in the low-permeability domain do not contribute significantly to the overall circulation.

#### 12.1.4 Extent of low-permeability blocks of crystalline rock

A geological question of key importance is the size and location of blocks of low-permeability crystalline rock, because the intention is to dispose of radioactive waste in these blocks at a sufficient distance from laterally bounding major water-conducting faults (layout-determining faults).

Data from Nagra's vertical boreholes do not contain any information on the spacing between steeply-dipping major water-conducting faults. Reflection seismics studies were able to improve this situation only slightly, because only those faults that significantly displace the Mesozoic sediments can be interpreted from the seismic data.

Based on studies in the crystalline basement in the neighboring Black Forest, a schematic network of major, steeply-dipping fault zones was postulated for Northern Switzerland, and information derived on the directions, frequencies, dips and thicknesses of various fault families (Chapter 5). Statistical analysis was used to calculate the expected size distribution of the individual crystalline rock blocks between the faults (Chapter 11). Table 12-1 summarizes the results.

Size of crystalline block (horizontal surface area)	Probability that at least one crystalline block per km <sup>2</sup> is present
≥ 500'000 m <sup>2</sup>	47 %
≥ 250'000 m <sup>2</sup>	94 %
≥ 100'000 m <sup>2</sup>	100 %

**Tab. 12-1 :** Size distribution of low-permeability crystalline blocks between major water-conducting faults (basis: Table 11-6).

These values are valid if the following assumptions are correct:

- The network of major faults in area West corresponds to the fault pattern that is derived from the Black Forest.
- All the faults in this network are major water-conducting faults. If, as expected, some of the faults or fault families are not water-conducting, then larger low-permeability crystalline blocks are to be expected.
- In the low-permeability domain, smaller faults (cataclastic zones) and dykes are expected to have low transmissivities. If some of these faults or dykes were to have large transmissivities and a hydraulic connection with the major water-conducting faults or the higher-permeability domain, they would become layout-determining, and smaller blocks of suitable crystalline rock would be expected.
- In a marginal zone of the Permo-Carboniferous Trough, strong tectonic overprinting of the crystalline basement is expected and the fault network mentioned above should not be taken as representative for this zone.

Despite the uncertainties that still exist, it is highly likely that, in an area of a few square kilometers in area West, sufficiently large low-permeability crystalline blocks occur and can be located.

#### **12.1.5 Long-term changes of the geological setting**

It is assumed that the effects on the repository of climatic and geological-tectonic long-term changes will be negligible in the next 10,000 years. Much longer timescales, however, have also been considered in the studies presented in Chapter 9. Over a period of 1 million years, the maximum depth of erosion caused by the Rhine river and its tributaries in area West will be about 200 m. It is also possible that the Rhine will erode the sediments south of the present Rhine valley, which could have the effect of displacing the river bed up to 2 km further south. The crystalline basement would be exposed and eroded in this zone and it is possible that, due to decompaction effects, the top of the low-permeability domain might lower.

In the entire region of Northern Switzerland, large-scale erosion (denudation) will not exceed 50 m in one million years, even under adverse climatic conditions.

As also discussed in Chapter 9, tectonic movements are possible. The largest component of these movements will be along existing major faults, with displacements of up to 100 m in one million years. Movements along smaller faults (cataclastic zones), which are also expected in the low-permeability domain, probably will not exceed 1 m in a million years.

Long-term geological changes are not expected to significantly alter the groundwater flow characteristics or the water chemistry in the low-permeability domain away from the groundwater discharge zone of the Rhine valley.

In the vicinity of the Rhine river, changes are to be expected due to the possible shift of the river bed to the south; for example, the groundwater discharge zone would also be shifted accordingly to the south. However, groundwater flow and hydrochemical conditions in the repository area would not be significantly affected as long as the position of the repository remains south of the future Rhine river.

## **12.2 Repository design and safety concept**

### **12.2.1 Repository design**

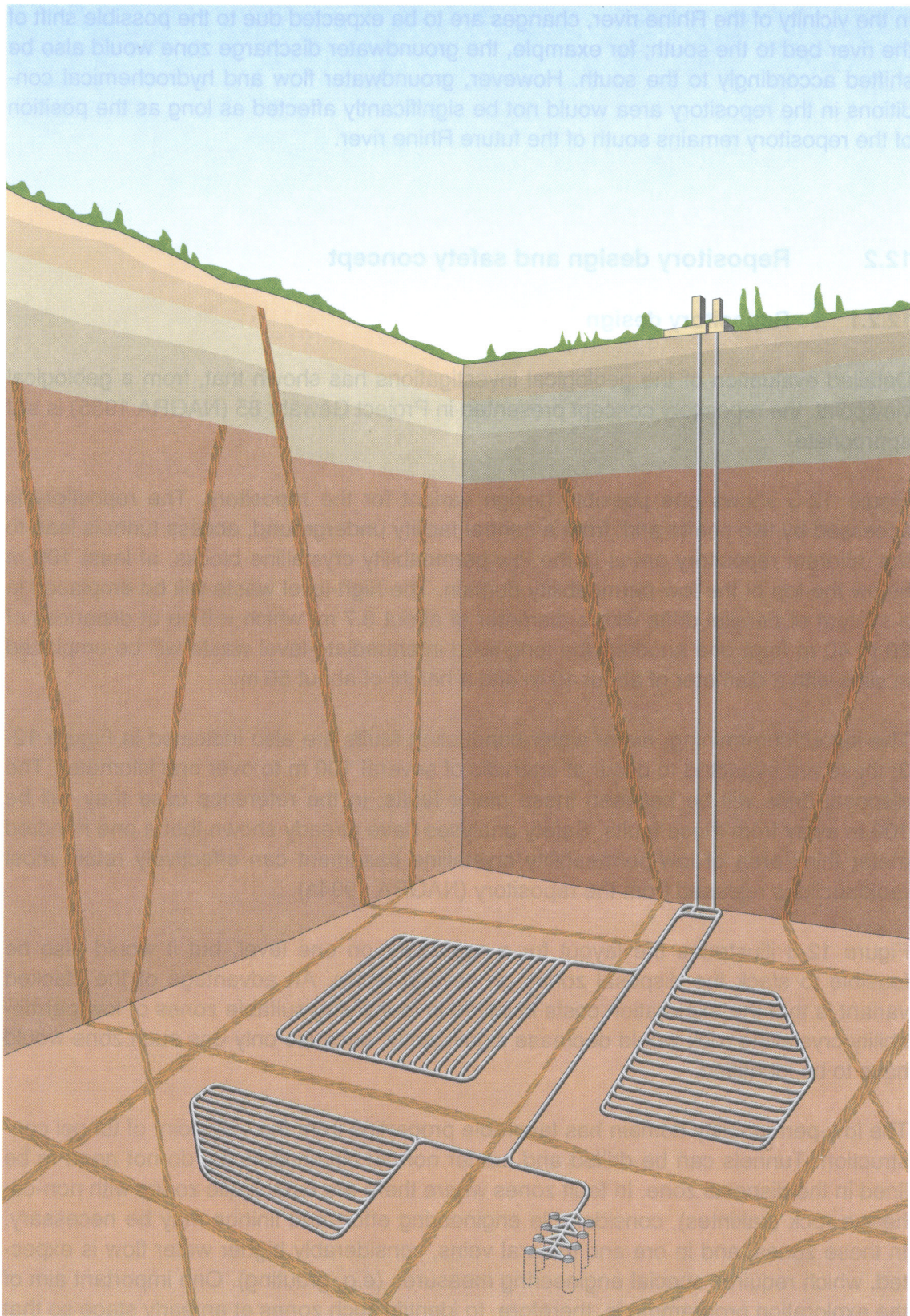
Detailed evaluation of the geological investigations has shown that, from a geological viewpoint, the repository concept presented in Project Gewähr 85 (NAGRA 1985) is still appropriate.

Figure 12-3 shows one possible design variant for the repository. The repository is accessed by two shafts and, from a central facility underground, access tunnels lead to the different repository areas in the low-permeability crystalline blocks, at least 100 m below the top of the low-permeability domain. The high-level waste will be emplaced in a system of parallel drifts with a diameter of about 3.7 m, which will be at distances of 20 to 40 m from one another; the long-lived intermediate-level waste will be emplaced in silos with a diameter of about 10 m and a height of about 50 m.

The layout-determining, major water-conducting faults are also indicated in Figure 12-3; these are expected to occur at intervals of several 100 m to over one kilometer. The disposal drifts will be between these major faults; in the reference case they will be 100 m away from these faults. Safety analyses have already shown that a one hundred meter thick area of low-permeability crystalline basement can effectively retain most radionuclides released from the repository (NAGRA 1994a).

Figure 12-3 illustrates the layout for a repository on one level, but it would also be feasible to stack the disposal zones on several levels. An advantage of the stacked variant is that the exploration costs involved in identifying suitable zones of low-permeability crystalline rock would decrease significantly, because only one such zone would have to be identified.

The low-permeability domain has favorable properties from the viewpoint of tunnel construction. Tunnels can be drilled and, under normal circumstances, do not need to be lined in the disposal zone. In fault zones where there are cataclastic zones with non-cohesive rock (kakirites), considerable engineering effort and linings may be necessary. In these zones, and in ore and mineral veins, considerably higher water flow is expected, which requires special engineering measures (e.g. grouting). One important aim of the exploration programme is, therefore, to identify such zones at an early stage so that they can be avoided wherever possible.



**Fig. 12-3 :** Sketch showing a repository concept for HLW/TRU in the crystalline basement of Northern Switzerland (variant with repository on one level).

### 12.2.2 Safety concept and contribution of the crystalline basement to repository safety

The safety concept for the repository for high-level waste is based on the multibarrier principle. Various engineered and geological barriers should ensure containment of the radionuclides within the engineered barriers over a long period of time and thereafter restrict their releases to low levels.

High-level waste from the reprocessing of spent fuel is vitrified, i.e. the radioactive materials are distributed homogeneously throughout a borosilicate glass matrix. Each glass block is enclosed in a thick steel canister that is intended to ensure isolation of the waste for more than 1000 years. The canister in turn is surrounded by a barrier of highly compacted bentonite clay which is expected to retard the release of any radionuclides leached from the glass, so that most of the inventory decays completely within the engineered barriers (NAGRA 1994a).

The geosphere makes the following contributions to the safety of the repository:

- physical protection of the disposal system for long periods of time
- ensuring longevity of the engineered barriers and restricting radionuclide release from the repository
- radionuclide retention in the rock due to sorption and matrix diffusion
- dilution of contaminated water in aquifers and surface waters.

- *Physical protection of the disposal system for long periods of time*

Once backfilling is complete and the shafts are sealed, an underground repository will be offered a high level of protection by the geosphere from intentional or unintentional human intrusion, sabotage and the consequences of wars.

The repository should be located at a sufficient depth to ensure that it will not be exposed, or its protective geological milieu significantly disturbed, if maximum expected erosion were to occur.

*The studies presented in Chapter 9 show that, in the next million years, the estimated maximum depth of erosion caused by the Rhine river and its tributaries in the region Kaisten-Leuggern-Böttstein is 200 m. It is therefore recommended that the repository be located at least 400 m below ground surface.*

- *Ensuring engineered barrier longevity and restricting radionuclide release from the repository*

Engineered barriers prevent radionuclides from entering the geosphere for very long periods of time. Radionuclides are expected to diffuse out of the engineered barrier system at very low rates. However, this expectation is based on the precondition that the integrity and proper functioning of the barriers will be maintained.

The following demands are therefore made on the geosphere:

- There should be no significant tectonic movement in the disposal zone that could damage the integrity of the waste canister and the bentonite barrier.

*In area West, maximum displacements of 100 m are expected along existing major faults in a million years. These faults can be identified during exploration and are to be avoided when designing the repository. Movements along smaller faults (cataclastic zones) in the disposal zone will not exceed the permissible amount of 1 m in a million years. Canister emplacement at such potential movement zones will be avoided.*

- Groundwater should be reducing and should have a relatively low mineralization. These conditions ensure, for example, that the steel canister will corrode extremely slowly and that the bentonite will not undergo any significant mineralogical changes over the relevant time period and will thus retain its function as a diffusion barrier.

*The advectively circulating groundwater in the crystalline basement of Northern Switzerland is very favorable in terms of its hydrochemistry and has low concentrations of colloids and organic carbon. The groundwater composition is not expected to change unfavorably in the long term.*

- The rock in the repository area should have a low permeability and groundwater flow rates should be as low as possible. These conditions ensure that the mineralogical changes in the bentonite will be minimal, and that the bentonite will not be eroded by advectively circulating groundwater in the vicinity of water-conducting features.

*The low-permeability domain of the crystalline basement observed in the boreholes of Böttstein and Leuggern fulfils these requirements.*

- *Radionuclide retention in the rock due to sorption and matrix diffusion*

Groundwater flows advectively in the crystalline rock in various types of water-conducting features. Radionuclides should be sorbed on different mineral surfaces; they should also diffuse into the pore space of the rock surrounding the water-conducting features (matrix diffusion) and be retained effectively there.

*The mineralogy of the rock in the vicinity of water-conducting features is favorable to radionuclide sorption, and the rock matrix has a connected microporosity that also favors matrix diffusion processes. The safety analysis has shown that radionuclides can be retained extremely effectively in only 100 m of low-permeability crystalline rock, of the quality observed in the Böttstein and Leuggern boreholes (NAGRA 1994a). These studies also indicate that colloidal transport of radionuclides does not seem to be a significant perturbing factor at the very low colloid concentrations observed in these groundwaters.*

*The safety analysis (NAGRA 1994a) has shown that the effectiveness of the engineered barriers is significantly greater than was assumed at the time of Project Gewähr 85. Effective radionuclide retention in the geosphere is not now a*

*critical element of the "robust" safety concept. In such a case, a safe distance of 100 m between disposal tunnel and layout-determining fault is not absolutely necessary and the waste could be emplaced closer to the major water-conducting faults. If feasible in terms of engineering and tunnel sealing, disposal tunnels could then pass through major water-conducting faults and the waste would be emplaced only in those sections of the tunnel that are in low-permeability domain. This means that a safe repository could be constructed in a crystalline formation with only relatively small blocks of low-permeability rock.*

- *Dilution of contaminated water in aquifers and surface waters*

Groundwater containing radionuclides released from the repository should be diluted on the way to the groundwater exfiltration zone, because of the much greater quantities of water circulating in higher-permeability rocks, in aquifers and in surface water. This dilution would result in effective reduction of radionuclide concentrations.

*In area West, groundwater is diluted as it moves from the low-permeability domain into a major water-conducting fault or into the higher-permeability domain, where, because of their higher permeabilities, much greater volumes of water circulate.*

*Even greater dilution occurs when groundwater from the crystalline basement enters the Quaternary gravels of the Rhine valley or the Rhine river itself. The total water flux through the Quaternary gravels of the Rhine valley is about  $5E+6 \text{ m}^3$  per year (cf. Table 10-2). If it is assumed that around  $3 \text{ m}^3$  of water per year flows through the repository, this gives a dilution factor of around  $1E+6$ . Under present-day climatic conditions, the Rhine has a water flow of approximately  $3E+10 \text{ m}^3$  per year, resulting in a dilution of  $1E+10$ .*

*As indicated in Chapter 9, under a continuation of present-day climatic conditions the floor of the Rhine valley can be expected to contain gravels. These could be removed by the action of glaciers during major glaciations but, when the glaciers retreat, gravels and sands will be deposited once again on the valley floors.*

*In an arid climate, the water flow in the Rhine could be less than at present; under more humid conditions, flow would probably be greater than at present, and the dilution of groundwater coming from a repository would increase correspondingly.*

### **12.3 Siting possibilities for a repository in the crystalline basement of Northern Switzerland**

When identifying potential siting areas, among the key parameters to be considered are the minimum and maximum depth of the repository.

It is desirable that a repository in the low-permeability domain be placed significantly deeper than the maximum depth of erosion to be expected in a region over the next million years.

The maximum depth of the repository is determined principally by the rock temperature. Rock temperature is important mainly from the point of view of tunnel construction and repository operation. The air temperature in the tunnel should not exceed 28 °C; if the rock temperature is higher, the tunnel atmosphere has to be cooled. Up to a temperature of around 35 °C, this cooling can be done using conventional tunnel ventilation techniques. At higher rock temperatures, the ventilating air itself has to be cooled, which requires considerable additional effort. In deep mines in South Africa, tunnels have been constructed in rock with temperatures up to 55 °C. Based on these considerations, the maximum rock temperature is therefore fixed at 55 °C. It is desirable, however, to place a repository in rocks with temperatures as low as possible.

High-level radioactive waste generates heat. The heat production is initially high but decreases relatively rapidly. The high-level waste is therefore held in interim storage at the surface for several decades to allow the heat production to decline to an acceptable level. Even after emplacement in the repository, the waste will continue to generate a certain amount of heat and the rock in the vicinity will warm up. The natural rock temperature should be such that a sufficiently thick section of the bentonite will not reach a temperature significantly over 100°C. Calculations have shown that this requirement is easy to fulfil in the crystalline rock if the natural rock temperature is below 55°C.

Table 12-2 shows the rock temperatures in selected Nagra boreholes. Areas where the top of the crystalline basement is less than 1200 m below ground level are considered as potential siting areas.

Borehole	Depth of rock temperature	
	50 °C	55 °C
Böttstein	1010 m	1175 m
Leuggern	1100 m	1230 m
Kaisten	1010 m	1160 m
Siblingen	1150 m	1300 m

**Tab. 12-2 :** Depth of rock temperatures of 50 °C and 55 °C in selected Nagra boreholes.

In a large part of Nagra's investigation area, the top of the crystalline basement is significantly deeper than 1200 m below ground level; in the region of the Permo-Carboniferous Trough of Northern Switzerland, it is at a depth of several kilometers. In two areas, the top of the crystalline basement is less than 1200 m below ground level:

- *Area West:* Kaisten-Leuggern-Böttstein area
- *Area East:* Siblingen area

### 12.3.1 Potential siting area Kaisten - Leuggern - Böttstein (area West)

The location of the area is shown in Figure 12-4.

The northern and eastern boundaries of the area are represented by the Rhine river, which coincides with the Swiss border. The southern boundary is represented by the area where the top of the crystalline basement is at a maximum depth of 1200 m below ground level; this location coincides with the northern margin of the Permo-Carboniferous Trough of Northern Switzerland. The western boundary is at the edge of the area between Basel and Säckingen that was disturbed tectonically by the formation of the Rhine Graben and still shows significant earthquake activity today.

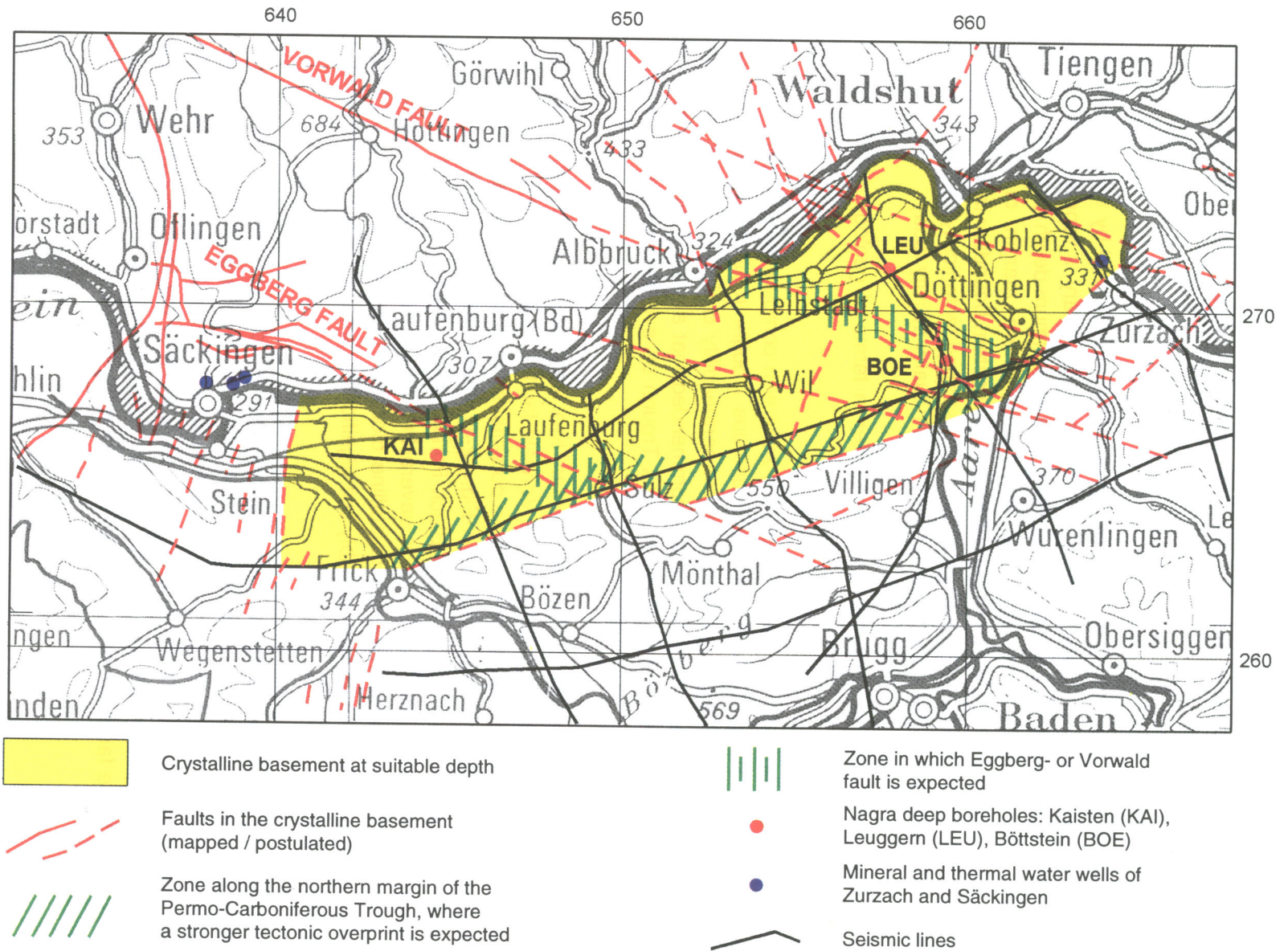
The area is divided into several zones that differ in terms of geology, tectonics and hydrogeology.

Along the southern boundary of the region, a zone with complex tectonic conditions is expected at the margin of the Permo-Carboniferous Trough. In this area, the likelihood of there being sufficiently large blocks of low-permeability crystalline rock is probably lower than farther north. It is therefore recommended that a zone 1 km wide north of the margin of the deep Permo-Carboniferous Trough be avoided (diagonally hatched zone in Fig. 12-4).

In the Black Forest north of the Rhine river, two significant fault zones of regional extent occur - the Eggberg fault and the Vorwald fault. It is expected that these faults extend into the crystalline basement of the potential siting area. Two zones have therefore been identified (vertical hatching in Fig. 12-4) where these faults are expected to occur. Based on observations in the Black Forest, these faults are either one single disturbed zone with a thickness of up to several hundred meters or several branches of thinner faults with low-permeability crystalline blocks in between. The sizes of these blocks between fault branches probably are significantly smaller than in zones outside these regional fault zones.

Except for these zones along the Permo-Carboniferous Trough and at the Eggberg and Vorwald faults, the conceptual model (section 12.1) shows an area of crystalline basement with major faults but, nevertheless, with sufficiently large blocks of low-permeability crystalline rocks in between. The presence of most of the faults shown in Figure 12-4 has been postulated on the basis of seismic interpretations. However, the exact location of these faults is not certain and it is not recommended to try to avoid them at present.

Fig. 12-4 : Potential sining area Kaisten - Leuggern - Böttstein (area West).



Within the siting area, the top of the crystalline basement becomes deeper toward the south. If it is assumed that the higher-permeability domain of the crystalline basement is generally several 100 m thick, then the top of the low-permeability domain (host rock) will also be deeper towards the south. South of the siting area, it is therefore possible that suitable crystalline rock will only be identified at depths where the rock temperatures exceed the boundary value of 55°C. Even to the north it is possible that the suitable crystalline rock will be too deep at sites where the higher-permeability domain is unusually thick.

The Rhine valley is the discharge area for groundwater from the crystalline basement of the siting area. However, some near-surface groundwater from the crystalline basement of the Black Forest north of the Rhine river also exfiltrates into this valley. In the next million years it is possible that the Rhine will erode to a depth of 200 m (Chapter 9) and that the river bed will shift southwards. A first estimate indicates that the Rhine could move as much as 2 km farther south. The Rhine is the exfiltration zone of groundwater coming from southern areas (from the potential siting area) and groundwater coming from the north from the Black Forest. In a strip up to 2 km wide between the actual river bed and the expected future river bed of the Rhine, it is therefore possible that younger groundwater from the Black Forest with a different hydrochemical composition could flow through a repository located in this area. If a site is to be considered in this area, the erosion potential of the Rhine river and the associated changes in groundwater circulation should be clarified in special local studies. The crystalline basement could also be eroded in this area and it can not be excluded that decompaction of the rock could cause the top of the low-permeability domain to become deeper.

The boreholes of Zurzach and Säckinggen are at the edge of the siting area; the thermal and mineral water in these boreholes comes from the crystalline basement. Hydraulic calculations have shown that the thermal waters are not expected to be influenced adversely (i.e. temporary lowering of the groundwater table) by the construction and operation of a repository, provided that a sufficient distance is maintained and that during construction of the repository steps will be taken to seal off strongly water-conducting zones. A sealed repository is not expected to have any hydraulic influence on the thermal springs.

The thermal springs of Baden and Schinznach are supplied mainly by groundwater from the Muschelkalk aquifer and possibly contain components of water from the crystalline basement or the Permo-Carboniferous Trough. These thermal springs would not be influenced by a repository in the proposed area, because they are south of the low-permeability Permo-Carboniferous Trough which acts as a hydraulic barrier.

To summarize, in principle, all zones in area West may contain suitable areas for hosting a repository. The synthesis of the available data, however, indicates that the central zone between the Vorwald and Eggberg faults may be tectonically more simple than the areas of Leuggern and Böttstein, but there is no direct information on the crystalline basement of this central area.

The geological situation in the area of the Leuggern and Böttstein boreholes may be more complex than in the central zone; here, however, low-permeability sections of crystalline rock are known to occur in the boreholes at Leuggern and Böttstein. In deciding upon the next steps in exploration of the crystalline basement, these considerations should be evaluated, taking into account also the project-specific boundary conditions of the Swiss HLW programme. A reasonable approach, intended to maximize the chances of positive results in the immediate future investigation phase, would be to continue exploration in the Böttstein - Leuggern area.

### **12.3.2 Potential siting area Siblingen (area East)**

The location of the Siblingen area is shown in Figure 12-5.

The north-west boundary is formed by the Swiss border and the south-east boundary is defined by the zone in which the top of the crystalline basement is less than 1200 m below ground level.

Interpretation of the geological structure and hydrogeological conditions in the region is based on information from the Siblingen borehole and from two seismic lines.

No low-permeability domain was encountered in the Siblingen borehole. Down to the final depth of 1522 m, the hydraulic conductivities measured were 1000 times higher than those encountered in the low-permeability domain in the Leuggern and Böttstein boreholes.

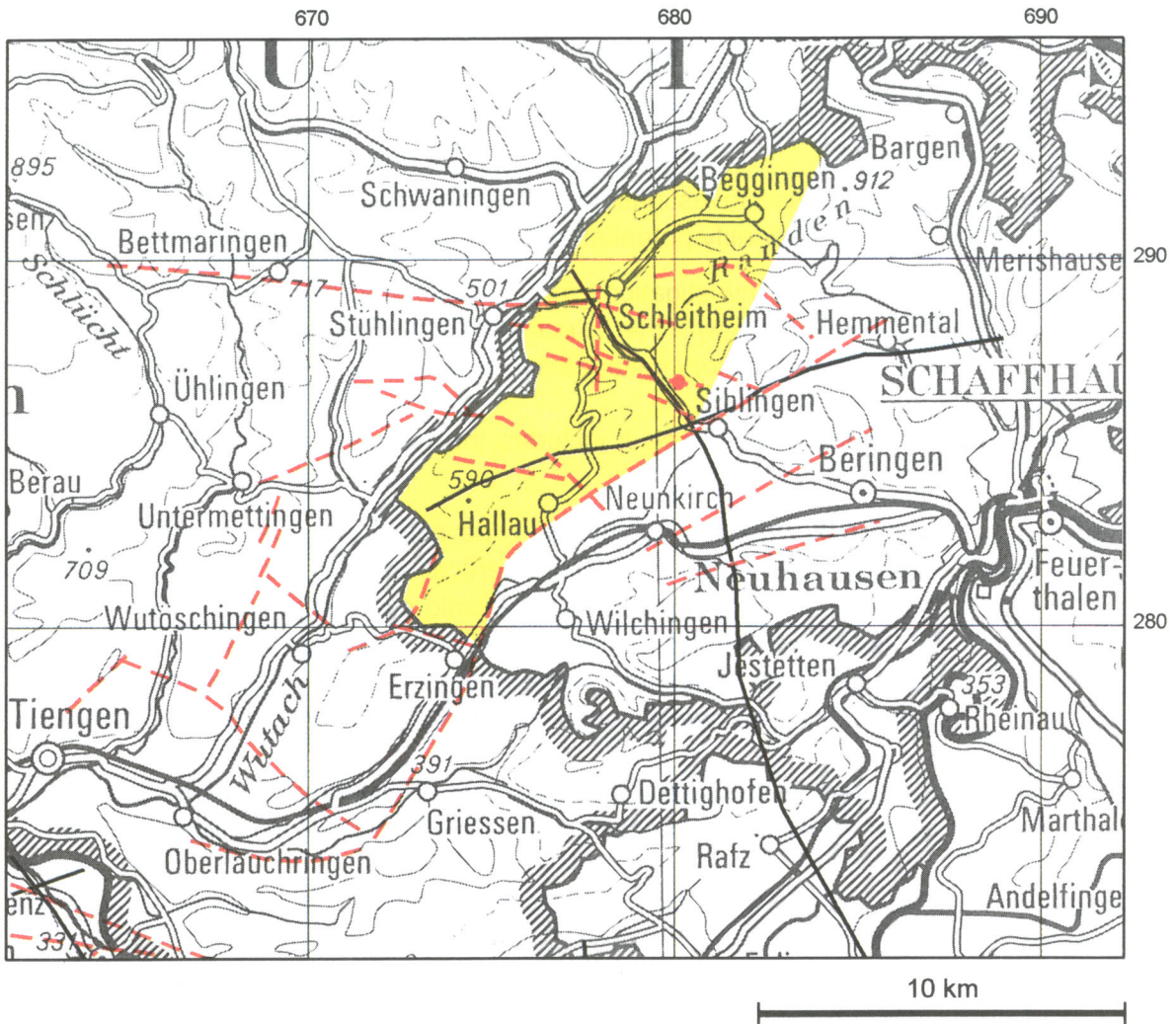
The question thus arises as to whether low-permeability domain can be expected in the Siblingen region at a suitable depth, or whether the crystalline rock in the whole region is generally more strongly tectonized and permeable than in area West. Further boreholes would have to be drilled before this question could be answered.

Based on the geological information currently available, it is recommended that this area be assigned second priority for further characterization.

## **12.4 Investigation concept**

The site investigation concept proposed for a repository in the crystalline basement of Northern Switzerland and the rationale leading to its definition are described in Chapter 11 (cf. Table 11-3 and Figure 11-1). The basis for the formulation of an investigation concept is:

- the conceptual geological model for flow and transport and the resulting key questions to be answered;
- the geometric and engineering characteristics of the repository (e.g. layout);
- the concept and requirements for the performance assessment;
- the available exploration methods.



-  Crystalline basement at suitable depth
-  Faults in the crystalline basement (postulated)
-  Nagra deep borehole Siblingen
-  Seismic lines

Fig. 12-5 : Potential siting area Siblingen (area East).

The investigation programme is divided into three phases:

- Phase I* regional investigations which are completed with the publication of this report.
- Phase II* surface-based investigations on a local scale to provide the information required to identify potential repository sites and shaft locations.
- Phase III* underground investigations at a specific site, commencing with a shaft and culminating with the selection of specific locations for the construction of the repository galleries and tunnels.

The investigation concept for *Phase II* includes the following steps (Table 11-3 and Figure 11-1):

- Step 1: Reflection seismics survey, with the main objective of identifying and locating major faults that have a vertical offset in the sedimentary cover. Although it is not possible with seismic surveys to clearly detect major faults in the crystalline basement and to make any statement on hydrogeological characteristics, these results are very valuable for the extrapolation of major water-conducting faults identified in the boreholes.
- Step 2: First vertical borehole, with the main objective of confirming the existence of the low-permeability crystalline basement at suitable depths.
- Step 3: Four inclined boreholes, in a star configuration (cf. Figure 11-1), with the objectives of:
- characterization of the crystalline basement and its water-conducting features;
  - identification of the upper limit of the low-permeability domain and definition of preliminary repository depth;
  - identification and characterization of the intersected major water-conducting faults;
  - confirmation or modification of the conceptual geological model.

In addition to the conventional investigation programme in these boreholes, plans include seismic tomography surveys and crosshole hydraulic testing.

- Step 4: Following the analysis of results, further exploration from the surface may be needed. If an area of suitable size has not yet been identified after evaluation of Step 3, additional boreholes may be required to increase the investigation area in a promising direction. If the location of the shaft is outside the investigation area of Step 3, boreholes will be needed in this step to confirm the acceptability of the shaft location and to characterize the area between the shaft and the repository.

The investigation concept for *Phase III* includes:

- Step 5: Shaft to provisional repository depth, preceded by boreholes for characterization of undisturbed hydrogeological conditions and for monitoring the effects of shaft sinking. Extended characterization of the crystalline basement will occur during sinking of the shaft.
- Step 6: Exploration with horizontal boreholes and pilot galleries. At a possible repository depth, exploration will start with horizontal boreholes, with the aim of detecting and characterizing major water-conducting faults. Through direct intersection, hydraulic testing and seismic tomography, all major water-conducting faults in the investigated area should be located in order to identify promising sites for the advancement of pilot galleries. This procedure (horizontal boreholes followed by pilot galleries) will be repeated until a sufficient volume of suitable rock for repository construction is identified.
- If the shaft is outside the potential repository area, then access tunnels towards the planned repository area will be constructed, preceded by horizontal boreholes.
- Step 7: Further detailed investigations during repository construction, with pilot boreholes and observations in pilot galleries, will aim at confirmation of the assumptions required for the repository design and fine-tuning of the layout.

With the new information gained during each step, the methodology developed for the investigation concept can be used to re-evaluate and optimize the remaining steps. Also, new and more effective tools may be developed as the project advances.



**REFERENCES**

- ABELIN, H., BIRGERSSON, L., WIDEN, H., ÅGREN, T., NERETNIEKS, I. & MORENO, L. 1992: Results of a channelling experiment in Stripa. - Proc. int. Migration Conf. Jerez de la Frontera.
- ABRECHT, J. 1980: Zur Bildung migmatitischer Schollenamphibolite aus dem Altkristallin des Aarmassivs. - Geol. Rdsch. 69, 695-725.
- ALAUX-NEGREL, G., BEAUCAIRE, C., MICHARD, G., TOULHOAT, P. & OUZOUNIAN, G. 1993: Trace-metal behaviour in natural granitic waters. - Contaminant Hydrol. 13, 309-325.
- ALEXANDER, R., BRUETSCH, R., DEGUELDRE, C. & HOFMANN, B. 1990: Evaluation of long distance transport of natural colloids in a crystalline groundwater. - PSI intern. rep. TM-43-90-20. Paul Scherrer Institute, Villigen.
- AMMANN, M., HUBER, M. & MÜLLER, W.H. 1992: Geologische Grundlagen für die hydrodynamische Modellierung des Kristallins der Nordschweiz. Dokumentierung der Arbeiten der Strukturgeologiegruppe. - Nagra intern. Ber. Nagra, Wettingen.
- ARTHAUD, F. & MATTE, P. 1977: Late Paleozoic strike-slip faulting in southern Europe and northern Africa: Result of a right-lateral shear zone between the Appalachians and the Urals. - Bull. geol. Soc. Amer. 88, 1305-1320.
- BACHMANN, G.H., MÜLLER, M. & WEGGEN, K. 1987: Evolution of the Molasse Basin (Germany, Switzerland). - Tectonophysics 137, 77-92.
- BAUBRON, J.C., JEBRAK, M., JOANNES, C., LHEGU, J., TOURAY, J.C. & ZISERMAN, A. 1980: Nouvelles datations K/Ar sur les filons à quartz et fluorine du Massif Central français. - C.R. Acad. Sci. (Paris) (D) 290, 951-953.
- BECKER, A., BLÜMLING, P. & MÜLLER, W.H. 1984: Rezenten Spannungsfeld in der zentralen Nordschweiz. - Nagra tech. Ber. NTB 84-37. Nagra, Wettingen.
- 1987: Recent stress field and neotectonics in the Eastern Jura Mountains, Switzerland. - Tectonophysics 135, 277-288.
- BECKER, A. & PALADINI, S. 1990: In situ-Spannungen in Nord- und Mitteleuropa. - Schriftenr. angew. Geol. Karlsruhe 10.
- 1992: In situ-Spannungen in Nord- und Mitteleuropa. In: UNIVERSITÄT KARLSRUHE (Ed.): Spannung und Spannungsumwandlung in der Lithosphäre (p. 605-656). - Berbd. Sonderforschungsbereich 108 für die Jahre 1990-1992 (Teil B) u. Schriftenr. angew. Geol. Karlsruhe 10 (1990), 1-63.

- BEHR, H.-J., ENGEL, W., FRANKE, W., GIESE, P. & WEBER, K. 1984: The Variscan Belt in Central Europe: main structures, geodynamic implications, open questions. - *Tectonophysics* 109, 15-40.
- BEHR, H.-J. & GERLER, J. 1987: Inclusions of sedimentary brines in post-Variscan mineralizations in the Federal republic of Germany - A study by neutron activation analysis. - *Chem. Geol.* 61, 65-77.
- BEHR, H.-J., HORN, E.E., FRENTZEL-BEYME, K., LÜDERS, V. & REUTEL, C. 1987: Fluid inclusion characteristics of the Variscan and post-Variscan vein deposits in the Federal Republic of Germany. - *Chem. Geol.* 61, 273-285.
- BELANGER, D.W., CAUFFMAN, T.L., LOLCAMA, J.L., LONGSINE, D.E. & PICKENS, J.F. 1989a: Interpretation of hydraulic testing in the sediments of the Riniken borehole. Intera Technologies, Inc. Austin/Texas. - Nagra tech. Rep. NTB 87-17. Nagra, Wettingen.
- BELANGER, D.W., FREEZE, G.A., LOLCAMA, J.L. & PICKENS, J.F. 1989b: Interpretation of hydraulic testing in crystalline rock at the Leuggern borehole. Intera Technologies Inc. Austin/Texas. - Nagra tech. Rep. NTB 87-19. Nagra, Wettingen.
- BELANGER, D.W., THOMPSON, B.M. & LONGSINE, D.E. 1990: Analysis of longterm pressure recovery data from the Böttstein, Weiach, Riniken and Leuggern boreholes. - Nagra tech. Rep. NTB 87-21. Nagra, Wettingen.
- BERGER, E. 1987: Konzeptionelle Überlegungen zum Verhalten von Untertagebauten während Erdbeben. - *Nagra informiert* 9/3, 15-20.
- BIEHLER, D. in prep.: Kluffgrundwässer im kristallinen Grundgebirge des Schwarzwaldes - Ergebnisse von Untersuchungen in Stollen. - Diss. Univ. Tübingen.
- BIEHLER, D., SCHMASSMANN, H., SCHNEEMANN, K. & SILLANPÄÄ, J. 1993: Hydrochemische Synthese Nordschweiz: Dogger-, Lias-, Keuper- und Muschelkalk-Aquifere. - Nagra tech. Ber. NTB 92-08. Nagra, Wettingen.
- BLACK, J., HOLMES, D. & BRIGHTMAN, M. 1987: Crosshole investigations - hydrogeological results and interpretations. - Nagra tech. Rep. NTB 87-37. Nagra, Wettingen.
- BLASER, P. & SCHOLTIS, A. 1991: Sondierbohrung Siblingen: Dokumentation der Wasserproben-Entnahmen und Interpretation der hydrochemischen und isopenhydrologischen Analysen. - Nagra tech. Ber. NTB 91-22. Nagra, Wettingen.
- BLÜM, W. 1989: Faciesanalyse im Rotliegenden des Nordschweizer Permokarbon-Trogs (Hochrhein-Region zwischen Basel und Laufenburg). - *Eclogae geol. Helv.* 82/2, 455-489.

- BLÜMLING, P. & HUFSCHMIED, P. 1989: Fluid Logging in Tiefbohrungen. - Nagra informiert 11/3+4, 24-38.
- BONHOMME, M.G., BÜHMANN, D. & BESNUS, Y. 1983: Reliability of K/Ar dating of clays and silicifications associated with vein mineralizations in Western Europe. - Geol. Rdsch. 72, 105-117.
- BONJER, K.-P. 1992: The southern part of the upper Rhinegraben area: seismicity and seismic dislocation pattern at the eastern masterfault system. In: UNIVERSITÄT KARLSRUHE (Ed.): Spannung und Spannungsumwandlung in der Lithosphäre (p. 985-1031). - Berbd. Sonderforschungsbereich 108 für die Jahre 1990-1992 (Teil B).
- BONJER, K.-P., FABER, S. & APOPEI, I. 1989: Seismizität als Zugang zu räumlichen und zeitlichen Anomalien der Spannungen in der Lithosphäre. In: UNIVERSITÄT KARLSRUHE (Ed.): Spannung und Spannungsumwandlung in der Lithosphäre (p. 65-137). - Berbd. Sonderforschungsbereich 108 für die Jahre 1987-1989 (Teil A).
- BRADBURY, M.H. 1989: Laboratory investigations in support of the migration experiments at the Grimsel Test Site. - Nagra tech. Rep. NTB 88-23. Nagra, Wettingen.
- BRANTLEY, S.L. 1992: Kinetics of dissolution and precipitation - Experimental and field results. In: KHARAKA, Y.K. & MAEST, A.S. (Ed.): Water-Rock Interaction WRI7 (p. 3-6): Proc. 7th int. Symp., Park City, Utah, 13-18 July 1992, A.A. Balkema, Rotterdam.
- BRISBIN, W.C. 1986: Mechanics of pegmatite intrusion. - Amer. Mineralogist 71, 644-651.
- BROCKAMP, O., CLAUER, N. & ZUTHER, M. (1994): K-Ar dating of episodic Mesozoic fluid migrations along the fault system of Gernsbach between the Moldanubian and Saxothuringian (Northern Black Forest, Germany). - Geol. Rdsch 83, 180-185.
- BROOKS, C. 1968: Relationship between feldspar alteration and the precise post-crystallization movement of rubidium and strontium isotopes in a granite. - J. geophys. Res. 73, 4751-4757.
- BROWN, S.R. 1987: Fluid flow through rock joints: The effect of surface roughness. - J. geophys. Res. 92/B2, 1337-1347.
- BRUETSCH, R., DEGUELDRE, C. & ULRICH, H.J. 1991: Kolloide in Thermalwasser vom Bad Zurzach. - PSI intern. rep. TM-43-91-19. Paul Scherrer Institute, Villigen.

- BUBNOFF, S. VON 1928: Der Werdegang einer Eruptivmasse. - Fortschr. Geol. Paläont. 7. 1-239.
- BÜCHI, E., BULETTI, M. & NIGGLI, E. 1984: Neue Aufschlüsse im schweizerischen Anteil des Schwarzwälder Grundgebirges. - Schweiz. mineral. petrogr. Mitt. 64, 49-65.
- BÜCHI, U.P., LEMCKE, K., WIENER, G. & ZIMDARS, J. 1965: Geologische Ergebnisse der Erdölexploration auf das Mesozoikum im Untergrund des schweizerischen Molassebeckens. - Bull. Ver. schweiz. Petroleum-Geol. u. -Ing. 32/82, 7-38.
- BUFFLE, J. 1988: Complexation reactions in aquatic systems, an analytical approach. E. Horwood Series in Analytical Chemistry. R. Chalmers and M. Masson, Chichester, UK.
- BUSER, M. & WILDI, W. 1981: Wege aus der Entsorgungsfalle. - Rep. Schweiz. Energiestift. 12.
- BUTLER, G.A., CAUFFMAN, T.L., LOLCAMA, J.L., LONGSINE, D.E. & McNEISH, J.A. 1989: Interpretation of hydraulic testing at the Weiach borehole. Intera Technologies Inc. Austin/Texas. - Nagra tech. Rep. NTB 87-20. Nagra, Wettingen.
- BUXTORF, A. 1916: Prognose und Befund beim Hauensteinbasis- und Grenchenbergtunnel und die Bedeutung der letzteren für die Geologie des Juragebirges. - Verh. natf. Ges. Basel 27, 184-254.
- CHALMERS, B.W. & CORREA, N.R. 1993: Hydraulic information at the sub-regional scale of the Grimsel Test Site. - Nagra intern. Rep. Nagra, Wettingen.
- CLAUSS, B. 1987: Numerische Modellierung der tektonischen Spannungen in der Nordschweiz. - Diplomarb. Univ. Karlsruhe.
- COSMA, C. & STANESCU, D. 1993: Exploration of crystalline rocks - Tomographic modelling. - Nagra intern. Rep. Nagra, Wettingen.
- DANECK, T. in prep.: Platznahme und mechanisches Verhalten von Ganggesteinen im Grundgebirge des Südschwarzwalds. - Diss. ETH Zürich.
- DEGUELDRE, C. 1994: Colloid properties in granitic groundwater systems. - Nagra tech. Rep. NTB 92-05. Nagra, Wettingen.
- DEGUELDRE, C., KEIL, R., MOHOS, M., VAN EYGEN, B. & WERNLI, B. 1990: Study of the Leuggern colloids. - PSI intern. Rep. TM-43-90-69. Paul Scherrer Institute, Villigen.

- DEGUELDRE, C., LONGWORTH, G., MOULIN, V., VILKS, P., ROSS, C., BIDOGLIO, G., CREMERS, A., KIM, J., PIERI, J., RAMSAY, J., SALBU, B. & VUORINEN, U. 1989: Grimsel Colloid Exercise: An international intercomparison exercise on the sampling and characterisation of groundwater colloids. - PSI Rep. No 39. Paul Scherrer Institute, Villigen, and Nagra tech. Rep. NTB 90-01. Nagra, Wettingen.
- DEGUELDRE, C. & WERNLI, B. 1987: Characterization of the natural inorganic colloids from a reference granitic ground water. - *Analyt. chim. Acta* 195, 211-223.
- DEICHMANN, N. 1987: Seismizität der Nordschweiz, 1983-1986. - Nagra tech. Ber. NTB 87-05. Nagra, Wettingen.
- 1990: Seismizität der Nordschweiz 1987-1989 und Auswertung der Erdbebenserien von Günsberg, Läufelfingen und Zeglingen. - Nagra tech. Ber. NTB 90-46. Nagra, Wettingen.
- DEICHMANN, N. & RENGGLI, K. 1984: Mikrobewen-Untersuchung Nordschweiz, Teil 2: Seismizität, Jan. 1983-Sept. 1984. - Nagra tech. Ber. NTB 84-12. Nagra, Wettingen.
- DEWEY, J.F. 1988: Extensional collapse of orogens. - *Tectonics* 7, 1123-1139.
- DIEBOLD, P. 1986: Erdwissenschaftliche Untersuchungen der Nagra in der Nordschweiz; Strömungsverhältnisse und Beschaffenheit der Tiefengrundwässer. - *Mitt. aarg. natf. Ges.* 31, 11-52.
- 1990: Die tektonische Entwicklung der Nordschweiz. - *Nagra informiert* 12/2, 47-55.
- DIEBOLD, P. & MÜLLER, W.H. 1985: Szenarien der geologischen Langzeitsicherheit: Risikoanalyse für ein Endlager für hochaktive Abfälle in der Nordschweiz. - Nagra tech. Ber. NTB 84-26. Nagra, Wettingen.
- DIEBOLD, P. & NAEF, H. 1990: Der Nordschweizer Permokarbon-Trog. - *Nagra informiert* 12/2, 29-36.
- DIEBOLD, P., NAEF, H. & AMMANN, M. 1991: Zur Tektonik der zentralen Nordschweiz. Interpretation aufgrund regionaler Seismik, Oberflächengeologie und Tiefbohrungen. - Nagra tech. Ber. NTB 90-04. Nagra, Wettingen.
- DÖBL, F. 1970: Die geothermischen Verhältnisse des Öfeldes Landau/Pfalz. In: ILLIES, J.H. & MÜLLER, S. (Ed.): *Graben problems* (p. 110-116) - *Int. Upper Mantle Project, sci. Rep.* 27, Stuttgart.

- ECHTLER, H.P. & CHAUVET, A. 1992: Carboniferous convergence and subsequent crustal extension in the southern Schwarzwald (SW Germany). In: UNIVERSITÄT KARLSRUHE (Ed.): Spannung und Spannungsumwandlung in der Lithosphäre (p. 1285-1304). - Berbd. Sonderforschungsbereich 108 für die Jahre 1990-1992 (Teil B).
- EISBACHER, G. & KROHE, A. 1985: The tectonic setting of the variscan Schwarzwald - A brief synopsis. In: INTER-UNION COMMISSION ON THE LITHOSPHERE (Ed.): Excursion-Guide Schwarzwald (p. 32-38). - 2nd int. Symp. Obs. cont. Crust through Drilling, Seehe.
- EISBACHER, G.H., LÜSCHEN, E. & WICKERT, F. 1989: Crustal-scale thrusting and extension in the Hercynian Schwarzwald and Vosges, central Europe. - *Tectonics* 8, 1-21.
- EMMERMANN, R. 1970: Geochemische Untersuchungen am Granit von St. Blasien (Südschwarzwald). *Jh. geol. Landesamt Bad.n-Württemb.* 12, 227-248.
- 1977: A Petrogenetic Model for the Origin and Evolution of the Hercynian Granite Series of the Schwarzwald. - *N. Jb. Mineral. [Abh.]* 128/3, 219-253.
- ERB, L. 1948: Die Geologie des Feldbergs. In: *Der Feldberg im Schwarzwald.* - L. Bielefelds Verlag K.G., Freiburg i. Br.
- FAURE, G. 1986: *Principles of isotope geology.* - John Wiley & Sons, New York.
- FISCHER, G., SCHNEGG, P.-A. & LE QUANG, B.V. 1984: Sondages Magnétotelluriques Pilotes 81; Programme d'Etudes Géophysiques du Nord de la Suisse. - *Nagra Rapp. tech. NTB 84-13.* Nagra, Wettingen.
- FISCHER, H. 1965: Geologie des Gebietes zwischen Blauen und Pfirter Jura. - *Beitr. geol. Karte Schweiz [N.F.]* 122.
- FLUCK, P. 1980: Métamorphisme et magmatisme dans les Vosges moyennes d'Alsace. Contribution à l'histoire de la chaîne varisque. - *Sci. géol. (Strasbourg) [Mém.]* 62, 1-248.
- FRAPE, S.K. & FRITZ, P. 1987: Geochemical trends for groundwaters from the Canadian Shield. In: FRITZ, P. & FRAOEM, S.K. (Ed.): *Saline Water and Gases in Crystalline Rocks* (p. 19-38). - *Spec. Pap. geol. Assoc. Canada* 33.
- FREEZE, R.A. & CHERRY, J.A. 1979: *Groundwater.* - Prentice-Hall, Englewood Cliffs, N.J. USA.
- FREI, R. 1912: *Monographie des Schweizerischen Deckenschotters.* - *Beitr. geol. Karte Schweiz [N.F.]* 37.

- FRICK, U., ALEXANDER, W.R., BAEYENS, B., BOSSART, P., BRADBURY, M.H., BÜHLER, C., EIKENBERG, J., FIERZ, T., HEER, W., HOEHN, E., McKINLEY, I.G. & SMITH, P.A. 1992: Grimsel Test Site - The radionuclide migration experiment - Overview of investigations 1985-1990. - Nagra tech. Rep. NTB 91-04. Nagra, Wettingen.
- FRICK, U., BÄRTSCHI, P. & HOEHN, E. 1988: Migration investigations. - Spec. Ed. Nagra Bull. 1988, 23-34.
- FRITZ, P., FRAPE, S.K., DRIMMIE, R.J., APPLEYARD, E.C., & HATTORI, K. 1994: Sulfate in brines in the crystalline rocks of the Canadian Shield. - *Geochim. cosmochim. Acta* 58, 57-65.
- FROMM, G., DRIESSEN, L. & LEHNEN, I. 1985: Geophysikalisches Untersuchungsprogramm Nordschweiz: Refraktionsseismische Messungen 84. - Nagra tech. Ber. NTB 84-43. Nagra, Wettingen.
- GALE, J.E., HERBERT, A.W., LANYON, G.W. & McLEOD, R. 1991: Modelling for the Stripa Site Characterisation and Validation Drift inflow: prediction of flow through fractured rock. - Stripa Proj. tech. Rep. 91-35. Swedish Nuclear Fuel and Waste Management Co., Stockholm.
- GAUTSCHI, A., MEYER, CH., PETERS, TJ., MEYER, J. & HOFMANN, B. 1986: Die geologische Charakterisierung der Wasserfließsysteme im kristallinen Grundgebirge der Nordschweiz; resp. Überlegungen zur Ausdehnung kristalliner Wirtgesteine für die Endlagerung radioaktiver Abfälle in der Nordschweiz. - Nagra informiert 1986/2, 15-21, und Nagra tech. Ber. NTB 86-26. Nagra, Wettingen.
- GAUTSCHI, A. & SCHOLTIS, A. 1989: Probenahmetechnik und Analyse von Grundwässern aus Tiefbohrungen. - Nagra informiert 11/3+4, 50-66.
- GEHLEN, K. VON, KLEINSCHMIDT, G., STENGER, R., WILHELM, H. & WIMMENAUER, W. 1986: Kontinentales Tiefbohrprogramm der Bundesrepublik Deutschland KTB. Ergebnisse der Vorerkundungsarbeiten Lokation Schwarzwald. - 2. KTB-Kolloq. Seeheim/Odenwald 1986.
- GEHLEN, K. VON 1989: Ore and mineral deposits of the Schwarzwald. In: EMMERMANN, R. & WOHLBERG, J. (Ed.): The German continental deep drilling program (KTB). - Springer, Berlin/Heidelberg.
- GEOLOGISCHES BÜRO DR. H. JÄCKLI AG, SCHMASSMANN, H. & MOTOR COLUMBUS INGENIEURUNTERNEHMUNG AG 1986: Überwachung bedeutender Mineralquellen und Thermen der Nordschweiz und angrenzender Gebiete: Resultate der Messstationen mit permanenter Aufzeichnung. - Nagra intern. Ber. Nagra, Wettingen.
- GEOLOGISCHES BÜRO KELLERHALS & HÄFELI 1989: Siblingen: Bohrstellengeologie. - Nagra intern. Ber. Nagra Wettingen.

- GEOLOGISCHES INSTITUT UNIVERSITÄT BERN 1989: Hydrochemische Analysen (11 Ordner); Isotopen- und Edelgasuntersuchungen (3 Ordner). - Nagra intern. Ber. Nagra, Wettingen.
- GERWECK, H., HEGELE, A., ROCKENBAUCH, K. & WIRTH, G. 1984: Geologie des Südschwarzwaldes. - Arb. geol.-paläont. Inst. Univ. Stuttgart [N.F.] 78, 1-9.
- GIGGENBACH, W. F. 1988: Geothermal solute equilibria. Derivation of Na-K-Mg-Ca geoindicators. - *Geochim. cosmochim. Acta* 52, 2749-2765.
- GONZALEZ, R. 1990: Geometrie und Kinematik der Zeiningen Bruch-Zone und eine Diskussion möglicher spätpaläozoischer Strukturen. - *Eclogae geol. Helv.* 83/3, 513-523.
- GORHAN, H.L. & GRIESSER, J.C. 1988: Geothermische Prospektion im Raume Schinznach Bad - Baden. - *Beitr. Geol. Schweiz, geotech. Ser.* 76.
- GRAUER, R. 1990: Zur Chemie von Kolloiden: Verfügbare Sorptionsmodelle und zur Frage der Kolloidhaftung. - *Nagra tech. Ber. NTB 90-37.* Nagra, Wettingen.
- GRIESSER, J.-C. 1989: Numerical thermohydraulic modelling of deep groundwater circulation in crystalline basement: an example of calibration. - *Geophys. Monogr.* 47, 65-74.
- GRINDROD, J.P., HERBERT, A., ROBERTS, D. & ROBINSON, P. 1991: NAPSAC Technical document. - *Stripa Proj. tech. Rep.* 91-31. Swedish Nuclear Fuel and Waste Management Co., Stockholm.
- GRISAK, G.E., PICKENS, J.F., BELANGER, D.W. & AVIS, J.D. 1985: Hydrogeologic testing of crystalline rocks during the Nagra deep drilling program. - *Nagra tech. Rep. NTB 85-08.* Nagra, Wettingen.
- GROSCHOPF, R., KESSLER, G., LEIBER, J., MAUS, H., OHMERT, W., SCHREINER, A. & WIMMENAUER, W. 1981: Erläuterungen zur Geologischen Karte von Freiburg i. Br. und Umgebung 1:50'000 (2. Aufl.). - *Geol. Landesamt Bad.-Württemb., Stuttgart.*
- GROSCHOPF, R. & SAWATZKI, G. 1989: Quartär und Grundgebirge im zentralen Hotzenwald (Exkursion E am 30. März 1989). - *Jber. Mitt. oberrh. geol. Ver.* [N.F.] 71, 85-109.
- GUBLER, E., SCHNEIDER, D. & KELLERHALS, P. 1984: Bestimmungen von rezenten Bewegungen der Erdkruste mit geodätischen Methoden. - *Nagra tech. Ber. NTB 84-17.* Nagra, Wettingen.
- GÜNTENSPERGER, M. (ED.) 1987: Die Erdbebengefährdung der Schweiz. - *Nagra informiert* 9/3, 4-14.

- GÜRLER, B., HAUBER, L. & SCHWANDER, M. 1987: Die Geologie der Umgebung von Basel mit Hinweisen über die Nutzungsmöglichkeiten von Erdwärme. - Beitr. geol. Karte Schweiz [N.F.] 160.
- HALDIMANN, P., NAEF, H. & SCHMASSMANN, H. 1984: Fluviale Erosions- und Akkumulationsformen als Indizien jungpleistozäner und holozäner Bewegungen in der Nordschweiz und angrenzenden Gebieten. - Nagra tech. Ber. NTB 84-16. Nagra, Wettingen.
- HALE, F.V. & TSANG, C.F. 1988: A code to compute borehole fluid conductivity profiles with multiple feed points. - Nagra tech. Rep. NTB 88-21. Nagra, Wettingen.
- HAMMERSCHMIDT, K. & WAGNER, M. 1983: K/Ar-Bestimmungen an Biotiten aus den kristallinen Gesteinen der Forschungsbohrung Urach 3. - N. Jb. Mineral. [Mh.] 1983/1, 35-48.
- HANTKE, R. 1978: Eiszeitalter 1: Die jüngste Erdgeschichte der Schweiz und ihrer Nachbargebiete. - Ott Verlag, Thun.
- 1984: Der Rhein-Durchbruch zwischen Rüdlingen und der Töss-Mündung (Kt. Schaffhausen und Zürich). - Ber. Scr. geogr. Inst. ETH Zürich 17.
- HAQ, B.U., HARDENBOL, J. & VAIL, P.R. 1987: Chronology of fluctuating sea levels since the Triassic. - Science 235, 1156-1167.
- HAUBER, L. 1971: Zur Geologie des Salzfeldes Schweizerhalle-Zinggibrunn (Kt. Baselland). - Eclogae geol. Helv. 64/1, 163-183.
- 1991: Ergebnisse der Geothermiebohrungen Riehen 1 und 2 sowie Reinach 1 im Südosten des Rheingrabens. - Geol. Jb., 167-184.
- 1993: Der Mittlere Muschelkalk am Hochrhein. - N. Jb. Geol. Paläont. [Abh.] 169, 1-3, 147-170.
- HAUG, A. 1985: Feldmethoden zur Grundwasserentnahme aus Tiefbohrungen und zur hydrochemischen Überwachung der Bohrspülung. - Nagra tech. Ber. NTB 85-07. Nagra, Wettingen.
- HEATH, M.J. 1985: Solute migration experiments in fractured granite, South West England. In: Designs and instrumentation of in situ experiments in underground laboratories for radioactive waste disposal (p. 191-200). - Proc. joint CEC-NEA workshop. Balkema, Rotterdam.
- HEGELE, A. 1984: Kleintektonik im Schweizer Jura zwischen Aare und Birs und ihre Beziehung zu Mittel- und Grosstektonik. - Arb. geol.-paläont. Inst. Univ. Stuttgart [N.F.] 78, 193-253.

- HEITZMANN, P. 1985: Kakirite, Kataklasite, Mylonite - Zur Nomenklatur der Metamorphite mit Verformungsgefügen. - *Eclogae geol. Helv.* 78/2, 273-286.
- HERBERT, A.W. & LANYON, G.W. 1992a: Evaluation of the effect of discrete fracture flow parameters in crystalline rock. - Nagra intern. Rep. Nagra, Wettingen.
- 1992b: Investigation of fracture flow path-ways through crystalline rock. - Nagra intern. Rep. Nagra, Wettingen.
- HERZOG, P. 1956: Die Tektonik des Tafeljura und der Rheintalflexur südöstlich von Basel. - *Eclogae geol. Helv.* 49/2, 317-362.
- HIMMELSBACH, T. 1993: Untersuchungen zum Wasser- und Stofftransportverhalten von Störungszonen im Grundgebirge (Albtalgranit, Südschwarzwald). - *Schr. angew. Geol. Karlsruhe* 23, 1-238, Karlsruhe.
- HINZE, W., JÄGGI, K. & SCHENKER, F. 1989: Sondierbohrungen Böttstein, Weiach, Riniken, Schafisheim, Kaisten, Leuggern - Gasmessungen. - Nagra tech. Ber. NTB 86-11. Nagra, Wettingen.
- HOENES, D. 1937: Die Gesteine und Erzlagerstätten im Schwarzwälder Grundgebirge zwischen Schauinsland, Münstertal und Belchen. - *N. Jb. Mineral. [Abh. A]* 72, 265-346.
- HOFMANN, A. & KÖHLER, H. 1973: Whole rock Rb-Sr ages of anatectic gneisses from the Schwarzwald, SW Germany. - *N. Jb. Mineral. [Abh.]* 119, 163-187.
- HOFMANN, B. 1989: Genese, Alteration und rezentes Fliess-System der Uranlagerstätte Krunkelbach (Menzenschwand, Südschwarzwald). - Nagra tech. Ber. NTB 88-30. Nagra, Wettingen.
- HOFMANN, B. & EIKENBERG, J. 1991: The Krunkelbach Uranium deposit, Schwarzwald, Germany: Correlation of radiometric ages (U-Pb, U-Xe-Kr, K-Ar,  $^{230}\text{Th}$ - $^{234}\text{U}$ ) with mineralogical stages and fluid inclusions. - *Econ. Geol.* 86, 1031-1049.
- HOFMANN, F. 1982: Die geologische Vorgeschichte der Bodenseelandschaft. *Schriftenr. Ver. f. Gesch. d. Bodensees u. Umgeb.* 99/100, Friedrichshafen 1981/2, 35-67.
- HOLDER, M.T. & LEVERIDGE, B.E. 1986: Correlation of the Rhenohercynian Variscides. - *J. geol. Soc. (London)* 143, 141-147.
- HRADETZKY, H., LIPPOLT, H.J. & HAUTMANN, S. 1989:  $^{40}\text{Ar}/^{39}\text{Ar}$ -Untersuchungen an Amphiboliten und gabbroiden Metabasiten des Schwarzwaldes. - *Ber. dtsh. mineral. Ges.* 1, 82.

- HSK 1987: Technischer Bericht zum Gutachten über das Projekt Gewähr 1985. - HSK Ber. 23/29 (KSA 23/66), Hauptabt. f. d. Sicherheit d. Kernanlagen, Würenlingen, Switzerland.
- HUBER-ALEFFI, M. & HUBER-ALEFFI, A. 1984: Das Kristallin des Südschwarzwaldes. - Nagra tech. Ber. NTB 84-30. Nagra, Wettingen.
- HUBER, M. & HUBER, A. 1986: Der Aufbau des kristallinen Grundgebirges - Kristallinkörper und Schollen. - Nagra informiert 8/2, 8-12.
- HUBER, M. & HUBER-ALEFFI, A. 1990: Zur Tektonik des Südschwarzwaldes. - Nagra tech. Ber. NTB 90-03. Nagra, Wettingen.
- HUCK, K. 1984: Die Beziehungen zwischen Tektonik und Paragenese unter Berücksichtigung geochemischer Kriterien in der Fluss- und Schwespatlagerstätte "Clara" bei Oberwolfach/Schwarzwald. - Unpubl. Diss. Univ. Heidelberg.
- HUFSCHMIED, P. & FRIEG, B. 1989: Beobachtung der hydraulischen Druckhöhen in den Nagra-Tiefbohrungen der Nordschweiz. - Nagra informiert 11/3+4, 39-49.
- HURFORD, A. 1993: Fission Track analysis of Apatite from the Nagra boreholes of Böttstein, Weiach, Schafisheim and Riniken, Northern Switzerland. - Nagra intern. Rep. Nagra, Wettingen.
- ILLIES, J.H. 1962: Oberrheinisches Grundgebirge und Rheingraben. - Geol. Rdsch. 52, 317-332.
- 1983: Der Hohenzollerngraben und Intraplatten-Seismizität infolge Vergitterung lamellärer Scherung mit einer Riftstruktur. - Oberrhein. geol. Abh. 31, 47-78.
- ILLIES, J.H. & GREINER, G. 1976: Regionales Stress-Feld und Neotektonik in Mitteleuropa. - Oberrh. geol. Abh. 25, 1-40.
- ISLER, A. 1984a: Zur effektiven Bedeutung der Satellitenbild-Lineamente im Raume Baden - Frick - Laufenburg - Zurzach. Zusammenfassender Bericht zur Studie "Lineamentanalyse Nordschweiz": Blätter 1050 Zurzach, 1049 Laufenburg, 1069 Frick, 1070 Baden. - Unpubl. Ber. Geolbüro Dres. P. Kellerhals & Ch. Haefeli z. H. der Nagra.
- 1984b: Literaturzusammenstellung zur Neotektonik. - Nagra tech. Ber. NTB 84-29. Nagra, Wettingen.
- ISLER, A., PASQUIER, F. & HUBER, M. 1984: Geologische Karte der zentralen Nordschweiz mit angrenzenden Gebieten von Baden-Württemberg. Geologische Spezialkarte Nr. 121, 1:100'000. - Nagra u. Schweiz. geol. Komm.
- JAQUET, O. 1991: Assessment of hydrogeological characteristics of the LEU, BOE and KAI boreholes. - Nagra intern. Rep. Nagra, Wettingen.

- JOHNSON, J.W., OELKERS, E.H. & HELGESON, H.C. 1992: SUPCRT92: A software package for calculating the standard molal thermodynamic properties of minerals, gases, aqueous species, and reactions from 1 to 5,000 bars and 0° to 1,000°C. - *Computers and Geosci.*, 899-947.
- JOHNS, R.A. & ROBERTS, P.V. 1991: A solute transport model for channelized flow in a fracture. - *Water Resour. Res.* 27, 1797-1808.
- JORDAN, P. & NÜESCH, R. 1989: Deformation Structures in the Muschelkalk Anhydrites of the Schafisheim Well (Jura Overthrust, Northern Switzerland). - *Eclogae geol. Helv.* 82/2, 429-454.
- KÄLIN, B. 1990: Gesteinsdichte und Kompaktion im schweizerischen Molassebecken, abgeleitet aus Bohrlochmessungen. - Unpubl. Diplomarb. ETH Zürich.
- KANZ, W. 1987: Grundwasserfließwege und Hydrogeochemie in tiefen Graniten und Gneisen. - *Geol. Rdsch.* 76/1, 265-284.
- KELLEY, V.A., LAVANCHY, J.M. & LÖW, S. 1991: Transmissivities and heads derived from detailed analysis of Siblingen 1989 fluid logging data. - *Nagra tech. Rep.* NTB 90-09. Nagra, Wettingen.
- KEMPTER, E.H.K. 1987: Fossile Maturität, Paläothermogradienten und Schichtlücken in der Bohrung Weiach im Lichte von Modellberechnungen der thermischen Maturität. - *Eclogae geol. Helv.* 80/2, 543-552.
- KIKUCHI, K., MITO, Y. & OKUNO, T. 1989: Experimental study for groundwater flow in an actual jointed rock mass. In: MAURY, V. & FOURMAINTRAUX, D. (Ed.): *Rock at Great Depth* (Vol. 1, p. 457-464). - *Proc. ISRM-SPE int. Symp. Pau 1989.* Balkema, Rotterdam/Brookfield.
- KIMMEIER, F., PERROCHET, P., ANDREWS, R. & KIRALY, L. 1985: Simulation par Modèle Mathématique des Ecoulements Souterrains entre les Alpes et la Forêt Noire - Partie A: Modèle Régional - Partie B: Modèle Local (Nord de la Suisse). - *Nagra Rapp. tech.* NTB 84-50. Nagra, Wettingen.
- KIRALY, L. 1985: FEM 301 - A three dimensional model for groundwater flow simulation. - *Nagra tech. Rep.* NTB 84-49. Nagra, Wettingen.
- KLEIN, H. & WIMMENAUER, W. 1984: Eclogites and their retrograde transformation in the Schwarzwald (Fed. Rep. Germany). - *N. Jb. Mineral. [Mh.]* 1984/1, 25-38.
- KLEINE BORNHORST, A., VON BANCHET, S. & BRÄUER, V. 1984: Aufstellung und ingenieurgeologische Beschreibung von Granitvorkommen in der Bundesrepublik Deutschland. 2. Teil: Die Schwarzwälder Granitmassive. - *Bundesanst. Geowiss. Rohst. (BGR)*, Hannover.

- KLEMENZ, W. 1991: Transmissivität der Zuflussstellen und Durchlässigkeit der Matrix im Kristallin der Tiefbohrungen Böttstein, Kaisten und Leuggern. - Nagra intern. Ber. Nagra, Wettingen.
- KLEMENZ, W. & GUYONNET, D. 1992: Transmissivität der Zuflussstellen und Durchlässigkeit der Matrix im Kristallin der Tiefbohrung Siblingen. - Nagra intern. Ber. Nagra, Wettingen.
- KLINGELE, E. & SCHWENDENER H. 1984: Geophysikalisches Untersuchungsprogramm Nordschweiz - Gravimetrische Messungen 81/82. - Nagra tech. Ber. NTB 84-22. Nagra, Wettingen.
- KLINGELE, E., SCHWENDENER, H. & HEIM, CH. 1984: Geophysikalisches Untersuchungsprogramm Nordschweiz - Aeromagnetische und bodenmechanische Messungen 81. - Nagra tech. Ber. NTB 84-14. Nagra, Wettingen.
- KOSSMAT, F. 1927: Gliederung des variskischen Gebirgsbaues. - Abh. sächs. geol. Landesamt 1.
- KRETSCHMAR, U. & SCOTT, S.D. 1984: Phase relations involving arsenopyrite in the system Fe-As-S and their application. - *Canad. Mineralogist* 14, 364-386.
- KROHE, A. & EISBACHER, G.H. 1988: Oblique crustal detachment in the Variscan Schwarzwald, southwestern Germany. - *Geol. Rdsch.* 77, 25-43.
- KTB 1986: Kontinentales Tiefbohrprogramm der Bundesrepublik Deutschland - Ergebnisse der Vorerkundungsarbeiten Lokation Schwarzwald. - 2. KTB-Kolloq. Seeheim/Odenwald, Sept. 1986.
- KÜPFER, TH., HUFSCHMIED, P. & PASQUIER, F. 1989: Hydraulische Tests in Tiefbohrungen der Nagra. - *Nagra informiert* 11/3+4, 7-23.
- LANYON, G.W. 1992a: NAPSAC modelling of crystalline fracture systems. - Nagra intern. Rep. Nagra, Wettingen.
- 1992b: Geometric simulations of fracture networks - Calculations based on data from the Siblingen borehole. - Nagra intern. Rep. Nagra, Wettingen.
- 1993: NAPSAC Modelling of the fault geometry of crystalline rocks in Northern Switzerland. - Nagra intern. Rep. Nagra, Wettingen.
- LANYON, G.W. & HOCH, A.R. 1993: A comparison of dynamic and geometric calculations of fluxes around a repository tunnel in crystalline rock. - Nagra intern. Rep. Nagra, Wettingen.
- LAUBSCHER, H.P. 1965: Ein kinematisches Modell der Jurafaltung. - *Eclogae geol. Helv.* 58/1, 231-318.

- 1977: Fold development in the Jura. - *Tectonophysics* 37, 337-362.
  - 1982: Die Südostecke des Rheingrabens - ein kinematisches und dynamisches Problem. - *Eclogae geol. Helv.* 75/1, 101-116.
  - 1985: The eastern Jura: Relations between thin-skinned and basement tectonics, local and regional. - Nagra tech. Rep. NTB 85-53. Nagra, Wettingen.
  - 1986: Expertenbericht zum Projekt Gewähr: Struktur des Grundgebirges und des Paläozoikums der Nordschweiz. - Unpubl. Ber. z.H. Bundesamt f. Energiewirtsch., Hauptabt. f.d. Sicherheit d. Kernanlagen (HSK), Würenlingen.
  - 1987: Die tektonische Entwicklung der Nordschweiz. - *Eclogae geol. Helv.* 80/2, 287-303.
  - 1992: Jura kinematics and the Molasse basin. - *Eclogae geol. Helv.* 85/3, 653-675.
- LEECH, R.E.J., KENNEDY, K.G. & GEVAERT, D. 1984: Sondierbohrung Böttstein, Hydrogeologic Testing of Crystalline Rocks. - Nagra tech. Rep. NTB 85-09. Nagra, Wettingen.
- LEUTWEIN, F. & SONNET, J. 1974: Geochronologische Untersuchungen im Südschwarzwald. - *N. Jb. Mineral. [Abh.]* 121, 252-271.
- LINDBERG, R.D. & RUNNELS, D.D. 1984: Groundwater redox reactions: An analysis of equilibrium state applied to Eh measurements and geochemical modeling. - *Science* 225, 925-927.
- LINDER, N. & VOBORNY, O. 1991: Statistische Auswertung der Matrixdurchlässigkeiten und der Transmissivitäten der Zuflussstellen im Kristallin der Tiefbohrungen BOE, KAI und LEU. - Nagra intern. Ber. Nagra, Wettingen.
- LINIGER, H. 1966: Das Plio-Altpleistozäne Flussnetz der Nordschweiz. - *Regio basil.* 7, 158-177.
- LIPPOLT, H.J., BARANYI, I. & RACZEK, I. 1975: Isotopische Untersuchungen an Lamprophyren des Südschwarzwaldes. - *Fortschr. Mineral.* 53, Beih. 1, 48.
- LIPPOLT, H.J., SCHLEICHER, H. & RACZEK, I. 1983: Rb-Sr systematics of Permian volcanites in the Schwarzwald (SW-Germany). Part I: Space of time between plutonism and late orogenic volcanism. - *Contr. Mineral. Petrol.* 84, 272-280.
- LORENZ, V. & NICHOLLS, I.A. 1976: The Permocarboneous Basin and Range Province of Europe. An Application of Plate Tectonics. In: FALKE, H. (Ed.): *The Continental Permian in Central, West, and South Europe* (p. 313-342). - D. Reidel publ. Co., Dordrecht/Boston.

- 1984: Plate and intraplate processes of Hercynian Europe during the late Paleozoic. - *Tectonophysics* 107, 25-56.
- LÜSCHEN, E., WENZEL, F., SANDMEIER, K.-J., MENGES, D., RÜHL, TH. & STILLER, M. 1987: Near-vertical and wide-angle seismic surveys in the Black Forest, SW Germany, - *J. Geophys.* 62, 1-30.
- LUTZ, M. 1964: Stratigraphische und tektonische Untersuchungen am südwestlichen Schwarzwaldrand zwischen Wiesental und Hochrhein. - *Oberrh. geol. Abh.* 13/1-2, 75-122.
- MAASS, R. 1983: Die tektonische Entwicklung im Schwarzwald. - *Kontinent. Tiefbohrprogramm d. BRD, Vorstud. Schwarzwald I*, 109-129.
- MÄLZER, H. 1988: Regional and local kinematics in SW-Germany by geodetic methods - geophysical and geological interpretation. - *J. Geodyn.* 9, 141-151.
- MÄLZER, H., RÖSCH, H., MISSELWITZ, I., EBERT, M. & MOOSMANN, D. 1988: Höhenänderungen in der Nordschweiz und im Südschwarzwald bis zum Bodensee. - *Nagra tech. Ber. NTB 88-05*. Nagra, Wettingen.
- MANDL, G. 1988: *Mechanics of tectonic faulting*. - Elsevier Science Publishers, Amsterdam.
- MATTER, A. 1987: Faciesanalyse und Ablagerungsmilieus des Permokarbons im Nordschweizer Trog. - *Eclogae geol. Helv.* 80/2, 345-368.
- MATTER, A., PETERS, T.J., BLÄSI, H.-R., MEYER, J., ISCHI, H. & MEYER, CH. 1988a: Sondierbohrung Weiach - Geologie; Text- und Beilagenband. - *Nagra tech. Ber. NTB 86-01*. Nagra, Wettingen.
- MATTER, A., PETERS, T.J., BLÄSI, H.-R., SCHENKER, F. & WEISS, H.-P. 1988b: Sondierbohrung Schafisheim - Geologie; Text- und Beilagenband. - *Nagra tech. Ber. NTB 86-03*. Nagra, Wettingen.
- MATTER, A., PETERS, T.J., ISENSCHMID, CH., BLÄSI, H.-R. & ZIEGLER, H.-J. 1987: Sondierbohrung Riniken - Geologie; Text- und Beilagenband. - *Nagra tech. Ber. NTB 86-02*. Nagra, Wettingen.
- MAUS, H. 1967: Ignimbrite des Schwarzwaldes. - *N. Jb. Geol. Paläont. [Mh.]* 1967, 461-489.
- MAYER-ROSA, D., BENZ, H., KRADOLFER, U. & RENGGLI, K. 1983: Inventar der Erdbeben 1910-1982 und Karten der Magnitudenschwellenwerte 1928-1982. - *Nagra tech. Ber. NTB 83-08*. Nagra, Wettingen.

- MAYER-ROSA, D., DIETIKER, M., DEICHMANN, N., RENGGLI, K., BRÄNDLI, J., STUDER, J. & RUTISHAUSER, G. 1984: Mikrobaben-Untersuchung Nordschweiz. Teil 1: Technische Unterlagen, Stationsnetz. - Nagra tech. Ber. NTB 84-11. Nagra, Wettingen.
- MAZUREK, M. 1989: Sondierbohrung Siblingen - Petrographie des Kristallins. - Nagra intern. Ber. Nagra, Wettingen.
- 1990a: Siblingen: Strukturen und Wasser-Fliesssysteme im Granit von Siblingen. - Nagra intern. Ber. Nagra, Wettingen.
- 1990b: Wasser-Fliesssysteme im Kristallin der Nordschweiz: Systematik diskreter Zuflusspunkte. - Nagra intern. Ber. Nagra, Wettingen.
- 1990c: Geochemical study of oxidation effects in Opalinus Clay from the Siblingen clay pit. - Nagra intern. Rep. Nagra, Wettingen.
- 1991: Geochemical interaction between groundwater and aplitic/pegmatitic dykes and leucocratic gneisses: Geological input parameters for safety performance analysis. - Nagra intern. Rep. Nagra, Wettingen.
- 1992: Phase equilibria and oxygen isotopes in the evolution of metapelitic migmatites: A case study from the Pre-Alpine basement of Northern Switzerland. - *Contr. Mineral. Petrol.* 109, 494-510.
- 1994: Geology of the crystalline basement of Northern Switzerland and derivation of geological input data for safety assessment models. - Nagra tech. Rep. NTB 93-12. Nagra, Wettingen.
- MAZUREK, M. & PETERS, T.J. 1992: Petrographie des kristallinen Grundgebirges der Nordschweiz und Systematik der herzynischen Granite. - *Schweiz. mineral. petrogr. Mitt.* 72/1, 11-35.
- MAZUREK, M., SMITH, P. & GAUTSCHI, A. 1992a: Application of a realistic geological database to safety assessment calculations: An exercise in interdisciplinary communication. In: KHARAKA, Y.K. & MAEST, A.S. (Ed.): *Water-Rock Interaction* (p. 407-411). - Proc. 7th int. Symp. Water-Rock Interaction, Park City (Utah). Balkema, Rotterdam.
- MAZUREK, M., GAUTSCHI, A. & VOMVORIS, S. 1992b: Deriving input data for solute transport models from deep borehole investigations - An approach for crystalline rocks. - Proc. int. Symp. on geol. Disposal of spent Fuel, high-level and alpha-bearing Wastes, Antwerp, Belgium, 19-23 Oct.; Int. Atomic Energy Agency.

- McCARTHY, J. & DEGUELDRE, C. 1993: Sampling and characterization of colloids in groundwater for studying their role in the subsurface transport of contaminants. In *Characterization of Environmental Particles*, In: BUFFLE, J. & LEEUWEN, H.P. VAN (Ed.): Environmental Analytical Chemistry Series, vol. 1. - Lewis Publ. inc.
- McCOMBIE, C., LAMBERT, A. & McKINLEY, I.G. 1993: Swiss strategy for developing a high-level waste disposal system. - Proc. int. Symp. on geol. Disposal of spent Fuel, high-level and alpha-bearing Wastes, Antwerp, Belgium, 19-23 Oct.; int. atomic Energy Agency, 365-375.
- McCORD, J.P. & MOE, H. 1990: Interpretation of hydraulic testing at the Kaisten borehole. - Nagra tech. Rep. NTB 89-18. Nagra, Wettingen.
- McKINLEY, I.G., McCOMBIE, C., THURY, M. & ZUIDEMA, P. 1993: Conclusions from a total system assessment within Kristallin-I. - Proc. int. Conf. on nuclear Waste Management and environmental Remediation, Prague, Czechoslovakia, 709-720.
- McNEISH, J.A., McCORD, J.P. & ANDREWS, R.W. 1990: Analyses of long-term monitoring data from the Schafisheim, Kaisten and Leuggern boreholes. - Nagra intern. Rep. Nagra, Wettingen.
- MEIER, B.P. 1994: Untere Süsswassermolasse des zentralen und östlichen Mittellandes. - Nagra intern. Ber. Nagra, Wettingen.
- METZ, R. 1980: Geologische Landeskunde des Hotzenwaldes. - Moritz Schauenburg, Lahr.
- MEYER, J. 1987: Die Kataklyse im kristallinen Untergrund der Nordschweiz. - *Ecologae geol. Helv.* 80/2, 323-334.
- MICHALSKI 1987: Apatit-Spaltspuren - Datierungen des Grundgebirges von Schwarzwald und Vogesen: Die post-variskische Entwicklung. - Diss. Univ. Heidelberg.
- MICHARD, G. 1987: Controls of the chemical composition of geothermal waters. In: HELGESON, H.C. (Ed.): *Chemical Transport in Metasomatic Processes* (p. 323-353), NATO adv. Stud. Inst. Ser. (C). math. phys. Sci. 218.
- 1990a: Behaviour of major elements and some trace elements (Li, Rb, Cs, Sr, Fe, Mn, W, F) in deep hot waters from granitic areas. - *Chem. Geol.* 89, 117-134.
- 1990b: La composition chimique des eaux thermominérales et géothermales (Chemical composition of thermal and geothermal waters). - *Hydrogéol.* 4, 253-266.

- MILANKOVITCH, M. 1930: Mathematische Klimalehre und astronomische Theorie der Klimaschwankungen. In: KÖPPEN, W. & GEIGER, R. (Ed.): Handbuch der Klimatologie I. - Gebr. Bornträger, Berlin.
- MILNES, A.G. 1990: Fault and fracture systems in the crystalline basement of Northern Switzerland and adjacent Southern Schwarzwald. A discussion paper with respect to the Swiss programme for high-level radioactive waste disposal. - Unpubl. Ber. Geologiebüro Milnes (Geol. & Environ. Assessments, GEA) z.H. Hauptabt. f. d. Sicherheit d. Kernanlagen (HSK).
- MOE, H., McNEISH, J.A., McCORD, J.P. & ANDREWS, R.W. 1990: Interpretation of hydraulic testing at the Schafisheim borehole. - Nagra tech. Rep. NTB 89-09. Nagra, Wettingen.
- MONNINGER, R. 1985: Neotektonische Bewegungsmechanismen im mittleren Oberrheingraben. - Diss. Univ. Karlsruhe.
- MUIRWOOD, R. & KING, G.C.P. 1993: The impact of earthquakes on fluids in the crust. In: PARNELL, J., RUFFELI, A.H. & MOLES, N.R. (Ed.): Geofluids '93 - Contr. to an int. Conf. on Fluid Evolution, Migration and Interaction in Rocks, 144-147.
- MULLIS, J. 1987: Fluideinschluss-Untersuchungen in den Nagra-Bohrungen der Nordschweiz. - *Eclogae geol. Helv.* 80/2, 553-568.
- MÜLLER, H.D. 1984: Die Lamprophyre des Schwarzwaldes. - *Fortschr. Mineral.* 62, Beih. 2, 106-111.
- 1989: Geochemistry of metasediments in the Hercynian and Pre-Hercynian crust of the Schwarzwald, the Vosges and Northern Switzerland. - *Tectonophysics* 157, 97-108.
- MÜLLER, W.H., BLÜMLING, P., BECKER, A. & CLAUSS, B. 1987: Die Entkopplung des tektonischen Spannungsfeldes an der Jura-Überschiebung. - *Eclogae geol. Helv.* 80/2, 473-489.
- MÜLLER, W.H., HUBER, M., ISLER, A. & KLEBOTH, P. 1984: Erläuterung zur Geologischen Karte der zentralen Nordschweiz 1:100'000. - Nagra tech. Ber. NTB 84-25. Nagra, Wettingen.
- NAEF, H. 1992: Geologische Langzeitszenarien Kristallin Nordschweiz 1992. - Nagra intern. Ber. Nagra, Wettingen.
- NAEF, H. & DIEBOLD, P. 1990: Tektonik des östlichen Tafeljuras und der angrenzenden Molasse. - *Nagra informiert* 2/90, 37-46.
- NAEF, H., DIEBOLD, P. & SCHLANKE, S. 1985: Sedimentation und Tektonik im Tertiär der Nordschweiz. - Nagra tech. Ber. NTB 85-14. Nagra, Wettingen.

- NAGRA 1985a: Sondierbohrung Böttstein, Untersuchungsbericht. (Text- und Beilagenband). - Nagra tech. Ber. NTB 85-01. Nagra, Wettingen.
- 1985b: Project Gewähr 1985: Nuclear Waste Management in Switzerland: Feasibility Studies and Safety Analysis. - Nagra Project Rep. NGB 85-09 (Extended German Version in 8 Volumes: NGB 85-01 to NGB 85-08). Nagra, Wettingen.
- 1985c: Sondierbohrung Böttstein - Bau- und Umweltaspekte, Bohrtechnik. - Nagra tech. Ber. NTB 85-12. Nagra, Wettingen.
- 1986a: Überwachung bedeutender Mineralquellen und Thermen der Nordschweiz und angrenzender Gebiete: Resultate der Messstationen mit permanenter Aufzeichnung. - Nagra intern. Ber. Nagra, Wettingen.
- 1986b: Sondierbohrung Weiach - Bau- und Umweltaspekte, Bohrtechnik. - Nagra tech. Ber. NTB 86-06. Nagra, Wettingen.
- 1986c: Sondierbohrung Kaisten - Bau- und Umweltaspekte, Bohrtechnik. - Nagra tech. Ber. NTB 86-09. Nagra, Wettingen.
- 1987: Beiträge zur Geologie der Nordschweiz: Symposium vom 9. Oktober 1986 der Schweizerischen Geologischen Gesellschaft, der Schweizerischen Mineralogischen und Petrographischen Gesellschaft und der Schweizerischen Paläontologischen Gesellschaft. - Sonderdr. Eclogae geol. Helv. 80/2 1987. Nagra tech. Ber. NTB 87-15. Nagra, Wettingen.
- 1988a: Sondierbohrungen Böttstein, Weiach, Riniken, Schafisheim, Kaisten, Leuggern. Fluid-Logging: Temperatur-, Leitfähigkeits- und Spinner-Flowmeter-Messungen (Text- und Beilagenband). - Nagra tech. Ber. NTB 85-10. Nagra, Wettingen.
- 1988b: Sedimentstudie - Zwischenbericht 1988. Möglichkeiten zur Endlagerung langlebiger radioaktiver Abfälle in den Sedimenten der Schweiz (Text- und Beilagenband). - Nagra tech. Ber. NTB 88-25/NTB 88-25E. Nagra, Wettingen.
- 1988c: Sondierbohrung Riniken - Bau- und Umweltaspekte, Bohrtechnik. - Nagra tech. Ber. NTB 86-07. Nagra, Wettingen.
- 1989a: Hydrochemische Analysen (formatierte Ausdrücke der hydrochemischen Datenbank, mit Berechnung von Äquivalentkonzentrationen). - Nagra intern. Ber. Nagra, Wettingen (9 Bände).
- 1989b: Sondierbohrung Leuggern - Bau- und Umweltaspekte, Bohrtechnik. - Nagra tech. Ber. NTB 86-10. Nagra, Wettingen.
- 1989c: Sondierbohrung Weiach - Untersuchungsbericht (Text- und Beilagenband). - Nagra tech. Ber. NTB 88-08. Nagra, Wettingen.

- 1990: Sondierbohrung Riniken - Untersuchungsbericht (Text- und Beilagenband). - Nagra tech. Ber. NTB 88-09. Nagra, Wettingen.
  - 1991a: Sondierbohrung Schafisheim - Bau- und Umweltaspekte, Bohrtechnik. - Nagra tech. Ber. NTB 86-08. Nagra, Wettingen.
  - 1991b: Sondierbohrung Leuggern - Untersuchungsbericht (Text- und Beilagenband). - Nagra tech. Ber. NTB 88-10. Nagra, Wettingen.
  - 1991c: Sondierbohrung Kaisten - Untersuchungsbericht (Text- und Beilagenband). - Nagra tech. Ber. NTB 88-12. Nagra, Wettingen.
  - 1991d: Sedimentstudie - Zwischenbericht 1990. - Nagra tech. Ber. NTB 91-19. Nagra, Wettingen.
  - 1992a: Sondierbohrung Siblingen - Untersuchungsbericht (Text- und Beilagenband). - Nagra tech. Ber. NTB 90-34. Nagra, Wettingen.
  - 1992b: Sondierbohrung Schafisheim - Untersuchungsbericht (Text- und Beilagenband). - Nagra tech. Ber. NTB 88-11. Nagra, Wettingen.
  - 1993: Geologische Grundlagen und Datensatz zur Beurteilung der Langzeitsicherheit des Endlagers für schwach- und mittelaktive Abfälle am Standort Wellenberg. - Nagra tech. Ber. NTB 93-28. Nagra, Wettingen.
  - 1994a: Kristallin-I: Safety Analysis Overview. - Nagra tech. Rep. NTB 93-22. Nagra, Wettingen.
  - 1994b: Kristallin-I: Conclusions from the regional investigation programme for siting a HLW repository in the crystalline basement of Northern Switzerland. - Nagra tech. Rep. NTB 93-09. Nagra, Wettingen.
- NERETNIEKS, I., ERIKSEN, T. & TÄHTINEN, P. 1982: Tracer movement in a single fissure in granitic rock: some experimental results and their interpretation. - Water Resour. Res. 18, 849-858.
- NORDSTROM, D.K., ANDREWS, J.N., CARLSSON, L., FONTES, J.CH., FRITZ, P., MOSER, H. & OLSSON, T. 1985: Hydrogeological and hydrochemical investigations in boreholes - Final report of the Phase I geochemical investigations of the Stripa groundwaters. - SKB tech. Rep. 85-06. Swedish Nuclear Fuel and Waste Management Co., Stockholm.
- NORDSTROM, D.K., BALL, J.W., DONAHOE, R.J. & WHITTEMORE, D. 1989a: Groundwater chemistry and water-rock interactions at Stripa. - Geochim. cosmochim. Acta 53, 1727-1740.

- NORDSTROM, D.K., LINDBLOM, S., DONAHOE, R.J. & BARTON, C.C. 1989b: Fluid inclusions in the Stripa granite and their possible influence on the groundwater chemistry. - *Geochim. cosmochim. Acta* 53, 1741-1756.
- OBERHÄNSLI, R., SCHENKER, F. & MERCOLLI, I. 1988: Indications of Variscan nappe tectonics in the Aar Massif. - *Schweiz. mineral. petrogr. Mitt.* 68, 509-520.
- ORTLAM, D. 1970: Die Randfazies des germanischen Buntsandsteins im südlichen Schwarzwald. - *Geol. Jb.* 89, 135-168.
- 1974: Inhalt und Bedeutung fossiler Bodenkomplexe in Perm und Trias von Mitteleuropa. - *Geol. Rdsch.* 63, 850-884.
- OSTROWSKI, L.P. & KLOSKA, M.B. 1989: Final interpretation of hydraulic testing at the Siblingen borehole. ITA, Institute of Petroleum Eng., TU Clausthal. - Nagra tech. Rep. NTB 89-10. Nagra, Wettingen.
- PAHL, A., HEUSERMANN, ST., BRÄUER, V. & GLÖGGLER, W. 1989: Felslabor Grimsel. Gebirgsspannungs-Untersuchungen. - Nagra tech. Ber. NTB 88-39. Nagra, Wettingen.
- PARKHURST, D.L., THORSTENSON, D.C. & PLUMMER, L.N. 1980: PHREEQE - A Computer Program for Geochemical Calculations (original publication 1980; revised and reprinted 1982, 1985, and 1990). - *U.S. geol. Surv., Water-Resour. Invest. Rep.* 80-96.
- PASQUIER, F., WILSON, W. & VOMVORIS, S. 1993: Reference set of hydraulic-head values at the Böttstein, Kaisten, Leuggern, Riniken, Schafisheim, Siblingen and Weiach boreholes, Northern Switzerland. - Nagra intern. Rep. Nagra, Wettingen.
- PAVONI, N. 1984: Seismotektonik Nordschweiz. - Nagra tech. Ber. NTB 84-45. Nagra, Wettingen.
- 1987: Zur Seismotektonik der Nordschweiz. - *Eclogae geol. Helv.* 80/2, 461-472.
- PEARSON, F.J. 1985: Sondierbohrung Böttstein - Results of hydrochemical investigations: Analysis and Interpretation. - Nagra tech. Rep. NTB 85-05. Nagra, Wettingen.
- PEARSON, F.J., BALDERER, W., LOOSLI, H.H., LEHMANN, B.E., MATTER, A., PETERS, T.J., SCHMASSMANN, H. & GAUTSCHI, A. 1991: Applied isotope hydrogeology - A case study in Northern Switzerland. - Nagra tech. Rep. NTB 88-01. Nagra, Wettingen.

- PEARSON, F.J. & BERNER, U. 1991: Nagra thermochemical data base. I. Core data. - Nagra tech. Rep. NTB 91-17. Nagra, Wettingen.
- PEARSON, F.J., BERNER, U. & HUMMEL, W. 1992: Nagra Thermochemical Data Base II. Supplemental Data 05/92. - Nagra tech. Rep. NTB 91-18. Nagra, Wettingen.
- PEARSON, F.J., LOLCAMA, J.L. & SCHOLTIS, A. 1989: Chemistry of Waters in the Böttstein, Weiach, Riniken, Schafisheim, Kaisten and Leuggern Boreholes: A Hydrochemically Consistent Data Set. - Nagra tech. Rep. NTB 86-19. Nagra, Wettingen.
- PEARSON, F.J. & SCHOLTIS, A. 1993: Chemistry of reference waters of the crystalline basement of Northern Switzerland for safety assessment studies. - Nagra tech. Rep. NTB 93-07. Nagra, Wettingen.
- PETERS, T.J. 1986: Structurally incorporated and water extractable chlorine in the Böttstein granite (N. Switzerland). - *Contr. Mineral. Petrogr.* 94, 272-273.
- 1987: Das Kristallin der Nordschweiz: Petrographie und hydrothermale Umwandlungen. - *Eclogae geol. Helv.* 80/2, 305-322.
- 1991: Distribution of exchangeable cations in Mesozoic and Permo-Carboniferous sediments in the subsurface of Northern Switzerland. - *Schweiz. mineral. petrogr. Mitt.* 71/1, 143-150.
- PETERS, T.J., MATTER, A., BLÄSI, H.-R. & GAUTSCHI, A. 1986: Sondierbohrung Böttstein - Geologie; Text- und Beilagenband. - Nagra tech. Ber. NTB 85-02. Nagra, Wettingen.
- PETERS, T.J., MATTER, A., BLÄSI, H.-R., ISENSCHMID, CH., KLEBOTH, P., MEYER, CH. & MEYER, J. 1989a: Sondierbohrung Leuggern - Geologie; Text- und Beilagenband. - Nagra tech. Ber. NTB 86-05. Nagra, Wettingen.
- PETERS, T.J., MATTER, A., MEYER, J., ISENSCHMID, CH. & ZIEGLER, H.-J. 1989b: Sondierbohrung Kaisten - Geologie; Text- und Beilagenband. - Nagra tech. Ber. NTB 86-04. Nagra, Wettingen.
- PFANNENSTIEL, M. 1957: Der Graben von Rüsswihl im Hotzenwald. - *Jh. geol. Landesamt Bad.-Württemb.* 2, 291-298.
- PICKENS, J.F., BELANGER, D.W. & SAULNIER, G.J. 1985: Analysis of pressure and flow data from the long-term monitoring tool in Böttstein borehole. GTC Geologic Testing Consultants, Ottawa. - Nagra tech. Rep. NTB 85-39. Nagra, Wettingen.
- RASMUSON, A. & NERETNIEKS, I. 1986: Radionuclide transport in fast channels in crystalline rock. - *Water Resour. Res.* 22, 1247-1256.

- RAUMER, J.F. VON 1983: Die Metapelite von Emosson (Aiguilles Rouges-Massiv) als Beispiel spätkaledonisch-frühvariszischer Metamorphose im Altkristallin des helvetischen Bereichs. - Schweiz. mineral. petrogr. Mitt. 63, 421-455.
- RAYMO, M.E., RUDDIMAN, W.F., SHACKLETON, N.J. & OPPO, D.W. 1990: Evolution of Atlantic-Pacific  $\delta^{13}\text{C}$  gradients over the last 2.5 m.y. - Earth and planet. Sci. Lett. 97, 353-368.
- REST, H. 1977: Ein Beitrag zur Tektonik des Wolfristkopfs nördlich Wehr. - Ber. natf. Ges. Freiburg i. Br. 67, 277-285.
- ROCKENBAUCH, K. 1984: Bruchtektonik im Granitgebiet des südwestlichen Schwarzwalds und im angrenzenden Deckgebirge (Dinkelbergscholle, Vorbergzone). - Arb. geol. paläont. Inst. Univ. Stuttgart [N.F.] 78, 137-191.
- ROEDDER, E. 1984: Fluid inclusions. - Reviews in Mineralogy 12, Min. Soc. America.
- ROMETSCH, R., ISSLER, H., McCOMBIE, C. & PLUSIEURS CONSULTANT 1983: Elimination des déchets nucléaires en Suisse - Concept et état des travaux en 1982. - Nagra Rapp. tech. NTB 83-02F. Nagra, Wettingen.
- RYBACH, L., EUGSTER, W. & GRIESSER, J.-C. 1987: Die geothermischen Verhältnisse in der Nordschweiz. - Eclogae geol. Helv. 80/2, 521-534.
- SATO, M. 1960: Oxidation of sulfide ore bodies: 1. Geochemical environments in terms of Eh and pH. Econ. Geol. 55, 928-961.
- SAUER, A. 1893: Der Granitit von Durbach im nördlichen Schwarzwalde und seine Grenzfacies von Glimmersyenit (Durbachit). - Mitt. bad. geol. Landesanst. 2, 231-275.
- SCHALTEGGER, U. 1986: Voralpine und alpine Mineralbildungen in der Gneiszone von Erstfeld (Sustenpass, Aarmassiv), der Mechanismus der K/Ar- und Rb/Sr-Verjüngung alpin umgewandelter Biotite. - Schweiz. mineral. petrogr. Mitt. 66, 395-412.
- SCHÄRLI, U. 1989: Geothermische Detailkartierung (1:100'000) in der zentralen Nordschweiz mit besonderer Berücksichtigung petrophysikalischer Parameter. - Diss. ETH Zürich Nr. 8941.
- SCHINDLER, C. 1985: Geologisch-geotechnische Verhältnisse in Schaffhausen und Umgebung. - Beitr. Geol. Schweiz, klein. Mitt. 74.
- SCHLEICHER, H. 1978: Petrologie der Granitporphyre des Schwarzwaldes. - N. Jb. Mineral. [Abh.] 132/2, 153-181.

- SCHLEICHER, H., LIPPOLT, H.J. & RACZEK, I. 1983: Rb-Sr systematics of Permian volcanites in the Schwarzwald (SW-Germany). Part II: Age of eruption and the mechanism of Rb-Sr whole rock age distortions. - *Contrib. Mineral. Petrol.* 84, 281-291.
- SCHLEICHER, H. & KRAMM, U. 1986: Altersbestimmungen nach der U/Pb-Methode an mittel- bis hochdruckmetamorphen Gesteinen des Schwarzwaldes. - 76. Jtag. geol. Vereinigung Giessen, Abstr., 69.
- SCHMASSMANN, H. 1990: The hydrogeochemical programme and observation network for projects of radioactive waste disposal in Northern Switzerland. - *Mem. 22nd Congr. IAH, Lausanne Vol. 22*, 711-718.
- SCHMASSMANN, H., BALDERER, W., KANZ, W. & PEKDEGER, A. 1984: Beschaffenheit der Tiefengrundwässer in der zentralen Nordschweiz und angrenzenden Gebieten. - *Nagra tech. Ber. NTB 84-21*. Nagra, Wettingen.
- SCHMASSMANN, H., KULLIN, M. & SCHNEEMANN, K. 1992: Hydrochemische Synthese Nordschweiz. Buntsandstein-, Perm- und Kristallin-Aquifere. - *Nagra tech. Ber. NTB 91-30*. Nagra, Wettingen.
- SCHNEIDER, A. & SCHLANKE, S. 1986: Sondierbohrungen Böttstein, Schafisheim, Weiach, Kaisten, Riniken - Langzeit-Beobachtung der Tiefengrundwässer. - *Nagra tech. Ber. NTB 85-11*. Nagra, Wettingen.
- SCHNEIDER, D., MATTLI, B. & GUBLER, E. 1992: Neotektonische Untersuchungen der Nagra im Hauensteingebiet: Nivellements-Messungen 1990/91 und kinematische Ausgleichungen der relativen Höhenänderungen 1911 bis 1991. - *Nagra intern. Ber. Nagra, Wettingen*.
- SCHNEIDER, D. & WIGET, A. 1990: GPS-Netz "NEOTEKTONIK" 1988. - *Nagra intern. Ber. Nagra Wettingen*.
- SCHREINER, A. 1992: Einführung in die Quartärgeologie. - Schweizerbart, Stuttgart.
- SCHWEINGRUBER, M. 1984: Deep-crystalline reference water for project "Gewähr". *Eidg. Inst. Reaktorforsch., Tech. Rep. TM-45-84-21*.
- SCHWEIZERISCHER INGENIEUR- UND ARCHITEKTENVEREIN (SIA) 1975: Erfassen des Grundgebirges im Untertagebau. SIA-Norm 199, Schweizer Norm 531 199. - Bauwesen, Zürich.
- SHAPIRO, A.M. & NICHOLAS, J.R. 1989: Assessing the validity of the channel model of fracture aperture under field conditions. - *Water Resour. Res.* 25, 817-828.
- SIBSON, R.H. 1993: Crustal stress, faulting, and fluid flow. In: PARNELL, J., RUFFELL, A.H. & MOLES, N.R. (Ed.): *Geofluids '93 - Contr. to an int. Conf. on Fluid Evolution, Migration and Interaction in Rocks*, 137-140.

- SIERRO, N., BINDSCHÄDLER, A., ANSORGE, J. & MÜLLER, S. 1983: Geophysikalisches Untersuchungsprogramm Nordschweiz - Regionale Refraktionsseismische Messungen. - Nagra tech. Ber. NTB 83-21. Nagra, Wettingen.
- SILLIMAN, S.E. 1989: An interpretation of the difference between aperture estimates derived from hydraulic and tracer tests in a single fracture. - Water Resour. Res. 25, 2275-2283.
- SIMON, K. 1990: Hydrothermal alteration of Variscan granites, southern Schwarzwald, Federal Republic of Germany. - Contr. Mineral. Petrol. 105, 177-196.
- SIMON, K. & HOEFS, J. 1987: Effects of meteoric water interaction on Hercynian granites from the Südschwarzwald, Southwest Germany. - Chem. Geol. 61, 253-261.
- SMITH, P.A. 1993: A model for colloid facilitated radionuclide transport through fractured media. - Nagra tech. Rep. NTB 93-32. Nagra, Wettingen.
- SNOW, D.T. 1968: Rock fracture spacings, openings and porosities. - J. Soil Mech. Found. Div. amer. Soc. civ. Eng. 94 (SM1), 73-91.
- 1970: The frequency and aperture of fractures in rock. - Int. J. Rock Mech. Min. Sci. 7, 23-40.
- SPANE, F.A. Jr. 1990: Description and results of tracer tests conducted for a deep fracture zone within granitic rock at the Leuggern borehole. - Nagra tech. Rep. NTB 90-05. Nagra, Wettingen.
- SPRECHER, C. & MÜLLER, W.H. 1986: Geophysikalisches Untersuchungsprogramm Nordschweiz: Reflexionsseismische Messungen 82. - Nagra tech. Ber. NTB 84-15. Nagra, Wettingen.
- STÄUBLE, J. 1993: Hydrogeologische Charakterisierung der Schottergrundwässer im unteren Aaretal und Rheintal. - Nagra intern. Ber. Nagra, Wettingen.
- STEIGER, R.H., BÄR, M.T. & BÜSCH, W. 1973: The zircon age of an anatectic rock in the Central Schwarzwald. - Fortschr. Mineral. 50, 131-132.
- STENGER, R. 1983: Geochronologische Tabellen. - Kontinent. Tiefbohrprogr. d. Bundesrep. Dtschl., Vorstudie Schwarzwald I, 130-144.
- STENGER, R., BAATZ, K., KLEIN, H. & WIMMENAUER, W. 1989: Metamorphic evolution of the Pre-Hercynian basement of the Schwarzwald (Federal Republic of Germany). - Tectonophysics 157, 117-121.
- STENHOUSE, M.J. 1994: Compilation and review of experimental sorption data with recommended Kd values. - Nagra tech. Rep. NTB 93-06. Nagra, Wettingen.

- STIEFEL, A. & WILHELM, H. 1989: Geothermische Untersuchungen im Schwarzwald. In: UNIVERSITÄT KARLSRUHE (Ed.): Spannung und Spannungsumwandlung in der Lithosphäre (p. 213-232). - Berbd. Sonderforschungsbereich 108 für die Jahre 1984-1986 (Teil A).
- STOBER, I. in Vorb.: Die Wasserführung des kristallinen Grundgebirges. - Habilschr. Univ. Freiburg i.Br. (erscheint voraussichtlich 1994).
- STOBER, I. & VILLINGER, E. in Vorb.: Hydraulisches Potential und Durchlässigkeit des höheren Malmes und des Oberen Muschelkalks im baden-württembergischen Molassebecken. - Jh. geol. Landesamt. Bad.-Württemb. (erscheint voraussichtlich 1994).
- STUMM, W. 1992: Chemistry of the Solid-Water Interface. - John Wiley and Sons, New York.
- THEOBALD, N., VOGT, H. & WITTMANN, D. 1977: Neotectonique de la partie méridionale du bloc rhénois. - Bull. Bur. Rech. géol. min. (Sect. IV) 2, 121-140.
- THURY, M. 1980: Erläuterungen zum Nagra-Tiefbohrprogramm als vorbereitende Handlung im Hinblick auf das "Projekt Gewähr". - Nagra tech. Ber. NTB 80-07. Nagra, Wettingen.
- THURY, M. & AMMANN, M. 1990: Die sieben Tiefbohrungen der Nagra in der Nordschweiz. Zusammenstellung der Untersuchungen. - Nagra informiert 12/7, 7-15.
- TODOROV, I., SCHEGG, R. & WILDI, W. 1993.: Thermal maturity and modelling of Mesozoic and Cenozoic sediments in the south of the Rhine Graben and the Eastern Jura (Switzerland). - Eclogae geol. Helv. 86/3, 667-692.
- TODT, W. & BÜSCH, W. 1981: U-Pb investigations of zircons from pre-Variscan gneisses. I: A study from the Schwarzwald, West Germany. - Geochim. cosmochim. Acta 45, 1789-1801.
- TRUESDELL, A.H. & HULSTON, J.R. 1980: Isotopic evidence on environments of geothermal systems. In: FRITZ, P. & FONTES J.C. (Ed.): Handbook of Environmental Isotope Geochemistry, vol. 1, - The Terrestrial Environment, A (p. 179-226). Elsevier, Amsterdam.
- TRÜMPY, R. 1980: Geology of Switzerland. Part A: An Outline of the Geology of Switzerland. - Wepf & Co., Basel/New York.
- TSANG, Y.W., TSANG, C.F., NERETNIEKS, I. & MORENO, L. 1988: Flow and tracer transport in fractured media: a variable aperture channel model and its properties. - Water Resour. Res. 24, 2049-2060.

- VAN MIERLO, J., OPPEN, S., RAUHUT, P. & VOGEL, M. 1992: Kriechende Spannungsumwandlungen: Rezente vertikale und horizontale Bewegungen. In: UNIVERSITÄT KARLSRUHE (Ed.): Spannung und Spannungsumwandlung in der Lithosphäre (p. 657-664). - Berbd. Sonderforschungsbereich 108 für die Jahre 1990 - 1992 (Teil B).
- VENZLAFF, V. 1971: Altersbestimmungen nach der Rb/Sr-Methode an Biotiten aus Gesteinen des Schwarzwaldes. - Z. Natf. 26a, 1372-1373.
- VILKS, P. & DEGUELDRE, C. 1991: Sorption behaviour of  $^{85}\text{Sr}$ ,  $^{131}\text{I}$  and  $^{137}\text{Cs}$  on colloids and suspended particles from the Grimsel Test Site. - Appl. Geochem. 6, 553-563.
- VOBORNY, O. 1992: Regional groundwater flow in crystalline rocks of Northern Switzerland: Preliminary results of a numerical model using an equivalent porous-medium approach. - Nagra intern. Rep. Nagra, Wettingen.
- VOBORNY, O., ADANK, P., HÜRLIMANN, W., VOMVORIS, S. & MISHRA, S. 1991: Grimsel Test Site - Modeling of groundwater flow in the rock body surrounding the underground laboratory. - Nagra tech. Rep. NTB 91-03. Nagra, Wettingen.
- VOBORNY, O., VOMVORIS, S. & RESELE, G. 1993a: Hydrogeology of crystalline rocks of Northern Switzerland: Synthesis of hydraulic borehole data and assessment of effective properties. - Nagra intern. Rep. Nagra, Wettingen.
- VOBORNY, O., VOMVORIS, S., WILSON, W., RESELE, G. & HÜRLIMANN, W. 1993b: Hydrodynamic modeling of crystalline rocks, Northern Switzerland. - Nagra tech. Rep. NTB 92-04. Nagra, Wettingen.
- VOBORNY, O., WILSON, W.E., HÜRLIMANN, W. & VOMVORIS, S. 1992: Analysis of regional groundwater flow in crystalline rocks of Northern Switzerland: Results of a numerical model using an equivalent porous medium. - Nagra intern. Rep. Nagra, Wettingen.
- VOGT, U. 1983: Gesteine des Grundgebirges nordöstlich von Wehr, südlichster Schwarzwald. - Unpubl. Diplomarb. Albert-Ludwigs-Univ. Freiburg i. Br.
- VOLLMAYR, T. 1983: Temperaturmessungen in Erdölbohrungen der Schweiz. - Bull. Ver. schweiz. Petroleum-Geol. u. -Ing. 49/116, 15-28.
- VOMVORIS, S. & ANDREWS, R. (Ed.) 1993: Crystalline explorability: Documentation of key assumptions, questions and interim synthesis of results. - Nagra intern. Rep. Nagra, Wettingen.

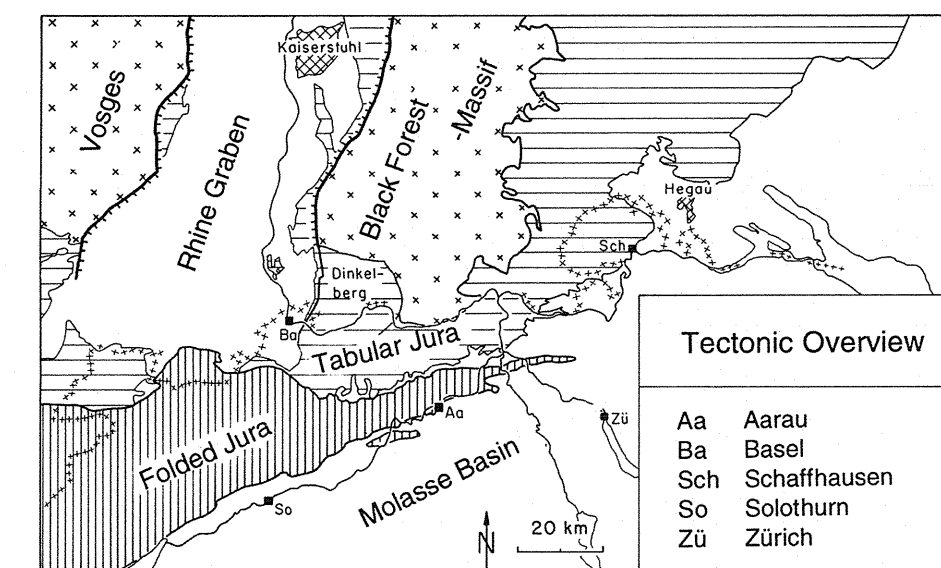
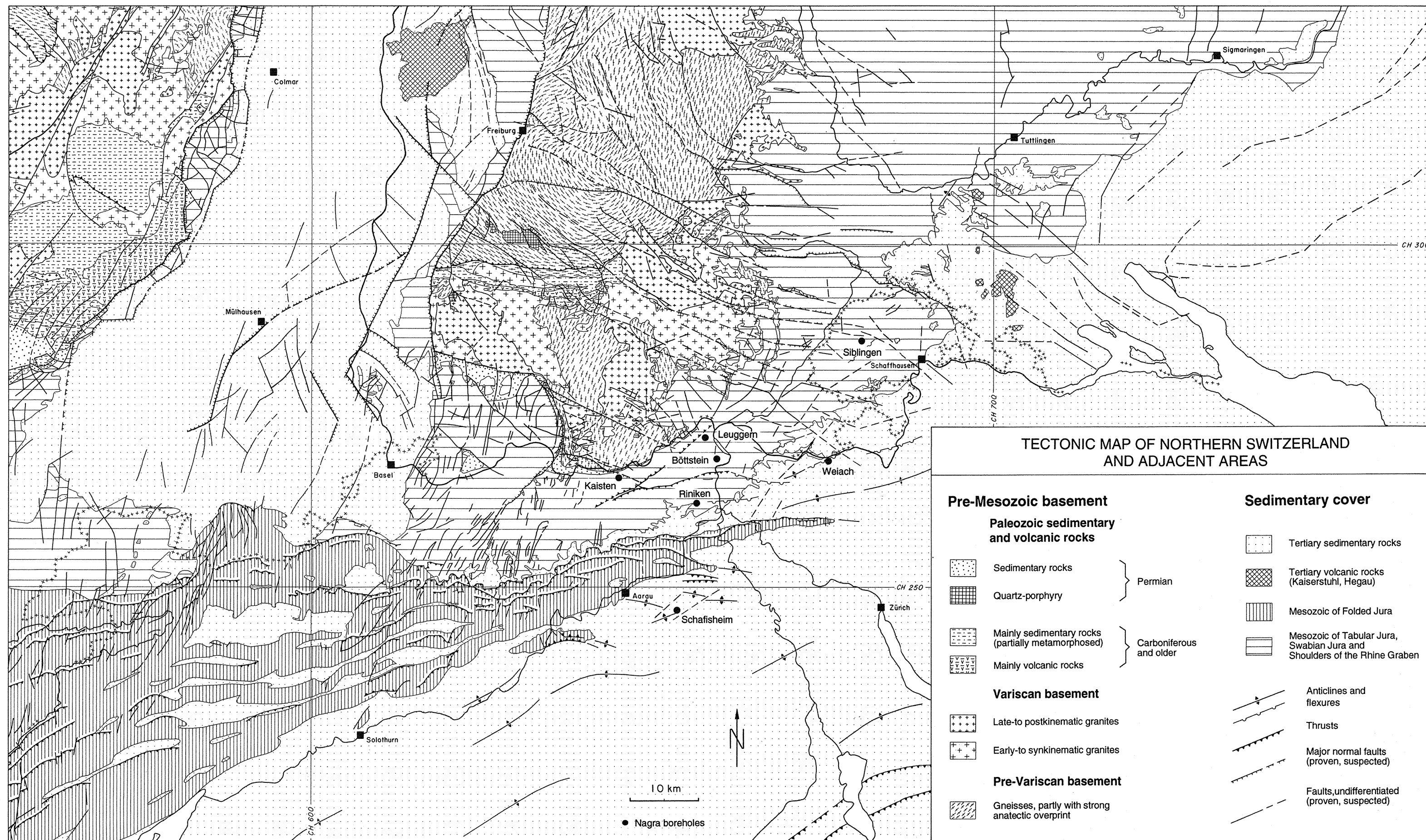
- VOMVORIS, S., ANDREWS, R.W., BLÜMLING, P., MÜLLER, W.H., SCHINDLER, M., TAKEUCHI, K., UMEKI, H., VOBORNY, O. & WILSON, W. 1993b: Northern Switzerland Crystalline Rocks: Preliminary assessment of changes in groundwater flow and their implications on the geo-dataset due to the excavation-disturbed zone around a repository tunnel. - Nagra intern. Rep. Nagra, Wettingen.
- VOMVORIS, S., VOBORNY, O., LANYON, W., WILSON, W. & ANDREWS, R.W. 1993c: Methodology for deriving hydrogeological input parameters for safety analysis models and application to fractured rocks in Switzerland. - Nagra tech. Rep. NTB 93-14. Nagra, Wettingen (expected to appear in 1994).
- VOMVORIS, S., VOBORNY, O., WILSON, W. & ANDREWS, R. 1993a: Hydrogeology of crystalline rocks of Northern Switzerland: Synthesis of results relevant to safety analysis, Reference Area East. - Nagra intern. Rep. Nagra, Wettingen.
- VOMVORIS, S., VOBORNY, O., WILSON, W., ANDREWS, R. & HÜRLIMANN, W. 1992: Hydrogeology of crystalline rocks of Northern Switzerland: Synthesis of results relevant to safety analysis, Reference Area West. - Nagra intern. Rep. Nagra, Wettingen.
- VSE/GKBP/UeW/NAGRA 1978: Konzept für die nukleare Entsorgung in der Schweiz. - Verb. Schweiz. Elektrizitätswerke (VSE), Gruppe der KKW-Betreiber u. -Projektanten (GKBP), Konferenz der Überlandw. (UeW), Nagra.
- VUATAZ, F.-D. 1982: Hydrogéologie, géochimie et géothermie des eaux thermales de Suisse et des régions alpines limitrophes. - Matér. Géol. Suisse, Hydrol. 29.
- WALLACE, R.E. & MORRIS H.T. 1979: Characteristics of faults and shear zones as seen in mines at depths as much as 2.5 km below the surface. In: Analysis of actual fault zones in bedrock (p. 79-100). - Conf. Proc. U.S. geol. Surv. Open File Rep. 79-1239.
- WALTHER, H.W. & 26 co-authors 1986: Federal Republic of Germany. In: DUNNING, F.W. & EVANS, A.M. (Ed.): Mineral deposits of Europe, Vol. 3: Central Europe (p. 175-301). - Instn. Mining Metal Mineral. Soc. London.
- WEBER, H.P., SATTEL, G. & SPRECHER, C. 1986: Sondierbohrungen Weiach, Riniken, Schafisheim, Kaisten, Leuggern - Geophysikalische Daten, Textband. - Nagra tech. Ber. NTB 85-50. Nagra, Wettingen.
- WERCHAU, A., SCHLEICHER, H. & KRAMM, U. 1989a: Geochronologische Untersuchungen an Eklogitamphiboliten des Schwarzwaldes. - Ber. dtsh. mineral. Ges. 1, 198.
- 1989b: Erste Altersbestimmungen an Monaziten des Schwarzwaldes. - Ber. dtsh. mineral. Ges. 1, 197.

- WEXSTEEN, P. & MATTER, A. 1989: Isotopic geothermometry and flow regimes in the Muschelkalk aquifer from Northern Switzerland (Nagra deep drilling programme). In: MILES, D.L. (Ed.): Water-Rock Interaction WRI-6 (p. 761-764). - A.A. Balkema, Rotterdam.
- WICKERT, F., ALTHERR, R. & DEUTSCH, M. 1990: Polyphase Variscan tectonics and metamorphism along a segment of the Saxothuringian-Moldanubian boundary: The Baden-Baden Zone, northern Schwarzwald (F.R.G.). - *Geol. Rdsch.* 79, 627-647.
- WILDI, W. 1975: Die Mettaufer Überschiebung im aargauischen Tafeljura (Nordschweiz). - *Eclogae geol. Helv.* 68/3, 483-489.
- WIMMENAUER, W. 1980: Lithology of the Precambrian in the Schwarzwald. An interim report. - *N. Jb. Mineral. [Mh.]* 1980, 364-372.
- 1984: Das prävariskische Kristallin im Schwarzwald. - *Fortschr. Mineral.* 62, Beih. 2, 69-86.
- 1985: Hydrothermal vein deposits of the Schwarzwald. - 2nd int. Symp. Obs. continental Crust through Drilling (4th Alfred Wegener Conf.), Exc. Guide Schwarzwald, 45-54.
- WIMMENAUER, W. & STENGER, R. 1989: Acid and intermediate HP metamorphic rocks in the Schwarzwald (Federal Republic of Germany). - *Tectonophysics* 157, 109-116.
- WIRTH, G. 1984: Kleintektonische Untersuchungen im Grund- und Deckgebirge des Südostschwarzwaldes (Baden-Württemberg). - *Arb. geol.-paläont. Inst. Univ. Stuttgart [N.F.]* 78, 85-135.
- WITHERSPOON, P.A., WANG, J.S.Y., IWAI, K. & GALE, J.E. 1980: Validity of cubic law for fracture flow in a deformable rock fracture. - *Water Resour. Res.* 16, 1016-1024.
- WITTWER, C. 1986: Probenahmen und chemische Analysen von Grundwässern aus den Sondierbohrungen Böttstein, Weiach, Riniken, Schafisheim, Kaisten, Leuggern. - *Nagra tech. Ber. NTB* 85-49. Nagra, Wettingen.
- WOLERY, T.J. 1992: EQ3NR, A Computer Program for Geochemical Aqueous Speciation-Solubility Calculations: Theoretical Manual, User's Guide, and Related Documentation (Version 7.0). - Rep. UCRL-MA-110662PTIII, Lawrence Livermore natl. Lab., Livermore, California, USA.
- ZIEGLER, P.A. 1982: Geological Atlas of Western and Central Europe (Textband u. Atlas). - *Shell int. Petroleum Maatsch. Elsevier*, Amsterdam/New York.

## LIST OF ABBREVIATIONS

Codes for the identification of water samples are included in Table 7-1

BOE	Nagra borehole at Böttstein
BST	Buntsandstein
DZ	Tectonically disturbed zone (along northern margin of PCT)
EPM	Equivalent porous medium
GOE	Borehole at Göhrwil
HLW	High-level waste
HPD	Higher-permeability domain
K	Hydraulic conductivity [m/s]
KAI	Nagra borehole at Kaisten
KRI	Crystalline basement
LC	Lower crystalline rock unit
LEU	Nagra borehole at Leuggern
LPD	Low-permeability domain
MWCF	Major water-conducting fault
MWCF1	First order MWCF
MWCF2	Second order MWCF
P	Permian
PCT	Permo-Carboniferous Trough of Northern Switzerland
PCTs	Shoulder of PCT
RKK	Boreholes at Koblenz
SHA	Nagra borehole at Schafisheim
SIB	Nagra borehole at Siblingen
T	Transmissivity [ $m^2/s$ ]
TE	Transmissive element
TRU	Transuranic-containing waste (= long-lived intermediate-level waste)
UC	Upper crystalline rock unit
U2	Boundary at the bottom of the tectonically disturbed zone (DZ)
VE	Vertical east boundary of the regional or local groundwater flow model
VN	Vertical north boundary of the regional or local groundwater flow model
VS	Vertical south boundary of the regional or groundwater flow local model
VW	Vertical west boundary of the regional or local groundwater flow model
WCF	Water-conducting feature
WEI	Nagra borehole at Weiach
ZUR	Boreholes at Zurzach



**TECTONIC MAP OF NORTHERN SWITZERLAND AND ADJACENT AREAS**

**Pre-Mesozoic basement**

**Paleozoic sedimentary and volcanic rocks**

- Sedimentary rocks } Permian
- Quartz-porphry } Permian
- Mainly sedimentary rocks (partially metamorphosed) } Carboniferous and older
- Mainly volcanic rocks } Carboniferous and older

**Variscan basement**

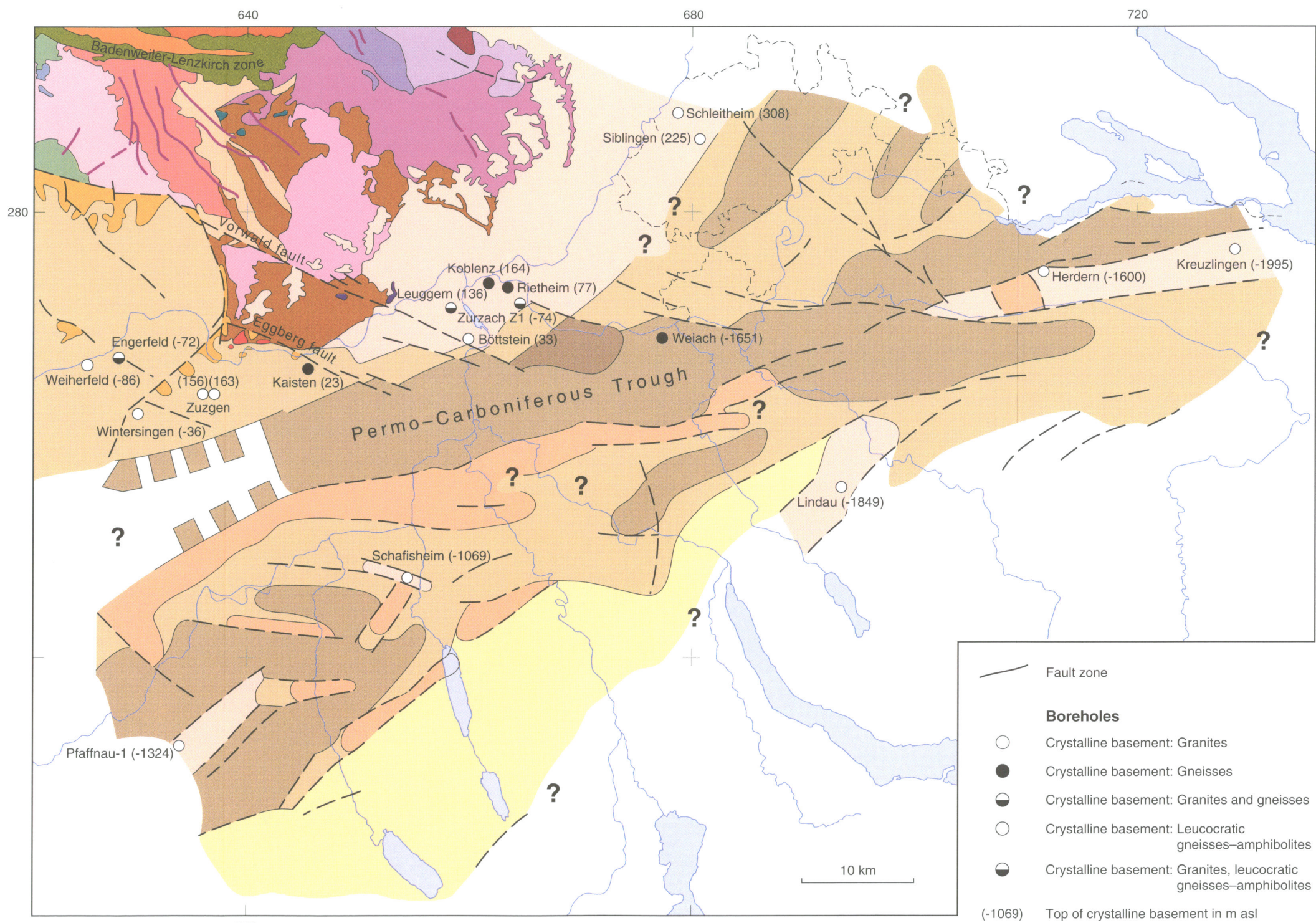
- Late-to postkinematic granites
- Early-to synkinematic granites

**Pre-Variscan basement**

- Gneisses, partly with strong anatectic overprint

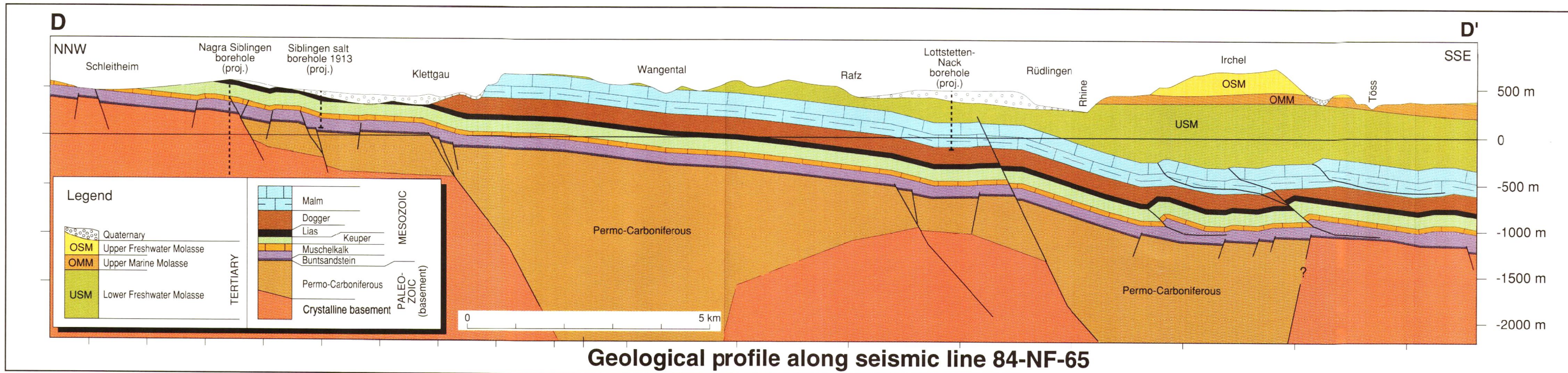
**Sedimentary cover**

- Tertiary sedimentary rocks
- Tertiary volcanic rocks (Kaiserstuhl, Hegau)
- Mesozoic of Folded Jura
- Mesozoic of Tabular Jura, Swabian Jura and Shoulders of the Rhine Graben
- Anticlines and flexures
- Thrusts
- Major normal faults (proven, suspected)
- Faults, undifferentiated (proven, suspected)



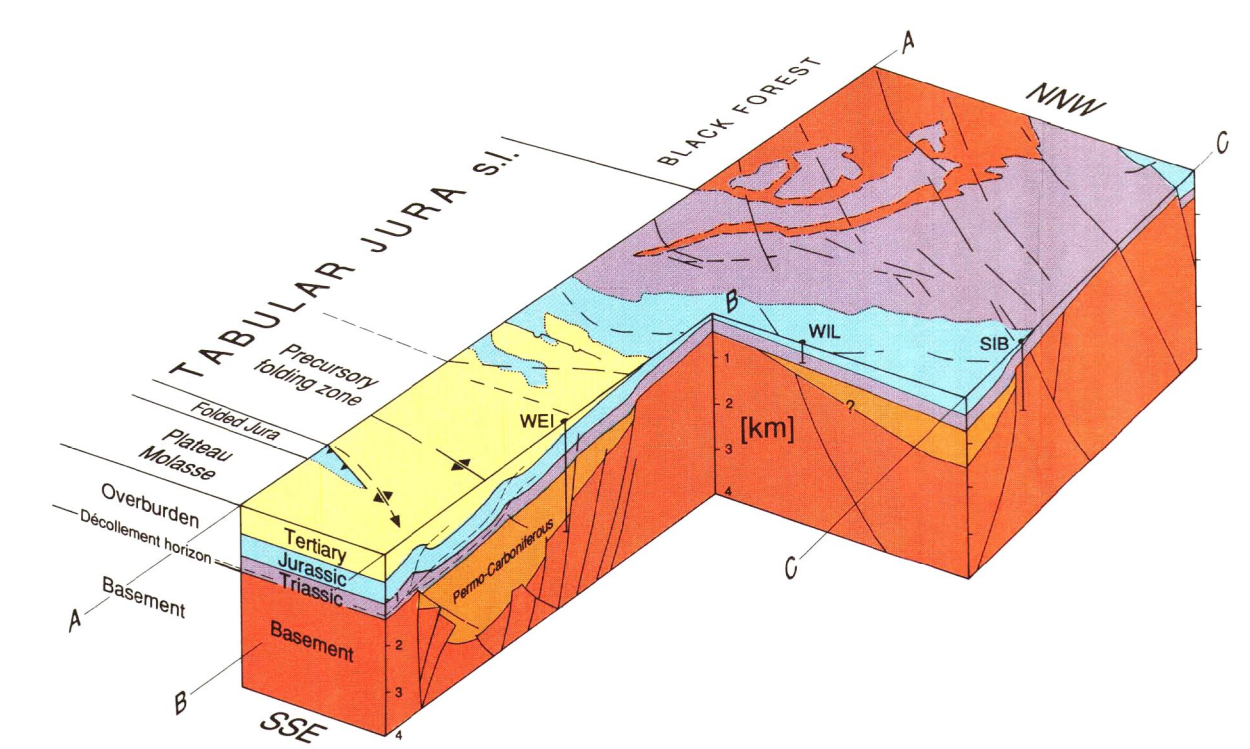
- SEDIMENTS**
- Permo-Carboniferous**
- Upper trough fill and Permian of the trough shoulders
  - Permo-Carboniferous sediments assumed
  - Deep Permo-Carboniferous trough
  - Shallow trough (upper trough fill missing)
  - Upper Rotliegendes exposed
- Upper Devonian – Lower Carboniferous**
- Sediments, volcanites and metamorphites of the Badenweiler-Lenzkirch zone
- BASEMENT**
- Crystalline basement or thin Permian (sediments) of the trough shoulders
  - Crystalline basement s.l. verified / assumed
- Variscan Basement**
- Upper Carboniferous – Permian**
- Dykes of quartz, granite porphyry and granophyre
  - Quartz porphyry of Stockberg
- Upper Carboniferous**
- Bärhalde granite
  - Schluchsee granite
  - Säcking granite
- Upper Devonian – Lower Carboniferous**
- Granites of Blauen, Klemmbach and Schlächtenhaus
  - Münsterhalden granite
  - «Rand» granite («Rand-Anatexite»)
  - Malsburg granite
  - Albtal granite
  - St. Blasien granite
  - Mambach granite
  - Lenzkirch-Steina granite
  - Hauenstein granite
- Pre-Variscan Basement**
- Gneisses, with weak anatectic overprint
  - Gneisses, with strong anatectic overprint
  - Amphibolites, serpentinites, peridotites, pyroxenites

- Fault zone**
- Boreholes**
- Crystalline basement: Granites
  - Crystalline basement: Gneisses
  - Crystalline basement: Granites and gneisses
  - Crystalline basement: Leucocratic gneisses-amphibolites
  - Crystalline basement: Granites, leucocratic gneisses-amphibolites
- (-1069) Top of crystalline basement in m asl
- Ref. :** DIEBOLD & NAEF (1990)  
ISLER ET AL. (1984)  
MEIER (1994)

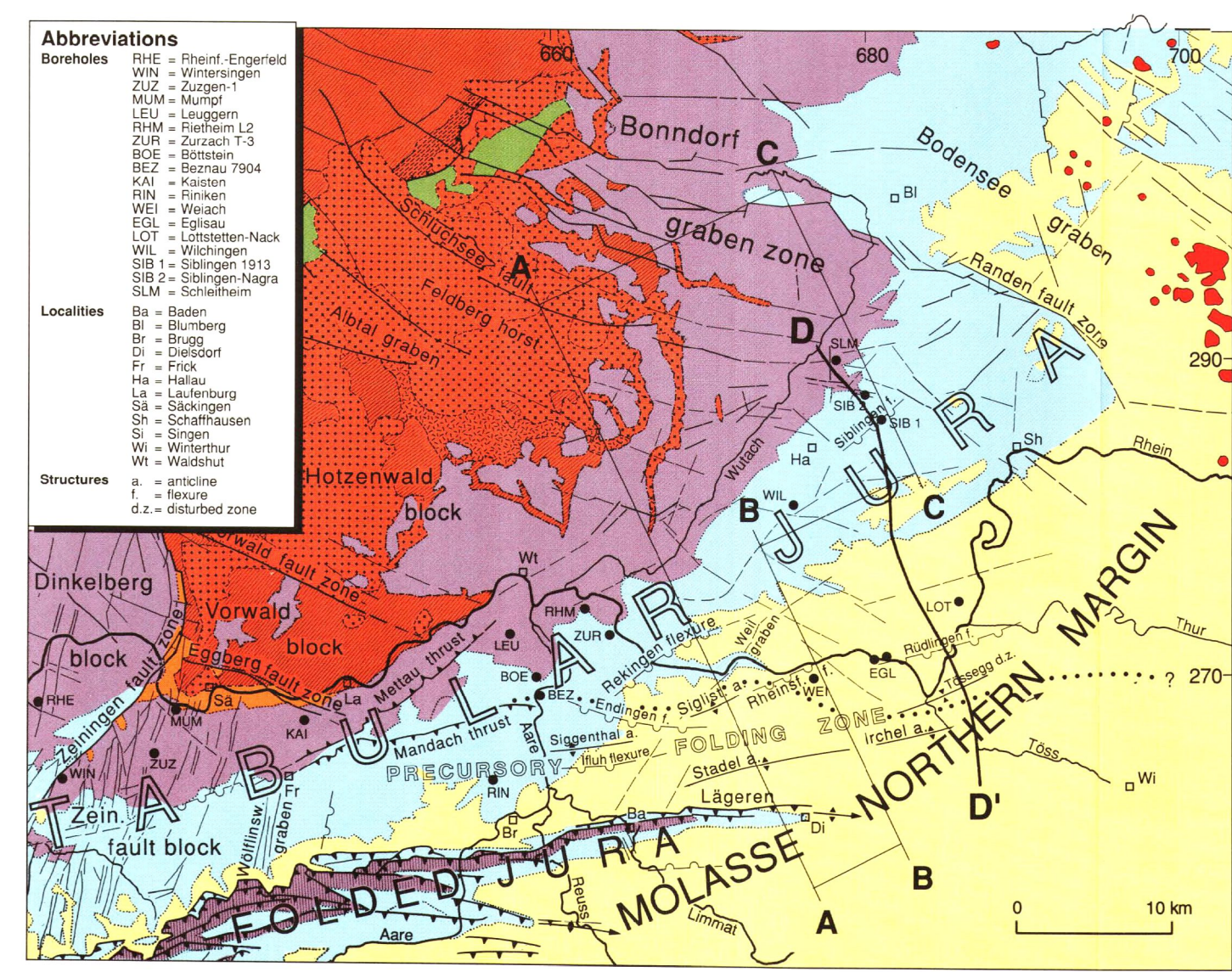


- LEGEND:**
- Variscan basement** (division according to Gerwecke et al. 1984, Appendix 1)
- Post-tectonic (undeformed) granites
    - M Mambach-granite
    - A Albtal-granite
    - U Ursee-granite
    - S Schluchsee-granite
    - B Bärhalden-granite
  - Syntectonic granites, granitoids and contact zones of the Badenweiler-Lenzkirch Zone
  - Syntect. complexes and mixed zones
    - Be Belchen
    - Bl Blauen
    - Sb St. Basien
    - We Wehratal syenites
    - Ww Wiesen- and Wehratal diorites
    - Ma Mambach syntectites

- Key to tectonic map**
- Post-Variscan overburden** (Quaternary not represented)
- Tertiary
  - Volcanism
  - Jurassic
  - Triassic
  - Permian (Upper Rotliegendes)
- Late Variscan overburden**
- Acid volcanism, ignimbrites, rhyolites, sheet porphyries
  - Sediments and volcanites of the Badenweiler-Lenzkirch Zone (Upp. Devonian-Viséan)
  - Pre-Variscan basement; mainly gneisses and anatectic gneisses
- Signatures**
- Disturbed zones (mostly faults, detected seismically underground)
  - Flexure
  - Overthrust
  - Muschelkalk imbrication zone (Folded Jura)
  - Fold axis (partly from seismic evidence)
  - Northern margin of distant push

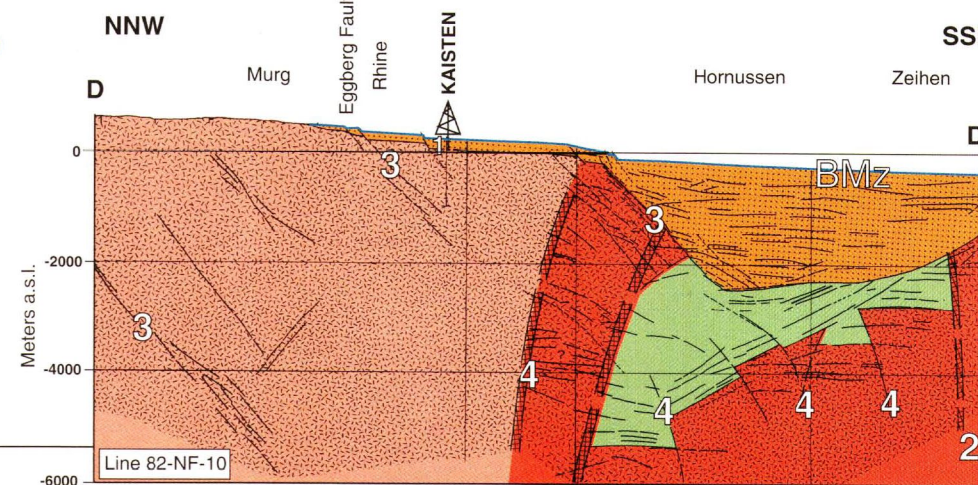
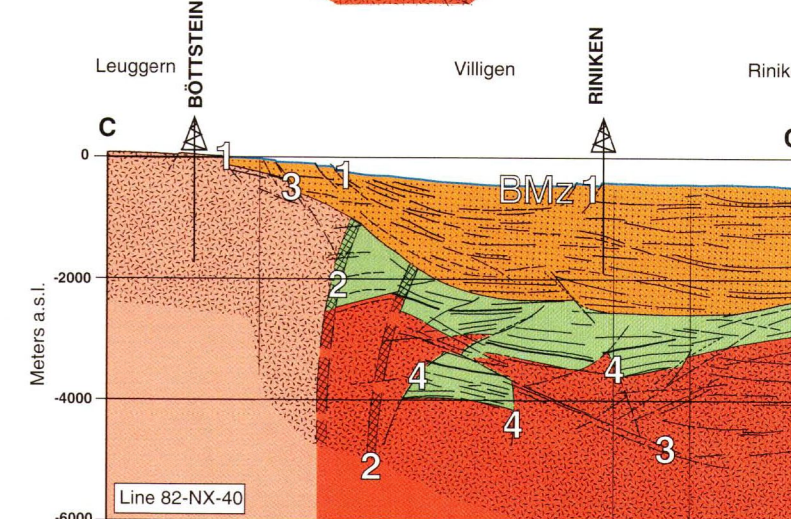
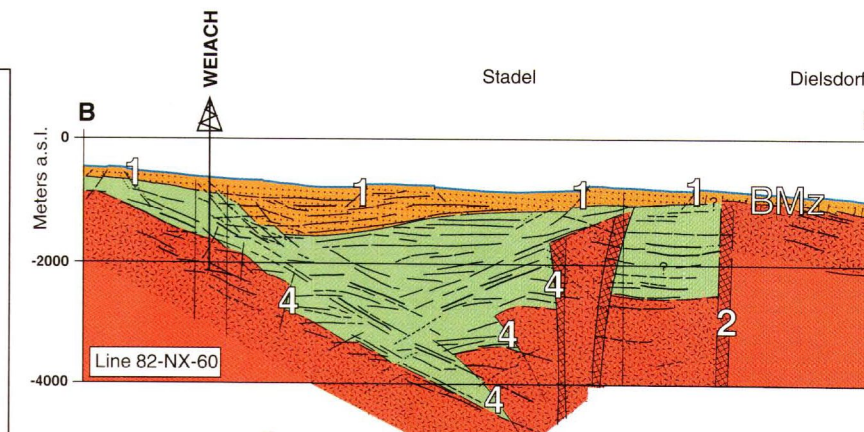
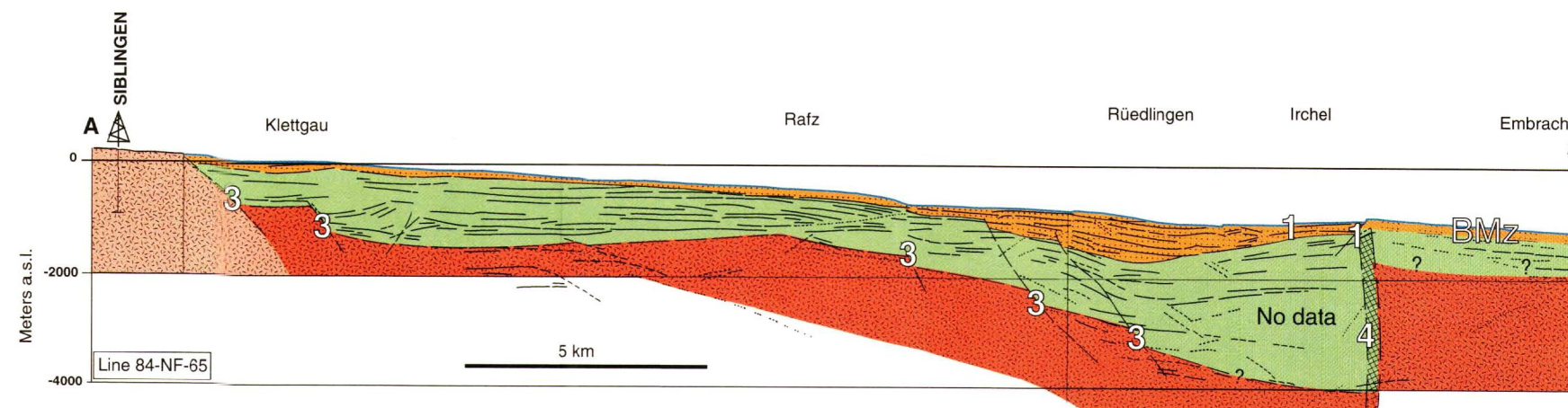


**Schematic block diagram of eastern Tabular Jura**



**TECTONIC OVERVIEW OF CENTRAL NORTHERN SWITZERLAND: Structures in the sedimentary overburden of the eastern Tabular Jura s.l.**

Figures from Nagra bulletin No. 2/1990

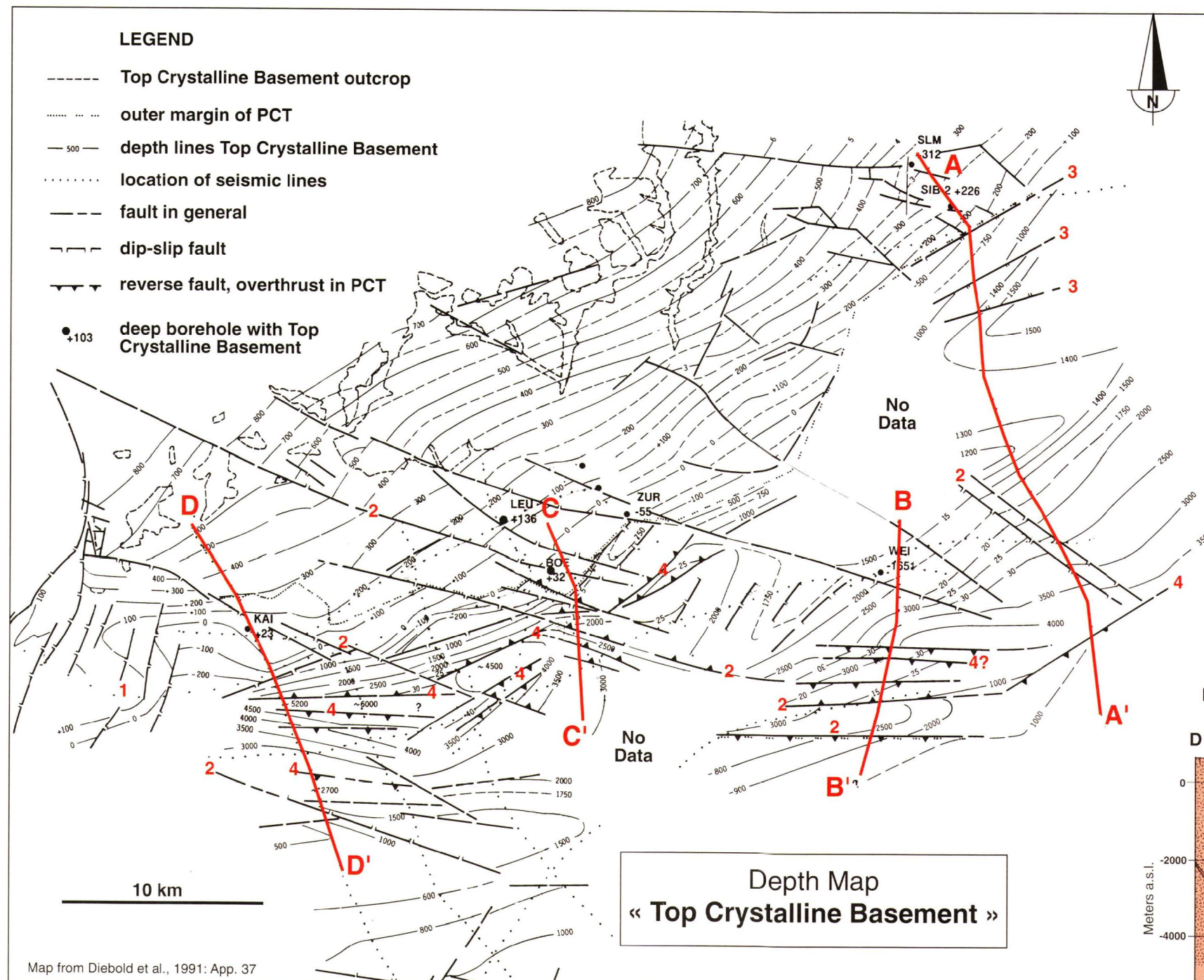


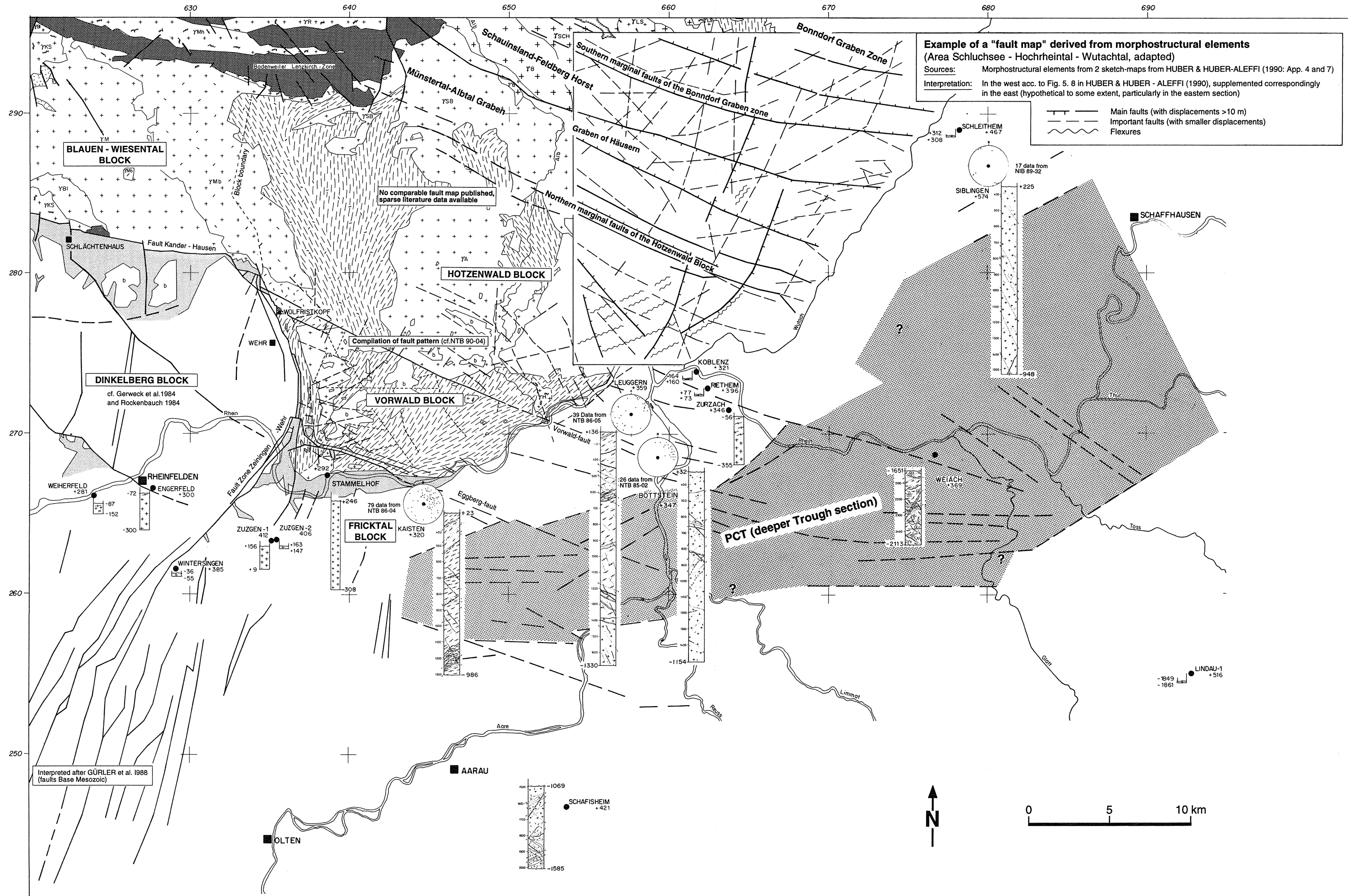
**LITHOLOGIES IN PROFILES A to D:**

- Base of Mesozoic BMz
- Upper trough infill (Late Permian)
- Lower trough infill (Upper Carboniferous - Permian)
- Crystalline Basement north of PCT
- Crystalline Basement below PCT

**FAULT ZONES:**

- 1 Late to post-Permian faults, partly reactivated during the Tertiary
- 2 Transverse faults of Saalian phase
- 3 Stephanian extensional faults; partly reactivated during the Tertiary
- 4 Stephanian extensional faults, transpressively overprinted during the Early Permian





**Example of a "fault map" derived from morphostructural elements**  
 (Area Schluchsee - Hochrheintal - Wutachtal, adapted)  
 Sources: Morphostructural elements from 2 sketch-maps from HUBER & HUBER-ALEFFI (1990: App. 4 and 7)  
 Interpretation: In the west acc. to Fig. 5, 8 in HUBER & HUBER - ALEFFI (1990), supplemented correspondingly in the east (hypothetical to some extent, particularly in the eastern section)

— Main faults (with displacements >10 m)  
 - - - Important faults (with smaller displacements)  
 ~~~~~ Flexures

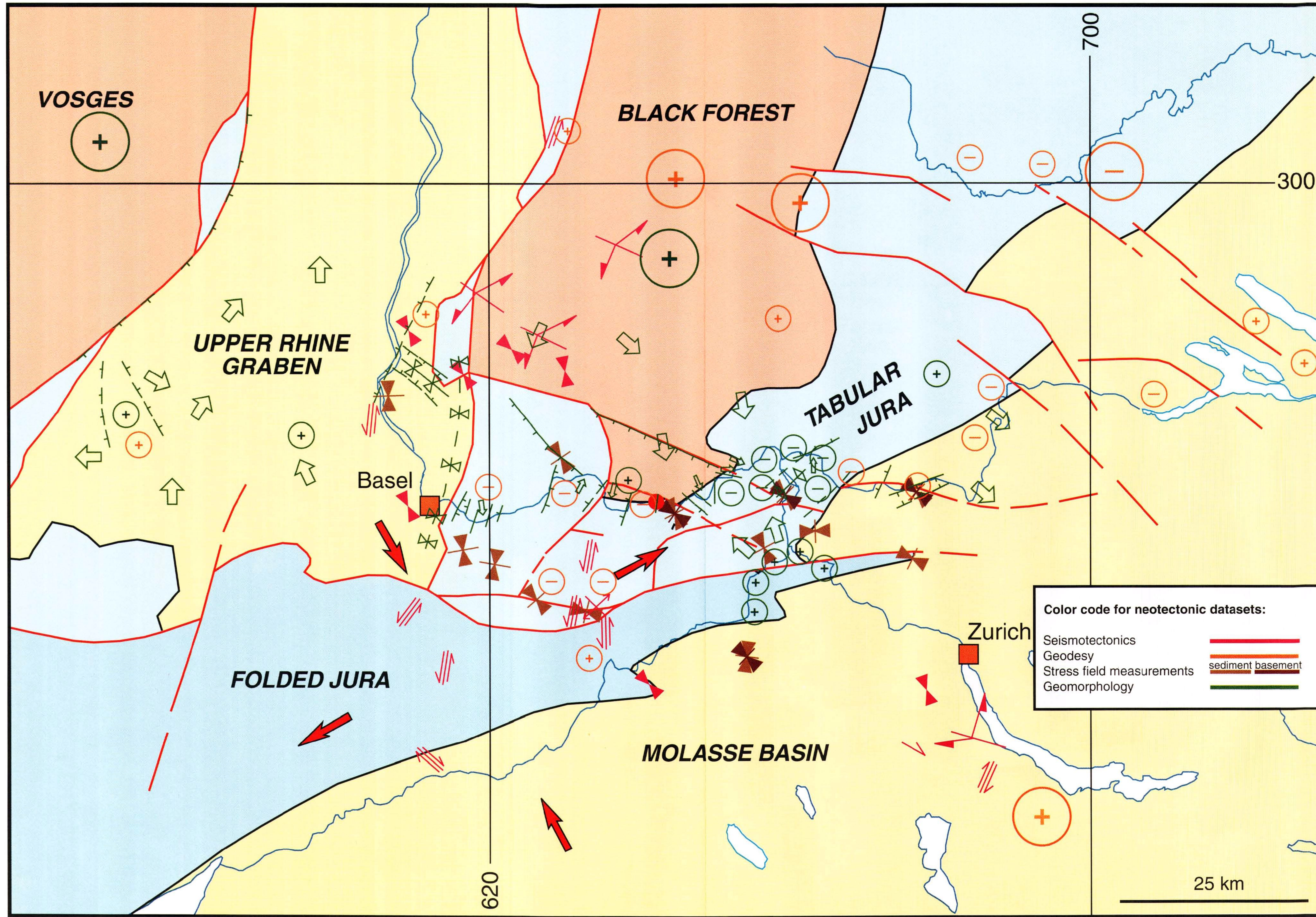
No comparable fault map published, sparse literature data available

Compilation of fault pattern (cf. NTB 90-04)

DINKELBERG BLOCK  
 cf. Gerweck et al. 1984 and Rothenbach 1984

Interpreted after GÜRLER et al. 1988 (faults Base Mesozoic)

- SURFACE GEOLOGY** (without Quaternary)
- Mesozoic and Tertiary
  - Buntsandstein (only isolated deposits on crystalline basement and Permian)
  - Permian in the Rhine Valley and Dinkelberg Block
  - Occurrence of Paleozoic sediments, volcanites and metamorphites (age partly unknown) in the Black Forest
    - Badenweiler-Lenzkirch Zone (BLZ)
    - Schlächtenhaus (metamorphites)
    - Wolfristkopf (occurrence uncertain)
  - Nappe-like quartz porphyry of Stockberg
- Variscan Basement**
- Upper Carboniferous granites
    - Y<sub>B</sub> Bärhalde Granites
    - Y<sub>Sch</sub> Schluchsee Granites
  - Lower Carboniferous granites (only locally cataclastically overprinted, or not all)
    - Y<sub>S</sub> Granite of Säkingen
    - Y<sub>A</sub> Albtal Granite
    - Y<sub>SB</sub> Granite of St. Blasien
    - Y<sub>M</sub> Malsburg Granite
    - Y<sub>BL</sub> Blauen Granite
  - Upper Devonian-Lower Carboniferous granites (extensively cataclastically overprinted)
    - Y<sub>S</sub> Klemmbach Granite, Granite of Schlächtenhaus
    - Y<sub>Mh</sub> Münsterhalden Granite
    - Y<sub>SH</sub> Granite of Schönau-Herrenschwand
    - Y<sub>MB</sub> Granite of Mambach
    - Y<sub>LS</sub> Lenzkirch-Steina Granite
    - Y<sub>H</sub> Granite of Hauenstein
    - Y<sub>R</sub> Marginal Granite
  - Cataclastic overprinting
  - Anatectic overprinting
- Pre-Variscan Basement**
- Gneiss antexite with cleavage direction, marked anatectic overprinting
  - Gneiss antexite with cleavage direction, marked anatectic overprinting
  - Wiesen-Wehratal complex
  - Anatexites of the lower Wehratal
  - Presence of faults certain
  - Presence of faults presumed
  - Presence of faults presumed (based on morphotectonic criteria)
- BOREHOLES**
- Presence of faults presumed
  - Data on terrain level (in m.a.s.l.), level of top of crystalline basement and level of borehole bottom
  - Granite
  - Gneiss, schist
  - Monzonite, diorite, syenite
- In the Nagra boreholes BÖTTSTEIN, KAISTEN, LEUGGERN, SCHAFISHEIM, SIBLINGEN and WEIACH:
- A: Aplites, aplitic-granites
  - P: Pegmatites
  - L: Lamprophyres
  - Rh: Rhyolitic porphyries
- Faults, fracturing.
  - Presentation of the (fault) plane poles projection, lower hemisphere. Only orientated faults shown.



**Color code for neotectonic datasets:**

|                           |                        |
|---------------------------|------------------------|
| Seismotectonics           | Red line               |
| Geodesy                   | Orange line            |
| Stress field measurements | Green line             |
| Geomorphology             | Blue line              |
|                           | Red line (sediment)    |
|                           | Orange line (basement) |

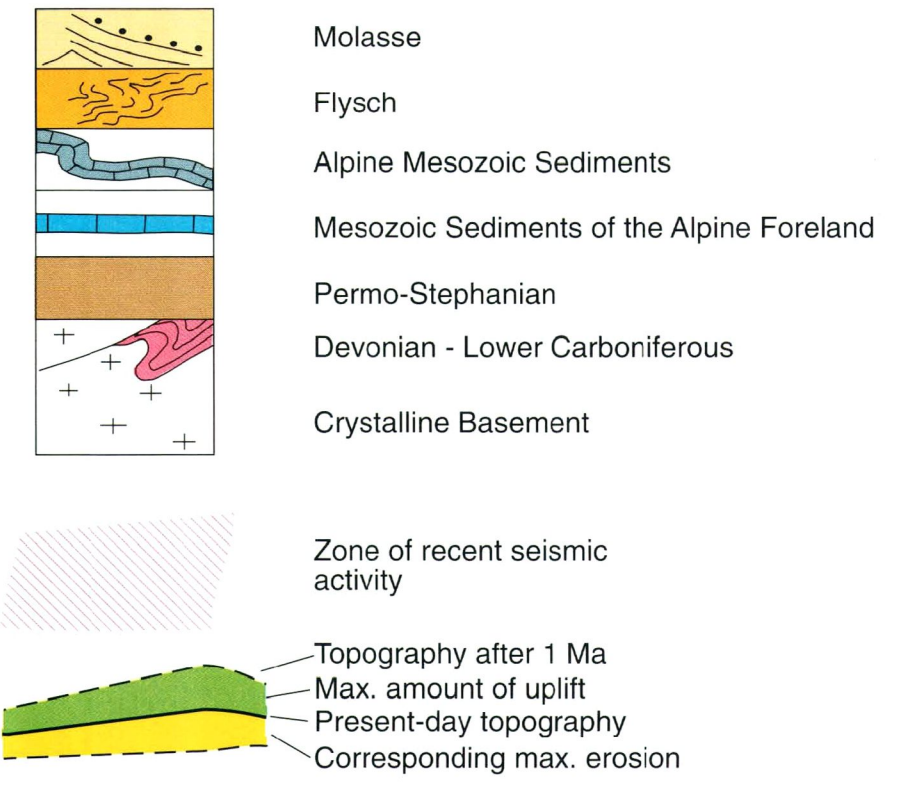
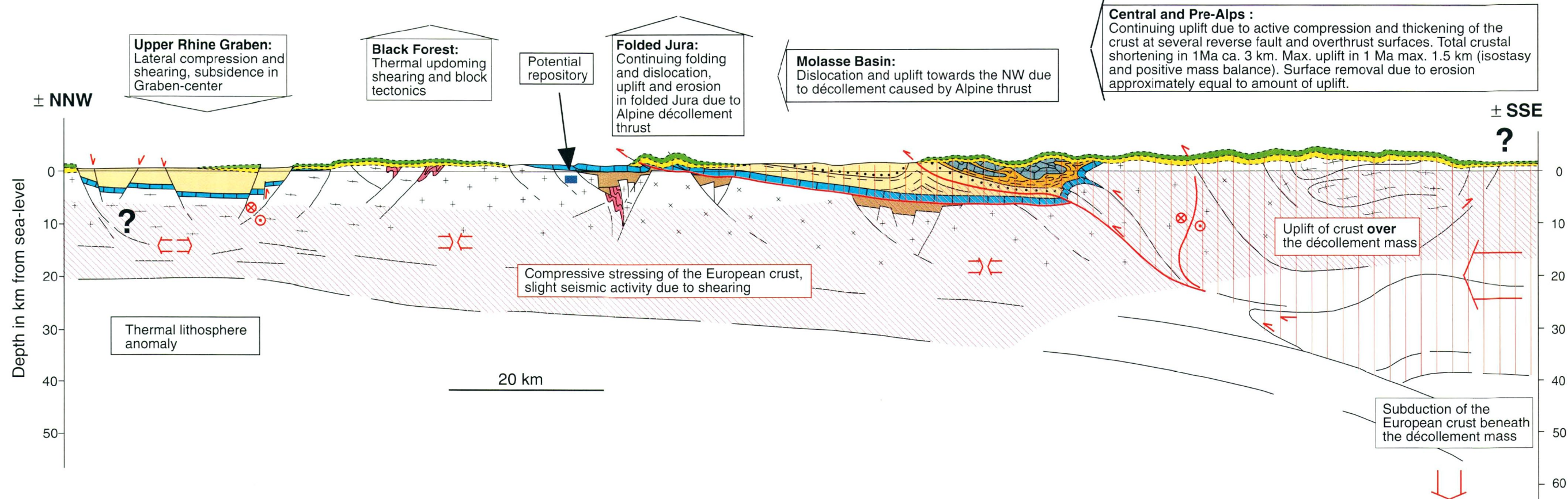
- Types of movement:**
- Normal fault, dislocation, fracture
  - Flexure
  - ⇌ Lateral movement, transverse fault
  - ◇ Anticline, updoming
  - ▽ Syncline, subsidence
  - ▽ Overthrust
  - ⊕ ⊖ Local uplift, subsidence
  - ⊕ ⊖ Large-scale regional uplift, subsidence
  - ⇒ Local tilt
  - ⇒ Regional large-scale tilt
  - Levelling reference point Laufenburg
  - ⊗ In situ stress measurements sediments / basement
  - ⊗ Seismotectonics, fault plane solutions Stress determination
  - Main faults and overthrusts
  - ⊗ Regional stress field derived from neotectonic information

**Main References:**

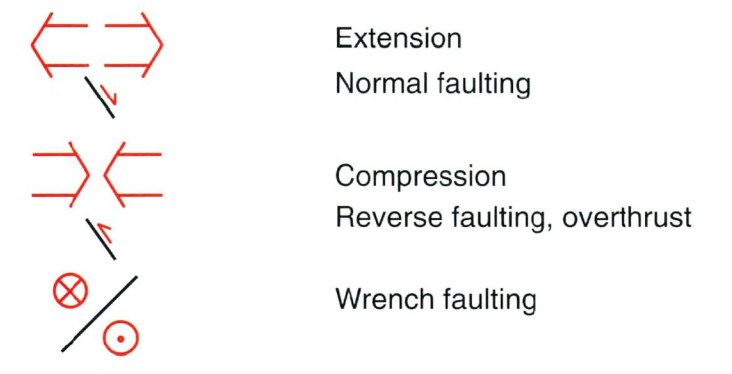
|                                   |                             |
|-----------------------------------|-----------------------------|
| ECKER, A. et al., 1984            | ISLER, A., 1984             |
| BONJER et al., 1989               | MÄLZER, H. et al., 1988     |
| DEICHMANN, N., 1987               | MIERLO, J. van et al., 1992 |
| DEICHMANN, N., 1990               | MÜLLER, W.H. et al., 1987   |
| DEICHMANN, N. & RENGGLI, K., 1984 | NEUGEBAUER, et al., 1980    |
| DIEBOLD, P. & MÜLLER, W.H., 1985  | PAVONI, N., 1984            |
| GUBLER et al., 1984               | SCHNEIDER, et al., 1992     |
| GWINNER, M.P., 1955               | SCHNEIDER, G., 1967         |
| HALDIMANN et al., 1984            | SCHNEIDER, G., 1979         |
| ILLIES, J.H. & GREINER, G., 1979  | THEOBALD, N. et al., 1977   |

**SCENARIO B in 1 Ma**

- Continuing compression and active crustal shortening in the Alps



**Stress state and movements :**



**SCENARIO B in 10 Ma**

